Impact of Emerging SARS-CoV-2 Variants on Humoral Immune Responses of COVID-19-Infected and Vaccinated Individuals

Dissertation

der Mathematisch-Naturwissenschaftlichen Fakultät

der Eberhard Karls Universität Tübingen

zur Erlangung des Grades eines

Doktors der Naturwissenschaften

(Dr. rer. nat.)

vorgelegt von

Daniel Junker

aus Reutlingen

Tübingen

2024

Gedruckt mit Genehmigung der Mathematisch-Naturwissenschaftlichen Fakultät der Eberhard Karls Universität Tübingen.

Tag der mündlichen Qualifikation:	16.10.2024
Dekan:	Prof. Dr. Thilo Stehle
1. Berichterstatter/-in:	Prof. Dr. Ulrich Rothbauer
2. Berichterstatter/-in:	Prof. Dr. Katja Schenke-Layland
3. Berichterstatter/-in:	PD Dr. Markus Löffler

Table of Contents

Abstract

The COVID-19 pandemic caused by the previously unknown SARS-CoV-2 presented the scientific community with the challenging task of understanding the basic properties of the virus under rapidly evolving and changing circumstances, in order to pave the way for effective therapies and vaccines.

To assess the humoral immune response to SARS-CoV-2, we developed and validated a multiplex serological immunoassay, MULTICOV-AB, for the reliable detection of antibodies against SARS-CoV-2 key antigens including the receptor binding domain (RBD) and nucleocapsid, demonstrating high sensitivity and specificity for the classification of infection. As the seroprevalence of SARS-CoV-2 in the population continuously increased and vaccination campaigns progressed, the quality of the antibody response, including longevity and immune protection, became the focus of research. This has been reinforced by the continuous emergence of new SARS-CoV-2 variants that differ in their ability to evade existing immune responses and thus make reinfection more likely.

Therefore, we have developed RBDCoV-ACE2, a multiplex surrogate neutralisation assay that investigates the presence of neutralising antibodies (NAbs) that interfere with the binding of the SARS-CoV-2 RBD to the host cellular receptor angiotensin-converting enzyme 2 (ACE2), which is equivalent to preventing infection *in vivo*.

Using both assays, we were able to show that variants with the E484K mutation, for example Beta, Gamma and Theta, are more likely to evade existing humoral immune responses, as antibodies formed against the RBD of the wild-type virus exhibited up to 14-fold lower ACE2 binding inhibition against these variants. Furthermore, we were able to compare vaccination regimens and show that mRNA-based vaccination led to a superior humoral immune response compared to homologous vector-based vaccine regimens. We were able to show that the long-term humoral immune response to SARS-CoV-2 infection lasts longer in children than in adults, even after asymptomatic infection. With the emergence of the highly mutated Omicron variants, we were able to show that both antigen binding and ACE2 binding inhibition of antibodies induced by vaccination or/and infection were greatly reduced, with booster doses and breakthrough infections causing a significant increase in both levels. This reduction in neutralising capacity was particularly noticeable in serum from immunocompromised individuals, such as hemodialysis or inflammatory bowel disease (IBD) patients, where we were able to contribute indications for future vaccination strategies. Both MULTICOV-AB and RBDCoV-ACE2 continue to provide valuable knowledge about the humoral immune response to novel emerging SARS-CoV-2 variants.

Zusammenfassung

Die COVID-19-Pandemie, die durch das bis dahin unbekannte SARS-CoV-2 verursacht wurde, stellte die Wissenschaft vor die schwierige Aufgabe, die grundlegenden Eigenschaften des Virus unter sich rasch entwickelnden und verändernden Bedingungen zu verstehen, um den Weg für wirksame Therapien und Impfstoffe zu ebnen.

Zur Bewertung der humoralen Immunantwort auf SARS-CoV-2 haben wir einen serologischen, multiplexen Immunassay, MULTICOV-AB, für den zuverlässigen Nachweis von Antikörpern gegen SARS-CoV-2-Schlüsselantigene, einschließlich der Rezeptorbindungsdomäne (RBD) und Nukleokapsid, entwickelt und validiert, der eine hohe Sensitivität und Spezifität für die Klassifizierung einer Infektion aufweist. Mit dem kontinuierlichen Anstieg der Seroprävalenz von SARS-CoV-2 in der Bevölkerung und dem Fortschreiten der weltweiten Impfkampagne rückte die Qualität der Antikörperreaktion, einschließlich Langlebigkeit und Immunschutz, in den Mittelpunkt der Forschung. Dies wurde durch das kontinuierliche Auftauchen neuer SARS-CoV- 2-Varianten verstärkt, die sich in ihrer Fähigkeit unterscheiden, bestehenden Immunantworten zu entgehen und somit eine Reinfektion wahrscheinlicher machen.

Daher haben wir RBDCoV-ACE2 entwickelt, einen multiplexen Surrogat-Neutralisationstest, der das Vorhandensein neutralisierender Antikörper (NAbs) untersucht, die die Bindung der SARS-CoV-2 RBD an den zellulären Wirtsrezeptor Angiotensin-konvertierendes Enzym 2 (ACE2) beeinträchtigen, was einer Verhinderung der Infektion *in vivo* gleichkommt.

Mit Hilfe beider Assays konnten wir zeigen, dass Varianten mit der E484K-Mutation, z. B. Beta, Gamma und Theta, eher in der Lage sind, bestehende humorale Immunantworten zu umgehen, da Antikörper, die gegen die RBD des Wildtyp-Virus gebildet werden, eine bis zu 14-fach geringere ACE2-Bindungshemmung gegen diese Varianten aufwiesen. Außerdem konnten wir Impfschemata vergleichen und zeigen, dass die mRNA-basierte Impfung zu einer stärkeren humoralen Immunantwort führte als homologe vektorbasierte Impfstoffschemata. Wir konnten zeigen, dass die langfristige humorale Immunantwort auf eine SARS-CoV-2-Infektion bei Kindern auch nach einer asymptomatischen Infektion länger anhält als bei Erwachsenen. Mit dem Auftreten der stark mutierten Omikron-Varianten konnten wir zeigen, dass sowohl die Antigenbindung als auch die ACE2-Bindungshemmung von Antikörpern, die durch eine Impfung oder/und eine Infektion induziert wurden, stark reduziert waren, wobei Auffrischungsdosen und Durchbruchsinfektionen zu einem deutlichen Anstieg beider Werte führten. Diese Verringerung der Neutralisierungskapazität war besonders auffällig im Serum von immungeschwächten Personen, wie z. B. Hämodialyse-Patienten oder Personen mit chronisch-entzündlichen Darmerkrankungen, wo wir Hinweise für künftige Impfstrategien liefern konnten. Sowohl MULTICOV-AB als auch RBDCoV-ACE2 liefern weiterhin wertvolle Erkenntnisse über die humorale Immunantwort auf neu auftretende SARS-CoV-2-Varianten.

Abbreviations

SARS-CoV-2	Severe-acute-respiratory-syndrome-related coronavirus 2
COVID-19	Coronavirus disease 2019
RBD	Receptor binding domain
ACE2	Angiotensin-converting enzyme 2
WHO	World Health Organization
PHEIC	Public health emergency of international concern
MERS-CoV	Middle east respiratory syndrome coronavirus
ORF	Open reading frame
kb	Kilo bases
NSP	Non-structural protein
CMA	Conditional marketing authorisation
EMA	European Medicines Agency
FDA	United States Food and Drug Administration
STIKO	German Standing Committee on Vaccination
IBD	Inflammatory bowel disease
VOI	Variant of interest
VOC	Variant of concern
VUM	Variant under monitoring
PRR	Pattern recognition receptors
BCR	B-cell receptor
MHC	Major histocompatibility complex
IgG	Immunoglobulin G
IgA	Immunoglobulin A
IgM	Immunoglobulin M
TCR	T-cell receptor
NAbs	Neutralising antibodies
ADCC	Antibody-dependent cellular cytotoxicity
xMAP	x = analyte, MAP = Multi-Analyte Profiling
VNT	Virus neutralisation test
BSL3	Biosafety level 3
%CV	Coefficient of variation in percent (Standard deviation divided by the mean multiplied by 100)
WT	Wild-type
BLI	Biolayer Interferometry

List of Figures

List of Tables

List of Publications

Accepted publications that are part of this thesis

* = Authors contributed equally

1. Becker M*, Strengert M*, **Junker D**, Kaiser PD, Kerrinnes T, Traenkle B, Dinter H, Häring J, Ghozzi S, Zeck A, Weise F, Peter A, Hörber S, Fink S, Ruoff F, Dulovic A, Bakchoul T, Baillot A, Lohse S, Cornberg M, Illig T, Gottlieb J, Smola S, Karch A, Berger K, Rammensee HG, Schenke-Layland K, Nelde A, Märklin M, Heitmann JS, Walz JS, Templin M, Joos TO, Rothbauer U, Krause G, Schneiderhan-Marra N. **Exploring beyond clinical routine SARS-CoV-2 serology using MultiCoV-Ab to evaluate endemic coronavirus cross-reactivity**. *Nat Commun.* 2021. 12(1):1152. https://doi.org/10.1038/s41467-021-20973-3

2. **Junker D**, Dulovic A, Becker M, Wagner TR, Kaiser PD, Traenkle B, Kienzle K, Bunk S, Struemper C, Haeberle H, Schmauder K, Ruetalo N, Malek N, Althaus K, Koeppen M, Rothbauer U, Walz JS, Schindler M, Bitzer M, Göpel S, Schneiderhan-Marra N. **COVID-19 patient serum less potently inhibits ACE2-RBD binding for various SARS-CoV-2 RBD mutants.** *Sci Rep.* 2022. 12(1):7168. https://doi.org/10.1038/s41598-022-10987-2

3. Dulovic A*, Kessel B*, Harries M*, Becker M, Ortmann J, Griesbaum J, Jüngling J, **Junker D**, Hernandez P, Gornyk D, Glöckner S, Melhorn V, Castell S, Heise JK, Kemmling Y, Tonn T, Frank K, Illig T, Klopp N, Warikoo N, Rath A, Suckel C, Marzian AU, Grupe N, Kaiser PD, Traenkle B, Rothbauer U, Kerrinnes T, Krause G, Lange B, Schneiderhan-Marra N, Strengert M. **Comparative Magnitude and Persistence of Humoral SARS-CoV-2 Vaccination Responses in the Adult Population in Germany**. *Front Immunol.* 2022. 13:828053. https://doi.org/10.3389/fimmu.2022.828053

4. Becker M*, Dulovic A*, **Junker D**, Ruetalo N, Kaiser PD, Pinilla YT, Heinzel C, Haering J, Traenkle B, Wagner TR, Layer M, Mehrlaender M, Mirakaj V, Held J, Planatscher H, Schenke-Layland K, Krause G, Strengert M, Bakchoul T, Althaus K, Fendel R, Kreidenweiss A, Koeppen M, Rothbauer U, Schindler M, Schneiderhan-Marra N. **Immune response to SARS-CoV-2 variants of concern in vaccinated individuals.** *Nat Commun***.** 2021. 12(1):3109. https://doi.org/10.1038/s41467-021-23473-6

5. Renk H*, Dulovic A*, Seidel A*, Becker M, Fabricius D, Zernickel M, **Junker D**, Groß R, Müller J, Hilger A, Bode SFN, Fritsch L, Frieh P, Haddad A, Görne T, Remppis J, Ganzemueller T, Dietz A, Huzly D, Hengel H, Kaier K, Weber S, Jacobsen EM, Kaiser PD, Traenkle B, Rothbauer U, Stich M, Tönshoff B, Hoffmann GF, Müller B, Ludwig C, Jahrsdörfer B, Schrezenmeier H, Peter A, Hörber S, Iftner T, Münch J, Stamminger T, Groß HJ, Wolkewitz M, Engel C, Liu W, Rizzi M, Hahn BH, Henneke P, Franz AR, Debatin KM, Schneiderhan-Marra N, Janda A, Elling R. **Robust and durable serological response following pediatric SARS-CoV-2 infection.** *Nat Commun.* 2022. 13(1):128. https://doi.org/10.1038/s41467-021-27595-9

6. **Junker D***, Becker M*, Wagner TR*, Kaiser PD, Maier S, Grimm TM, Griesbaum J, Marsall P, Gruber J, Traenkle B, Heinzel C, Pinilla YT, Held J, Fendel R, Kreidenweiss A, Nelde A, Maringer Y, Schroeder S, Walz JS, Althaus K, Uzun G, Mikus M, Bakchoul T, Schenke-Layland K, Bunk S, Haeberle H, Göpel S, Bitzer M, Renk H, Remppis J, Engel C, Franz AR, Harries M, Kessel B, Lange B, Strengert M, Krause G, Zeck A, Rothbauer U, Dulovic A, Schneiderhan-Marra N. **Antibody Binding and Angiotensin-Converting Enzyme 2 Binding Inhibition Is Significantly Reduced for Both the BA.1 and BA.2 Omicron Variants**. *Clin Infect Dis*. 2023. 76(3):e240-e249. https://doi.org/10.1093/cid/ciac498

7. Dulovic A*, Strengert M*, Ramos GM*, Becker M, Griesbaum J, **Junker D**, Lürken K, Beigel A, Wrenger E, Lonnemann G, Cossmann A, Stankov MV, Dopfer-Jablonka A, Kaiser PD, Traenkle B, Rothbauer U, Krause G, Schneiderhan-Marra N, Behrens GMN. **Diminishing Immune Responses against Variants of Concern in Dialysis Patients 4 Months after SARS-CoV-2 mRNA Vaccination.** *Emerg Infect Dis*. 2022. 28(4):743-750. https://doi.org/10.3201/eid2804.211907

8. Becker M*, Cossmann A*, Lürken K, **Junker D**, Gruber J, Juengling J, Ramos GM, Beigel A, Wrenger E, Lonnemann G, Stankov MV, Dopfer-Jablonka A, Kaiser PD, Traenkle B, Rothbauer U, Krause G, Schneiderhan-Marra N, Strengert M, Dulovic A, Behrens GMN. **Longitudinal cellular and humoral immune responses after triple BNT162b2 and fourth full-dose mRNA-1273 vaccination in haemodialysis patients.** *Front Immunol*. 2022. 13:1004045. https://doi.org/10.3389/fimmu.2022.1004045

9. Woelfel S, Dütschler J, König M, Dulovic A, Graf N, **Junker D**, Oikonomou V, Krieger C, Truniger S, Franke A, Eckhold A, Forsch K, Koller S, Wyss J, Krupka N, Oberholzer M, Frei N, Geissler N, Schaub P; STAR SIGN Study Investigators; Albrich WC, Friedrich M, Schneiderhan-Marra N, Misselwitz B, Korte W, Bürgi JJ, Brand S. **STAR SIGN study: Evaluation of COVID-19 vaccine efficacy against the SARS-CoV-2 variants BQ.1.1 and XBB.1.5 in patients with inflammatory bowel disease.** *Aliment Pharmacol Ther*. 2023. 58(7):678-691. https://doi.org/10.1111/apt.17661

The following unpublished manuscript is part of this thesis:

10. Becker M*, Dulovic A*, Uzun G, Bareiß A, Mikus M, **Junker D**, Griesbaum J, Michel T, Fandrich M, Schenke-Layland K, Althaus K, Bakchoul T, Schneiderhan-Marra N. **Dynamics of humoral response towards SARS-CoV-2 from vaccination and breakthrough infection**. Unpublished Manuscript

Author Contribution

Table 1: Personal contribution to publications that are part of this thesis

Manuscript Number	**1**	**2**	**3**	**4**	**5**	**6**	**7**	**8**	**9**	**10**
Accepted for publication	yes	yes	yes	yes	yes	yes	yes	yes	yes	no
Number of authors	36	21	32	26	50	41	19	20	20	13
Position of candidate in author list	3	1	8	3	7	1	6	4	4	6
Scientific ideas by candidate (%)	50	70	10	30	10	50	10	20	20	10
Data generation by candidate (%)	50	70	50	60	60	50	50	50	50	50
Interpretation and analysis by candidate (%)	20	60	20	20	10	50	10	20	20	20
Paper writing by candidate (%)	20	60	10	30	10	25	10	10	10	10

Accepted publications that are not part of this thesis

11. Wagner TR*, Ostertag E*, Kaiser PD, Gramlich M, Ruetalo N, **Junker D**, Haering J, Traenkle B, Becker M, Dulovic A, Schweizer H, Nueske S, Scholz A, Zeck A, Schenke-Layland K, Nelde A, Strengert M, Walz JS, Zocher G, Stehle T, Schindler M, Schneiderhan-Marra N, Rothbauer U. **NeutrobodyPlex-monitoring SARS-CoV-2 neutralising immune responses using nanobodies**. *EMBO Rep.* 2021. 22(5):e52325. https://doi.org/10.15252/embr.202052325

12. Fink S*, Ruoff F*, Stahl A, Becker M, Kaiser P, Traenkle B, **Junker D**, Weise F, Ruetalo N, Hörber S, Peter A, Nelde A, Walz J, Krause G, Baillot A, Schenke-Layland K, Joos TO, Rothbauer U, Schneiderhan-Marra N, Schindler M, Templin MF. **Multiplexed Serum Antibody Screening Platform Using Virus Extracts from Endemic Coronaviridae and SARS-CoV-2**. *ACS Infect Dis.* 2021. 7(6):1596-1606. https://doi.org/10.1021/acsinfecdis.0c00725

13. Wratil PR, Schmacke NA, Karakoc B, Dulovic A, **Junker D**, Becker M, Rothbauer U, Osterman A, Spaeth PM, Ruhle A, Gapp M, Schneider S, Muenchhoff M, Hellmuth JC, Scherer C, Mayerle J, Reincke M, Behr J, Kääb S, Zwissler B, von Bergwelt-Baildon M, Eberle J, Kaderali L, Schneiderhan-Marra N, Hornung V, Keppler OT. **Evidence for increased SARS-CoV-2 susceptibility and COVID-19 severity related to pre-existing immunity to seasonal coronaviruses**. *Cell Rep.* 2021. 37(13):110169. https://doi.org/10.1016/j.celrep.2021.110169

14. Wagner TR*, Schnepf D*, Beer J*, Ruetalo N*, Klingel K, Kaiser PD, **Junker D**, Sauter M, Traenkle B, Frecot DI, Becker M, Schneiderhan-Marra N, Ohnemus A, Schwemmle M, Schindler M, Rothbauer U. **Biparatopic nanobodies protect mice from lethal challenge with SARS-CoV-2 variants of concern**. *EMBO Rep.* 2022. 23(2):e53865. https://doi.org/10.15252/embr.202153865

15. Häring J, Hassenstein MJ, Becker M, Ortmann J, **Junker D**, Karch A, Berger K, Tchitchagua T, Leschnik O, Harries M, Gornyk D, Hernández P, Lange B, Castell S, Krause G, Dulovic A, Strengert M, Schneiderhan-Marra N. **Borrelia multiplex: a bead-based multiplex assay for the simultaneous detection of Borrelia specific IgG/IgM class antibodies**. *BMC Infect Dis.* 2022. 22(1):859. https://doi.org/10.1186/s12879-022-07863-9

16. Jacobsen H*, Strengert M*, Maaß H, Ynga Durand MA, Katzmarzyk M, Kessel B, Harries M, Rand U, Abassi L, Kim Y, Lüddecke T, Metzdorf K, Hernandez P, Ortmann J, Heise JK, Castell S, Gornyk D, Glöckner S, Melhorn V, Kemmling Y, Lange B, Dulovic A, Marsall P, Häring J, **Junker D**, Schneiderhan-Marra N, Hoffmann M, Pöhlmann S, Krause G, Cicin-Sain L. **Diminished neutralisation responses towards SARS-CoV-2 Omicron VoC after mRNA or vector-based COVID-19 vaccinations**. *Sci Rep.* 2022. 12(1):19858. https://doi.org/10.1038/s41598-022-22552-y

17. Uzun G, Müller R, Althaus K, Becker M, Marsall P, **Junker D**, Nowak-Harnau S, Schneiderhan-Marra N, Klüter H, Schrezenmeier H, Bugert P, Bakchoul T. **Correlation between Clinical Characteristics and Antibody Levels in COVID-19 Convalescent Plasma Donor Candidates**. *Viruses*. 2023. 15(6):1357. https://doi.org/10.3390/v15061357

18. Häring J*, Michel T*, Becker M, **Junker D**, Tchitchagua T, Leschnik O, Lange B, Castell S, Krause G, Strengert M, Dulovic A, Schneiderhan-Marra N. **Simultaneous Detection of Different Antibody Classes in a Multiplexed Serological Test**. *J Vis Exp*. 2023. (197). https://doi.org/10.3791/65323

19. Uzun G, Bareiß A, Becker M, Althaus K, Dulovic A, **Junker D**, Schenke-Layland K, Martus P, Borst O, Schneiderhan-Marra N, Bakchoul T. **Characteristics Associated with COVID-19 Breakthrough Infections after Booster Vaccinations in Healthcare Workers: Insights from the TüSeRe:exact Study.** *J Clin Med*. 2024. 13(6):1571. https://doi.org/10.3390/jcm13061571

1 Introduction

1.1 SARS-CoV-2 and the COVID-19 pandemic

1.1.1 Emergence and early phase of the pandemic

Severe Acute Respiratory Syndrome Coronavirus 2 (SARS-CoV-2) is the responsible pathogen for Coronavirus disease 2019 (COVID-19) that rapidly spread across the globe, triggering a pandemic that caused over 7,000,000 confirmed deaths as of February 2024[1]. Following its emergence in Wuhan, China in December 2019, SARS-CoV-2 initially caused a cluster of severe, often fatal, pneumonia[2,3]. Exacerbating factors such as the ease of transmission through respiratory droplets, high infectivity, travel and global connectivity led to an unprecedented global outbreak with over 150,000 cases by March 2020[4]. Consequently, the COVID-19 outbreak, which was already classified as public health emergency of international concern (PHEIC) by the World Health Organization (WHO) in January 2020[5], was declared a pandemic on 11 March 2020[6]. In response, many countries undertook drastic non-pharmaceutical interventions (e.g. lockdowns), to slow the spread of the virus and prevent healthcare systems from being overburdened. By April 2020, already a third of the global population was under some form of lockdown[7]. **Figure 1** summarises the key events in the first ten months of the pandemic.

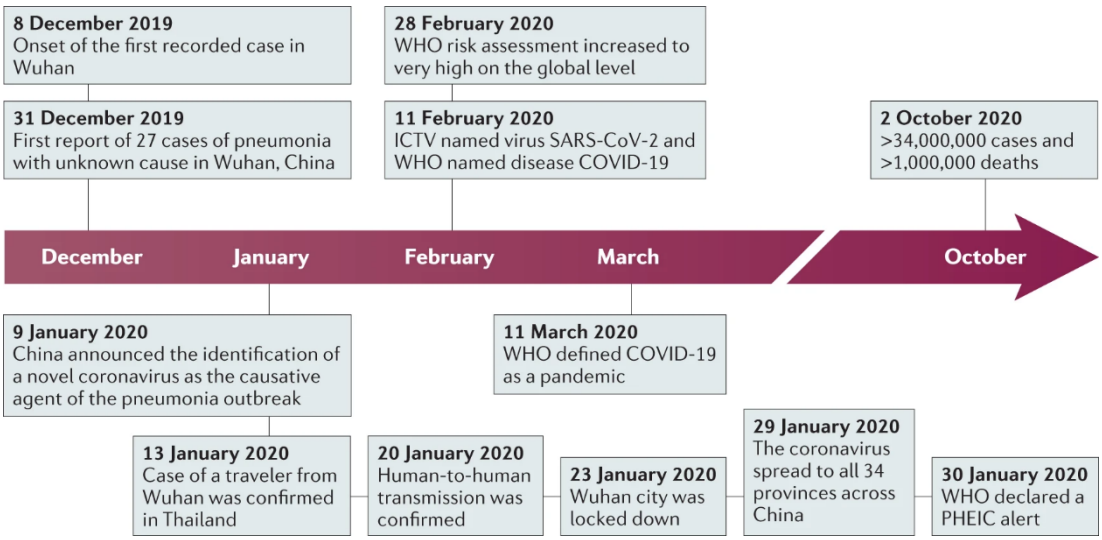

Figure 1: Key events in the early phase of the COVID-19 pandemic
Timeline showing developments of the COVID-19 pandemic from December 2019 to October 2020. Reprinted with permission by Springer Nature: Ben Hu et al., Characteristics of SARS-CoV-2 and COVID-19, Nature Reviews Microbiology, © 2020, Springer Nature Limited[8]

SARS-CoV-2 belongs to the genus *Betacoronavirus* of the *Coronaviridae* family and is closely related to the zoonotic Severe Acute Respiratory Syndrome Coronavirus (SARS-CoV) and Middle East Respiratory Syndrome Coronavirus (MERS-CoV) that were responsible for outbreaks of severe respiratory disease in 2002 and 2012[9,10]. Genomically, it shares 79 % and 50 % genome sequence identity with both pathogens, respectively[11]. Other members of the *Coronaviridae* family include four frequently circulating human coronaviruses 229E, OC43, NL63 and HKU1, which usually cause mild respiratory illnesses like the common cold and are therefore considered endemic[12].

A high proportion of early SARS-CoV-2 infections in Wuhan could be traced back to the Huanan Seafood Market, where the spillover event was first suspected to have occurred[2,3]. Since the closest relative of SARS-CoV-2 is a horseshoe bat coronavirus that shares over 96 % genomic sequence identity[13], it is thought the spillover to humans occurred from bats, either directly or via an intermediate animal host[14]. Such zoonotic spillovers from one species to another are common events and the origin of 60 - 75 % of all human infectious diseases[15]. As of February 2024, the zoonotic origin of SARS-CoV-2 is still to be determined and subject of ongoing research.

1.1.2 Virus structure and life cycle

SARS-CoV-2 virions are enveloped and have a spherical shape with an average diameter of 108 nm[16]. Like most other coronaviruses, SARS-CoV-2 virions comprise four structural proteins, spike (S), nucleocapsid (N), envelope (E) and membrane (M), as illustrated in **Figure 2**[17].

The surface of the virion contains heavily glycosylated S proteins that form trimers, which are crucial for viral infection. The S protein is responsible for binding to cellular entry receptor angiotensin-converting enzyme 2 (ACE2) on the host cell membrane and initiates membrane fusion. Located within the viral envelope, the N protein is an abundant, mostly disordered RNA-binding protein and is critical for genome packaging and unwinding. Embedded into the viral membrane, the E protein is a small protein consisting of 75 amino acids which is a structural protein in the viral capsid and is also thought to be involved in virus assembly and alteration of the membrane permeability of the host cell[18]. Another transmembrane protein, the M protein is the most abundant viral structural protein and is the driver of virus assembly[19].

The genome of SARS-CoV-2 has a size of approximately 30 kb and is one of the largest of all known RNA viruses. It contains 14 open reading frames (ORFs) that encode 29 viral proteins. Two thirds of the genomic RNA are occupied by two large ORFs (ORF1a and ORF1b) encoding for two overlapping polyproteins that are digested by viral proteases into 16 non-structural proteins (NSPs). These proteins together form the transcription and replication machinery. Nine accessory proteins encoded at the 3'-end are involved in host antiviral immune modulation[20,21].

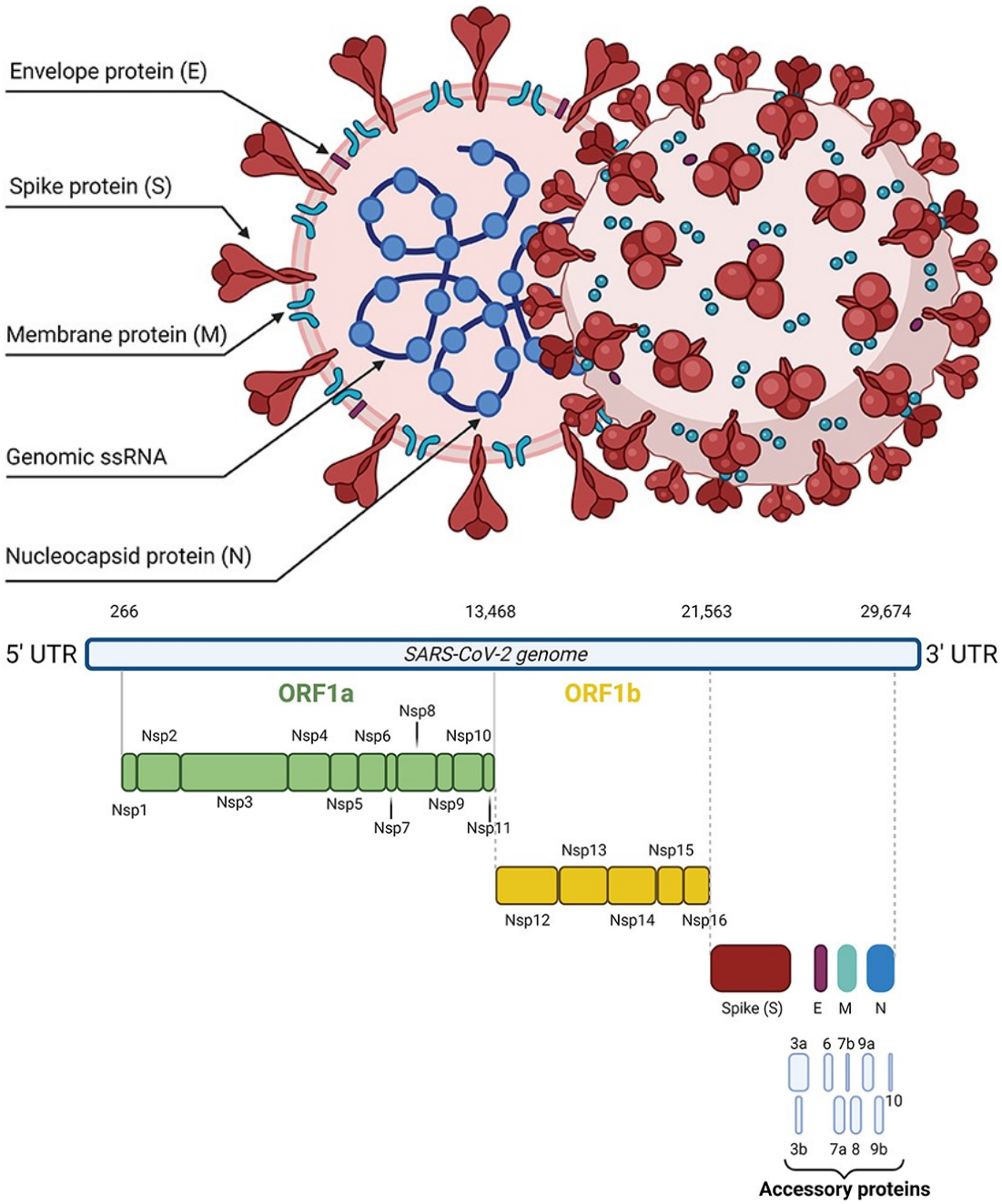

Figure 2: Schematic structure of SARS-CoV-2 virus particle and genome organisation
Schematic structure of SARS-CoV-2 virus particle and genome. Adapted from Massimo Pizzato et al., SARS-CoV-2 and the Host Cell: A Tale of Interactions, Frontiers in Virology, 2022[17]. Licensed for use under Creative Commons 4.0: https://creativecommons.org/licenses/by/4.0/

SARS-CoV-2 is mainly transmitted by inhalation of virus-laden respiratory droplets and aerosols (airborne transmission) or infected droplets coming into direct contact with eyes, nose or mouth (droplet transmission)[22,23].

Figure 3 illustrates the life cycle of SARS-CoV-2. Binding of SARS-CoV-2 is mediated by the trimeric S protein protruding from the virus membrane. The S protein binds to the ACE2 receptor on the target cell, which leads to a conformational change of the S1 subunit that exposes the S2' cleavage site in the S2 subunit. Cleavage of the S2 subunit by the serine protease TMPRSS2

exposes the fusion peptide which initiates fusion of the viral membrane with the host cellular membrane[24]. Besides ACE2, other potential receptors were found that might facilitate viral cell entry, such as CD147 or neuropilin-1 (NRP1), however, ACE2 is known as the primary receptor site[25-27]. After membrane fusion, the viral RNA is released into the cytoplasm and ORF1a and ORF1ab are translated by host ribosomes. Afterwards, the polyproteins are cleaved into 16 NSPs by virus-encoded proteases which form the transcription and replication complexes. After transcription, messenger RNAs (mRNA) encoding for structural proteins are translated by ribosomes and SARS-CoV-2 virions are assembled in the endoplasmic reticulum and Golgi body. Finally, the assembled viruses are released by exocytosis to complete the life cycle[28].

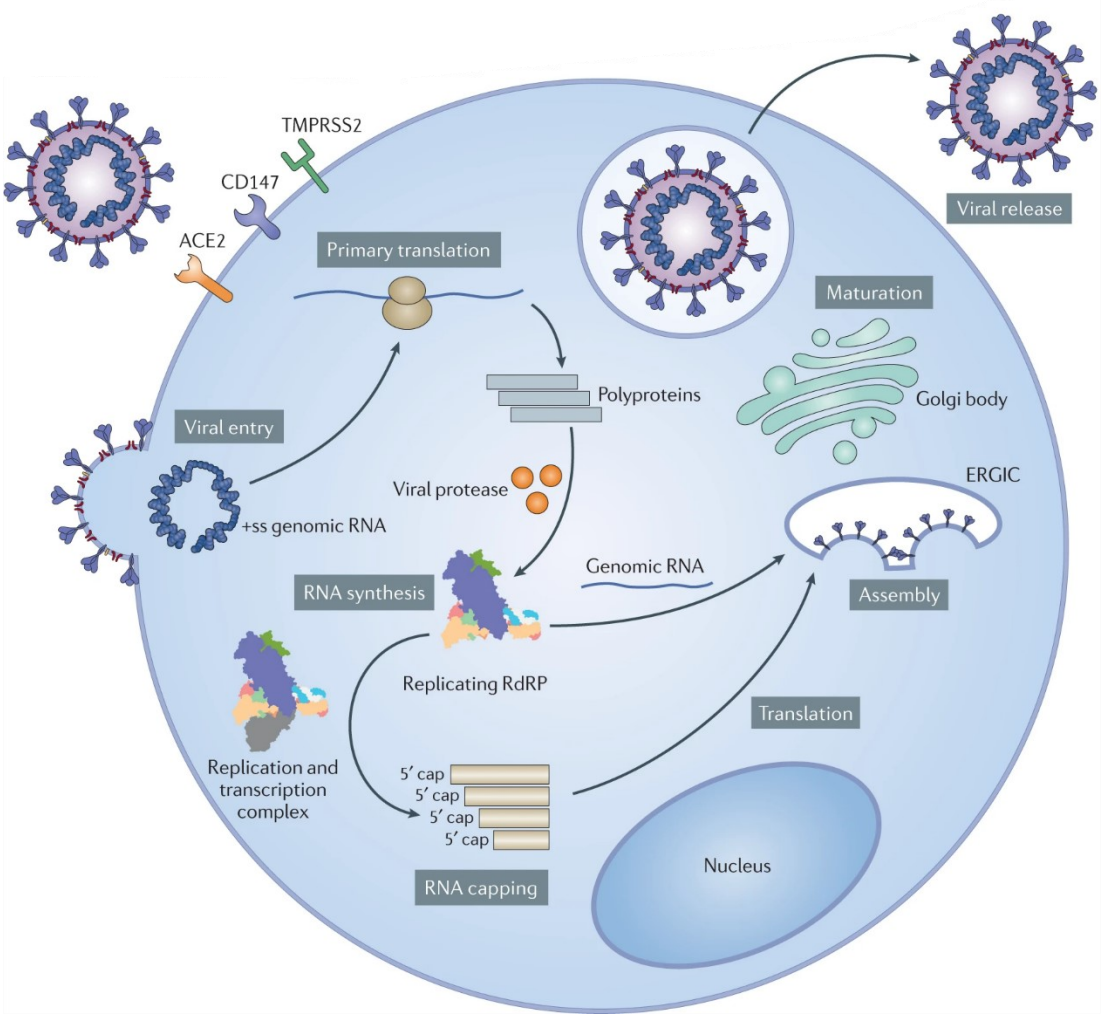

Figure 3: SARS-CoV-2 life cycle
The life cycle of SARS-CoV-2 including viral entry, replication and transcription, virus assembly and release. Reprinted with permission by Springer Nature: Haitao Yang & Zihe Rao, Structural biology of SARS-CoV-2 and implications for therapeutic development, Nature Reviews Microbiology, © 2021, Springer Nature Limited[28]

1.1.3 SARS-CoV-2 vaccines

Early measures available to tackle the COVID-19 pandemic mainly consisted of socioeconomical measures such as lockdowns and self-isolation in an effort to "flatten the curve"[29] and were not feasible as a long-term strategy to sustainably combat SARS-CoV-2. However, they fulfilled their purpose to mitigate the deathly impact of the virus on the global health infrastructure until therapeutics and vaccines were developed to broadly immunise the population. Effective vaccines against SARS-CoV-2 would prevent severe illness, therefore lifting its toll on public health systems. Thus, in June 2020 already 157 vaccine candidates utilising different platforms were in development by companies and institutions[30]. After the SARS-CoV epidemic from 2002 to 2004, several vaccines were developed and two candidates were tested in phase I clinical trials[31,32]. This provided valuable structural and functional knowledge that could be transferred to SARS-CoV-2, accelerating the research and development of SARS-CoV-2 vaccine candidates[33]. Following an unprecedented scientific effort, BNT162b2, developed in partnership by the pharmaceutical companies BioNTech and Pfizer, was the first vaccine to be given conditional marketing authorisation (CMA) by the European Medicines Agency (EMA) on 21 December 2020[34], only one year after the first global COVID-19 hospital admissions in Wuhan[35]. A second vaccine, mRNA-1273 by Moderna, was granted a CMA two weeks later[36] followed by the viral vector-based ChAdOx1-S by AstraZeneca AB in cooperation with Oxford University that received CMA on 29 January 2021[37]. Another viral vector-based vaccine named Ad26.COV2.S developed by Janssen-Cilag International NV in the Netherlands was approved on 11 March 2021[38]. Those four vaccines accounted for more than 96% of all administered doses in Germany until 8 April 2023[39] and are therefore the focus of this thesis (see **Table 2**).

Table 2: Overview of SARS-CoV-2 vaccines approved by the EMA with the most administered doses in Germany

Name (Commercial name)	Developer/ Manufacturer	Vaccine Type	Dosage (Number of vaccinations)[40]	Date of EMA Approval [34,36-38]	Vaccine efficacy against infection [41-44]	% of doses administered in Germany as of 08.04.23[39]
BNT162b2 (Comirnaty)	BioNTech Manufacturing GmbH	mRNA	30 µg RNA (2x)	21.12.2020	95 %	73.5 %
mRNA-1273 (Spikevax)	Moderna Biotech Spain, S.L.	mRNA	100 µg RNA (2x)	06.01.2021	94 %	16.8 %
ChAdOx1-S (Vaxzeriva)	AstraZeneca AB	Vector-based	$5x10^{10}$ adenovirus vector particles (2x)	29.01.2021	70 %	6.4 %
Ad26.COV2.S (Jcovden)	Janssen-Cilag International NV	Vector-based	$5x10^{10}$ adenovirus vector particles (1x)	11.03.2021	66 %	2.4 %

The urgency of the pandemic spurred the advance of new vaccine technologies besides the traditional vaccine development approaches. Thus, BNT162b2 and mRNA-1273 became the first mRNA-based vaccines ever licensed by the EMA and FDA. Both vaccines contain mRNA encoding the S protein of SARS-CoV-2 which is enclosed in lipid nanoparticles to enhance mRNA stability and cell absorption[45-47]. After intramuscular injection, the nanoparticles fuse with cellular membranes and release the mRNA into the cytoplasm, where it is translated into SARS-CoV-2 S proteins. The S proteins are then presented on the cell membrane and elicit an immune reaction[48]. The vaccinated mRNA is structurally analogue to the mRNA produced by RNA polymerases of eukaryotic cells *in vivo* – it contains a 5'-cap, an ORF, a 3' polyadenylation tail and two untranslated regions (5' and 3'). To stimulate the production of neutralising antibodies, the spike protein was stabilised in its pre-fused state by the introduction of two proline substitutions (K986P and V987P)[40]. Furthermore, the base uridine was exchanged by 1-methyl-3'-pseudouridylyl to reduce activation of an innate immune response[49,50]. One dose of BNT162b2 contains 30 μg of mRNA whereas one dose of mRNA-1273 contains 100 μg[40].

ChAdOx1-S and Ad26.COV2.S are both viral vector vaccines using a replication-deficient adenovirus containing the full-length DNA sequence of the SARS-CoV-2 S protein. After intramuscular injection, the adenovirus vector enters the cell and releases its DNA into the cytoplasm. The DNA is then transported into the nucleus where it is transcribed into mRNA. Afterwards, the mRNA coding for the spike protein is channelled to the cytoplasm and translated into S proteins that subsequently elicit the desired immune response. The adenoviral vector in ChAdOx1-S is derived from the chimpanzee adenovirus serotype Y25, whereas the viral vector in Ad26.COV2.S is derived from a human recombinant adenovirus type 26 (Ad26)[51]. Adenoviruses are particularly suitable as a viral vector due to their well-defined biology, low pathogenicity, lack of integration into the host genome and ease of large scale production[52]. AstraZeneca's ChAdOx1-S is administered in two doses of $5x10^{10}$ adenovirus vector particles each[43], while Janssen's Ad26.COV2.S is administered in a single dose of $5x10^{10}$ adenovirus vector particles[53].

BNT162b2 accounted for most of the doses administered in Germany with over 73 %, followed by mRNA-1273, which accounted for 16 % of all doses. Vector-based ChAdOx1-S and Ad26.COV2.S represented 6.4 % and 2.4 % of all doses respectively (**Table 2**).
Recommendations for the use of vaccines in Germany are given on the basis of research and epidemiological data by the Standing Committee on Vaccination (STIKO) since its foundation in 1972[54]. Shortly after the above-mentioned vaccines were approved in Europe in early 2021, the STIKO published a phased plan for the distribution of limited vaccine doses based on the priority of population groups to be vaccinated, in order to limit further damage from SARS-CoV-2 as effectively as possible[55]. Highly prioritised were elderly adults over the age of 70 years, healthcare

workers with a high risk of virus exposition and individuals with pre-existing medical conditions. For all vaccines in **Table 2** except Ad26.COV2.S, which was administered as a single dose, two doses 4-12 weeks apart were recommended for all persons aged 12 years and older to acquire basic immunity against SARS-CoV-2[56]. Later in 2021, the use in children younger than 12 years was authorised.

Recommendations have been updated throughout the pandemic in reaction to changing circumstances, such as the emergence of new variants or research results on the effectiveness and side effects of vaccines. For instance, administration of Ad26.COV2.S in Germany was temporarily halted in March 2021 due to rare occurrences of cerebral venous sinus thrombosis after vaccination, predominantly in people under 60 years of age[57]. Following a risk assessment by the EMA with the result of a positive benefit-risk balance for the vaccine, Ad26.COV2.S was re-authorised for use in Germany on March 18 2021 and shortly afterwards recommended by the STIKO exclusively for the vaccination of people over 65 years of age[58,59]. With the highly transmissible Delta variant becoming dominant in the second half of 2021, breakthrough infections of vaccinated individuals became more frequent, with individuals who had been vaccinated with Ad26.COV2.S being most affected. Accordingly, researchers found that the protection against infection with COVID-19 waned to the greatest extent for the Janssen vaccine, with 13 % protection remaining seven months after vaccination[60]. In comparison, the protection by vaccines of BioNTech/Pfizer and Moderna declined to 43 % and 58 % respectively[60]. As a result, the STIKO considered the effectiveness of a single dose of Ad26.COV2.S to be insufficient and recommended additional vaccination with a mRNA vaccine[61].

In November 2021, the STIKO recommended a booster dose (third dose) of exclusively mRNA vaccines to further boost and maintain immunity against SARS-CoV-2[62]. In response to waning neutralising antibody levels over time and the continuous emergence of immune evasive variants such as Omicron, several vaccine companies have adapted their vaccines to Omicron subvariants. The first Omicron BA.1 and BA.4/5 adapted mRNA vaccines were administered bivalently in combination with the original vaccine. The first adapted monovalent vaccine receiving CMA by the EMA was Comirnaty Omicron XBB.1.5 by BioNTech/Pfizer on 31 August 2023[63].

Immunocompromised patients were designated a priority group for vaccination, due to previous studies indicating reduced seroconversion following vaccination, as well as impracticalities in self-isolating while also requiring frequent medical attention[64-67]. Hemodialysis patients with insufficient kidney function are immunocompromised, as decreased renal function leads to increased oxidative stress and the release of inflammatory cytokines that disturb the function of innate and adaptive immunity[68]. Their underlying medical conditions mean that they often are transplant recipients and require immunosuppressive treatment[69]. Inflammatory bowel disease (IBD) caused mainly by Crohn's disease and ulcerative colitis, is characterised by a chronic inflammation of the gastrointestinal tract[70]. It is commonly treated with immunomodulators such

as TNF-alpha antagonists and corticosteroids that suppress the immune system[71]. The STIKO continues to recommend annual booster vaccinations for immunocompromised individuals after basic immunity has been built up through three encounters of the immune system with parts of the virus, with at least one occurring through vaccination[72]. Monitoring humoral immunity through serological assays can help assess antibodies generated through vaccination and provide valuable information to take into consideration when formulating further vaccination recommendations.

Beyond mRNA and viral-vector-based vaccines, various other technologies are utilised in the development of COVID-19 vaccines. Traditional protein subunit vaccines use antigenic parts of the virus such as the spike protein to elicit an immune response. Nuvaxovid by Novavax CZ, a.s. and Bimervax by HIPRA Human Health S. L. U are currently the only licensed protein subunit vaccine against COVID-19[63].

SARS-CoV-2 vaccines played an important role in reducing the severity and death related to COVID-19. A study from June 2022 estimated, an additional 14.4. to 19.8 million deaths in 185 countries could be prevented by COVID-19 vaccines from 8 December 2020 to 8 December 2021[73]. As of January 2024, 71 % of the world population received at least one vaccine dose and over 13.5 billion doses have been administered[74].

1.1.4 SARS-CoV-2 variants

The development of a virus is mainly determined by the stability of its genome, which in turn depends on the fidelity of the replication machinery. The RNA-dependent RNA polymerase of SARS-CoV-2 produces around $1x10^{-6}$ – $2x10^{-6}$ mutations per nucleotide per replication cycle, lower than in other RNA viruses such as Hepatitis C Virus but still significantly higher than DNA-dependent polymerases that usually have mutation rates of $1x10^{-6}$ to $1x10^{-8}$ per nucleotide[75,76]. Although most of the mutations occurring during viral replication are neutral or have minimal effects, selective mutations lead to significant differences in viral properties such as transmission, disease severity or immune evasion and can provide a selective advantage to the virus[77]. For example, the D614G mutation of the SARS-CoV-2 spike protein was found to enhance viral replication in human lung epithelial cells and increase the infectivity of the virus, therefore elevating transmissibility[78]. Additional to the genetic error susceptibility, the high number of infections and global distribution of SARS-CoV-2 provides a lot of opportunity for the introduction of mutations and diverging evolutionary paths. The selective pressure based on factors such as antiviral treatments, vaccination regimes and socioeconomic restrictions can also influence the emergence and persistence of variants[79,80]. Furthermore, a spill-over from a natural host to humans and vice versa (spill-back) can provide the virus with opportunities to adapt to the new host environment and acquire mutations, leading to variants with altered characteristics. One such example is the SARS-CoV-2 variant "Cluster 5" which was associated with farmed minks and was detected in COVID-19 patients in November 2020 in Denmark. It harboured

several mutations within the S protein, but had no significant consequences on the pandemic[81]. However, it has raised awareness of the importance of genomic surveillance of SARS-CoV-2 by sequencing the viral genomes of infected individuals and highlighted its crucial role in detecting changes in the viral genome and tracking viral variants that have emerged during the pandemic.

Since late 2020, the Technical Advisory Group on SARS-CoV-2 Virus Evolution by the WHO characterises emerging variants based on their potential impact on public health. Emerging variants that have certain changes known to affect viral behaviour or impact human health, such as increased transmission, immune evasion or COVID-19 disease severity, are classified as variants of interest (VOIs) or variants under investigation (VUIs) if their impact on public health is not fully understood and they require further monitoring. Variants of concern (VOCs) additionally have the potential to cause a detrimental change in disease severity, serious impact on public health systems and impaired effectiveness of available vaccines to prevent the disease. With the continuous evolution of the Omicron variant into divergent sublineages, the WHO updated their variant classification system to better represent the variant landscape. Whereas all Omicron sublineages were previously classified as part of the Omicron VOC, Omicron sublineages were classified independently as either variants under monitoring (VUMs), VOIs or VOCs from 15 March 2023 onwards[82].

Table 3 is listing all variants that were classified as VUMs, VOIs and VOCs by the WHO during the pandemic and that were studied in the context of our publications. Therefore, XBB.1.5 is the most recent variant discussed in this thesis.

Table 3: Overview of SARS-CoV-2 variants classified as VOCs, VOIs and VUMs by the WHO

Variant	Lineage[83]	WHO desig-nation*[83]	First occurence[83]	Date of designation[83]	Basis for designation†
Alpha	B.1.1.7	VOC	09.2020	18.12.2020	↑ Transmission[84] ↑ Disease severity[85]
Beta	B.1.351	VOC	05.2020	18.12.2020	↑ Immune escape[86,87]
Gamma	P.1	VOC	11.2020	11.01.2021	↑ Immune escape[88]
Epsilon	B.1.427	VOI	03.2020	05.03.2021	↑ Immune escape[89]
Zeta	P.2	VOI	04.2020	17.03.2021	↑ Immune escape[86]
Eta	B.1.525	VOI	12.2020	17.03.2021	↑ Immune escape[86,90]
Theta	P.3	VOI	01.2021	24.03.2021	↑ Immune escape[86]
Iota	B.1.526	VOI	11.2020	24.03.2021	↑ Immune escape[86,91]
Kappa	B.1.617.1	VOI	10.2020	04.04.2021	↑ Transmission[92] ↑ Immune escape[93]
Delta	B.1.617.2	VOC	10.2020	11.05.2021	↑ Transmission[94] ↑ Disease severity[95]
Lambda	C.37	VOI	12.2020	14.06.2021	↑ Immune escape[96]
Mu	B.1.621	VOI	01.2021	30.08.2021	↑ Immune escape[97]
Omicron BA.1	B.1.1.529	VOC	11.2021	26.11.2021	↑ Transmission[98] ↑ Immune escape[99]
Omicron BA.2	B.1.1.529	VOC	11.2021	26.11.2021	↑ Transmission[100] ↑ Immune escape[99]
Omicron BA.4/BA.5	B.1.1.529	VOC	01.2022	12.05.2022‡	↑ Immune escape[102]
Omicron BQ.1	B.1.1.529	VUM	10.2022	21.09.2022	↑ Immune escape[103]
Omicron XBB	B.1.1.529	VUM	08.2022	12.10.2022	↑ Transmission[104] ↑ Immune escape[105]
Omicron XBB.1.5	B.1.1.529	VOI	10.2022	11.01.2023	↑ Transmission[104] ↑ Immune escape[104,106]

SARS-CoV-2 variants have different numbers of mutations in different structural proteins (e.g. N, M or S) and non-structural proteins (e.g. NSP3). Mutations in the S protein are the most interesting for assessing the epidemiological impact of a variant, as it plays a crucial role in viral entry and is therefore the main target of neutralising antibodies. In addition, most of the approved SARS-CoV-2 vaccines are based on S proteins. Mutations in the S proteins of the SARS-CoV-2 variants summarised in **Table 2** are illustrated in **Figure 4**.

* This designation was subject to change as the pandemic progressed. Here, the most relevant WHO designation is listed for each variant.

† Based on either variant-specific evidence or, if not available, mutation-specific findings. "↑" represents an increase in the following parameter.

‡ The WHO has summarised Omicron variants BA.1, BA.2. BA.4 and BA.5 as VOC "Omicron" until March 15, 2023. This date corresponds to the classification of the ECDC[101].

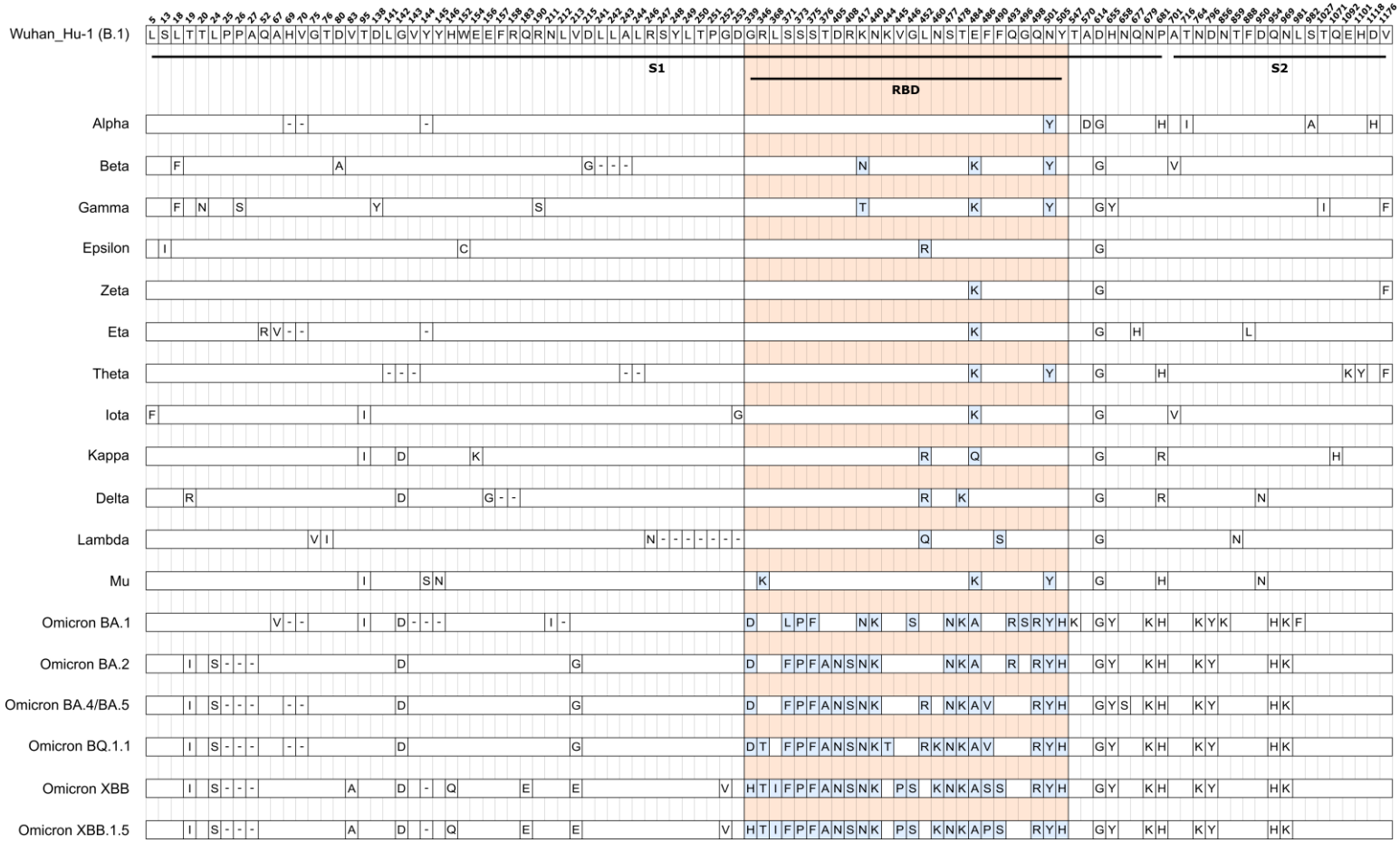

Figure 4: Overview of spike mutations of SARS-CoV-2 variants
Overview of mutations in the S proteins of SARS-CoV-2 variants classified as VOCs, VOIs and VUMs by the WHO. Included are mutations with a minimal prevalence of 40 %. Sequence data for lineage comparison was obtained from GISAID based on Karthik Gangavarapu et al., Outbreak.info genomic reports: scalable and dynamic surveillance of SARS-CoV-2 variants and mutations, Nature Methods, 2023[107].

The proportion of sequences assigned to defined variants over time in Germany is illustrated in **Figure 5**. The SARS-CoV-2 Alpha variant (lineage B.1.1.7) was first detected in the United Kingdom in early December 2020 and rapidly displaced the ancestral strain Wuhan_Hu-1 (hereinafter referred to as wild-type or WT) becoming the first variant to dominate global infection events. It contains a single N501Y mutation in the RBD, which was found to increase binding affinity towards ACE2[108]. Furthermore, a deletion of six nucleotides in the S gene, which results in the loss of amino acids at position 69 and 70, is present in the N-terminal domain of the S protein. Both mutations are leading to an increase in transmissibility estimated up to 80 % compared to the ancestral strain[84,109]. The more transmissible Alpha variant, which encountered a largely unvaccinated population in winter 2020/2021, caused a large and rapid increase in infections and hospitalisations in the UK, followed by most European countries[110]. Studies showed that the newly approved vaccines would provide sufficient protection against the Alpha variant[111,112]. The increasing number of vaccinations as well as public health measures (e.g. physical distancing) could mitigate the burden on healthcare systems. In January 2021, two further variants, Beta and Gamma, were classified as variants of concern[83].

The Beta variant was first detected in South Africa, where it was responsible for the majority of infections until June 2021, while Gamma was mainly circulating in Brazil where it remained the dominant variant until August 2021[113]. In addition to the N501Y mutation, both variants carry the E484K mutation within the RBD. Furthermore, the lysine at position 417 is exchanged with asparagine in Beta (K417N) and with threonine in Gamma (K417T). E484K, located in the ACE2 binding site of the RBD, was identified as immune escape mutation. High reinfection rates and significantly reduced neutralisation by monoclonal antibodies and antibodies induced by infection or vaccination with the wild-type strain supported this assessment[86,87]. Consequently, both Beta and Gamma variants were believed to considerably reduce vaccine efficacy[114]. Germany and major parts of western Europe did not report substantial numbers of infections with Beta or Gamma, with Alpha instead accounting for almost all infections until April 2021[115]. Alpha, Beta and Gamma variants were reclassified as previously circulating variants in March 2022 due to a lack of confirmed cases detected in the weeks and months prior[116].

The dominance of the Alpha variant was broken by the Delta variant which caused a high wave of infection in India during April and May 2021, after which it spread globally[115]. Numerous studies attributed a higher transmissibility compared to the Alpha variant and significantly increased risk for hospitalisation, resulting in its classification as a VOC in June 2021[94,95]. By August 2021, Delta was responsible for 99 % of all recorded infections in Germany[115]. It contains eight point mutations and two deletions in the S protein of which two are located within the RBD. The L452R mutation was shown to impair neutralisation by antibodies induced by infection and vaccination[117], while the substitution of the threonine at position 478 with lysine (T478K) was shown to increase RBD-ACE2 binding by increasing the electrostatic potential[118].

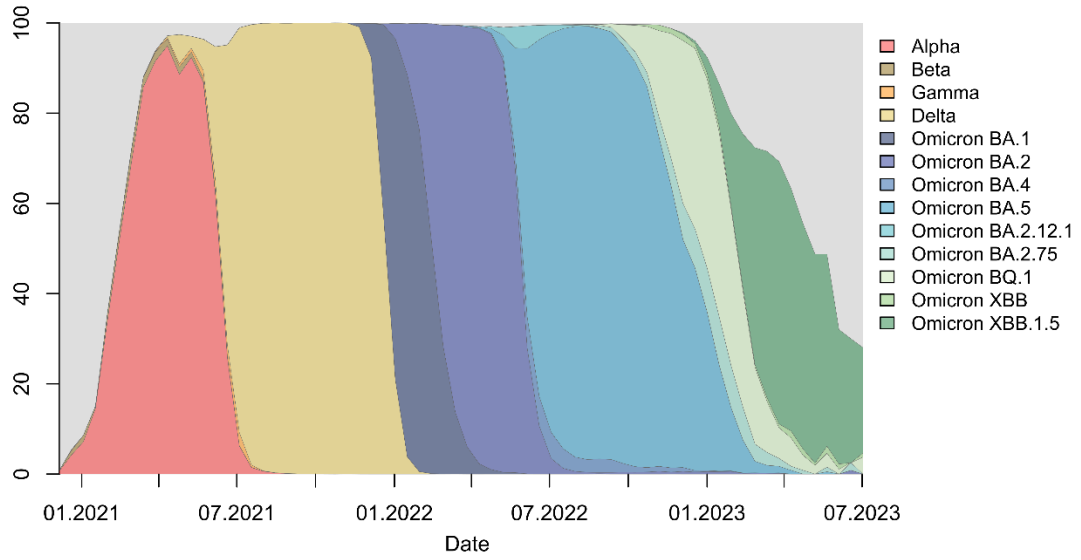

Figure 5: SARS-CoV-2 variant frequency during the COVID-19 pandemic in Germany
Variant frequency in percent from the emergence of the first VOC (Alpha) in Germany until July 2023. Variant frequency was determined by dividing the number of sequenced genomes of a variant by the total number of sequenced genomes in an interval of 14 days. Data was obtained through GISAID[119] and was provided by Hodcroft et al.[115].

Delta maintained its dominant status until the end of 2021, when the Omicron variant emerged and quickly became dominant, with 90 % of all sequenced infections confirmed as Omicron within six weeks of the first detected case[120]. Omicron was classified as a VOC immediately after its discovery in November 2021, as it had an unprecedented number of mutations. It contained over 30 mutations in the S protein, 15 of which located within the RBD, compared to two mutations in Delta's RBD.

The Omicron parent lineage B.1.1.529 branched out into two sublineages in December 2021, of which BA.1 was the first sublineage to dominate global infection events, before being replaced by BA.2 in March 2022. Originating from BA.2, variants BA.4 and BA.5, which have identical S proteins and only differ in other genomic regions such as M and N, became dominant from May to December 2022. Descending from the BA.5 variant, sublineage BQ.1.1 became the dominant variant in January 2023 due to further mutations within the RBD (N460K and K444T) and its enhanced ability to escape existing immunity[121]. At the same time as BQ.1.1, XBB was discovered in Germany, which resulted from a recombination of the sublines BA.2.10.1 and BA.2.75, but accounted for only 1 % of all sequences analysed in December 2022.[120]. However, the XBB.1.5 sublineage, which in turn emerged from XBB, was able to establish itself as the dominant variant in Germany from February 2023[115]. It carries an additional F486P mutation within the RBD which is associated with higher ACE2 affinity[122].

In general, Omicron variants were attributed a higher transmissibility compared to Delta[98]. Between January and May 2022, when BA.1 and BA.2 were the predominant variants in Germany, the highest daily case numbers during the pandemic were recorded with over 290,000 new cases

per day, resulting in 18 million registered infections during this period, which corresponded to approximately 21% of the entire German population[123,124]. The fact that 70 % of the German population had received two vaccine doses by January 1st 2022[125], and many individuals previously infected with earlier circulating variants were reinfected, suggested that Omicron variants effectively escape immunity induced by vaccination based on the ancestral Wuhan_Hu-1 strain and infection with pre-Omicron variants. However, the severity of COVID-19 caused by Omicron was greatly reduced compared to the Delta variant, with the risk of hospitalisation decreased by 56 %[126].

As of February 2024, new variants are still continuously emerging, and the rapid evolution of SARS-CoV-2 is ongoing. It is therefore crucial to continue monitoring the development of the virus and to recognise changes that may have a negative impact on public health at an early stage.

1.2 Serology and immune response

1.2.1 Immune response to SARS-CoV-2

The first line of defence against pathogens such as SARS-CoV-2 is the epidermis of the skin and the epithelium of mucosa, whose task is to limit the penetration of the virus into the body. When the virus breaks through this barrier, pattern recognition receptors (PRRs), which are located on the cell surface, in the cytosol and in the endosomes of epithelial and immune cells, are activated by pathogen-associated molecular patterns (PAMPs). Those receptors are the starting-switch of inflammatory cascades that lead to the expression and secretion of cytokines, such as interleukins and antiviral interferons like TNF-α and type I interferons[127]. The secretion of cytokines communicates the viral threat to neighbouring cells and immune cells and leads to the activation of cellular anti-viral defences such as impairment of protein synthesis and up-regulation of important immunological proteins, including major histocompatibility complex (MHC) molecules[128]. Attracted by cytokines, innate myeloid immune cells, such as antigen presenting macrophages and dendritic cells, internalise pathogens and process their antigens, e.g. the SARS-CoV-2 structural and non-structural proteins, into peptide fragments to display them on MHC class II molecules to lymphoid B- and T-cells of the adaptive immune system in secondary lymph organs such as the lymph nodes[129].

The B-cell recognises the antigen either presented by a professional APC or in free form via its specific B-cell receptor (BCR) and is internalising the antigen-BCR complex. The antigen is processed into peptide fragments and bound to MHC class II molecules. This MHC-II-antigen complex is returned to the B-cell surface and can be recognised by a T follicular helper (T_{FH}) cell activated by the same antigen in a process called linked recognition. Co-stimulation by surface receptors and cytokines of T_{FH}-cells (e.g. IL-4) promote activation, differentiation and proliferation of B-cells[130].

Activated B-cells differentiate into either antibody producing plasma cells or memory B-cells. Memory B-cells are long-lived and circulate the blood stream in a quiescent state. They are memorising the specific antigen their parent B-cell was activated with and trigger an accelerated and strong secondary immune response upon re-encountering the same antigen[131].

Within germinal centers in secondary lymphoid tissue, activated B-cells accumulate mutations in the variable regions of immunoglobulin genes by a process called somatic hypermutation. These diversified B-cell clones subsequently undergo affinity maturation which involves the positive selection of clones with BCRs of higher affinity through repeated exposure to the target antigen.

The antibody-mediated immune response is carried out by multiple classes of antibodies (IgM, IgA, IgD) that are all characterised by their functions, tissue distribution and half-lifes. The first expressed antibodies in a naïve B-cell after activation and before class switching are IgM and IgD antibodies. Class switching through the recombination of the constant region in the immunoglobulin heavy chain gene locus allows the production of different isotypes with different

effector functions, while retaining antigen specificity. IgM antibodies have a low antigen affinity compared to IgG due to limited affinity maturation, but a high avidity because of their pentameric structure with which they form multimeric interactions with the antigen[132].

IgA antibodies are present in higher concentrations in human serum compared to IgM and are mainly found in mucosal surfaces and secretions. In their secreted form, they occur as dimers and therefore have increased avidity. In the respiratory tract, they can neutralise a pathogen through aggregation and prevent infection[133].

IgG antibodies only occur in monomeric form and make up 75 % of all antibodies in serum[134]. They occur later during the immune response because they undergo affinity maturation through somatic mutations that increases their affinity and capacity to neutralise pathogens[135]. They have a longer half-life and are produced by memory B-cells and are therefore associated with long-term immunity[132]. Besides neutralisation, IgG fulfils important other functions through the Fc-region, such as activation of other immune cells with Fc-receptors and antibody-dependent cellular cytotoxicity (ADCC)[136].

The second arm of adaptive immunity against pathogens is cellular immunity mediated by T-cells. Like B-cells, T-cells circulate between blood and peripheral lymphoid tissue until they encounter their specific antigen[129]. After encountering an APC such as dendritic cells, carrying the specific antigen on its MHC-II molecule, the naïve T-cell is activated and proliferates into effector cells in a process called clonal expansion. The most common types of T-cells are the CD4+ (helper) T-cells and CD8+ (cytotoxic) T-cells. CD4+ T-cells recognise MHC-II-bound antigens on APCs and are modulating the immune response by producing cytokines (i.e. IFN-y) that communicate with other immune cells. They are also activating B-cells resulting in antibody production. CD8+ T-cells bind exclusively to antigens presented on MHC-I with their T-cell receptor (TCR) and utilise their killing function by releasing cytotoxins such as perforin and granzymes and thus induce apoptosis. In this way, infected or malignantly altered host cells are eliminated[137]. In **Figure 6**, the immune response against SARS-CoV-2 is illustrated schematically.

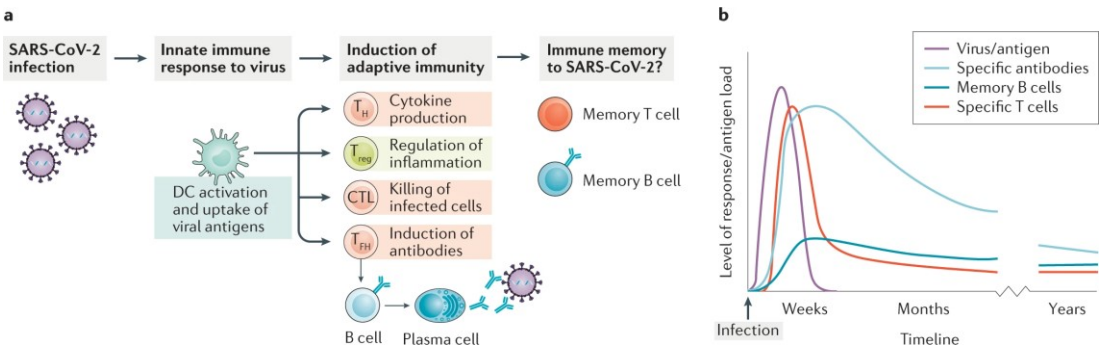

Figure 6: Immune response to SARS-CoV-2
(a) Pattern associated molecular patterns (PAMPs) of SARS-CoV-2 are recognised by pattern recognition receptors (PRRs) on innate immune cells and epithelial cells which leads to their activation. Antigen presenting cells (APCs) migrate to lymphoid organs and activate T-cells, which then activate B-cells, therefore launching the adaptive immune response. (b) Schematic timeline of the adaptive immune response to SARS-CoV-2. Memory B- and T-cells remain after the pathogen is cleared, able to quickly proliferate in the case of reinfection. Reprinted with permission by Springer Nature: Rebecca J. Cox et al., Not just antibodies: B-cells and T cells mediate immunity to COVID-19, Nature Reviews Microbiology, © 2020, Springer Nature Limited

1.2.2 Neutralising antibodies

The three main functions of antibodies in pathogen defence are neutralisation, opsonisation and complement activation[129]. Antibodies that inhibit the infectivity of viruses, bacteria or toxins are called neutralising antibodies (NAbs) and are a main focus of this dissertation. NAbs are part of the humoral immune response of the adaptive immune system and bind to structures on infectious particles needed for cell entry, therefore preventing host cell infection[138]. Pathogens including SARS-CoV-2 use protein or carbohydrate structures on their surface to interact with host cell surface receptors in order to enter the cell and start the replication cycle. NAbs most commonly bind to epitopes within those viral surface proteins and inhibit the interaction between the viral protein and the cell surface receptor. In the case of SARS-CoV-2, the virus binds to the cell surface receptor ACE2 via the RBD of the glycosylated trimeric S protein to achieve cell entry. Especially at the beginning of the pandemic, treatment of severe and/or immunocompromised COVID-19 patients with convalescent plasma containing NAbs proved to be an effective therapy to decrease mortality[139]. In 2021, nine anti-SARS-CoV-2 prophylactic and/or therapeutic antibody-based drugs were granted Emergency Use Authorisation by the EMA[140]. The treatment with monoclonal antibodies was however mostly discontinued since January 2022, due to their ineffectiveness to neutralise circulating Omicron variants[141-143]. In addition to blocking the interaction of viruses with their entry receptors, NAbs also act in other ways such as preventing conformational changes of viral proteins that are necessary for infection (e.g. membrane fusion). While non-neutralising antibodies also bind to specific epitopes of antigens, they do not interfere with the infectivity of the pathogen. However, they also play a crucial rule in the humoral immune response as their main principle is opsonisation, where pathogens are tagged for elimination by other immune cells[144].

1.2.3 Bead-based multiplex immunoassays

Multiplexing is the simultaneous analysis of multiple analytes in a single reaction mixture. In contrast to standard ELISAs that can only measure a single analyte at once, multiplexing provides a material- and cost-saving alternative that generates complex datasets. The serological analysis of pathogen-specific antibodies using multiplex immunoassays can therefore give a more accurate picture of the humoral immune response against the whole pathogen.

xMAP© technology (x = analyte, MAP = Multi-Analyte Profiling) by Luminex (Austin, USA) allows the simultaneous analysis of up to 500 analytes in one reaction mixture. This is enabled by 500 spectrally distinct polystyrene bead populations (hereinafter simply referred to as beads) that are labelled with three fluorescent dyes (infrared, red and orange) at different ratios located inside of the microspheres (**Figure 7a**). xMAP© technology provides many applications in numerous bioanalytical fields, and assays using the technology differ in their components depending on the specific application. For serological assays, immobilised antigens on the beads are used to capture antibodies from a sample such as human blood serum or saliva. The captured antibodies are then detected by a reporter system, usually comprised of secondary antibodies conjugated with a fluorophore. However, the detection is not limited to bound antibodies, as all analytes bound to the immobilised antigen can be recognised (e.g. receptor molecules).

The beads are analysed using a FLEXMAP 3D instrument that works similar to a dual-detection flow cytometer. The beads are aligned in a single file through a flow cell where they are individually excited by two lasers. The red classification laser (λ = 638 nm) excites the internal colour code of each bead population allowing its identification. The green laser (λ = 532 nm) excites the fluorophore-tag of the reporter molecule (e.g. R-phycoerythrin) for signal quantification (**Figure 7b**). For each bead population, the instrument calculates the median fluorescence intensity (MFI) of all beads measured per population[145].

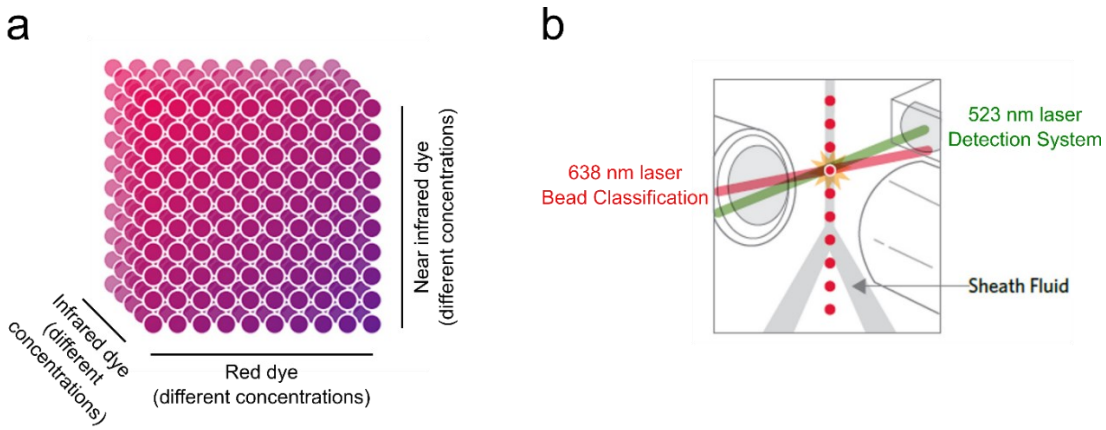

Figure 7: xMAP© technology for multiplex immunoassays
(a) 500 distinct bead populations are obtained by combining three fluorescent dyes (infrared, red and orange) at different ratios inside of the microspheres. (b) Two sequential lasers identify the bead population (red, λ=633 nm) and signal intensity (green, λ=532 nm). Figure modified and used with permission from Luminex, a Diasorin company.

1.2.3.1 Analysing antibody binding with MULTICOV-AB

Utilising xMAP© technology, we developed MULTICOV-AB, a serological multiplex antibody binding assay to accurately characterise the antigen-specific antibody response against SARS-CoV-2 and endemic human coronaviruses OC43, NL63, HKU1 and 229E.

We selected antigens from every virus and immobilised them on MagPlex© microspheres. The beads were incubated with diluted serum or saliva and the bound antigen-specific antibodies were detected with secondary antibodies specific for the isotype to be analysed (IgG or IgA). The antigen panel of SARS-CoV-2 consisted of the full-length S protein as well as the spike-derived domains RBD, S1 and S2 and the N protein. For endemic coronaviruses, antigen-specific antibodies against the S1 domain and N protein were analysed. **Figure 8** gives an overview of SARS-CoV-2 antigens included in MULTICOV-AB.

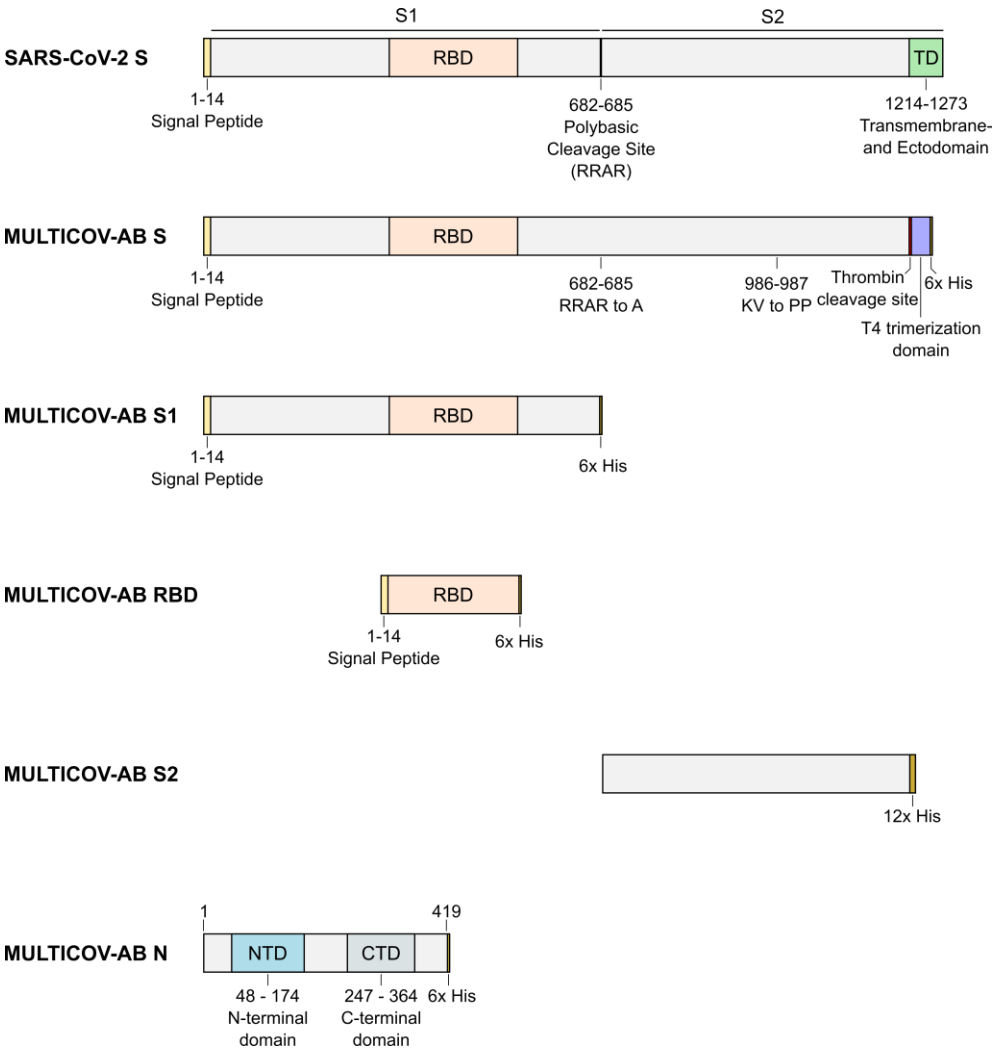

Figure 8: SARS-CoV-2 antigen panel of MULTICOV-AB
The SARS-CoV-2 antigen panel of the bead-based multiplex immunoassay MULTICOV-AB consists of the full-length S protein, the S domains S1, RBD and S2 as well as the N protein.

1.2.3.2 Analysing ACE2 binding inhibition with RBDCoV-ACE2

Virus neutralisation tests (VNTs) present the gold standard for assessing the ability of antibodies to neutralise viruses. Typically, a cell line is exposed to live viruses in the presence of antibodies (e.g. patient blood serum). Here, the neutralising capacity of the serum is directly correlated with the survival rate of the cultured cell line.

While the VNT is testing the functionality of NAbs to prevent infection events, it is very labour-intensive, time-consuming and is not suitable for high-throughput screenings. Additionally, it requires live viruses that demand handling in biosafety level 3 (BSL3) laboratories, as well as access to variant strains especially in the case of SARS-CoV-2.

To combine the valuable information of neutralising activity with a material-, time- and cost-saving method that is also scalable for high-throughput applications, we developed a surrogate virus neutralisation assay based on xMAP technology called RBDCoV-ACE2.

This protein-based assay is founded upon the antibody-mediated inhibition of ACE2-RBD binding, the first and crucial step of the SARS-CoV-2 infection cycle. In **Figure 9**, the assay principle is illustrated, mimicking the way NAbs function *in vivo*.

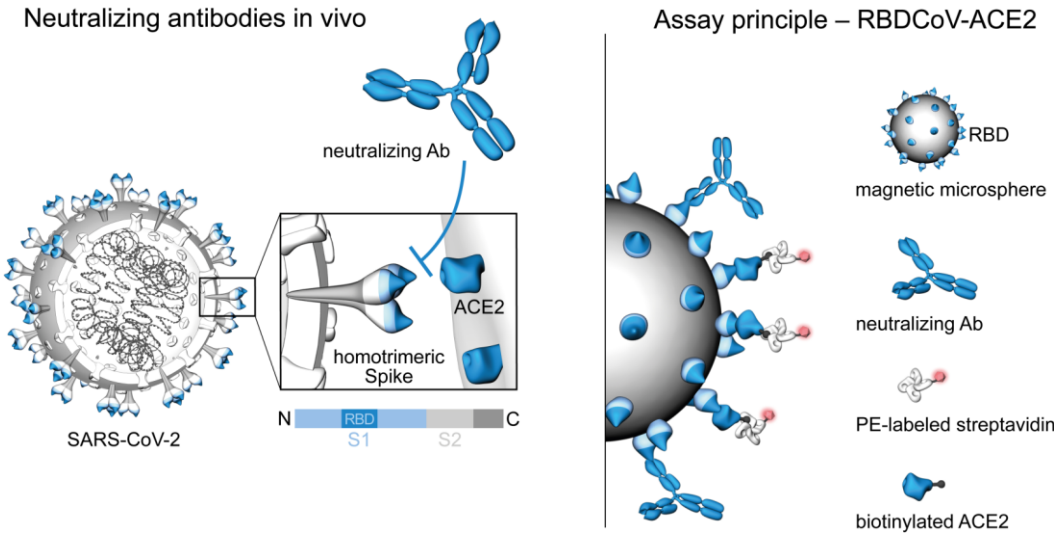

Figure 9: Assay principle of RBDCoV-ACE2
Neutralising antibodies (NAbs) *in vivo* bind to epitopes within the RBD crucial for the binding of ACE2 (left panel). RBDCoV-ACE2 mimics the way of function of NAbs *in vitro* by co-incubating RBD-coated beads with diluted serum and biotinylated ACE2. ACE2 bound to RBD is detected with phycoerythrin (PE)-labeled streptavidin (right panel). Figure adapted and extended from Wagner et al.[146] (© NMI Natural and Medical Sciences Institute at the University of Tübingen).

In **Figure 10**, the assay procedure of RBDCoV-ACE2 is illustrated. RBDs of SARS-CoV-2 variants are immobilised on MagPlex© microspheres and incubated with diluted serum in the presence of biotinylated ACE2 proteins, resulting in a competition for binding of the RBD between the ACE2 proteins and the NAbs (if present) in the sample. The detection of bound ACE2 by streptavidin labelled with phycoerythrin (PE), and the normalisation to a control without added serum yields the remaining portion of bound ACE2-RBD complexes. By subtracting this value from 1 and multiplying with 100, ACE2 binding inhibition in percent is obtained.

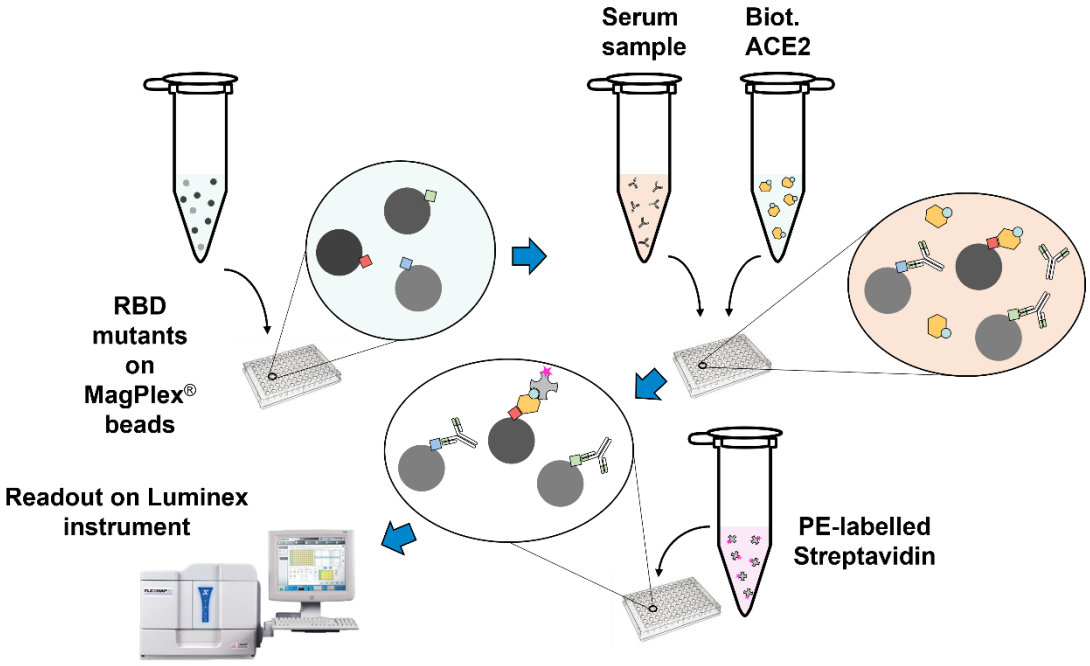

Figure 10: Assay procedure of RBDCoV-ACE2
Assay procedure of the multiplex surrogate neutralisation assay RBDCoV-ACE2. Beads coated with RBDs of different SARS-CoV-2 variants are incubated with diluted serum in a buffer containing biotinylated ACE2. After incubation, bound ACE2 is detected with streptavidin-PE and the beads are analysed with a FLEXMAP 3D instrument. The MFI of each measurement is normalised to the mean MFI of control measurements containing only biotinylated ACE2. Subtracting this value from 1 and multiplying with 100 results in the ACE2 binding inhibition (%). Figure concept adapted from Matthias Becker, Serological Analysis to Accompany Clinical Research, Vaccination and Evolution of the COVID-19 Pandemic, Doctoral Dissertation, 2023, University of Tübingen[147].

2 Objective of the Thesis

With the emergence of SARS-CoV-2 in late 2019, the world was confronted with a highly infectious and contagious virus that causes severe respiratory disease. As the initial outbreak turned into a pandemic in early 2020 and public health infrastructure was overwhelmed, an unprecedented collaborative effort by the scientific community was required to expand the limited knowledge of the virus and develop therapeutics and vaccines.

In order to close these knowledge gaps, we set ourselves the goal of developing serological multiplex tests that can be used for research into the humoral immune response to SARS-CoV-2 as well as in clinical practice and in the development of therapeutics and vaccines.

Therefore, I co-developed MULTICOV-AB, a bead-based multiplex assay to analyse antibody binding towards antigens of SARS-CoV-2 and the endemic coronaviruses 229E, OC43, NL63 and HKU1. After validating the assay to FDA and EMA guidelines, we could utilise it to assess the seroprevalence of SARS-CoV-2 in the German population and differentiate between antibody responses induced by infection and vaccination with superior sensitivity and specificity compared to commercially available ELISAs.

As the pandemic progressed and seroprevalence in the population steadily increased, the functional characterisation of the immune response to SARS-CoV-2 became increasingly the focus of research. Especially with regard to newly emerging SARS-CoV-2 variants with altered characteristics such as transmissibility and disease severity, it is crucial to determine whether the antibody responses induced by previous infections or vaccinations are still able to effectively neutralise the virus.

To address this, I developed RBDCoV-ACE2, a multiplex surrogate neutralisation assay based on the inhibition of the interaction between the RBD of SARS-CoV-2 and the host receptor ACE2 by NAbs in the probe serum. RBDCoV-ACE2 is capable of analysing the neutralising capacity of blood serum against all circulating SARS-CoV-2 variants simultaneously in one reaction mixture, requiring minimal amounts of material (5 µL of sample) in a time-efficient manner (total assay time < 4 hours). It correlates well with the gold standard VNT and is suitable to be processed under biosafety level 2 conditions as it does not require infectious live virus. RBDCoV-ACE2 was utilised in over ten publications since 2021 and beyond application in clinical practice, was also used in pre-clinical tests of a SARS-CoV-2 vaccine candidate adapted to Omicron variants.

3 Results and Discussion

Parts of this dissertation have been previously published. Publications discussed in this dissertation are listed below in the order in which they are covered in this chapter. The publications and supplementary material (if available) are reprinted in the Appendix.

1. Becker M*, Strengert M*, **Junker D**, Kaiser PD, Kerrinnes T, Traenkle B, Dinter H, Häring J, Ghozzi S, Zeck A, Weise F, Peter A, Hörber S, Fink S, Ruoff F, Dulovic A, Bakchoul T, Baillot A, Lohse S, Cornberg M, Illig T, Gottlieb J, Smola S, Karch A, Berger K, Rammensee HG, Schenke-Layland K, Nelde A, Märklin M, Heitmann JS, Walz JS, Templin M, Joos TO, Rothbauer U, Krause G, Schneiderhan-Marra N. **Exploring beyond clinical routine SARS-CoV-2 serology using MultiCoV-Ab to evaluate endemic coronavirus cross-reactivity**. *Nat Commun.* 2021. 12(1):1152. https://doi.org/10.1038/s41467-021-20973-3

2. **Junker D**, Dulovic A, Becker M, Wagner TR, Kaiser PD, Traenkle B, Kienzle K, Bunk S, Struemper C, Haeberle H, Schmauder K, Ruetalo N, Malek N, Althaus K, Koeppen M, Rothbauer U, Walz JS, Schindler M, Bitzer M, Göpel S, Schneiderhan-Marra N. **COVID-19 patient serum less potently inhibits ACE2-RBD binding for various SARS-CoV-2 RBD mutants.** *Sci Rep.* 2022. 12(1):7168. https://doi.org/10.1038/s41598-022-10987-2

3. Dulovic A*, Kessel B*, Harries M*, Becker M, Ortmann J, Griesbaum J, Jüngling J, **Junker D**, Hernandez P, Gornyk D, Glöckner S, Melhorn V, Castell S, Heise JK, Kemmling Y, Tonn T, Frank K, Illig T, Klopp N, Warikoo N, Rath A, Suckel C, Marzian AU, Grupe N, Kaiser PD, Traenkle B, Rothbauer U, Kerrinnes T, Krause G, Lange B, Schneiderhan-Marra N, Strengert M. **Comparative Magnitude and Persistence of Humoral SARS-CoV-2 Vaccination Responses in the Adult Population in Germany**. *Front Immunol.* 2022. 13:828053. https://doi.org/10.3389/fimmu.2022.828053

4. Becker M*, Dulovic A*, **Junker D**, Ruetalo N, Kaiser PD, Pinilla YT, Heinzel C, Haering J, Traenkle B, Wagner TR, Layer M, Mehrlaender M, Mirakaj V, Held J, Planatscher H, Schenke-Layland K, Krause G, Strengert M, Bakchoul T, Althaus K, Fendel R, Kreidenweiss A, Koeppen M, Rothbauer U, Schindler M, Schneiderhan-Marra N. **Immune response to SARS-CoV-2 variants of concern in vaccinated individuals.** *Nat Commun***.** 2021. 12(1):3109. https://doi.org/10.1038/s41467-021-23473-6

5. Renk H*, Dulovic A*, Seidel A*, Becker M, Fabricius D, Zernickel M, **Junker D**, Groß R, Müller J, Hilger A, Bode SFN, Fritsch L, Frieh P, Haddad A, Görne T, Remppis J, Ganzemueller T, Dietz A, Huzly D, Hengel H, Kaier K, Weber S, Jacobsen EM, Kaiser PD, Traenkle B, Rothbauer U, Stich M, Tönshoff B, Hoffmann GF, Müller B, Ludwig C, Jahrsdörfer B, Schrezenmeier H, Peter A, Hörber S, Iftner T, Münch J, Stamminger T, Groß HJ, Wolkewitz M, Engel C, Liu W, Rizzi M, Hahn BH, Henneke P, Franz AR, Debatin KM, Schneiderhan-Marra N, Janda A, Elling R. **Robust and durable serological response following pediatric SARS-CoV-2 infection.** *Nat Commun.* 2022. 13(1):128. https://doi.org/10.1038/s41467-021-27595-9

6. **Junker D***, Becker M*, Wagner TR*, Kaiser PD, Maier S, Grimm TM, Griesbaum J, Marsall P, Gruber J, Traenkle B, Heinzel C, Pinilla YT, Held J, Fendel R, Kreidenweiss A, Nelde A, Maringer Y, Schroeder S, Walz JS, Althaus K, Uzun G, Mikus M, Bakchoul T, Schenke-Layland K, Bunk S, Haeberle H, Göpel S, Bitzer M, Renk H, Remppis J, Engel C, Franz AR, Harries M, Kessel B, Lange B, Strengert M, Krause G, Zeck A, Rothbauer U, Dulovic A, Schneiderhan-Marra N. **Antibody Binding and Angiotensin-Converting Enzyme 2 Binding Inhibition Is Significantly Reduced for Both the BA.1 and BA.2 Omicron Variants**. *Clin Infect Dis*. 2023. 76(3):e240-e249. https://doi.org/10.1093/cid/ciac498

7. Dulovic A*, Strengert M*, Ramos GM*, Becker M, Griesbaum J, **Junker D**, Lürken K, Beigel A, Wrenger E, Lonnemann G, Cossmann A, Stankov MV, Dopfer-Jablonka A, Kaiser PD, Traenkle B, Rothbauer U, Krause G, Schneiderhan-Marra N, Behrens GMN. **Diminishing Immune Responses against Variants of Concern in Dialysis Patients 4 Months after SARS-CoV-2 mRNA Vaccination.** *Emerg Infect Dis*. 2022. 28(4):743-750. https://doi.org/10.3201/eid2804.211907

8. Becker M*, Cossmann A*, Lürken K, **Junker D**, Gruber J, Juengling J, Ramos GM, Beigel A, Wrenger E, Lonnemann G, Stankov MV, Dopfer-Jablonka A, Kaiser PD, Traenkle B, Rothbauer U, Krause G, Schneiderhan-Marra N, Strengert M, Dulovic A, Behrens GMN. **Longitudinal cellular and humoral immune responses after triple BNT162b2 and fourth full-dose mRNA-1273 vaccination in haemodialysis patients.** *Front Immunol*. 2022. 13:1004045. https://doi.org/10.3389/fimmu.2022.1004045

9. Woelfel S, Dütschler J, König M, Dulovic A, Graf N, **Junker D**, Oikonomou V, Krieger C, Truniger S, Franke A, Eckhold A, Forsch K, Koller S, Wyss J, Krupka N, Oberholzer M, Frei N, Geissler N, Schaub P; STAR SIGN Study Investigators; Albrich WC, Friedrich M, Schneiderhan-Marra N, Misselwitz B, Korte W, Bürgi JJ, Brand S. **STAR SIGN study: Evaluation of COVID-19 vaccine efficacy against the SARS-CoV-2 variants BQ.1.1 and XBB.1.5 in patients with inflammatory bowel disease.** *Aliment Pharmacol Ther*. 2023. 58(7):678-691. https://doi.org/10.1111/apt.17661

The following unpublished manuscript is part of this dissertation:

10. Becker M*, Dulovic A*, Uzun G, Bareiß A, Mikus M, **Junker D**, Griesbaum J, Michel T, Fandrich M, Schenke-Layland K, Althaus K, Bakchoul T, Schneiderhan-Marra N. **Dynamics of humoral response towards SARS-CoV-2 from vaccination and breakthrough infection**. Unpublished Manuscript

3.1 Multiplex serological immunoassay development

In my master thesis, which I submitted on the 7th of September 2020, I wrote about the early development of the antibody binding assay MULTICOV-AB and a bead-based ACE2-RBD competition assay, which would later be named RBDCoV-ACE2[148]. The focus of this work laid on antigen testing and the selection of immunogenic antigens (self-produced or commercially available) for both tests as well as the determination of cut-off values to reliably differentiate between SARS-CoV-2 positive and healthy negative individuals. In addition, I established the test principle of RBDCoV-ACE2 and tested convalescent sera and anti-RBD nanobodies for their neutralising capabilities. In September 2020, neither SARS-CoV-2 vaccines nor variants were available or relevant and both MULTICOV-AB and RBDCoV-ACE2 assay developments had not yet been completed. This dissertation is the follow-up of this work and includes the finalised assay development and validation as well as all major publications in which both assays were used.

3.1.1 MULTICOV-AB

In February 2020, one month before the SARS-CoV-2 outbreak was classified a pandemic, I began working as part of a group on the development of a serological bead-based multiplex immunoassay, later named MULTICOV-AB, to analyse the humoral antibody immune response against SARS-CoV-2.

Initially, we evaluated SARS-CoV-2 proteins for their antigenic properties. Following this, we immobilised all structural SARS-CoV-2 proteins on carboxylated MagPlex© beads and tested a set of sera from SARS-CoV-2 infected and healthy individuals for antibody binding of antibody isotypes IgG and IgA. We found that antigens derived from S and N proteins showed a specific antibody binding response in the samples of infected individuals and no binding response in the samples of healthy individuals. Antigens based on E and M proteins, on the other hand, showed unspecific antibody binding and were therefore excluded from the antigen panel. The final panel consisted of the full-length S protein, the S1, S2 and RBD of the S protein as well as the full-length N protein (see **Figure 8**). Furthermore, we included the S1 domains and N proteins of the endemic coronaviruses 229E, OC43, NL63 and HKU1 to assess potential cross-reactivity and cross-protection between endemic human coronaviruses and SARS-CoV-2.

Following the definition of the MULTICOV-AB antigen panel, we screened a set of serum and plasma samples from 310 infected and 866 healthy, uninfected individuals (described in **Appendix I**). Overall, we found that the full-length S protein and RBD achieved the best distinction between positive and negative samples for both IgG and IgA (see **Figure 11a**). We could maximise assay sensitivity and specificity to 90 % and 100 % respectively by integrating the results of both antigens into a combined cut-off for both IgG and IgA detection (see **Appendix I: Figure 2a, b; Table 3**). Since the aim of serological assays is to avoid false positive test results which would falsely attribute an existing immune response, the classification cut-off of MULTICOV-AB was

refined to maximise assay specificity to 100 %. In contrast, diagnostic tests such as PCR analysis aim for high sensitivity to avoid false negative test results, which would lead to further spread of the virus and put other people at risk. Furthermore, we measured a subset of 205 infected and 72 non-infected samples with commercially available serological tests from Roche, Siemens and Euroimmun and compared their performance to MULTICOV-AB (see **Figure 11b**). Here, we could show that MULTICOV-AB has superior sensitivity (90 %) over all tested commercial assays (**Appendix I: Table 1, Supplementary Figure 3**).

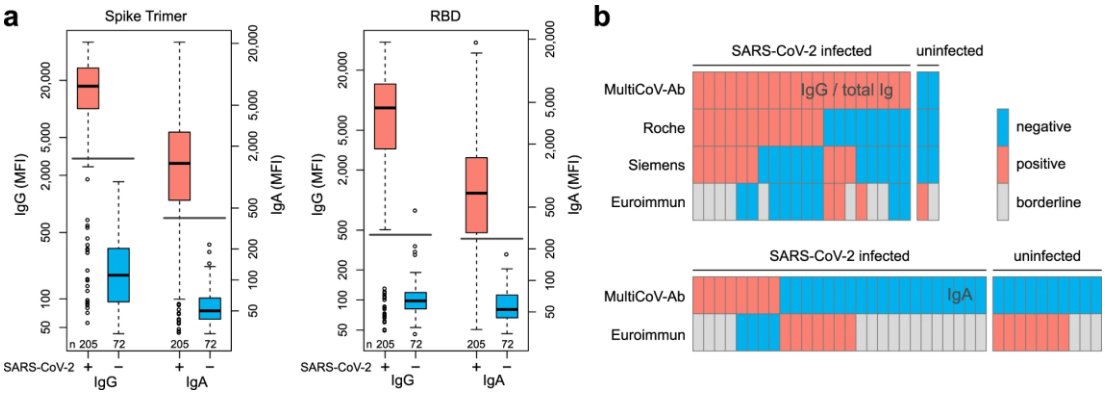

Figure 11: Analysing SARS-CoV-2 antibody responses with MULTICOV-AB
(a) Control sera (blue, n = 72) and sera from individuals with PCR-confirmed SARS-CoV-2 infection (red, n = 205) were screened in a multiplex bead-based assay using Luminex technology (MULTICOV-AB) to quantify IgG or IgA responses to various antigens. Reactivity towards trimeric SARS-CoV-2 spike protein (Spike Trimer) or SARS-CoV-2 receptor binding domain of spike (RBD) was found to be the best predictor of SARS-CoV-2 infection. Data are presented as Box-Whisker plots of a sample's median fluorescence intensity (MFI) on a logarithmic scale. Box represents the median and the 25th and 75th percentiles, whiskers show the largest and smallest values. Outliers determined by 1.5 times IQR of log-transformed data are depicted as circles. Cut-off values for classification for single antigens are displayed as horizontal lines (Spike Trimer IgG: 3,000 MFI, IgA: 400 MFI; RBD IgG: 450 MFI, IgA: 250 MFI). (b) Sample set from a, was used to compare assay performance of the MultiCoV-Ab using Spike Trimer and RBD antigens with commercially available single analyte SARS-CoV-2 IVD assays which detect total Ig (Elecsys Anti-SARS-CoV-2 (Roche); ADVIA Centaur SARS-CoV-2 Total (COV2T) (Siemens Healthineers)) or IgG (Anti-SARS-CoV-2-ELISA - IgG (Euroimmun)) or IgA (Anti-SARS-CoV-2-ELISA - IgA (Euroimmun)). SARS-CoV-2 infection status of samples based on PCR diagnostic is indicated as SARS-CoV-2 positive or negative. Antibody test results were classified as negative (blue), positive (red), or borderline (grey) as per the manufacturer's definition. Only samples with divergent antibody test results are shown. Figure and caption reproduced from **Appendix I: Figure 1**.

To ensure technical stability of MULTICOV-AB, we validated the assay based on EMA and FDA guidelines by analysing intra-assay variance, inter-assay variance, limit of detection, parallelism and matrix effects from serum or plasma samples. Stable assay performance was confirmed with coefficients of variation (%CV) values not exceeding 8.5 % for the intra-and inter-assay variance of all SARS-CoV-2 antigens (see **Appendix I: Supplementary Table 1**).

The multiplex analysis of antibody binding to SARS-CoV-2 antigens including domains of the S and N proteins provided valuable insight into the humoral immune response of infected and vaccinated individuals. Important basic research questions such as the potential cross-reactivity of antibodies generated by infection with seasonal coronaviruses (**Appendix I: Figures 4 and 5**) and the analysis of antibodies induced by vaccination could be explored with MULTICOV-AB.

3.1.2 RBDCoV-ACE2

As the pandemic unfolded and the seroprevalence in the global population progressively increased, research on SARS-CoV-2 humoral immunity increasingly focused on the ability of the antibodies to prevent (serious) infection, especially in the light of newly available vaccines and the emergence of new virus variants.

The most valuable antibodies to have for protection against SARS-CoV-2 infection are NAbs that mainly function by binding to epitopes within the RBD that overlap with binding sites of the host cell receptor ACE2, therefore blocking the RBD-ACE2 interaction and preventing infection before the virus can attach to the cell. Nevertheless, non-neutralising antibodies also have important immune functions in opsonisation, complement activation and ADCC. Since only a fraction of all spike-binding antibodies are NAbs, the antibody binding signal provides insufficient information about the neutralising functionality of the bound antibodies.

To analyse the effect of NAbs in blood serum, I developed RBDCoV-ACE2, a multiplex surrogate neutralisation assay based on the inhibition of RBD-ACE2 binding by NAbs. RBDCoV-ACE2 is a material-, time- and cost-saving alternative to VNTs that require infectious live virus particles and therefore can only be performed in BSL3 laboratories. In contrast, RBDCoV-ACE2 enables significant higher throughput and reproducibility and was also automated to run on pipetting robots. The multiplex format of RBDCoV-ACE2 is optimal for assessing the neutralising capacity against all circulating SARS-CoV-2 variants simultaneously, generating a high amount of data in a short time (total assay time < 4 hours) using minimal amount of serum (5 µL per measurement).

I tested and optimised the concentration of biotinylated ACE2 and serum dilution by performing titration experiments and choosing values that were within linear range. For the final ACE2 concentration I decided on 150 ng/mL and human serum was used at a 1:400 dilution.

To validate RBDCoV-ACE2, I compared its performance to a VNT, representing the gold standard in analysing virus neutralisation, and a commercially available surrogate neutralisation test (NeutraLISA, Euroimmun). Both VNT and NeutraLISA are not capable of measuring multiple analytes simultaneously and therefore only inhibitory effects towards the wild-type RBD could be compared with those assays (**Appendix II**).

I analysed a sample set of 266 sera from SARS-CoV-2 infected and healthy individuals with RBDCoV-ACE2. The sample set for comparison with the VNT consisted of 16 serum samples, 12 of which were from convalescent COVID-19 donors and 4 from healthy pre-pandemic donors. Initially, I compared the performance of RBDCoV-ACE2 to the VNT. The serum virus neutralisation titre in the VNT was defined as the reciprocal sample dilution at which 50 % of cell infection is inhibited, compared to a control without added serum. As illustrated in **Figure 12**, the ACE2 binding inhibition values of RBDCoV-ACE2 showed a strong correlation with the VNT50 values of the VNT (Spearman's r 0.95), confirming that the inhibition of ACE2-RBD binding can be linked to NAbs specifically and is not caused by other factors such as sample matrix effects.

I also confirmed that the binding of ACE2 was specific to the RBD by including SARS-CoV-2 S2 and N proteins, which showed no ACE2 binding.

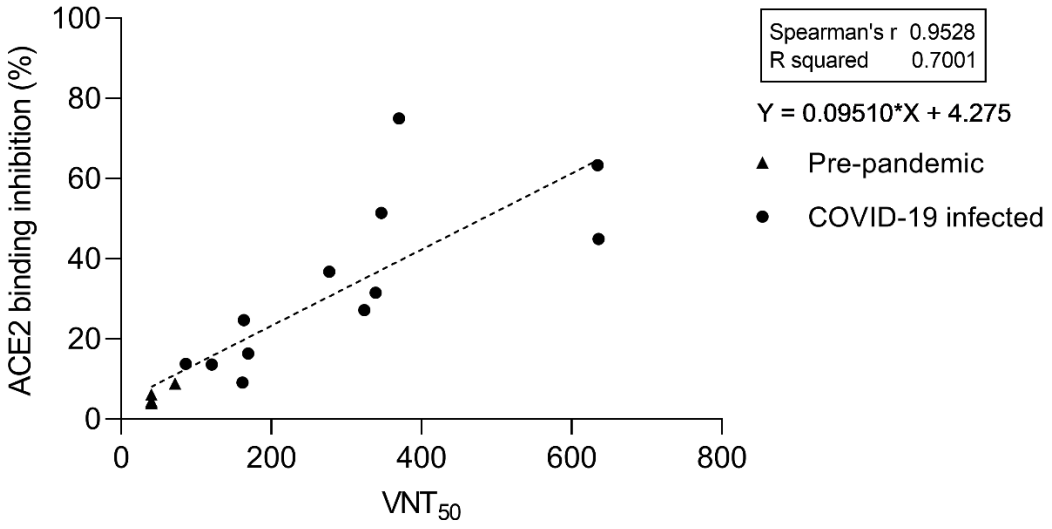

Figure 12: Comparison between RBDCoV-ACE2 and a virus neutralisation test (VNT)
Serum samples (n = 16) of pre-pandemic (n = 4) and COVID-19 convalescent (n = 12) individuals were measured using both assays and analysed by linear regression. The equation of the dashed regression line is shown next to the graph. VNT results are depicted as half-maximal inhibiting serum dilutions (VNT50), RBDCoV-ACE2 results are shown in percentage inhibition of ACE2 binding. Correlation analysis was performed after Spearman and the correlation coefficient r is shown. Figure and caption reproduced from **Appendix II: Figure 1**.

I further compared RBDCoV-ACE2 to the commercially available NeutraLISA by Euroimmun. This ELISA utilises a similar assay principle as RBDCoV-ACE2 by co-incubating diluted serum with biotinylated ACE2, however in a planar format using 96-well plates coated with wild-type SARS-CoV-2 RBD proteins. Thus, NeutraLISA is also a surrogate neutralisation assay analysing percentage inhibition of RBD-ACE2 binding and is therefore well suited for a comparison with RBDCoV-ACE2.

In **Figure 13**, the performance of NeutraLISA is compared to the VNT (**Figure 13a**) and to RBDCoV-ACE2 (**Figure 13b, c**). The results of NeutraLISA and the VNT show a strong correlation (Spearman's r 0.94), however, the inhibition percentage values of NeutraLISA appear to saturate at 100 % at the equivalent of VNT50 values of around 300 to 400 (**Figure 13a**). In contrast, RBDCoV-ACE2 is not reaching saturation for the whole dilution range tested (1:40 to 1:650, **Figure 12**).

This plateau effect can also be seen in the comparison of RBDCoV-ACE2 with NeutraLISA (**Figure 13b, c**). The data of both assays is strongly correlated (Spearman's r 0.84), however RBDCoV-ACE2 can distinguish all measured data points of strongly neutralising samples with high resolution, whereas the inhibitory percentage of NeutraLISA is already mostly saturated at the equivalent of 40 % in RBDCoV-ACE2.

When defining the cut-off percentage value below which a sample is classified as non-neutralising, we employed the same cut-off at 20 % as NeutraLISA, since both assays are based on ACE2 binding inhibition and ACE2 binding inhibition values below 20 % are more likely to fluctuate. RBDCoV-ACE2 assay performance was independently proven by other groups and the assay was also utilised in pre-clinical tests of an Omicron-adapted vaccine candidate in addition to VNTs[149]. If this cut-off is employed on the measurements of both assays, 30.4 % of all samples were considered negative (< 20 % ACE2 binding inhibition) and 55.4 % were classified positive (≥ 20 % ACE2 binding inhibition) in both assays. Of the 24 samples (14.3 %) that were classified differently between both assays, 4 samples (2.4 %) were only positive in RBDCoV-ACE2 while 20 samples (11.9 %) were only positive in NeutraLISA. In summary, RBDCoV-ACE2 is generally estimating a lower ACE2 binding inhibition compared to NeutraLISA but shows a stronger correlation to the gold-standard VNT results and has a broader dynamic range.

a

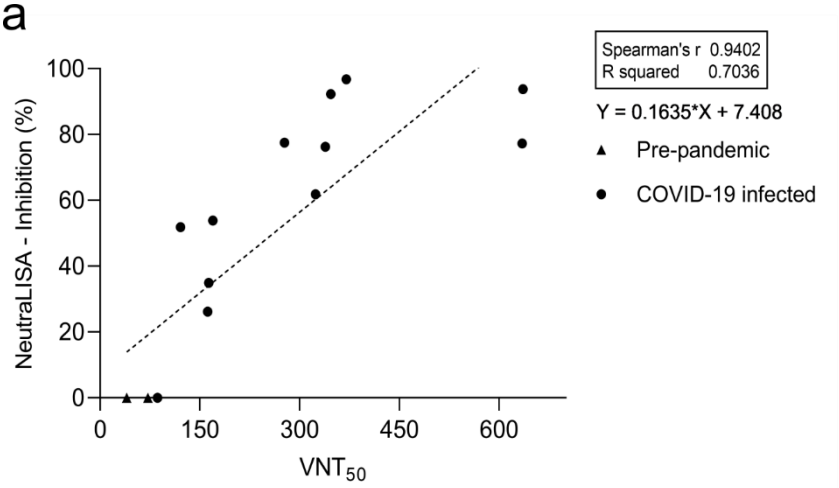

b

	RBDCoV-ACE2 (% ACE2 binding inhibition)		
NeutraLISA (% Inhibition)		≤ 20 %	> 20%
	≤ 20 %	51 (30.4 %)	4 (2.4 %)
	> 20 %	20 (11.9 %)	93 (55.4 %)
Spearman's r [95% CI]	0.8396 [0.7867; 0.8802]		

c

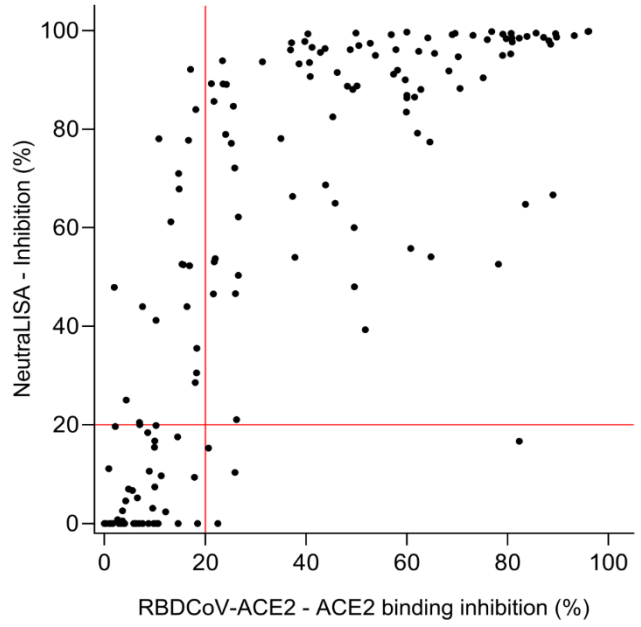

Figure 13: Comparison of RBDCoV-ACE2 to NeutraLISA (Euroimmun)
Correlation between SARS-CoV-2 NeutraLISA and VNT and comparison to RBDCoV-ACE2. (a) Correlation and linear regression between NeutraLISA and VNT results for pre-pandemic (n = 4) and COVID-19 infected (n = 12) samples. Correlation analyses were performed after Spearman and correlation coefficients r are shown. (b) Descriptive statistics of the (c) correlation between NeutraLISA and RBDCoV-ACE2. One sample from each individual (n = 168) was measured using both assays. Correlation was calculated after Spearman. Samples were classified as being negative (non-neutralising) if they had a value below 20% (red lines). Figure and caption reproduced from **Appendix II: Figure 2**.

To ensure that RBDCoV-ACE2 produces reproducible and reliable results and is stable under various working conditions, I performed technical validation based on EMA and FDA bioanalytical guidelines[150,151]. RBDCoV-ACE2 was tested for intra- and inter-assay stability, freeze-thaw stability, short-term stability and parallelism (see **Figure 14**). I also verified that multiplex measurements with RBDCoV-ACE2 produced the same results as singleplex measurements only using the respective analyte (**Appendix II: Supplementary Figure S2**).

The sample set for the technical validation consisted of six serum samples, four of which came from BNT162b2-vaccinated donors (n = 4), one sample from a COVID-19 infected individual (n = 1) and one sample from a pre-pandemic healthy donor (n = 1).

RBDCoV-ACE2 is highly reproducible as shown by the high intra- and inter-assay precision with percent coefficients of variation (%CV) of all samples below 5 % and 7 % respectively (**Figure 14a, b**). To prove that RBDCoV-ACE2 can be processed under various working conditions, I tested the stability of biotinylated ACE2 in assay buffer (ACE2 buffer) when stored for either 2h, 4h or 24h at either 4 °C or 21 °C (RT) before performing sample measurement. Again, the values remained stable for all tested conditions with the %CV of only one sample for WT RBD being higher than 10 % (11.6 %) and a mean %CV of all samples lower than 5 % (**Figure 14c**). Similarly, the frozen biotinylated ACE2 stock could be thawed and re-frozen 5 times and still produce highly stable results (mean %CV of all samples < 5 %, **Figure 14d**).

With the parallelism experiment, I optimised the concentration of biotinylated ACE2 and ensured that the chosen concentration was within linear range. Here, RBDCoV-ACE2 demonstrates a high flexibility towards potentially fluctuating ACE2 concentrations (e.g. due to pipetting errors), as the error is eliminated by normalisation with the ACE2 control.

The %CV values of the technical validation for all samples and all variant RBD are summarised in **Supplementary Table S3 of Appendix II**.

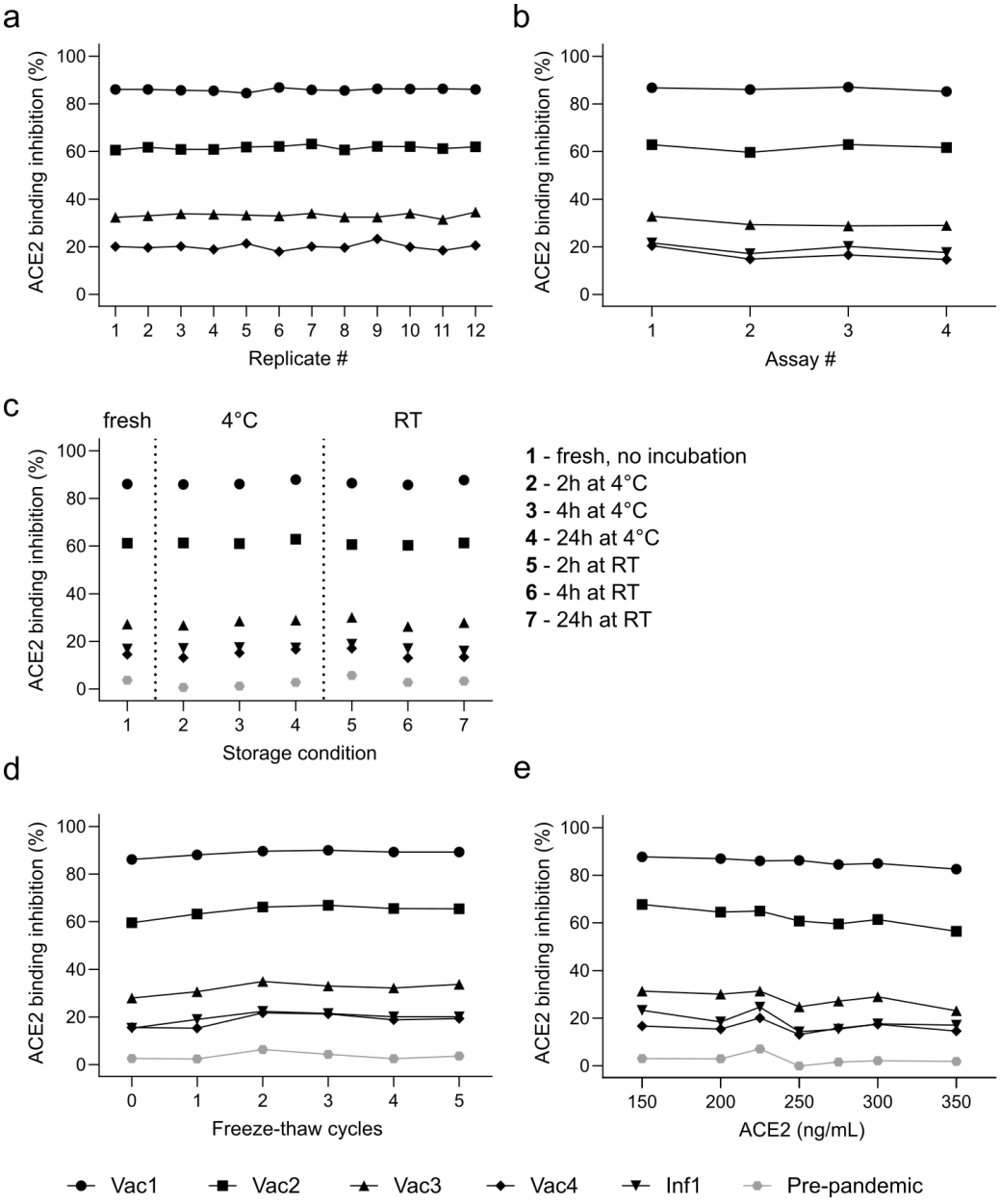

Figure 14: Stable assay performance of RBDCoV-ACE2
Results of intra-assay precision (a), inter-assay precision (b), short-term stability (c), freeze-thaw stability (d) and parallelism (e) experiments analysing ACE2 binding inhibition (displayed as %) using wild-type (WT) RBD. Four samples from donors vaccinated with Pfizer BNT-162b2 (n=4, black), one COVID-19 infected (n=1) and one pre-pandemic sample (n=1, grey) were analysed. Data points of each sample are illustrated by different symbols according to the figure key. Percent coefficients of variation (%CV) for all included RBD mutants are summarised in **Supplementary Table S3 of Appendix II**. Figure and caption reproduced from **Appendix II: Figure S1**.

RBDCoV-ACE2 was also employed in pre-clinical testing of a mRNA-based vaccine against SARS-CoV-2[149]. For this purpose, the assay had to be expanded to enable analysis of rat and mouse sera. To validate the assay for use with those species, I repeated the technical validation by testing different serum dilutions and performing intra- and inter assay precision experiments (**Figure 15**).

I analysed both rat and mouse serum in a dilution row ranging from 1:50 to 1:6400 and confirmed that the serum of both species can be analysed at a dilution of 1:400 (**Figure 15a, c**). No unspecific binding or matrix effects were observed with either rat or mouse serum, so that RBDCoV-ACE2 could be processed analogously to measurements with human serum.

Measurements of both rat and mouse serum were highly stable and showed minimal variance (**Figure 15b, d).**

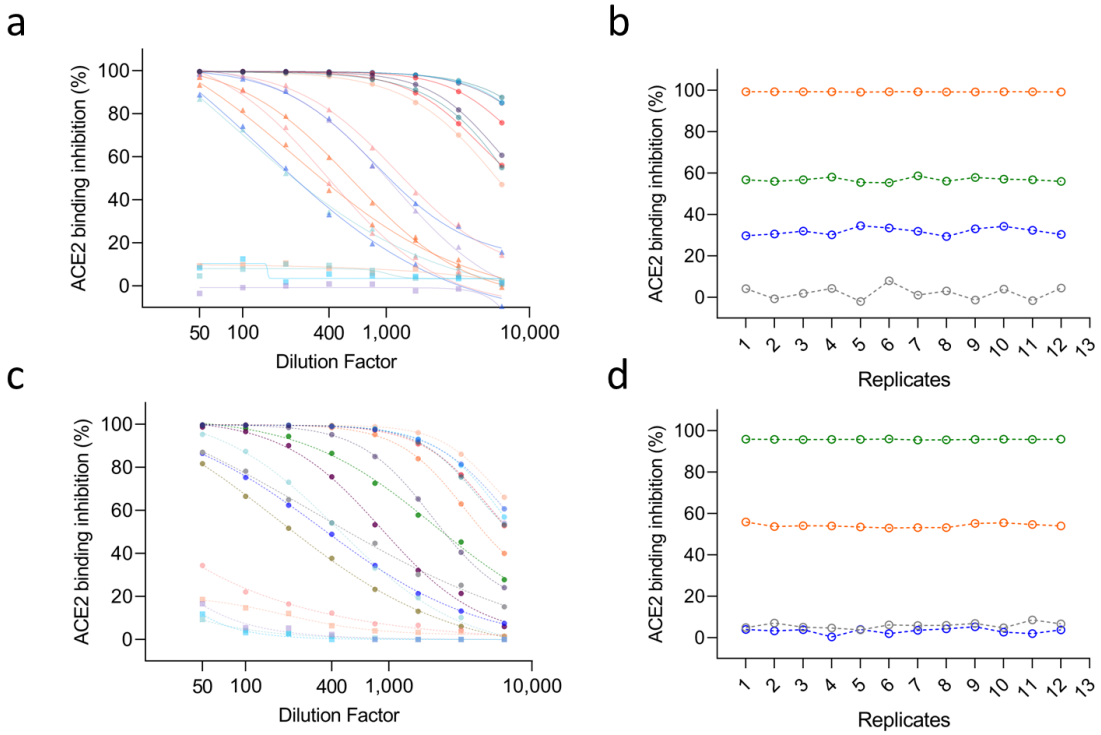

Figure 15: RBDCoV-ACE2 for measurements of rat and mouse serum
ACE2 binding inhibition was measured towards wild-type RBD with serially diluted rat (a) and mouse sera (c) from SARS-CoV-2 immunised (Rat: n=16, Mouse: n=14) and naïve (Rat: n=4, Mouse: n=5) animals. Assay performance of RBDCoV-ACE2 is stable illustrated by the results of intra-assay stability experiments for rat (b) and mouse (d) sera (n=4)

As the pandemic progressed, I continued to add numerous variants to RBDCoV-ACE2 and MULTICOV-AB shortly after their emergence. This also meant that the effects of the variants on infection events were often not yet known at the time of variant inclusion. **Table 4** summarises all RBD antigens that were included in RBDCoV-ACE2 and MULTICOV-AB and their use in publications.

Table 4: Overview of SARS-CoV-2 RBDs included in RBDCoV-ACE2 and MULTICOV-AB and their use in publications

Variant	Lineage	Publications (Appendix No.)									
		1	2	3	4	5	6	7	8	9	10
Wild-type	B.1	■	■	■	■	■	■	■	■	■	■
Alpha	B.1.1.7		■	■	■	■	■	■			
Beta	B.1.351		■	■	■	■	■	■			■
Gamma	P.1		■	■			■	■			
A.23.1	A23.1		■								
Cluster 5	B.1.1.298		■		■						
Epsilon	B.1.427		■		■						
Zeta	P.2										
Eta	B.1.525		■								
Theta	P.3		■								
Iota	B.1.526										
Kappa	B.1.617.1		■								
Lambda	C.37		■				■				
Delta	B.1.617.2		■	■			■	■	■		■
Mu	B.1.621						■				
Omicron BA.1	B.1.1.529						■		■	■	
Omicron BA.2	B.1.1.529						■				■
Omicron BA.4/BA.5	B.1.1.529									■	■
Omicron BA.2.12.1	B.1.1.529										
Omicron BA.2.75	B.1.1.529										
Omicron BF.7	B.1.1.529										
Omicron BA.2.75.2	B.1.1.529										
Omicron XBB	B.1.1.529										
Omicron BA.2.3.20	B.1.1.529										
Omicron BM.1.1.1	B.1.1.529										
Omicron BQ.1.1	B.1.1.529									■	
Omicron XBB.1.5	B.1.1.529									■	

3.2 Application of MULTICOV-AB and RBDCoV-ACE2

3.2.1 Vaccination schemes induce heterologous immune responses

SARS-CoV-2 vaccination campaigns started with the approval of four vaccines of different types in the EU between December 2020 and March 2021 (see **Table 2**). All four vaccines were based on inducing an immune response against the SARS-CoV-2 S protein. Until then, the presence of antibodies against SARS-CoV-2 could only imply a previous infection with the virus or recent treatment with COVID-19 convalescent plasma. The approval of multiple vaccines within a matter of weeks, combined with varying recommendations and availability and the subsequent withdrawal of vector-based vaccines ChAdOx1-S and Ad26.COV2.S due to safety concerns, led to an extremely heterogenous vaccination landscape.

To investigate this landscape and compare the humoral responses elicited by different SARS-CoV-2 vaccine regimens on a population basis, we analysed 1821 samples from 1731 participants in the MuSPAD (Multilocal and Serial Prevalence Study of Antibodies against (Respiratory) Infectious Diseases in Germany)[152] seroprevalence study who had received either a homologous vaccination regimen (consisting of two doses of mRNA- or vector-based vaccines) or heterologous vaccination regimens (consisting of one mRNA- and one vector-based dose) (**Appendix III**). In this study ChAdOx1-S by AstraZeneca is called AZD1222. While MuSPAD was a population-based study, we designed our study cohort for this publication to be representative of the proportion of each vaccine in the population at the time of the experiment (June 2021).

The analysed vaccination regimens induced significantly different IgG levels towards wild-type (WT) S-derived antigens. We observed a greater S, RBD and S1 IgG binding response for homologous mRNA-based vaccinations compared to vector-based ones (see **Figure 16a** and **Appendix III: Figure 1a - c**). Comparable results were achieved by heterologous vaccination schemes, consisting of one vector-based dose and one mRNA-based dose, with significantly higher titres than homologous vector-based vaccination.

We analysed the same sample set with RBDCoV-ACE2 (**Figure 16b**). ACE2 binding inhibition towards WT RBD behaved analogous to the induced IgG response with homologous mRNA vaccination and heterologous vaccination eliciting higher neutralisation responses than homologous vector-based vaccination.

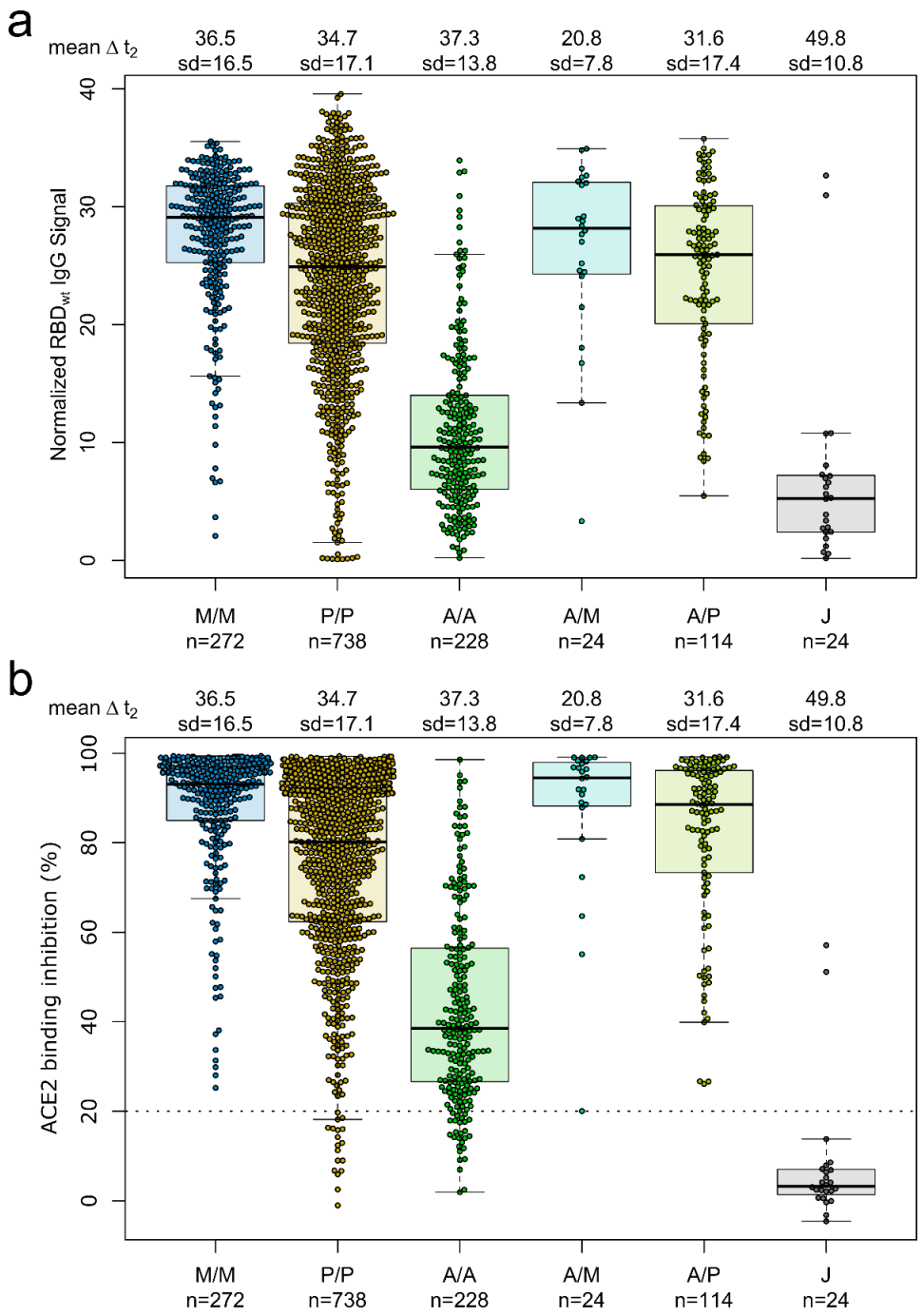

Figure 16: Analysis of the antibody response to various vaccination schemes
Different SARS-CoV-2 vaccination schemes result in distinct humoral responses. IgG antibody titre (a) and ACE2 binding inhibition (b), against the receptor-binding domain (RBD) were measured with MULTICOV-AB and RBDCoV-ACE2. Individuals received either homologous mRNA-1273 (M/M, blue, n = 272), BNT162b2 (P/P, orange, n = 738) or AZD1222 (A/A, green, n = 228), heterologous AZD1222-mRNA-1273 (A/M, light blue, n = 24), AZD1222-BNT162b2 (A/P, light green, n = 114), or a single dose of Ad26.CoV2.S (J, grey, n = 24). Raw MFI values were normalised against QC samples to generate signal ratios for each antigen (a). The threshold for non-responsive samples (ACE2 binding inhibition less than 20%) is shown as dotted line. All samples below this threshold can be considered non-responsive (b). Data is shown as box and whisker plots overlaid with strip charts. Boxes represent medians, 25th and 75th percentiles and whiskers show the largest and smallest non-outlier values based on 1.5 IQR calculation. Time between sampling and full vaccination is displayed as mean and SD for each group. Number of samples per vaccination scheme are stated below. Figure and caption adapted from **Appendix III: Figures 1 and 3**.

Our findings were consistent with other studies that observed reduced humoral and cellular immune responses of vector-based vaccination compared to mRNA-based vaccination[153,154]. Slomka et al. observed significantly higher IgG titres and neutralising activities in individuals vaccinated with two doses of BNT162b2 compared to a cohort that received ChAdOx1-S at any timepoint over the course of six months, with a 13.3-fold higher peak IgG titre in the first group[155].

Samples from individuals vaccinated with Ad26.COV2.S by Janssen showed only low antibody titres against all S-derived antigens, and most samples did not show a neutralising response, with 91 % of all samples analysed failing to respond (ACE2 binding inhibition < 20 %). In addition to the observed reduced humoral immune response induced by the single-dose vector-based Janssen vaccine, a comparative study of participants vaccinated with either BNT162b2 or Ad26.COV2.S found a 5.2-fold higher risk of hospitalisation for the group that received Ad26.COV2.S[156]. In consideration of those findings, the STIKO later recommended all people receiving vector-based vaccines to receive a booster vaccination with a mRNA vaccine[157].

3.2.2 Reduced antibody binding and ACE2 binding inhibition towards VOCs Alpha and Beta

The first SARS-CoV-2 VOCs dominated global infection events from early 2021, with Alpha accounting for the majority of infections in Europe and North America and Beta found predominantly in South Africa. The efficacy of SARS-CoV-2 vaccines against the newly emerged variants was therefore of great interest, as they harboured several mutations in crucial epitopes of the S protein.

Thus, we analysed antibody binding in the serum of infected and vaccinated individuals, before and after the second dose towards WT, Alpha (UK) and Beta (SA) RBDs using MULTICOV-AB (**Appendix IV**). While antibody binding to Alpha was nearly identical to WT in all groups (**Figure 17a**), we observed a significant decrease in IgG binding to Beta in both infected and vaccinated individuals compared to WT, regardless of the number of doses (**Figure 17b**). Regardless of the variant observed, the data points were clearly divided into two clusters depending on the number of doses received, with IgG binding signals being significantly higher after second vaccination. In contrast, samples from infected individuals showed highly individualised IgG binding responses covering the entire observed signal range, highlighting the individualised nature of the humoral immune response to natural infections compared to vaccinations of the same type and dose.

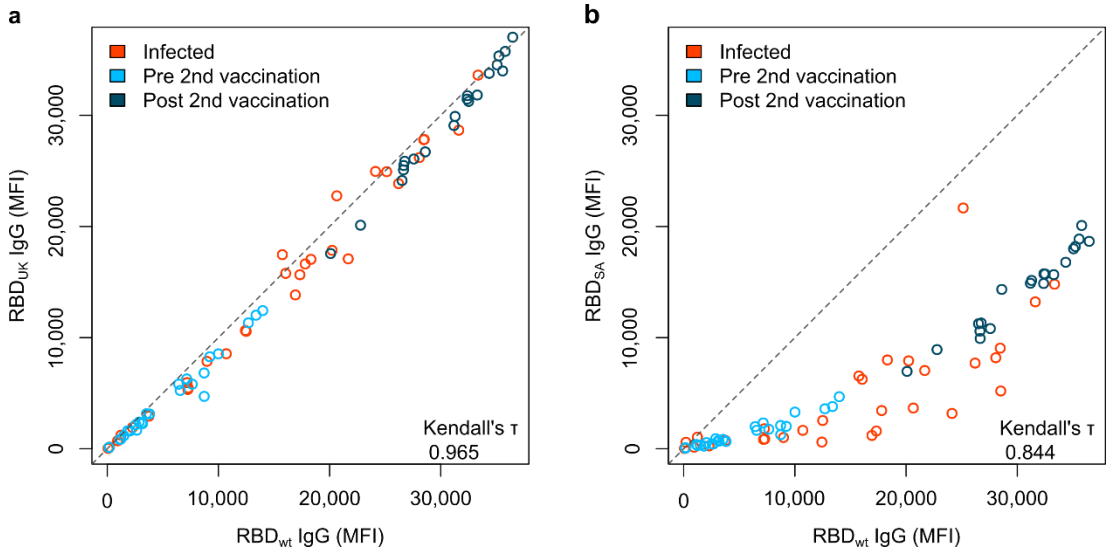

Figure 17: Antibody binding towards variants Alpha and Beta
UK (a) and South African (SA) RBD mutants (b) have differing effects upon antibody binding. RBD mutant antigens were generated and added to MULTICOV-AB to measure the immune response towards them in sera from vaccinated pre-second dose (light blue, n = 25), post second dose (dark blue, n = 20), and infected (red, n = 35) individuals, compared to the wild-type (wt) RBD. A linear curve (y = x) is shown as a dashed grey line to indicate an identical response between wild-type and mutant. Kendall's tau was calculated to measure the ordinal association between the mutant and wild-type. Figure and caption reproduced from **Appendix IV: Figure 3**.

Having established that antibody binding towards Beta was generally reduced, we investigated the effect of the second BNT162b2 dose on antibody binding against RBDs of WT and Beta in longitudinal samples before and after the second dose and analysed the neutralising antibody response with RBDCoV-ACE2 (see **Figure 18**).

Here, a positive correlation between time after the first dose and IgG and IgA antibody response could be observed, with a significant boost of antibody levels after the second dose (**Figure 18a, b**). ACE2 binding inhibition to WT RBD remained below 20 % in samples collected after the first dose and was greatly increased after the second dose, with all samples exceeding 20 % ACE2 binding inhibition (**Figure 18c**).

ACE2 binding inhibition of the same samples towards Beta RBD was significantly reduced compared to WT and only half of the samples taken after the second dose exceeded the 20 % cut-off (**Figure 18d**). Our observed reduction of neutralisation towards the Beta variant by antibodies induced by infection or vaccination was confirmed in a VNT experiment using a patient-derived Beta strain of SARS-CoV-2 (**Appendix IV: Figure 4a**). The negative impact of SARS-CoV-2 Beta on antibody binding and neutralising activity after infection and vaccination was reported by numerous other studies, confirming our findings[158-160].

The steep increase in antibody response after the second dose and the fact that the antibodies induced after the first dose are unable to exert a neutralising effect, reinforce the two-dose regimen of BNT162b2 and have also been reported in numerous other studies[161-163]. It further demonstrates the importance of analysing the neutralising capacity of serum instead of measuring antibody binding alone.

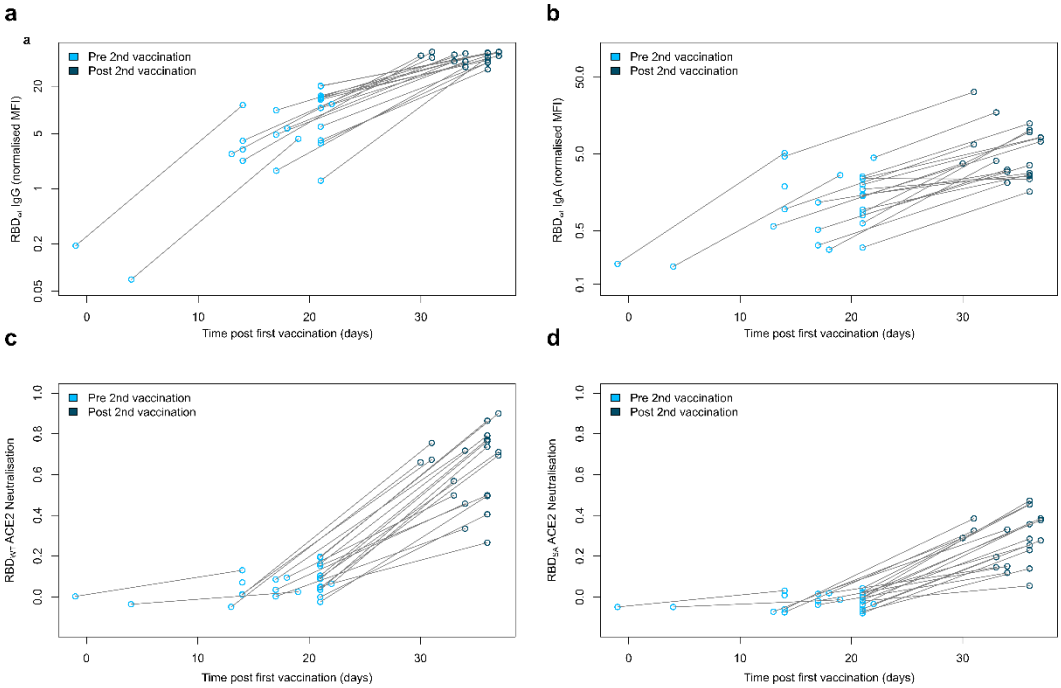

Figure 18: IgG and IgA responses before and after second vaccination
IgG (a) and IgA (b) binding response in sera from individuals pre second vaccination (light blue, n=25) and post second vaccination (dark blue, n=20)) shown as normalised MFI values for WT RBD. The same samples were analysed for ACE2 binding inhibition towards WT RBD (c) and beta (d) using RBDCoV-ACE2. Lines between data points indicate paired samples from the same donor. Figure and caption adapted from **Appendix IV: Figures 1 and 4**.

3.2.3 Children generate strong antibody responses after SARS-CoV-2 infection

Children play a significant role in the transmission of SARS-CoV-2 within communities, as they have a high number of social contacts and were found to be more likely to have asymptomatic cases of COVID-19[164]. It is therefore important to characterise SARS-CoV-2 infections in children in terms of symptoms, transmission and protective immunity including the humoral immune response to SARS-CoV-2.

Thus, we investigated 328 households each with at least one SARS-CoV-2 infected member within a multi-centre longitudinal study, which were followed for up to 12 months after the first infection in each household (**Appendix V**).

Analysing the antibody response following SARS-CoV-2 household exposure, we found that children produce significantly higher antibody titres against S, RBD, S1 and N antigens than adults at a median time of 96 days after positive PCR (**Appendix V: Figure 1**). This could be confirmed by other groups such as Jacobsen et al. who found higher antibody titres against S1 and N in children four months after infection compared to adults[165]. Consistent with our findings, Tomasi et al. measured higher antibody levels in children under 12 years old against S, S1 and RBD but not against the S2 domain[166].

Similar to other authors, we found no significant difference in antibody levels between symptomatic and asymptomatic COVID-19 cases in both adults and children (**Appendix V:**

Figure 2). Dufloo et al. showed that asymptomatic SARS-CoV-2 infections elicit a robust neutralising antibody response that activates the complement system and kills infected cells by ADCC[167].

We further investigated if the higher antibody titres against S-derived antigens in children also led to a stronger neutralisation capacity using a commercial surrogate neutralisation test by GenScript that also analyses ACE2 binding inhibition (**Figure 19a**). Analogously to antibody binding, we found a significantly increased ACE2 binding inhibition in children compared to adults at both tested timepoints (T1: $p < 0.001$ and T2: $p = 0.02$), that was strongly correlating with the elevated anti-S1 IgG levels in children (**Figure 19b**). No differences in antibody binding to Alpha and Beta RBDs between adults and children were found, with almost identical binding for Alpha compared to wild-type (**Figure 19c**). In contrast, antibody binding was significantly reduced for the Beta variant in both adults and children (**Figure 19d**).

In summary, both the increased antibody titres as well as the strong neutralising capacity of convalescent children indicate that children with mild or asymptomatic COVID-19 can elicit a durable and robust immune response.

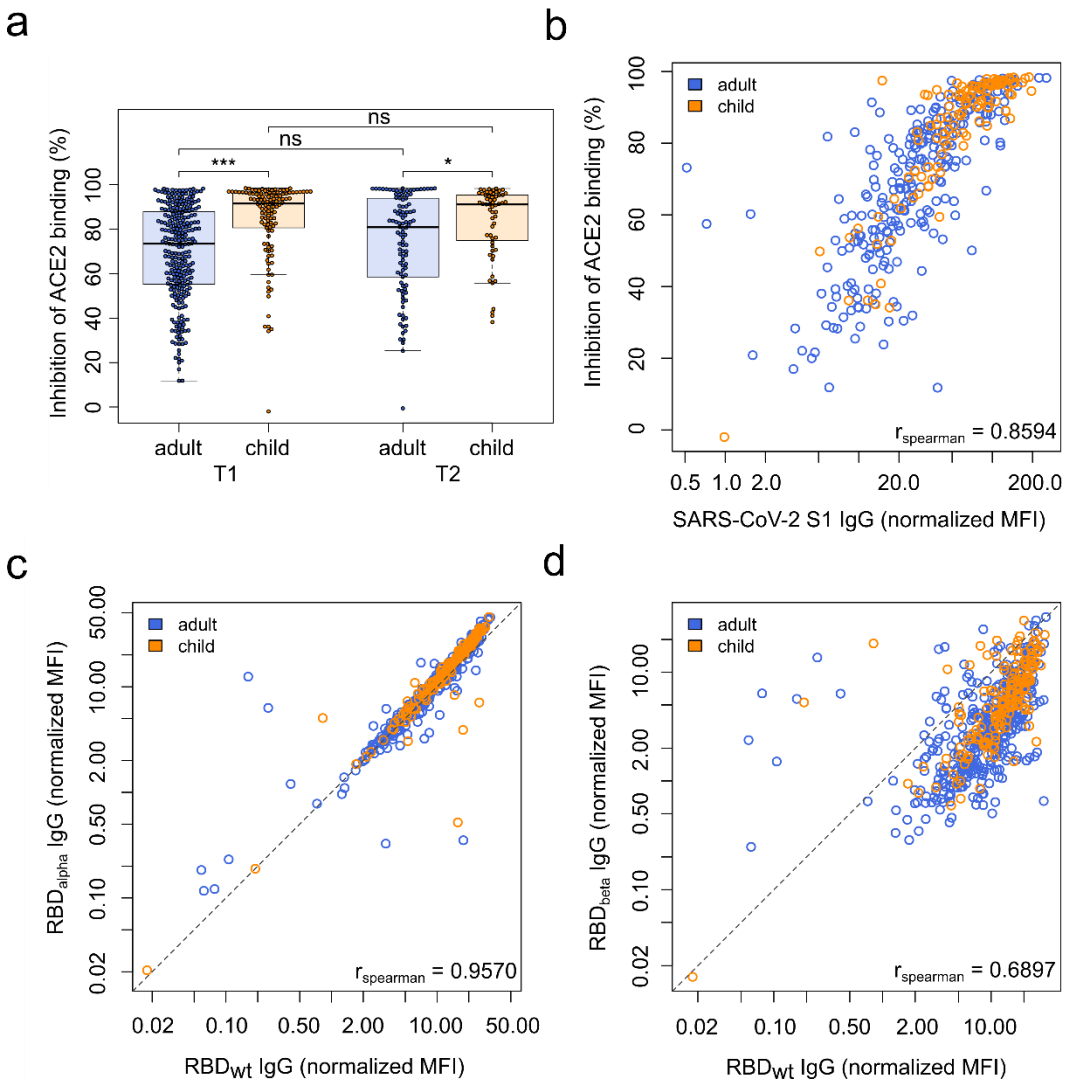

Figure 19: SARS-CoV-2 antibody responses in infected adults and children
(a) Box and whisker plot showing that antibodies produced by children (orange, n = 118) have a significantly higher inhibition of ACE2 binding than those produced by adults (blue, n = 267, p = 4.37 x 10−13) at T1 and T2 (p = 0.02, child n = 59, adult n = 106) as determined by the sVNT assay. Boxes represent the median, 25th and 75th percentiles, while whiskers show the largest and smallest non-outlier values. Outliers were identified using upper/lower quartile ±1.5 times IQR. Statistical significance was calculated using Mann–Whitney-U (two-sided) with *** indicating a p value < 0.001, * indicating a p value < 0.05, and ns indicating a non-significant p value > 0.05. To determine whether this was due to the higher titres in children, SARS-CoV-2 S1 humoral response was determined using MULTICOV-AB for T1 and plotted against the results of the sVNT assay (b). Spearman's rank was calculated to measure the ordinal association between them, confirming that the increase in neutralisation is due to higher titres. Protection against the Alpha (c) and Beta (d) VOCs was determined by MULTICOV-AB and plotted as a linear regression against the antibody binding response to the wild-type (wt) receptor binding domain (RBD), with Spearman's rank calculated to measure the ordinal association. There was no difference in antibody response between children (n = 166, T1 samples only) and adults (n = 381, T1 samples only) for either variant. Figure and caption adapted from **Appendix V: Figure 3**.

3.2.4 Impaired ACE2 binding inhibition towards SARS-CoV-2 VOCs and VOIs

With the emergence of SARS-CoV-2 variants, the effectiveness of antibodies generated against the WT strain through infection or/and vaccination became a major point of interest. Especially amino acid substitutions in the RBD of the spike protein can have significant impact on virus characteristics such as transmission, infectivity and immune evasion. Therefore, I analysed the ACE2 binding inhibition of sera from COVID-19 patients with varying disease severity using RBDCoV-ACE2. The multiplex assay platform enabled the inclusion and simultaneous analysis of RBDs including WT and every circulating SARS-CoV-2 variant up to the time of publication (Delta was the dominant variant at the time). I analysed 266 serum samples from 168 COVID-19 patients, of which 35 individuals donated at multiple timepoints after positive PCR (**Appendix II**). In general, we found a strong positive correlation between anti-RBD IgG responses and ACE2 binding inhibition, suggesting a proportional NAb response as part of the total antibody response (**Appendix II: Figure 4**). **Figure 20** shows the ACE2 binding inhibition against all twelve variant RBDs of serum from individual donors collected 7 to 49 days after positive PCR, including a mutation profile for each variant. I could show that the median ACE2 binding inhibition of all variants except A.23.1 is reduced in relation to WT RBD with Eta (5.7-fold), Gamma (6.4-fold), Theta (9.0-fold) and Beta (14.1-fold) showing the greatest reduction. Examining the mutation profile of these variants revealed that they all contain the E484K mutation, from which we concluded that it plays an important role in the evasion of the antibody response. The E484K mutation, identified by several studies as escape mutation[86,114,160], has been shown to result in enhanced binding affinity of the RBD to ACE2 by altering electrostatic interactions and the conformation of the loop in the RBD-ACE2 binding interface while simultaneously weaken the binding interaction to NAbs, and also provides resistance to neutralisation by monoclonal antibodies such as bamlanivimab[168].

The additional N501Y mutation in the RBD of variants Gamma, Theta and Beta appears to amplify this effect further, whereas the presence of the mutation alone in the Alpha variant results in a weaker, 1.2-fold reduction. The N501Y mutation was shown to enhance affinity of the RBD to ACE2 (5-10 times higher than WT), which in turn makes it harder for NAbs to inhibit the RBD-ACE2 interaction and contributes to the higher transmission rate of the Alpha variant (estimated up to 80 % higher than WT strain) that dominated the global infection events from late 2020 until June 2021[84,108,109,169].

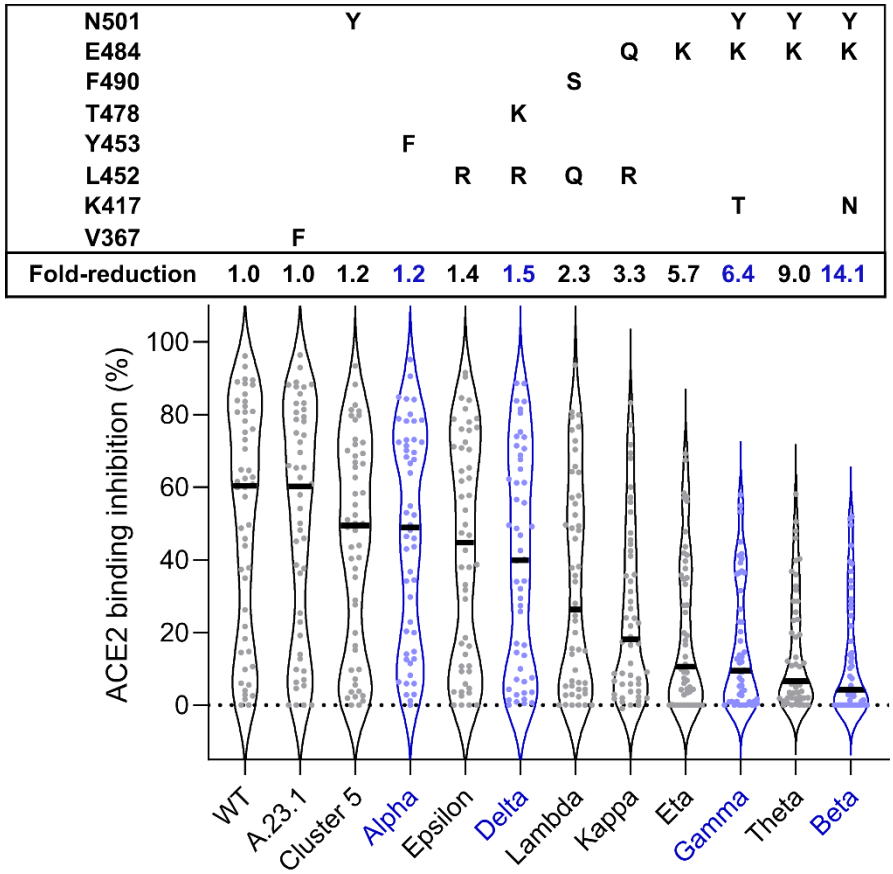

Figure 20: ACE2 binding inhibition towards SARS-CoV-2 variants
ACE2 binding inhibition varies between RBD mutants. Violin plots showing ACE2 binding inhibition (%) of individual serum samples from 7 to 49 days post PCR (n = 50, depicted as dots) against RBD mutants. Black horizontal lines represent medians. Fold-reduction of ACE2 binding inhibition in comparison to wild-type corresponds to the ratio between the medians of wild-type and the respective RBD mutant. VOC-RBDs are shown in blue. Mutations of each RBD mutant are shown in the box above the violin plot. Figure and caption reproduced from **Appendix II: Figure 3**

After Alpha, the Delta variant was the second dominant strain that dominated global infection events in the second half of 2021, carrying the mutations T478K and L452R in the RBD. Both mutations resulted in a 1.5-fold reduced ACE2 binding inhibition compared to WT RBD, placing it in the mid-range of all tested RBDs. The T478K mutation was also shown to increase the electrostatic potential of the RBD, therefore increasing the binding affinity to ACE2 while L452R was linked to increased fusogenicity and infectivity of SARS-CoV-2[170-172].

In summary, we could utilise RBDCoV-ACE2 to assess the impact of emerging SARS-CoV-2 variants on the humoral immune response induced by infection with wild-type SARS-CoV-2. In agreement with the results of other groups, our results suggest that protection against reinfection with the then dominant Alpha variant was still sufficient.[173], while variants carrying the E484K variant strongly evaded neutralisation by NAbs[174,175].

3.2.5 COVID-19 disease severity correlates with antibody titre and neutralising capacity

I further investigated whether there is a correlation between the severity of COVID-19 and the neutralising capacity of serum by ACE2 binding inhibition (**Appendix II**). For this, I divided our sample set of COVID-19 infected individuals admitted to the intensive care unit (ICU) into two timeframes, 7 – 49 post initial positive PCR and ≥ 50 days post initial positive PCR and plotted both ACE2 binding inhibition and IgG binding to the RBDs of WT and Delta against disease severity indicated by WHO grades (see **Figure 21**).

Again, we observed the general reduction of ACE2 binding inhibition for Delta in comparison to WT as seen previously (**Figure 21a–d**). Antibody binding to Delta RBD was reduced as well (**Figure 21e-h**). Due to waning antibody levels, the samples taken at a later timepoint post positive PCR (≥ 50 days) showed lower ACE2 binding inhibition (**Figure 21c, d**) and antibody binding (**Figure 21g, h**) compared to samples taken within the first 49 days post positive PCR. We observed a positive correlation of COVID-19 disease severity from WHO grade 1 to WHO grade 7 for both ACE2 binding inhibition and IgG binding for both WT and Delta RBDs. Although most of the differences in ACE2 binding inhibition between WHO severity grades were not significant, this finding is in line with previous reports, that SARS-CoV-2 anti-S IgG and NAb-titres are higher in patients with severe COVID-19[169,176-178].

Interestingly however, this progressively increasing trend is interrupted in patients with fatal disease course (WHO grade 8). Other groups also found that individuals with fatal COVID-19 had lower antibody responses to the SARS-CoV-2 spike protein than non-fatal disease outcomes[161,179]. Lucas, Klein et al. reported that the neutralising antibody response in patients with fatal COVID-19 was delayed, initially being lower than in discharged patients within the first 3 weeks after symptom onset but reaching higher maximum antibody levels afterwards[176]. Since our sample set only contained samples of fatal COVID-19 patients taken at maximum 26 days after positive PCR result and lacked samples at later timepoints, this could explain the decreased antibody response in our samples from patients with fatal COVID-19. Together with the positive correlation found between disease severity and T-cell responses in COVID-19 patients, our findings suggests that both the humoral and cellular immune responses are amplified in more severe forms of the disease[180-182].

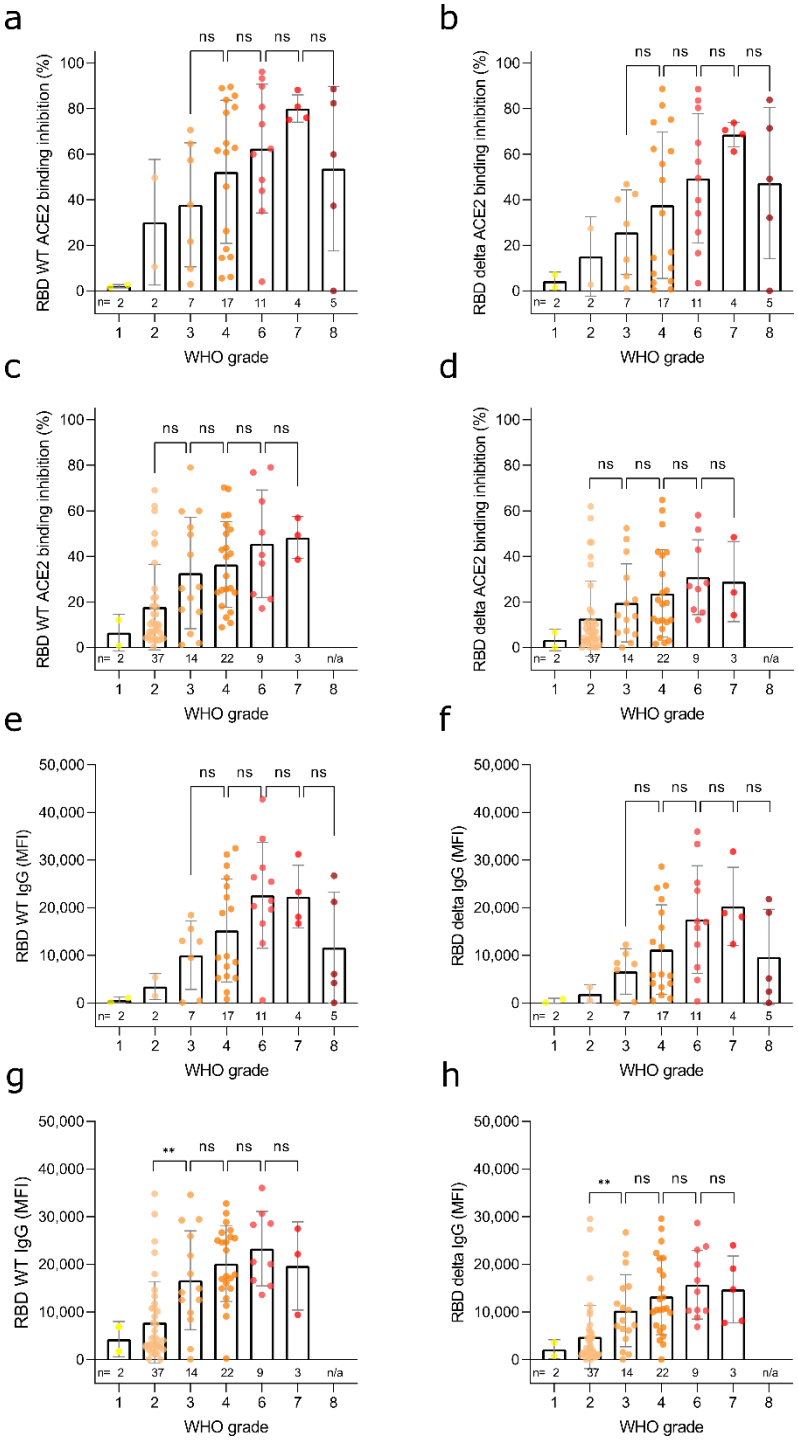

Figure 21: Correlation between antibody response and COVID-19 disease severity
Correlation of anti-RBD IgG levels and ACE2 binding inhibition with SARS-CoV-2 disease severity. Bar charts showing mean ACE2 binding inhibitions (%) against wild-type and delta RBD are correlated with WHO grades for disease severity for samples 7–49 days post PCR (a,b) and ≥ 50 days post PCR (c,d). Mean anti-WT RBD IgG and anti-RBD delta IgG levels are shown for samples 7–49 days post PCR (e,f) and ≥ 50 days post PCR (g,h). Individual samples are displayed as coloured dots, bars indicate the mean of the dataset with error bars representing standard deviation. Number of samples is given below the columns (n). If no samples for a group were available, the column is labelled with "n/a". WHO grade 1—ambulatory/no limitations of activities, 2—ambulatory/limitation of activities, 3—hospitalised, mild disease/no oxygen therapy, 4—hospitalised, mild disease/mask or nasal prongs, 6—hospitalised, severe disease/intubation + mechanical ventilation, 7—hospitalised, severe disease/ventilation + additional organ support (pressors, RRT, ECMO), 8—Death. The study did not contain samples of WHO grade 5. Figure and caption reproduced from **Appendix II: Figure 6**.

3.2.6 Impaired humoral immune response to Omicron VOCs induced by infection and vaccination

When Omicron variants emerged and became globally dominant by December 2021, public health authorities feared a substantial decrease in immune protection by vaccination or infection with previous SARS-CoV-2 variants, since Omicron BA.1 and BA.2 carried an unprecedented high number of mutations in the RBD (15 and 16 mutations respectively, see **Figure 4**). To investigate the impact of Omicron subvariants in addition to other relevant VOCs and VOIs, we analysed IgG binding and ACE2 binding inhibition in sera of pre-pandemic negative, COVID-19 infected and vaccinated individuals (**Appendix VI**). For both vaccinated and convalescent samples, IgG binding and ACE2 binding inhibition was significantly reduced for BA.1 and BA.2 compared to WT, to a similar extent as the statistically significant reduction in binding towards Beta and Mu variants (see **Figure 22a, b**). We found that IgG binding towards BA.1 was significantly more reduced compared to BA.2. Analysing ACE2 binding inhibition, we again observed the reduction of both ACE2 binding inhibition for all tested variants compared to WT as illustrated in **Figure 20**. BA.2 had the lowest rate of responsive samples (ACE2 binding inhibition > 20 %) of all tested variants in both the infected and vaccinated sample groups, while BA.1 had a higher responsive rate than Beta, Gamma and Mu.

We further included full-length S proteins of BA.1 and BA.2 as well as WT in our RBDCoV-ACE2 measurements, to analyse the effect of spike mutations outside the RBD (**Appendix VI: Figure 2a**). ACE2 binding inhibition towards Omicron S proteins was significantly reduced compared to WT. The RBDCoV-ACE2 response rate towards S compared to RBD was reduced for both WT and BA.2 by 30 %. Interestingly, we observed no difference in the IgG binding towards the nucleocapsid of BA.2 compared to WT (**Appendix VI: Figure 2f**).

Since both MULTICOV-AB and RBDCoV-ACE2 are endpoint assays, we used biolayer interferometry (BLI) analysis to assess the binding kinetics of RBD-specific antibodies induced by vaccination (two doses BNT162b2) and infection (WT) in serum samples to RBDs of WT and VOCs Delta, BA.1 and BA.2 (see **Figure 22c, d**). The antibody binding response towards BA.1 and BA.2 was reduced compared to WT and Delta for all samples and the dissociation constant, despite variation between samples, was increased for most samples.

Using BLI analysis, we also confirmed that both BA.1 an BA.2 RBDs bound to ACE2 with high affinity (**Appendix VI: Supplementary Figure 2**).

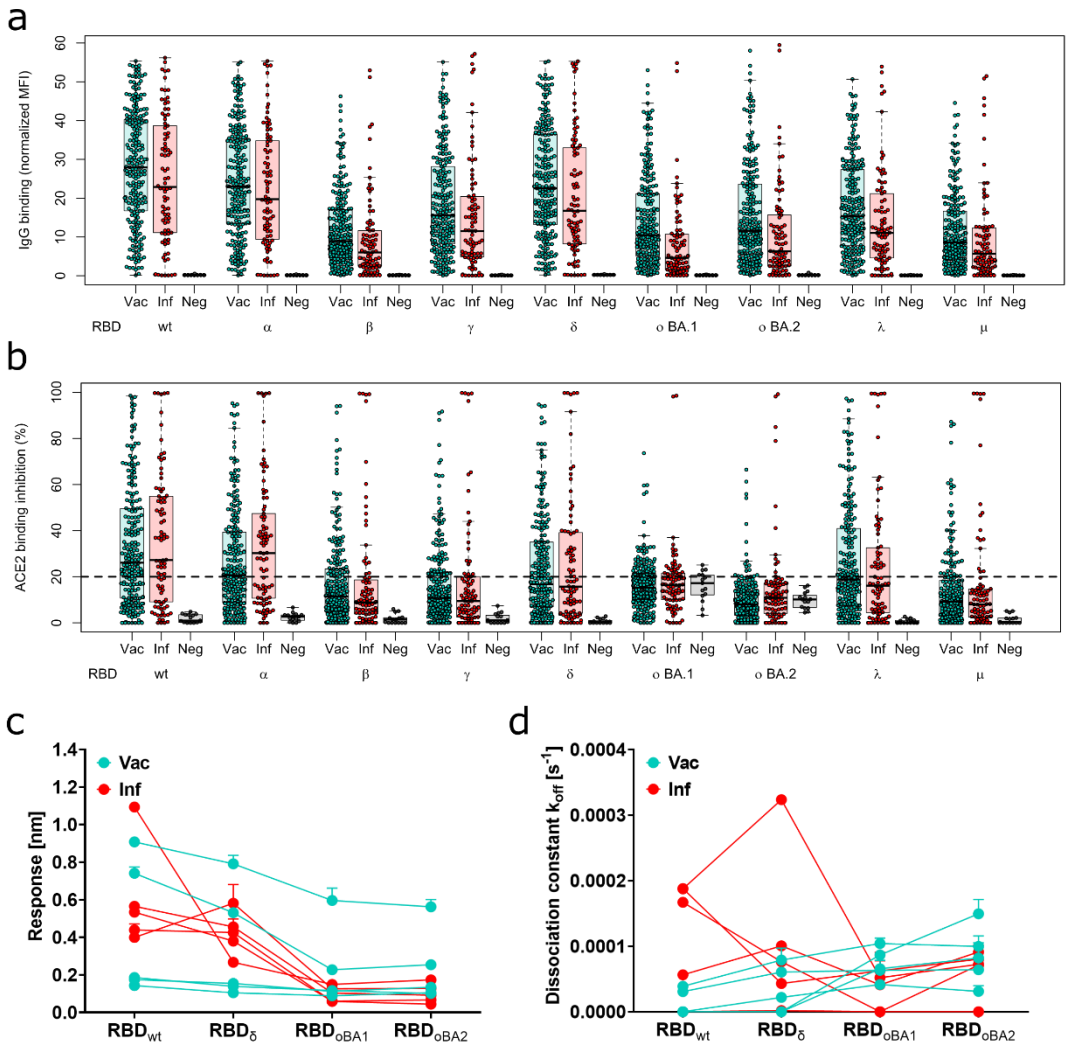

Figure 22: Significantly reduced antibody responses towards Omicron BA.1 and BA.2
Antibody binding response is significantly reduced for both BA.1 and BA.2. Binding response by preexisting antibodies generated through either infection or vaccination was measured with MULTICOV-AB (a) and RBDCoV-ACE2 (b) assays and Biolayer interferometry (c and d). (a) Boxplot showing that immunoglobulin G binding is significantly reduced for both BA.1 and BA.2 as compared to other variants of concern (VOCs)/variants of interest (VOIs) for convalescent (n = 86) and vaccinated (n = 226) samples. Negative samples are included as controls (n = 15). (b) Boxplot showing that ACE2 binding inhibition is significantly reduced for both BA.1 and BA.2 as compared to other VOCs/VOIs for both convalescent and vaccinated samples. Boxes represent the median with 25th and 75th percentiles; whiskers show the largest and smallest nonoutlier values. Outliers were determined by 1.5 interquartile range. (c and d) Binding kinetics of receptor-binding domain (RBD)–specific antibodies from serum samples of convalescent and vaccinated individuals (both n = 5). Binding response (c) and dissociation constant (d) were determined by 1:1 fitting model of the individual serum samples between the different RBD variants. Figure and caption reproduced from **Appendix VI: Figure 1**.

To get a more detailed insight into the immune protection against Omicron BA.2 induced by vaccination, we analysed IgG binding and ACE2 binding inhibition in sera from individuals receiving different vaccine combinations in **Figure 23** (analogous to **Figure 16**). Similar to the response to WT RBD, we could confirm that homologous mRNA-based vaccination was resulting in a higher and longer lasting median IgG titre compared to vector-based vaccination and was only surpassed by the antibody response of infected and vaccinated individuals (**Figure 23a**). In contrast to the IgG binding response, which was still present, albeit reduced, we observed

a drastic reduction of ACE2 binding inhibition towards Omicron BA.2 regardless of the received vaccine type or infection status, with the median ACE2 binding inhibition of all examined groups classified as non-responsive (< 20%) by RBDCoV-ACE2 (**Figure 23b**). This drastically impaired neutralising activity towards Omicron BA.2 was also reported by other studies[143,183,184].

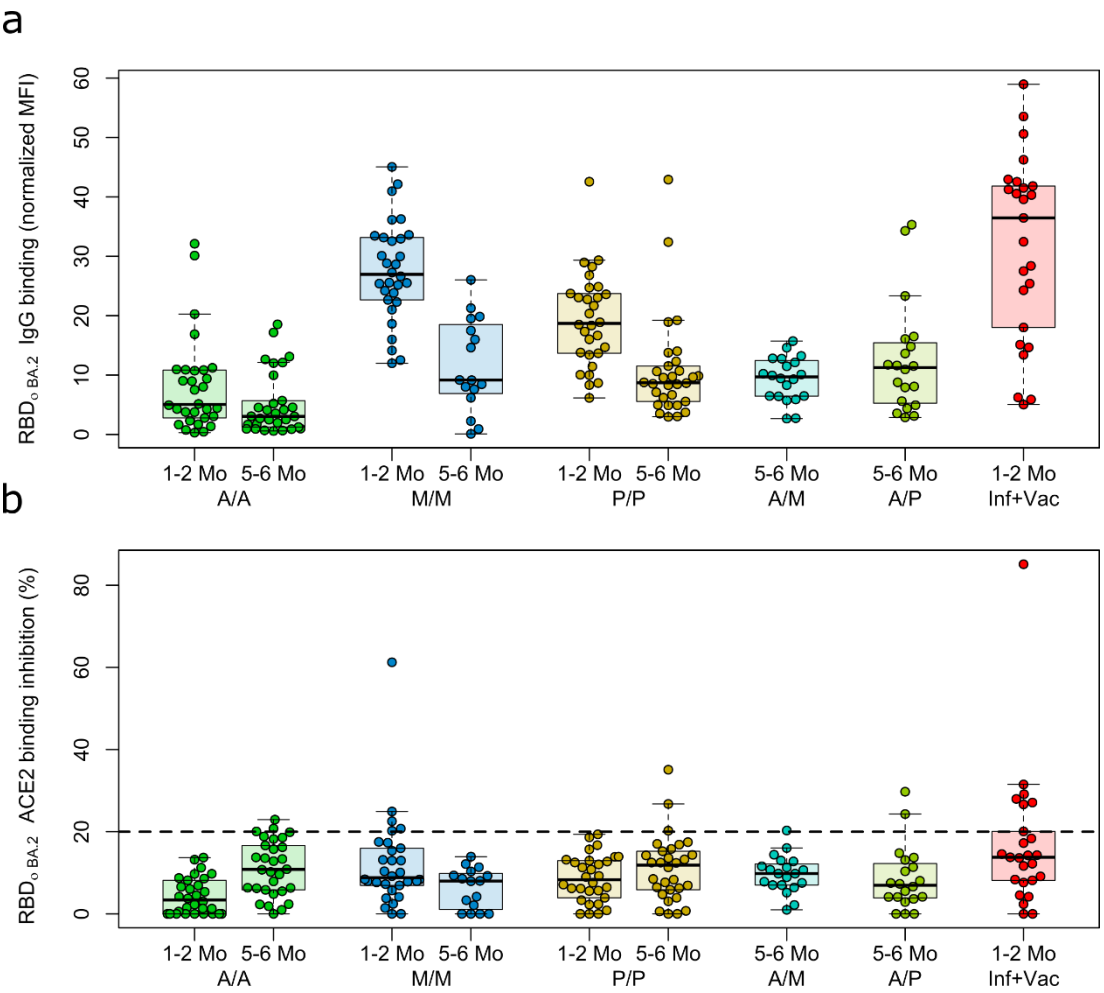

Figure 23: Binding and inhibitory response of vaccine-induced antibodies towards Omicron BA.2 Differences in Omicron binding response among different populations of vaccinated samples. Binding response toward Omicron BA.2 was analysed by either MULTICOV-AB (a) or RBDCoV-ACE2 (b) assays for samples from different vaccine schemes (n = 30 for all samples, except for mRNA-1273 at 5–6 months (n = 16), heterologous vaccine schemes (both n = 20), and infected and vaccinated (n = 25). To determine the effect of time postvaccination, samples from both 1–2 months and 5–6 months postvaccination were included. Boxes represent the median with 25th and 75th percentiles; whiskers show the largest and smallest nonoutlier values. Outliers were determined by 1.5 interquartile range. The 20% cutoff for non-responders is indicated by the dashed line on (b). The equivalent data for BA.1 are provided as Supplementary Figure 3. Abbreviations: A/A, AZD1222; A/M, first dose AZD1222, second dose mRNA-1273; A/P, first dose AZD1222, second dose BNT162b2; Inf, infected; M/M, mRNA-1273; P/P, BNT162b2; Vac, vaccinated. Figure and caption reproduced from **Appendix VI: Figure 3**.

After we established, that the antibodies elicited by two vaccine doses were still able to bind to Omicron RBDs but showed a strongly reduced neutralising capacity, we investigated the effect of a booster (third) vaccine dose on both antibody binding and ACE2 binding inhibition towards Omicron BA.1 and BA.2 and all current and previously circulating VOCs (**Figure 24**). Administration of a third dose increased ACE2 binding inhibition towards all VOCs significantly, including BA.1 and BA.2 (**Figure 24a**). Whereas 27 % and 0 % of samples post second dose showed neutralisation activity toward BA.1 and BA.2 respectively 1 - 2 months post second dose (**Figure 24b**), it increased to 55 % and 25 % after receiving the booster dose in a similar timeframe post vaccination. Median ACE2 binding inhibition of samples 5 - 6 months after second dose was significantly lower for all VOCs compared to 1 – 2 months after second vaccination (**Figure 24c**). This strong boost of neutralisation activity indicates that a booster dose with mRNA-based vaccines provides increased protection against Omicron BA.1 and BA.2[185-188].

In summary, we found that antibodies induced by vaccination or infection with WT or previously circulating variants did not completely lose their ability to bind to the extensively mutated Omicron RBDs, however IgG binding responses were significantly reduced. As numerous other studies have reported, neutralisation of BA.1 and BA.2 by sera from infected and vaccinated individuals was severely impaired, which could explain the large wave of infections in Germany during the dominance of BA.1 and BA.2 including frequent breakthrough infections[123,124].

Our study provided additional evidence that the recommendation of a third vaccine dose by the STIKO in Germany was justified and necessary to retain partial neutralising responses against Omicron[62]. In response to those findings, vaccine manufacturers started the development of vaccines adapted to Omicron sublineages BA.1 and BA.2 and did further adapt their vaccines to following subvariants[63].

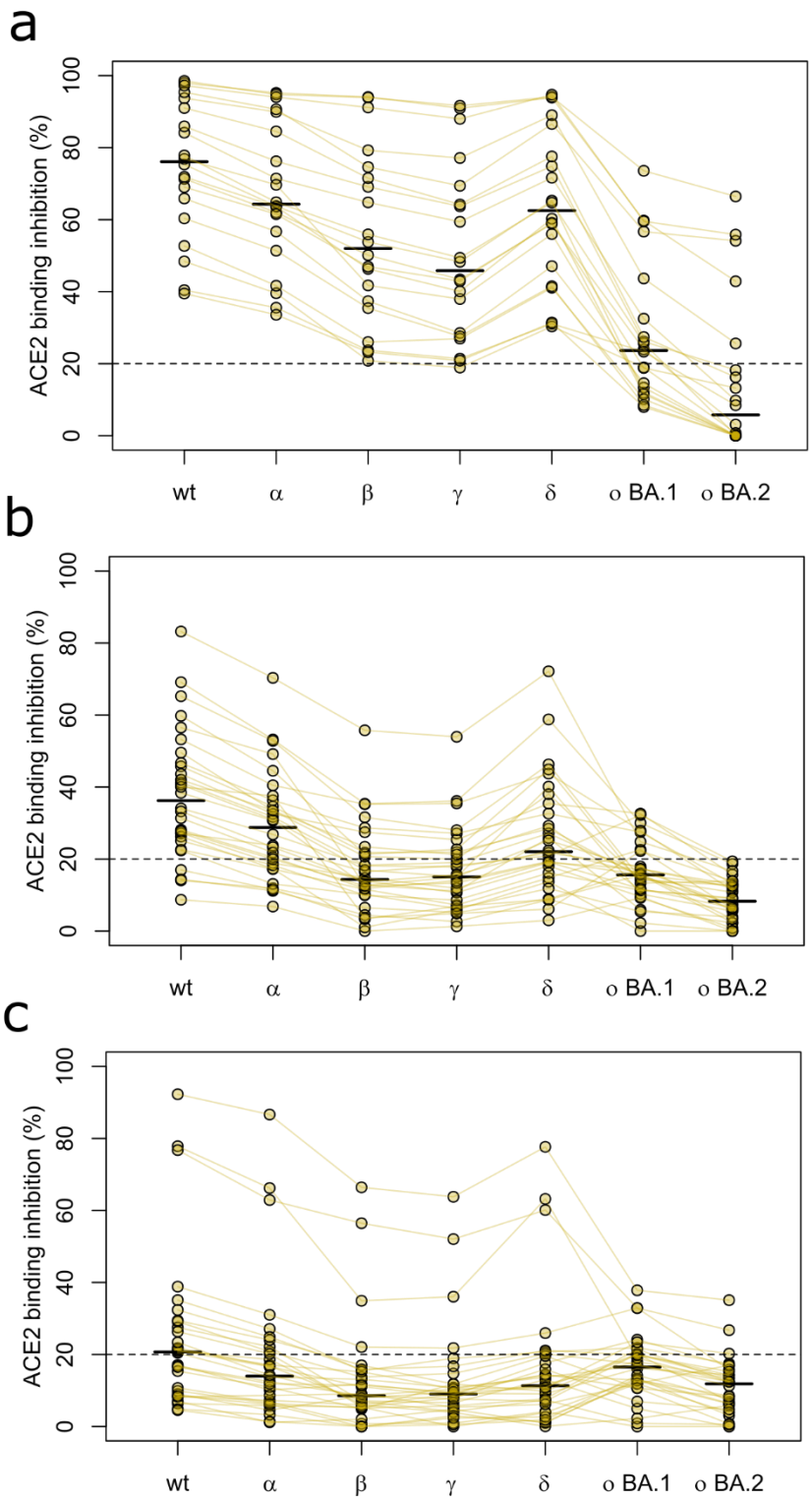

Figure 24: ACE2 binding inhibition responses after second vaccine dose wane within 5 - 6 months and are significantly boosted after third dose

Angiotensin-converting enzyme 2 (ACE2) binding inhibition toward Omicron is boosted by a third vaccine dose. (a) Changes in ACE2 binding inhibition response following the third dose of BNT162b2 for all variants within the study. Samples come from either boosted (n = 20), 1–2 months post–second dose of BNT162b2 (n = 20, b), or 5–6 months post–second dose of BNT162b2 (n = 20, c). Individual samples are highlighted by connected lines with bars representing medians. The 20% cutoff for non-responders is indicated by the dashed line. Figure and caption reproduced from **Appendix VI: Figure 4**.

3.2.7 The effect of breakthrough infections on antibody responses

The limited vaccine availability especially in the early pandemic, regularly changing vaccine recommendations due to safety concerns and new insights on vaccine effectiveness against emerging VOCs and breakthrough infections resulted in a highly heterogenous immune response to SARS-CoV-2 in the German population. We examined a cohort of vaccinated healthcare workers and medical researchers as part of the TüSeRe:exact study in Southwest Germany, to assess potential differences in their humoral immune responses and have summarised the results in an unpublished manuscript (**Appendix X**).

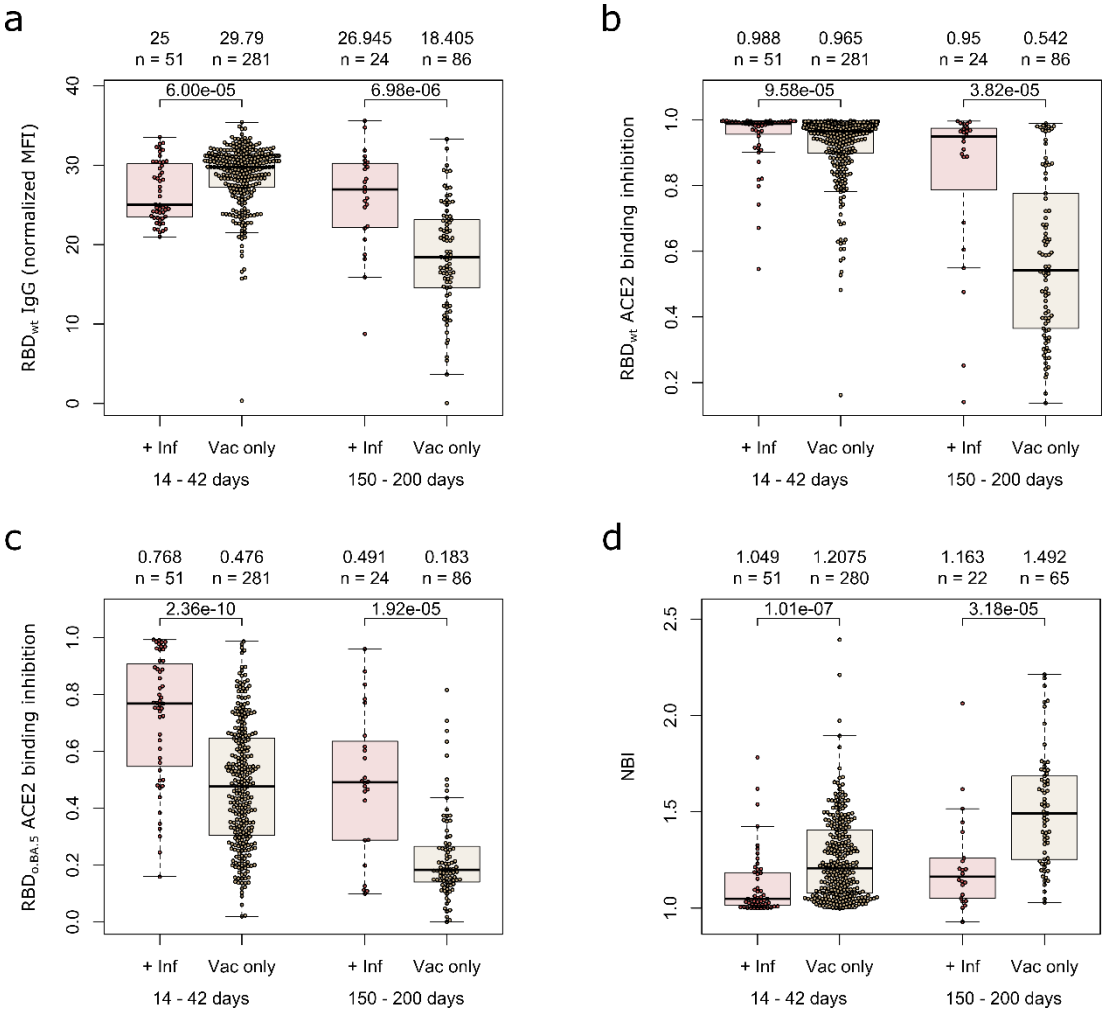

Figure 25: Breakthrough Infections lead to increased breadth and longevity of the antibody response

Antibody titre (a), ACE2 binding inhibition towards WT (b) and BA.5 (c), neutralising breadth index (d) were compared in samples from individuals with or without a breakthrough infection following 3 vaccine doses. Samples were compared at two timepoints: 14 to 42 days post most recent immunising event to capture the peak response and 150 to 200 days to capture the long term "lag" response (see Supplementary Figure 4 for further details on sample selection). box and whisker plots where boxes represent the 1st to 3rd quartiles, whiskers represent 1.5 IQR and the line represents the median. Outliers are shown. MWU was used to identify statistically significant differences between the two groups with *** indicating $p<0.001$ and n.s. indicating a non-significant p value >0.05. N's and medians for each group are included within the figure panels. Figure and caption adapted from **Appendix X: Figure 2**.

While vaccinated-only individuals initially had a higher median IgG titre to WT RBD shortly after their last dose compared to individuals with an additional SARS-CoV-2 infection, it already waned significantly 150 – 200 days after the third dose. In contrast, IgG titres induced by three vaccine doses and breakthrough infection sustained and even increased during the same time (**Figure 25a**). Similarly, ACE2 binding inhibition to Omicron BA.5 and WT RBD was also showing significant slower waning over time in individuals with both vaccination and infection (**Figure 25b, c**). To assess the breadth of the antibody response towards SARS-CoV-2 variants, we specified the neutralising breadth index (NBI) as the WT ACE2 binding inhibition divided by the median ACE2 binding inhibition of Beta, Delta and Omicron BA.2[189].

As shown in **Figure 25d**, NBI for individuals with previous infection and vaccination was significantly lower compared to vaccinated only individuals, indicating a broader neutralising antibody response to current and previously circulating VOCs established by breakthrough infection.

Furthermore, we examined the antibody response of individuals who were not recommended a booster dose due to a previous SARS-CoV-2 infection, therefore having received two doses and an infection with SARS-CoV-2 (hereinafter referred to as "hybrid immunity"). We also compared this group to the vaccinated-only individuals who received three vaccine doses (**Appendix X: Figure 3**). We again observed a significantly slower waning rate of IgG titre and ACE2 binding inhibition induced by hybrid immunity compared to the vaccinated-only group towards RBD WT. Interestingly, hybrid immunity also led to a broader neutralisation response even though most of the infections in this group occurred during earlier infection waves when either the Alpha or Delta variant were dominating infection events.

In summary, we found that SARS-CoV-2 vaccination and infection with either two or three vaccine doses resulted in a significantly more sustainable IgG titre and ACE2 binding inhibition response than vaccination alone, although the median IgG titre initially is higher in the vaccinated-only group. Moreover, both vaccinated and previously infected individuals have a broader inhibitory response to SARS-CoV-2 VOCs, which is in accordance with numerous other studies[190-193].

These findings are backed by a study in Great Britain which found that individuals with two vaccine doses and a breakthrough infection with Delta or Omicron had better protection against infection with omicron BA.4/BA.5 compared to SARS-CoV-2 naïve individuals who received three doses[194]. Infection rates have been found to be significantly lower for individuals with both previous SARS-CoV-2 infection and vaccination in several studies[195-198].

Taken together, our results emphasise the high individuality of the humoral immune response to SARS-CoV-2 dependent on the previous infection and vaccination history, which should be taken into consideration for the formulation of new vaccine recommendations.

3.2.8 Weakened humoral immune response in immunocompromised individuals

Immunocompromised individuals were among the highly prioritised groups to receive SARS-CoV-2 vaccines since they often have reduced immune responses to common vaccinations (e.g. Influenza) and had significantly higher mortality rates for COVID-19 during the early stages of the pandemic[199-201]. With their immune system either weakened by medical conditions or drugs, immunocompromised individuals are highly reliant on effective vaccination programs that provide them with protective immunity.

The compromised immune system of hemodialysis patients is often the result of decreased renal function that leads to chronic inflammation, or it is induced by medications in transplant recipients[68,69]. After approval of the first generation of SARS-CoV-2 vaccines in 2021, hemodialysis patients received standard immunisation with two vaccine doses, however it was unclear whether this was sufficient to elicit a protective immune response, especially regarding the reduced effectiveness of the first-generation vaccines against new SARS-CoV-2 variants. We tested this by comparing B- and T-cell responses from 76 hemodialysis patients to the immune response of 23 healthcare workers from the dialysis centre with no underlying medical conditions 3 weeks (T1) and 16 weeks (T2) after basic immunisation with two doses of BNT162b2 (**Appendix VII**).

We could show that both mucosal and systemic wild-type RBD-specific IgG responses at T2 were significantly reduced compared to T1 for both groups (**Figure 26**). Furthermore, titres in plasma and saliva were significantly reduced in the hemodialysis group compared to the control group at both T1 and T2 after second vaccination (**Figure 26a, b**). This reduction effect could also be observed with ACE2 binding inhibition in the serum of hemodialysis patients especially at T1. At T2, ACE2 binding inhibition for both groups was significantly reduced compared to T1 and most samples were classified non-neutralising by RBDCoV-ACE2 (**Figure 26c**). In addition, ACE2 binding inhibitions of samples from both groups towards VOCs Alpha, Beta, Gamma and Delta were reduced for all tested variants (**Appendix VII: Figure 2**) in accordance to our previous findings (**Figure 22 - 24**) and to other studies on the neutralising antibody response of hemodialysis patients towards VOCs[202,203].

To examine spike-specific T-cell responses, we analysed the release of IFN-γ in whole-blood induced by vaccination (**Figure 26d**). Here, we observed a reduced, albeit not significant, release of IFN-γ in hemodialysis patients at both timepoints. These findings are in line with reports of significantly lower SARS-CoV-2 specific T-cell responses in dialysis patients and kidney transplant recipients after two doses of mRNA-1273 or BNT162b2[204,205].

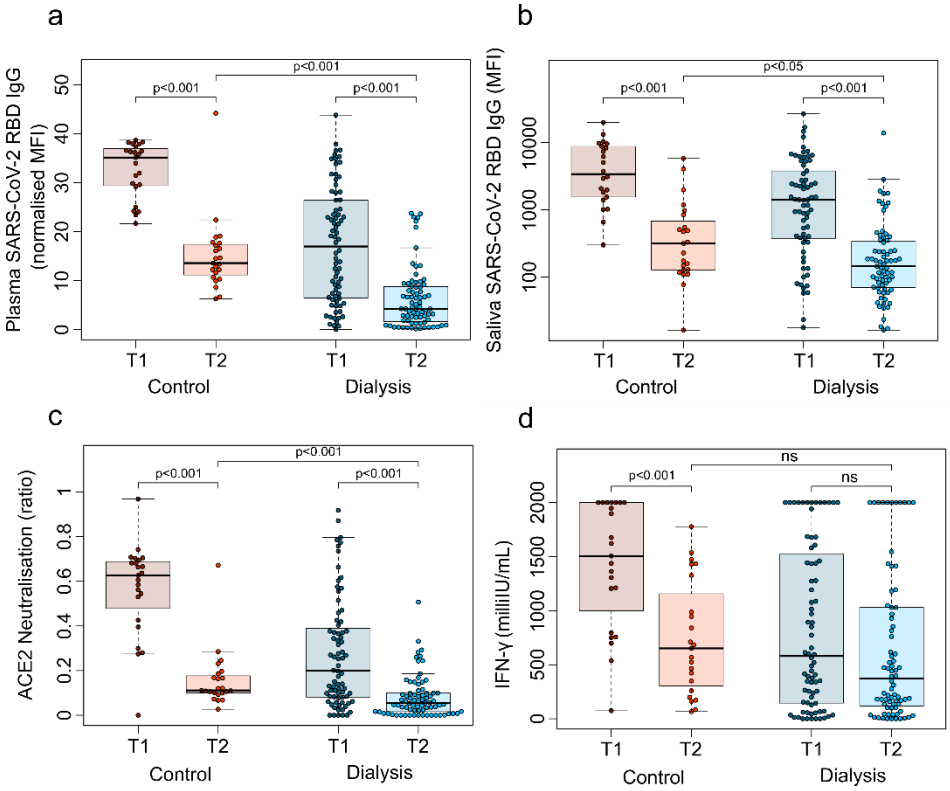

Figure 26: Impaired vaccine-induced immune responses in dialysis patients
Significant decrease in humoral and cellular responses induced by Pfizer-BioNTech vaccine BNT162b2 (https://www.pfizer.com) against SARS-CoV-2 from 3 weeks to 16 weeks after second vaccination, observed in a study of immune response against variants of concern in dialysis patients 4 months after SARS-CoV-2 mRNA vaccination. a) IgG response in plasma; b) IgG response in saliva; c) neutralising capacity toward SARS-CoV-2 wild-type B.1; d) T-cell response measured by IFN-γ release assay. Blue circles indicate dialysis patients (n = 76) and red circles controls (n = 23). Samples were taken 3 weeks (T1) and 16 weeks (T2) after vaccination. Saliva (panel B) has reduced sample numbers in both groups because of issues in sample collection (T1 control, n = 22; T1 dialysis, n = 69; T2 control, n = 23; T2 dialysis. n = 71). T1 timepoint data has been published previously (13) and is reproduced here for clarity. Horizontal lines within boxes indicate medians; box tops and bottoms indicate the 25th and 75th percentiles; whiskers show the largest and smallest nonoutlier values. Outliers were determined by 1.5 times interquartile range. Statistical significance was calculated by Wilcoxon matched-pairs signed rank test when comparing T1 and T, and 2-sided Mann–Whitney–U test when comparing control and dialysis groups. Figure and caption reproduced from **Appendix VII: Figure 1**.

Subsequently to our initial study, hemodialysis patients in our sample cohort received booster vaccinations according to the recommendations by the STIKO, during the subsequent infection waves caused by the Delta and Omicron variants. In a follow-up study, we analysed their humoral immune response to the RBDs of B.1 (WT), Delta and Omicron BA.1 after a third dose of BNT162b2 as well as before and after receiving a fourth dose of mRNA-1273 (**Appendix VIII**). Consistent with our previous results, we found that both IgG binding and ACE2 binding inhibition to RBD WT were significantly reduced in hemodialysis patients compared to the healthy control group shortly after the second vaccination and declined to similarly low levels with time after vaccination. After receiving a third BNT162b2 dose after six to eight months, the median IgG binding and ACE2 binding inhibition reached a new peak in both groups, with the values of the hemodialysis patients showing a higher variability (**Appendix VIII: Figure 2**).

Again, both median IgG titre and ACE2 binding inhibition waned as time passed post third vaccination, but with higher residual values compared to the timepoint three months after the second dose. Administration of a fourth dose strongly elevated anti-RBD IgG and ACE2 binding inhibition responses to a new maximum (**Figure 27**). Especially ACE2 binding inhibition towards Omicron BA.1, which was largely absent prior to the fourth dose, was significantly elevated. This further boost of humoral immunity after the fourth dose of either BNT162b2 or mRNA-1273 against WT and Omicron variants was also reported by other groups, with cross-immunisation schemes of both vaccines inducing the highest responses[206-209]. However, in line with other studies, humoral immunity against Omicron subvariants after four vaccine doses was still significantly reduced compared to wild-type and Delta, which potentially affects the duration and quality of vaccine-induced protection against Omicron VOCs[206,210]. Additional doses with updated vaccines directed against Omicron such as the bivalent BA.4/BA.5 or monovalent XBB.1.5 mRNA-vaccines available since 2023[63], may help to achieve a higher immunity against Omicron subvariants. Available studies on the effect of a fifth dose of adapted vaccines provided promising results, finding increased antibody titres and neutralisation against both the wild-type virus and Omicron subvariants BA.4, BA.5, BQ.1.1 and XBB.1.5 in hemodialysis patients[211,212].

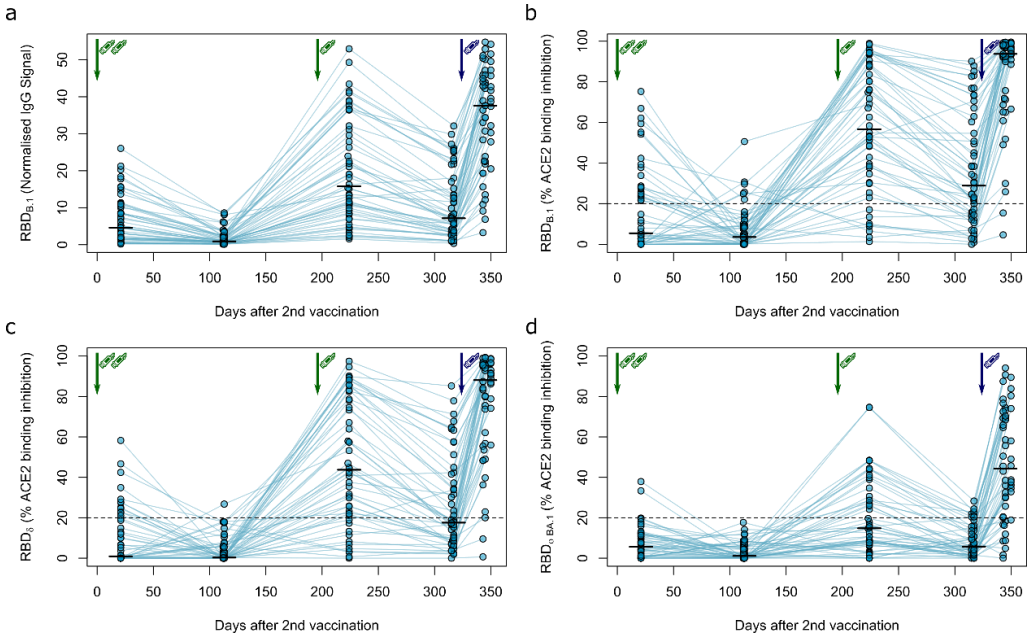

Figure 27: Effects of third and fourth vaccine doses on humoral immune response in hemodialysis patients

Longitudinal humoral immune response in haemodialysis patients after a triple vaccination with BNT162b2 and a fourth full-dose of mRNA-1273. IgG response (a) and ACE2 binding inhibition (b-d) towards the SARS-CoV-2 RBD of B.1 (a, b), δ (c) and O BA.1 (d) isolates were measured in plasma from haemodialysis patients (n = 50) using MULTICOV-AB (a) or an ACE2-RBD competition assay (b-d) after immunisation with a triple dose of BNT162b2 (green syringe) and a fourth full-dose of mRNA-1273 (blue syringe). Data is displayed as normalised median fluorescence intensity (MFI) signal for IgG binding (a) or as % ACE2 binding inhibition where 100% indicates maximum inhibition and 0% no inhibition (b-d). Samples with an ACE2 binding inhibition of less than 20 % (dashed line) are classified as non-responders (b-d). Interconnecting lines represent samples from the same individual. Sampling time points in days after the standard complete two-dose BNT162b2 vaccination is stated below the graph. Statistical significance was calculated by two-sided paired Wilcoxon rank test. Significance was defined as $p < 0.05$. Figure and caption reproduced from **Appendix VIII: Figure 3**.

Altogether, we could follow a cohort of immunocompromised hemodialysis patients from basic immunisation with two vaccine doses to booster vaccinations up to four doses and found a significantly impaired humoral immune response compared to healthy individuals.

Using MULTICOV-AB and RBDCoV-ACE2, we could contribute evidence for the recommendation of further vaccinations for immunocompromised individuals.

We further examined the vaccine efficacy in patients with inflammatory bowel disease (IBD) that require immunomodulatory medication, 2 - 16 weeks and 22 - 40 weeks after receiving the third mRNA vaccine dose (**Appendix IX**). Using RBDCoV-ACE2, we could show that ACE2 binding inhibition was significantly reduced for BA.1, BA.5, BQ.1.1 and XBB.1.5 compared to wild-type. Treatment with Anti-TNF biologics led to a significantly impaired neutralising capacity against wild-type and all tested Omicron variants after vaccination, compared to non-anti-TNF treated patients (**Appendix IX: Figure 2**), which was also reported in other studies[213-215]. This attenuated immune response in anti-TNF treated IBD patients was associated with a higher risk of breakthrough infection and a shorter time to reinfection with Omicron VOCs[216,217].

We further compared the longitudinal antibody response post third dose in patients with and without breakthrough infection (**Figure 28**). ACE2 binding inhibition of serum from patients without previous breakthrough infection declined between visits 1 and 2, in accordance with our previous findings. In contrast, patients with Omicron breakthrough infection between visit 1 and 2 counteracted this waning response and exhibited strongly increased ACE2 binding inhibition against wild-type and all tested Omicron variants (**Figure 28a**). Consequently, in the group of patients with breakthrough infections, the proportions of non-inhibitory samples towards wild-type and all variants were strongly reduced at the second visit compared to the first (**Figure 28b**). Similar to our findings in hemodialysis patients, the occurrence of breakthrough infections could broaden and lengthen the neutralising immune response against omicron VOCs.

In summary, our findings underlined the importance of vaccine efficacy surveillance in IBD patients in the context of emerging highly infectious SARS-CoV-2 variants such as BQ.1 and XBB.1.5, especially in those treated with anti-TNF. Our results supported the administration of a fourth vaccine dose optionally updated to novel variants.

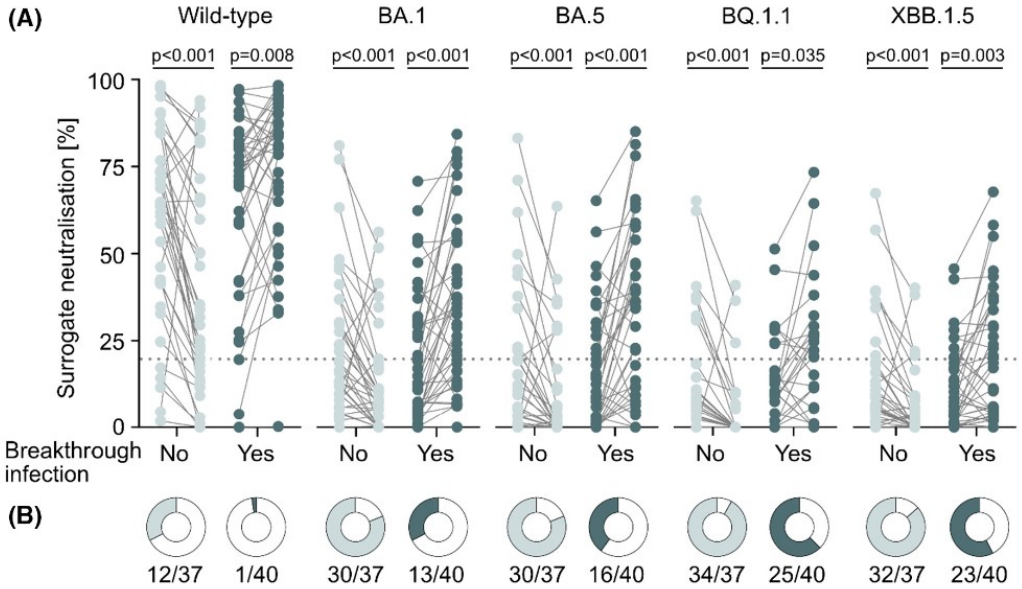

Figure 28: ACE2 binding inhibition towards Omicron VOCs in IBD patients
Vaccine-elicited ACE2 binding inhibition against BQ.1.1 and XBB.1.5 wanes over time but is increased by omicron breakthrough infection. (A) Surrogate neutralisation against wild-type and omicron sublineages BA.1, BA.5, BQ.1.1 and XBB.1.5 at visit 1 (2-16 weeks) and visit 2 (22-40 weeks) after SARS-CoV-2 vaccination, in SARS-CoV-2 naïve study participants (light teal) and participants with SARS-CoV-2 breakthrough infection between visit 1 and 2 (dark teal). Individuals with fourth vaccination, SARS-CoV-2 infection before vaccination, or with breakthrough infection before visit 1 were excluded from this analysis. Dotted line at 20 % indicates threshold for inhibitory ACE2 binding inhibition. Statistical analysis is based on Wilcoxon signed rank test (B) Proportions of individuals with non-inhibitory ACE2 binding inhibition against indicated SARS-CoV-2 variants at visit 2 in Individuals without (light teal) and with (dark teal) breakthrough infection between visits 1 and 2. Figure and caption reproduced from **Appendix IX: Figure 4**

.

4 Conclusion and Outlook

With MULTICOV-AB and RBDCoV-ACE2, I have developed two multiplex serological immunoassays during the COVID-19 pandemic that have numerous advantages over commercially available or standard methods.

Using MULTICOV-AB, I was able to contribute to the exploration of the humoral immune response to SARS-CoV-2 in the early phase of the pandemic, investigate seroprevalence in nationwide cohorts and characterise and differentiate the immune response of vaccinated and infected individuals. The application of a binary cut-off for IgG and IgA classification led to a superior performance of MULTICOV-AB compared to commercially available test systems.

With the progression of the pandemic and the emergence of new SARS-CoV-2 variants with partly altered properties such as infectivity, transmissibility and disease severity, I developed the surrogate neutralisation assay RBDCoV-ACE2, which can simultaneously determine the NAb-mediated neutralisation capacity of serum against all circulating SARS-CoV-2 VOCs, VOIs and VUMs. Hereby, in addition to antibody binding, I gained a functional insight into the neutralising antibody response induced by infection or/and vaccination.

Using RBDCoV-ACE2, I was able to show that the neutralisation capacity is reduced in a variant-specific manner and that mutations of certain amino acids in the RBD, especially E484, lead to a strong reduction. Furthermore, I was able to analyse the vaccination regimens administered during the pandemic and confirm that mRNA-based vaccines induce a stronger humoral immune response than vector-based vaccines, but that this immune response is strongly reduced towards Omicron variants. The administration of a third dose of mRNA vaccines (booster dose) resulted in a significant increase in neutralising capacity against all analysed variants but remained largely unreactive in RBDCoV-ACE2 against Omicron.

I also investigated the immunocompromised immune response of hemodialysis and IBD patients, who represent a particularly vulnerable group for severe COVID-19 courses. Here, I found significantly reduced IgG responses in serum and saliva and a greatly reduced neutralisation capacity compared to individuals without underlying medical conditions, providing evidence for the need for regular booster vaccination, preferably with variant-updated vaccines.

In summary, I have developed two assays, MULTICOV-AB and RBDCoV-ACE2, which have been used in relevant research questions on the immune response to the previously unknown SARS-CoV-2, as well as in clinical practice and in nationwide seroprevalence studies. Furthermore, RBDCoV-ACE2 was used in pre-clinical studies for the development of an Omicron-adapted vaccine candidate.

Although its status as a global health emergency was officially ended by the WHO in May 2023, SARS-CoV-2 continues to cause thousands of infections every day as of February 2024 with new variants constantly emerging that can suddenly impact the infection rate. It is therefore important that new virus variants, and the immune response to them, continue to be monitored in order to re-evaluate the impact on existing immunity, also with regard to the effectiveness of vaccination regimens.

References

1 *Number of COVID-19 deaths reported to WHO (cumulative total)* https://data.who.int/dashboards/covid19/deaths?n=c, last accessed 13.02.2024.

2 Zhu, N. *et al.* A Novel Coronavirus from Patients with Pneumonia in China, 2019. *N Engl J Med* **382**, 727-733 (2020). https://doi.org:10.1056/NEJMoa2001017

3 Pneumonia of unknown cause – China (World Health Organization, 2020) https://www.who.int/emergencies/disease-outbreak-news/item/2020-DON229, last accessed 07.04.2024.

4 Coronavirus disease 2019 (COVID-19) Situation Report – 55. (World Health Organization, 2020) https://www.who.int/docs/default-source/coronaviruse/situation-reports/20200315-sitrep-55-covid-19.pdf, last accessed 07.04.2024.

5 Statement on the second meeting of the International Health Regulations (2005) Emergency Committee regarding the outbreak of novel coronavirus (2019-nCoV). (World Health Organization, 2020) https://www.who.int/news-room/detail/30-01-2020-statement-on-the-second-meeting-of-the-international-health-regulations-(2005)-emergency-committee-regarding-the-outbreak-of-novel-coronavirus-(2019-ncov), last accessed 13.02.2024.

6 WHO Director-General's opening remarks at the media briefing on COVID-19 - 11 March 2020. (World Health Organization, 2020) https://www.who.int/director-general/speeches/detail/who-director-general-s-opening-remarks-at-the-media-briefing-on-covid-19---11-march-2020, last accessed 13.02.2024.

7 Koh, D. COVID-19 lockdowns throughout the world. *Occupational Medicine* **70**, 322-322 (2020). https://doi.org:10.1093/occmed/kqaa073

8 Hu, B., Guo, H., Zhou, P. & Shi, Z.-L. Characteristics of SARS-CoV-2 and COVID-19. *Nature Reviews Microbiology* **19**, 141-154 (2021). https://doi.org:10.1038/s41579-020-00459-7

9 Feng, D. *et al.* The SARS epidemic in mainland China: bringing together all epidemiological data. *Trop Med Int Health* **14 Suppl 1**, 4-13 (2009). https://doi.org:10.1111/j.1365-3156.2008.02145.x

10 Zumla, A., Hui, D. S. & Perlman, S. Middle East respiratory syndrome. *Lancet* **386**, 995-1007 (2015). https://doi.org:10.1016/s0140-6736(15)60454-8

11 Lu, R. *et al.* Genomic characterisation and epidemiology of 2019 novel coronavirus: implications for virus origins and receptor binding. *Lancet* **395**, 565-574 (2020). https://doi.org:10.1016/s0140-6736(20)30251-8

12 Harrison, C. M. *et al.* Evaluating the Virology and Evolution of Seasonal Human Coronaviruses Associated with the Common Cold in the COVID-19 Era. *Microorganisms* **11** (2023). https://doi.org:10.3390/microorganisms11020445

13 Zhou, P. *et al.* A pneumonia outbreak associated with a new coronavirus of probable bat origin. *Nature* **579**, 270-273 (2020). https://doi.org:10.1038/s41586-020-2012-7

14 Worobey, M. *et al.* The Huanan Seafood Wholesale Market in Wuhan was the early epicenter of the COVID-19 pandemic. *Science* **377**, 951-959 (2022). https://doi.org:10.1126/science.abp8715

15 Ellwanger, J. H. & Chies, J. A. B. Zoonotic spillover: Understanding basic aspects for better prevention. *Genet Mol Biol* **44**, e20200355 (2021). https://doi.org:10.1590/1678-4685-gmb-2020-0355

16 Hardenbrook, N. J. & Zhang, P. A structural view of the SARS-CoV-2 virus and its assembly. *Curr Opin Virol* **52**, 123-134 (2022). https://doi.org:10.1016/j.coviro.2021.11.011

17 Pizzato, M. *et al.* SARS-CoV-2 and the Host Cell: A Tale of Interactions. *Frontiers in Virology* **1** (2022).

18 Liu, D. X., Yuan, Q. & Liao, Y. Coronavirus envelope protein: a small membrane protein with multiple functions. *Cell Mol Life Sci* **64**, 2043-2048 (2007). https://doi.org:10.1007/s00018-007-7103-1

19 Zhang, Z. *et al.* Structure of SARS-CoV-2 membrane protein essential for virus assembly. *Nature Communications* **13**, 4399 (2022). https://doi.org:10.1038/s41467-022-32019-3

20 Shang, J. *et al.* Compositional diversity and evolutionary pattern of coronavirus accessory proteins. *Brief Bioinform* **22**, 1267-1278 (2021). https://doi.org:10.1093/bib/bbaa262

21 Zandi, M. *et al.* The role of SARS-CoV-2 accessory proteins in immune evasion. *Biomed Pharmacother* **156**, 113889 (2022). https://doi.org:10.1016/j.biopha.2022.113889

22 Johnson, T. J. *et al.* Viral load of SARS-CoV-2 in droplets and bioaerosols directly captured during breathing, speaking and coughing. *Scientific Reports* **12**, 3484 (2022). https://doi.org:10.1038/s41598-022-07301-5

23 *Coronavirus disease (COVID-19): How is it transmitted?* (2021), https://www.who.int/news-room/questions-and-answers/item/coronavirus-disease-covid-19-how-is-it-transmitted, last accessed 16.02.2024.

24 Hoffmann, M. *et al.* SARS-CoV-2 Cell Entry Depends on ACE2 and TMPRSS2 and Is Blocked by a Clinically Proven Protease Inhibitor. *Cell* **181**, 271-280.e278 (2020). https://doi.org:10.1016/j.cell.2020.02.052

25 Wang, K. *et al.* CD147-spike protein is a novel route for SARS-CoV-2 infection to host cells. *Signal Transduction and Targeted Therapy* **5**, 283 (2020). https://doi.org:10.1038/s41392-020-00426-x

26 Fenizia, C. *et al.* SARS-CoV-2 Entry: At the Crossroads of CD147 and ACE2. *Cells* **10**, 1434 (2021).

27 Cantuti-Castelvetri, L. *et al.* Neuropilin-1 facilitates SARS-CoV-2 cell entry and infectivity. *Science* **370**, 856-860 (2020). https://doi.org:doi:10.1126/science.abd2985

28 Yang, H. & Rao, Z. Structural biology of SARS-CoV-2 and implications for therapeutic development. *Nat Rev Microbiol* **19**, 685-700 (2021). https://doi.org:10.1038/s41579-021-00630-8

29 Roberts, S. *Flattening the Coronavirus Curve* (2020), https://www.nytimes.com/article/flatten-curve-coronavirus.html, last accessed 22.02.2024.

30 Shin, M. D. *et al.* COVID-19 vaccine development and a potential nanomaterial path forward. *Nature Nanotechnology* **15**, 646-655 (2020). https://doi.org:10.1038/s41565-020-0737-y

31 Martin, J. E. *et al.* A SARS DNA vaccine induces neutralizing antibody and cellular immune responses in healthy adults in a Phase I clinical trial. *Vaccine* **26**, 6338-6343 (2008). https://doi.org:10.1016/j.vaccine.2008.09.026

32 Lin, J. T. *et al.* Safety and immunogenicity from a phase I trial of inactivated severe acute respiratory syndrome coronavirus vaccine. *Antivir Ther* **12**, 1107-1113 (2007).

33 Krammer, F. SARS-CoV-2 vaccines in development. *Nature* **586**, 516-527 (2020). https://doi.org:10.1038/s41586-020-2798-3

34 *Comirnaty* https://www.ema.europa.eu/en/medicines/human/EPAR/comirnaty, last accessed 18.02.2024.

35 Huang, C. *et al.* Clinical features of patients infected with 2019 novel coronavirus in Wuhan, China. *Lancet* **395**, 497-506 (2020). https://doi.org:10.1016/s0140-6736(20)30183-5

36 *Spikevax (previously COVID-19 Vaccine Moderna)* https://www.ema.europa.eu/en/medicines/human/EPAR/spikevax-previously-covid-19-vaccine-moderna, last accessed 18.02.2024.

37 *Vaxzevria (previously COVID-19 Vaccine AstraZeneca)* https://www.ema.europa.eu/en/medicines/human/EPAR/vaxzevria-previously-covid-19-vaccine-astrazeneca, last accessed 18.02.2024.

38 *Jcovden (previously COVID-19 Vaccine Janssen)* https://www.ema.europa.eu/en/medicines/human/EPAR/jcovden-previously-covid-19-vaccine-janssen, last accessed 18.02.2024.

39 *Current Vaccination Status -Deliveries by manufacturer and vaccine type* (2023), https://impfdashboard.de/en, last accessed 18.02.2024.

40 Heinz, F. X. & Stiasny, K. Distinguishing features of current COVID-19 vaccines: knowns and unknowns of antigen presentation and modes of action. *npj Vaccines* **6**, 104 (2021). https://doi.org:10.1038/s41541-021-00369-6

41 Polack, F. P. *et al.* Safety and Efficacy of the BNT162b2 mRNA Covid-19 Vaccine. *N Engl J Med* **383**, 2603-2615 (2020). https://doi.org:10.1056/NEJMoa2034577

42 Baden, L. R. *et al.* Efficacy and Safety of the mRNA-1273 SARS-CoV-2 Vaccine. *N Engl J Med* **384**, 403-416 (2021). https://doi.org:10.1056/NEJMoa2035389

43 Voysey, M. *et al.* Safety and efficacy of the ChAdOx1 nCoV-19 vaccine (AZD1222) against SARS-CoV-2: an interim analysis of four randomised controlled trials in Brazil, South Africa, and the UK. *Lancet* **397**, 99-111 (2021). https://doi.org:10.1016/s0140-6736(20)32661-1

44 Sadoff, J. *et al.* Safety and Efficacy of Single-Dose Ad26.COV2.S Vaccine against Covid-19. *N Engl J Med* **384**, 2187-2201 (2021). https://doi.org:10.1056/NEJMoa2101544

45 Walsh, E. E. *et al.* Safety and Immunogenicity of Two RNA-Based Covid-19 Vaccine Candidates. *New England Journal of Medicine* **383**, 2439-2450 (2020). https://doi.org:10.1056/NEJMoa2027906

46 Baden, L. R. *et al.* Efficacy and Safety of the mRNA-1273 SARS-CoV-2 Vaccine. *New England Journal of Medicine* **384**, 403-416 (2020). https://doi.org:10.1056/NEJMoa2035389

47 Cheng, F. *et al.* Research Advances on the Stability of mRNA Vaccines. *Viruses* **15** (2023). https://doi.org:10.3390/v15030668

48 Rijkers, G. T. *et al.* Antigen Presentation of mRNA-Based and Virus-Vectored SARS-CoV-2 Vaccines. *Vaccines (Basel)* **9** (2021). https://doi.org:10.3390/vaccines9080848

49 Nance, K. D. & Meier, J. L. Modifications in an Emergency: The Role of N1-Methylpseudouridine in COVID-19 Vaccines. *ACS Central Science* **7**, 748-756 (2021). https://doi.org:10.1021/acscentsci.1c00197

50 Nelson, J. *et al.* Impact of mRNA chemistry and manufacturing process on innate immune activation. *Science Advances* **6**, eaaz6893 (2020). https://doi.org:doi:10.1126/sciadv.aaz6893

51 Bos, R. *et al.* Ad26 vector-based COVID-19 vaccine encoding a prefusion-stabilized SARS-CoV-2 Spike immunogen induces potent humoral and cellular immune responses. *npj Vaccines* **5**, 91 (2020). https://doi.org:10.1038/s41541-020-00243-x

52 Travieso, T., Li, J., Mahesh, S., Mello, J. D. F. R. E. & Blasi, M. The use of viral vectors in vaccine development. *npj Vaccines* **7**, 75 (2022). https://doi.org:10.1038/s41541-022-00503-y

53 Sadoff, J. *et al.* Safety and Efficacy of Single-Dose Ad26.COV2.S Vaccine against Covid-19. *New England Journal of Medicine* **384**, 2187-2201 (2021). https://doi.org:10.1056/NEJMoa2101544

54 *Ständige Impfkommission - Aufgaben und Methodik* https://www.rki.de/DE/Content/Kommissionen/STIKO/Aufgaben_Methoden/methoden_node.html, last accessed 19.02.2024.

55 *Stufenplan der STIKO zur Priorisierung der COVID-19-Impfung* (2021), https://www.rki.de/DE/Content/Infekt/Impfen/ImpfungenAZ/COVID-19/Stufenplan.pdf?__blob=publicationFile, last accessed 19.02.2024.

56 Durchführung der COVID-19-Impfung (Stand 26.1.2024). (Robert Koch Institute, 2024) https://www.rki.de/SharedDocs/FAQ/COVID-Impfen/FAQ_Liste_Durchfuehrung_Impfung.html, last accessed 19.02.2024.

57 Das Paul-Ehrlich Institut informiert – Vorübergehende Aussetzung der Impfung mit dem COVID-19 Impfstoff AstraZeneca (Paul-Ehrlich-Institute, Langen, 2021) https://www.pei.de/DE/newsroom/hp-meldungen/2021/210315-voruebergehende-aussetzung-impfung-covid-19-impfstoff-astra-zeneca.html, last accessed 26.03.2024.

58 Pressemitteilung der STIKO zum AstraZeneca-Impfstoff (30.03.2021). (Robert Koch Institute, 2021) https://www.rki.de/DE/Content/Kommissionen/STIKO/Empfehlungen/AstraZeneca-Impfstoff-2021-03-30.html, last accessed 26.02.2024.

59 COVID-19 Vaccine AstraZeneca – Safety Assessment Result: The Vaccine is Safe and Effective in the Fight against COVID-19. (Paul-Ehrlich-Institute, Langen, 2021) https://www.pei.de/EN/newsroom/hp-news/2021/210319-covid-19-vaccine-astrazeneca-safety-assessment-result-vaccine-safe-and-effective.html, last accessed 26.03.2024.

60 Cohn, B. A., Cirillo, P. M., Murphy, C. C., Krigbaum, N. Y. & Wallace, A. W. SARS-CoV-2 vaccine protection and deaths among US veterans during 2021. *Science* **375**, 331-336 (2022). https://doi.org:doi:10.1126/science.abm0620

61 Pressemitteilung der STIKO zur COVID-19-Auffrischimpfung und zur Optimierung der Janssen-Grundimmunisierung (7.10.2021). (Robert Koch Institute, 2021) https://www.rki.de/DE/Content/Kommissionen/STIKO/Empfehlungen/PM_2021-10-07.html, last accessed 26.02.2024.

62 Pressemitteilung der STIKO zur Auffrischimpfung einer COVID-19-Impfung bei Personen ab 18 Jahren (18.11.2021). (Robert Koch Institute, 2021) https://www.rki.de/DE/Content/Kommissionen/STIKO/Empfehlungen/PM_2021-11-18.html, last accessed 19.02.2024.

63 *COVID-19 medicines* (2024), https://www.ema.europa.eu/en/human-regulatory-overview/public-health-threats/coronavirus-disease-covid-19/covid-19-medicines, last accessed 22.02.2024.

64 Shoham, S. *et al.* Vaccines and therapeutics for immunocompromised patients with COVID-19. *eClinicalMedicine* **59** (2023). https://doi.org:10.1016/j.eclinm.2023.101965

65 Boyarsky, B. J. *et al.* Antibody Response to 2-Dose SARS-CoV-2 mRNA Vaccine Series in Solid Organ Transplant Recipients. *Jama* **325**, 2204-2206 (2021). https://doi.org:10.1001/jama.2021.7489

66 Abbasi, J. Researchers Tie Severe Immunosuppression to Chronic COVID-19 and Virus Variants. *Jama* **325**, 2033-2035 (2021). https://doi.org:10.1001/jama.2021.7212

67 Bordry, N. *et al.* SARS-CoV-2 m-RNA Vaccine Response in Immunocompromised Patients: A Monocentric Study Comparing Cancer, People Living with HIV, Hematopoietic Stem Cell Transplant Patients and Lung Transplant Recipients. *Vaccines (Basel)* **11** (2023). https://doi.org:10.3390/vaccines11081284

68 Steiger, S., Rossaint, J., Zarbock, A. & Anders, H. J. Secondary Immunodeficiency Related to Kidney Disease (SIDKD)-Definition, Unmet Need, and Mechanisms. *J Am Soc Nephrol* **33**, 259-278 (2022). https://doi.org:10.1681/asn.2021091257

69 Szumilas, K. *et al.* Current Status Regarding Immunosuppressive Treatment in Patients after Renal Transplantation. *Int J Mol Sci* **24** (2023). https://doi.org:10.3390/ijms241210301

70 *What is inflammatory bowel disease (IBD)?* https://www.cdc.gov/ibd/what-is-IBD.htm#symptoms, last accessed 22.02.2024.

71 Peyrin-Biroulet, L. *et al.* Tumour necrosis factor inhibitors in inflammatory bowel disease: the story continues. *Therapeutic Advances in Gastroenterology* **14**, 17562848211059954 (2021). https://doi.org:10.1177/17562848211059954

72 *Impfung bei Immunschwäche (Immundefizienz) (Stand: 11.1.2024)* (2024), https://www.rki.de/SharedDocs/FAQ/COVID-Impfen/FAQ_Liste_Impfung_Immundefizienz.html, last accessed 19.02.2024.

73 Watson, O. J. *et al.* Global impact of the first year of COVID-19 vaccination: a mathematical modelling study. *The Lancet Infectious Diseases* **22**, 1293-1302 (2022). https://doi.org:10.1016/S1473-3099(22)00320-6

74 Mathieu, E. R., Hannah; Rodés-Guirao, Lucas; Appel, Cameron; Giattino, Charlie; Hasell, Joe; Macdonald, Bobbie; Dattani, Saloni; Beltekian, Diana; Ortiz-Ospina, Esteban; Roser, Max (Published online at OurWorldInData.org., 2020).

75 Markov, P. V. *et al.* The evolution of SARS-CoV-2. *Nature Reviews Microbiology* **21**, 361-379 (2023). https://doi.org:10.1038/s41579-023-00878-2

76 Peck, K. M. & Lauring, A. S. Complexities of Viral Mutation Rates. *Journal of Virology* **92**, 10.1128/jvi.01031-01017 (2018). https://doi.org:doi:10.1128/jvi.01031-17

77 Harvey, W. T. *et al.* SARS-CoV-2 variants, spike mutations and immune escape. *Nature Reviews Microbiology* **19**, 409-424 (2021). https://doi.org:10.1038/s41579-021-00573-0

78 Plante, J. A. *et al.* Spike mutation D614G alters SARS-CoV-2 fitness. *Nature* **592**, 116-121 (2021). https://doi.org:10.1038/s41586-020-2895-3

79 López-Cortés, G. I. *et al.* The Spike Protein of SARS-CoV-2 Is Adapting Because of Selective Pressures. *Vaccines (Basel)* **10** (2022). https://doi.org:10.3390/vaccines10060864

80 Nielsen, B. F., Eilersen, A., Simonsen, L. & Sneppen, K. Lockdowns exert selection pressure on overdispersion of SARS-CoV-2 variants. *Epidemics* **40**, 100613 (2022). https://doi.org:10.1016/j.epidem.2022.100613

81 Disease Outbreak News – -COVID-19 - Denmark (World Health Organization, 2020) https://www.who.int/emergencies/disease-outbreak-news/item/2020-DON297, last accessed 01.03.2024.

82 Updated working definitions and primary actions for SARS-CoV-2 variants, 4 October 2023. (World Health Organization, 2023) https://www.who.int/publications/m/item/updated-working-definitions-and-primary-actions-for--sars-cov-2-variants, last accessed 01.03.2024.

83 *Tracking SARS-CoV-2 variants* (2021-2024), https://www.who.int/activities/tracking-SARS-CoV-2-variants, last accessed 15.02.2024.

84 Leung, K., Shum, M. H., Leung, G. M., Lam, T. T. & Wu, J. T. Early transmissibility assessment of the N501Y mutant strains of SARS-CoV-2 in the United Kingdom, October to November 2020. *Euro Surveill* **26** (2021). https://doi.org:10.2807/1560-7917.Es.2020.26.1.2002106

85 Grint, D. J. *et al.* Severity of Severe Acute Respiratory System Coronavirus 2 (SARS-CoV-2) Alpha Variant (B.1.1.7) in England. *Clin Infect Dis* **75**, e1120-e1127 (2022). https://doi.org:10.1093/cid/ciab754

86 Jangra, S. *et al.* SARS-CoV-2 spike E484K mutation reduces antibody neutralisation. *The Lancet Microbe* **2**, e283-e284 (2021). https://doi.org:10.1016/S2666-5247(21)00068-9

87 Weisblum, Y. *et al.* Escape from neutralizing antibodies by SARS-CoV-2 spike protein variants. *Elife* **9** (2020). https://doi.org:10.7554/eLife.61312

88 Garcia-Beltran, W. F. *et al.* Multiple SARS-CoV-2 variants escape neutralization by vaccine-induced humoral immunity. *Cell* **184**, 2372-2383.e2379 (2021). https://doi.org:10.1016/j.cell.2021.03.013

89 Deng, X. *et al.* Transmission, infectivity, and neutralization of a spike L452R SARS-CoV-2 variant. *Cell* **184**, 3426-3437.e3428 (2021). https://doi.org:10.1016/j.cell.2021.04.025

90 Liu, Q. *et al.* Antibody neutralization to SARS-CoV-2 and variants after 1 year in Wuhan, China. *Innovation (Camb)* **3**, 100181 (2022). https://doi.org:10.1016/j.xinn.2021.100181

91 Annavajhala, M. K. *et al.* Emergence and expansion of SARS-CoV-2 B.1.526 after identification in New York. *Nature* **597**, 703-708 (2021). https://doi.org:10.1038/s41586-021-03908-2

92 Ren, W. *et al.* Characterization of SARS-CoV-2 Variants B.1.617.1 (Kappa), B.1.617.2 (Delta), and B.1.618 by Cell Entry and Immune Evasion. *mBio* **13**, e00099-00022 (2022). https://doi.org:doi:10.1128/mbio.00099-22

93 Hoffmann, M. *et al.* SARS-CoV-2 variant B.1.617 is resistant to bamlanivimab and evades antibodies induced by infection and vaccination. *Cell Reports* **36**, 109415 (2021). https://doi.org:https://doi.org/10.1016/j.celrep.2021.109415

94 Bhattacharya, M., Chatterjee, S., Sharma, A. R., Lee, S. S. & Chakraborty, C. Delta variant (B.1.617.2) of SARS-CoV-2: current understanding of infection, transmission, immune escape, and mutational landscape. *Folia Microbiol (Praha)* **68**, 17-28 (2023). https://doi.org:10.1007/s12223-022-01001-3

95 Bast, E., Tang, F., Dahn, J. & Palacio, A. Increased risk of hospitalisation and death with the delta variant in the USA. *The Lancet Infectious Diseases* **21**, 1629-1630 (2021). https://doi.org:10.1016/S1473-3099(21)00685-X

96 Acevedo, M. L. *et al.* Differential neutralizing antibody responses elicited by CoronaVac and BNT162b2 against SARS-CoV-2 Lambda in Chile. *Nature Microbiology* **7**, 524-529 (2022). https://doi.org:10.1038/s41564-022-01092-1

97 Arora, P. *et al.* SARS-CoV-2 variants C.1.2 and B.1.621 (Mu) partially evade neutralization by antibodies elicited upon infection or vaccination. *Cell Reports* **39**, 110754 (2022). https://doi.org:https://doi.org/10.1016/j.celrep.2022.110754

98 Bálint, G., Vörös-Horváth, B. & Széchenyi, A. Omicron: increased transmissibility and decreased pathogenicity. *Signal Transduction and Targeted Therapy* **7**, 151 (2022). https://doi.org:10.1038/s41392-022-01009-8

99 Wang, L., Møhlenberg, M., Wang, P. & Zhou, H. Immune evasion of neutralizing antibodies by SARS-CoV-2 Omicron. *Cytokine Growth Factor Rev* **70**, 13-25 (2023). https://doi.org:10.1016/j.cytogfr.2023.03.001

100 Lyngse, F. P. *et al.* Household transmission of SARS-CoV-2 Omicron variant of concern subvariants BA.1 and BA.2 in Denmark. *Nature Communications* **13**, 5760 (2022). https://doi.org:10.1038/s41467-022-33498-0

101 *SARS-CoV-2 variants of concern as of 15 March 2024* (2024), https://www.ecdc.europa.eu/en/covid-19/variants-concern, last accessed 08.04.2024.

102 Khan, K. *et al.* Omicron BA.4/BA.5 escape neutralizing immunity elicited by BA.1 infection. *Nat Commun* **13**, 4686 (2022). https://doi.org:10.1038/s41467-022-32396-9

103 Dewald, F. *et al.* Impaired humoral immunity to BQ.1.1 in convalescent and vaccinated patients. *Nat Commun* **14**, 2835 (2023). https://doi.org:10.1038/s41467-023-38127-y

104 Yue, C. *et al.* ACE2 binding and antibody evasion in enhanced transmissibility of XBB.1.5. *Lancet Infect Dis* **23**, 278-280 (2023). https://doi.org:10.1016/s1473-3099(23)00010-5

105 Kurhade, C. *et al.* Low neutralization of SARS-CoV-2 Omicron BA.2.75.2, BQ.1.1 and XBB.1 by parental mRNA vaccine or a BA.5 bivalent booster. *Nat Med* **29**, 344-347 (2023). https://doi.org:10.1038/s41591-022-02162-x

106 Uriu, K. *et al.* Enhanced transmissibility, infectivity, and immune resistance of the SARS-CoV-2 omicron XBB.1.5 variant. *Lancet Infect Dis* **23**, 280-281 (2023). https://doi.org:10.1016/s1473-3099(23)00051-8

107 Gangavarapu, K. *et al.* Outbreak.info genomic reports: scalable and dynamic surveillance of SARS-CoV-2 variants and mutations. *Nature Methods* **20**, 512-522 (2023). https://doi.org:10.1038/s41592-023-01769-3

108 Tian, F. *et al.* N501Y mutation of spike protein in SARS-CoV-2 strengthens its binding to receptor ACE2. *Elife* **10** (2021). https://doi.org:10.7554/eLife.69091

109 Liu, Y. *et al.* The N501Y spike substitution enhances SARS-CoV-2 infection and transmission. *Nature* **602**, 294-299 (2022). https://doi.org:10.1038/s41586-021-04245-0

110 *SARS-CoV-2 Alpha variant* (2024), https://en.wikipedia.org/wiki/SARS-CoV-2_Alpha_variant, last accessed 27.03.2024.

111 Planas, D. *et al.* Sensitivity of infectious SARS-CoV-2 B.1.1.7 and B.1.351 variants to neutralizing antibodies. *Nature Medicine* **27**, 917-924 (2021). https://doi.org:10.1038/s41591-021-01318-5

112 Shen, X. *et al.* SARS-CoV-2 variant B.1.1.7 is susceptible to neutralizing antibodies elicited by ancestral spike vaccines. *Cell Host Microbe* **29**, 529-539.e523 (2021). https://doi.org:10.1016/j.chom.2021.03.002

113 Duong, D. Alpha, Beta, Delta, Gamma: What's important to know about SARS-CoV-2 variants of concern? *Cmaj* **193**, E1059-e1060 (2021). https://doi.org:10.1503/cmaj.1095949

114 Uwamino, Y. *et al.* The effect of the E484K mutation of SARS-CoV-2 on the neutralizing activity of antibodies from BNT162b2 vaccinated individuals. *Vaccine* **40**, 1928-1931 (2022). https://doi.org:10.1016/j.vaccine.2022.02.047

115 Hodcroft, E. B. *CoVariants: SARS-CoV-2 Mutations and Variants of Interest* (2021), https://covariants.org/, last accessed 23.02.2024.

116 Rettner, R. L., Nicoletta *Coronavirus variants: Facts about omicron, delta and other SARS-CoV-2 mutants* (2023), https://www.livescience.com/coronavirus-variants.html, last accessed 24.02.2024.

117 Planas, D. *et al.* Reduced sensitivity of SARS-CoV-2 variant Delta to antibody neutralization. *Nature* **596**, 276-280 (2021). https://doi.org:10.1038/s41586-021-03777-9

118 Di Giacomo, S., Mercatelli, D., Rakhimov, A. & Giorgi, F. M. Preliminary report on severe acute respiratory syndrome coronavirus 2 (SARS-CoV-2) Spike mutation T478K. *J Med Virol* **93**, 5638-5643 (2021). https://doi.org:10.1002/jmv.27062

119 Khare, S. *et al.* GISAID's Role in Pandemic Response. *China CDC Wkly* **3**, 1049-1051 (2021). https://doi.org:10.46234/ccdcw2021.255

120 Hodcroft, E. *Overview of Variants in Countries* (2024), https://covariants.org/per-country, last accessed 23.02.2024.

121 Qu, P. *et al.* Distinct Neutralizing Antibody Escape of SARS-CoV-2 Omicron Subvariants BQ.1, BQ.1.1, BA.4.6, BF.7 and BA.2.75.2. *bioRxiv* (2022). https://doi.org:10.1101/2022.10.19.512891

122 Parums, D. V. Editorial: The XBB.1.5 ('Kraken') Subvariant of Omicron SARS-CoV-2 and its Rapid Global Spread. *Med Sci Monit* **29**, e939580 (2023). https://doi.org:10.12659/msm.939580

123 *Coronavirus Resource Center - Cumulative Cases* (2023), https://coronavirus.jhu.edu/data/cumulative-cases, last accessed 24.02.2024.

124 *Coronavirus Resource Center - Number of Daily Cases* (2023), https://coronavirus.jhu.edu/region/germany, last accessed 24.02.2024.

125 *Current Vaccination Status - Vaccination progress* (2023), https://impfdashboard.de/en, last accessed 24.02.2024.

126 Relan, P. *et al.* Severity and outcomes of Omicron variant of SARS-CoV-2 compared to Delta variant and severity of Omicron sublineages: a systematic review and metanalysis. *BMJ Glob Health* **8** (2023). https://doi.org:10.1136/bmjgh-2023-012328

127 Mogensen, T. H. Pathogen recognition and inflammatory signaling in innate immune defenses. *Clin Microbiol Rev* **22**, 240-273, Table of Contents (2009). https://doi.org:10.1128/cmr.00046-08

128 Katze, M. G., He, Y. & Gale, M. Viruses and interferon: a fight for supremacy. *Nature Reviews Immunology* **2**, 675-687 (2002). https://doi.org:10.1038/nri888

129 Murphy, K. M. & Weaver, C. *Janeway's immunobiology*. 9th edn, 399-411 (New York: Garland Science, 2017).

130 Avalos, A. M. & Ploegh, H. Early BCR Events and Antigen Capture, Processing, and Loading on MHC Class II on B Cells. *Frontiers in Immunology* **5** (2014). https://doi.org:10.3389/fimmu.2014.00092

131 Zou, Y.-R., Grimaldi, C. & Diamond, B. in *Kelley and Firestein's Textbook of Rheumatology (Tenth Edition)* (eds Gary S. Firestein *et al.*) 207-230.e203 (Elsevier, 2017).

132 Schroeder, H. W., Jr. & Cavacini, L. Structure and function of immunoglobulins. *J Allergy Clin Immunol* **125**, S41-52 (2010). https://doi.org:10.1016/j.jaci.2009.09.046

133 Woof, J. M. & Mestecky, J. Mucosal immunoglobulins. *Immunol Rev* **206**, 64-82 (2005). https://doi.org:10.1111/j.0105-2896.2005.00290.x

134 Majidi, J., Baradaran, B., Hassan, Z. M. & Mostafaie, A. Production and characterization of monoclonal antibodies against human IgG in Balb/c mouse. *Hum Antibodies* **14**, 1-5 (2005).

135 Zan, H. & Casali, P. in *Encyclopedia of Medical Immunology: Autoimmune Diseases* (eds Ian R. Mackay, Noel R. Rose, Betty Diamond, & Anne Davidson) 517-528 (Springer New York, 2014).

136 Lu, L. L., Suscovich, T. J., Fortune, S. M. & Alter, G. Beyond binding: antibody effector functions in infectious diseases. *Nat Rev Immunol* **18**, 46-61 (2018). https://doi.org:10.1038/nri.2017.106

137 Janeway CA Jr, T. P., Walport M, et al. Ch. Chapter 8, T Cell-Mediated Immunity, (2001).

138 Freund, N. T. Antibodies: what makes us stronger. *Hum Vaccin Immunother* **17**, 3551-3553 (2021). https://doi.org:10.1080/21645515.2021.1929034

139 Senefeld, J. W. *et al.* COVID-19 Convalescent Plasma for the Treatment of Immunocompromised Patients: A Systematic Review and Meta-analysis. *JAMA Network Open* **6**, e2250647-e2250647 (2023). https://doi.org:10.1001/jamanetworkopen.2022.50647

140 Almagro, J. C., Mellado-Sánchez, G., Pedraza-Escalona, M. & Pérez-Tapia, S. M. Evolution of Anti-SARS-CoV-2 Therapeutic Antibodies. *International Journal of Molecular Sciences* **23**, 9763 (2022).

141 *FDA updates Sotrovimab emergency use authorization* (2022), https://www.fda.gov/drugs/drug-safety-and-availability/fda-updates-sotrovimab-emergency-use-authorization?utm_medium=email&utm_source=govdelivery, last accessed 06.04.2024.

142 VanBlargan, L. A. *et al.* An infectious SARS-CoV-2 B.1.1.529 Omicron virus escapes neutralization by therapeutic monoclonal antibodies. *Nat Med* **28**, 490-495 (2022). https://doi.org:10.1038/s41591-021-01678-y

143 Wilhelm, A. *et al.* Limited neutralisation of the SARS-CoV-2 Omicron subvariants BA.1 and BA.2 by convalescent and vaccine serum and monoclonal antibodies. *eBioMedicine* **82** (2022). https://doi.org:10.1016/j.ebiom.2022.104158

144 Thau L, A. E., Mahajan K. *Physiology, Opsonization*. (StatPearls Publishing, 2023).

145 *Luminex xMAP Technology* https://int.diasorin.com/en/licensed-technologies/xmap-technology, last accessed 07.04.2024.

146 Wagner, T. R. *et al.* NeutrobodyPlex—monitoring SARS-CoV-2 neutralizing immune responses using nanobodies. *EMBO reports* **22**, e52325 (2021). https://doi.org:https://doi.org/10.15252/embr.202052325

147 Becker, M. *Serological Analysis to Accompany Clinical Research, Vaccination and Evolution of the COVID-19 Pandemic*, University of Tübingen,Doctoral Dissertation (2023).

148 Junker, D. *Development and Application of a Bead-Based Multiplex Assay System to analyze the humoral Immune Response of SARS-CoV-2 infected individuals*, University of Tübingen,Master Thesis (2020).

149 Roth, N. *et al.* Assessment of Immunogenicity and Efficacy of CV0501 mRNA-Based Omicron COVID-19 Vaccination in Small Animal Models. *Vaccines (Basel)* **11** (2023). https://doi.org:10.3390/vaccines11020318

150 *ICH guideline M10 on bioanalytical method validation and study sample analysis* https://www.ema.europa.eu/en/documents/scientific-guideline/guideline-bioanalytical-method-validation_en.pdf, last accessed 06.04.2024.

151 *M10 Bioanalytical Method Validation and Study Sample Analysis - Guidance for Industry* (2022), https://www.fda.gov/media/162903/download, last accessed 06.04.2024.

152 *MuSPAD - Nationwide antibody study on the spread of SARS-CoV-2 infections* https://hzi-c19-antikoerperstudie.de/en/, last accessed 07.04.2024.

153 Liu, X. *et al.* Safety and immunogenicity of heterologous versus homologous prime-boost schedules with an adenoviral vectored and mRNA COVID-19 vaccine (Com-COV): a single-blind, randomised, non-inferiority trial. *The Lancet* **398**, 856-869 (2021). https://doi.org:10.1016/S0140-6736(21)01694-9

154 Schmidt, T. *et al.* Immunogenicity and reactogenicity of heterologous ChAdOx1 nCoV-19/mRNA vaccination. *Nature Medicine* **27**, 1530-1535 (2021). https://doi.org:10.1038/s41591-021-01464-w

155 Slomka, S., Zieba, P., Rosiak, O. & Piekarska, A. Comparison of Post-Vaccination Response between mRNA and Vector Vaccines against SARS-CoV-2 in Terms of Humoral Response after Six Months of Observation. *Vaccines (Basel)* **11** (2023). https://doi.org:10.3390/vaccines11101625

156 Botton, J. *et al.* Effectiveness of Ad26.COV2.S Vaccine vs BNT162b2 Vaccine for COVID-19 Hospitalizations. *JAMA Network Open* **5**, e220868-e220868 (2022). https://doi.org:10.1001/jamanetworkopen.2022.0868

157 Vygen-Bonnet, S. e. a. Beschluss der STIKO zur 8. Aktualisierung der COVID-19-Impfempfehlung und die dazugehörige wissenschaftliche Begründung. 14-31 (Robert Koch Institut, 2021) https://www.rki.de/DE/Content/Infekt/EpidBull/Archiv/2021/Ausgaben/27_21.pdf?__blob=publicationFile, last accessed 07.04.2024.

158 Madhi, S. A. *et al.* Efficacy of the ChAdOx1 nCoV-19 Covid-19 Vaccine against the B.1.351 Variant. *New England Journal of Medicine* **384**, 1885-1898 (2021). https://doi.org:10.1056/NEJMoa2102214

159 Shinde, V. *et al.* Efficacy of NVX-CoV2373 Covid-19 Vaccine against the B.1.351 Variant. *New England Journal of Medicine* **384**, 1899-1909 (2021). https://doi.org:10.1056/NEJMoa2103055

160 Zhou, D. *et al.* Evidence of escape of SARS-CoV-2 variant B.1.351 from natural and vaccine-induced sera. *Cell* **184**, 2348-2361.e2346 (2021). https://doi.org:https://doi.org/10.1016/j.cell.2021.02.037

161 Atyeo, C. *et al.* Distinct Early Serological Signatures Track with SARS-CoV-2 Survival. *Immunity* **53**, 524-532.e524 (2020). https://doi.org:10.1016/j.immuni.2020.07.020

162 Fernández-Ciriza, L. *et al.* Humoral and cellular immune response over 9 months of mRNA-1273, BNT162b2 and ChAdOx1 vaccination in a University Hospital in Spain. *Scientific Reports* **12**, 15606 (2022). https://doi.org:10.1038/s41598-022-19537-2

163 Kontopoulou, K. *et al.* Second dose of the BNT162b2 mRNA vaccine: Value of timely administration but questionable necessity among the seropositive. *Vaccine* **39**, 5078-5081 (2021). https://doi.org:10.1016/j.vaccine.2021.07.065

164 Karron, R. A. *et al.* Assessment of Clinical and Virological Characteristics of SARS-CoV-2 Infection Among Children Aged 0 to 4 Years and Their Household Members. *JAMA Network Open* **5**, e2227348-e2227348 (2022). https://doi.org:10.1001/jamanetworkopen.2022.27348

165 Jacobsen, E.-M. *et al.* High antibody levels and reduced cellular response in children up to one year after SARS-CoV-2 infection. *Nature Communications* **13**, 7315 (2022). https://doi.org:10.1038/s41467-022-35055-1

166 Tomasi, L. *et al.* Younger Children Develop Higher Effector Antibody Responses to SARS-CoV-2 Infection. *Open Forum Infect Dis* **9**, ofac554 (2022). https://doi.org:10.1093/ofid/ofac554

167 Dufloo, J. *et al.* Asymptomatic and symptomatic SARS-CoV-2 infections elicit polyfunctional antibodies. *Cell Rep Med* **2**, 100275 (2021). https://doi.org:10.1016/j.xcrm.2021.100275

168 Wang, W. B. *et al.* E484K mutation in SARS-CoV-2 RBD enhances binding affinity with hACE2 but reduces interactions with neutralizing antibodies and nanobodies: Binding free energy calculation studies. *J Mol Graph Model* **109**, 108035 (2021). https://doi.org:10.1016/j.jmgm.2021.108035

169 Ahmad, A., Fawaz, M. A. M. & Aisha, A. A comparative overview of SARS-CoV-2 and its variants of concern. *Infez Med* **30**, 328-343 (2022). https://doi.org:10.53854/liim-3003-2

170 Thakur, S. *et al.* SARS-CoV-2 Mutations and Their Impact on Diagnostics, Therapeutics and Vaccines. *Frontiers in Medicine* **9** (2022). https://doi.org:10.3389/fmed.2022.815389

171 Goher, S. S., Ali, F. & Amin, M. The Delta Variant Mutations in the Receptor Binding Domain of SARS-CoV-2 Show Enhanced Electrostatic Interactions with the ACE2. *Med Drug Discov*, 100114 (2021). https://doi.org:10.1016/j.medidd.2021.100114

172 Zhang, Y. *et al.* SARS-CoV-2 spike L452R mutation increases Omicron variant fusogenicity and infectivity as well as host glycolysis. *Signal Transduction and Targeted Therapy* **7**, 76 (2022). https://doi.org:10.1038/s41392-022-00941-z

173 Graham, M. S. *et al.* Changes in symptomatology, reinfection, and transmissibility associated with the SARS-CoV-2 variant B.1.1.7: an ecological study. *The Lancet Public Health* **6**, e335-e345 (2021). https://doi.org:10.1016/S2468-2667(21)00055-4

174 Dejnirattisai, W. *et al.* Antibody evasion by the P.1 strain of SARS-CoV-2. *Cell* **184**, 2939-2954.e2939 (2021). https://doi.org:10.1016/j.cell.2021.03.055

175 Hoffmann, M. *et al.* SARS-CoV-2 variants B.1.351 and P.1 escape from neutralizing antibodies. *Cell* **184**, 2384-2393.e2312 (2021). https://doi.org:10.1016/j.cell.2021.03.036

176 Lucas, C. *et al.* Delayed production of neutralizing antibodies correlates with fatal COVID-19. *Nature Medicine* **27**, 1178-1186 (2021). https://doi.org:10.1038/s41591-021-01355-0

177 Guthmiller, J. J. *et al.* SARS-CoV-2 Infection Severity Is Linked to Superior Humoral Immunity against the Spike. *mBio* **12**, 10.1128/mbio.02940-02920 (2021). https://doi.org:doi:10.1128/mbio.02940-20

178 Legros, V. *et al.* A longitudinal study of SARS-CoV-2-infected patients reveals a high correlation between neutralizing antibodies and COVID-19 severity. *Cellular & Molecular Immunology* **18**, 318-327 (2021). https://doi.org:10.1038/s41423-020-00588-2

179 McNaughton, A. L. *et al.* Fatal COVID-19 outcomes are associated with an antibody response targeting epitopes shared with endemic coronaviruses. *JCI Insight* **7** (2022). https://doi.org:10.1172/jci.insight.156372

180 Du, J. *et al.* Persistent High Percentage of HLA-DR(+)CD38(high) CD8(+) T Cells Associated With Immune Disorder and Disease Severity of COVID-19. *Front Immunol* **12**, 735125 (2021). https://doi.org:10.3389/fimmu.2021.735125

181 Georg, P. *et al.* Complement activation induces excessive T cell cytotoxicity in severe COVID-19. *Cell* **185**, 493-512.e425 (2022). https://doi.org:10.1016/j.cell.2021.12.040

182 Mathew, D. *et al.* Deep immune profiling of COVID-19 patients reveals distinct immunotypes with therapeutic implications. *Science* **369** (2020). https://doi.org:10.1126/science.abc8511

183 Nemet, I. *et al.* Third BNT162b2 Vaccination Neutralization of SARS-CoV-2 Omicron Infection. *N Engl J Med* **386**, 492-494 (2022). https://doi.org:10.1056/NEJMc2119358

184 Schmidt, F. *et al.* Plasma Neutralization of the SARS-CoV-2 Omicron Variant. *N Engl J Med* **386**, 599-601 (2022). https://doi.org:10.1056/NEJMc2119641

185 Wan, J. *et al.* Booster vaccination protection against SARS-CoV-2 infections in young adults during an Omicron BA.1-predominant period: A retrospective cohort study. *PLoS Med* **20**, e1004153 (2023). https://doi.org:10.1371/journal.pmed.1004153

186 Assawakosri, S. *et al.* Omicron BA.1, BA.2 and COVID-19 Booster Vaccination *The Journal of Infectious Diseases* **226**, 1480-1481 (2022). https://doi.org:10.1093/infdis/jiac158

187 Gruell, H. *et al.* mRNA booster immunization elicits potent neutralizing serum activity against the SARS-CoV-2 Omicron variant. *Nat Med* **28**, 477-480 (2022). https://doi.org:10.1038/s41591-021-01676-0

188 Pajon, R. *et al.* SARS-CoV-2 Omicron Variant Neutralization after mRNA-1273 Booster Vaccination. *N Engl J Med* **386**, 1088-1091 (2022). https://doi.org:10.1056/NEJMc2119912

189 Moriyama, S. *et al.* Temporal maturation of neutralizing antibodies in COVID-19 convalescent individuals improves potency and breadth to circulating SARS-CoV-2 variants. *Immunity* **54**, 1841-1852.e1844 (2021). https://doi.org:10.1016/j.immuni.2021.06.015

190 Hoffmann, M. *et al.* Effect of hybrid immunity and bivalent booster vaccination on omicron sublineage neutralisation. *The Lancet Infectious Diseases* **23**, 25-28 (2023). https://doi.org:10.1016/S1473-3099(22)00792-7

191 Muik, A. *et al.* Omicron BA.2 breakthrough infection enhances cross-neutralization of BA.2.12.1 and BA.4/BA.5. *Sci Immunol* **7**, eade2283 (2022). https://doi.org:10.1126/sciimmunol.ade2283

192 Quandt, J. *et al.* Omicron BA.1 breakthrough infection drives cross-variant neutralization and memory B cell formation against conserved epitopes. *Sci Immunol* **7**, eabq2427 (2022). https://doi.org:10.1126/sciimmunol.abq2427

193 Hornsby, H. *et al.* Omicron infection following vaccination enhances a broad spectrum of immune responses dependent on infection history. *Nature Communications* **14**, 5065 (2023). https://doi.org:10.1038/s41467-023-40592-4

194 Wei, J. *et al.* Protection against SARS-CoV-2 Omicron BA.4/5 variant following booster vaccination or breakthrough infection in the UK. *Nature Communications* **14**, 2799 (2023). https://doi.org:10.1038/s41467-023-38275-1

195 Ntziora, F. *et al.* Protection of vaccination versus hybrid immunity against infection with COVID-19 Omicron variants among Health-Care Workers. *Vaccine* **40**, 7195-7200 (2022). https://doi.org:10.1016/j.vaccine.2022.09.042

196 Altarawneh, H. N. *et al.* Effects of Previous Infection and Vaccination on Symptomatic Omicron Infections. *N Engl J Med* **387**, 21-34 (2022). https://doi.org:10.1056/NEJMoa2203965

197 de Gier, B. *et al.* Effects of COVID-19 vaccination and previous infection on Omicron SARS-CoV-2 infection and relation with serology. *Nature Communications* **14**, 4793 (2023). https://doi.org:10.1038/s41467-023-40195-z

198 Bobrovitz, N. *et al.* Protective effectiveness of previous SARS-CoV-2 infection and hybrid immunity against the omicron variant and severe disease: a systematic review and meta-regression. *Lancet Infect Dis* **23**, 556-567 (2023). https://doi.org:10.1016/s1473-3099(22)00801-5

199 Evans, R. A. *et al.* Impact of COVID-19 on immunocompromised populations during the Omicron era: insights from the observational population-based INFORM study. *The Lancet Regional Health – Europe* **35** (2023). https://doi.org:10.1016/j.lanepe.2023.100747

200 Turtle, L. *et al.* Outcome of COVID-19 in hospitalised immunocompromised patients: An analysis of the WHO ISARIC CCP-UK prospective cohort study. *PLoS Med* **20**, e1004086 (2023). https://doi.org:10.1371/journal.pmed.1004086

201 Zbinden, D. & Manuel, O. Influenza vaccination in immunocompromised patients: efficacy and safety. *Immunotherapy* **6**, 131-139 (2014). https://doi.org:10.2217/imt.13.171

202 Ling, T. C. *et al.* Trajectory of Humoral Responses to Two Doses of ChAdOx1 nCoV-19 Vaccination in Patients Receiving Maintenance Hemodialysis. *Microbiol Spectr* **11**, e0344522 (2023). https://doi.org:10.1128/spectrum.03445-22

203 Speer, C. *et al.* Neutralizing antibody response against variants of concern after vaccination of dialysis patients with BNT162b2. *Kidney International* **100**, 700-702 (2021). https://doi.org:10.1016/j.kint.2021.07.002

204 Imhof, C. *et al.* SARS-CoV-2 Spike-specific IFN-γ T-cell Response After COVID-19 Vaccination in Patients With Chronic Kidney Disease, on Dialysis, or Living With a Kidney Transplant. *Transplant Direct* **8**, e1387 (2022). https://doi.org:10.1097/txd.0000000000001387

205 Sattler, A. *et al.* Impaired humoral and cellular immunity after SARS-CoV-2 BNT162b2 (tozinameran) prime-boost vaccination in kidney transplant recipients. *J Clin Invest* **131** (2021). https://doi.org:10.1172/jci150175

206 Affeldt, P. *et al.* Immune Response to Third and Fourth COVID-19 Vaccination in Hemodialysis Patients and Kidney Transplant Recipients. *Viruses* **14**, 2646 (2022).

207 Housset, P. *et al.* Humoral response after a fourth "booster" dose of a Coronavirus disease 2019 vaccine following a 3-dose regimen of mRNA-based vaccination in dialysis patients. *Kidney Int* **101**, 1289-1290 (2022). https://doi.org:10.1016/j.kint.2022.04.006

208 Einbinder, Y. *et al.* Humoral Response and SARS-CoV-2 Infection Risk following the Third and Fourth Doses of the BNT162b2 Vaccine in Dialysis Patients. *Am J Nephrol* **53**, 586-590 (2022). https://doi.org:10.1159/000525309

209 Cheng, C. C. *et al.* Improved SARS-CoV-2 Neutralization of Delta and Omicron BA.1 Variants of Concern after Fourth Vaccination in Hemodialysis Patients. *Vaccines (Basel)* **10** (2022). https://doi.org:10.3390/vaccines10081328

210 Anft, M. *et al.* Inferior cellular and humoral immunity against Omicron and Delta variants of concern compared with SARS-CoV-2 wild type in hemodialysis patients immunized with 4 SARS-CoV-2 vaccine doses. *Kidney Int* **102**, 207-208 (2022). https://doi.org:10.1016/j.kint.2022.05.004

211 Liao, B.-H. *et al.* SARS-CoV-2 Neutralization Capacity in Hemodialysis Patients with and without a Fifth Vaccination with the Updated Comirnaty Original/Omicron BA.4-5 Vaccine. *Vaccines* **12**, 308 (2024).

212 Huth, L. *et al.* Immunologic Effect of Bivalent mRNA Booster in Patients Undergoing Hemodialysis. *N Engl J Med* **388**, 950-952 (2023). https://doi.org:10.1056/NEJMc2216309

213 Alexander, J. L. *et al.* COVID-19 vaccine-induced antibody and T-cell responses in immunosuppressed patients with inflammatory bowel disease after the third vaccine dose (VIP): a multicentre, prospective, case-control study. *Lancet Gastroenterol Hepatol* **7**, 1005-1015 (2022). https://doi.org:10.1016/s2468-1253(22)00274-6

214 Schell, T. L. *et al.* Humoral Immunogenicity of 3 COVID-19 Messenger RNA Vaccine Doses in Patients With Inflammatory Bowel Disease. *Inflamm Bowel Dis* **28**, 1781-1786 (2022). https://doi.org:10.1093/ibd/izac082

215 Wellens, J. *et al.* Combination therapy of infliximab and thiopurines, but not monotherapy with infliximab or vedolizumab, is associated with attenuated IgA and neutralisation responses to SARS-CoV-2 in inflammatory bowel disease. *Gut* **71**, 1919-1922 (2022). https://doi.org:10.1136/gutjnl-2021-326312

216 Kennedy, N. A. *et al.* Vaccine escape, increased breakthrough and reinfection in infliximab-treated patients with IBD during the Omicron wave of the SARS-CoV-2 pandemic. *Gut* **72**, 295-305 (2023). https://doi.org:10.1136/gutjnl-2022-327570

217 Lin, S. *et al.* Antibody decay, T cell immunity and breakthrough infections following two SARS-CoV-2 vaccine doses in inflammatory bowel disease patients treated with infliximab and vedolizumab. *Nat Commun* **13**, 1379 (2022). https://doi.org:10.1038/s41467-022-28517-z

Acknowledgements

I want to thank all the people who have accompanied me on my way to this exciting point in my scientific career.

I would especially like to thank Dr. Nicole Schneiderhan-Marra for the opportunity she gave me to write my doctoral thesis in her group. I am very grateful for the trust placed in me during my work on various projects, especially the research on SARS-CoV-2, through which I was able to gain a lot of knowledge and interesting insights.

I would also like to thank Dr. Alex Dulovic for his great support as a supervisor, and his constant availability to answer my questions. I wish him all the best for his new position as group leader at the NMI.

I want to thank Prof. Dr. Ulrich Rothbauer and Prof. Dr. Katja Schenke-Layland for supervising my doctoral thesis and supporting me during my time at the NMI.

I would also like to thank our cooperation partners from clinics and research institutes for their interesting and productive collaboration, without which this dissertation would not have been possible. I would particularly like to mention Prof. Dr. Bitzer and Dr. Siri Göpel from the University Hospital Tübingen and the group of Prof. Dr. Georg Behrens at Hannover Medical School.

I would like to give special thanks to my colleagues at the Multiplex Immunoassays group, who have become wonderful friends and have provided so much fun in the lab and office, while always lending me a helping hand. I couldn't have wished for a better working atmosphere, especially in the sometimes stressful day-to-day life of science. I would particularly like to thank Matthias Becker, who gave me great support in my early days at the NMI as Master's student and with whom it was great fun to work on the SARS-CoV-2 projects. Our time in and out of the lab bonded us together and a close friendship developed.

I would like to thank Michelle Knodel for her full support of my work and her great patience with me, and gratefully mention our cat Debbie, who always made sure that I got up early on the weekends so that I could continue working on my dissertation.

Finally, I would like to thank my family for their unconditional support throughout my time at university. With your warmth and care, I could always rely on you, and you always encouraged me to pursue my goals.

Appendix

Appendix I: Exploring beyond clinical routine SARS-CoV-2 serology using MultiCoV-Ab to evaluate endemic coronavirus cross-reactivity

Becker M*, Strengert M*, **Junker D**, Kaiser PD, Kerrinnes T, Traenkle B, Dinter H, Häring J, Ghozzi S, Zeck A, Weise F, Peter A, Hörber S, Fink S, Ruoff F, Dulovic A, Bakchoul T, Baillot A, Lohse S, Cornberg M, Illig T, Gottlieb J, Smola S, Karch A, Berger K, Rammensee HG, Schenke-Layland K, Nelde A, Märklin M, Heitmann JS, Walz JS, Templin M, Joos TO, Rothbauer U, Krause G, Schneiderhan-Marra N.

Nature Communications. 2021. 12(1):1152

https://doi.org/10.1038/s41467-021-20973-3

nature COMMUNICATIONS

ARTICLE

https://doi.org/10.1038/s41467-021-20973-3 OPEN

Exploring beyond clinical routine SARS-CoV-2 serology using MultiCoV-Ab to evaluate endemic coronavirus cross-reactivity

Matthias Becker[1,24], Monika Strengert[2,3,24], Daniel Junker[1], Philipp D. Kaiser[1], Tobias Kerrinnes[4], Bjoern Traenkle[1,5], Heiko Dinter[1,5], Julia Häring[1], Stéphane Ghozzi[2], Anne Zeck[1], Frank Weise[1], Andreas Peter[6,7,8], Sebastian Hörber[6,7,8], Simon Fink[1], Felix Ruoff[1], Alex Dulovic[1], Tamam Bakchoul[9], Armin Baillot[10], Stefan Lohse[11], Markus Cornberg[12], Thomas Illig[13], Jens Gottlieb[14,15], Sigrun Smola[11], André Karch[16], Klaus Berger[16], Hans-Georg Rammensee[17,18,19], Katja Schenke-Layland[1,19,20,21], Annika Nelde[17,19,22], Melanie Märklin[19,21], Jonas S. Heitmann[19,21], Juliane S. Walz[17,19,23,22], Markus Templin[1], Thomas O. Joos[1], Ulrich Rothbauer[1,5,24], Gérard Krause[2,3] & Nicole Schneiderhan-Marra[1✉]

The humoral immune response to SARS-CoV-2 is a benchmark for immunity and detailed analysis is required to understand the manifestation and progression of COVID-19, monitor seroconversion within the general population, and support vaccine development. The majority of currently available commercial serological assays only quantify the SARS-CoV-2 antibody response against individual antigens, limiting our understanding of the immune response. To overcome this, we have developed a multiplex immunoassay (MultiCoV-Ab) including spike and nucleocapsid proteins of SARS-CoV-2 and the endemic human coronaviruses. Compared to three broadly used commercial in vitro diagnostic tests, our MultiCoV-Ab achieves a higher sensitivity and specificity when analyzing a well-characterized sample set of SARS-CoV-2 infected and uninfected individuals. We find a high response against endemic coronaviruses in our sample set, but no consistent cross-reactive IgG response patterns against SARS-CoV-2. Here we show a robust, high-content-enabled, antigen-saving multiplex assay suited to both monitoring vaccination studies and facilitating epidemiologic screenings for humoral immunity towards pandemic and endemic coronaviruses.

A full list of author affiliations appears at the end of the paper.

Since its first characterization in late 2019, SARS-CoV-2, the seventh known coronavirus to infect humans, has developed into a worldwide pandemic with dramatic socio-economic consequences[1–3]. While the majority of individuals suffer only from mild symptoms, approximately 14% of infected adults experience particularly severe disease outcomes (i.e., pneumonia) of COVID-19[4]. Of these 14%, 5% will progress into a critical condition characterized by hypoxaemic respiratory failure, acute respiratory distress syndrome and multiorgan failure[4]. To date, the large number of infected individuals and of those requiring urgent intensive care has put a high burden on public healthcare infrastructures[3].

In contrast to the recently emerged SARS-CoV-2, the four endemic human coronaviruses (hCoVs) NL63 and 229E (α-hCoVs) as well as OC43 and HKU1 (β-hCoVs), regularly circulate in the population[5] (one study reported a 91% prevalence for OC43 in the adult population[6]) and are thought to cause up to 20% of mild colds[7]. As humoral immune responses are in general seen as protective by production of neutralizing antibodies to viral surface proteins[8], it would be tempting to speculate that a previous infection with an endemic strain offers protection against infection with the β-coronavirus SARS-CoV-2, as already seen in in vitro studies[9]. However, it has also been reported that for both SARS coronaviruses and MERS-CoV, disease severity and fatal outcome correlates with early seroconversion and/or increased antibody titers by a yet undefined mechanism[10–13]. Consequentially, a detailed understanding of the humoral SARS-CoV-2 immune response is of importance to provide insights into COVID-19 disease biology[12,14].

Serological tests are essential tools in cohort-based epidemiological studies to determine seroprevalence and precisely assess mortality rates, the extent of asymptomatic or mild infections not currently detectable by molecular testing, and ultimately determine the effectiveness of population-based interventions and direct future preventive strategies. Furthermore, serological testing is a companion diagnostic to monitor vaccination efficacy and mode of action in vaccine trials[15,16]. As a result, there is a need for robust serological tests to quantify antibody production against SARS-CoV-2 in detail. Currently, most commercially available serological assays utilize single analyte technologies (i.e., ELISA) to measure antibodies against SARS-CoV-2 spike (S) or nucleocapsid (N) antigens[16–19]. Few tests combine and correlate N- and S-antigen-based detection[20–22] or attempt global profiling of antibody responses against the entire SARS-CoV-2 genome[23]. To this end, we developed a multiplexed SARS-CoV-2 immunoassay (MultiCoV-Ab) which included not only S and N protein-based antigens of SARS-CoV-2, but also from endemic hCoVs (NL63, 229E, OC43, HKU1) based on findings of numerous SARS-CoV-1 serological studies, which reported on cross-reactive antibodies to antigens from circulating hCoVs[24]. Such an expanded antigen panel allows to both resolve the SARS-CoV-2 antibody response in detail and to assess and correlate potential cross-protection mechanisms between coronaviruses. We measured both IgA and IgG responses, as these isotypes in contrast to IgM can persist for extended periods in the serum and in nasal fluids[25]. Further, SARS-CoV-2 is a mucosal-targeted virus, and reports indicate that IgA, as the dominant antibody isotype in the mucosal defense is a good indicator for early immune defense mechanisms in this case[26].

In this study, to determine how well MultiCoV-Ab performs, we compare our assay to broadly applied commercial in vitro diagnostic (IVD) tests with well-characterized sample sets for clinical validation and further analyze potential sources of cross-reactivity with hCoVs. For the sample set examined, we were able to reach a specificity of 100% with MultiCoV-Ab and achieved an improved sensitivity compared to commercial tests, confirming its value as a serological screening assay.

Results

MultiCoV-Ab: a highly sensitive test for SARS-CoV-2 seroconversion. To investigate the antibody response of SARS-CoV-2-infected individuals, we developed and established a high-throughput and automatable bead-based multiplex assay, termed MultiCoV-Ab. We expressed and immobilized six different SARS-CoV-2-specific antigens on Luminex MAGPLEX beads with distinct color codes, specifically the trimeric full-length spike protein (Spike Trimer), receptor-binding domain (RBD), S1 domain (S1), S2 domain (S2), full-length nucleocapsid (N), and the N-terminal domain of nucleocapsid (N-NTD) (Supplementary Fig. 1). Immunoglobulins from serum and plasma samples were detected using phycoerythrin-labeled anti-human IgG or IgA antibodies. To ensure assay stability and comparability, quality control samples were processed in parallel within every assay run. Quality control and assay performance data sets are provided in Supplementary Fig. 2 and Supplementary Table 1.

To analyze SARS-CoV-2-induced seroconversion, we used the Spike Trimer and RBD (previously described by Amanat et al.[27]) as key antigens for classification, and initially screened a sample set of 205 reconvalescent SARS-CoV-2-infected and 72 uninfected individuals with the MultiCoV-Ab. To critically assess assay performance, we compared our results with three commercially available IVD tests widely used in clinical routine SARS-CoV-2 antibody testing namely: Elecsys Anti-SARS-CoV-2 (antibodies including IgG; Roche[28]), SARS-CoV-2 Total (total antibodies IgM and IgG; Siemens Healthineers[29]) and Anti-SARS-CoV-2 ELISA (IgG/IgA; Euroimmun[30]). Using a combined cut-off of both antigens, we identified all uninfected samples as negative (Fig. 1a). In accordance with our MultiCoV-Ab, none of the uninfected samples was classified as false positive by the Roche and Siemens tests, while one sample was classified as false positive and one as "borderline" by the Euroimmun IgG test. Of the 205 infected samples, both MultiCoV-Ab and commercial IVD tests for total Ig or IgG identified 24 (11.7%) as IgG antibody-negative. However, the IVD tests missed an additional 8 (Roche), 11 (Siemens Healthineers), and 9 (Euroimmun IgG) samples of SARS-CoV-2-infected individuals. Furthermore, the Euroimmun IgG test classified 8 additional samples as "borderline" (Fig. 1b, Supplementary Fig. 3a–c). When testing for IgA antibodies in serum/plasma of SARS-CoV-2-infected individuals, our MultiCoV-Ab classified 47 (22.9%) as IgA-negative, whereas the Euroimmun test classified 32 (15.6%) as IgA-negative, and 16 (7.8%) as borderline (Fig. 1b and Supplementary Fig. 3d). For the uninfected samples, the Euroimmun IgA test identified 7 (9.7%) as false positives and 3 (4.2%) as "borderline", whereas no samples were classified as false positives by the MultiCoV-Ab. Overall, the MultiCoV-Ab achieved a sensitivity of 88.3% and a specificity of 100% in this initial set of samples using IgG detection (Table 1). When comparing the results of the commercial IVD tests to the respective manufacturers' specifications, all tests were unable to reach their stated sensitivity of 100%. In contrast, for all commercial tests, the found specificities were close to the manufacturers' stated specificity in our sample set (Table 1). This demonstrates that antigen selection and assay setup are crucial in achieving optimal performance and must be considered when screening for SARS-CoV-2, particularly in low prevalence scenarios.

Multiplex serology improves assay specificity. Next, to perform a more detailed clinical validation of our MultiCoV-Ab, we expanded our sample set to a total of 310 SARS-CoV-2-infected and 866 uninfected donors (a simplified overview of this set is shown in Table 2; a complete breakdown is displayed in Supplementary Table 2). We performed a ROC analysis[31,32] per

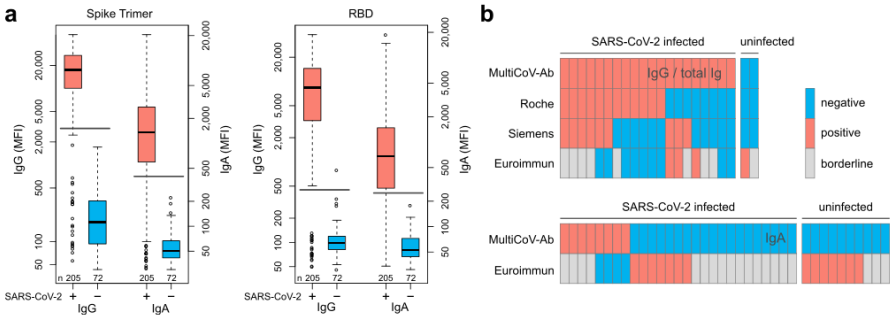

Fig. 1 MultiCoV-Ab, a sensitive and specific tool to monitor SARS-CoV-2 antibody responses. a Control sera (blue, $n = 72$) and sera from individuals with PCR-confirmed SARS-CoV-2 infection (red, $n = 205$) were screened in a multiplex bead-based assay using Luminex technology (MultiCoV-Ab) to quantify IgG or IgA responses to various antigens. Reactivity towards trimeric SARS-CoV-2 spike protein (Spike Trimer) or SARS-CoV-2 receptor binding domain of spike (RBD) was found to be the best predictor of SARS-CoV-2 infection. Data are presented as Box-Whisker plots of a sample's median fluorescence intensity (MFI) on a logarithmic scale. Box represents the median and the 25th and 75th percentiles, whiskers show the largest and smallest values. Outliers determined by 1.5 times IQR of log-transformed data are depicted as circles. Cut-off values for classification for single antigens are displayed as horizontal lines (Spike Trimer IgG: 3,000 MFI, IgA: 400 MFI; RBD IgG: 450 MFI, IgA: 250 MFI). **b** Sample set from **a**, was used to compare assay performance of the MultiCoV-Ab using Spike Trimer and RBD antigens with commercially available single analyte SARS-CoV-2 IVD assays which detect total Ig (Elecsys Anti-SARS-CoV-2 (Roche); ADVIA Centaur SARS-CoV-2 Total (COV2T) (Siemens Healthineers)) or IgG (Anti-SARS-CoV-2-ELISA - IgG (Euroimmun)) or IgA (Anti-SARS-CoV-2-ELISA - IgA (Euroimmun)). SARS-CoV-2 infection status of samples based on PCR diagnostic is indicated as SARS-CoV-2 positive or negative. Antibody test results were classified as negative (blue), positive (red), or borderline (gray) as per the manufacturer's definition. Only samples with divergent antibody test results are shown. **c** Performance and specifications as stated in the manufacturer's IVD assay manual. For the manufacturer sensitivity specification, information for samples >14 days post-infection are presented. Respective sensitivity and specificity values calculated in this study are given with 95% Clopper-Pearson confidence intervals[52]. Positive and negative predictive values (PPV/NPV) were calculated based on a seropositivity of 3%. Source data are provided as a Source Data file.

SARS-CoV-2 antigen and detection system (Supplementary Fig. 4), which confirmed that Spike Trimer and RBD were the best predictors of SARS-CoV-2 infection. We, therefore, decided to use a combination of both antigens (IgG or IgA overall cut-off) to define overall SARS-CoV-2 reactivity for IgG or IgA, for which the two independent cut-offs for Spike Trimer and RBD had to be met (Table 3). Cut-offs were chosen with focus on maximum specificity for the overall classification (Spike Trimer$^+$/RBD$^+$) to prevent false positive results (Fig. 2a). With the overall IgG cut-off, we reached a specificity of 100%, which would not have been possible for either of the antigens individually, while still retaining acceptable sensitivity (88.7%). IgG detection was shown to be more specific and sensitive than IgA for determination of SARS-CoV-2 infection within our sample set. Only 8 samples which were IgA-positive showed no IgG response (Fig. 2b, dashed lines), 2 of which were uninfected and falsely classified as positive. Of the 6 remaining samples, metadata (including the time between the onset of symptoms and sample collection) was available for 4 (2, 6, 7, and 15 days). As a result, we hypothesized that IgA in these samples can be used to measure an early onset of antibody response as has been proposed by several groups[26,33,34]. Therefore, to give an overall measure of SARS-CoV-2 infection, we used the IgG classification as a basis and included samples with strong IgA positivity–signal to cut-off (S/CO) > 2 for Spike Trimer and RBD–as positive, irrespective of their detected IgG response (Fig. 2b, straight lines). With this combined IgG + IgA classification, we reached an optimal sensitivity of 90% while retaining a specificity of 100%.

Antigen selection affects SARS-CoV-2 serology test performance. While further analyzing the immune response detected towards our 4 additional SARS-CoV-2 antigens in our Multiplex panel, we assessed the IgG response towards the S1 and S2 subdomains of the spike, which both did not improve sample classification (Fig. 2c). Interestingly, RBD, which is a part of S1, showed fewer uninfected samples with increased IgG response compared to S1. For S2, even more, uninfected samples had increased signals, suggesting the presence of potential cross-reactive antibodies for this domain of the spike protein (Fig. 2c). These findings suggest that the RBD response is highly characteristic of the overall SARS-CoV-2 immune response. To further complement our assay, we included the N and N-NTD proteins. Although these antigens have been successfully used in single-analyte assays[35], we observed a high cross-reactivity in uninfected samples for both (Fig. 2d). Interestingly, across the entire data set, only one sample showed a distinct immune response to N and N-NTD, but not to all spike-derived antigens. This confirms that the performance of an antigen is specific to the assay setup and cannot be easily generalized, as commercial IVD tests (i.e., Roche) are able to use the N protein to great effect in a different assay setup.

Dynamics of antibody response in COVID-19 patients. Longitudinal samples from 5 hospitalized patients were used to perform a small-scale time-course analysis of IgG and IgA immune responses (Fig. 3a). Levels of both Ig classes strongly increased within the first ten days after the onset of symptoms. While IgG levels appeared constant over roughly two months, IgA levels started to decline between day 10 and 20 after the onset of symptoms. This reduction in IgA antibody levels was also observed with increased time post-infection in samples without longitudinal follow-up (Supplementary Figure 5). These effects were consistent for the majority of SARS-CoV-2 antigens.

Table 1 Comparison of MultiCoV-Ab and commercial IVD tests in screening results and manufacturer specifications as stated in the assay manuals.

			Manufacturer specification		Correctly classified		Found	Found			
		Antigen	>14 days post infection		Infected	Uninfected	sensitivity	specificity	PPV at 3%	NPV at 3%	
Assay	Detection	used	Sensitivity	Specificity	(of 205)	(of 72)	(95% CI)	(95% CI)	Prevalence	Prevalence	
MultiCoV-Ab	IgG	S Trimer + RBD	—	—	181	72	88.3% (83.1–92.4%)	100% (95.0–100%)	100%	99.6%	
Roche	Total Ig	N	100% $n = 29$	99.8% $n = 5272$	173	72	84.4% (78.7–89.1%)	100% (95.0–100%)	100%	99.5%	
Siemens	Total Ig	S1 RBD	100% $n = 47$	99.8% $n = 1589$	170	72	82.9% (77.1–87.8%)	100% (95.0–100%)	100%	99.5%	
Euroimmun	IgG	S1	100% $n = 13$	99.0% $n = 1261$	164	70	80.0% (73.9–85.2%)	97.2% (90.3–99.7%)	46.9%	99.4%	
MultiCoV-Ab	IgA	S Trimer + RBD	—	—	158	72	77.1% (70.7–82.6%)	100% (95.0–100%)	100%	99.3%	
Euroimmun	IgA	S1	100% $n = 13$	90.4% $n = 1261$	157	62	76.6% (70.2–82.2%)	86.1% (75.9–93.1%)	14.6%	99.2%	

Table 2 Extended Sample set used to further validate MultiCoV-Ab performance.

Age group	≤39				40–59				≥60				Not available				Σ
n	299 (25.4%)				241 (20.5%)				475 (40.4%)				161 (13.7%)				1176
Sex	Male		Female		Male		Female		Male		Female		Male		Female		Not available		
n	139	(11.8%)	160	(13.6%)	144	(12.2%)	97	(8.2%)	271	(23.0%)	204	(17.3%)	5	(0.4%)	3	(0.3%)	153	(13.0%)	1176
SARS-CoV-2 infected	60	(19.4%)	51	(16.5%)	71	(22.9%)	63	(20.3%)	42	(13.5%)	17	(5.5%)	3	(1.0%)	3	(1.0%)	0	(0.0%)	310
hospitalized	6	(10.9%)	2	(3.6%)	14	(25.5%)	6	(10.9%)	23	(41.8%)	4	(7.3%)	0	(0.0%)	0	(0.0%)	0	(0.0%)	55
non-hospitalized	52	(25.0%)	43	(20.7%)	49	(23.6%)	43	(20.7%)	13	(6.3%)	8	(3.8%)	0	(0.0%)	0	(0.0%)	0	(0.0%)	208
hospitalization NA	2	(4.3%)	6	(12.8%)	8	(17.0%)	14	(29.8%)	6	(12.8%)	5	(10.6%)	3	(6.4%)	3	(6.4%)	0	(0.0%)	47
SARS-CoV-2 uninfected	79	(9.1%)	109	(12.6%)	73	(8.4%)	34	(3.9%)	229	(26.4%)	187	(21.6%)	2	(0.2%)	0	(0.0%)	153	(17.7%)	866

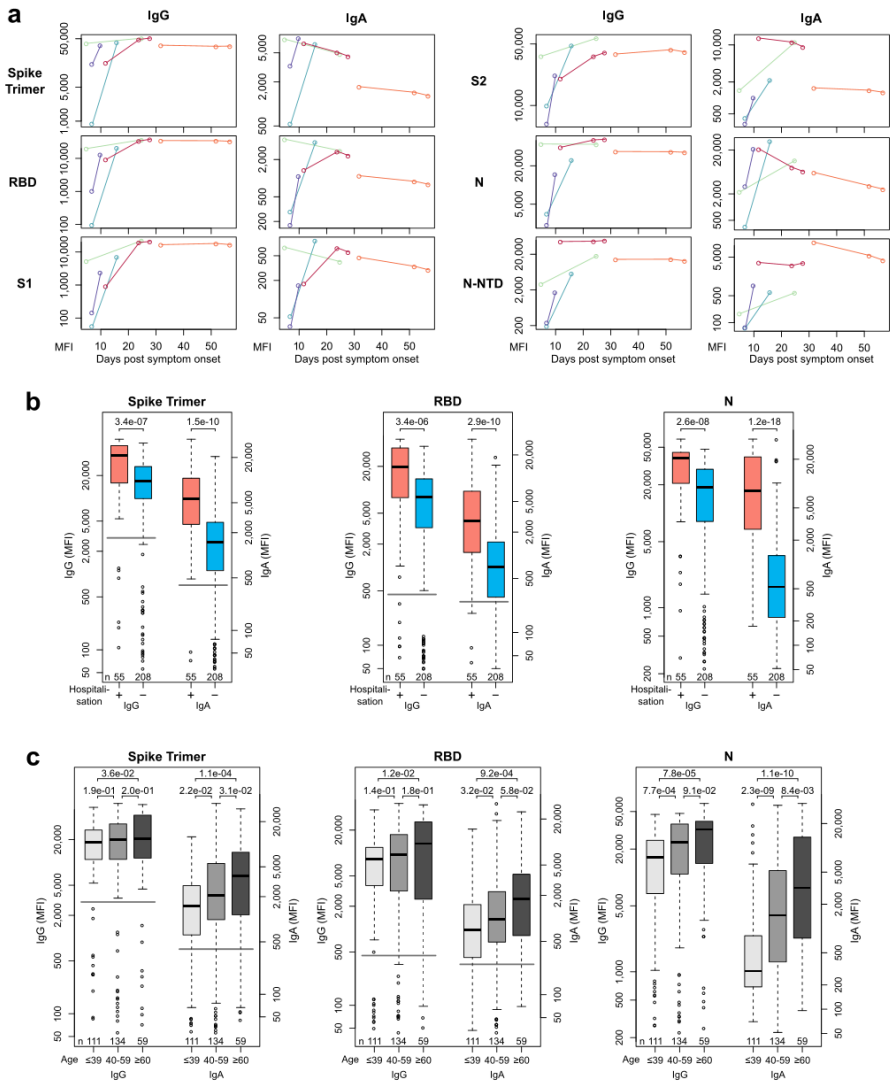

Fig. 3 Multiplex-based seroprofiling allows in-depth characterization of SARS-CoV-2 antibody responses. a Kinetic of SARS-CoV-2 antigen-specific IgA and IgG responses is shown for indicated days after symptom onset for six SARS-CoV-2-specific antigens for five different patients. Patients are indicated by color. **b**, **c** Samples of SARS-CoV-2-infected individuals were analyzed to identify antigen- and isotype-specific antibody responses based on hospitalization indicating disease severity (**b**) or age (**c**). Data is presented as Box-Whisker plots of sample MFI on a logarithmic scale. Box represents the median and the 25th and 75th percentiles, whiskers show the largest and smallest values. Outliers determined by 1.5 times IQR of log-transformed data are depicted as circles. *p*-value (Mann–Whitney U test, two-sided) is displayed at the top of the boxes, indicating differences between signal distribution for respective groups. Cut-off values for MultiCoV-Ab classification are displayed as horizontal lines (Spike Trimer IgG: 3,000 MFI, IgA: 400 MFI; RBD IgG: 450 MFI, IgA: 250 MFI). Source data are provided as a Source Data file.

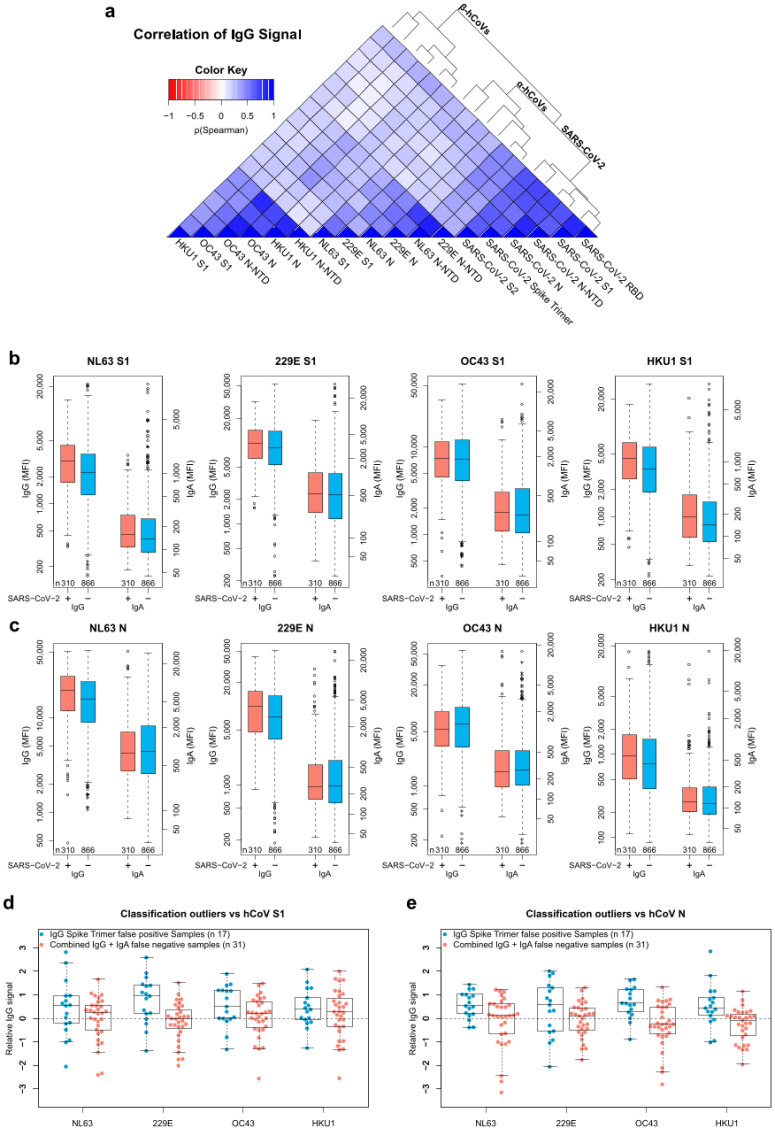

antigens from human α- (NL63 and 229E) and β-hCoVs (OC43 and HKU1) in our MultiCoV-Ab panel (Supplementary Fig. 1). The immune response towards all hCoV antigens was more dependent on coronavirus clade than on antigen choice. However, within the clades of α-hCoVs and β-hCoVs, types of antigens were more dominant than the virus subtype, as demonstrated by rank correlation analysis and hierarchical clustering (Fig. 4a, Supplementary Fig. 6a), suggesting there is potential cross-reactivity within the hCoV clades. Interestingly, IgG response against α-hCoVs clustered more closely to SARS-CoV-2 than to β-hCoVs. This is unexpected, since SARS-CoV-2 has been assigned to the clade of β-CoVs and is also more similar

Fig. 4 Correlation of seasonal hCoV and SARS CoV-2 antibody responses. a Correlation of IgG response for the entire sample set ($n = 1176$) is visualized as heatmap based on Spearman's ρ coefficient; dendrogram on the right side displays antigens after hierarchical clustering was performed. b-c, Immune responses (IgG and IgA) towards hCoV S1 (**b**) and N (**c**) proteins are presented as Box-Whisker plots of sample MFI on a logarithmic scale for SARS-CoV-2-infected (red, $n = 310$) and uninfected (blue, $n = 866$) individuals. Box represents the median and the 25th and 75th percentiles, whiskers show the largest and smallest values. Outliers determined by 1.5 times IQR of log-transformed data are depicted as circles. d-e, Relative levels of IgG-specific immune response towards hCoV S1 (**d**) and N (**e**) proteins are presented as Box-Whisker plots/strip chart overlays of log-transformed and per-antigen scaled and centered MFI for the sample subsets of Spike Trimer false positives (blue, $n = 17$) and combined IgG + IgA false negatives (red, $n = 31$). Box represents the median and the 25th and 75th percentiles, whiskers show the largest and smallest values, excluding outliers as determined by 1.5 times IQR. Source data are provided as a Source Data file.

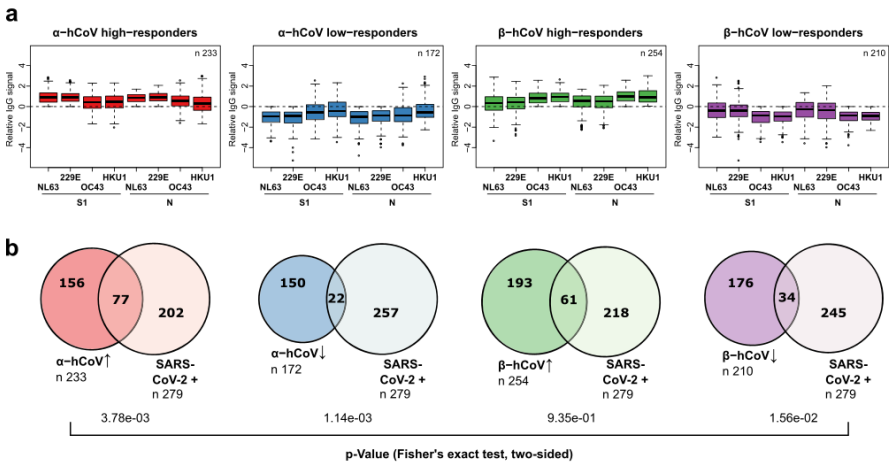

Fig. 5 Analysis of seasonal hCoV high and low responders. a From the entire study population, groups of α- or β-hCoV high and low responders were built as indicated. High responder were defined as samples with above average MFI values for S1 and N-specific IgGs of the respective hCoV clade. Low responders were defined with below MFI values, correspondingly. Responder groups (i) α-hCoV ↑, red, $n = 233$, (ii) β-hCoV ↑, green, $n = 254$, (iii) α-hCoV ↓, blue, $n = 172$ (iv) β-hCoV ↓, purple, $n = 210$ are shown as Box-Whisker plots of log-transformed and per-antigen scaled and centered MFI values across hCoV N and S1 antigens. Box represents the median and the 25th and 75th percentiles, whiskers show the largest and smallest values. Outliers determined by 1.5 times IQR are depicted as circles. **b** The over- or under-representation of SARS-CoV-2 responders (SARS-CoV-2 + , $n = 279$, as determined by positive MultiCoV-Ab classification) within the four sample groups is visualized in Venn diagrams, stochastic significance was calculated using Fisher's exact test (two-sided). Source data are provided as a Source Data file.

in sequence to the β-hCoVs (Supplementary Table 3). Overall, we identified a considerable immune response to hCoV antigens throughout the whole sample set with no notable differences between samples from SARS-CoV-2-infected and uninfected donors in IgG or IgA for S1 (Fig. 4b), N (Fig. 4c), or N-NTD (Supplementary Fig. 6b). We, therefore, used the IgG signal relative to the average response per antigen for further analyses, which allowed comparison among all hCoV antigens on one scale. For those uninfected samples which showed an IgG cross-reactivity towards Spike Trimer (Spike Trimer false positives), we partially observed increased responses towards hCoV antigens. Those samples, which did not show an immune response after SARS-CoV-2 infection (false negatives, as determined by MultiCoV-Ab, combined IgG + IgA) were closer to the baseline (Fig. 4d, e, Supplementary Fig. 6c). This indicates that cross-reactivity with hCoVs causes some of the observed SARS-CoV-2 immune response in samples taken from individuals not exposed to SARS-CoV-2. To investigate the correlation of hCoV and SARS-CoV-2 immune response further, we grouped samples into high and low responders for α-hCoVs and β-hCoVs, as the antigens were shown to correlate closely within a single hCoV clade. High responders were defined as having relative IgG signals > 0 for N and S1 antigens of both hCoV subtypes within the clade, while low-responders had signals < 0, respectively (Fig. 5a). Samples with SARS-CoV-2 immune response (as determined by MultiCoV-Ab, combined IgG + IgA classification) were significantly overrepresented within the group of α-hCoV high responders ($p = 3.78e-03$, Fisher's exact test, two-sided), while being significantly underrepresented within the group of α-hCoV and β-hCoV low responders ($p = 1.14e-03$ and $p = 1.56e-02$, respectively, Fisher's exact test, two-sided) (Fig. 5b). These results showed that while there were no discernible global effects for single antigens, there is a correlation between the SARS-CoV-2 immune response with high hCoV responses, especially towards α-hCoVs. This effect, and the clustering of α-hCoVs and SARS-CoV-2 in Fig. 4a may be a result of similar host-pathogen interaction (such as use of the same entry receptor as NL63, an α-hCoV) or similarities in the mode of action of host suppressive viral proteins. Interestingly, some longitudinal samples from Fig. 3a, showed increased hCoV response post SARS-CoV-2

exposure (Supplementary Fig. 7). However, to further explore cross-reactivity and correlation between CoV-induced immune responses, additional longitudinal samples from donors after SARS-CoV-2 infection are needed to generate meaningful conclusions.

Discussion

We demonstrated that our MultiCoV-Ab, a multiplex immunoassay, is highly suitable to classify seroconversion in SARS-CoV-2-infected individuals. With a combined cut-off using SARS-CoV-2 trimeric full-length spike protein and RBD, we were able to eliminate false positive responses and achieved a sensitivity of 90% with a specificity of 100% for 310 samples from SARS-CoV-2-infected and for 866 samples from uninfected individuals. We found that detection of IgG more accurately reflected infection compared to IgA, although both were highly specific. However, by simultaneously monitoring IgA, we additionally were able to detect an early immune response in some patients. Interestingly, Yu, et al.[26] found that enhanced IgA responses might confer damaging effects in severe COVID-19. This is consistent with the observed significant increase in N protein directed IgA in hospitalized COVID19-cases, and confirms that careful monitoring of serum IgA warrants further attention.

The MultiCoV-Ab approach allows the easy addition of SARS-CoV-2-specific antigens, here 6 in total, which provides an additional level of confidence in patient classification. Thus, for example, we noticed that the spike S1 domain showed fewer false-positive responses compared to the S2 domain. Interestingly, Ng *et al.*[9] reported reactivity towards SARS-CoV-2 S2 from sera of patients with recent seasonal hCoV infection. These sera prevented infection with SARS-CoV-2 pseudotypes in a neutralization assay. Additionally, we found that spike non-responders also did not show a response to nucleocapsid but not vice versa, where nucleocapsid has been described as the strongest inducer of antibody responses[35,36]. Interestingly, nucleocapsid showed significant unspecific Ig binding in our assay. It has been previously reported, that the SARS-CoV-2 N protein is highly positively charged which may facilitate binding of viral nucleic acid but also result in unspecific binding of negatively charged molecules[37]. In addition, N protein oligomerization which is required to form the capsid[38] could further contribute to non-specific protein-protein interactions Therefore, our results highlight that the performance of an antigen is highly specific to the assay setup and cannot be easily generalized.

Another study measuring comparable numbers of serum/plasma samples using multiplex Luminex technology reports similar sensitivities and specificities for SARS-CoV-2 classification[20]. In our comparison to commercially available IVD tests, the MultiCoV-Ab classified fewer samples from SARS-CoV-2 infected donors as negative. However, for 10% of all infected samples, we could not detect a SARS-CoV-2 specific immune response, both in our measurement with MultiCoV-Ab and the commercial IVD kits. Intriguingly, others have already reported that up to 10% of SARS-CoV-2 patients do not develop detectable Ig levels[12,20,39]. Whether those non-responders are able to limit viral replication by innate immune mechanisms[40], forms of pre-existing immunity[41], or cellular immunity[42–44] is dominant in mediating viral clearance remains however to be determined.

One of the strengths of our study, compared to earlier studies[17,20,27], is the relatively large number of control and SARS-CoV-2 infected sera. However, a limitation is the potential bias introduced by an uneven age distribution across the study population. The uninfected control cohort was heavily skewed towards the age group of >60, whereas non-hospitalized COVID-19 cases were over-represented in the age groups below 60. Despite this, MultiCoV-Ab specificity will still be accurate as all uninfected samples were identified correctly and all age groups were well represented with >100 samples per group.

Expanding our MultiCoV-Ab to the endemic hCoVs NL63, 229E, OC43, and HKU1 revealed a clear IgG immune response for all tested samples. Furthermore, we did not observe a difference for the samples from PCR-confirmed hCoV-infected individuals, compared to all others, suggesting that there is a significant degree of pre-exposure in the general population for all endemic hCoVs. Due to the general lack of availability of samples from hCoV-naive individuals, it was difficult to analyze hCoV-mediated cross-reactivity, set a cut-off and subsequently calculate specificities and sensitives for the hCoV S1, N-NTD, N antigens used here. Nevertheless, our multiplexed readout indicates a correlation between the SARS-CoV-2 immune response and high hCoV responses. Currently, we are identifying population groups which were highly exposed and showed different susceptibility to SARS-CoV-2 infection, e.g., the "Ischgl-study group" (unpublished data)[45], in order to elucidate potential cross-protection derived from immune responses towards endemic hCoVs in more detail. Alternatively, studies analyzing hCoV signatures in samples from individuals before and after SARS-CoV-2 infection using the MultiCoV-Ab would help to gain insight into a potential cross-protection.

A multiplex setup such as in MultiCoV-Ab is especially suited to vaccination studies, since the flexibility and broad antigen coverage allows to efficiently map vaccine immune responses to an immunoglobulin isotype and subtype level for the target pathogen and related species[17]. Interestingly, previous SARS-CoV-1 vaccine studies clearly indicated that a detailed characterization of vaccine-induced antibody responses is mandatory for efficient coronavirus vaccine development[46,47]. For instance, Yasui *et al.*[46] reported that although vector vaccines encoding SARS-CoV-1 S or N protein lead to comparable levels of anti-S and anti-N IgG in the respective study groups, N protein-immunized mice showed vaccine-induced pathology characterized by more severe lung damage, increased pulmonary neutrophil and eosinophil infiltration, and a significant upregulation of pro-inflammatory cytokine secretion upon challenge[43].

In summary, we have established and clinically validated the MultiCoV-Ab, a robust, high-content-enabled, and antigen-saving multiplex assay. This assay is suitable for comprehensive characterization of SARS-CoV-2 infection on the humoral immune response and for epidemiological screenings to accurately measure SARS-CoV-2 seroprevalence in large cohort studies. It could also provide the unique opportunity to assess and correlate immunity for both endemic and pathogenic coronaviruses. Finally, a broad and flexible antigen range through the multiplex nature of the MultiCoV-Ab can deliver urgently needed data to help guide decisions for SARS-CoV-2 vaccination strategies.

Methods

Generation of expression constructs for viral antigen production. The sequence optimized cDNAs encoding the full-length nucleocapsid proteins of SARS-CoV-2, hCoV-OC43, hCoV-NL63, hCoV-229E, and hCoV-HKU1 (GenBank accession numbers "QHD43423.2"; "YP_009555245.1"; "YP_003771.1"; "NP_073556.1"; "YP_173242.1") were produced with an N-terminal hexahistidine (His_6)-tag by DNA synthesis (ThermoFisher Scientific). The cDNAs were cloned by standard techniques into NdeI/HindIII sites of the bacterial expression vector pRSET2b (ThermoFisher Scientific). The N-terminal domains (NTDs) of all nucleocapsid proteins were designed based upon previously published structural data[48]. Through this we were able to monitor the immune response against a rigid folded domain and exclude potential unspecific interactions with the largely unstructured region located between N-NTD and N-CTD of the nucleocapsid proteins. Furthermore, by depleting the N-CTD which is responsible for oligomerization of the nucleocapsid, we aimed to monitor antibody binding of a monomeric version of the

nucleocapsid. To generate NTDs of the respective nucleocapsid proteins (SARS-CoV-2 NTD aa 1-189; hCoV-OC43 NTD aa 1-204; hCoV-NL63 NTD aa 1 - 154; hCoV-229E NTD aa 1-156; hCoV-HKU1 NTD aa 1- 203), a stop codon located N-terminally to the Serine-Arginine (SR)-rich linker site[49] was introduced via PCR mutagenesis of the nucleocapsid encoding plasmids using the forward primer pRSET2b down-for and respective reverse primers: SARS-CoV2_NTD-rev, OC43_NTD-rev, NL63_NTD-rev, 229E_NTD-rev, and HKU1_NTD-rev.

Primer sequences are shown in Supplementary Table 4.

The pCAGGS plasmids encoding the stabilized trimeric Spike protein and the receptor binding domain (RBD) of SARS-CoV-2 were kindly provided by F. Krammer[27].

The cDNA encoding the S1 domain (aa 1–681) of the SARS-CoV-2 spike protein was obtained by PCR amplification using the forward primer S1_CoV2-for and reverse primer S1_CoV2-rev and the full length SARS-CoV-2 spike cDNA as template and cloned into the XbaI/NotI-digested backbone of the pCAGGS vector, thereby adding a C-terminal His_6-Tag.

The cDNAs encoding the S1 domains of hCoV-OC43 (aa 1–760), hCoV-NL63 (aa 1–744), hCoV-229E (aa 1–561) and hCoV-HKU1 (aa 1–755) (GenBank accession numbers "AVR40344.1"; "APF29071.1"; "APT69883.1"; "AGW27881.1") were produced by DNA synthesis (ThermoFisher Scientific), digested using XbaI/NotI and ligated into the pCAGGS vector. All expression constructs were verified by sequence analysis. An overview of all expressed constructs can be found in Supplementary Table 5.

Protein expression and purification. For the expression of the viral nucleocapsid proteins (full-length nucleocapsid and N-NTDs), the respective expression constructs were used to transform *E.coli* BL21 (DE3) cells. Protein expression was induced in 1 L TB medium at an optical density (OD_{600}) of 2.5–3 by addition of 0.2 mM isopropyl-β-D-thiogalactopyranoside (IPTG) for 16 h at 20 °C. Cells were harvested by centrifugation (10 min at 6,000 × g) and the pellets were then suspended in binding buffer (1x PBS, ad 0.5 M NaCl, 50 mM imidazole, 2 mM phenylmethylsulfonyl fluoride, 2 mM $MgCl_2$, 150 µg/mL lysozyme (Merck) and 625 µg/mL DNaseI (Applichem)). Cell suspensions were sonified for 15 min (Bandelin Sonopuls HD70 - power MS72/D, cycle 50%) on ice, incubated for 1 h at 4 °C in a rotary shaker followed by a second sonification step for 15 min. After centrifugation (30 min at 20,000 × *g*), urea was added to a final concentration of 6 M to the soluble protein extract. The extract was filtered through a 0.45 µm filter and loaded on a pre-equilibrated 1-mL $HisTrap^{FF}$ column (GE Healthcare). The bound His-tagged nucleocapsid proteins were eluted by a linear gradient (30 mL) ranging from 50 to 500 mM imidazole in elution buffer (1x PBS, pH 7.4, 0.5 M NaCl, 6 M urea). Elution fractions (0.5 mL) containing the His-tagged nucleocapsid proteins were pooled and dialyzed (D-Tube Dialyzer Mega, Novagen) against PBS.

The viral S1-domains, SARS-CoV-2 RBD, and the stabilized trimeric SARS-CoV-2 spike protein were expressed in Expi293 cells following the protocol as described in Stadlbauer et al.[19]. In brief, Expi293F-cells were cultivated (37 °C, 125 rpm, 8% (v/v) CO_2) to a density of 5.5×10^6 cells/mL. The cells were diluted with Expi293F expression medium to a density of 3.0×10^6 cells/mL, followed by transfection of the corresponding expression plasmids (1 µg per mL cell culture) with Expifectamine dissolved in Opti-MEM medium, according to the manufacturer's instructions. After 20 h post-transfection, transfection enhancers were added as documented in the Expi293F-cells manufacturer's instructions. The cell suspensions were cultivated for 2–5 days (37 °C, 125 rpm, 8% (v/v) CO_2) and centrifuged (4 °C, 23,900 × *g*, 20 min) to clarify the supernatant. The supernatants were filtered using a 0.22 µm membrane filter (Millipore, Darmstadt, Germany) and supplemented with His-A buffer stock solution (final concentration in the medium: 20 mM Na_2HPO_4, 300 mM NaCl, 20 mM imidazole, pH 7.4), before the solution was applied to a HisTrap FF crude column on a Äkta pure system (GE Healthcare, Freiburg, Germany). The columns were extensively washed with His-buffer-A (20 mM Na_2HPO_4, 300 mM NaCl, 20 mM imidazole, pH 7.4) before bound proteins were eluted with a imidazole gradient ranging from 50 mM – 400 mM. Eluted proteins were dialyzed against PBS and concentrated to 1 mg/mL.

All purified proteins were analyzed via standard SDS-PAGE followed by staining with InstantBlue Coomassie stain (Expedeon) and immunoblotting using an anti-His antibody (Penta-His Antibody, #34660, Qiagen, used at 1:1,000 dilution) in combination with a donkey-anti-mouse antibody labeled with AlexaFluor647 (#A31571, Invitrogen, used at 1:1,000 dilution) on a Typhoon Trio (GE-Healthcare, Freiburg, Germany; excitation 633 nm, emission filter settings 670 nm BP 30) to confirm protein integrity. To further confirm correct expression, integrity, and purity, proteins were analyzed by mass spectrometry. To control the production reproducibility of the antigens, potential aggregation and melting temperatures of the proteins were investigated by nano differential scanning fluorimetry (nanoDSF) using a Prometheus (Nanotemper, Munich, Germany).

Commercial antigens. Two commercial antigens were used to complement the in-house-produced antigen panel.

The S2 ectodomain of the SARS-CoV-2 spike protein (aa 686–1213) was purchased from Sino Biological, Eschborn, Germany (cat # 40590, lot # LC14MC3007). A full-length nucleocapsid protein of SARS-CoV-2 was purchased from Aalto Bioreagents, Dublin, Ireland (cat # 6404-b, lot # 4629).

Bead-based serological multiplex assay. All antigens were covalently immobilized on spectrally distinct populations of carboxylated paramagnetic beads (MagPlex Microspheres, Luminex Corporation, Austin, TX) using 1-ethyl-3-(3-dimethylaminopropyl)carbodiimide (EDC)/sulfo-N-hydroxysuccinimide (sNHS) chemistry. For immobilization, a magnetic particle processor (KingFisher 96, Thermo Scientific, Schwerte, Germany) was used.

Bead stocks were vortexed thoroughly and sonicated for 15 s. Subsequently, 83 µL of 0.065% (v/v) Triton X-100 and 1 mL of bead stock containing 12.5×10^7 beads of one single bead population were pipetted into each well. The beads were then washed twice with 500 µL of activation buffer (100 mM Na_2HPO_4, pH 6.2, 0.005% (v/v) Triton X-100) and beads were activated for 20 min in 300 µL of activation mix containing 5 mg/mL EDC and 5 mg/mL sNHS in activation buffer. Following activation, the beads were washed twice with 500 µL of coupling buffer (500 mM MES, pH 5.0, 0.005% (v/v) Triton X-100) and the antigens were added to the activated beads and incubated for 2 h at 21 °C to immobilize the antigens on the surface.

Antigen-coupled beads were washed twice with 800 µL of wash buffer (1x PBS, 0.005% (v/v) Triton X-100) and were finally resuspended in 1000 µL of storage buffer (1x PBS, 1% (w/v) BSA, 0.05% (v/v) ProClin). The beads were stored at 4°C until further use.

To detect human IgG and IgA responses against SARS-CoV-2 and the endemic human coronaviruses (hCoV-NL63, hCoV-229E, hCoV-OC43 and hCoV-HKU1), the purified trimeric spike protein (S), S1-domain, S2-domain (Sino Biological GmbH, Europe), RBD, nucleocapsid (N) and the N-terminal domain of nucleocapsid (N-NTD) of SARS-CoV-2 as well as the S1-domain, N, and N-NTD of the endemic hCoVs were immobilized on different bead populations as described above. The individual bead populations were combined into a bead mix. A bead-based multiplex assay was performed. Briefly, samples were incubated at a 1:400 dilution for 2 hours at 21 °C. Unbound antibodies were removed and the beads were washed three times with 100 µL of wash buffer (1x PBS, 0.05% (v/v) Tween20) per well using a microplate washer (Biotek 405TS, Biotek Instruments GmbH). Bound antibodies were detected with R-phycoerythrin labeled goat-anti-human IgG (Dianova, Cat# 109-116-098, Lot#148837, used at 3 µg/mL) or IgA (Dianova, Cat# 109-115-011, Lot#143454, used at 5 µg/mL) antibodies (incubation for 45 min at 21 °C). For each sample, a single measurement was performed. Readout was done using a Luminex FLEXMAP 3D instrument and the Luminex xPONENT Software 4.3 (settings: sample size: 80 µL, 50 events, Gate: 7,500–15,000, Reporter Gain: Standard PMT).

Quality control and technical assay validation steps. In order to test the repeatability of the MultiCoV-Ab three quality control samples (QCs) were processed in duplicate on each test plate ($n = 17$) during the sample screening and inter-assay variance was assessed for each antigen in the multiplex. For intra-assay variance, 24 replicates for each of the three QC samples were analyzed on one plate. Results from this are presented in Supplementary Table 1 and Supplementary Fig. 2. A limit of detection (LOD) for each antigen was determined by processing a blank in 24 replicates and the LOD was set as mean MFI + 3 standard deviations. Sample parallelism and comparability of paired serum and plasma samples were assessed over eight dilution steps ranging from 1:100 to 1:12,800 (Supplementary Fig. 2). A set of samples derived from 205 SARS-CoV-2-infected and 72 uninfected individuals was tested repeatedly with two different kit batches. The samples classification in both runs matched 100%. Furthermore, as part of our negative sample panel, we have analyzed samples with potentially interfering characteristics (i.e., samples from patients with PCR-confirmed hCoV infection, presences of HAMA (human anti-mouse antibodies) and rheumatoid factor (RF), with high procalcitonin values (> 3 ng/mL), as well as from pregnant women and patients with neuroinflammatory diseases) (Supplementary Table 2).

Samples. A total of 1176 sera and plasma samples were used for the MultiCoV-Ab assay development. Ethical approval was granted from the Ethics Committee of Hannover Medical School (#9122_BO_K2020). Only de-identified samples were used for the MultiCoV-Ab assay development. All samples were pre-existing. Cohort age was 5-88 years; age was not known for 161 samples.

310 samples were from COVID-19 patients or convalescents. Samples were classified as SARS-CoV-2 infected, if a positive SARS-CoV-2 RT-PCR was reported and/or if hospitalization/quarantine for COVID-19 was indicated as part of the samples metadata. dT defined as time between PCR test or symptom onset and blood draw was 0–73 days (median= 38 d; $n = 258$). dT was not provided for 52 samples. SARS-CoV-2 infected samples used in this study were collected after ethical review (9001_BO_K, Hannover Medical School; 179/2020/BO2, University Hospital Tübingen; 85/20, Ärztekammer des Saarlandes).

866 control samples were from non-SARS-CoV-2 infected individuals and were classified as non-infected as they were obtained prior to the emergence of SARS-CoV-2 in December 2019 or because they were taken from individuals who had not reported cold symptoms since the beginning of 2020.

The majority of non-SARS-COV-2 infected samples were randomly selected and consisted of pre-pandemic blood donors, commercially available (Central BioHub GmbH, Berlin, Germany and BBI Solutions, Crumlin, UK) or bio-banked specimens. 365 samples were from the Memory and Morbidity in Augsburg Elderly (MEMO) study (a sub-cohort of the MONICA S2 cohort (WHO 1988)) and were included based on available serological titers for HSV-1, HSV-2, HHV-6, and

EBV[50]. 88 samples were obtained from transplanted patients with chronic respiratory conditions.

Collection of non-SARS-CoV-2 infected control samples had been approved by several ethic committees: 3232-2016 (Ethics Committee of Hannover Medical School); 62/20 (Ethics Committees of the Medical Faculty of the Saarland University at the Saarland Ärztekammer); WUM 17.02.1997 (Joint ethics committee of the University of Münster and the Westphalian Chamber of Physicians).

All necessary patient/participant consent has been obtained and the appropriate institutional forms have been archived. Additional sample details can be found in Supplementary Table 2. Serum and plasma samples were handled in Class II-laminar flow benches in L2 laboratories[51]. Samples were not heat-inactivated. All incubation steps took place in fully sealed assay plates.

Data analysis. Data analysis and visualization were performed with R Studio (Version 1.2.5001, using R version 3.6.1) using the Median Fluorescent Intensity (MFI). Statistical analysis was performed using R package "stats" from the base repository. Mann-Whitney U test was used to determine the difference between signal distributions from different sample groups. Spearman's ρ coefficient was calculated in order to correlate antigens by response from the entire sample set, followed by hierarchical clustering to group antigens. Fishers' exact test was used to calculate the significance of overlap between sample groups. 95% Confidence intervals for sensitivity and specificity values calculated in this study were calculated after Clopper-Pearson[52] and associated positive and negative predictive values (PPV/NPV) were calculated based on a seropositivity of 3%. Sequence alignments and sequence identity scores were calculated with version 1.2.4. of Clustal Omega[53].

Reporting summary. Further information on research design is available in the Nature Research Reporting Summary linked to this article.

Data availability

Data relating to the findings of this study are available from the corresponding author upon request. Source data have been deposited on GitHub alongside the analysis code: https://github.com/BeckerMatthias/MULTICOV-AB_Publication/. Source data are provided with this paper.

Code availability

Analysis code and required input files have been deposited on GitHub: https://github.com/BeckerMatthias/MULTICOV-AB_Publication/

Received: 27 July 2020; Accepted: 6 January 2021;
Published online: 19 February 2021

References

1. Gorbalenya, A. E. et al. The species Severe acute respiratory syndrome-related coronavirus: classifying 2019-nCoV and naming it SARS-CoV-2. *Nat. Microbiol.* **5**, 536–544 (2020).
2. Mofijur, M. et al. Impact of COVID-19 on the social, economic, environmental and energy domains: Lessons learnt from a global pandemic. *Sustain. Prod. Consum.* **26**, 343–359 (2021).
3. Hu, B., Guo, H., Zhou, P. & Shi, Z.-L. Characteristics of SARS-CoV-2 and COVID-19. *Nat. Rev. Microbiol.* https://doi.org/10.1038/s41579-020-00459-7 (2020).
4. Wu, Z. & McGoogan, J. M. Characteristics of and important lessons from the coronavirus disease 2019 (COVID-19) outbreak in China: summary of a report of 72 314 cases from the Chinese Center for Disease Control and Prevention. *Jama* **323**, 1239–1242 (2020).
5. Huang, A. T. et al. A systematic review of antibody mediated immunity to coronaviruses: kinetics, correlates of protection, and association with severity. *Nat. Commun.* **11**, 4704 (2020).
6. Severance, E. G. et al. Development of a nucleocapsid-based human coronavirus immunoassay and estimates of individuals exposed to coronavirus in a US metropolitan population. *Clin. Vaccin. Immunol.* **15**, 1805–1810 (2008).
7. Corman, V. M., Muth, D., Niemeyer, D. & Drosten, C. in *Advances in virus research* Vol. 100 163–188 (Elsevier, 2018).
8. Murin, C. D., Wilson, I. A. & Ward, A. B. Antibody responses to viral infections: a structural perspective across three different enveloped viruses. *Nat. Microbiol.* **4**, 734–747 (2019).
9. Ng, K. W. *et al.* Preexisting and de novo humoral immunity to SARS-CoV-2 in humans. *Science*, eabe1107, https://doi.org/10.1126/science.abe1107 (2020).
10. Lee, N. et al. Anti-SARS-CoV IgG response in relation to disease severity of severe acute respiratory syndrome. *J. Clin. Virol.* **35**, 179–184 (2006).
11. Ho, M.-S. et al. Neutralizing antibody response and SARS severity. *Emerg. Infect. Dis.* **11**, 1730 (2005).
12. Tan, W. et al. Viral Kinetics and Antibody Responses in Patients with COVID-19. Preprint at: https://www.medrxiv.org/content/10.1101/2020.03.24.20042382v1. (2020).
13. Ko, J.-H. et al. Serologic responses of 42 MERS-coronavirus-infected patients according to the disease severity. *Diagnostic Microbiol. Infect. Dis.* **89**, 106–111 (2017).
14. Long, Q. X. et al. Antibody responses to SARS-CoV-2 in patients with COVID-19. *Nat. Med.* **26**, 845–848 (2020).
15. Amanat, F. & Krammer, F. SARS-CoV-2 vaccines: status report. *Immunity* **52**, 583–589 (2020).
16. Robbiani, D. F. et al. Convergent antibody responses to SARS-CoV-2 in convalescent individuals. *Nature* **584**, 437–442 (2020).
17. Okba, N. M. A. et al. Severe acute respiratory syndrome coronavirus 2-specific antibody responses in coronavirus disease patients. *Emerg. Infect. Dis.* **26**, 1478–1488 (2020).
18. Lassaunière, R. et al. Evaluation of nine commercial SARS-CoV-2 immunoassays. Preprint at: https://www.medrxiv.org/content/10.1101/2020.04.09.20056325v1. (2020).
19. Stadlbauer, D. et al. SARS-CoV-2 seroconversion in humans: a detailed protocol for a serological assay, antigen production, and test setup. *Curr. Protoc. Microbiol* **57**, e100 (2020).
20. den Hartog, G. et al. SARS-CoV-2–specific antibody detection for seroepidemiology: a multiplex analysis approach accounting for accurate seroprevalence. *J. Infect. Dis.* **222**, 1452–1461 (2020).
21. Norman, M. et al. Ultra-sensitive high-resolution profiling of anti-SARS-CoV-2 antibodies for detecting early seroconversion in COVID-19 patients. Preprint at https://www.medrxiv.org/content/10.1101/2020.04.28.20083691v1. (2020).
22. Rudberg, A.-S. et al. SARS-CoV-2 exposure, symptoms and seroprevalence in healthcare workers in Sweden. *Nat. Commun.* **11**, 5064 (2020).
23. Jiang, H.-w et al. SARS-CoV-2 proteome microarray for global profiling of COVID-19 specific IgG and IgM responses. *Nat. Commun.* **11**, 3581 (2020).
24. Meyer, B., Drosten, C. & Müller, M. A. Serological assays for emerging coronaviruses: challenges and pitfalls. *Virus Res.* **194**, 175–183 (2014).
25. Callow, K., Parry, H., Sergeant, M. & Tyrrell, D. The time course of the immune response to experimental coronavirus infection of man. *Epidemiol. Infect.* **105**, 435–446 (1990).
26. Yu, H.-q. *et al.* Distinct features of SARS-CoV-2-specific IgA response in COVID-19 patients. *Eur. Resp. J.* 2001526, https://doi.org/10.1183/13993003.01526-2020 (2020).
27. Amanat, F. et al. A serological assay to detect SARS-CoV-2 seroconversion in humans. *Nat. Med.* **26**, 1033–1036 (2020).
28. Elecsys® Anti-SARS-CoV-2, https://diagnostics.roche.com/global/en/products/params/elecsys-anti-sars-cov-2.html (2020).
29. SARS-CoV-2-Gesamtantikörpertest, https://www.siemens-healthineers.com/de/laboratory-diagnostics/assays-by-diseases-conditions/infectious-disease-assays/cov2t-assay (2020).
30. SARS-CoV-2, https://www.coronavirus-diagnostik.de/antikoerpertestsysteme-fuer-covid-19.html (2020).
31. Fawcett, T. An introduction to ROC analysis. *Pattern Recognit. Lett.* **27**, 861–874 (2006).
32. Zou, K. H., O'Malley, A. J. & Mauri, L. Receiver-operating characteristic analysis for evaluating diagnostic tests and predictive models. *Circulation* **115**, 654–657 (2007).
33. Guo, L. et al. Profiling early humoral response to diagnose novel coronavirus disease (COVID-19). *Clin. Infect. Dis.* **71**, 778–785 (2020).
34. Iyer, A. S. et al. Persistence and decay of human antibody responses to the receptor binding domain of SARS-CoV-2 spike protein in COVID-19 patients. *Sci Immunol.* **5**, eabe0367 (2020).
35. Burbelo, P. D. et al. Sensitivity in Detection of Antibodies to Nucleocapsid and Spike Proteins of Severe Acute Respiratory Syndrome Coronavirus 2 in Patients With Coronavirus Disease 2019. *J Infect Dis.* **222**, 206–213 (2020).
36. Sun, B. et al. Kinetics of SARS-CoV-2 specific IgM and IgG responses in COVID-19 patients. *Emerg. Microbes Infect.* **9**, 940–948 (2020).
37. Zeng, W. et al. Biochemical characterization of SARS-CoV-2 nucleocapsid protein. *Biochem. Biophys. Res Commun.* **527**, 618–623 (2020).
38. McBride, R., Van Zyl, M. & Fielding, B. C. The coronavirus nucleocapsid is a multifunctional protein. *Viruses* **6**, 2991–3018 (2014).
39. Wang, H. et al. SARS-CoV-2 Proteome microarray for mapping COVID-19 antibody interactions at amino acid resolution. *ACS Central Science*, https://doi.org/10.1021/acscentsci.0c00742 (2020).
40. Angka, L., Market, M., Ardolino, M. & Auer, R. C. Is innate immunity our best weapon for flattening the curve? *J. Clin. Investig.* **130**, 3954–3956 (2020).
41. Sette, A. & Crotty, S. Pre-existing immunity to SARS-CoV-2: the knowns and unknowns. *Nat. Rev. Immunol.* **20**, 457–458 (2020).
42. Nelde, A. *et al.* SARS-CoV-2-derived peptides define heterologous and COVID-19-induced T cell recognition. *Nat. Immunol.* https://doi.org/10.1038/s41590-020-00808-x (2020).

43. Liu, L. et al. Anti-spike IgG causes severe acute lung injury by skewing macrophage responses during acute SARS-CoV infection. *JCI Insight* **4**, e123158 (2019).
44. Gallais, F. *et al.* Intrafamilial exposure to SARS-CoV-2 induces cellular immune response without seroconversion. Preprint at https://www.medrxiv.org/content/10.1101/2020.06.21.20132449v1. (2020).
45. Ischgl: 42,4 Prozent sind Antikörper-positiv, https://www.deutsche-apotheker-zeitung.de/news/artikel/2020/06/26/viele-buerger-ischgls-waren-infiziert (2020).
46. Yasui, F. et al. Prior immunization with severe acute respiratory syndrome (SARS)-associated coronavirus (SARS-CoV) nucleocapsid protein causes severe pneumonia in mice infected with SARS-CoV. *J. Immunol.* **181**, 6337–6348 (2008).
47. Bolles, M. et al. A double-inactivated severe acute respiratory syndrome coronavirus vaccine provides incomplete protection in mice and induces increased eosinophilic proinflammatory pulmonary response upon challenge. *J. Virol.* **85**, 12201–12215 (2011).
48. Chen, I.-J. et al. Crystallization and preliminary X-ray diffraction analysis of the N-terminal domain of human coronavirus OC43 nucleocapsid protein. *Acta Crystallogr. Sect. F: Struct. Biol. Crystallization Commun.* **66**, 815–818 (2010).
49. Kang, S. *et al.* Crystal structure of SARS-CoV-2 nucleocapsid protein RNA binding domain reveals potential unique drug targeting sites. *Acta Pharm Sin B*, https://doi.org/10.1016/j.apsb.2020.04.009 (2020).
50. Zeeb, M. *et al.* Seropositivity for pathogens associated with chronic infections is a risk factor for all-cause mortality in the elderly: findings from the Memory and Morbidity in Augsburg Elderly (MEMO) Study. *GeroScience*, https://doi.org/10.1007/s11357-020-00216-x (2020).
51. Offergeld, R. *Stellungnahme des AK Blut (S20) zu SARS-Coronavirus-2 (17.3.2020)*, https://www.rki.de/DE/Content/Kommissionen/AK_Blut/Stellungnahmen/download/COVID.pdf?__blob=publicationFile (2020).
52. Clopper, C. J. & Pearson, E. S. The use of confidence or fiducial limits illustrated in the case of the binomial. *Biometrika* **26**, 404–413 (1934).
53. Madeira, F. et al. The EMBL-EBI search and sequence analysis tools APIs in 2019. *Nucleic acids Res.* **47**, W636–W641 (2019).

Acknowledgements

This work was supported by the Initiative and Networking Fund of the Helmholtz Association of German Research Centres (Grant number SO-96). This work has further received funding from the European Union's Horizon 2020 research and innovation programme under Grant agreement no. 101003480–CORESMA. We thank Florian Krammer for providing us with expression plasmids for the Spike Trimer and RBD. We thank Shannon Layland for critically proofreading of the manuscript.

Author contributions

M.B. designed and performed experiments and data analysis; M.S. designed experiments; D.J., J.H., S.F., F.R., planned and performed experiments; A.Z. performed mass spectrometry analysis; J.H. performed nanoDSF analyses; H.D., B.T., P.D.K., F.W., U.R. designed, cloned, expressed and purified the antigens; S.H. and A.P. performed sample analysis; T.B., A.B., S.L., S.S., M.C., T.I., J.G., A.K., K.B., H-G.R., A.N., M.M., J.S.H., J.S.W., M.T., T.O.J. arranged sample and data collection; K.S-L., M.T., T.O.J, T.K., G.K. supported the study planning; S.G. reviewed the analysis code; N.S-M. planned the study, assay development, and validation and designed experiments; M.B., M.S., A.D., U.R., and N.S-M. wrote the manuscript. All authors reviewed the manuscript.

Competing interests

The authors declare the following competing interests: T.O.J. is a scientific advisor for Luminex. N.S-M. was a speaker at Luminex user meetings in the past. The Natural and Medical Sciences Institute at the University of Tübingen is involved in applied research projects as a fee for services with Luminex. The remaining authors declare no competing interests.

Additional information

Supplementary information The online version contains supplementary material available at https://doi.org/10.1038/s41467-021-20973-3.

Correspondence and requests for materials should be addressed to N.S.-M.

Peer review information *Nature Communications* thanks the anonymous reviewers for their contribution to the peer review of this work. Peer reviewer reports are available.

Reprints and permission information is available at http://www.nature.com/reprints

Publisher's note Springer Nature remains neutral with regard to jurisdictional claims in published maps and institutional affiliations.

[1]NMI Natural and Medical Sciences Institute at the University of Tübingen, Reutlingen, Germany. [2]Department of Epidemiology, Helmholtz Centre for Infection Research, Braunschweig, Germany. [3]TWINCORE GmbH, Centre for Experimental and Clinical Infection Research, a joint venture of the Hannover Medical School and the Helmholtz Centre for Infection Research, Hannover, Germany. [4]Helmholtz-Institute for RNA-based Infection Research (HIRI), Würzburg, Germany. [5]Pharmaceutical Biotechnology, University of Tübingen, Tübingen, Germany. [6]Institute for Clinical Chemistry and Pathobiochemistry, Department for Diagnostic Laboratory Medicine, University Hospital Tübingen, Tübingen, Germany. [7]Institute for Diabetes Research and Metabolic Diseases of the Helmholtz Center Munich at the University of Tübingen, Tübingen, Germany. [8]German Center for Diabetes Research (DZD), München-Neuherberg, Germany. [9]Institute for Clinical and Experimental Transfusion Medicine, University Hospital Tübingen, Tübingen, Germany. [10]Niedersächsisches Landesgesundheitsamt, Department of Virology/Serology, Hannover, Germany. [11]Institute of Virology, Saarland University Medical Center, Homburg/Saar, Germany. [12]Department of Gastroenterology, Hepatology, Endocrinology, Hannover Medical School, Hannover, Germany; Centre for Individualized Infection Medicine (CiiM), Hannover, Germany. [13]Hannover Unified Biobank (HUB), Hannover Medical School, Hannover, Germany. [14]Department of Respiratory Medicine, Hannover Medical School, Hannover, Germany. [15]Biomedical Research in End-stage and obstructive Lung Disease Hannover (BREATH), Member of the German Center for Lung Research (DZL), Hannover, Germany. [16]Institute of Epidemiology and Social Medicine, University of Münster, Münster, Germany. [17]Institute for Cell Biology, Department of Immunology, University of Tübingen, Tübingen, Germany. [18]German Cancer Consortium (DKTK) and German Cancer Research Center (DKFZ), partner site Tübingen, Tübingen, Germany. [19]Cluster of Excellence iFIT (EXC2180) "Image-Guided and Functionally Instructed Tumor Therapies", University of Tübingen, Tübingen, Germany. [20]Department of Women's Health, Research Institute for Women's Health, Eberhard-Karls-University, Tübingen, Germany. [21]Department of Medicine/Cardiology, Cardiovascular Research Laboratories, David Geffen School of Medicine at UCLA, Los Angeles, CA, USA. [22]Clinical Collaboration Unit Translational Immunology, German Cancer Consortium (DKTK), Department of Internal Medicine, University Hospital Tübingen, Tübingen, Germany. [23]Dr. Margarete Fischer-Bosch Institute of Clinical Pharmacology (IKP) and Robert Bosch Center for Tumor Diseases (RBCT), both Stuttgart, Germany. [24]These authors contributed equally: Matthias Becker, Monika Strengert, Ulrich Rothbauer. ✉email: Nicole.Schneiderhan@nmi.de

Supplementary Information

Exploring beyond clinical routine SARS-CoV-2 serology using MultiCoV-Ab to evaluate endemic coronavirus cross-reactivity

Matthias Becker[1,#], Monika Strengert[2,3,#], Daniel Junker[1], Philipp D. Kaiser[1], Tobias Kerrinnes[4], Bjoern Traenkle[1,5], Heiko Dinter[1,5], Julia Häring[1], Stéphane Ghozzi[2], Anne Zeck[1], Frank Weise[1], Andreas Peter[6,7,8], Sebastian Hörber[6,7,8], Simon Fink[1], Felix Ruoff[1], Alex Dulovic[1], Tamam Bakchoul[9], Armin Baillot[10], Stefan Lohse[11], Markus Cornberg[12], Thomas Illig[13], Jens Gottlieb[14,15], Sigrun Smola[11], André Karch[16], Klaus Berger[16], Hans-Georg Rammensee[17,18,19], Katja Schenke-Layland[1,19,20,21], Annika Nelde[17,19,22], Melanie Märklin[19,21], Jonas S. Heitmann[19,21], Juliane S. Walz[17,19,23,22], Markus Templin[1], Thomas O. Joos[1], Ulrich Rothbauer[1,5,#], Gérard Krause[2,3], Nicole Schneiderhan-Marra[1,*]

Affiliations

[1] NMI Natural and Medical Sciences Institute at the University of Tübingen, Reutlingen, Germany

[2] Department of Epidemiology, Helmholtz Centre for Infection Research, Braunschweig, Germany

[3] TWINCORE GmbH, Centre for Experimental and Clinical Infection Research, a joint venture of the Hannover Medical School and the Helmholtz Centre for Infection Research, Hannover, Germany

[4] Helmholtz-Institute for RNA-based Infection Research (HIRI), Würzburg, Germany

[5] Pharmaceutical Biotechnology, University of Tübingen, Germany

[6] Institute for Clinical Chemistry and Pathobiochemistry, Department for Diagnostic Laboratory Medicine, University Hospital Tübingen, Tübingen, Germany

[7] Institute for Diabetes Research and Metabolic Diseases of the Helmholtz Center Munich at the University of Tübingen, Tübingen, Germany

[8] German Center for Diabetes Research (DZD), München-Neuherberg, Germany

[9] Institute for Clinical and Experimental Transfusion Medicine, University Hospital Tübingen, Tübingen, Germany

[10] Niedersächsisches Landesgesundheitsamt, Department of Virology/Serology, Hannover, Germany

[11] Institute of Virology, Saarland University Medical Center, Homburg/Saar, Germany

[12] Department of Gastroenterology, Hepatology, Endocrinology, Hannover Medical School, Hannover, Germany; Centre for Individualized Infection Medicine (CiiM), Hannover, Germany

[13] Hannover Unified Biobank (HUB), Hannover Medical School, Hannover, Germany

[14] Department of Respiratory Medicine, Hannover Medical School, Hannover Germany

[15] Biomedical Research in End-stage and obstructive Lung Disease Hannover (BREATH), member of the German Center for Lung Research (DZL), Hannover, Germany

[16] Institute of Epidemiology and Social Medicine, University of Münster, Münster, Germany

[17] Institute for Cell Biology, Department of Immunology, University of Tübingen, Tübingen, Germany

[18] German Cancer Consortium (DKTK) and German Cancer Research Center (DKFZ), partner site Tübingen, Tübingen, Germany.

[19] Cluster of Excellence iFIT (EXC2180) “Image-Guided and Functionally Instructed Tumor Therapies”, University of Tübingen, Tübingen, Germany

[20] Department of Women’s Health, Research Institute for Women’s Health, Eberhard-Karls-University, Tübingen, Germany

[21] Department of Medicine/Cardiology, Cardiovascular Research Laboratories, David Geffen School of Medicine at UCLA, Los Angeles, CA, USA

[22] Clinical Collaboration Unit Translational Immunology, German Cancer Consortium (DKTK), Department of Internal Medicine, University Hospital Tübingen, Tübingen, Germany

[23] Dr. Margarete Fischer-Bosch Institute of Clinical Pharmacology (IKP) and Robert Bosch Center for Tumor Diseases (RBCT), both Stuttgart, Germany

[#] These authors contributed equally to this work.

* Corresponding author:

Dr. Nicole Schneiderhan-Marra

Markwiesenstrasse 55, 72770 Reutlingen, Germany

Phone: 0049 7121 51530 815

Fax: 0049 7121 51530 16

E-Mail: Nicole.Schneiderhan@nmi.de

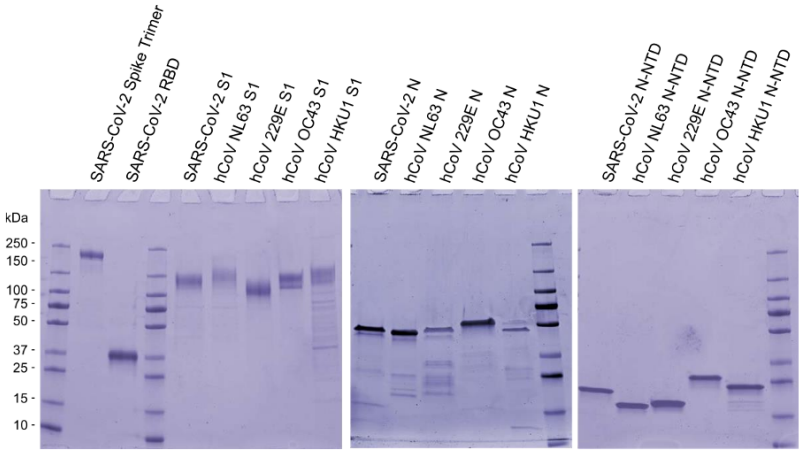

Supplementary Figure 1

SDS-PAGE analysis of the recombinant viral antigens used in this study. To test for purity and integrity 1 - 2 µg of indicated recombinant proteins were boiled in reducing SDS-sample buffer and subjected to a gradient (4 – 20 %) SDS-PAGE followed by Coomassie staining. SARS-CoV-2 Spike Trimer, SARS-CoV-2 RBD and the S1-domains of SARS-CoV-2, hCoV-NL63, hCoV-229E, hCoV-OC43 and hCoV-HKU1 were produced in ExpiHEK™ cells. Nucleocapsid (N) and N-terminal domain of nucleocapsid (N-NTD) of SARS-CoV-2, hCoV-NL63, hCoV-229E, hCoV-OC43 and hCoV-HKU1 were produced in *E.coli*. The image is an assembly of all expressed proteins and is representative for single protein purity after purification. Source data are provided as a Source Data file.

4

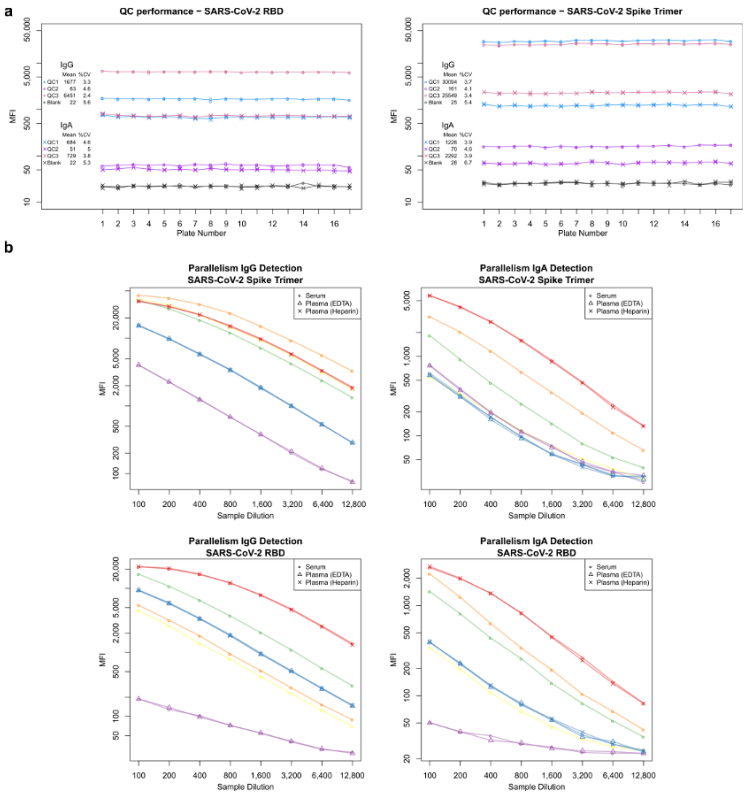

Supplementary Figure 2

a, Three quality control (QC) samples, as well as a sample of assay buffer (blank sample) were processed in duplicates on every plate. Performance across 17 assay runs is depicted and mean and %CVs are shown on the left side (n=34). For plate 14, a processing error lead to exclusion of one blank sample from this evaluation. **b,** To assess parallelism of signals from different samples, 6 unique serum samples were processed over a dilution series of 8 steps from 1:100 to 1:12,800. For 3 samples, paired plasma (EDTA and/or Heparin) were available and processed together. For IgG and IgA detection of Spike Trimer and RBD, MFI are plotted against sample dilution. Color indicates unique sample and shapes indicate sample type. The data represent a single measurement per sample and dilution (n=1). Source data are provided as a Source Data file.

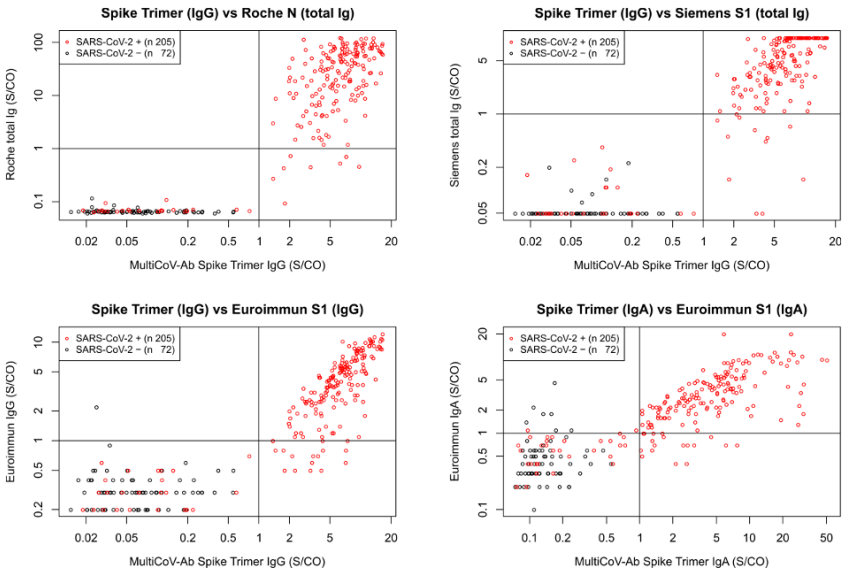

Supplementary Figure 3

Scatterplots of sample set with defined SARS-CoV-2 infection status (infected: red, n=205; uninfected: black, n=72) to compare performance of the MultiCoV-Ab Spike Trimer vs indicated antigens of commercial SARS-CoV-2 test kits. Signals are depicted as Signal to cut-off ratios (S/CO) on a logarithmic scale. Lines indicate the respective cut-off values as defined by the manufacturer to determine positive and negative test results. Source data are provided as a Source Data file.

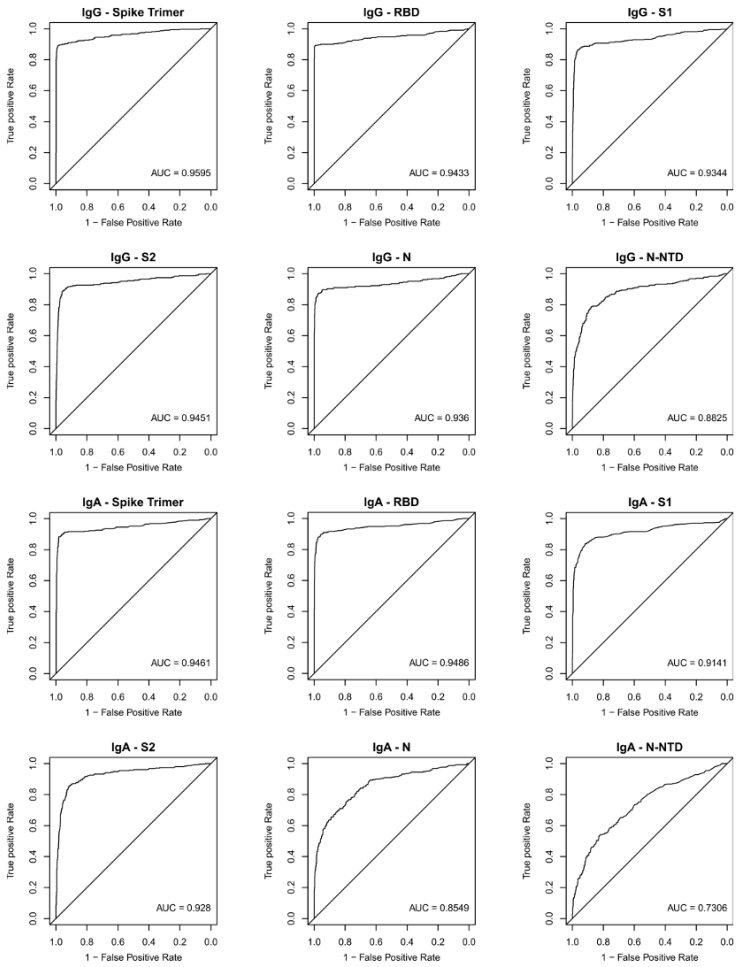

Supplementary Figure 4

ROC analysis[1,2] for IgG and IgA detection of SARS-CoV-2 antigens based on the extended sample set of 866 uninfected and 310 infected samples used for clinical validation for MultiCoV-Ab. True positive rate is displayed against 1 - false positive rate, corresponding to sensitivity and specificity at a given cut-off. AUC-values indicating individual antigen performance are shown. Source data are provided as a Source Data file.

7

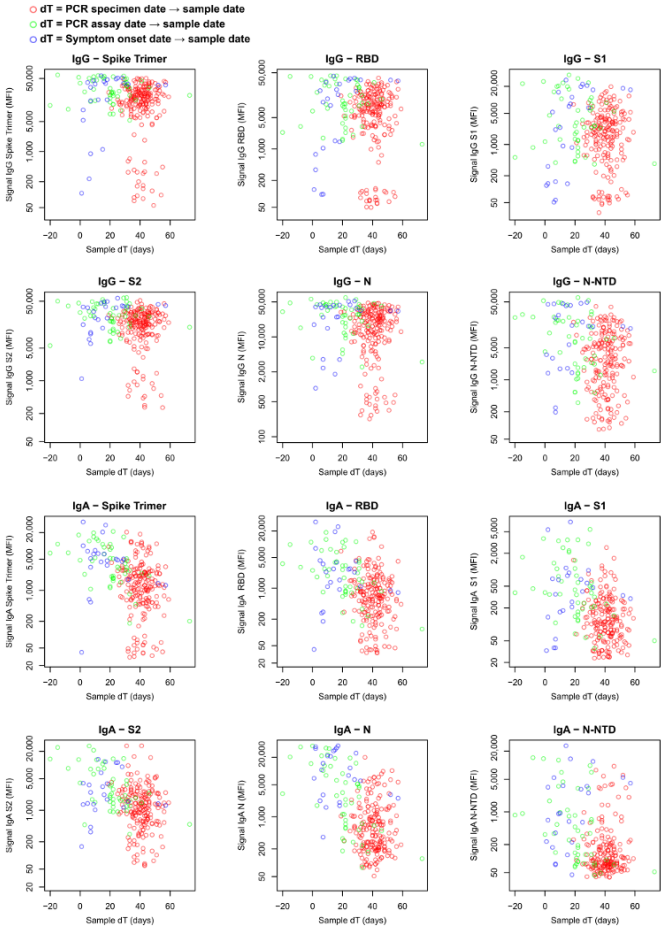

Supplementary Figure 5

Impact of sample time on antibody response is visualized by scatter plots. Sample dT in days is displayed against the observed MFI signal per antigen. Definition of dT is not consistent as samples measured in this study were taken from various sources. dT was calculated from the day of a positive PCR result (red circles), from the day of the PCR test itself (green circles) or from the day of symptom onset (blue circles). Source data are provided as a Source Data file.

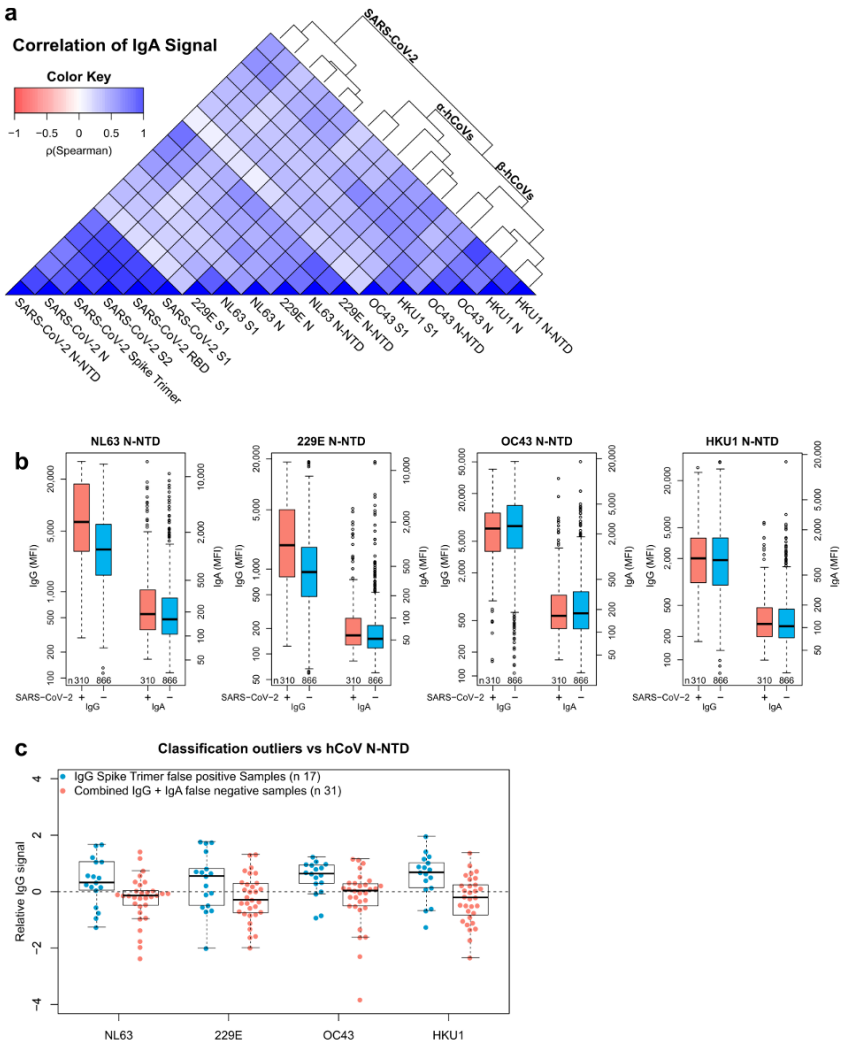
a
Correlation of IgA Signal
Color Key
−1 −0.5 0 0.5 1
ρ(Spearman)
SARS-CoV-2
α-hCoVs
β-hCoVs
SARS-CoV-2 N-NTD
SARS-CoV-2 N
SARS-CoV-2 Spike Trimer
SARS-CoV-2 S2
SARS-CoV-2 RBD
SARS-CoV-2 S1
229E S1
NL63 S1
NL63 N
229E N
NL63 N-NTD
229E N-NTD
OC43 S1
HKU1 S1
OC43 N-NTD
OC43 N
HKU1 N
HKU1 N-NTD
b
NL63 N-NTD
229E N-NTD
OC43 N-NTD
HKU1 N-NTD
IgG (MFI)
IgA (MFI)
SARS−CoV−2
IgG
IgA
c
Classification outliers vs hCoV N-NTD
IgG Spike Trimer false positive Samples (n 17)
Combined IgG + IgA false negative samples (n 31)
Relative IgG signal
NL63
229E
OC43
HKU1

Supplementary Figure 6

a, Correlation of IgA response for the entire sample set (n=1176) is visualized as heatmap based on Spearman's ρ coefficient; dendrogram on the right side displays antigens after hierarchical clustering was performed. **b,** Immune response (IgG and IgA) towards hCoV N-NTD proteins are presented as Box-Whisker plots of sample MFI on a logarithmic scale for SARS-CoV-2-infected (red, n=310) and uninfected (blue, n=866) individuals. Box represents the median and the 25th and 75th percentiles, whiskers show the largest and smallest values. Outliers determined by 1.5 times IQR of log-transformed data are depicted as circles. **c,** Relative levels of IgG-specific immune response towards hCoV N-NTD proteins are presented as Box-Whisker plots / stripchart overlays of log-transformed and per-antigen scaled and centred MFI for the sample subsets of Spike Trimer false positives (blue, n=17) and combined IgG + IgA false negatives (red, n=31). Box represents the median and the 25th and 75th percentiles, whiskers show the largest and smallest values, excluding outliers as determined by 1.5 times IQR. Source data are provided as a Source Data file.

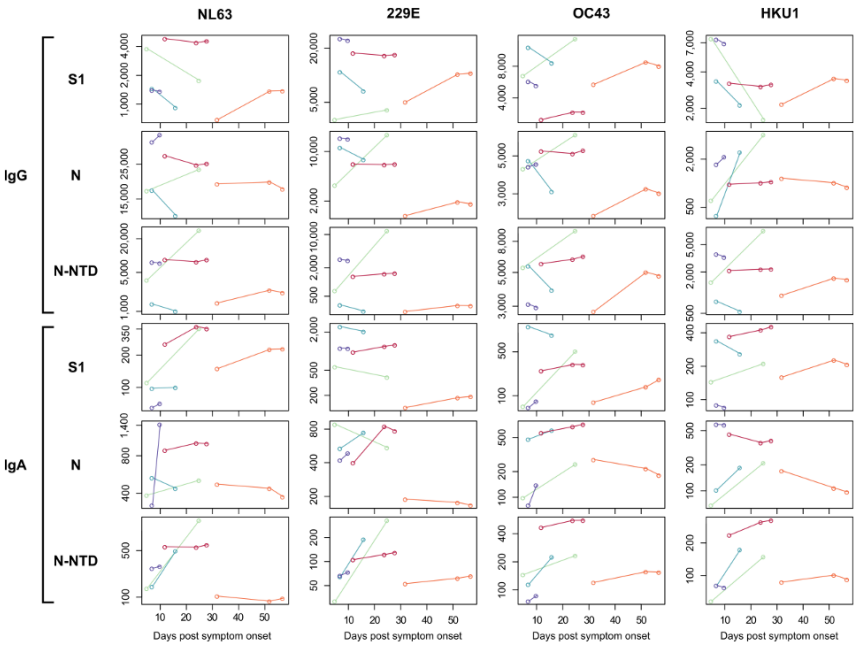

Supplementary Figure 7

Kinetic of hCoV antigen-specific IgA and IgG responses is shown for indicated days after symptom onset for the three used hCoV antigens across five different patients. Colored lines indicated kinetic of respective SARS-CoV-2 antigen per patient. Source data are provided as a Source Data file.

Supplementary Table 1 | Assay Variance and LOD

Intra- and inter-assay variance were determined by repeated measurement of QC samples and blank sample as replicates on one plate and in duplicates over 17 plates, respectively. Standard deviation relative to mean (%CV) is given for each antigen. A limit of detection (LOD) was calculated from 24 blank sample replicates on the same plate as the mean MFI + 3 times standard deviation.

			SARS-CoV-2						hCoV NL63			hCoV 229E			hCoV OC43			hCoV HKU1		
			Spike Trimer	RBD	S1	S2	N	N-NTD	S1	N	N-NTD	S1	N	N-NTD	S1	N	N-NTD	S1	N	N-NTD
Inter-assay variance (%CV) n = 34, duplicates, 17 plates	IgG	QC1	3.7	3.3	3.4	3.7	2.8	7.4	3.5	3.2	4.4	3.3	2.8	5.2	3.1	6.0	4.4	3.4	4.7	5.4
		QC2	4.1	4.6	6.9	3.4	5.3	4.8	3.0	2.2	6.3	2.4	2.1	6.7	2.7	4.5	2.3	2.7	5.1	2.8
		QC3	3.4	2.4	2.3	3.6	2.1	4.6	3.1	2.5	3.5	2.9	2.0	4.7	2.9	6.4	4.6	3.2	3.2	3.5
		Blank	5.4	5.6	6.7	6.4	5.6	6.1	6.3	7.1	5.7	9.1	6.1	6.1	5.6	7.3	4.1	4.9	6.1	8.3
	IgA	QC1	3.9	4.6	4.9	4.0	5.1	5.0	4.2	3.6	3.9	4.0	5.3	7.4	4.3	7.4	5.0	4.2	6.0	5.0
		QC2	4.6	5.0	5.1	3.9	3.9	4.2	3.7	2.4	7.6	2.9	2.2	6.0	4.1	16.4	4.2	4.3	5.5	3.9
		QC3	3.9	3.8	4.5	3.4	3.4	4.8	3.9	2.8	4.0	3.0	5.1	4.5	3.6	6.1	4.1	3.7	4.5	5.1
		Blank	6.7	5.3	8.2	6.3	5.3	5.3	3.3	5.0	5.0	6.7	7.0	6.1	5.3	7.1	4.7	6.0	6.8	6.3
Intra-assay variance (%CV) n = 24	IgG	QC1	2.5	1.9	2.0	2.1	1.8	2.1	2.4	1.7	2.8	2.0	2.7	3.2	1.9	2.0	2.2	2.7	2.4	2.2
		QC2	5.9	4.3	4.1	2.8	2.7	3.2	1.9	1.9	2.6	2.0	2.2	2.7	2.2	1.6	2.1	2.5	3.1	2.5
		QC3	1.6	4.3	5.1	1.9	1.9	4.5	4.2	1.7	3.2	3.3	4.1	5.7	3.2	3.1	5.5	5.6	6.0	8.4
		Blank	6.0	5.6	5.2	5.8	5.2	4.2	5.0	4.8	4.8	7.3	6.2	6.3	6.5	6.2	4.4	6.1	6.0	6.2
	IgA	QC1	2.5	3.3	5.2	3.8	3.7	4.2	3.2	2.3	2.2	2.0	4.8	4.7	2.9	4.7	3.4	3.3	4.5	4.3
		QC2	4.8	5.7	5.7	3.2	4.1	4.3	3.4	2.0	5.7	2.1	2.1	6.1	3.0	3.1	1.9	3.9	6.4	3.8
		QC3	3.1	4.7	5.5	3.0	4.1	4.4	3.7	2.7	3.7	2.7	5.4	5.8	2.6	4.1	3.1	2.4	4.5	4.3
		Blank	5.8	5.3	6.3	5.0	5.4	5.5	4.5	5.6	5.3	7.2	6.3	7.0	6.7	9.5	7.3	5.2	8.8	7.0
LOD (MFI) n = 24	IgG		32	26	23	29	38	33	29	28	26	65	35	24	33	30	33	37	33	25
	IgA		31	26	26	27	37	32	57	28	40	28	36	22	35	28	32	33	39	28

Supplementary Table 2 | Complete overview of study sample set divided into columns by age groups and sex.
Samples from SARS-CoV-2-infected donors are further split up by hospitalization status. Age and gender of patients from which multiple samples were available for time course analyses are indicated. SARS-CoV-2-uninfected samples are further divided into samples drawn during the pandemic, which was defined as all samples taken on 01.01.2020 or later, and pre-pandemic samples. 147 samples with previous hCoV infection were included in the SARS-CoV-2-uninfected group. Detailed diagnosis of hCoV subspecies is indicated where available. Other sample conditions for special groups of uninfected samples are listed. NA: Information was not available.

Age	≤39				40-59				≥60				NA				∑
n	299 (25.4 %)				241 (20.5 %)				475 (40.4 %)				161 (13.7 %)				1176
Sex	male		female		male		female		male		female		male		female		NA		
n	139	(11.8 %)	160	(13.6 %)	144	(12.2 %)	97	(8.2 %)	271	(23.0 %)	204	(17.3 %)	5	(0.4 %)	3	(0.3 %)	153	(13.0 %)	1176
SARS-CoV-2-infected (total)	60	(19.4 %)	51	(16.5 %)	71	(22.9 %)	63	(20.3 %)	42	(13.5 %)	17	(5.5 %)	3	(1.0 %)	3	(1.0 %)	0	(0.0 %)	310
Hospitalized (for COVID19)	6	(10.9 %)	2	(3.6 %)	14	(25.5 %)	6	(10.9 %)	23	(41.8 %)	4	(7.3 %)	0	(0.0 %)	0	(0.0 %)	0	(0.0 %)	55
Non-Hospitalized	52	(25.0 %)	43	(20.7 %)	49	(23.6 %)	43	(20.7 %)	13	(6.3 %)	8	(3.8 %)	0	(0.0 %)	0	(0.0 %)	0	(0.0 %)	208
Hospitalisation NA	2	(4.3 %)	6	(12.8 %)	8	(17.0 %)	14	(29.8 %)	6	(12.8 %)	5	(10.6 %)	3	(6.4 %)	3	(6.4 %)	0	(0.0 %)	47
Patients with time series	2	(40.0 %)	0	(0.0 %)	0	(0.0 %)	0	(0.0 %)	2	(40.0 %)	1	(20.0 %)	0	(0.0 %)	0	(0.0 %)	0	(0.0 %)	5
SARS-CoV-2-uninfected (total)	79	(9.1 %)	109	(12.6 %)	73	(8.4 %)	34	(3.9 %)	229	(26.4 %)	187	(21.6 %)	2	(0.2 %)	0	(0.0 %)	153	(17.7 %)	866
Sample during pandemic	10	(15.4 %)	10	(15.4 %)	12	(18.5 %)	14	(21.5 %)	7	(10.8 %)	5	(7.7 %)	1	(1.5 %)	0	(0.0 %)	6	(9.2 %)	65
Sample pre-pandemic	69	(8.6 %)	99	(12.4 %)	61	(7.6 %)	20	(2.5 %)	222	(27.7 %)	182	(22.7 %)	1	(0.1 %)	0	(0.0 %)	147	(18.4 %)	801
Previous hCoV Infection	19	(12.9 %)	18	(12.2 %)	45	(30.6 %)	20	(13.6 %)	29	(19.7 %)	16	(10.9 %)	0	(0.0 %)	0	(0.0 %)	0	(0.0 %)	147
confirmed NL63	2	(20.0 %)	0	(0.0 %)	3	(30.0 %)	1	(10.0 %)	2	(20.0 %)	2	(20.0 %)	0	(0.0 %)	0	(0.0 %)	0	(0.0 %)	10
confirmed 229	5	(25.0 %)	1	(5.0 %)	4	(20.0 %)	1	(5.0 %)	5	(25.0 %)	4	(20.0 %)	0	(0.0 %)	0	(0.0 %)	0	(0.0 %)	20
confirmed OC43	0	(0.0 %)	1	(3.7 %)	14	(51.9 %)	1	(3.7 %)	6	(22.2 %)	5	(18.5 %)	0	(0.0 %)	0	(0.0 %)	0	(0.0 %)	27
confirmed HKU1	3	(20 %)	1	(6.7 %)	4	(26.7 %)	2	(13.3 %)	5	(33.3 %)	0	(0.0 %)	0	(0.0 %)	0	(0.0 %)	0	(0.0 %)	15
unknown hCoV	9	(12 %)	15	(20.0 %)	20	(26.7 %)	15	(20.0 %)	11	(14.7 %)	5	(6.7 %)	0	(0.0 %)	0	(0.0 %)	0	(0.0 %)	75
Pregnant	0	(0.0 %)	9	(90.0 %)	0	(0.0 %)	1	(10.0 %)	0	(0.0 %)	0	(0.0 %)	0	(0.0 %)	0	(0.0 %)	0	(0.0 %)	10
RF/HAMA samples	0	(0.0 %)	0	(0.0 %)	0	(0.0 %)	0	(0.0 %)	0	(0.0 %)	0	(0.0 %)	0	(0.0 %)	0	(0.0 %)	6	(100 %)	6
PCT > 3 ng/mL	0	(0.0 %)	0	(0.0 %)	0	(0.0 %)	0	(0.0 %)	0	(0.0 %)	0	(0.0 %)	0	(0.0 %)	0	(0.0 %)	21	(100 %)	21
Neuroinflammatory disease	6	(40.0 %)	6	(40.0 %)	1	(6.7 %)	0	(0.0 %)	1	(6.7 %)	1	(6.7 %)	0	(0.0 %)	0	(0.0 %)	0	(0.0 %)	15

Supplementary Table 3 - Percentage Identity of sequence alignments of used hCoV and corresponding SARS-CoV-2.
Alignments were calculated using version 1.2.4. of Clustal Omega[3]. Sequences of constructs used in alignment are provided as a Source Data file.

		% of sequence identity of corresponding antigen				
Protein	Identifier	hCoV-NL63	hCoV-229E	SARS-CoV-2	hCoV-OC43	hCoV-HKU1
hCoV-NL63 S1	APF29071.1	100.0	50.2	17.8	19.7	18.1
hCoV-229E S1	APT69883.1	50.2	100.0	18.5	20.2	18.7
SARS-CoV-2 S1	QHD43416.1	17.8	18.5	100.0	24.2	24.2
hCoV-OC43 S1	AVR40344.1	19.7	20.2	24.2	100.0	58.0
hCoV-HKU1 S1	AGW27881.1	18.1	18.7	24.2	58.0	100.0
hCoV-NL63 N	YP_003771.1	100.0	47.5	30.9	29.0	29.7
hCoV-229E N	NP_073556.1	47.5	100.0	30.4	30.1	32.2
SARS-CoV-2 N	QHD43423.2	30.9	30.4	100.0	37.1	36.7
hCoV-OC43 N	YP_009555245.1	29.0	30.1	37.1	100.0	65.5
hCoV-HKU1 N	YP_173242.1	29.7	32.2	36.7	65.5	100.0
hCoV-NL63 N-NTD	YP_003771.1	100.0	63.4	35.3	34.4	35.8
hCoV-229E N-NTD	NP_073556.1	63.4	100.0	38.2	37.9	39.2
SARS-CoV-2 N-NTD	QHD43423.2	35.3	38.2	100.0	42.0	42.8
hCoV-OC43 N-NTD	YP_009555245.1	34.4	37.9	42.0	100.0	68.3
hCoV-HKU1 N-NTD	YP_173242.1	35.8	39.2	42.8	68.3	100.0

Supplementary Table 4 | Overview of primers used in this study with respective sequence.

Primer	Sequence
pRSET2b down-for	GGTAAGCTTGATCCGGCTGCTAA
SARS-CoV2_NTD-rev	GGGAAGCTTACTCAGCATAGAAGCCCTTTGG
OC43_NTD-rev	GGGAAGCTTATTCGATATAATAGCCCTGCGG
NL63_NTD-rev	GGGAAGCTTATTCAACAACGCTCAGTTCCG
229E_NTD-rev	GGGAAGCTTATTCAACAACGGTAACACCATTC
HKU1_NTD-rev	GGGAAGCTTATTCCACATAGTAGCCCTGAGGC
S1 CoV2-for	CTTCTGGCGTGTGACCGG
S1 CoV2-rev	GTTGCGGCCGCTTAGTGGTGGTGGTGGTGGGGGCTGTTTGTCTGTGTCTG

Supplementary Table 5 | Overview of antigens used in this study.

Construct	Manufacturer	Sequence Identifier	Fragment	Mutations	Expression system	Tag	Tag position
SARS-CoV-2 Spike Trimer	In-house expressed	QHD43416.1	1-1213	^{682}RRAR to A, K986P and V987P	Expi293	Thrombin cleavage-site/ T4 foldon/ His_6	C-terminus
SARS-CoV-2 RBD	In-house expressed	QHD43416.1	1-14 + 319-541		Expi293	His_6	C-terminus
SARS-CoV-2 S2	Sino Biological #40590-V08B	YP_009724390.1	686-1213		Baculovirus-Insect cells	His_6	C-terminus
SARS-CoV-2 S1	In-house expressed	QHD43416.1	1-681		Expi293	His_6	C-terminus
hCoV-OC43 S1	In-house expressed	AVR40344.1	1-760		Expi293	His_6	C-terminus
hCoV-NL63 S1	In-house expressed	APF29071.1	1-744		Expi293	His_6	C-terminus
hCoV-229E S1	In-house expressed	APT69883.1	1-561		Expi293	His_6	C-terminus
hCoV-HKU1 S1	In-house expressed	AGW27881.1	1-755		Expi293	His_6	C-terminus
SARS-CoV-2 N	Aalto Bioreagents #CK 6406-b	NA	full length		*E. coli*	His_6	C-terminus
SARS-CoV-2 N-NTD	In-house expressed	QHD43423.2	1-174		*E.coli* BL21	His_6	N-terminus
hCoV-OC43 N	In-house expressed	YP_009555245.1	1-448		*E.coli* BL21	His_6	N-terminus
hCoV-OC43 N-NTD	In-house expressed	YP_009555245.1	1-189		*E.coli* BL21	His_6	N-terminus
hCoV-NL63 N	In-house expressed	YP_003771.1	1-377		*E.coli* BL21	His_6	N-terminus
hCoV-NL63 N-NTD	In-house expressed	YP_003771.1	1-139		*E.coli* BL21	His_6	N-terminus
hCoV-229E N	In-house expressed	NP_073556.1	1-389		*E.coli* BL21	His_6	N-terminus
hCoV-229E N-NTD	In-house expressed	NP_073556.1	1-141		*E.coli* BL21	His_6	N-terminus
hCoV-HKU1 N	In-house expressed	YP_173242.1	1-441		*E.coli* BL21	His_6	N-terminus
hCoV-HKU1 N-NTD	In-house expressed	YP_173242.1	1-188		*E.coli* BL21	His_6	N-terminus

For commercial antigens, catalogue number is given and information is provided as available from the data sheets. NA: Information was not available.

Supplementary References

1 Fawcett, T. An introduction to ROC analysis. *Pattern recognition letters* **27**, 861-874 (2006).

2 Zou, K. H., O'Malley, A. J. & Mauri, L. Receiver-operating characteristic analysis for evaluating diagnostic tests and predictive models. *Circulation* **115**, 654-657 (2007).

3 Madeira, F. *et al.* The EMBL-EBI search and sequence analysis tools APIs in 2019. *Nucleic acids research* **47**, W636-W641 (2019).

Appendix II: COVID-19 patient serum less potently inhibits ACE2-RBD binding for various SARS-CoV-2 RBD mutants

Junker D, Dulovic A, Becker M, Wagner TR, Kaiser PD, Traenkle B, Kienzle K, Bunk S, Struemper C, Haeberle H, Schmauder K, Ruetalo N, Malek N, Althaus K, Koeppen M, Rothbauer U, Walz JS, Schindler M, Bitzer M, Göpel S, Schneiderhan-Marra N.
Scientific Reports. 2022. 12(1):7168
https://doi.org/10.1038/s41598-022-10987-2

www.nature.com/scientificreports

scientific reports

Check for updates

OPEN

COVID-19 patient serum less potently inhibits ACE2-RBD binding for various SARS-CoV-2 RBD mutants

Daniel Junker[1], Alex Dulovic[1], Matthias Becker[1], Teresa R. Wagner[1,2], Philipp D. Kaiser[1], Bjoern Traenkle[1], Katharina Kienzle[3], Stefanie Bunk[3], Carlotta Struemper[3], Helene Haeberle[4], Kristina Schmauder[5,6], Natalia Ruetalo[7], Nisar Malek[3,8], Karina Althaus[9], Michael Koeppen[4], Ulrich Rothbauer[1,2], Juliane S. Walz[10,11,12,13], Michael Schindler[7], Michael Bitzer[3,8], Siri Göpel[3,6,14]✉ & Nicole Schneiderhan-Marra[1,14]✉

As global vaccination campaigns against SARS-CoV-2 proceed, there is particular interest in the longevity of immune protection, especially with regard to increasingly infectious virus variants. Neutralizing antibodies (Nabs) targeting the receptor binding domain (RBD) of SARS-CoV-2 are promising correlates of protective immunity and have been successfully used for prevention and therapy. As SARS-CoV-2 variants of concern (VOCs) are known to affect binding to the ACE2 receptor and by extension neutralizing activity, we developed a bead-based multiplex ACE2-RBD inhibition assay (RBDCoV-ACE2) as a highly scalable, time-, cost-, and material-saving alternative to infectious live-virus neutralization tests. By mimicking the interaction between ACE2 and the RBD, this serological multiplex assay allows the simultaneous analysis of ACE2 binding inhibition to the RBDs of all SARS-CoV-2 VOCs and variants of interest (VOIs) in a single well. Following validation against a classical virus neutralization test and comparison of performance against a commercially available assay, we analyzed 266 serum samples from 168 COVID-19 patients of varying severity. ACE2 binding inhibition was reduced for ten out of eleven variants examined compared to wild-type, especially for those displaying the E484K mutation such as VOCs beta and gamma. ACE2 binding inhibition, while highly individualistic, positively correlated with IgG levels. ACE2 binding inhibition also correlated with disease severity up to WHO grade 7, after which it reduced.

Neutralizing antibodies (Nabs) prevent infection of the cell with pathogens or foreign particles by neutralizing them, eliminating a potential threat and rendering the pathogen or particle harmless[1]. The longevity of a Nab response has important implications for immune protection and vaccination strategies. In SARS-CoV-2, Nabs interfere with the cell entry mechanism primarily by blocking the interaction of the receptor binding domain

[1]NMI Natural and Medical Sciences Institute at the University of Tübingen, Markwiesenstrasse 55, 72770 Reutlingen, Germany. [2]Pharmaceutical Biotechnology, Eberhard Karls University, Tübingen, Germany. [3]Department Internal Medicine I, University Hospital Tübingen, Otfried-Müller-Strasse 10, 72076 Tübingen, Germany. [4]Department of Anesthesiology and Intensive Care Medicine, University Hospital Tübingen, Tübingen, Germany. [5]Institute for Medical Microbiology and Hygiene, University Hospital Tübingen, Tübingen, Germany. [6]German Center for Infection Research (DZIF), Partner Site Tübingen, Tübingen, Germany. [7]Institute for Medical Virology and Epidemiology, University Hospital Tübingen, Tübingen, Germany. [8]Center for Personalized Medicine, Eberhard Karls University, Tübingen, Germany. [9]Institute for Clinical and Experimental Transfusion Medicine, University Hospital Tübingen, Tübingen, Germany. [10]Department of Internal Medicine, Clinical Collaboration Unit Translational Immunology, German Cancer Consortium (DKTK), University Hospital Tübingen, Tübingen, Germany. [11]Department of Immunology, Institute for Cell Biology, University of Tübingen, Tübingen, Germany. [12]Cluster of Excellence iFIT (EXC2180) "Image-Guided and Functionally Instructed Tumor Therapies", University of Tübingen, Tübingen, Germany. [13]Dr. Margarete Fischer-Bosch-Institute for Clinical Pharmacology, Robert Bosch Center for Tumor Diseases (RBCT), Stuttgart, Germany. [14]These authors contributed equally: Siri Göpel and Nicole Schneiderhan-Marra. ✉email: siri.goepel@med.uni-tuebingen.de; Nicole.schneiderhan@nmi.de

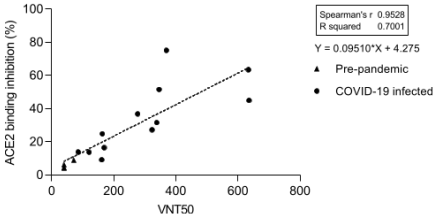

Figure 1. Comparison between RBDCoV-ACE2 and a virus neutralization test (VNT). Serum samples (n = 16) of pre-pandemic (n = 4) and COVID-19 convalescent (n = 12) individuals were measured using both assays and analyzed by linear regression. The equation of the dashed regression line is shown next to the graph. VNT results are depicted as half-maximal inhibiting serum dilutions (VNT50), RBDCoV-ACE2 results are shown in percentage inhibition of ACE2 binding. Correlation analysis was performed after Spearman and the correlation coefficient r is shown.

(RBD) with the human cell receptor angiotensin converting enzyme 2 (ACE2)[2,3]. The RBD of SARS-CoV-2 is target of approximately 90% of the neutralizing activity present in immune sera[4], with a lack of Nabs correlating with risk of fatal outcome[5,6]. Passive transfer of Nabs through convalescent serum or as monoclonal antibodies have been shown to provide protection from infection[7–9], with several Nabs drugs granted emergency use authorization by the U.S. Food and Drug Administration[10–13].

Since the first documented infections in Wuhan China[14], SARS-CoV-2 has continually evolved, with the emergence of global variants of concern (VOCs) being of particular importance. As of this moment, the WHO lists the alpha (B.1.1.7)[15], beta (B.1.351)[16], gamma (P.1)[17], delta (B.1.617.2)[18] and omicron (B.1.1.529)[19] strains as VOCs[20], in addition to further variants of interest (VOIs) such as lambda (C.37) [21]. The emergence and disappearance of variants and continual mutation of SARS-CoV-2 is of particular relevance for vaccine development, as all currently licensed vaccines[22–25] only elicit an immune response against the spike protein based on the original Wuhan-Hu-1 isolate (hereon referred to as "wild-type")[26,27]. Several studies have already found that both convalescent and post-vaccinated sera have lower neutralization capacities against beta and gamma VOCs[28–30]. Of particular concern are mutations on amino acid residue (aa) 484 (e.g. E484K), which seem to confer escape from vaccine control, with an additional mutation on aa 501 (e.g. N501Y) increasing this effect[31].

In order to lead development of new vaccines and safely lift social restrictions, definitive correlates of protective immunity are necessary[32]. The gold standard for Nabs assessment are virus neutralization tests (VNTs), however these require live infectious virions which must be handled in biosafety level 3 (BSL3) laboratories, as well as access to variant strains of SARS-CoV-2. In this study, we developed and applied RBDCoV-ACE2, a multiplex ACE2-RBD inhibition assay based upon the antibody-mediated inhibition of ACE2-RBD binding. This automatable assay enables simultaneous screening of serum samples for the presence of Nabs against a great number of VOCs/VOIs in a single well, making it a time-, material- and cost-effective alternative to live VNTs or classical ELISAs. Following in-depth validation of the assay, we analyzed the IgG antibody response and ACE2 binding inhibition of 266 serum samples from 168 COVID-19 patients with mild to severe disease progression towards eleven different SARS-CoV-2 variant RBDs including the alpha, beta, gamma and delta VOCs.

Results

ACE2-RBD inhibition assay (RBDCoV-ACE2) validation. To investigate the inhibition of ACE2 binding by SARS-CoV-2 VOCs, we developed and established a high-throughput bead-based multiplex ACE2-RBD inhibition assay (from here on referred to as "RBDCoV-ACE2"). This assay mimics the ACE2-RBD interaction and thereby detects the presence of Nabs against SARS-CoV-2 that inhibit this interaction. At the time of experimentation, RBDCoV-ACE2 contained the RBDs of SARS-CoV-2 wild-type and 11 different variants (alpha, beta, gamma, epsilon, eta, theta, kappa, delta, lambda, Cluster 5 and A.23.1).

To validate the assay, we both compared performance to a standard VNT (Fig. 1), as well as completed technical validation to FDA bioanalytical guidelines verifying reagent stability, assay precision, freeze–thaw stability and parallelism (Figure S1). An assay validation sample set of 16 samples (12 convalescent, 4 pre-pandemic) was measured by VNT against wild-type and with RBDCoV-ACE2. The results of both assays showed a strong correlation (Spearman's rank 0.95), confirming that RBDCoV-ACE2 is measuring neutralizing antibodies specifically (Fig. 1). Technical validation performed with a set of 6 samples (4 vaccinated, 1 infected, 1 pre-pandemic) confirmed that RBDCoV-ACE2 is highly reproducible, as seen by the low intra- and inter-assay variation (all CVs under 5% and 7% respectively, Figure S1a and b, Table S3). ACE2 buffer was shown to be stable both in storage (4 °C) and at room temperature (21 °C), with minimal loss in performance compared to freshly prepared buffer (Figure S1c). Similarly, the biotinylated ACE2 stock solution showed high freeze–thaw stability (all CVs under 13%, Figure S1d). Parallelism was used to optimize the assay conditions and to ensure that the ACE2 concentration was in linear range (Figure S1e). Percentage coefficients of variation (%CV) of all technical validation experiments for every analyzed sample are summarized in Table S3. Lastly, to ensure that the multiplex nature of the assay was not causing competition between beads for ACE2 which would have resulted in artificially

a

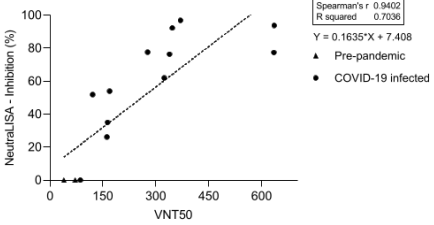

b

		RBDCoV-ACE2 (% ACE2 binding inhibition)	
NeutraLISA (% Inhibition)		≤ 20 %	> 20%
	≤ 20 %	51 (30.4 %)	4 (2.4 %)
	> 20 %	20 (11.9 %)	93 (55.4 %)
Spearman's r [95% CI]		0.8396 [0.7867; 0.8802]	

c

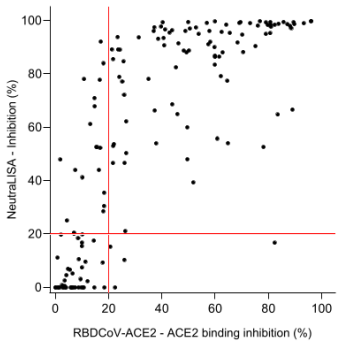

Figure 2. Correlation between SARS-CoV-2 NeutraLISA and VNT and comparison to RBDCoV-ACE2. (**a**) Correlation and linear regression between NeutraLISA and VNT results for pre-pandemic (n = 4) and COVID-19 infected (n = 12) samples. Correlation analyses were performed after Spearman and correlation coefficients r are shown. (**b**) Descriptive statistics of the (**c**) correlation between NeutraLISA and RBDCoV-ACE2. One sample from each individual (n = 168) was measured using both assays. Correlation was calculated after Spearman. Samples were classified as being negative (non-neutralizing) if they had a value below 20% (red lines).

deflated values, the assay was performed as both a singleplex (for all VOCs) and multiplex with 24 samples (19 COVID-19 infected, 5 pre-pandemic), with no difference in performance between the two bead compositions found (Figure S2).

RBDCoV-ACE2 comparison to commercially available assay. To compare RBDCoV-ACE2 performance to a similar commercially available inhibition assay, we initially tested our assay validation sample set on NeutraLISA and compared its performance to the VNT (Fig. 2a). While the results of the two assays did correlate (Spearman's rank 0.94), the NeutraLISA appeared to reach a plateau and saturate, as seen by the high inhibition percentage for all samples with a VNT50 greater than 350. To confirm this plateau effect, we analyzed a subset of samples from our COVID-19 sample collection on both RBDCoV-ACE2 and the NeutraLISA, finding that while a strong correlation between the results existed (Spearman's rank 0.84, Fig. 2b), the saturation plateau was still present (Fig. 2c). This suggests that RBDCoV-ACE2 has a more dynamic range and better resolution, especially in the higher inhibition percentages. When classifying samples as being either positive or negative, samples with an inhibition percentage under 20% are considered negative for the NeutraLISA[33]. As both assays detect bound ACE2, we implemented a similar cut-off for RBDCoV-ACE2. Overall, 30.4% of samples (51/168) were considered negative in both assays, while a further 55.4% (93/168) were considered positive in both (Fig. 2b). Of the remaining samples, 4 (2.4%) exceeded 20% binding inhibition only in RBDCoV-ACE2, while 20 (11.9%)

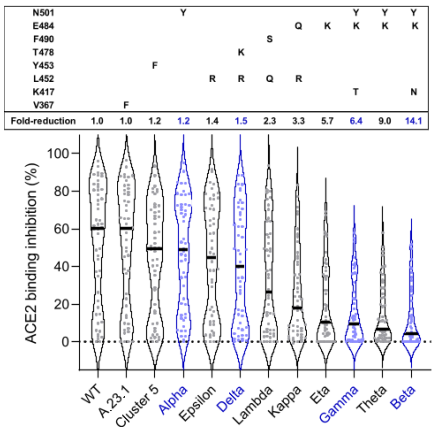

Figure 3. ACE2 binding inhibition varies between RBD mutants. Violin plots showing ACE2 binding inhibition (%) of individual serum samples from 7 to 49 days post PCR (n = 50, depicted as dots) against RBD mutants. Black horizontal lines represent medians. Fold-reduction of ACE2 binding inhibition in comparison to wild-type corresponds to the ratio between the medians of wild-type and the respective RBD mutant. VOC-RBDs are shown in blue. Mutations of each RBD mutant are shown in the box above the violin plot.

exceeded 20% inhibition in the NeutraLISA only. Overall, the stronger correlation between RBDCoV-ACE2 and VNT (Fig. 1) compared to NeutraLISA and VNT, as well as the increased dynamic range, proves RBDCoV-ACE2 has superior assay performance.

ACE2 binding inhibition is reduced for mutant RBDs. Having developed and validated RBDCoV-ACE2, as well as identifying superior performance to a commercially available kit, we then analyzed ACE2 binding inhibition within 266 serum samples from 168 COVID-19 patients (COVID-19 sample collection), including longitudinal samples from 35 donors. Samples were measured against RBD wild-type and 11 variants (hereafter referred to as "RBD mutants") of SARS-CoV-2. All RBD mutants except A.23.1 showed reduced ACE2 binding inhibition compared to wild-type (1.2-fold (Cluster 5) to 14.1-fold (beta), Fig. 3) in serum samples taken within the first 49 days post initial positive PCR test. In the set of tested VOCs, alpha had the lowest reduction in ACE2 binding inhibition (1.2-fold), followed by delta (1.5-fold), gamma (6.4-fold) and beta (14.1-fold). While reduction in ACE2 binding inhibition was variant-specific, mutations at critical residues (e.g. E484K) appeared to have the largest effect (Fig. 3). Among the current and former VOIs, epsilon had the lowest reduction (1.4 fold), followed by lambda (2.3 fold), kappa (3.3 fold), eta (5.7 fold) and theta (9.0 fold).

ACE2 binding inhibition correlates with antibody production against spike domains. To determine if a correlation existed between ACE2 binding inhibition and RBD-specific antibody levels, we analyzed all samples with MULTICOV-AB[34]. ACE2 binding inhibition and SARS-CoV-2 RBD IgG antibody responses were positively correlated (all Spearman's correlation coefficients above 0.70, Fig. 4) with variant-specific differences still present and reflecting. Additionally, we could show the positive correlation between ACE2 binding inhibition and S1/trimeric spike antibody production (Figure S3a and b). The ACE2 binding inhibitions of both S1 and trimeric spike coated beads compared to the inhibition of RBD beads were strongly correlated (all Spearman's correlation coefficients above 0.95) (Figure S3c and d). In contrast, beads coated with the SARS-CoV-2 spike S2 domain, which does not interact with ACE2 in vivo, showed no ACE2 binding in our assay. Those findings confirm specific binding of ACE2 to its natural binding partners and therefore reaffirms that the presence of neutralizing antibodies is being detected. For all RBD mutants, the increase in ACE2 binding inhibition most commonly occurred once IgG RBD MFI levels exceeded 10,000 (Fig. 4). Notably, there was individual variation among the samples, with some having high ACE2 binding inhibition but relatively low IgG responses. For RBD mutants with a E484K mutation (eta, gamma, theta and beta), more than 78% of all samples were considered negative, compared to 42% for wild-type (Fig. 4).

ACE2 binding inhibition decreases over time. To examine whether ACE2 binding inhibition changes over time, we analyzed longitudinal samples from 35 study participants (range 1–290 days post-initial positive PCR). ACE2 binding inhibition and RBD antibody titers originally remained low directly following a positive

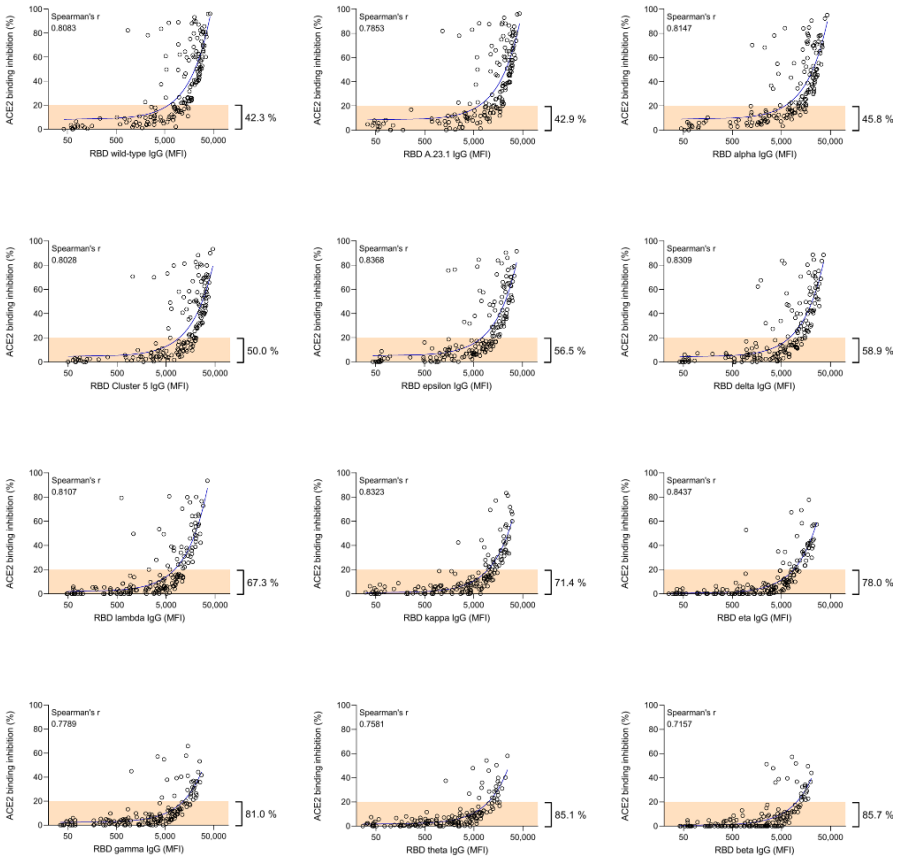

Figure 4. Correlation between anti-RBD IgG MFI signals and ACE2 binding inhibition (%) of serum samples from COVID-19 patients for wild-type and 11 RBD mutants. Regression analysis comparing ACE2 binding inhibition (%) and IgG responses (MFI) for wild-type and all RBD mutants included in the study. Each circle represents one sample (n = 168). For longitudinal donors with more than one sample available, the sample closest to 20 days post positive PCR diagnosis was selected. The percentage next to the bracket indicates the proportion of samples with ACE2 binding inhibition ≤ 20% (in orange). Spearman's correlation coefficient (r) is specified for every correlation.

test, before rapidly increasing (mean peak at day 23 post-PCR) and then decreasing (Fig. 5a,b). Due to the highly individualistic nature of the responses, we confirmed this pattern by analyzing a subset of six individuals with similar sample collection points (Fig. 5c,d). As delta represents the current dominant global strain, we then examined whether any differences in ACE2 binding inhibition and antibody binding were present within this variant compared to wild-type. Overall, ACE2 binding inhibition and IgG response followed the same pattern for all samples as for wild-type (Fig. 5e,f). We then confirmed that this pattern was true for all RBD variants (Fig. 5g,h). As expected, while there were differences in reduction in binding inhibition between the variants, all variants examined follow the same pattern of binding inhibition over time.

ACE2 binding inhibition correlates with disease severity. We then examined correlations between ACE2 binding inhibition and COVID-19 disease severity within our population of COVID-19 patients. The severity of COVID-19 infection was determined according to the WHO grading scale. For analysis purposes,

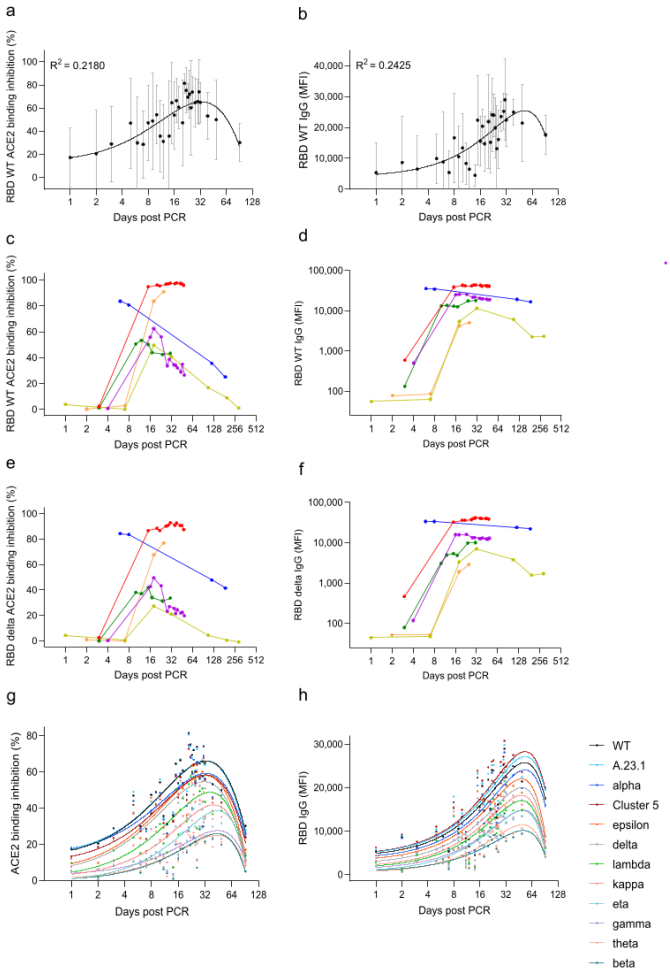

Figure 5. Longitudinal analysis of ACE2 binding inhibition and anti-RBD IgG levels in COVID-19 patients. Mean ACE2 binding inhibition (%) and IgG responses (MFI) for wild-type RBD against time post positive PCR test for samples (n = 149) taken from 1 to 92 days post PCR are shown (**a**,**b**). Black dots indicate mean responses with standard deviation indicated by the error bars. The same analysis is then shown for longitudinal samples of selected donors (n = 6) for wild-type (**c**,**d**) and RBD delta (**e**,**f**). For all RBD mutants, mean ACE2 binding inhibition (%) and mean IgG responses (MFI) 1 to 92 days post PCR are shown (**g**,**h**). Each variant is illustrated by a different color according to the figure key.

samples were split into two separate timeframes, 7–49 days post-initial positive PCR and ≥ 50 days post-initial positive PCR, in order to examine both the log and lag stages of infection. While all WHO grades (except for 5 and 8 for samples ≥ 50 days post-initial positive PCR) were represented within both timeframes, the early

log timeframe consisted mostly of samples in WHO grades 4 and 6, while the later lag timeframe samples were mostly WHO grades 2 to 4. ACE2 binding inhibition was examined for both WT and delta to confirm no differences between wild-type and the variants existed. Regardless of timeframe, ACE2 binding inhibition increased as disease severity increased. Within the early log timeframe, ACE2 binding inhibition for wild-type and delta RBD increased steadily with disease severity up to grade 7 (WHO grading scale, hospitalized patients needing intubation and mechanical ventilation), before decreasing for patients of grade 8 (fatal disease course) (Fig. 6a,b). Within the later lag timeframe, ACE2 binding inhibitions increased with disease severity (Fig. 6c,d), however there was an overall reduction for grades 4 to 7 compared to the early timeframe for both wild-type and delta (Fig. 6c,d). As expected, anti-RBD IgG levels also correlated with disease severity in both timeframes for wild-type and delta (Fig. 6e–h). Peak mean IgG levels were observed at grade 6 severity for wild-type and grade 7 for delta, 7–49 days post PCR. Post 49 days, mean IgG levels peaked for patients with grade 6 severity. As confirmation, confounding variables (age, gender, BMI) were examined for any potential effect on the results (Figure S4). While gender had no effect, we did find correlations between ACE2 binding inhibition and donor age for samples taken ≥ 50 days post-positive PCR ($p = 0.0001$), as well as BMI for samples collected in both timeframes (< 49 days $p = 0.0330$, ≥ 50 days $p = 0.0017$) (Figure S4d-f).

Discussion

With vaccination campaigns now increasingly focusing on the role of booster doses, the quality of immune protection against SARS-CoV-2 in view of constantly emerging variants is of great interest. Whereas in the early-phase of the pandemic SARS-CoV-2 antibody assays were helpful in determining seroprevalence and support vaccine development, now a reliable correlate of immune protection is needed to securely lift social restrictions and guide future vaccine developments.

We show here that the performance of RBDCoV-ACE2 correlates strongly with classical VNTs, confirming that the assay is measuring the activity of neutralizing antibodies, while our technical validation also confirms RBDCoV-ACE2 is stable and reproducible. While cell-culture based VNTs (e.g. plaque reduction neutralization test) are the gold standard for neutralization assays, they have many disadvantages over conventional protein-based surrogate assays. Such assays require rapid access to continually changing virus variants and as such special biosafety level 3 laboratories are necessary. Additionally, VNTs are cell-culture based and therefore it takes multiple days to conduct an experiment with reproducibility potentially affected by either the cells or their long culture conditions. Consequently, highly reproducible assays under substantially faster and safer working conditions (e.g. BSL 1) would be highly beneficial. RBDCoV-ACE2 is finished in under 4 h and only requires 5 µL of patient sample to measure ACE2 binding inhibition simultaneously against multiple SARS-CoV-2 VOCs and VOIs. As a protein-based assay, it does not require enhanced safety protocols to be followed and can be completed safely in a BSL1 laboratory. Due to the bead-based nature and plate format, it is automatable, suitable for high-throughput, standardized and highly reproducible. The protein-based nature also allows for the rapid inclusion of emerging variants or single mutations. In comparison to the commercially available inhibition assay examined (NeutraLISA), RBDCoV-ACE2 did not have an apparent saturation phase, and therefore has a resolution range that enables greater separation of samples, particularly those that are strongly inhibiting ACE2 binding. The stronger correlation of RBDCoV-ACE2 to the VNT compared to NeutraLISA makes it a more accurate alternative to commercially available inhibition assays.

Similarly to other authors[35,36], we identified a positive correlation between anti-RBD IgG levels and ACE2 binding inhibition, suggesting that neutralizing antibodies represent a consistent portion of all antibodies produced. Similar correlations between anti-S1 and anti-trimeric spike IgG levels and ACE2 binding inhibition as well as no ACE2 binding to the S2 domain reinforce this conclusion. There is, however, a large degree of individualism in responses, with some samples having low titers yet high ACE2 binding inhibition for specific RBD mutants. We also identified, as other have done previously[6,37], a correlation between disease severity and ACE2 binding inhibition. However, the decrease in IgG levels and ACE2 binding inhibition of patients with WHO disease grade 8 (death) has not to our knowledge been reported before. This decrease requires further investigation to determine its cause, given its likely role in patient mortality.

As expected, ACE2 binding inhibition towards VOCs was highly variable. The strongest reductions in binding inhibition compared to wild-type were all from variants with a E484K mutation (eta, gamma, theta and beta). This specific mutation has been reported in multiple studies as an escape mutation that enhances the RBD-ACE2 affinity[38]. ACE2 binding inhibition was further reduced among these variants for those which additionally had a N501Y mutation (gamma, theta and beta), which is known to further enhance RBD-ACE2 binding[39]. These results are in-line with previous findings that have reported significant reductions in neutralization for gamma and beta[40–43]. The gamma and beta RBDs in our assays are only separated by a single K417N mutation, which is known to significantly reduce both the RBD-ACE2 binding affinity as well as the binding affinity to monoclonal therapeutic antibodies or other human antibodies[44]. Among recently emerged strains (delta, kappa, lambda), ACE2 binding inhibition compared to wild-type was reduced for all. The reduction in ACE2 binding inhibition seen for kappa and delta are comparable to recent findings[45], although we could not confirm the reduction seen by other authors for Lambda[46]. This is likely due to the 7-amino acid deletion in the N-terminal domain of lambda's spike protein, which is not present in the RBD and is thought to contribute to its immune evading properties[47]. Overall, the reduction in ACE2 binding inhibition against RBDs of all analyzed variants compared to wild-type has important implications for the design of second generation vaccines.

RBDCoV-ACE2 has limitations similar to other protein-based in vitro neutralization assays, such as only accounting for the Nabs that block the RBD-ACE2 interaction site through steric hindrance, and not for Nabs that interfere with cell entry mechanisms as would be analyzed in a VNT. Furthermore, the binding assay is also more prone to non-specific binding events. However, a major advantage of RBDCoV-ACE2 over VNTs is the

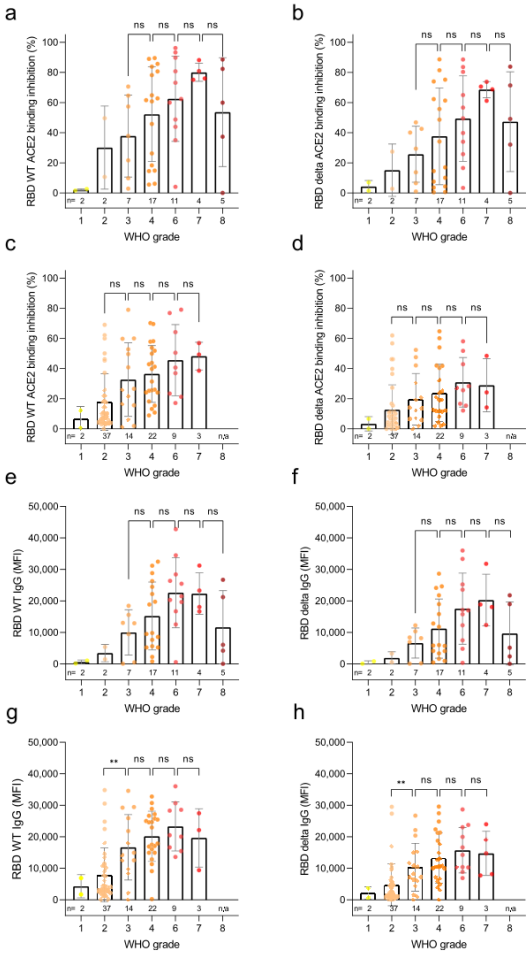

Figure 6. Correlation of anti-RBD IgG levels and ACE2 binding inhibition with SARS-CoV-2 disease severity. Bar charts showing mean ACE2 binding inhibitions (%) against wild-type and delta RBD are correlated with WHO grades for disease severity for samples 7–49 days post PCR (**a**,**b**) and ≥ 50 days post PCR (**c**,**d**). Mean anti-RBD WT IgG and anti-RBD delta IgG levels are shown for samples 7–49 days post PCR (**e**,**f**) and ≥ 50 days post PCR (**g**,**h**). Individual samples are displayed as colored dots, bars indicate the mean of the dataset with error bars representing standard deviation. Number of samples is given below the columns (n). If no samples for a group were available, the column is labeled with "n/a". WHO grade 1—ambulatory/no limitations of activities, 2—ambulatory/limitation of activities, 3—hospitalized, mild disease/no oxygen therapy, 4—hospitalized, mild disease/mask or nasal prongs, 6—hospitalized, severe disease/intubation + mechanical ventilation, 7—hospitalized, severe disease/ventilation + additional organ support (pressors, RRT, ECMO), 8—Death. The study did not contain samples of WHO grade 5.

speed of response toward viral evolution such as emerging variants of concern. The bead-based format of the assay is also highly reproducible and not susceptible to changes in experimental conditions, as is the case for cell culture based VNTs. The plate format of the assay also enables automation and high-throughput screening. Our assay only requires recombinant expressed RBD proteins, which can be quickly and easily produced. Additionally, this assay has the possibility of introducing artificial mutants to screen for possible escape variants that could arise in the future. Among our COVID-19 study population, the majority were admitted to the intensive care unit, meaning that the more serious grades of COVID-19 infection are heavily overrepresented in our population, while asymptomatic infections, which are known to be the most common form of disease progression[48], are severely underrepresented. Our sample set for longitudinal analysis is also highly variable in sampling times post-PCR. However, this large variation is also beneficial as it clearly demonstrates the individual variability in ACE2 binding inhibition.

In conclusion, we have developed and validated RBDCoV-ACE2, an ACE2-RBD inhibition assay that analyzes current variants of concern/under investigation/interest of SARS-CoV-2. Assay performance showed good correlation to VNT, confirming that neutralizing antibodies are being analyzed. ACE2 binding inhibition was highly variable among all variants examined, with the 484 aa residue appearing to be critical in reducing ACE2 binding inhibition. ACE2 binding inhibition correlated with both antibody titers and disease severity, although responses were highly individualistic. Overall, the protein-based format of the assay allows for the fast and simple incorporation of new SARS-CoV-2 variants, enabling rapid screening to identify how ACE2 binding inhibition is altered for emerging variants, or in guiding next-generation vaccine development to target a range of SARS-CoV-2 variants.

Materials and methods

Sample collection for assay validation. 16 serum samples consisting of 12 samples from COVID-19 patients (ethical approval #179/2020/BO2, University Hospital Tübingen) and four negative pre-pandemic samples (Central BioHub) were measured by both virus neutralization test and RBDCoV-ACE2 as part of the assay validation.

For technical assay validation, negative pre-pandemic serum samples were purchased from Central BioHub and four previously collected vaccinated samples from healthcare workers vaccinated with the Pfizer BNT-162b2 vaccine[30] (222/2020/BO2, University Hospital Tübingen) as well as one sample from a COVID-19 patient (#179/2020/BO2, University Hospital Tübingen) were used.

COVID-19 sample collection. 266 serum samples were collected from 168 patients hospitalized at the University Hospital Tübingen, Germany, between April 17, 2020 and May 12, 2021. Longitudinal samples were measured from 35 of the 168 patients ranging from 2 to 12 samples per patient. All individuals were tested positive by SARS-CoV-2 PCR. Key characteristics of the study population are summarized in Table S1.

For serum collection, blood was extracted by venipuncture, with the serum blood collection tube rotated 180° two to three times to extract possible air bubbles in the sample. After a minimum coagulation time of 30 min at room temperature, serum was extracted by centrifugation for 15 min at 2000×*g* (RT) and then stored at − 80 °C until analysis. Time between blood sampling and centrifugation did not exceed 2 h.

Ethical approval. Collection of samples and the execution of this study was approved by the Ethics committee of the Eberhard Karls University Tübingen and the University Hospital Tübingen under the ethical approval numbers 188/2020A and 764/2020/BO2 to Prof. Dr. Michael Bitzer. All participants signed the broad informed written consent of the Medical Faculty Tübingen for sample collection and all methods were performed in accordance with the relevant guidelines and regulations. Samples that were used for assay validation had their collection approved by the Ethics committee of the Eberhard Karls University Tübingen and the University Hospital Tübingen under the ethical approval numbers 222/2020/BO2 to Dr. Karina Althaus and 179/2020/BO2 to Prof. Dr. Juliane Walz. For collection of assay validation samples, informed written consent was obtained and all methods were performed in accordance with the relevant guidelines and regulations.

Expression and purification of SARS-CoV-2 RBD mutants. The expression plasmid pCAGGS, encoding the receptor-binding domain (RBD) of SARS-CoV-2 spike protein (amino acids 319–541), was kindly provided by F. Krammer[49]. Expression and purification of VOCs alpha, beta and epsilon was carried out as previously described[30,50]. RBDs of SARS-CoV-2 VOCs gamma, delta, eta, theta, kappa and A.23.1 were generated by PCR amplification of fragments from wild-type or cognate DNA templates and subsequent fusion PCR by overlap extension to introduce described mutations. Based on RBD wild-type sequence, primer pairs RBDfor, E484Krev and E484Kfor, RBDrev for VOC eta and RBDfor, V367Frev and V367Ffor, RBDrev for A.23.1 were used. VOC lambda was generated based on RBD wild-type sequence using primer pairs L452Qfor, L452Qrev and F490Sfor, F490Srev. VOC delta was generated based on VOC epsilon using primer pairs RBDfor, T478Krev and T478Kfor, RBDrev. Based on VOC alpha sequence, VOC theta was generated using primer pairs RBDfor, E484Krev and E484Kfor, RBDrev. VOC kappa was generated based on VOC eta sequence using primer pairs RBDfor, L452Rrev and L452Rfor, RBDrev. VOC gamma was generated based on VOC theta sequence using primer pairs RBDfor, K417Trev and K417Tfor, RBDrev. Amplificates were inserted into the pCDNA3.4 expression vector using XbaI and NotI restriction sites. The integrity of all expression constructs was confirmed by standard sequencing analysis. An overview of the primer sequences is shown in Table S2. Confirmed constructs were expressed in Expi293 cells[30,34]. Briefly, cells were cultivated (37 °C, 125 rpm, 8% (v/v) CO_2) to a density of 5.5×10^6 cells/mL and diluted with Expi293F expression medium. Transfection of the corresponding plasmids (1 µg/mL) with Expifectamine was performed as per the manufacturer's instructions. Enhancers were added as

per the manufacturer's instructions 20 h post transfection. Cell suspensions were cultivated for 2–5 days (37 °C, 125 rpm, 8% (v/v) CO_2) and centrifuged (4 °C, 23,900 × *g*, 20 min) to clarify the supernatant. Afterwards, supernatants were filtered with a 0.22 µm membrane (Millipore, Darmstadt, Germany) and supplemented with His-A buffer stock solution (20 mM Na_2HPO_4, 300 mM NaCl, 20 mM imidazole, pH 7.4). The solution was applied to a HisTrap FF crude column on an Äkta pure system (GE Healthcare, Freiburg, Germany), extensively washed with His-A buffer, and eluted with an imidazole gradient (50–400 mM). Amicon 10 K centrifugal filter units (Millipore, Darmstadt, Germany) were used for buffer exchange to PBS and concentration of eluted proteins.

Bead coupling. The in-house expressed RBD mutants were immobilized on magnetic MagPlex beads (Luminex) using the AMG Activation Kit for Multiplex Microspheres (# A-LMPAKMM-400, Anteo Technologies). In brief, 1 mL of spectrally distinct MagPlex beads (1.25 *10^7 beads) were activated in 1 mL of AnteoBind Activation Reagent for 1 h at room temperature. The beads were washed twice with 1 mL of conjugation buffer using a magnetic separator, before being resuspended in 1 mL of antigen solution diluted to 25 µg/mL in conjugation buffer. After 1 h incubation at room temperature the beads were washed twice with 1 mL conjugation buffer and incubated for 1 h in 0.1% (w/v) BSA in conjugation buffer for blocking. Following this, the beads were washed twice with 1 mL storage buffer. Finally, the beads were resuspended in 1 mL storage buffer and stored at 4 °C until further use.

RBDCoV-ACE2. Assay buffer (1:4 Low Cross Buffer (Candor Bioscience GmbH) in CBS (1 × PBS + 1% BSA) + 0.05% Tween20) was supplemented with biotinylated human ACE2 (Sino Biological, # 10108-H08H-B) to a final concentration of 342.9 ng/mL to produce ACE2 buffer. Working inside a sterile laminar flow cabinet, serum samples were thawed and diluted 1:25 in assay buffer before being further diluted 1:8 in ACE2 buffer resulting in a final concentration of 300 ng/mL ACE2 in all 1:200 diluted samples. Spectrally distinct populations of MagPlex beads (Luminex) coupled with RBD proteins of SARS-CoV-2 wild-type and variants alpha, beta, gamma, epsilon, eta, theta, kappa, delta, lambda, Cluster 5 and A.23.1 were pooled in assay buffer to create a bead mix (40 beads/µL per bead population). 25 µL of diluted serum was added to 25 µL of bead mix in each well of a 96-well plate (Corning, #3642). To allow comparison of ACE2 binding inhibition between different RBD mutants on a relative scale, 300 ng/mL ACE2 without added serum was measured in triplicates on every plate as normalization control. Additionally, one quality control sample was analyzed in triplicates on every plate. For blank measurement, 25 µL assay buffer instead of diluted sample was added to two wells per plate. Samples were incubated for 2 h at 21 °C while shaking at 750 rpm on a thermomixer. Following incubation, the beads were washed three times with 100 µL wash buffer (1 × PBS + 0.05 Tween20) using a microplate washer (Biotek 405TS, Biotek Instruments GmbH). For detection of bound biotinylated ACE2, 30 µL of 2 µg/mL RPE-Streptavidin was added to each well and the plate was incubated for 45 min at 21 °C while shaking at 750 rpm on a thermomixer. Afterwards, the beads were washed again three times with 100 µL wash buffer. The 96-well plate was placed for 3 min on the thermomixer at 1000 rpm to resuspend the beads before analysis using a FLEXMAP 3D instrument (Luminex) with the following settings: 80 µL (no timeout), 50 events, Gate: 7500–15,000, Reporter Gain: Standard PMT. MFI values of each sample were divided by the mean of the ACE2 normalization control. The normalized values were converted into percent and subtracted from 100 resulting in the percentage of ACE2 binding inhibition. Negative values were manually set to zero.

MULTICOV-AB. MULTICOV-AB[34], an in-house produced SARS-CoV-2 antibody assay, was performed with all serum samples to measure RBD/S1/trimeric spike-specific IgG levels. The antigen panel was expanded to include RBD proteins from 11 different SARS-CoV-2 variants from which all, except the Cluster 5 variant from Sino Biological (# 40592-V08H80), were produced in-house. The assay was carried out as previously described[30].

Viruses. All experiments associated with the SARS-CoV-2 virus were conducted in a Biosafety Level 3 laboratory. The recombinant infectious SARS-CoV-2 clone expressing mNeonGreen (icSARS-CoV-2-mNG)[51], corresponding to the 2019-nCoV/USA_WA1/2020 isolate, was obtained from the World Reference Center for Emerging Viruses and Arboviruses (WRCEVA) at the UTMB (University of Texas Medical Branch). The mNeon Green reporter gene introduced into ORF7 allows the differentiation between infected and uninfected cells.

The generation of icSARSCoV-2-mNG stocks and the MOI determination was performed as previously described[52].

Virus Neutralization Assay (VNT). VNTs were determined previously[53]. Briefly, 1×10^4 Caco-2 cells/well were seeded in 96-well plates the day before infection in media containing 5% FCS. Caco-2 cells were co-incubated with the SARS-CoV-2 strain icSARS-CoV-2-mNG[51] at a MOI = 1.1 and serum samples in two-fold serial dilutions ranging from 1:40 to 1:5120. 48 h post infection, cells were fixed with 2% PFA and stained with Hoechst33342 (1 µg/mL final concentration) for 10 min at 37 °C. Following this, the staining solution was removed and exchanged for PBS. To quantify infection rates, images were taken with the Cytation3 (Biotek Instruments GmbH) and Hoechst + and mNG + cells were automatically counted by the Gen5 Software (Biotek Instruments GmbH). Infection rate was determined by dividing the number of infected cells through total cell count per condition. Virus-neutralizing titers (VNT50s) were calculated as the half-maximal inhibitory serum dilution.

Assay validation experiments. To determine the intra-assay precision of RBDCoV-ACE2, 12 replicates of four serum samples (Vac1–Vac4) were measured on a 96-well plate (Corning, #3642). Additionally, 15 replicates of the 300 ng/mL ACE2 normalization control and 12 replicates of the blank control containing only assay

buffer without sample or ACE2 were measured. For inter-assay precision, five serum samples (Vac1–Vac4 and Inf1) were measured in triplicates in four independent experiments. Additionally, the quality control, the ACE2 normalization control and blank were also processed in triplicates in the same four experiments. Short-term stability was determined by storing ACE2 buffer under six different conditions before proceeding with the assay protocol. The prepared ACE2 buffer was stored 2 h, 4 h and 24 h at both 4 °C and room temperature and compared to ACE2 buffer without storage (fresh). Replicate MFI values of every sample (Vac1–Vac4 (vaccinated), Inf1 (infected) and pre-pandemic) were normalized to the values of the respective ACE2 normalization control. Freeze–thaw stability of the biotinylated ACE2 stocks was determined by analyzing six serum samples (Vac1–Vac4 (vaccinated), Inf1 (infected) and pre-pandemic) in triplicates, with ACE2 stocks undergoing 1 to 5 cycles. In addition to that, every sample was also processed with ACE2 not re-frozen once thawed (fresh, 0 freeze–thaw cycles). The MFI values of every sample were normalized to the values of the respective ACE2 normalization control. To investigate the stability of RBDCoV-ACE2 against variations of the used ACE2 concentration, six samples (Vac1–Vac4 (vaccinated), Inf1 (infected) and pre-pandemic) were analyzed with ACE2 concentrations ranging from 150 ng/mL to 350 ng/mL. Replicate MFI values of every sample were normalized to the values of the respective ACE2 normalization control. For analysis, the mean, standard deviation and coefficient of variation in percent of all replicates were calculated.

To confirm that the multiplex assay format has no undesirable effect on ACE2 binding inhibition values compared to singleplex measurements, 24 samples (pre-pandemic (n = 5) and COVID-19 infected (n = 19)) were analyzed in both singleplex and multiplex (for all VOCs).

NeutraLISA. One sample from each individual donor (n = 168) was analyzed with the commercially available in-vitro diagnostic test SARS-CoV-2 NeutraLISA (Euroimmun). The assay was performed according to the manufacturer's instructions. For longitudinal donors with more than one sample available, the sample closest to 20 days after positive PCR diagnosis was picked. Negative values were manually set to zero.

Statistical analysis. Data collection and assignment to metadata was performed with Microsoft Excel 2016. Data analysis, visualization and curve fitting was performed with Graphpad Prism (version 9.1.2). Virus-neutralizing titers (VNT50s) as the half-maximal inhibitory serum dilution were calculated using 4-parameter nonlinear regression. Longitudinal curves were fitted using a one-site total binding equation. Correlations were analyzed using Spearman's correlation coefficient. Significances were calculated (where appropriate) using Mann–Whitney U tests. Figures were edited with Inkscape (version 0.92.4). Data generated for this manuscript is available from the authors upon request.

Received: 6 December 2021; Accepted: 22 March 2022
Published online: 03 May 2022

References

1. Forthal, D. N. Functions of antibodies. *Microbiol. Spectrum* https://doi.org/10.1128/microbiolspec.AID-0019-2014 (2014).
2. Jiang, S., Zhang, X., Yang, Y., Hotez, P. J. & Du, L. Neutralizing antibodies for the treatment of COVID-19. *Nat. Biomed. Eng.* **4**, 1134–1139. https://doi.org/10.1038/s41551-020-00660-2 (2020).
3. Shi, R. *et al.* A human neutralizing antibody targets the receptor-binding site of SARS-CoV-2. *Nature* **584**, 120–124. https://doi.org/10.1038/s41586-020-2381-y (2020).
4. Piccoli, L. *et al.* Mapping neutralizing and immunodominant sites on the SARS-CoV-2 spike receptor-binding domain by structure-guided high-resolution serology. *Cell* **183**, 1024-1042.e1021. https://doi.org/10.1016/j.cell.2020.09.037 (2020).
5. Dispinseri, S. *et al.* Neutralizing antibody responses to SARS-CoV-2 in symptomatic COVID-19 is persistent and critical for survival. *Nat. Commun.* **12**, 2670. https://doi.org/10.1038/s41467-021-22958-8 (2021).
6. Garcia-Beltran, W. F. *et al.* COVID-19-neutralizing antibodies predict disease severity and survival. *Cell* **184**, 476-488.e411. https://doi.org/10.1016/j.cell.2020.12.015 (2021).
7. McMahan, K. *et al.* Correlates of protection against SARS-CoV-2 in rhesus macaques. *Nature* **590**, 630–634. https://doi.org/10.1038/s41586-020-03041-6 (2021).
8. Kim, Y. I. *et al.* Critical role of neutralizing antibody for SARS-CoV-2 reinfection and transmission. *Emerg. Microbes Infect.* **10**, 152–160. https://doi.org/10.1080/22221751.2021.1872352 (2021).
9. Rogers, T. F. *et al.* Isolation of potent SARS-CoV-2 neutralizing antibodies and protection from disease in a small animal model. *Science* **369**, 956–963. https://doi.org/10.1126/science.abc7520 (2020).
10. Weinreich, D. M. *et al.* REGN-COV2, a neutralizing antibody cocktail, in outpatients with Covid-19. *N. Engl. J. Med.* **384**, 238–251. https://doi.org/10.1056/NEJMoa2035002 (2021).
11. (FDA), F. a. D. A. *Coronavirus (COVID-19) Update: FDA Authorizes Monoclonal Antibodies for Treatment of COVID-19*, <https://www.fda.gov/news-events/press-announcements/coronavirus-covid-19-update-fda-authorizes-monoclonal-antibodies-treatment-covid-19> (2020).
12. Gottlieb, R. L. *et al.* Effect of bamlanivimab as monotherapy or in combination with etesevimab on viral load in patients with mild to moderate COVID-19: A randomized clinical trial. *JAMA* **325**, 632–644. https://doi.org/10.1001/jama.2021.0202 (2021).
13. (FDA), F. a. D. A. *Coronavirus (COVID-19) Update: FDA Authorizes Monoclonal Antibodies for Treatment of COVID-19*, <https://www.fda.gov/news-events/press-announcements/coronavirus-covid-19-update-fda-authorizes-monoclonal-antibodies-treatment-covid-19-0> (2021).
14. Zhou, P. *et al.* A pneumonia outbreak associated with a new coronavirus of probable bat origin. *Nature* **2**, 1–4 (2020).
15. Graham, M. S. *et al.* Changes in symptomatology, reinfection, and transmissibility associated with the SARS-CoV-2 variant B.1.1.7: An ecological study. *Lancet. Public health* **6**, e335–e345. https://doi.org/10.1016/s2468-2667(21)00055-4 (2021).
16. Tegally, H. *et al.* Detection of a SARS-CoV-2 variant of concern in South Africa. *Nature* **592**, 438–443. https://doi.org/10.1038/s41586-021-03402-9 (2021).
17. Sabino, E. C. *et al.* Resurgence of COVID-19 in Manaus, Brazil, despite high seroprevalence. *Lancet (Lond., Engl.)* **397**, 452–455. https://doi.org/10.1016/s0140-6736(21)00183-5 (2021).

18. Control, E. C. f. D. P. a. *Threat Assessment Brief: Emergence of SARS-CoV-2 B.1.617 variants in India and situation in the EU/EEA*, <https://www.ecdc.europa.eu/en/publications-data/threat-assessment-emergence-sars-cov-2-b1617-variants> (2021).
19. (WHO), W. H. O. *Classification of Omicron (B.1.1.529): SARS-CoV-2 Variant of Concern*, <https://www.who.int/news/item/26-11-2021-classification-of-omicron-(b.1.1.529)-sars-cov-2-variant-of-concern> (2021).
20. (WHO), W. H. O. *Tracking SARS-CoV-2 variants*, <https://www.who.int/en/activities/tracking-SARS-CoV-2-variants/> (2021).
21. O'Toole, A. & Hill, V. *Lineage C.37*, <https://cov-lineages.org/lineage.html?lineage=C.37> (2021).
22. Skowronski, D. M. & De Serres, G. Safety and efficacy of the BNT162b2 mRNA Covid-19 vaccine. *N. Engl. J. Med.* **384**, 1576–1577. https://doi.org/10.1056/NEJMc2036242 (2021).
23. Baden, L. R. *et al.* Efficacy and safety of the mRNA-1273 SARS-CoV-2 vaccine. *N. Engl. J. Med.* **384**, 403–416. https://doi.org/10.1056/NEJMoa2035389 (2021).
24. Voysey, M. *et al.* Safety and efficacy of the ChAdOx1 nCoV-19 vaccine (AZD1222) against SARS-CoV-2: an interim analysis of four randomised controlled trials in Brazil, South Africa, and the UK. *Lancet (London, England)* **397**, 99–111. https://doi.org/10.1016/s0140-6736(20)32661-1 (2021).
25. Sadoff, J. *et al.* Safety and efficacy of single-dose Ad26.COV2.S vaccine against Covid-19. *N. Engl. J. Med.* **384**, 2187–2201. https://doi.org/10.1056/NEJMoa2101544 (2021).
26. Krammer, F. SARS-CoV-2 vaccines in development. *Nature* **586**, 516–527. https://doi.org/10.1038/s41586-020-2798-3 (2020).
27. Stamatatos, L. *et al.* mRNA vaccination boosts cross-variant neutralizing antibodies elicited by SARS-CoV-2 infection. *Science* https://doi.org/10.1126/science.abg9175 (2021).
28. Jalkanen, P. *et al.* COVID-19 mRNA vaccine induced antibody responses against three SARS-CoV-2 variants. *Nat. Commun.* **12**, 3991. https://doi.org/10.1038/s41467-021-24285-4 (2021).
29. Shen, X. *et al.* Neutralization of SARS-CoV-2 Variants B1429 and B1351. *N. Engl. J. Med.* **384**, 2352–2354. https://doi.org/10.1056/NEJMc2103740 (2021).
30. Becker, M. *et al.* Immune response to SARS-CoV-2 variants of concern in vaccinated individuals. *Nat. Commun.* **12**, 3109. https://doi.org/10.1038/s41467-021-23473-6 (2021).
31. Hoffmann, M. *et al.* SARS-CoV-2 variants B.1.351 and P.1 escape from neutralizing antibodies. *Cell* **184**, 2384–2393. https://doi.org/10.1016/j.cell.2021.03.036 (2021).
32. Krammer, F. A correlate of protection for SARS-CoV-2 vaccines is urgently needed. *Nat. Med.* https://doi.org/10.1038/s41591-021-01432-4 (2021).
33. Euroimmun. *SARS-CoV-2 NeutraLISA: Produkt-Datenblatt*, <https://www.coronavirus-diagnostik.de/documents/Indications/Infections/Coronavirus/EI_2606_D_DE_F.pdf> (2021).
34. Becker, M. *et al.* Exploring beyond clinical routine SARS-CoV-2 serology using MultiCoV-Ab to evaluate endemic coronavirus cross-reactivity. *Nat. Commun.* **12**, 1152. https://doi.org/10.1038/s41467-021-20973-3 (2021).
35. Mendrone-Junior, A. *et al.* Correlation between SARS-COV-2 antibody screening by immunoassay and neutralizing antibody testing. *Transfusion* **61**, 1181–1190. https://doi.org/10.1111/trf.16268 (2021).
36. Grenache, D. G., Ye, C. & Bradfute, S. B. Correlation of SARS-CoV-2 neutralizing antibodies to an automated chemiluminescent serological immunoassay. *J. Appl. Lab. Med.* **6**, 491–495. https://doi.org/10.1093/jalm/jfaa195 (2021).
37. Legros, V. *et al.* A longitudinal study of SARS-CoV-2-infected patients reveals a high correlation between neutralizing antibodies and COVID-19 severity. *Cell. Mol. Immunol.* **18**, 318–327. https://doi.org/10.1038/s41423-020-00588-2 (2021).
38. Nelson, G. *et al.* Molecular dynamic simulation reveals E484K mutation enhances spike RBD-ACE2 affinity and the combination of E484K, K417N and N501Y mutations (501Y.V2 variant) induces conformational change greater than N501Y mutant alone, potentially resulting in an escape mutant. *Biorxiv* https://doi.org/10.1101/2021.01.13.426558 (2021).
39. Luan, B., Wang, H. & Huynh, T. Enhanced binding of the N501Y-mutated SARS-CoV-2 spike protein to the human ACE2 receptor: Insights from molecular dynamics simulations. *FEBS Lett.* **595**, 1454–1461. https://doi.org/10.1002/1873-3468.14076 (2021).
40. Shen, X. *et al.* SARS-CoV-2 variant B.1.1.7 is susceptible to neutralizing antibodies elicited by ancestral spike vaccines. *Cell Host Microbe* **29**, 529–539. https://doi.org/10.1016/j.chom.2021.03.002 (2021).
41. Wall, E. C. *et al.* Neutralising antibody activity against SARS-CoV-2 VOCs B.1.617.2 and B.1.351 by BNT162b2 vaccination. *Lancet (Lond., Engl.)* **397**, 2331–2333. https://doi.org/10.1016/s0140-6736(21)01290-3 (2021).
42. Wang, P. *et al.* Antibody resistance of SARS-CoV-2 variants B.1.351 and B.1.1.7. *Nature* **593**, 130–135. https://doi.org/10.1038/s41586-021-03398-2 (2021).
43. Heggestad, J. T. *et al.* Rapid test to assess the escape of SARS-CoV-2 variants of concern. *Sci. Adv.* **7**, 7682. https://doi.org/10.1126/sciadv.abl7682 (2021).
44. Luan, B. & Huynh, T. Insights into SARS-CoV-2's Mutations for Evading Human Antibodies: Sacrifice and Survival. *J. Med. Chem.* https://doi.org/10.1021/acs.jmedchem.1c00311 (2021).
45. Edara, V. V. *et al.* Infection and vaccine-induced neutralizing-antibody responses to the SARS-CoV-2 B.1.617 variants. *N. Engl. J. Med.* **385**, 664–666. https://doi.org/10.1056/NEJMc2107799 (2021).
46. Kimura, I. *et al.* The SARS-CoV-2 Lambda variant exhibits enhanced infectivity and immune resistance. *Cell Rep.* **38**, 110218. https://doi.org/10.1016/j.celrep.2021.110218 (2022).
47. Acevedo, M. L. *et al.* Infectivity and immune escape of the new SARS-CoV-2 variant of interest Lambda. *Medrxiv* https://doi.org/10.1101/2021.06.28.21259673 (2021).
48. Subramanian, R., He, Q. & Pascual, M. Quantifying asymptomatic infection and transmission of COVID-19 in New York City using observed cases, serology, and testing capacity. *Proc. Natl. Acad. Sci. U.S.A.* https://doi.org/10.1073/pnas.2019716118 (2021).
49. Amanat, F. *et al.* A serological assay to detect SARS-CoV-2 seroconversion in humans. *Nat. Med.* **26**, 1033–1036. https://doi.org/10.1038/s41591-020-0913-5 (2020).
50. Wagner, T. R. *et al.* Biparatopic nanobodies protect mice from lethal challenge with SARS-CoV-2 variants of concern. *EMBO Rep.* **23**, e53865. https://doi.org/10.15252/embr.202153865 (2022).
51. Xie, X. *et al.* An infectious cDNA clone of SARS-CoV-2. *Cell Host Microbe* **27**, 841-848.e843. https://doi.org/10.1016/j.chom.2020.04.004 (2020).
52. Ruetalo, N. *et al.* Antibody response against SARS-CoV-2 and seasonal coronaviruses in nonhospitalized COVID-19 patients. *MSphere* https://doi.org/10.1128/mSphere.01145-20 (2021).
53. Wagner, T. R. *et al.* NeutrobodyPlex-monitoring SARS-CoV-2 neutralizing immune responses using nanobodies. *EMBO Rep.* **22**, e52325. https://doi.org/10.15252/embr.202052325 (2021).

Acknowledgements

We thank Johanna Griesbaum, Jennifer Jüngling and Christine Geisler for excellent technical assistance. This work was financially supported by the State Ministry of Baden-Württemberg for Economic Affairs, Labour and Housing Construction (Grant number FKZ 3-4332.62-NMI-68) and the EU Horizon 2020 research and innovation program (Grant agreement number 101003480-CORESMA). The funders had no role in study design, data collection and interpretation, or the decision to submit the work for publication.

Author contributions

D.J. and A.D. conceived the study and designed the experiments. N.S.M. supervised the study. D.J. and Ma.B. performed the experiments. D.J., A.D., Ma.B. produced components for RBDCoV-ACE2. K.K., S.B., C.S., H.H., K.S., N.M., K.A., M.K., J.W., M.B. and S.G. collected samples or organized their collection and provided clinical metadata. N.R. and M.S. provided virus neutralization test data. P.D.K., B.T., T.W. and U.R. produced and designed recombinant assay proteins. M.B., S.G. and N.S.M. procured funding. D.J. performed data analysis and generated the figures. D.J. and A.D. wrote the manuscript. All authors critically reviewed and approved the final manuscript.

Competing interests

NSM was a speaker at Luminex user meetings in the past. The Natural and Medical Sciences Institute at the University of Tübingen is involved in applied research projects as a fee for services with the Luminex Corporation. The other authors declare no competing interest.

Additional information

Supplementary Information The online version contains supplementary material available at https://doi.org/10.1038/s41598-022-10987-2.

Correspondence and requests for materials should be addressed to S.G. or N.S.-M.

Reprints and permissions information is available at www.nature.com/reprints.

Publisher's note Springer Nature remains neutral with regard to jurisdictional claims in published maps and institutional affiliations.

COVID-19 patient serum less potently inhibits ACE2-RBD binding for various SARS-CoV-2 RBD mutants

Daniel Junker[1], Alex Dulovic[1], Matthias Becker[1], Teresa R. Wagner[1,2], Philipp D. Kaiser[1], Bjoern Traenkle[1], Katharina Kienzle[3], Stefanie Bunk[3], Carlotta Struemper[3], Helene Haeberle[4], Kristina Schmauder[5,6], Natalia Ruetalo[7], Nisar Malek[3,8], Karina Althaus[9], Michael Koeppen[4], Ulrich Rothbauer[1,2], Juliane S. Walz[10,11,12,13], Michael Schindler[7], Michael Bitzer[3,8], Siri Göpel[3,6]*, Nicole Schneiderhan-Marra[1]*

Author Affiliations

[1] NMI Natural and Medical Sciences Institute at the University of Tübingen, Reutlingen, Germany

[2] Pharmaceutical Biotechnology, Eberhard Karls University, Tübingen, Germany

[3] Department Internal Medicine I, University Hospital Tübingen, Tübingen, Germany

[4] Department of Anesthesiology and Intensive Care Medicine, University Hospital Tübingen, Tübingen, Germany

[5] Institute for Medical Microbiology and Hygiene, University Hospital Tübingen, Tübingen, Germany

[6] German Centre for Infection Research (DZIF), Partner Site Tübingen, Tübingen, Germany

[7] Institute for Medical Virology and Epidemiology, University Hospital Tübingen, Tübingen, Germany

[8] Center for Personalized Medicine, Eberhard Karls University, Tübingen, Germany

[9] Institute for Clinical and Experimental Transfusion Medicine, University Hospital Tübingen, Tübingen, Germany

[10] Clinical Collaboration Unit Translational Immunology, German Cancer Consortium (DKTK), Department of Internal Medicine, University Hospital Tübingen, Tübingen, Germany

[11] Institute for Cell Biology, Department of Immunology, University of Tübingen, Tübingen, Germany

[12] Cluster of Excellence iFIT (EXC2180) "Image-Guided and Functionally Instructed Tumor Therapies", University of Tübingen, Tübingen, Germany

[13] Dr. Margarete Fischer-Bosch-Institute for Clinical Pharmacology and Robert Bosch Center for Tumor Diseases (RBCT), Stuttgart, Germany

Running Head: Less potent ACE2 binding inhibition against SARS-CoV-2 RBD mutants

* denotes shared senior authorship and corresponding authors.

Contact Information

Nicole Schneiderhan-Marra – Phone number +49 (0)7121 51530 815. Email Address Nicole.schneiderhan@nmi.de Postal Address – Markwiesenstrasse 55, 72770 Reutlingen, Germany.

Siri Göpel – Phone number +49 (0)7071 29 85415. Email Address siri.goepel@med.uni-tuebingen.de Postal Address – Otfried-Müller-Strasse 10, 72076 Tübingen, Germany.

Table S1 - Characteristics of the analyzed COVID-19 serum sample collection set.

Characteristic	
Number of donors	168
Number of samples	266
Median age (IQR) -years	62 (23)
Female sex (%)	78 (46.4)
Median ΔT post first positive PCR test (range)	91 (1-348)
Median BMI (range)	26.9 (18.4 – 50.2)

Table S2 - Primer sequences used for expression of RBD mutants.

Primer Name	Sequence (5‘ to 3‘)
RBDfor	ATATCTAGAGCCACCATGTTCGTGTTTCTGG
E484Krev	GCAGTTGAAGCCTTTCACGCCGTTACAAGGGGT
E484Kfor	GTAACGGCGTGAAAGGCTTCAACTGCTACTTCCC
RBD rev	AAGATCTGCTAGCTCGAGTCGC
V367Frev	CGGAGTTGTACAGGAAGGAGTAGTCGGCCACGCA
V367Ffor	CGACTACTCCTTCCTGTACAACTCCGCCAGCTTC
L452Qfor	GGCAACTACAATTACCAGTACCGGCTGTTCCGGAAG
L452Qrev	CGGTACTGGTAATTGTAGTTGCCGCCG
F490Sfor	TCAACTGCTACTCCCCACTGCAGTCCTACGGC
F490Srev	CTGCAGTGGGGAGTAGCAGTTGAAGCCTTCCAC
T478Krev	CGTTACAAGGCTTGCTGCCGGCCTGATAGA
T478Kfor	CCGGCAGCAAGCCTTGTAACGGCGTGGAAG
L452Rrev	CGGTACCGGTAATTGTAGTTGCCGCCG
L452Rfor	GGCAACTACAATTACCGGTACCGGCTGTTCCGGAAG
K417Trev	GTTGTAGTCGGCGATGGTGCCTGTCTGTCCAGGGG)
K417Tfor	GACAGACAGGCACCATCGCCGACTACAACTACAAG

Table S3 - RBDCoV-ACE2 technical validation results. Percentage coefficients of variation (%CV) of normalized MFI values for every SARS-CoV-2 RBD for all analyzed samples (n=6) including the mean of all samples.

	Samples	RBD WT	alpha	beta	gamma	epsilon	Cluster 5	A.23.1	eta	theta	kappa
Intra-assay precision (%CV)	Vac1	1.4	1.5	2.6	2.5	1.3	1.5	1.7	1.4	2.1	1.1
	Vac2	2.2	2.1	1.1	1.6	1.7	1.2	1.5	1.9	1.6	2.0
	Vac3	2.8	4.0	3.8	2.1	4.2	3.0	3.5	2.1	1.6	4.3
	Vac4	2.2	2.1	3.4	1.9	2.0	2.0	2.3	1.7	2.1	2.4
	Mean	**2.2**	**2.4**	**2.7**	**2.0**	**2.3**	**1.9**	**2.3**	**1.8**	**1.9**	**2.5**
Inter-assay precision (%CV)	Vac1	1.9	2.7	3.0	2.9	2.8	2.3	3.5	2.7	2.9	2.9
	Vac2	2.6	3.0	3.9	2.8	3.5	2.4	2.7	3.0	2.1	3.0
	Vac3	5.7	6.9	6.9	3.5	6.4	4.6	5.5	4.9	3.6	5.2
	Vac4	4.4	3.5	4.6	2.9	4.3	2.5	1.9	3.0	2.7	3.3
	Inf1	1.9	2.5	2.9	2.9	2.8	2.4	1.6	1.8	1.8	2.4
	Mean	**3.3**	**3.7**	**4.3**	**3.0**	**4.0**	**2.8**	**3.0**	**3.1**	**2.6**	**3.4**
Short-term stability (%CV)	Vac1	2.5	3.9	3.2	2.3	2.5	2.3	2.6	2.1	2.8	3.2
	Vac2	2.3	3.1	4.5	2.3	2.3	2.8	2.6	2.0	2.4	2.6
	Vac3	8.6	9.3	6.4	3.0	6.9	4.4	4.9	7.1	3.2	7.3
	Vac4	11.6	4.9	3.4	3.2	3.0	2.4	3.1	3.2	2.3	3.3
	Inf1	1.4	2.6	3.5	2.5	1.9	2.4	2.2	1.8	1.7	1.7
	Pre-pandemic	1.6	2.3	3.7	1.9	1.9	1.8	2.2	1.8	2.4	2.1
	Mean	**4.7**	**4.4**	**4.1**	**2.5**	**3.1**	**2.7**	**2.9**	**3**	**2.5**	**3.4**
Freeze-thaw stability (%CV)	Vac1	2.7	3.8	4.5	3.1	4.0	2.7	3.3	2.1	2.9	3.2
	Vac2	4.0	3.2	2.5	2.5	3.8	2.8	2.9	2.6	3.2	2.9
	Vac3	9.3	10.2	4.7	5.8	12.1	8.9	7.3	9.8	5.5	10.6
	Vac4	7.6	6.2	6.1	5.3	7.2	5.8	6.6	6.3	4.9	6.3
	Inf1	3.6	2.6	4.1	3.1	3.1	2.9	2.4	2.5	2.4	3.5
	Pre-pandemic	1.8	1.8	3.2	3.7	1.8	1.4	2.1	2.3	2.3	2.0
	Mean	**4.8**	**4.6**	**4.2**	**3.9**	**5.3**	**4.1**	**4.1**	**4.3**	**3.5**	**4.8**
Parallelism (%CV)	Vac1	4.1	3.9	5.0	4.0	4.5	4.2	4.2	3.2	2.6	3.9
	Vac2	4.2	2.5	4.0	3.4	2.7	2.5	4.2	2.6	2.8	4.2
	Vac3	12.0	11.7	4.0	5.3	11.9	11.8	9.3	13.6	4.5	12.7
	Vac4	11.3	9.6	6.5	6.9	10.0	8.7	8.6	9.9	4.4	9.3
	Inf1	5.2	3.4	5.5	3.4	4.8	4.1	4.0	4.2	4.2	3.6
	Pre-pandemic	2.1	1.2	3.6	2.8	2.3	2.1	2.4	1.9	2.7	1.4
	Mean	**6.5**	**5.4**	**4.8**	**4.3**	**6.0**	**5.6**	**5.5**	**5.9**	**3.5**	**5.9**

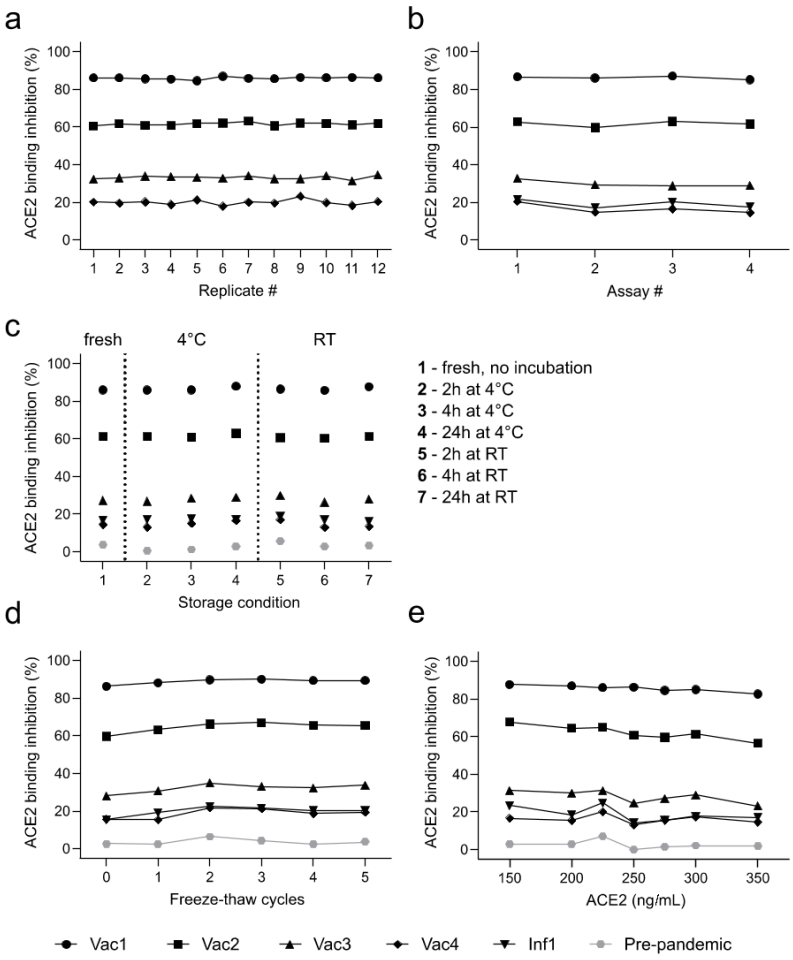

Figure S1 - RBDCoV-ACE2 technical validation results. Results of intra-assay precision (a), inter-assay precision (b), short-term stability (c), freeze-thaw stability (d) and parallelism (e) experiments analyzing ACE2 binding inhibition (displayed as %) using wild-type (WT) RBD. Four samples from donors vaccinated with Pfizer BNT-162b2 (n=4), one COVID-19 infected (n=1) and one pre-pandemic sample (n=1, grey) were analyzed. Data points of each sample are illustrated by different shapes according to the figure key. Percent coefficients of variation (%CV) for all included RBD mutants are summarized in **Table S3**.

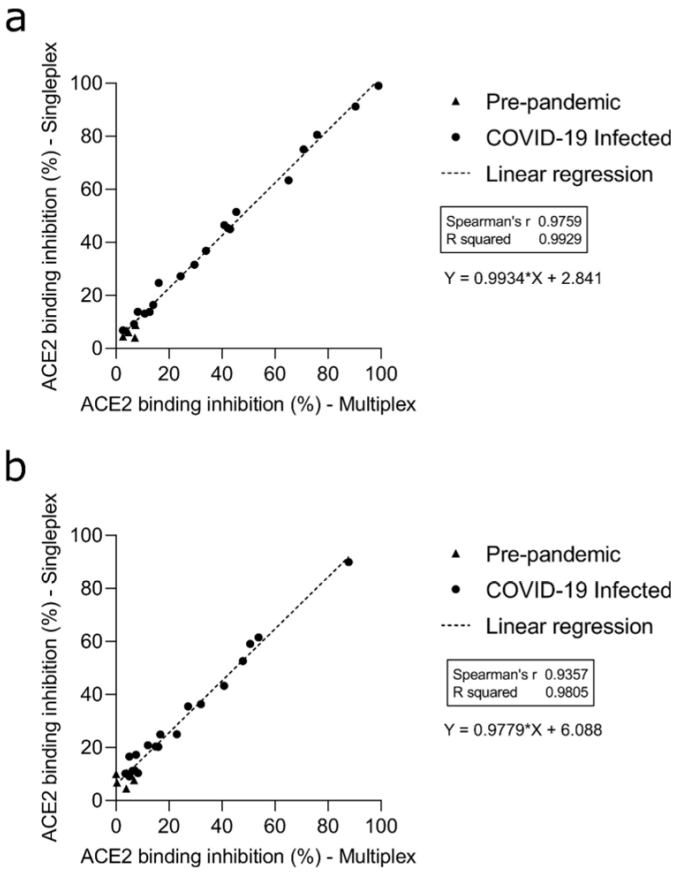

Figure S2 - Comparison of multiplex and singleplex assay formats. Linear regression analysis between ACE2 binding inhibition (%) values of samples from pre-pandemic (n=5) and COVID-19 infected (n=19) individuals analyzed in both multiplex and singleplex for RBD WT (a) and RBD delta (b). Correlation analysis was performed after Spearman and the correlation coefficient r is shown.

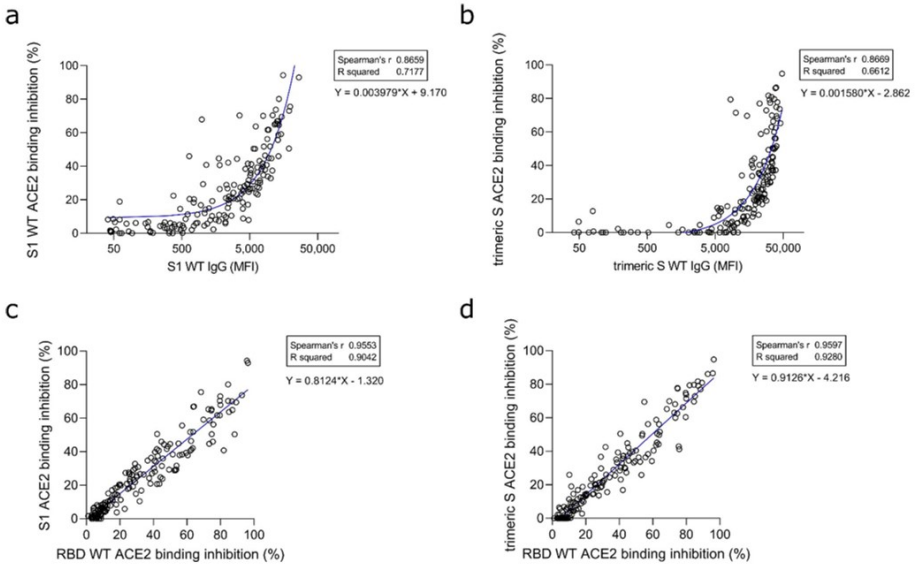

Figure S3 - Correlation between IgG MFI signals and ACE2 binding inhibition (%) against SARS-CoV-2 S1-domain (a) and trimeric spike (b) of serum samples from COVID-19 patients (n= 168). Regression analysis comparing ACE2 binding inhibitions (%) for S1 and trimeric spike with RBDCoV-ACE2 results of RBD WT (c and d). Each circle represents one sample (n=168). For longitudinal donors with more than one sample available, the sample closest to 20 days post positive PCR diagnosis was selected. Spearman's correlation coefficient (r) as well as the equation of the linear regression is specified for every correlation.

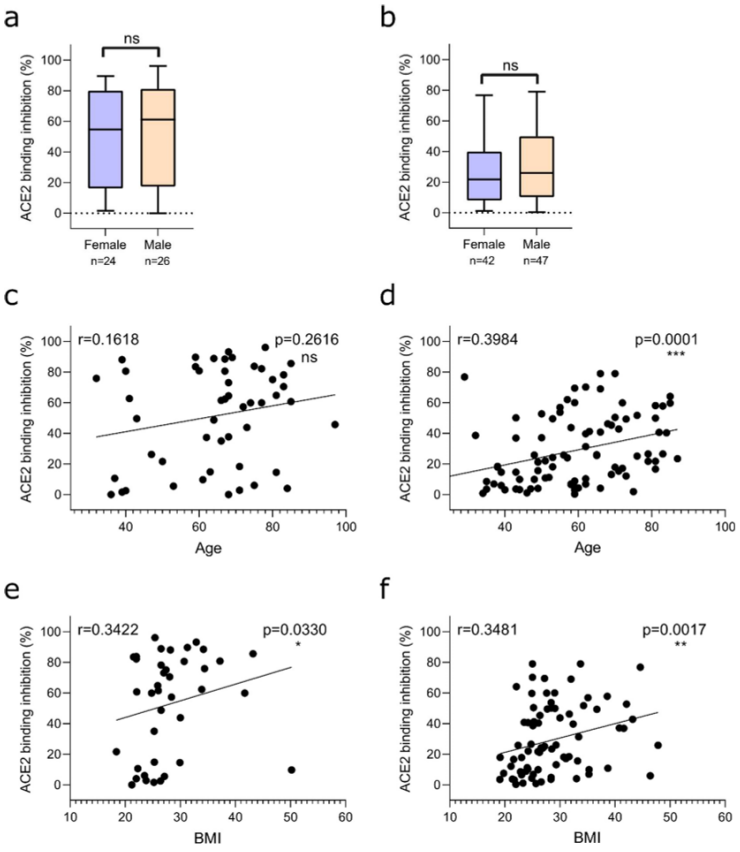

Figure S4 - Relation between ACE2 binding inhibition (%) and gender, donor age and Body-mass-index (BMI). Correlation between wild-type ACE2 binding inhibition (%) and gender (a, b), age (c, d) and BMI (e, f) for samples 7-49 days post PCR (a, c, e) and ≥ 50 days post PCR (b, d, f). P-values, when significant, are shown for all panels. Spearman's r was used to determine correlations.

Appendix III: Comparative Magnitude and Persistence of Humoral SARS-CoV-2 Vaccination Responses in the Adult Population in Germany

Dulovic A*, Kessel B*, Harries M*, Becker M, Ortmann J, Griesbaum J, Jüngling J, **Junker D**, Hernandez P, Gornyk D, Glöckner S, Melhorn V, Castell S, Heise JK, Kemmling Y, Tonn T, Frank K, Illig T, Klopp N, Warikoo N, Rath A, Suckel C, Marzian AU, Grupe N, Kaiser PD, Traenkle B, Rothbauer U, Kerrinnes T, Krause G, Lange B, Schneiderhan-Marra N, Strengert M.

Frontiers in Immunology. 2022. 13:828053

https://doi.org/10.3389/fimmu.2022.828053

frontiers in Immunology

ORIGINAL RESEARCH
published: 16 February 2022
doi: 10.3389/fimmu.2022.828053

Comparative Magnitude and Persistence of Humoral SARS-CoV-2 Vaccination Responses in the Adult Population in Germany

Alex Dulovic[1†], Barbora Kessel[2†], Manuela Harries[2†], Matthias Becker[1], Julia Ortmann[2], Johanna Griesbaum[1], Jennifer Jüngling[1], Daniel Junker[1], Pilar Hernandez[2], Daniela Gornyk[2], Stephan Glöckner[2], Vanessa Melhorn[2], Stefanie Castell[2], Jana-Kristin Heise[2], Yvonne Kemmling[2], Torsten Tonn[3], Kerstin Frank[3], Thomas Illig[4], Norman Klopp[4], Neha Warikoo[2], Angelika Rath[2], Christina Suckel[2], Anne Ulrike Marzian[2], Nicole Grupe[2], Philipp D. Kaiser[1], Bjoern Traenkle[1], Ulrich Rothbauer[1,5], Tobias Kerrinnes[6], Gérard Krause[2,7,8], Berit Lange[2,8‡], Nicole Schneiderhan-Marra[1*‡] and Monika Strengert[2,7*‡]*

[1] NMI Natural and Medical Sciences Institute at the University of Tübingen, Reutlingen, Germany, [2] Department of Epidemiology, Helmholtz Centre for Infection Research, Braunschweig, Germany, [3] German Red Cross Blood Donation Service North East, Dresden, Germany, [4] Hannover Unified Biobank, Hannover Medical School, Hannover, Germany, [5] Pharmaceutical Biotechnology, Department of Pharmacy and Biochemistry, University of Tübingen, Tübingen, Germany, [6] Department of RNA-Biology of Bacterial Infections, Helmholtz Institute for RNA-Based Infection Research, Würzburg, Germany, [7] TWINCORE, Centre for Experimental and Clinical Infection Research, a Joint Venture of the Hannover Medical School and the Helmholtz Centre for Infection Research, Hannover, Germany, [8] German Centre for Infection Research (DZIF), Partner Site Hannover-Braunschweig, Braunschweig, Germany

Recent increases in SARS-CoV-2 infections have led to questions about duration and quality of vaccine-induced immune protection. While numerous studies have been published on immune responses triggered by vaccination, these often focus on studying the impact of one or two immunisation schemes within subpopulations such as immunocompromised individuals or healthcare workers. To provide information on the duration and quality of vaccine-induced immune responses against SARS-CoV-2, we analyzed antibody titres against various SARS-CoV-2 antigens and ACE2 binding inhibition against SARS-CoV-2 wild-type and variants of concern in samples from a large German population-based seroprevalence study (MuSPAD) who had received all currently available immunisation schemes. We found that homologous mRNA-based or heterologous prime-boost vaccination produced significantly higher antibody responses than vector-based homologous vaccination. Ad26.CoV2S.2 performance was particularly concerning with reduced titres and 91.7% of samples classified as non-responsive for ACE2 binding inhibition, suggesting that recipients require a booster mRNA vaccination. While mRNA vaccination induced a higher ratio of RBD- and S1-targeting antibodies, vector-based vaccines resulted in an increased proportion of S2-targeting antibodies. Given the role of RBD- and S1-specific antibodies in neutralizing SARS-CoV-2, their relative over-representation after mRNA vaccination may explain why these vaccines have increased efficacy compared to vector-based formulations. Previously infected individuals

OPEN ACCESS

Edited by:
Ingo Drexler,
Heinrich Heine University, Germany

Reviewed by:
Lisa Müller,
Heinrich-Heine-University, Germany
Agatha Jassem,
University of British Columbia, Canada

***Correspondence:**
Berit Lange
berit.lange@helmholtz-hzi.de
Nicole Schneiderhan-Marra
nicole.schneiderhan@nmi.de
Monika Strengert
monika.strengert@helmholtz-hzi.de

†These authors have contributed equally to this work and share first authorship

‡These authors have contributed equally to this work and share last authorship

Specialty section:
This article was submitted to Vaccines and Molecular Therapeutics, a section of the journal Frontiers in Immunology

Received: *02 December 2021*
Accepted: *17 January 2022*
Published: *16 February 2022*

Citation:
Dulovic A, Kessel B, Harries M, Becker M, Ortmann J, Griesbaum J, Jüngling J, Junker D, Hernandez P, Gornyk D, Glöckner S, Melhorn V, Castell S, Heise J-K, Kemmling Y, Tonn T, Frank K, Illig T, Klopp N, Warikoo N, Rath A, Suckel C, Marzian AU, Grupe N, Kaiser PD, Traenkle B, Rothbauer U, Kerrinnes T, Krause G, Lange B, Schneiderhan-Marra N and Strengert M (2022) Comparative Magnitude and Persistence of Humoral SARS-CoV-2 Vaccination Responses in the Adult Population in Germany. Front. Immunol. 13:828053. doi: 10.3389/fimmu.2022.828053

had a robust immune response once vaccinated, regardless of which vaccine they received, which could aid future dose allocation should shortages arise for certain manufacturers. Overall, both titres and ACE2 binding inhibition peaked approximately 28 days post-second vaccination and then decreased.

Keywords: SARS-CoV-2, mRNA vaccines, vector-based vaccines, variants of concern, protective immunity, population-based study, longitudinal study, antibody persistence

INTRODUCTION

In response to the global SARS-CoV-2 pandemic, multiple vaccines have been developed, tested and licensed for use within record time (1–4). As vaccination coverage became more widespread at the beginning of 2021, countries experienced a reduction in SARS-CoV-2 infections (5, 6), although case numbers have again begun to increase in recent months due to spread among and by unvaccinated individuals (7) as well as longevity-related reductions in vaccine protection (8–11). Although a measurable correlate of protection that either prevents SARS-CoV-2 infection or limits COVID-19 disease progression is not yet defined, sufficient levels of neutralizing antibodies are assumed to be a key element (12, 13). As in most other countries, the German national vaccination strategy (until June 7th 2021) was based on prioritisation by occupation, underlying medical conditions or advanced age. Currently, 56.8 million German residents are reported to be completely vaccinated (68.3% coverage), with a further 2.4 million having so far received one dose. The majority of doses administered based on delivery numbers in Germany are BNT162b2 from Pfizer (77.0%), followed by Astra Zeneca´s AZD1222 (11.3%), Moderna's mRNA-1273 (8.7%) and Janssen's single-shot Ad26.CoV2.S (3.0%; impfdashboard.de and rki.de as of November 25th 2021). However, based on a lack of efficacy data from phase III clinical trials, the German Standing Committee on Vaccination (STIKO) recommended AZD1222 only for use in those below the age of 60. Following reports of moderate to severe thrombocytopenia and atypical thrombosis cases after AZD1222 vaccination in spring 2021 (14–16), temporary suspensions and eligibility restrictions were not only enacted in Germany (on March 15th 2021) but in 12 other EU member states (17). Administration of AZD1222 was resumed by the 1st of April 2021 in Germany, however only for those above the age of 60 or after an individual risk analysis. Individuals who had received a first dose of AZD1222 and were below the age of 60 were instead offered a mRNA-based vaccine as second dose which resulted in a heterologous prime-boost vaccination scheme (18). Although these "mix and match" approaches were not covered by the initial licensing terms, it has by now been shown that they result in a more robust humoral and cell-mediated immune response compared to the homologous AZD1222 immunisation (19, 20). While multiple studies have so far investigated vaccine-induced responses, predominantly in at-risk groups such as dialysis or transplant recipients (21, 22), groups with increased exposure risk such as health care workers (23–25) or as part of the initial clinical efficacy trials which in general enroll healthier than average populations (26), we report immunological vaccination response data from the general adult population. By using samples from a population-based seroprevalence study (MuSPAD), which assessed SARS-CoV-2 seroprevalence from July 2020 to August 2021 in eight regions in Germany (27), we examined the dynamics of vaccine-induced humoral responses using MULTICOV-AB (28) and an ACE2-RBD competition assay (29) to analyze ACE2 binding inhibition.

MATERIAL AND METHODS

MuSPAD Study Recruitment

Vaccination responses were analyzed in participants of the multi-local and serial cross-sectional prevalence study on antibodies against SARS-CoV-2 in Germany (MuSPAD) study, a nationwide population-based SARS-CoV-2 seroprevalence study (27) from July 2020 to August 2021. The study was approved by the Ethics Committee of the Hannover Medical School (9086_BO_S_2020). MuSPAD participants were recruited by age- and gender-stratified random sampling based on records from the respective local residents' registration offices. Study locations in eight regions across Germany were selected in spring 2020 based on differing epidemic activity at that time. In addition to the successive cross-sectional study design, certain study locations were sampled longitudinally within a 3-4 month interval. At the study center, following written informed consent, all eligible participants (>18 years) were subject to a standardised computer-based interview using the digital eResearch system PIA (Prospective Monitoring and Management-App) to gather basic sociodemographic data, information on pre-existing medical conditions including a previously confirmed SARS-CoV-2 infection or a SARS-CoV-2 vaccination, once it became available in Germany in late December 2020. Information about SARS-CoV-2 infections or vaccinations are self-reported. After serum was obtained by venipuncture from a serum gel S-Monovette (Sarstedt), samples were aliquoted in Matrix 2D Barcoded Screw Top Tubes (Thermo Scientific) at the Institute of Transfusion Medicine and Immunohematology and frozen at -20°C before being transported on dry ice to the Hannover Unified Biobank (Germany). After registration and quality control, one serum aliquot was shipped to the Natural and Medical Sciences Institute (Reutlingen, Germany) where they were stored at -80°C until analysis.

Study Design and Eligibility

Our study contains a total of 1821 samples from 1731 MuSPAD participants which were divided into three subgroups to examine different aspects of the vaccine-induced humoral response. Based on our inclusion criteria, individual samples can be part of several subgroups.

1. Individuals who received a homologous or heterologous complete two-dose vaccination with AZD1222, BNT162b2 and mRNA-1273 or the one-dose vaccine Ad26.CoV2.S with a blood sample taken at least 7 days but no more than 65 days post the last vaccination (hereon referred to as "mix and match sample cohort").
2. Individuals who donated one blood sample following a two-dose homologous vaccination with BNT162b2 or mRNA-1273 within the defined time frames of day 5 to 12, day 26 to 30, day 54 to 58, day 94 to 103, day 129 to 146 or day 176 to 203 after the second dose to monitor antibody kinetics (hereon referred to as "time point sample cohort").
3. Individuals with paired blood samples taken at two separate successive time points where the first sample had to be taken a minimum of seven days after the second homologous dose of BNT162b2 (hereon referred to as "longitudinal sample cohort").

All samples originated from the following locations where the MuSPAD study had previously been scheduled to take place and were collected from January to August 2021: Aachen (Städteregion), Magdeburg (Stadtkreis), Osnabrück (Stadt- und Landkreis), Chemnitz (Stadtkreis) or Landkreis Vorpommern-Greifswald. A flow chart to illustrate sample selection form the entire MuSPAD cohort can be found in **Supplementary Figure 1**. Basic sociodemographic information and details of comorbidities (hypertension, cardiovascular disease, diabetes, lung disease, immunosuppression, cancer) for each group are provided in more detail in **Table 1** and **Supplementary Table 1**. Apart from the homologous BNT162b2 samples which are part of our mix and match sample cohort, the maximum available sample number meeting the specified criteria in groups 1-3 was used. For the homologous BNT162b2 vaccination samples within our mix and match sample cohort, we applied a random selection from the entire available sample pool of BNT162b2 vaccinees who took part in the MuSPAD study to select 771 sera. Individuals with a previous SARS-CoV-2 infection either defined by a positive SARS-CoV-2 PCR or antigen test result, or a MULTICOV-AB nucleocapsid IgG normalisation ratio above 1 are listed separately (hereon referred to as "recovered") within the mix and match sample cohort. Additional sample eligibility criteria were having a complete vaccination record (manufacturer and vaccination dates) and information on age and gender as part of the participant's metadata.

MULTICOV-AB

Vaccine-induced humoral responses were analyzed using MULTICOV-AB (28), a previously published semi-quantitative multiplex immunoassay that includes both antigens of SARS-CoV-2 (e.g. Spike, Receptor Binding Domain (RBD), S1 domain, S2 domain and nucleocapsid) and the endemic coronaviruses (OC43, HKU1, NL63 and 229E). While samples were processed using an automated platform on a Beckman Coulter i7 pipetting robot as previously described (30) with minor modifications, all sample and reagent dilutions were already established and verified as part of the initial MULTICOV-AB technical assay validation process which is detailed in (28). Briefly, samples were thawed at room temperature, vortexed and then centrifuged at 2000 g for 3 mins to pellet any cell debris within the sample. Samples were then opened using a LabElite DeCapper SL (Hamilton Company). Opened sample matrix racks were then loaded into the pipetting robot, where the sample was diluted 1:200 in assay buffer, before being combined in a 384-well plate and mixed 1:1 with 1x bead mix (see **Supplementary Table 2** for antigen panel), resulting in a final dilution of 1:400. Samples were then incubated in a Thermomixer (Eppendorf) for 2 h at 1400 rpm, 20°C, in darkness. Following this initial incubation, samples were washed to remove unbound antibodies using an automated magnetic plate washer (Biotek). Bound IgG was detected by adding R-phycoerythrin labelled goat-anti-human IgG (3 µg/mL; #109-116-098, Jackson Immunoresearch Labs) and incubating for a further 45 mins at 1400 rpm, 20°C, in darkness. Following a further washing step, beads were resuspended in 100 µl of wash buffer, shaken for 1 min at 1400 rpm and then measured once on a FLEXMAP 3D instrument (Luminex Corporation) using the following settings: Timeout 100 sec, Gate 7500-15000, Reporter Gain: Standard PMT, 40 events. To ensure reproducibility, 3 quality control (QC) samples were included in octuplicate per plate. Additionally, each plate had to pass 3 QC criteria to be considered as valid run: first, throughout acquisition each sample had to reach a minimum bead count of 35 per bead ID, second median fluorescence intensity (MFI) values of sample and signal system control beads and third plate-by-plate QC sample controls had to be within normal range. Beads coupled with human IgG and goat-anti-human IgG were utilized to control for sample and signal system addition. Any sample that failed QC was remeasured for MULTICOV-AB and the ACE2-RBD competition assay (30/1821). Raw MFI values were normalised to a QC sample for all antigens as in (24, 31). A Signal to Cutoff ratio (S/CO) of 1 or above for both the trimeric Spike and RBD antigen was defined as reactive for SARS-CoV-2 Spike-specific IgG.

ACE2-RBD Competition Assay

To enable high-throughput screening of ACE2-RBD binding inhibition in the presence of sera, a previously established ACE2-RBD competition assay (29) was automated on a Beckmann Coulter i7 pipetting robot with minor modifications. 1:20 previously diluted samples from MULTICOV-AB were diluted 1:200 in ACE2 buffer (29) containing 150 ng/mL biotinylated ACE2. Samples were then mixed 1:1 with 1x VoC (Variant of Concern) bead mix containing RBDs of SARS-CoV-2 wild-type and the Alpha, Beta, Gamma, Delta VoCs (**Supplementary Table 3**), resulting in a final dilution of 1:400. Samples were then incubated in a Thermomixer for 2 h at 1400 rpm, 20°C, in darkness. Following this initial incubation, samples were washed to remove unbound ACE2 using an automated magnetic plate

TABLE 1 | Demographics of study population (n. a., not applicable; NA, not available).

Sample cohort (n)	SARS-CoV-2 infection status* (n)	Vaccine (n)	Mean ΔT (SD) in days post-vaccination	Mean ΔT (SD) in days between doses	Age (y), median (IQR)	Female (n, %)	Comorbidities (min. 1/person) (n, %)	Number of comorbidities (mean, SD)
Mix and match (1470)	+ (70)	M/M (13)	34.7 (16.3)	42.5 (27.9)	59 (11)	8 (61.5)	5 (38.5)	0.5 (0.8)
		P/P (33)	31.5 (13.5)	25.3 (9.6)	66 (29)	25 (75.8)	13 (39.4)	0.6 (0.9)
		A/A (12)	35.3 (13.5)	70.3 (19.8)	69 (7)	7 (58.3)	10 (83.3)	1.3 (0.9)
		A/M (1)**	17.0 (0.0)	66.0 (0.0)	age group 66-79	0 (0.0)	1 (100.0)	1.0 (0.0)
		A/P (6)	47.8 (14.5)	72.0 (11.6)	57 (25)	3 (50.0)	4 (66.7)	0.8 (0.7)
		J (5)	42.2 (18.0)	n. a.	40 (15)	3 (60.0)	3 (60.0)	0.6 (0.5)
	- (1400)	M/M (272)	36.5 (16.5)	31.2 (7.1)	56 (26)	162 (59.6)	108 (39.7)	0.6 (0.8)
		P/P (738)	34.7 (17.1)	27.9 (9.7)	59 (26)	456 (61.8)	438 (4 NA; 46.1)	0.7 (1.0)
		A/A (228)	37.3 (13.8)	73.6 (10.9)	66 (10)	122 (53.5)	114 (50.0)	0.7 (0.9)
		A/M (24)	20.8 (7.8)	69.6 (16.9)	68 (5)	15 (62.5)	14 (58.3)	0.8 (0.8)
		A/P (114)	31.6 (17.4)	72.2 (14.8)	59 (20)	64 (56.1)	55 (48.3)	0.8 (1.0)
		J (24)	49.8 (10.8)	n. a.	62 (14)	15 (62.5)	11 (45.8)	0.8 (1.2)
Time points (597)	–	P/P (107)	6.9 (1.4)	34.7 (13.5)	64 (26)	57 (53.3)	61 (57.0)	0.8 (0.9)
		M/M (40)	6.7 (1.3)	39.7 (11.2)	58 (27)	20 (50.0)	15 (37.5)	0.5 (0.8)
		P/P (103)	27.9 (1.4)	28.2 (9.9)	52 (42)	60 (58.3)	42 (1 NA; 41.2)	0.8 (1.1)
		M/M (8)	28.1 (1.4)	30.3 (4.7)	67 (39)	5 (62.5)	3 (37.5)	0.5 (0.7)
		P/P (92)	55.9 (1.5)	29.1 (9.6)	61 (20)	60 (65.2)	45 (48.9)	0. 8 (1.0)
		M/M (22)	55.5 (1.2)	28.0 (0.3)	57 (15)	17 (77.3)	5 (22.7)	0.3 (0.6)
		P/P (139)	97.7 (2.6)	22.3 (4.0)	60 (22)	87 (62.6)	72 (51.8)	0.8 (1.0)
		M/M (7)	98.1 (2.6)	28.9 (2.3)	64 (8)	5 (71.4)	3 (42.9)	0.9 (1.1)
		P/P (38)	138.0 (3.8)	21.0 (2.2)	80 (24)	25 (68.8)	24 (63.1)	1.2 (1.2)
		M/M (5)	141.0 (5.1)	29.2 (1.6)	83 (4)	2 (40.0)	3 (60.0)	1.2 (1.2)
		P/P (36)	189.0 (5.6)	21.7 (1.4)	50 (13)	30 (83.3)	11 (30.6)	0.4 (0.6)
		M/M (0)	n. a	n. a.	n. a.	n. a.	n. a.	n. a.
Longitudinal (180)	–	P/P T1 (90)	27.9 (14.8)	21.3 (1.2)	58 (34)	65 (72.2)	45 (2 NA; 51.1)	0.8 (1.0)
		P/P T2 (90)	166.4 (19.4)		58 (33)	65 (72.2)	48 (53.3)	0.7 (1.0)

Different vaccines and combinations are abbreviated as follows: M/M (two-dose mRNA-1273), P/P (two-dose BNT162b2), A/A (two-dose AZD1222), A/M (first dose AZD1222, second dose mRNA-1273), A/P (first dose AZD1222, second dose BNT162b2) and J (one-dose Ad26.CoV2.S). The time points sample cohort contains only homologous BNT162b2 and mRNA-1273 samples. The longitudinal sample cohort contains only paired homologous BNT162b2 taken at time 1 (T1) or 2 (T2).

**Based on self-reported positive PCR/antigen test result at study center visit and/or MULTICOV-AB nucleocapsid IgG S/CO ratio above 1; **only age group reported as n=1.*

washer. ACE2 was detected using R-phycoerythrin labelled streptavidin (2 µg/mL, #SAPE-001, Moss) by incubating the bead-sample mix for a further 45 mins at 1400 rpm, 20°C, in darkness. Following a further washing step, beads were resuspended in 100 µl of wash buffer, shaken for 1 min at 1400 rpm and then measured once on a FLEXMAP 3D instrument using the following settings: Timeout 100 sec, Gate 7500-15000, Reporter Gain: Standard PMT, 40 events. As controls, 12 blank wells, 10 wells with 150 ng/mL ACE2 alone and 10 wells with an ACE2 QC sample were included. ACE2 binding inhibition was calculated as percentage ACE2 inhibition as in (29) with 100% indicating maximum ACE2 binding inhibition and 0% no ACE2 binding inhibition. Samples with an ACE2 binding inhibition less than 20% are classified as non-responders (29).

Data Analysis and Statistics

Initial results collation and matching to metadata was done in Excel 2016 and R 4.1.0 (32).

For pair-wise comparisons of titres and ACE2 binding inhibition between vaccination schemes within our mix and match sample cohort, we used a two-sided generalized Wilcoxon test also referred to as Brunner-Munzel test (33) with a significance level of 0.05 as part of the lawstat package (34). In each comparison of two vaccination schemes, the test assesses if a titre (or ACE2 binding inhibition) tends to larger (smaller) values under one vaccination scheme in comparison to the other. Where indicated, we adjusted for multiple testing by using the Bonferroni-Holm's procedure (35) to control the family-wise error rate to be at most 0.05.

To investigate the impact of age, sex, comorbidities and time post-vaccination on the ACE2 binding inhibition between the different vaccination schemes, we used a normal linear mixed model for logit-transformed ACE2 binding inhibition. Negative measurement values were replaced by 0.001 to enable the transformation. The model included additive effects of age, sex, time post-vaccination (peak response period: 7-27 days vs plateau response period: 28-65 days) and comorbidities [cardiovascular disease, hypertension, diabetes, lung disease and cancer/immunosuppression (which were combined to a binary indicator based on low sample numbers)]. The model further included a random effect defined by the variable "plate number" to account for dependencies due to the measurement procedure, and allowed for heteroscedastic variances for younger (<=70) and older (>70) ages and vaccination types. REML estimation was implemented using the lme function [nlme library (36)]. Statistical testing was based on the asymptotic normality of the estimates. As part of a sensitivity analysis, we extended the model with interaction terms between each confounder and the time post-vaccination, allowing for possibly differing effects in the peak (7-27 days) and plateau (28-65 days) period after the last vaccination.

Since the effects of the considered covariates were allowed to differ between the individual vaccination schemes, we analyzed only four vaccination schemes (BNT162b2-BNT162b2, mRNA-1273-mRNA-1273, AZD1222-BNT162b2, AZD1222-AZD1222) with a reasonable sample size in the mix and match study cohort, while we excluded immunisation with AZD1222-mRNA-1273 and Ad26.CoV2.S due to the low sample number of 24 per scheme. Additionally, four individuals with a BNT162b2-BNT162b2 vaccination with missing comorbidity metadata were excluded from this analysis. The described statistical comparison of vaccination schemes within the mix and match cohort was performed after the exclusion of recovered individuals.

To assess the impact of a previous SARS-CoV-2 infection on RBD antibody titres and wild-type ACE2 binding inhibition among the different vaccination schemes, we also used a two-sided generalized Wilcoxon (Brunner-Munzel) test.

To generate a heat map for comparing antigen-specific antibody formation across different vaccination schemes within the mix and match sample cohort, normalised antibody responses were initially scaled using the function "z-score", before being plotted as a heat map. To evaluate longitudinal changes in antibody response and ACE2 binding inhibition within our longitudinal sample cohort, changes from T1 to T2 were calculated using log2 fold change. Any increase in titre or binding is represented by a positive value, while decreases in titre or binding are represented by negative values.

Data visualization was done in RStudio (Version 1.2.5001 running R version 3.6.1). Additional packages "gplots" (37) and "beeswarm" (38) were used for specific displays (22). Graphs were exported from RStudio and further edited in Inkscape (Version 0.92.4) to generate final figures.

RESULTS

First, we examined differences in humoral responses between individuals who received homologous or heterologous immunisation schemes within our mix and match sample cohort where vaccine dose distribution is similar to the German vaccine coverage. Using MULTICOV-AB, we compared vaccination-induced antibody titres generated against the full-length Spike trimer, RBD, S1 and S2 domains and found that mRNA-based homologous vaccinations induced a greater Spike (median normalised MFI: mRNA-1273 13.78, BNT162b2 12.49, AZD1222 5.68, Ad26.CoV2.S 3.65), RBD (median normalised MFI: mRNA-1273 29.12, BNT162b2 24.89, AZD1222 9.61, Ad26.CoV2.S 5.25) and S1 response (median normalised MFI: mRNA-1273 195.9, BNT162b2 139.8, AZD1222 56.40, Ad26.CoV2.S 10.14) than vector-based ones (**Figure 1**). When comparing between the two vector-based vaccinations, the two-dose immunisation with AZD1222 resulted in higher titres than the one-dose Ad26.CoV2.S from Janssen. For mRNA vaccines, Moderna's mRNA-1273 produced a significantly higher response than Pfizer's BNT162b2 (p-values <0.001, **Supplementary Table 5**). Heterologous dose vaccination schemes resulted in comparable titres (for Spike and RBD) as homologous mRNA vaccine regimens among our study group independent of the origin of the second dose (Spike normalised MFI: AZD1222-mRNA-1273 13.59, AZD1222-BNT162b2 13.27, RBD normalised MFI: AZD1222-mRNA-1273 28.17, AZD1222-BNT162b2 25.93). Heterologous titres were in addition significantly higher than those after a homologous AZD1222 two-dose immunisation (p-values <0.001, **Supplementary Table 5**). In line with their lower titres, serological non-responder rate (defined as a Signal to Cutoff ratio (S/CO) below 1 for either Spike or RBD antigen) was highest for vector-based homologous vaccination schemes (**Table 2**).

As multiplex-based serology tests such as MULTICOV-AB offer the unique opportunity for in-depth profiling of polyclonal antibody reactivity towards multiple viral antigens, we then assessed differences in antibody specificities between the different vaccines. Within the mix and match sample cohort, we observed that mRNA-based SARS-CoV-2 vaccinations resulted in reduced S2-specific antibody titres compared to vector-based ones (**Figure 1**). To investigate this unequal antibody distribution further, we initially scaled titres for each individual antigen (**Figure 2**), and found that while Spike, RBD, S1 titres were low for both AZD1222 and Ad26.CoV2.S, S2-specific titres were considerably higher than expected. We then calculated proportional ratios between antigens (**Table 3**), confirming that homologous mRNA vaccination resulted in significantly higher proportion of RBD- (mRNA-1273 14.01-fold, BNT162b2 18.63-fold, AZD1222 5.23-fold) and S1-targeted antibodies (mRNA-1273 97.21-fold, BNT162b2 110.10-fold, AZD1222 33.48-fold) compared to S2-targeted immunoglobulins. This over-representation of S1-targeting antibodies following mRNA vaccination, was also present in those who received a heterologous immunisation scheme (AZD1222-mRNA-1273 47.60-fold, AZD1222-BNT162b2 65.06-fold).

Having determined that mRNA vaccines produce a significantly higher proportion of RBD and S1 antibodies, we next investigated their ACE2 binding inhibition as these antigens are predominantly responsible for antibody-mediated virus neutralization (12, 13). For this, we used a previously published ACE2-RBD competition assay (22, 29, 30), which detects neutralizing antibody activity only and is comparable to classical viral neutralization assays (24, 29). As expected, homologous mRNA vaccination resulted in higher ACE2 binding inhibition than homologous vector-based vaccination (median ACE2 binding inhibition mRNA-1273 93.1%, BNT162b2 80.1%, AZD1222 38.5%, Ad26.CoV2.S 3.3%, **Figure 3**). Neutralizing antibodies generated following vaccination with Ad26.CoV2.S resulted in minimal ACE2 binding inhibition, with only 8.3% being classified as responders (29). As variants of concern now comprise the majority of infections globally (39), we also assessed ACE2 binding inhibition against the Alpha, Beta, Gamma and Delta SARS-CoV-2 VoC strains. ACE2 binding inhibition was most similar to wild-type for the Alpha variant, followed by Delta whereas Beta and Gamma variants had the largest reductions in ACE2 binding inhibition (**Supplementary Figure 2**).

Due to the range of responses recorded for each dose combination and likely differences in population characteristics

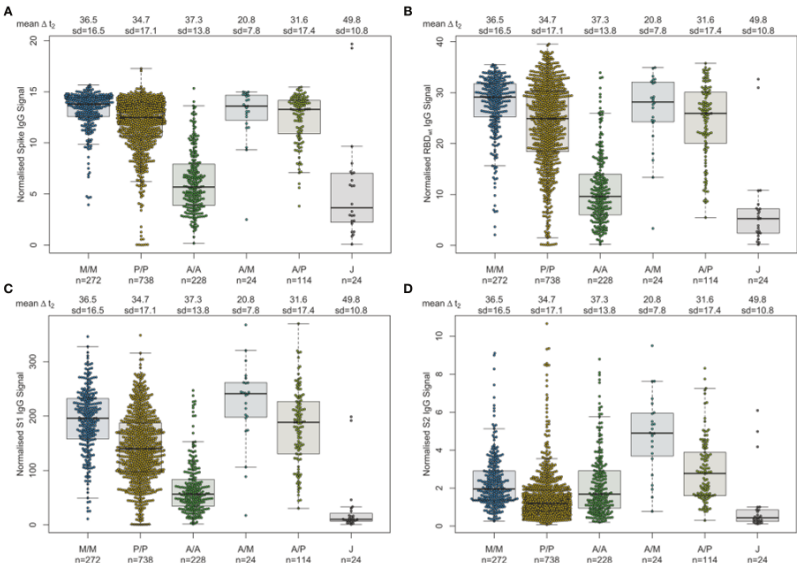

FIGURE 1 | Different SARS-CoV-2 vaccination schemes result in distinct humoral responses. IgG antibody titres against full-length Spike trimer **(A)**, receptor-binding domain (RBD) **(B)**, S1 domain **(C)** and S2 domain **(D)** were measured with MULTICOV-AB. Individuals received either homologous mRNA-1273 (M/M, blue, n = 272), BNT162b2 (P/P, orange, n = 738) or AZD1222 (A/A, green, n = 228), heterologous AZD1222-mRNA-1273 (A/M, light blue, n = 24), AZD1222-BNT162b2 (A/P, light green, n = 114), or a single dose of Ad26.CoV2.S (J, grey, n = 24). Raw MFI values were normalised against QC samples to generate signal ratios for each antigen. Data is shown as box and whisker plots overlaid with strip charts. Boxes represent medians, 25th and 75th percentiles and whiskers show the largest and smallest non-outlier values based on 1.5 IQR calculation. Time between sampling and full vaccination is displayed as mean and SD for each group. Number of samples per vaccination scheme are stated below.

as a result of changing vaccine recommendations, we examined whether confounders (sampling time post-vaccination (ΔT), age, gender or comorbidities) were instead responsible. To analyze impact of ΔT, we separated samples into 7 to 27 days post-final dose to capture peak response and 28 to 65 days post-final dose to capture plateau response (**Figure 4**). While there was a reduction in median response for samples from individuals collected within the plateau phase, the pattern between the vaccines remained consistent. While increasing age did result in small reductions in ACE2 binding inhibition (only significant for BNT162b2, $p<0.001$), the vaccine dosing scheme received had a substantially larger effect, with the eldest age group (>79) of homologous mRNA vaccine recipients still having increased IgG titres and ACE2 inhibition capacities than the youngest (26 to 45) AZD1222 recipients (**Figure 4**). Regression modelling for ACE2 binding inhibition against wild-type confirmed the decrease of ACE2 binding inhibition with time post-vaccination for all vaccination types except homologous AZD1222 (**Supplementary Table 4A**). While age did not cause a significant decrease for homologous AZD1222, this may have been due to the low number of samples at both ends of the age range within our cohort. For mRNA-1273, while age did result in a significant decrease during the peak period ($p=0.029$), this was not present within the plateau phase ($p=0.615$). For homologous BNT162b2 vaccination, male sex seemed to be associated with a decreased ACE2 binding inhibition, although the same was not true for mRNA-1273. Similar patterns were observed for the ACE2 binding inhibition against Alpha, Beta, Gamma and Delta VoCs (**Supplementary Tables 4B–E**). As we observed serological non-responders within our mix and match study cohort, we systematically evaluated their distribution among the different immunisation schemes (**Table 2**). Overall, vector-based homologous vaccination (2.8%) resulted in a higher proportion of non-responders than homologous mRNA-based vaccination (0.9%). Neither age nor gender was a determining factor in being a non-responder.

As our population-based cohort also contained individuals who had been previously infected and then vaccinated, we examined what effect this had upon their vaccine-induced response. As previously observed (40), recovered and then

TABLE 2 | Vaccine non-responder rates across study population.

Sample cohort (n)	ΔT range post-vaccination (days)	Vaccine (n)	Non-responders MULTICOV-AB (n, %)	Non-responders ACE2-RBD WT (n, %)
Mix and match (1400)	7-65	M/M (272)	0 (0.0)	0 (0.0)
		P/P (738)	9 (1.2)	18 (2.4)
		A/A (228)	4 (1.8)	26 (11.4)
		A/M (24)	0 (0.0)	0 (0.0)
		A/P (114)	0 (0.0)	0 (0.0)
		J (24)	3 (12.5)	22 (91.7)
Time points (597)	5-12	P/P (107)	6 (5.6)	13 (12.2)
		M/M (40)	1 (2.5)	1 (2.5)
	26-30	P/P (103)	1 (1.0)	2 (1.9)
		M/M (8)	0 (0.0)	0 (0.0)
	54-58	P/P (92)	1 (1.1)	3 (3.3)
		M/M (22)	0 (0.0)	0 (0.0)
	94-103	P/P (139)	2 (1.4)	8 (5.8)
		M/M (7)	0 (0.0)	0 (0.0)
	129-146	P/P (38)	3 (7.9)	2 (5.3)
		M/M (5)	1 (20.0)	1 (20.0)
	176-203	P/P (36)	0 (0.0)	8 (22.2)
		M/M (0)	n. a.	n. a.
Longitudinal (180)	T1: 7-63	P/P T1 (90)	2 (2.2)	3 (3.3)
	T2: 121-203	P/P T2 (90)	2 (2.2)	17 (18.9)

MULTICOV-AB non-responders were determined as in (28), with samples that had a signal to cutoff ratio below 1 for either the Spike or RBD being considered non-responders. ACE2-RBD non-responders were determined as in (29), with samples that had a ACE2 binding inhibition less than 20% being considered non-responders. Different vaccines and combinations are abbreviated as follows: M/M (two-dose mRNA-1273), P/P (two-dose BNT162b2), A/A (two-dose AZD1222), A/M (first dose AZD1222, second dose mRNA-1273), A/P (first dose AZD1222, second dose BNT162b2) and J (one-dose Ad26.CoV2.S). The time points sample cohort contains only homologous BNT162b2 and mRNA-1273 samples. The longitudinal sample cohort contains only paired homologous BNT162b2 taken at time 1 (T1) or 2 (T2).

vaccinated individuals developed high levels of IgG with strong ACE2 binding inhibition (**Figure 5** and **Supplementary Table 6**). While mRNA or heterologous vaccination of recovered individuals still elevated median RBD IgG titres (mRNA-1273 31.81, BNT162b2 32.23, AZD1222-mRNA-1273 35.18, AZD1222-BNT162b2 30.49, **Supplementary Figure 3**) and median ACE2 binding inhibition (mRNA-1273 98.1%, BNT162b2 98.8%, AZD1222-mRNA-1273 99.3%, AZD1222-BNT162b2 97.7%, **Figure 5**), increases were particularly apparent for the vector-based vaccinations where median RBD IgG titres (AZD1222 24.69, Ad26.CoV2.S 36.53, **Supplementary Figure 3**) and median ACE2 binding inhibition (AZD1222 92.9%, Ad26.CoV2.S 70.8%, **Figure 5**) were significantly higher than in SARS-CoV-2 naïve vaccinated individuals (median RBD IgG mRNA-1273 29.12, BNT162b2 24.89, AZD1222-mRNA-1273 28.17, AZD1222-BNT162b2 25.93, AZD1222 9.61, Ad26.CoV2.S 5.25, **Figure 1**) and median ACE2 binding inhibition (mRNA-1273 93.1%, BNT162b2 80.1%, AZD1222-mRNA-1273 94.5%, AZD1222-BNT162b2 88.6%, AZD1222 38.5%, Ad26.CoV2.S 3.3%, **Figure 3**).

Having determined that mRNA-based vaccination resulted in an increased humoral response, we evaluated lifespan and antibody response kinetics using our time point sample cohort which were selected to mimic key response periods for antibody-producing B-cell activity such as expansion, peak and plateau phase after a complete vaccination scheme. Vaccine-induced titres and ACE2 binding inhibition both initially increased, peaked during the second time point (26 to 30 days post-second dose), and then decreased linearly as time increased (**Figure 6** and **Supplementary Table 7**). ACE2 binding inhibition followed the same pattern of decrease as time increased. In contrast to antibody levels, the percentage of non-responders showed however a trend for increased decline already from time point 94 to 103 days post-second vaccination onwards for BNT162b2, with 22.2% of samples considered as non-responders at 176-203 days post-second vaccination (**Table 2**). As already observed in **Figure 1**, mRNA-1273 (blue line) resulted in higher titres and ACE2 binding inhibition compared to BNT162b2 (yellow line) for all monitored time points. To validate this pattern of decreasing antibody titres and ACE2 inhibition activity, we examined samples from a cohort of longitudinal donors (longitudinal sample cohort). Unlike the time point sample cohort, this cohort contained paired samples from each donor which allows to directly compare changes in titre and neutralization activity from the first sampling to the second sampling. While these samples had a variable initial ΔT post-full vaccination (7-63 days), the sampling intervals between first and second donation were more comparable (114-163 days). Overall, mean reduction in RBD-specific antibody titres were 66.3% between their first and second sampling (**Figure 7**). Among the different SARS-CoV-2 antigens, RBD and S1 antibodies had the largest decrease, while Spike Trimer and S2 had the smallest. This reduction in titre was also reflected in ACE2 binding inhibition from the first to second sampling for both the wild-type RBD which was reduced substantially (mean difference of 42%) and for all the VoC RBDs (mean difference: Alpha 36%, Beta 30%, Gamma 29%, Delta 38%).

DISCUSSION

We report both significant and substantial differences in humoral responses generated by the different vaccines and immunisation schemes currently available in Germany, with homologous

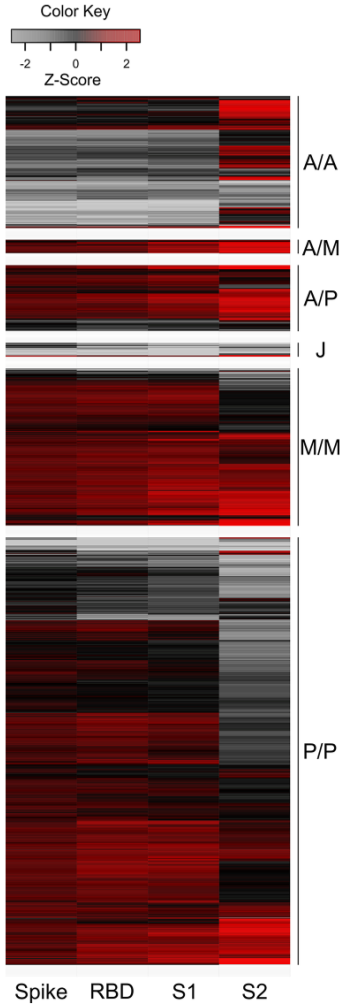

FIGURE 2 | Humoral immune response after mRNA vaccination is skewed towards increased RBD and S1 titres, while vector-based vaccination results in increased S2 antibody levels. Antigen-specific antibody titres measured in the mix and match sample cohort were scaled and centered per antigen. Resulting values greater than 2.5 and smaller than -2.5 were set to these extreme values instead. Samples were then clustered within their subgroups based on immunisation scheme and are displayed as a heat map. Negative values represent below average titres and positive values represent positive above average titres per antigen. Colour shades indicate low (grey) to high (red) value distribution. A/A – two-dose AZD1222. A/M – first dose AZD1222, second dose mRNA-1273. A/P – first dose AZD1222, second dose BNT162b2. M/M – two-dose mRNA-1273. P/P – two-dose BNT162b2. J – one-dose Ad26.CoV2.S.

TABLE 3 | Antigen-specific ratios for different vaccination schemes.

	Antibody target (95% CI)					
Vaccine	**RBD vs S**	**S1 vs S**	**S1 vs RBD**	**S vs S2**	**RBD vs S2**	**S1 vs S2**
A/A	1.72 (1.66-1.78)	10.09 (9.72-10.47)	5.89 (5.73-6.11)	3.38 (3.04-3.60)	5.23 (4.65-6.07)	33.48 (27.92-37.56)
A/M	1.97 (1.85-2.26)	16.71 (15.04-18.37)	8.15 (7.86-8.68)	2.76 (2.15-3.48)	5.86 (4.58-6.28)	47.60 (41.28-53.66)
A/P	1.97 (1.90-2.04)	14.16 (13.42-14.64)	7.17 (6.95-7.36)	4.76 (4.08-5.46)	8.60 (7.85-10.53)	65.06 (58.95-69.61)
M/M	2.10 (2.06-2.12)	14.19 (13.67-14.47)	6.80 (6.61-6.93)	6.88 (6.24-7.55)	14.01 (12.74-15.09)	97.21 (92.07-100.90)
P/P	2.00 (1.96-2.04)	11.21 (10.95-11.52)	5.72 (5.64-5.78)	9.99 (9.48-10.43)	18.63 (17.82-20.00)	110.10 (104.20-114.10)
J	1.23 (0.97-1.61)	3.30 (2.72-4.18)	2.79 (2.35-4.06)	8.89 (3.71-13.27)	6.83 (4.70-22.35)	31.53 (15.53-38.63)

Ratios were calculated by dividing normalised MFI values for the two targets for all samples. RBD – receptor-binding domain, S – full-length trimeric Spike protein. Median values with 95% CI in brackets are shown. A/A – two-dose AZD1222. A/M – first dose AZD1222, second dose mRNA-1273. A/P – first dose AZD1222, second dose BNT162b2. M/M – two-dose mRNA-1273. P/P – two-dose BNT162b2. J – one-dose Ad26.CoV2.S.

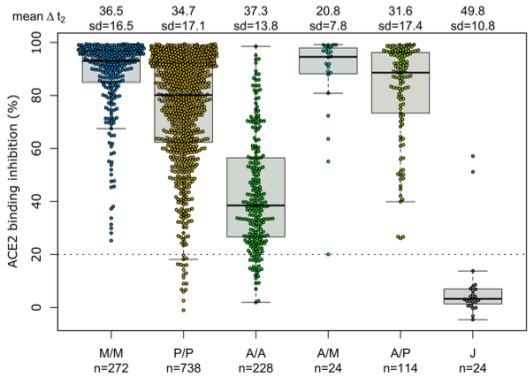

FIGURE 3 | Different vaccination schemes impact ACE2 binding inhibition against SARS-CoV-2 wild-type. ACE2 binding inhibition against the SARS-CoV-2 wild-type (B.1 isolate) RBD was assessed by an ACE2-RBD competition assay for homologous mRNA [mRNA-1273 (M/M, blue), BNT162b2 (P/P, orange)], heterologous prime-boost (AZD1222-mRNA-1273 (A/M, light blue), AZD1222-BNT162b2 (A/P, light green) or vector-based [AZD1222-AZD1222 (A/A, green), Ad26.CoV2.S (J, grey)] vaccination schemes in the mix and match cohort. Data is shown as box and whisker plots overlaid with strip charts. Boxes represent medians, 25th and 75th percentiles and whiskers show the largest and smallest non-outlier values based on 1.5 IQR calculation. The threshold for non-responsive samples (ACE2 binding inhibition less than 20%) is shown as dotted line. All samples below this threshold can be considered non-responsive. Time between sampling and full vaccination is displayed as mean and SD for each group. Number of samples per vaccination scheme are stated below. ACE2 binding inhibition towards VoCs can be found in **Supplementary Figure 2**.

mRNA or combined heterologous vector and mRNA vaccination approaches inducing significantly higher titres and ACE2 binding inhibition compared to homologous vector-based vaccination schemes. This expands on results from on-going randomized and observational trials such as the ComCoV (41) or CoCo (42) study which provided only information on AZD1222-BNT162b2 schemes (20, 43). Further, as expected titres and ACE2 binding inhibition for AZD1222 were reduced compared to mRNA-based vaccination (43). Among homologous mRNA regimens, we identified like others, that mRNA-1273 resulted in higher antibody titres and ACE2 binding inhibition than BNT162b2 (40, 44). Extending time periods between successive doses of mRNA and vector-based vaccinations also positively impacted on serological and cellular response levels or vaccine efficiency and effectiveness (1, 45–49). The German STIKO recommended at the time of the study dosing intervals of six weeks between mRNA vaccines, 12 weeks for vector vaccines and 9-12 weeks for heterologous vaccination approaches (18). While heterologous and vector vaccination dosing intervals in our mix and match cohort adhere more closely to those extended intervals (1), time periods for mRNA vaccine dosing across our study population mimic 21 or 28 days from clinical trials (3, 4) and licensing agreements (50, 51) making them unlikely contributors to the observed differences in humoral responses. While we have used an ACE2-RBD competition assay to measure ACE2 binding inhibition as opposed to classic virus neutralization assays, this assay analyses neutralizing antibodies as seen by its similar performance to VNT (24, 29). ACE2

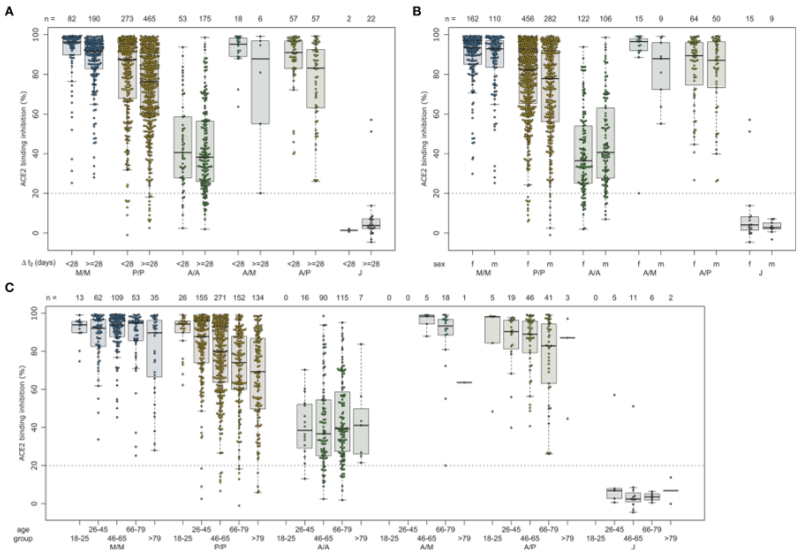

FIGURE 4 | Effect of time post-vaccination, gender and age on ACE2 binding inhibition for different SARS-CoV-2 vaccination schemes. ACE2 binding inhibition against the SARS-CoV-2 wild-type (B.1 isolate) RBD was assessed by an ACE2-RBD competition assay. Samples were split according to vaccination scheme (homologous mRNA [mRNA-1273 (M/M, blue), BNT162b2 (P/P, orange)], heterologous prime-boost (AZD1222-mRNA-1273 (A/M, light blue), AZD1222-BNT162b2 (A/P, light green) or vector-based [AZD1222-AZD1222 (A/A, green), Ad26.CoV2.S (J, grey)]. To display impact of potential confounders, samples were further split in time post-vaccination up to 27 and above 27 days **(A)**, gender **(B)** and indicated age groups **(C)**. Boxes represent medians, 25th and 75th percentiles and whiskers show the largest and smallest non-outlier values based on 1.5 IQR calculation. The threshold for non-responsive samples (ACE2 binding inhibition less than 20%) is shown as dotted line. All samples below this threshold can be considered non-responsive. Time between sampling and full vaccination is displayed as mean and SD for each group. Number of samples per vaccination scheme are stated below the figure. Statistical significance was calculated by a regression model (**Supplementary Table 4**).

inhibition assays instead of a VNT have also already been used successfully by other groups to determine neutralizing antibody activity (52). Methodically, MULTICOV-AB and the ACE2-RBD competition assay are also complementary and are measured using a single initial sample dilution which further reduces variability between their results. By multiplex-based antibody profiling, we were able to further investigate titre differences and determined that vector- and mRNA-based vaccines induced a distinct pattern of Spike subdomain-targeted antibodies. While vector-based formulations result in a significantly larger proportion of S2-domain antibodies, RBD- and S1-domain antibodies dominated in mRNA vaccines. While these observations require further detailed investigation, the relative over-representation of RBD- and S1-targeting antibodies within mRNA vaccines is particularly intriguing as these two antigens comprise the majority of neutralizing antibody activity (13, 53). Although a series of modelling studies have now linked levels of neutralizing antibodies to vaccine efficacy (12, 54), a clearly defined correlation of vaccine efficacy and neutralizing antibody levels is still lacking. Nevertheless it appears logical that increased antibody levels specific to virus proteins-mediating cell attachment could result in enhanced levels of protection from infection and contribute to observed differences in vaccine efficacy and effectiveness levels (3, 55, 56). Interestingly, our conclusions are strengthened by studies examining the relative immunogenicity of the different Spike subdomains. By immunising rabbits with SARS-CoV-2 S2, S1 or RBD proteins, Ravichandran et al. were able to show that S2 protein elicited considerable lower neutralizing antibody levels compared to the S1 and RBD antigens (57). Similar results were obtained from isolating immunoglobulins of COVID-19 convalescents where S2 subunit-targeting antibodies showed weaker SARS-CoV-2 neutralization activity compared to the RBD-targeting ones (58). While the Spike protein surface is extensively glycosylated, including the membrane-proximal S2 domain, the RBD completely lacks N-glycans which might explain its immunodominance (59–61).

An additional finding of our study requiring further investigation is the relatively poor performance of Ad26.CoV2.S, particularly for induction of neutralizing antibodies for both SARS-CoV-2 wild-type and VoC RBDs. While some studies have reported

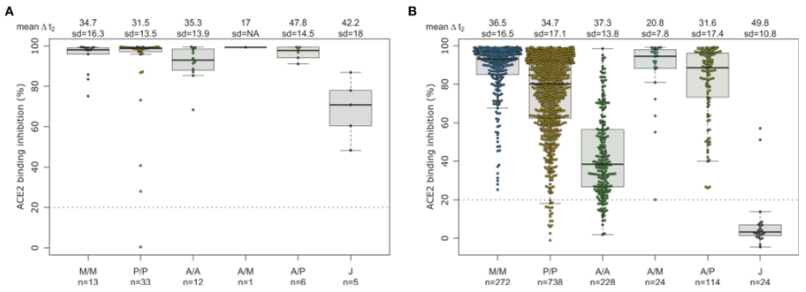

FIGURE 5 | SARS-CoV-2 vaccination boosts ACE2 binding inhibition among recovered individuals independent of vaccination scheme. Differences in vaccination responses of recovered previously SARS-CoV-2 infected individuals from our mix and match cohort were analyzed using an ACE2-RBD competition assay **(A)**. SARS-CoV-2 infection status was based on a previous self-reported positive PCR/antigen test or a MULTICOV-AB nucleocapsid IgG normalisation ratio above 1. Samples were split according to vaccination scheme in homologous mRNA (mRNA-1273 (M/M, blue), BNT162b2 (P/P, orange)), heterologous prime-boost (AZD1222-mRNA-1273 (A/M, light blue), AZD1222-BNT162b2 (A/P, light green) or vector-based (AZD1222-AZD1222 (A/A, green), Ad26.CoV2.S (J, grey)). For clarity and comparison, ACE2 inhibition of SARS-CoV-2 naïve individuals are displayed **(B)**. Boxes represent medians, 25th and 75th percentiles and whiskers show the largest and smallest non-outlier values based on 1.5 IQR calculation. If not enough sample to generate a box were present (minimum 5), then only the median is indicated by a line. The threshold for non-responsive samples (ACE2 binding inhibition less than 20%) is shown as dotted line. All samples below this can be considered non-responsive. Time between sampling and full vaccination is displayed as mean and SD for each group. Number of samples per vaccination scheme are stated below the graph. Results of a formal statistical comparison of recovered-vaccinated and SARS-CoV-2 naïve-vaccinated individuals are shown in **Supplementary Table 6**.

sufficient levels of neutralizing activity after vaccination with Ad26.CoV2.S (2), others identified minimal neutralizing activity, particularly when compared to other COVID-19 vaccines from Pfizer or Moderna (44). The relatively poor performance of Ad26.CoV2.S in inducing an antibody response has also been identified by researchers studying other bodily fluids (e.g. breast milk), who found that Ad26.CoV2.S produced significantly fewer IgA antibodies than BNT162b2 or mRNA-1273 (62). While our Ad26.CoV2.S sample group size is low (n=29), it is three times larger than a recent study from the manufacturer which reported neutralizing activity against Delta and other VoCs [n=8 (63)]. It should be noted that four of the eight individuals within their cohort were reported as being spike seropositive at baseline which is a consistent finding with our cohort, where strong ACE2 binding inhibition was only achieved in those individuals who had been previously infected. Our median time point is however earlier than the reported peak of antibody activity (2, 64). Further independent investigations into the neutralizing activity generated by single-dose Ad26.CoV2.S to clarify those differing results within SARS-CoV-2 naïve individuals are therefore urgently needed.

Among confounding variables, we identified like others that age resulted in a general reduction in titre and ACE2 binding inhibition (11, 40, 65), although the vaccination scheme received had a more significant effect. While recovered individuals developing high titres and ACE2 binding inhibition once vaccinated has been previously reported (40, 43), we found that these responses were similar among all vaccines and immunisation schemes. Given that current German guidelines require a six month post-positive PCR waiting period before receiving a first dose, this suggests that such individuals would be suitable for all currently licensed vaccines, assuming they meet pre-existing EMA and STIKO criteria. This ability to use all vaccines and generate a substantial response will be of particular public health importance, given the on-going booster dose administration which could impact availability for some vaccine brands, as happened earlier in 2021.

Our results on the longevity of the humoral response post-vaccination is similar to others, in identifying an initial peak from approximately 28 days post-second dose onwards followed by a gradual reduction over time (66). As expected, ACE2 binding inhibition and titre are mostly mirrored in their decline over time. However, the increased numbers of non-responders from BNT162b2-vaccinated individuals from six months after the second vaccine needs further careful monitoring until a precise correlate of protection has been defined. Among the different SARS-CoV-2 antibodies, it is unsurprising that the RBD and S1 underwent the greatest reductions as they had the largest titres to begin with. Between VoCs, we did not identify any apparent differences in ACE2 binding inhibition between the differing immunisation schemes for confounders. Instead, again vaccine type or regimen (homologous vs heterologous) received had the largest effect upon ACE2 binding inhibition. The VoCs themselves followed a previously published pattern (9, 22, 67), with the lowest reduction for the Alpha variant, and the highest for the Beta and Gamma variants. It should be stated that in our analysis of longitudinal samples, there is a wide variety of timeframes post-vaccination, meaning that initial samples are collected both before, during and after the initial peak response at around 28 days. While we have then made the assumption that decreases in responses would be linear to the second sampling, this is not the case as some

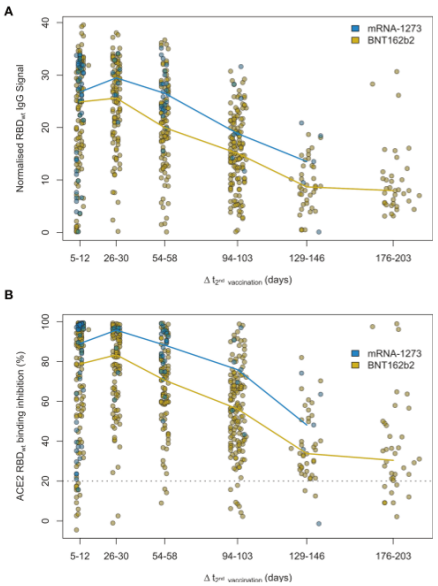

FIGURE 6 | Antibody and neutralization response kinetic up to 7 months after SARS-CoV-2 mRNA vaccination. Humoral vaccine response was assessed by MULTICOV-AB **(A)** and an ACE2-RBD competition assay **(B)** using the time point sample set. Samples were either 5 to 12, 26 to 30, 54 to 58, 94 to 103, 129 to 146 and 176 to 203 days post-second dose of either a two-dose BNT162b2 (yellow, n = 515) or mRNA-1273 (blue, n = 82) vaccination. Colored line connects median response per time point and vaccine. Data is displayed as normalised IgG RBD ratio or as % ACE2 binding inhibition where 100% indicates maximum binding inhibition and 0% no binding inhibition. The threshold for non-responsive samples (ACE2 binding inhibition less than 20%) is shown as dotted line. All samples below this threshold can be considered non-responsive. Median values with 95% CI and IQR of RBD_{wt} IgG signal and ACE2 binding inhibition are shown in **Supplementary Table 7**.

of the early collected samples (e.g. 7 days post-second vaccination) would have initially increased before later decreasing. However, our purpose of this analysis was to measure changes over a larger timeframe (4 months) and the difference in time from first to second sampling, means that all samples should be in the decline phase by their second sampling.

Our manuscript has several limitations, namely that we are only measuring antibodies (including neutralizing antibodies) that are present within serum. As previously stated, we have used an ACE2-RBD competition assay to measure inhibition of ACE2 binding instead of classical virus neutralization assays, although the results of this assay have already been shown to be similar to VNT and are known to be specific to neutralizing antibody responses only. While neutralizing antibodies themselves are considered a strong correlate for protection (13), other components that are not measured within our assays such as T-cell mediated immunity will also offer protection (68, 69). Our use of serum also means that memory B-cells, which are involved in protection against severe disease progression (70), are equally excluded from our analysis. Our study cohort consists of relatively low sample numbers for both heterologous and Ad26.CoV2.S vaccinations whereas BNT162b2 samples are overrepresented. However, our sample numbers are similar or in case of Ad26.CoV2.S exceed other previously published work making our study one of the largest independent evaluation studies of this vaccine. Our BNT162b2 sample size mimics dose distribution in Germany where approximately 70% of delivered vaccine doses were from Pfizer. Our study population is also relatively similar in regard to age and gender. Last, self-reported information about a previous SARS-CoV-2 infection or vaccination could bias study outcome. However, recent studies have found a good correlation between self-reported and administrative records with 98% consistency for vaccination type and 95% for vaccination date or detection of SARS-CoV-2 antibodies with a positive predictive value of 98.2% and a negative predictive value of 97.3%, respectively (71, 72). Additionally, our data on persistence and magnitude of vaccine-induced humoral responses is consistent with several other cohort-based studies (11, 20, 41, 66) which did not rely on self-reported vaccination records, therefore stressing the validity of our approach.

Next to an increasing number of observational studies including ours which examine vaccine-induced protection by assessing levels of humoral immunity, several large scale test-negative design (TND) studies have by now been conducted to determine vaccine effectiveness against a laboratory-confirmed SARS-CoV-2 infection requiring medical attention outside of randomized clinical trials (45, 73, 74). While readouts between those study types are fundamentally different and both are subject to different limitations (75–79), results are comparable. For instance, our findings of significantly higher titres and ACE2 binding inhibition after mRNA or heterologous immunisation schemes compared vector-based ones also translate to differing levels of vaccine effectiveness against SARS-CoV-2 infection of above 90% with at least one mRNA vaccine dose or of less than 70% with two doses of AZD1222 in a TND study from Canada (45). Equally, our results of decreasing humoral response levels after a full BNT162b2 vaccination correlate with increases in PCR-confirmed SARS-CoV-2 infections up to six month post-vaccination with BNT162b2 in an Israeli TND study (73).

Overall, we provide data on the vaccine-induced humoral response for all currently available mRNA-, vector-based and heterologous immunisation schemes in Germany. Within our population-based cohort, mRNA homologous or heterologous vaccination resulted in increased humoral responses. Our multiplex approach identified differences in quantities and ratios of RBD- and S1-targeting antibodies following mRNA homologous or heterologous vaccination. Further investigation into this targeting will be of particular interest to improve vaccine performance particularly for next generation vector-based vaccines.

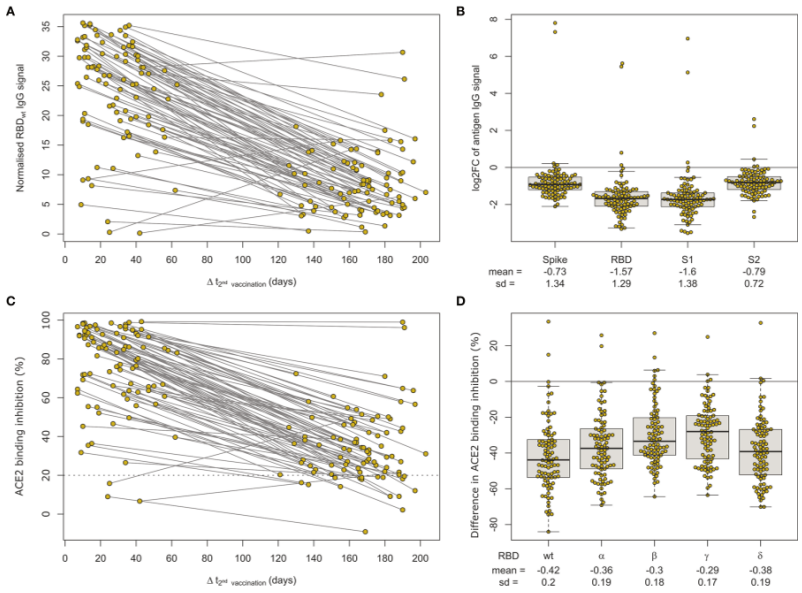

FIGURE 7 | Longitudinal mRNA vaccine response monitoring defines decreases over time. Humoral response was assessed by MULTICOV-AB **(A, B)** and an ACE2-RBD competition assay **(C, D)** for all samples of the paired longitudinal sample set at indicated time points post-second dose of 90 individuals after a two-dose BNT162b2 vaccination. Line graph illustrates longitudinal development of RBD-specific antibody levels **(A)** or ACE2 binding inhibition **(C)** towards WT RBD as time post-vaccination increases. The threshold (less than 20% ACE2 binding inhibition) for non-responsive samples within the ACE2-RBD competition assay is shown (dotted line). All samples below this threshold are considered non-responsive. SARS-CoV-2 antigen-specific differences in longitudinal humoral response are expressed as log2 fold changes **(B)**. Reduction in ACE2 binding inhibition for RBD of Alpha, Beta, Gamma and Delta VoC between sampling times is shown as difference **(D)**.

DATA AVAILABILITY STATEMENT

Source data and the analysis code have been deposited on GitHub (https://github.com/BeckerMatthias/MuSPAD_VaccStudy).

ETHICS STATEMENT

The studies involving human participants were reviewed and approved by the Ethics Committee of Hannover Medical School (9086_BO_S_2020). The participants provided their written informed consent to participate in this study.

AUTHOR CONTRIBUTIONS

MS, AD, BL, GK, and NS-M conceived the study. NS-M, MS, BL, VM, SC, and GK procured funding. AD, MS, MB, and NS-M designed the experiments. AD, JG, JJ, and DJ performed the experiments. AD, MS, MB, MH, JO, SC, NW, SG, J-KH, and BK performed data collection and analysis. AD, MB, MH, and BK generated figures and tables. TT, KF, TI, and NK organized sample collection and processing. AD, MS, MH, and BK verified the underlying data. AD, MS, and MB wrote the manuscript. AD, MH, JO, PH, BL, NS-M, MS, YK, DG, VM, DJ, PK, BT, UR, TT, KF, NK, TI, TK, AR, CS, AR, AM, and NG contributed resources or were involved in project administration. All authors critically reviewed and approved the final manuscript.

FUNDING

This work was financially supported by the Initiative and Networking Fund of the Helmholtz Association of German Research Centres (grant number SO-96), the EU Horizon 2020 research and innovation program (grant agreement number 101003480 - CORESMA), intramural funds of the Helmholtz Centre for Infection Research and the State Ministry of Baden-

Württemberg for Economic Affairs, Labour and Tourism (grant numbers FKZ 3-4332.62-NMI-67 and FKZ 3-4332.62-NMI-68). The funders had no role in study design, data collection and analysis, decision to publish, or preparation of the manuscript.

ACKNOWLEDGMENTS

First and foremost, we would like to thank the MuSPAD participants for their willingness and commitment to make this study possible. We also want to thank all laboratory members and administrative staff at the Institute of Transfusion Medicine and Immunohematology in Plauen for continued excellent technical and organizational support in sample processing. We are grateful to the entire team of BOS112 for running of MuSPAD study sites. We sincerely thank all participating counties, cities and local health care authorities for their support. We thank Astrid Hans and Carina Lützow for administrative assistance. We thank members of the Multiplex Immunoassays Group at the NMI for their assistance in sample arrival and storage.

SUPPLEMENTARY MATERIAL

The Supplementary Material for this article can be found online at: https://www.frontiersin.org/articles/10.3389/fimmu.2022.828053/full#supplementary-material

REFERENCES

1. Voysey M, Clemens SAC, Madhi SA, Weckx LY, Folegatti PM, Aley PK, et al. Safety and Efficacy of the ChAdOx1 Ncov-19 Vaccine (AZD1222) Against SARS-CoV-2: An Interim Analysis of Four Randomised Controlled Trials in Brazil, South Africa, and the UK. *Lancet* (2021) 397(10269):99–111. doi: 10.1016/S0140-6736(20)32661-1
2. Sadoff J, Gray G, Vandebosch A, Cárdenas V, Shukarev G, Grinsztejn B, et al. Safety and Efficacy of Single-Dose Ad26.Cov2.S Vaccine Against Covid-19. *New Engl J Med* (2021) 384(23):2187–201. doi: 10.1056/NEJMoa2101544
3. Baden LR, El Sahly HM, Essink B, Kotloff K, Frey S, Novak R, et al. Efficacy and Safety of the mRNA-1273 SARS-CoV-2 Vaccine. *N Engl J Med* (2020) 384 (5):403–16. doi: 10.1056/NEJMoa2035389
4. Polack FP, Thomas SJ, Kitchin N, Absalon J, Gurtman A, Lockhart S, et al. Safety and Efficacy of the BNT162b2 mRNA Covid-19 Vaccine. *N Engl J Med* (2020) 383(27):2603–15. doi: 10.1056/NEJMoa2034577
5. RKI COVID-19 Dashboard. Available at: https://experience.arcgis.com/experience/478220a4c454480e823b17327b2bf1d4/page/page_1/2021.
6. Statistisches Beratungslabor, Institut für Statistik and LMU München. (2021): Corona.stat.uni-muenchen.de/maps/
7. Scobie HM, Johnson AG, Suthar AB, Severson R, Alden NB, Balter S, et al. Monitoring Incidence of COVID-19 Cases, Hospitalizations, and Deaths, by Vaccination Status - 13 U.S. Jurisdictions, April 4-July 17, 2021. *MMWR Morb Mortal Wkly Rep* (2021) 70(37):1284–90. doi: 10.15585/mmwr.mm7037e1
8. Israeli Government. (2021) Report available under: https://www.gov.il/BlobFolder/reports/vaccine-efficacy-safety-follow-up-committee/he/files_publications_corona_two-dose-vaccination-data.pdf2021.
9. Dulovic A, Strengert M, Ramos GM, Becker M, Griesbaum J, Junker D, et al. Diminishing Immune Responses Against Variants of Concern in Dialysis Patients Four Months After SARS-CoV-2 mRNA Vaccination. *medRxiv* (2021) 2021.08.16.21262115. doi: 10.1101/2021.08.16.21262115
10. Kustin T, Harel N, Finkel U, Perchik S, Harari S, Tahor M, et al. Evidence for Increased Breakthrough Rates of SARS-CoV-2 Variants of Concern in BNT162b2-mRNA-Vaccinated Individuals. *Nat Med* (2021) 27(8):1379–84. doi: 10.1038/s41591-021-01413-7
11. Naaber P, Tserel L, Kangro K, Sepp E, Jürjenson V, Adamson A, et al. Dynamics of Antibody Response to BNT162b2 Vaccine After Six Months: A Longitudinal Prospective Study. *Lancet Regional Health - Europe* (2021) 10:100208. doi: 10.1016/j.lanepe.2021.100208
12. Earle KA, Ambrosino DM, Fiore-Gartland A, Goldblatt D, Gilbert PB, Siber GR, et al. Evidence for Antibody as a Protective Correlate for COVID-19 Vaccines. *Vaccine* (2021) 39(32):4423–8. doi: 10.1016/j.vaccine.2021.05.063
13. Khoury DS, Cromer D, Reynaldi A, Schlub TE, Wheatley AK, Juno JA, et al. Neutralizing Antibody Levels Are Highly Predictive of Immune Protection From Symptomatic SARS-CoV-2 Infection. *Nat Med* (2021) 27(7):1205–11. doi: 10.1038/s41591-021-01377-8
14. Althaus K, Möller P, Uzun G, Singh A, Beck A, Bettag M, et al. Antibody-Mediated Procoagulant Platelets in SARS-CoV-2-Vaccination Associated Immune Thrombotic Thrombocytopenia. *Haematologica* (2021) 106 (8):2170–9. doi: 10.3324/haematol.2021.279000
15. Greinacher A, Thiele T, Warkentin TE, Weisser K, Kyrle PA, Eichinger S. Thrombotic Thrombocytopenia After ChAdOx1 Ncov-19 Vaccination. *New Engl J Med* (2021) 384(22):2092–101. doi: 10.1056/NEJMoa2104840
16. Pottegård A, Lund LC, Karlstad Ø, Dahl J, Andersen M, Hallas J, et al. Arterial Events, Venous Thromboembolism, Thrombocytopenia, and Bleeding After Vaccination With Oxford-AstraZeneca ChAdOx1-S in Denmark and Norway: Population Based Cohort Study. *BMJ* (2021) 373:n1114. doi: 10.1136/bmj.n1114
17. Wise J. Covid-19: European Countries Suspend Use of Oxford-AstraZeneca Vaccine After Reports of Blood Clots. *BMJ* (2021) 372:n699. doi: 10.1136/bmj.n699
18. Vygen-Bonnet S, Koch J, Bogdan C, Harder T, Heininger U, Kling K, et al. Beschluss Der STIKO Zur 5. Aktualisierung Der COVID-19-Impfempfehlung Und Die Dazugehörige Wissenschaftliche Begründung. *Epid Bull* (2021) (19):24–36. doi: 10.25646/8467
19. Schmidt T, Klemis V, Schub D, Mihm J, Hielscher F, Marx S, et al. Immunogenicity and Reactogenicity of Heterologous ChAdOx1 Ncov-19/mRNA Vaccination. *Nat Med* (2021) 27(9):1530–5. doi: 10.1038/s41591-021-01464-w
20. Barros-Martins J, Hammerschmidt SI, Cossmann A, Odak I, Stankov MV, Morillas Ramos G, et al. Immune Responses Against SARS-CoV-2 Variants After Heterologous and Homologous ChAdOx1 Ncov-19/BNT162b2 Vaccination. *Nat Med* (2021) 27(9):1525–9. doi: 10.1038/s41591-021-01449-9
21. Carr EJ, Wu M, Harvey R, Wall EC, Kelly G, Hussain S, et al. Neutralising Antibodies After COVID-19 Vaccination in UK Haemodialysis Patients. *Lancet* (2021) 398(10305):1038–41. doi: 10.1016/S0140-6736(21)01854-7
22. Strengert M, Becker M, Ramos GM, Dulovic A, Gruber J, Juengling J, et al. Cellular and Humoral Immunogenicity of a SARS-CoV-2 mRNA Vaccine in Patients on Haemodialysis. *EBioMedicine* (2021) 70:103524. doi: 10.1016/j.ebiom.2021.103524
23. Harsch IA, Ortloff A, Reinhöfer M, Epstude J. Symptoms, Antibody Levels and Vaccination Attitude After Asymptomatic to Moderate COVID-19 Infection in 200 Healthcare Workers. *GMS Hygiene Infect Control* (2021) 16:Doc15. doi: 10.3205/dgkh000386
24. Becker M, Dulovic A, Junker D, Ruetalo N, Kaiser PD, Pinilla YT, et al. Immune Response to SARS-CoV-2 Variants of Concern in Vaccinated Individuals. *Nat Commun* (2021) 12(1):3109. doi: 10.1038/s41467-021-23473-6
25. Galanis P, Vraka I, Fragkou D, Bilali A, Kaitelidou D. Seroprevalence of SARS-CoV-2 Antibodies and Associated Factors in Healthcare Workers: A Systematic Review and Meta-Analysis. *J Hosp Infect* (2021) 108:120–34. doi: 10.1016/j.jhin.2020.11.008
26. Tregoning JS, Flight KE, Higham SL, Wang Z, Pierce BF. Progress of the COVID-19 Vaccine Effort: Viruses, Vaccines and Variants Versus Efficacy, Effectiveness and Escape. *Nat Rev Immunol* (2021) 21(10):626–36. doi: 10.1038/s41577-021-00592-1

27. Gornyk D, Harries M, Glöckner S, Strengert M, Kerrinnes T, Heise J-K, et al. SARS-CoV-2 Seroprevalence in Germany. *Dtsch Arztebl Int* (2021) 0 (OnlineFirst):1–. doi: 10.3238/arztebl.m2021.0364
28. Becker M, Strengert M, Junker D, Kaiser PD, Kerrinnes T, Traenkle B, et al. Exploring Beyond Clinical Routine SARS-CoV-2 Serology Using MultiCoV-Ab to Evaluate Endemic Coronavirus Cross-Reactivity. *Nat Commun* (2021) 12(1):1152. doi: 10.1038/s41467-021-20973-3
29. Junker D, Dulovic A, Becker M, Wagner TR, Kaiser PD, Traenkle B, et al. Reduced Serum Neutralization Capacity Against SARS-CoV-2 Variants in a Multiplex ACE2 RBD Competition Assay. *medRxiv* (2021) 2021.08.20.21262328. doi: 10.1101/2021.08.20.21262328
30. Renk H, Dulovic A, Seidel A, Becker M, Fabricius D, Zernickel M, et al. Robust and Durable Serological Response Following Pediatric SARS-CoV-2 Infection. *Nat Commun* (2022) 13(1):128. doi: 10.1038/s41467-021-27595-9
31. Planatscher H, Rimmele S, Michel G, Potz O, Joos T, Schneiderhan-Marra N. Systematic Reference Sample Generation for Multiplexed Serological Assays. *Sci Rep* (2013) 3. doi: 10.1038/srep03259
32. R Core Team. *R: A Language and Environment for Statistical Computing*. Vienna, Austria: R Foundation for Statistical Computing (2021).
33. Brunner E, Munzel U. (2000). The Nonparametric Behrens-Fischer Problem: Asymptotic Theory and A Small-Sample Approximation. *Biometrical J* 42 (1):17-25.
34. Gastwirth JL, Gel YR, Wallace Hui WL, Lyubchich V, Miao W, Noguchi K. (2020). lawstat: Tools for biostatistics, public policy, and law. R-package version 3.4, https://CRAN.R-project.org/package=lawstat
35. Holm S. A Simple Sequentially Rejective Multiple Test Procedure. *Scandinavian J Stat* (1979) 6(2):65–70.
36. Pinheiro J, Bates D, DebRoy S, Sarkar D. R Core Team (2022). nlme: Linear and nonlinear mixed effects models. R-package version 3.1-155, https://Cran.R-project.org/package=nlme
37. Warnes GR, Bolker B, Bonebakker L, Gentleman R, Huber W, Liaw A, et al. *Gplots: Various R Programming Tools for Plotting Data. R package version 3.1.1*. (2021) https://CRAN.R-project.org/package=gplots.
38. Eklund A, Trimble J. *Beeswarm: The Bee Swarm Plot, an Alternative to Stripchart. R Package Version 0.4.0*. (2021) https://CRAN.R-project.org/package=beeswarm.
39. CoVariants. *Shared Mutations*. Available at: https://covariants.org/shared-mutations.
40. Steensels D, Pierlet N, Penders J, Mesotten D, Heylen L. Comparison of SARS-CoV-2 Antibody Response Following Vaccination With BNT162b2 and mRNA-1273. *JAMA* (2021) 326(15):1533–35. doi: 10.1001/jama.2021.15125
41. Liu X, Shaw RH, Stuart ASV, Greenland M, Aley PK, Andrews NJ, et al. Safety and Immunogenicity of Heterologous Versus Homologous Prime-Boost Schedules With an Adenoviral Vectored and mRNA COVID-19 Vaccine (Com-COV): A Single-Blind, Randomised, Non-Inferiority Trial. *Lancet (London England)* (2021) 398(10303):856–69. doi: 10.1016/S0140-6736(21)01694-9
42. Behrens GMN, Cossmann A, Stankov MV, Schulte B, Streeck H, Förster R, et al. Strategic Anti-SARS-CoV-2 Serology Testing in a Low Prevalence Setting: The COVID-19 Contact (CoCo) Study in Healthcare Professionals. *Infect Dis Ther* (2020) 9(4):837–49. doi: 10.1007/s40121-020-00334-1
43. Eyre DW, Lumley SF, Wei J, Cox S, James T, Justice A, et al. Quantitative SARS-CoV-2 Anti-Spike Responses to Pfizer-BioNTech and Oxford-AstraZeneca Vaccines by Previous Infection Status. *Clin Microbiol Infect* (2021) 27(10):1516.e7–.14. doi: 10.1016/j.cmi.2021.05.041
44. Tada T, Zhou H, Samanovic MI, Dcosta BM, Cornelius A, Mulligan MJ, et al. Comparison of Neutralizing Antibody Titers Elicited by mRNA and Adenoviral Vector Vaccine Against SARS-CoV-2 Variants. *bioRxiv* (2021) 2021.07.19.452771. doi: 10.1101/2021.07.19.452771
45. Skowronski DM, Setayeshgar S, Febriani Y, Ouakki M, Zou M, Talbot D, et al. Two-Dose SARS-CoV-2 Vaccine Effectiveness With Mixed Schedules and Extended Dosing Intervals: Test-Negative Design Studies From British Columbia and Quebec, Canada. *medRxiv* (2021) 2021.10.26.21265397. doi: 10.1101/2021.10.26.21265397
46. Amirthalingam G, Bernal JL, Andrews NJ, Whitaker H, Gower C, Stowe J, et al. Higher Serological Responses and Increased Vaccine Effectiveness Demonstrate the Value of Extended Vaccine Schedules in Combatting COVID-19 in England. *medRxiv* (2021) 2021.07.26.21261140. doi: 10.1101/2021.07.26.21261140
47. Grunau B, Asamoah-Boaheng M, Lavoie PM, Karim ME, Kirkham TL, Demers PA, et al. A Higher Antibody Response Is Generated With a 6- to 7-Week (vs Standard) Severe Acute Respiratory Syndrome Coronavirus 2 (SARS-CoV-2) Vaccine Dosing Interval. *Clin Infect Dis* (2021) ciab938. doi: 10.1093/cid/ciab938
48. Payne RP, Longet S, Austin JA, Skelly DT, Dejnirattisai W, Adele S, et al. Immunogenicity of Standard and Extended Dosing Intervals of BNT162b2 mRNA Vaccine. *Cell* (2021) 184(23):5699–714.e11. doi: 10.1016/j.cell.2021.10.011
49. Tauzin A, Gong SY, Beaudoin-Bussières G, Vézina D, Gasser R, Nault L, et al. Strong Humoral Immune Responses Against SARS-CoV-2 Spike After BNT162b2 mRNA Vaccination With a 16-Week Interval Between Doses. *Cell Host Microbe* (2021). doi: 10.1016/j.chom.2021.12.004
50. European Medicines Agency, Committee for Medicinal Products for Human Use (CHMP, 2021): Assessment report Comirnaty. EMA/707383/2020 Corr1.
51. European Medicines Agency, Committee for Medicinal Products for Human Use (CHMP, 2021): Assessment report COVID-19 Vaccine Moderna. EMA/702084/2021; EMEA/H/C/005735.
52. Lopez E, Haycroft ER, Adair A, Mordant FL, O'Neill MT, Pymm P, et al. Simultaneous Evaluation of Antibodies That Inhibit SARS-CoV-2 Variants via Multiplex Assay. *JCI Insight* (2021) 6(16). doi: 10.1172/jci.insight.150012
53. Zost SJ, Gilchuk P, Case JB, Binshtein E, Chen RE, Nkolola JP, et al. Potently Neutralizing and Protective Human Antibodies Against SARS-CoV-2. *Nature* (2020) 584(7821):443–9. doi: 10.1038/s41586-020-2548-6
54. Feng S, Phillips DJ, White T, Sayal H, Aley PK, Bibi S, et al. Correlates of Protection Against Symptomatic and Asymptomatic SARS-CoV-2 Infection. *Nat Med* (2021) 27:2032–40. doi: 10.1101/2021.06.21.21258528
55. Madhi SA, Baillie V, Cutland CL, Voysey M, Koen AL, Fairlie L, et al. Efficacy of the ChAdOx1 nCoV-19 Covid-19 Vaccine against the B.1.351 Variant. *New Engl J Med* (2021) 384(20):1885–98.
56. Self WH, Tenforde MW, Rhoads JP, Gaglani M, Ginde AA, Douin DJ, et al. Comparative Effectiveness of Moderna, Pfizer-BioNTech, and Janssen (Johnson & Johnson) Vaccines in Preventing COVID-19 Hospitalizations Among Adults Without Immunocompromising Conditions - United States, March-August 2021. *MMWR Morb Mortal Wkly Rep* (2021) 70(38):1337–43. doi: 10.15585/mmwr.mm7038e1
57. Ravichandran S, Coyle Elizabeth M, Klenow L, Tang J, Grubbs G, Liu S, et al. Antibody Signature Induced by SARS-CoV-2 Spike Protein Immunogens in Rabbits. *Sci Trans Med* (2020) 12(550):eabc3539. doi: 10.1126/scitranslmed.abc3539
58. Wec AZ, Wrapp D, Herbert AS, Maurer DP, Haslwanter D, Sakharkar M, et al. Broad Neutralization of SARS-Related Viruses by Human Monoclonal Antibodies. *Science* (2020) 369(6504):731–6. doi: 10.1126/science.abc7424
59. Watanabe Y, Allen JD, Wrapp D, McLellan JS, Crispin M. Site-Specific Glycan Analysis of the SARS-CoV-2 Spike. *Science* (2020) 369(6501):330–3. doi: 10.1126/science.abb9983
60. Walls AC, Park Y-J, Tortorici MA, Wall A, McGuire AT, Veesler D. Structure, Function, and Antigenicity of the SARS-CoV-2 Spike Glycoprotein. *Cell* (2020) 181(2):281–92.e6. doi: 10.1016/j.cell.2020.02.058
61. Grant OC, Montgomery D, Ito K, Woods RJ. Analysis of the SARS-CoV-2 Spike Protein Glycan Shield Reveals Implications for Immune Recognition. *Sci Rep* (2020) 10(1):14991. doi: 10.1038/s41598-020-71748-7
62. Fox A, DeCarlo C, Yang X, Norris C, Powell RL. Comparative Profiles of SARS-CoV-2 Spike-Specific Milk Antibodies Elicited by COVID-19 Vaccines Currently Authorized in the USA. *medRxiv* (2021) 2021.07.19.21260794. doi: 10.1101/2021.07.19.21260794
63. Jongeneelen M, Kaszas K, Veldman D, Huizingh J, van der Vlugt R, Schouten T, et al. Ad26.COV2.S Elicited Neutralizing Activity Against Delta and Other SARS-CoV-2 Variants of Concern. *bioRxiv* (2021) 2021.07.01.450707. doi: 10.1101/2021.07.01.450707
64. Barouch DH, Stephenson KE, Sadoff J, Yu J, Chang A, Gebre M, et al. Durable Humoral and Cellular Immune Responses 8 Months After Ad26.COV2.S Vaccination. *N Engl J Med* (2021) 385(10):951–3. doi: 10.1056/NEJMc2108829
65. Shrotri M, Fragaszy E, Geismar C, Nguyen V, Beale S, Braithwaite I, et al. Spike-Antibody Responses to ChAdOx1 and BNT162b2 Vaccines by Demographic and Clinical Factors (Virus Watch Study). *medRxiv* (2021) 2021.05.12.21257102. doi: 10.1101/2021.05.12.21257102
66. Doria-Rose N, Suthar MS, Makowski M, O'Connell S, McDermott AB, Flach B, et al. Antibody Persistence Through 6 Months After the Second Dose of

mRNA-1273 Vaccine for Covid-19. *N Engl J Med* (2021) 384(23):2259–61. doi: 10.1056/NEJMc2103916
67. van Gils MJ, Lavell AHA, van der Straten K, Appelman B, Bontjer I, Poniman M, et al. Four SARS-CoV-2 Vaccines Induce Quantitatively Different Antibody Responses Against SARS-CoV-2 Variants. *medRxiv* (2021) 2021.09.27.21264163. doi: 10.1101/2021.09.27.21264163
68. Mateus J, Dan Jennifer M, Zhang Z, Rydyznski Moderbacher C, Lammers M, Goodwin B, et al. Low-Dose mRNA-1273 COVID-19 Vaccine Generates Durable Memory Enhanced by Cross-Reactive T Cells. *Science* (2021) eabj9853. doi: 10.1126/science.abj9853
69. Israelow B, Mao T, Klein J, Song E, Menasche B, Omer Saad B, et al. Adaptive Immune Determinants of Viral Clearance and Protection in Mouse Models of SARS-CoV-2. *Sci Immunol* (2021) eabl4509. doi: 10.1126/sciimmunol.abl4509
70. Goel RR, Apostolidis SA, Painter MM, Mathew D, Pattekar A, Kuthuru O, et al. Distinct Antibody and Memory B Cell Responses in SARS-CoV-2 Naïve and Recovered Individuals Following mRNA Vaccination. *Sci Immunol* (2021) 6(58):abm0829. doi: 10.1126/sciimmunol.abi6950
71. Pritchard E, Matthews PC, Stoesser N, Eyre DW, Gethings O, Vihta K-D, et al. Impact of Vaccination on New SARS-CoV-2 Infections in the United Kingdom. *Nat Med* (2021) 27(8):1370–8. doi: 10.1038/s41591-021-01410-w
72. Siegler AJ, Luisi N, Hall EW, Bradley H, Sanchez T, Lopman BA, et al. Trajectory of COVID-19 Vaccine Hesitancy Over Time and Association of Initial Vaccine Hesitancy With Subsequent Vaccination. *JAMA Network Open* (2021) 4(9):e2126882–e. doi: 10.1001/jamanetworkopen.2021.26882
73. Israel A, Merzon E, Schäffer AA, Shenhar Y, Green I, Golan-Cohen A, et al. Elapsed Time Since BNT162b2 Vaccine and Risk of SARS-CoV-2 Infection: Test Negative Design Study. *BMJ* (2021) 375:e067873. doi: 10.1136/bmj-2021-067873
74. Thompson MG, Stenehjem E, Grannis S, Ball SW, Naleway AL, Ong TC, et al. Effectiveness of Covid-19 Vaccines in Ambulatory and Inpatient Care Settings. *N Engl J Med* (2021) 385(15):1355–71. doi: 10.1056/NEJMoa2110362
75. Houlihan CF, Beale R. The Complexities of SARS-CoV-2 Serology. *Lancet Infect Dis* (2020) 20(12):1350–1. doi: 10.1016/S1473-3099(20)30699-X
76. Dean NE, Hogan JW, Schnitzer ME. Covid-19 Vaccine Effectiveness and the Test-Negative Design. *N Engl J Med* (2021) 385(15):1431–3. doi: 10.1056/NEJMe2113151
77. Vandenbroucke JP, Brickley EB, Vandenbroucke-Grauls CMJE, Pearce N. A Test-Negative Design With Additional Population Controls Can Be Used to Rapidly Study Causes of the SARS-CoV-2 Epidemic. *Epidemiology* (2020) 31 (6). doi: 10.1097/EDE.0000000000001251
78. Galipeau Y, Greig M, Liu G, Driedger M, Langlois M-A. Humoral Responses and Serological Assays in SARS-CoV-2 Infections. *Front Immunol* (2020) 11:3382. doi: 10.3389/fimmu.2020.610688
79. Patel MK, Bergeri I, Bresee JS, Cowling BJ, Crowcroft NS, Fahmy K, et al. Evaluation of Post-Introduction COVID-19 Vaccine Effectiveness: Summary of Interim Guidance of the World Health Organization. *Vaccine* (2021) 39 (30):4013–24. doi: 10.1016/j.vaccine.2021.05.099

Conflict of Interest: NS-M was a speaker at Luminex user meetings in the past. The Natural and Medical Sciences Institute at the University of Tübingen is involved in applied research projects as a fee for services with the Luminex Corporation.

The remaining authors declare that the research was conducted in the absence of any commercial or financial relationships that could be construed as a potential conflict of interest.

Supplementary Material - Comparative magnitude and persistence of humoral SARS-CoV-2 vaccination responses in the adult population in Germany

Alex Dulovic[1,#], Barbora Kessel[2,#], Manuela Harries[2,#], Matthias Becker[1], Julia Ortmann[2], Johanna Griesbaum[1], Jennifer Jüngling[1], Daniel Junker[1], Pilar Hernandez[2], Daniela Gornyk[2], Stephan Glöckner[2], Vanessa Melhorn[2], Stefanie Castell[2], Jana-Kristin Heise[2], Yvonne Kemmling[2], Torsten Tonn[3], Kerstin Frank[3], Thomas Illig[4], Norman Klopp[4], Neha Warikoo[2], Angelika Rath[2], Christina Suckel[2], Anne Ulrike Marzian[2], Nicole Grupe[2], Philipp D. Kaiser[1], Bjoern Traenkle[1], Ulrich Rothbauer[1,5], Tobias Kerrinnes[6], Gérard Krause[2,7,8], Berit Lange[2,8,§,*], Nicole Schneiderhan-Marra[1,§,*], Monika Strengert [2,7,§,*]

[1] NMI Natural and Medical Sciences Institute at the University of Tübingen, Reutlingen, Germany
[2] Helmholtz Centre for Infection Research, Department of Epidemiology, Braunschweig, Germany
[3] German Red Cross Blood Donation Service North East, Dresden, Germany
[4] Hannover Unified Biobank, Hannover Medical School, Hannover, Germany
[5] Pharmaceutical Biotechnology, Department of Pharmacy and Biochemistry, University of Tübingen, Tübingen, Germany
[6] Helmholtz Institute for RNA-based Infection Research, Department of RNA-Biology of Bacterial Infections, Würzburg, Germany
[7] TWINCORE, Centre for Experimental and Clinical Infection Research, a joint venture of the Hannover Medical School and the Helmholtz Centre for Infection Research, Hannover, Germany
[8] German Centre for Infection Research (DZIF), partner site Hannover-Braunschweig, Braunschweig, Germany

# these authors have contributed equally to this work and share first authorship.
§ these authors have contributed equally to this work and share last authorship.
* corresponding authors.

* Correspondence:

Monika Strengert
monika.strengert@helmholtz-hzi.de

Berit Lange
berit.lange@helmholtz-hzi.de

Nicole Schneiderhan-Marra
nicole.schneiderhan@nmi.de

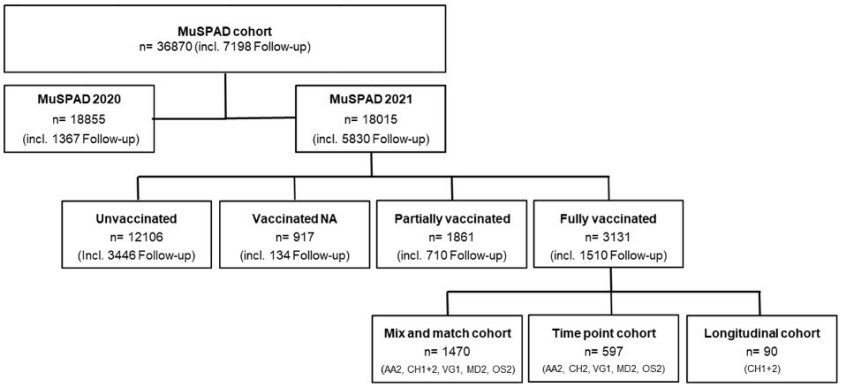

Supplementary Figure 1. Flow chart for sample selection from MuSPAD cohort.
Sample selection for our vaccine response study from the entire MuSPAD cohort is displayed in a flow chart. Samples were selected based on selection criteria outlined in method section to examine impact of vaccination scheme, length and persistence of antibody response. Samples originated from the following study locations: Aachen 2 (AA2), Chemnitz 1(CH1), Chemnitz 2 (CH2), Vorpommern-Greifswald 1 (VG1), Osnabrück 2 (OS2), and Magdeburg 2 (MD2). Number of participants is given per group (n), NA: not available.

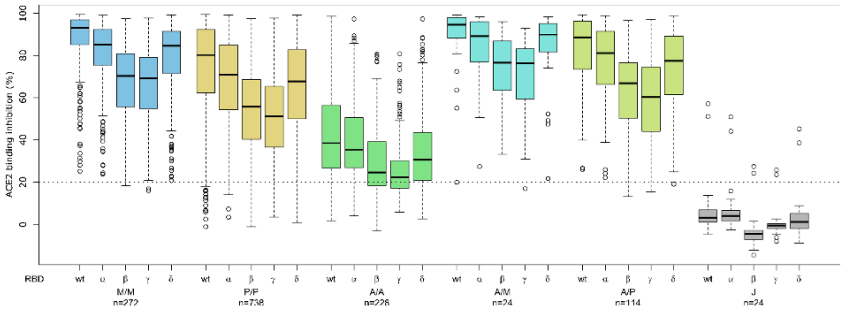

Supplementary Figure 2. Different VoCs reduce antibody ACE2 binding inhibition comparably between SARS-CoV-2 vaccination schemes.
ACE2 binding inhibition against the SARS-CoV-2 VoC Alpha (B.1.1.7), Beta (B.1.351), Gamma (P1) and Delta (B.1.617.2) RBDs was assessed by an ACE2-RBD competition assay for homologous mRNA (mRNA-1273 (M/M, blue), BNT162b2 (P/P, orange)), heterologous prime-boost (AZD1222-mRNA-1273 (A/M, light blue), AZD1222-BNT162b2 (A/P, light green) or vector-based (AZD1222-AZD1222 (A/A, green), Ad26.CoV2.S (J, grey)) vaccination schemes in the mix and match cohort. SARS-CoV-2 RBD WT (Figure 3) is again shown for clarity and comparison. Data is shown as box and whisker plots. Boxes represent medians, 25th and 75th percentiles and whiskers show the largest and smallest non-outlier values based on 1.5 IQR calculation. Outlier values are shown in clear circles. The threshold for non-responsive samples (ACE2 binding inhibition less than 20%) is shown as dotted line. All samples below this can be considered non-responsive. Number of samples per vaccination scheme are stated below the figure.

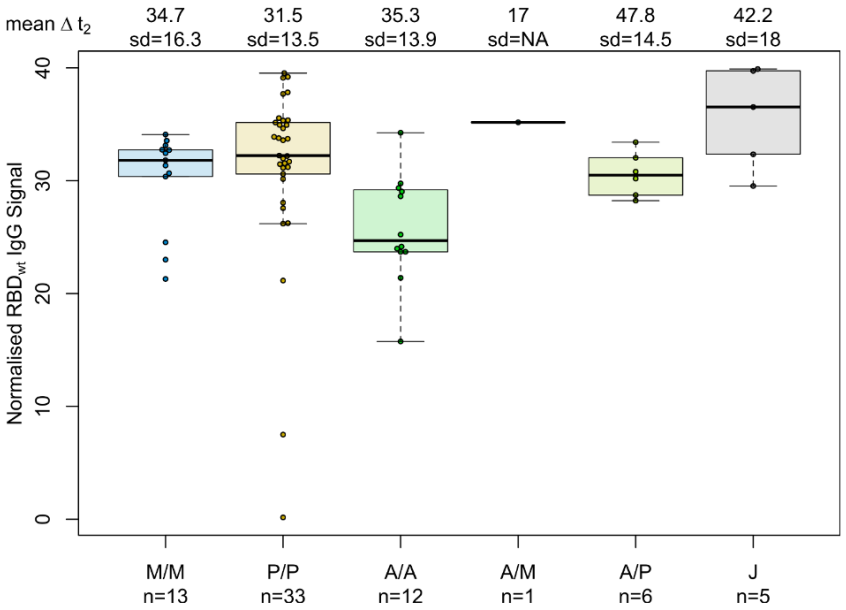

Supplementary Figure 3. SARS-CoV-2 vaccination boosts humoral response among recovered individuals independent of vaccination scheme.
Differences in vaccination responses of recovered previously SARS-CoV-2 infected individuals from our mix and match cohort were analyzed using MULTICOV-AB. SARS-CoV-2 infection status was based on a previous self-reported positive PCR/antigen test or a MULTICOV-AB nucleocapsid IgG normalisation ratio above 1. Samples were split according to vaccination scheme (homologous mRNA (mRNA-1273 (M/M, blue), BNT162b2 (P/P, orange)), heterologous prime-boost (AZD1222-mRNA-1273 (A/M, light blue), AZD1222-BNT162b2 (A/P, light green) or vector-based (AZD1222-AZD1222 (A/A, green), Ad26CoV2.S (J, grey)). Boxes represent medians, 25th and 75th percentiles and whiskers show the largest and smallest non-outlier values based on 1.5 IQR calculation. When less than 5 samples were available per group, only the median is indicated by a line. Time between sampling and full vaccination is displayed as mean and SD for each group. Number of samples per vaccination scheme are stated below the figure. Results of a formal statistical comparison of recovered-vaccinated and SARS-CoV-2 naïve-vaccinated individuals is shown in Table S6.

Supplementary Table 1. Comorbidities in study participants (n. a.: not applicable; NA: not available; CVD: cardiovascular disease).

Sample cohort (n)	SARS-CoV-2 infection status (n) *	ΔT range in days post-vaccination	Vaccine (n)	Hyper-tension (n, %)	CVD (n, %)	Diabetes (n, %)	Lung disease (n, %)	Cancer (n, %)	Immuno-suppression (n, %)
Mix and match (1470)	+ (70)	7-65	M/M (13)	4 (30.8)	1 (7.7)	2 (15.4)	0 (0.0)	0 (0.0)	0 (0.0)
			P/P (33)	12 (36.0)	4 (12.0)	3 (9.1)	0 (0.0)	0 (0.0)	1 (3.0)
			A/A (33)	7 (58.3)	3 (25.0)	2 (16.7)	1 (8.3)	1 (8.3)	2 (16.7)
			A/M (1)	1 (100.0)	0 (0.0)	0 (0.0)	0 (0.0)	0 (0.0)	0 (0.0)
			A/P (6)	3 (50.0)	1 (16.7)	0 (0.0)	1 (16.7)	0 (0.0)	0 (0.0)
			J (5)	2 (40.0)	0 (0.0)	0 (0.0)	0 (0.0)	0 (0.0)	1 (20.0)
	- (1400)		M/M (272)	84 (30.9)	23 (8.5)	13 (4.8)	17 (6.3)	2 (0.7)	11 (4.0)
			P/P (734, 4 NA)	263 (35.8)	101 (13.8)	64 (8.7)	59 (8.1)	20 (2.7)	37 (5.0)
			A/A (228)	91 (39.9)	25 (11.1)	25 (11.0)	12 (5.3)	2 (0.9)	9 (4.0)
			A/M (24)	12 (50.0)	4 (16.7)	2 (8.3)	0 (0.0)	1 (4.2)	0 (0.0)
			A/P (114)	43 (37.7)	16 (14.0)	10 (8.8)	10 (8.8)	4 (3.5)	6 (5.3)
			J (24)	9 (37.5)	2 (8.3)	2 (8.3)	2 (8.3)	1 (4.2)	2 (8.3)
Time points (597)	-	5-12	P/P (107)	50 (46.7)	16 (15.0)	6 (5.6)	3 (2.8)	0 (0.0)	7 (6.5)
			M/M (40)	13 (32.5)	3 (7.5)	3 (7.5)	1 (2.5)	0 (0.0)	1 (2.5)
		26-30	P/P (102; 1 NA)	31 (30.4)	15 (14.7)	11 (10.8)	12 (11.8)	0 (0.0)	0 (0.0)
			M/M (8)	3 (37.5)	1 (12.5)	0 (0.0)	0 (0.0)	0 (0.0)	0 (0.0)
		54-58	P/P (92)	37 (40.2)	14 (15.2)	7 (7.6)	0 (0.0)	2 (2.2)	4 (4.4)
			M/M (22)	2 (9.1)	0 (0.0)	2 (9.1)	2 (9.1)	0 (0.0)	1 (4.6)
		94-103	P/P (139)	59 (42.5)	18 (13.0)	12 (8.6)	1 (0.7)	7 (5.0)	0 (0.0)
			M/M (7)	3 (42.9)	1 (14.3)	1 (14.3)	1 (14.3)	1 (14.3)	0 (0.0)
		129-146	P/P (38)	19 (50.0)	9 (23.7)	7 (18.4)	4 (10.5)	2 (5.3)	4 (10.5)
			M/M (5)	3 (60.0)	2 (40.0)	1 (20.0)	1 (20.0)	0 (0.0)	0 (0.0)
		176-203	P/P (36)	5 (13.9)	2 (5.6)	1 (2.8)	2 (5.6)	0 (0.0)	3 (8.3)
			M/M (0)	n. a.	n. a.	n. a.	n. a.	n. a.	n. a.
Longi-tudinal (180)	-	P/P T1: 7-63	P/P T1 (90; 2 NA)	35 (39.8)	15 (17.1)	11 (12.5)	4 (4.6)	2 (2.2)	3 (3.4)
		P/P T2: 121-203	P/P T2 (90)	33 (36.7)	12 (13.3)	8 (8.9)	3 (3.3)	1 (1.1)	9 (10.0)

Different vaccines and combinations are abbreviated as follows: M/M (two-dose mRNA-1273), P/P (two-dose BNT162b2), A/A (two-dose AZD1222), A/M (first dose AZD1222, second dose mRNA-1273), A/P (first dose AZD1222, second dose BNT162b2) and J (one-dose Ad26.CoV2.S). The time points sample cohort contains only homologous BNT162b2 and mRNA-1273 samples. The longitudinal sample cohort contains only paired homologous BNT162b2 taken at time 1 (T1) or 2 (T2).

***** based on self-reported positive PCR/antigen test result at study center visit and/or MULTICOV-AB nucleocapsid IgG S/CO ratio above 1

Supplementary Table 2. MULTICOV-AB antigen panel.

Virus	Antigen	Manufacturer	Product number
SARS-CoV-2	Spike Trimer	NMI	-
SARS-CoV-2	RBD B.1 (wild-type)	NMI	-
SARS-CoV-2	Nucleocapsid	Aalto	6404-b
SARS-CoV-2	RBD B.1.1.7 (Alpha)	NMI	
SARS-CoV-2	RBD B.1.351 (Beta)	NMI	
SARS-CoV-2	RBD P.3 (Gamma)	NMI	
SARS-CoV-2	RBD B.1.617.2 (Delta)	NMI	
hCoV-OC43	S1 domain	NMI	-
hCoV-OC43	Nucleocapsid	NMI	-
hCoV-HKU1	S1 domain	NMI	-
hCoV-HKU1	Nucleocapsid	NMI	-
hCoV-NL63	S1 domain	NMI	-
hCoV-NL63	Nucleocapsid	NMI	-
hCoV-229E	S1 domain	NMI	-
hCoV-229E	Nucleocapsid	NMI	-

List of antigens included in MULTICOV-AB as well as their manufacturer and, if applicable, their product number.

Supplementary Table 3. ACE2-RBD competition antigen panel.

Virus	Antigen	Manufacturer	Amino acid exchanges in RBD
SARS-CoV-2	RBD B.1 (wild-type)	NMI	-
SARS-CoV-2	RBD B.1.1.7 (Alpha)	NMI	N501Y
SARS-CoV-2	RBD B.1.351 (Beta)	NMI	N501Y, E484K, K417N
SARS-CoV-2	RBD P.1 (Gamma)	NMI	N501Y, E484K, K417T
SARS-CoV-2	RBD B.1.617.2 (Delta)	NMI	T478K, L452R

List of antigens included in ACE2-RBD competition assay as well as their manufacturer, and the mutations covered within the RBD.

Supplementary Table 4. Impact of confounders on ACE2 inhibition response towards SARS-CoV-2 wild-type and VoC RBDs.

A. WT ACE2 binding inhibition, logit	**P/P, n=734**		**M/M, n=272**		**A/P, n=114**		**A/A, n=228**	
scale	Est (sd)	p-value	Est (sd)	p-value	Est (sd)	p-value	Est (sd)	p-value
Intercept	3.50 (0.231)	---	3.39 (0.330)	---	3.07 (0.538)	---	-0.52 (0.496)	---
Male	-0.25 (0.103)	0.014	-0.05 (0.149)	0.752	-0.33(0.267)	0.218	0.30(0.152)	0.050
Age (per 1 year)	-0.03 (0.003)	<0.001	0.00 (0.005)	0.431	-0.01 (0.010)	0.251	0.00(0.008)	0.960
Days post-vaccination (ΔT)								
7-27	Ref.		Ref.		Ref.		Ref.	
28-65	-0.69 (0.104)	<0.001	-0.97 (0.169)	<0.001	-0.74 (0.260)	0.005	-0.10(0.188)	0.584
Comorbidities								
Cardiovascular	-0.12(0.158)	0.454	-0.54 (0.309)	0.083	-0.03(0.424)	0.937	0.02 (0.241)	0.943
Hypertension	0.19 (0.119)	0.109	-0.13 (0.180)	0.480	-0.08(0.301)	0.789	0.11(0.161)	0.485
Diabetes	-0.04 (0.185)	0.808	0.58(0.386)	0.136	0.84(0.501)	0.095	-0.15(0.242)	0.547
Lung disease*	-0.03(0.187)	0.853	0.53(0.324)	0.104	-0.87(0.513)	0.091	-0.11(0.349)	0.758
Cancer or Immunosuppression*	-0.26(0.192)	0.176	0.29(0.362)	0.418	0.22(0.508)	0.662	-0.61(0.368)	0.099

B. Alpha ACE2 binding inhibition, logit scale	**P/P, n=734**		**M/M, n=272**		**A/P, n=114**		**A/A, n=228**	
	Est (sd)	p-value	Est (sd)	p-value	Est (sd)	p-value	Est (sd)	p-value
Intercept	2.50(0.211)	---	2.64(0.301)	---	2.26(0.465)	---	-0.77(0.420)	---
Male	-0.22(0.083)	0.008	-0.02(0.130)	0.862	-0.27(0.226)	0.228	0.24(0.126)	0.060
Age (per 1 year)	-0.02(0.003)	<0.001	-0.01(0.004)	0.218	-0.01(0.009)	0.270	0.00(0.006)	0.826
Days post-vaccination (ΔT)								
7-27	Ref.		Ref.		Ref.		Ref.	
28-65	-0.56(0.083)	<0.001	-0.89(0.147)	<0.001	-0.58(0.219)	0.008	-.03(0.155)	0.842
Comorbidities								
Cardiovascular	-0.10(0.125)	0.434	-0.42(0.266)	0.112	-0.02(0.361)	0.961	0.04(0.202)	0.842
Hypertension	0.16(0.095)	0.087	-0.10(0.156)	0.524	-0.06(0.255)	0.800	0.05(0.134)	0.715
Diabetes	-0.03(0.149)	0.828	0.41(0.332)	0.216	0.81(0.425)	0.057	-0.05(0.204)	0.815
Lung disease*	-0.03(0.149)	0.851	0.40(0.281)	0.156	-0.78(0.433)	0.073	-0.08(0.288)	0.789
Cancer or Immunosuppression*	-0.15(0.153)	0.343	0.21(0.314)	0.510	0.15(0.428)	0.724	-0.45(0.302)	0.139

C. Beta ACE2 binding inhibition, logit scale	**P/P, n=734**		**M/M, n=272**		**A/P, n=114**		**A/A, n=228**	
	Est (sd)	p-value	Est (sd)	p-value	Est (sd)	p-value	Est (sd)	p-value
Intercept	1.27(0.259)	---	1.55(0.309)	---	1.12(0.420)	---	-1.18(0.432)	---
Male	-0.19(0.070)	0.006	-0.08(0.105)	0.448	-0.27(0.180)	0.131	0.11(0.116)	0.337
Age (per 1 year)	-0.02(0.002)	<0.001	0.00(0.004)	0.170	-0.01(0.007)	0.268	0.00(0.006)	0.584
Days post-vaccination (ΔT)								
7-27	Ref.		Ref.		Ref.		Ref.	
28-65	-0.44(0.070)	<0.001	-0.86(0.119)	<0.001	-0.59(0.175)	0.001	0.07(0.144)	0.645
Comorbidities								
Cardiovascular	0.00(0.106)	0.971	-0.37(0.216)	0.088	-0.04(0.294)	0.899	0.06(0.181)	0.741
Hypertension	0.08(0.081)	0.306	-0.12(0.126)	0.323	-0.02(0.205)	0.923	0.01(0.122)	0.940
Diabetes	0.01(0.124)	0.917	0.24(0.270)	0.380	0.48(0.345)	0.165	0.09(0.180)	0.636
Lung disease*	-0.08(0.126)	0.520	0.39(0.227)	0.087	-0.54(0.346)	0.117	0.10(0.268)	0.705
Cancer or Immunosuppression*	-0.19(0.130)	0.155	0.13(0.254)	0.606	0.27(0.340)	0.426	-0.40(0.286)	0.163

D. Gamma ACE2 binding inhibition,	**P/P, n=734**		**M/M, n=272**		**A/P, n=114**		**A/A, n=228**	
logit scale	Est (sd)	p-value	Est (sd)	p-value	Est (sd)	p-value	Est (sd)	p-value
Intercept	1.31(0.169)	---	1.64(0.250)	---	1.24(0.377)	---	-1.05(0.313)	---
Male	-0.20(0.067)	0.003	-0.06(0.109)	0.612	-0.36(0.183)	0.049	0.13(0.092)	0.165
Age (per 1 year)	-0.02(0.002)	<0.001	0.00(0.004)	0.222	-0.01(0.007)	0.183	0.00(0.005)	0.382
Days post-vaccination (ΔT)								
7-27	Ref.		Ref.		Ref.		Ref.	
28-65	-0.46(0.068)	<0.001	-0.91(0.124)	<0.001	-0.52(0.177)	0.004	-0.03(0.114)	0.769
Comorbidities								
Cardiovascular	-0.06(0.101)	0.556	-0.41(0.225)	0.069	-0.05(0.299)	0.862	0.13(0.145)	0.352
Hypertension	0.14(0.078)	0.063	-0.08(0.132)	0.548	0.04(0.208)	0.862	0.07(0.097)	0.496
Diabetes	-0.01(0.118)	0.960	0.21(0.281)	0.463	0.53(0.351)	0.134	0.03(0.145)	0.821
Lung disease*	-0.04(0.121)	0.770	0.27(0.237)	0.252	-0.62(0.351)	0.076	-0.13(0.212)	0.554
Cancer or Immunosuppression*	-0.17(0.125)	0.178	0.12(0.265)	0.654	0.17(0.344)	0.626	-0.45(0.225)	0.047

E. Delta ACE2 binding inhibition, logit	**P/P, n=734**		**M/M, n=272**		**A/P, n=114**		**A/A, n=228**	
scale	Est (sd)	p-value	Est (sd)	p-value	Est (sd)	p-value	Est (sd)	p-value
Intercept	2.34(0.218)	---	2.53(0.312)	---	2.16(0.468)	---	-1.10(0.430)	---
Male	-0.21(0.085)	0.013	-0.03(0.135)	0.830	-0.34(0.226)	0.132	0.20(0.128)	0.128
Age (per 1 year)	-0.02(0.003)	<0.001	0.00(0.004)	0.349	-0.01(0.009)	0.203	0.00(0.007)	0.698
Days post-vaccination (ΔT)								
7-27	Ref.		Ref.		Ref.		Ref.	
28-65	-0.55(0.086)	<0.001	-0.99(0.152)	<0.001	-0.70(0.220)	0.001	0.01(0.159)	0.938
Comorbidities								
Cardiovascular	-0.10(0.130)	0.445	-0.52(0.276)	0.058	0.12(0.365)	0.744	0.09(0.203)	0.641
Hypertension	0.15(0.099)	0.125	-0.11(0.162)	0.501	0.01(0.256)	0.957	-0.04(0.136)	0.762
Diabetes	-0.01(0.152)	0.969	0.42(0.345)	0.227	0.68(0.429)	0.116	-0.01(0.204)	0.953
Lung disease*	-0.02(0.155)	0.920	0.39(0.292)	0.182	-0.67(0.434)	0.125	-0.15(0.295)	0.604
Cancer or Immunosuppression*	-0.18(0.159)	0.261	0.17(0.326)	0.603	0.06(0.428)	0.888	-0.50(0.311)	0.111

ACE2 binding inhibition towards SARS-CoV-2 wild-type (A) and Alpha (B), Beta (C), Gamma (D), Delta (E) VoC in the mix and match sample cohort was modelled to assess the role of confounders (see methods for model details). Four samples (P/P) had missing information on comorbidities and were excluded from the analysis. Est=estimate, sd=standard deviation. Categories denoted with * were merged in the sensitivity analysis including interaction terms with time post-vaccination due to limited sample sizes (selected results reported in the main text). Different vaccines and combinations are abbreviated as follows: M/M (two-dose mRNA-1273), P/P (two-dose BNT162b2), A/A (two-dose AZD1222), A/M (first dose AZD1222, second dose mRNA-1273), A/P (first dose AZD1222, second dose BNT162b2) and J (one-dose Ad26.CoV2.S).

Supplementary Table 5. Statistical comparison of antibody titres between vaccination schemes.

Comparison X vs. Y		Full-length Spike trimer p'' (p-value)	RBD p'' (p-value)	S1 p'' (p-value)	S2 p'' (p-value)
J	M/M	0.91 (< 0.001) *	0.93 (<0.001) *	0.96 (<0.001) *	0.86 (< 0.001) *
	P/P	0.89 (<0.001) *	0.90 (<0.001) *	0.92 (<0.001) *	0.79 (< 0.001) *
	A/M	0.89 (<0.001) *	0.91 (<0.001) *	0.97 (<0.001) *	0.93 (<0.001) *
	A/P	0.90 (<0.001) *	0.92 (<0.001) *	0.95 (<0.001) *	0.88 (<0.001) *
	A/A	0.63 (<0.080)	0.74 (<0.001) *	0.86 (<0.001) *	0.81 (<0.001) *
A/A	M/M	0.96 (<0.001) *	0.94 (<0.001) *	0.93 (<0.001) *	0.57 (0.013) *
	P/P	0.91 (<0.001) *	0.87 (<0.001) *	0.83 (<0.001) *	0.39 (<0.001) *
	A/M	0.93 (<0.001) *	0.91 (<0.001) *	0.93 (<0.001) *	0.84 (< 0.001) *
	A/P	0.93 (<0.001) *	0.89 (<0.001) *	0.91 (<0.001) *	0.66 (< 0.001) *
A/P	M/M	0.60 (0.002) *	0.64 (<0.001) *	0.55 (0.114)	0.38 (< 0.001) *
	P/P	0.42 (0.012)	0.49 (0.608)	0.34 (<0.001) *	0.21 (< 0.001) *
	A/M	0.59 (0.204)	0.59 (0.155)	0.69 (0.004) *	0.77 (<0.001) *
A/M	M/M	0.50 (0.982)	0.53 (0.623)	0.33 (0.014) *	0.16 (<0.001) *
	P/P	0.33 (0.014)	0.40 (0.085)	0.18 (<0.001)*	0.09 (<0.001) *
P/P	M/M	0.69 (<0.001) *	0.64 (<0.001) *	0.72 (<0.001) *	0.71 (<0.001) *

Estimated probability (p'') that a random individual under one vaccination scheme in the mix and match sample cohort, has a larger titre than a random individual under another vaccination scheme. Two-sided generalized Wilcoxon also referred to as Brunner-Munzel test was used to determine statistical significance with Bonferroni-Holm's adjustment for multiple testing. For a comparison of a scheme X with a scheme Y, a significant p'' larger than ½ means that the vaccination-induced titres under Y tend to be higher and a significant p'' smaller than ½ means that the vaccination-induced titres under X tend to be higher. Different vaccines and combinations are abbreviated as follows: M/M (two-dose mRNA-1273), P/P (two-dose BNT162b2), A/A (two-dose AZD1222), A/M (first dose AZD1222, second dose mRNA-1273), A/P (first dose AZD1222, second dose BNT162b2) and J (one-dose Ad26.CoV2.S).

Supplementary Table 6. Statistical comparison of RBD antibody titres and wild-type ACE2 binding inhibition in recovered-vaccinated and SARS-CoV-2 naïve-vaccinated individuals for different vaccination schemes.

	M/M p'' (p-value)	**P/P p'' (p-value)**	**A/M p'' (p-value)**	**A/P p'' (p-value)**	**A/A p'' (p-value)**	**J p'' (p-value)**
RBD	0.66 (0.074)	0.79 (<0.001)	-- (only 1 convalescent)	0.79 (<0.001)	0.94 (<0.001)	0.98 (<0.001)
AC2 binding inhibition against WT	0.74 (0.016)	0.85 (<0.001)	-- (only 1 convalescent)	0.84 (0.004)	0.97 (<0.001)	0.98 (<0.001)

Estimated probability (p'') that a random recovered-vaccinated individual has a larger titre than a random SARS-CoV-2 naïve vaccinated individual under the respective vaccination scheme. Statistical analysis was determined by two-sided generalized Wilcoxon/Brunner-Munzel test. A significant p'' larger than ½ means that the vaccination-induced titres tend to be higher in recovered-vaccinated individuals. Different vaccines and combinations are abbreviated as follows: M/M (two-dose mRNA-1273), P/P (two-dose BNT162b2), A/A (two-dose AZD1222), A/M (first dose AZD1222, second dose mRNA-1273), A/P (first dose AZD1222, second dose BNT162b2) and J (one-dose Ad26.CoV2.S).

Supplementary Table 7. Antibody titres and ACE2 binding inhibition up to 7 months after SARS-CoV-2 mRNA vaccination.

Sample cohort (n)	ΔT range in days post-vaccination	Vaccine (n)	RBD_{wt} IgG signal (95% CI)	(%) ACE2 binding inhibition (95% CI)	RBD_{wt} IgG signal (IQR)	(%) ACE2 binding inhibition (IQR)
Time points (597)	5-12	P/P(107)	24.88 (20.02-27.10)	78.73 (64.37-87.92)	24.88 (15.09-31.17)	78.73 (52.27-94.27)
		M/M (40)	26.76 (21.38-30.47)	89.03 (65.66-97.16)	26.76 (12.24-31.69	89.03 (41.06-97.95)
	26-30	P/P (103)	25.60 (23.15-27.79)	83.34 (78.04-0.86.00)	25.60 (18.76-30.87)	83.34 (63.63-93.37)
		M/M (8)	29.45 (21.01-34.13)	95.75 (60.74-96.97)	29.45 (26.20-32.42)	95.75 (77.52-96.82)
	54-58	P/P (92)	19.96 (18.22-22.73)	70.59 (62.66-75.07)	19.96 (14.00-26.37)	70.59 (58.54-83.18)
		M/M (22)	26.52 (23.56-30.01)	88.22 (78.90-94.10)	26.52 (23.54-30.20)	88.22 (77.92-94.32)
	94-103	P/P (139)	15.07 (13.97-16.77)	56.22 (50.18-61.20)	15.07 (10.20-20.70)	56.22 (39.97-69.67)
		M/M (7)	18.85 (11.67-31.61)	75.94 (43.40-96.95)	18.85 (14.18-28.24)	75.94 (55.40-90.74)
	129-146	P/P (38)	8.67 (7.24-10.27)	33.82 (27.95-39.87)	8.67 (5.48-12.68)	33.82 (25.52-50.97)
		M/M (5)	13.51 (n. a)	48.16 (n. a.)	13.51 (4.78-19.64)	48.16 (17.95-68.86)
	176-203	P/P (36)	7.97 (5.98-10.03)	30.44 (23.38-42.16)	7.97 (5.51-11.36)	30.44 (20.50-48.77)
		M/M (0)	n. a.	n. a.	n. a.	n. a.

Median values with 95% CI and IQR are shown for normalised RBD_{wt} IgG signal or ACE2 binding inhibition. Data is graphically displayed in Figure 6. Different vaccines are abbreviated as follows: M/M – two-dose mRNA-1273. P/P – two-dose BNT162b2.

Appendix IV: Immune response to SARS-CoV-2 variants of concern in vaccinated individuals

Becker M*, Dulovic A*, Junker D, Ruetalo N, Kaiser PD, Pinilla YT, Heinzel C, Haering J, Traenkle B, Wagner TR, Layer M, Mehrlaender M, Mirakaj V, Held J, Planatscher H, Schenke-Layland K, Krause G, Strengert M, Bakchoul T, Althaus K, Fendel R, Kreidenweiss A, Koeppen M, Rothbauer U, Schindler M, Schneiderhan-Marra N.

Nature Communications. 2021. 12(1):3109

https://doi.org/10.1038/s41467-021-23473-6

nature COMMUNICATIONS

ARTICLE

https://doi.org/10.1038/s41467-021-23473-6 OPEN

Immune response to SARS-CoV-2 variants of concern in vaccinated individuals

Matthias Becker[1,14], Alex Dulovic[1,14], Daniel Junker[1], Natalia Ruetalo[2], Philipp D. Kaiser[1], Yudi T. Pinilla[3], Constanze Heinzel[3], Julia Haering[1], Bjoern Traenkle[1], Teresa R. Wagner[1,4], Mirjam Layer[2], Martin Mehrlaender[5], Valbona Mirakaj[5], Jana Held[3,6], Hannes Planatscher[7], Katja Schenke-Layland[1,8,9,10], Gérard Krause[11,12], Monika Strengert[11,12], Tamam Bakchoul[13], Karina Althaus[13], Rolf Fendel[3,6], Andrea Kreidenweiss[3,6], Michael Koeppen[5], Ulrich Rothbauer[1,4✉], Michael Schindler[2✉] & Nicole Schneiderhan-Marra[1✉]

SARS-CoV-2 is evolving with mutations in the receptor binding domain (RBD) being of particular concern. It is important to know how much cross-protection is offered between strains following vaccination or infection. Here, we obtain serum and saliva samples from groups of vaccinated (Pfizer BNT-162b2), infected and uninfected individuals and characterize the antibody response to RBD mutant strains. Vaccinated individuals have a robust humoral response after the second dose and have high IgG antibody titers in the saliva. Antibody responses however show considerable differences in binding to RBD mutants of emerging variants of concern and substantial reduction in RBD binding and neutralization is observed against a patient-isolated South African variant. Taken together our data reinforce the importance of the second dose of Pfizer BNT-162b2 to acquire high levels of neutralizing antibodies and high antibody titers in saliva suggest that vaccinated individuals may have reduced transmission potential. Substantially reduced neutralization for the South African variant further highlights the importance of surveillance strategies to detect new variants and targeting these in future vaccines.

[1] NMI Natural and Medical Sciences Institute at the University of Tübingen, Reutlingen, Germany. [2] Institute for Medical Virology and Epidemiology, University Hospital Tübingen, Tübingen, Germany. [3] Institute of Tropical Medicine, University of Tübingen, Tübingen, Germany. [4] Pharmaceutical Biotechnology, University of Tübingen, Tübingen, Germany. [5] Department of Anaesthesiology and Intensive Care Medicine, University Hospital Tübingen, Tübingen, Germany. [6] German Center for Infection Research (DZIF), partner site Tübingen, Tübingen, Germany. [7] Signatope GmbH, Reutlingen, Germany. [8] Cluster of Excellence iFIT (EXC2180) "Image-Guided and Functionally Instructed Tumor Therapies", University of Tübingen, Tübingen, Germany. [9] Department of Women's Health, Research Institute for Women's Health, University of Tübingen, Tübingen, Germany. [10] Department of Medicine/Cardiology, Cardiovascular Research Laboratories, David Geffen School of Medicine at UCLA, Los Angeles, USA. [11] Helmholtz Centre for Infection Research, Braunschweig, Germany. [12] TWINCORE GmbH, Centre for Experimental and Clinical Infection Research, a joint venture of the Hannover Medical School and the Helmholtz Centre for Infection Research, Hannover, Germany. [13] Institute for Clinical and Experimental Transfusion Medicine, University Hospital Tübingen, Tübingen, Germany. [14] These authors contributed equally: Matthias Becker, Alex Dulovic. ✉email: Ulrich.rothbauer@nmi.de; Michael.Schindler@med.uni-tuebingen.de; Nicole.schneiderhan@nmi.de

Since the initial outbreak in Wuhan, China in late 2019[1,2], SARS-CoV-2 has evolved into a global pandemic, with more than 138 million infections and nearly 3 million deaths (as per WHO, https://covid19.who.int/, accessed April 15, 2021), impacting severely on mental health[3,4] and global economics[5]. In response, the scientific community has made unprecedented progress, resulting in the generation of multiple vaccines, using a variety of different approaches[6–8], such as the Pfizer BNT-162b2 vaccine, which encodes a full-length trimerized spike protein[9]. In parallel, SARS-CoV-2 is continually evolving impacting its infectivity[10], transmission[11–13], and viral immune evasion[14,15]. To date, advanced genomic approaches have identified thousands of variants of SARS-CoV-2 with multiple RBD mutations circulating due to natural selection[16,17]. The variability of RBD epitopes is of specific concern as such mutations might reduce vaccine efficacy, increase viral transmission, or impair acquired immunity by neutralizing antibodies[10,18,19]. For the pandemic to be brought under control, herd immunity must be achieved through vaccination. However, there is a discourse about how long antibodies generated during the first wave persist, with some studies suggesting seroreversion between 2 and 3 months[20], while others find antibodies present for up to 7 or 8 months post infection[21–23]. Alarmingly, antibodies generated during the first wave also appear to have reduced immunoreactivity and neutralization potency toward emerging variants[22].

As the virus is known to continually mutate, particularly the emerging UK (B.1.1.7)[12], South African (B.1.351)[24], Brazil (P1)[25], Mink (Cluster 5)[26], and Southern California (hereon referred to as "LA" (B1.429)[27] variants are of concern. The UK variant has an increased risk of transmission[13] and mortality[13,28]. It further exhibits reduced neutralization susceptibility[29], which is most substantially related to a subset of RBD-specific monoclonal antibodies[14,29]. The N501Y mutation appears to mediate increased ACE2–RBD interaction[30] and is known to be critical for SARS-CoV-2 infection in vivo in mice[31]. Similarly, the South African variant, which is now spreading globally, has two escape mutations within the RBD (K417N and E484K)[24] in addition to the N501Y mutation. The combination of these three point mutations results in both a higher infection rate and reduced capacity of neutralizing antibodies produced against variants without RBD mutations of concern (hereon referred to as "wild-type")[32]. In light of these developments, and in spite of increasing data provided by vaccine companies, it remains unclear whether vaccines formulated against the original Wuhan strain of the virus will remain effective against new and emerging variants such as UK or South Africa. To understand this, we characterized the antibody response post vaccination with the Pfizer BNT-162b2 vaccine in both serum and saliva and then investigated the presence and efficacy of neutralizing antibodies against emerging variants of concern (UK, South Africa, Mink, and LA).

Results

To analyze the humoral response generated by vaccination, SARS-CoV-2 reactive antibody titers in serum samples from vaccinated, convalescent (hereon referred to as "infected"), and uninfected (hereon referred to as "negative") individuals were measured using MULTICOV-AB[33] (Fig. 1). Descriptions of all groups of donors can be found in Supplementary Table 1. Vaccinated individuals had not been previously infected with SARS-CoV-2 as demonstrated by the absence of anti-nucleocapsid IgG and IgA (Fig. 1a). As expected, there was a typical variation in antibody titers reflecting individual immune responses (Fig. 1a, b). When comparing between vaccine doses (Fig. 1c, d), all vaccinated subjects showed an enhanced antibody response with increasing time after the first dose and a further significant boost after the second dose. This boosting effect was so pronounced that it reached the upper limit of detection for MULTICOV-AB, as confirmed by a dilution series (Supplementary Fig. 1).

To expand our understanding of the immune response of vaccinated individuals, we analyzed their saliva for IgA and IgG antibodies. The saliva of infected and negative individuals served as controls. Infected individuals had significantly higher levels of IgA than negative (P value = 0.0008) or vaccinated individuals (P value = 0.03), with no significant difference seen between vaccinated and negative individuals (P value = 0.23) (Fig. 2a). Conversely, the IgG response in the saliva of vaccinated individuals was significantly higher than either infected (P value <0.0001) or negative individuals (P value <0.0001) (Fig. 2b). These results were verified using a second antibody test measuring IgG in saliva (Supplementary Fig. 2). We also identified that vaccination with Pfizer BNT-162b2 does not appear to offer any cross-protection against other endemic coronaviruses (Supplementary Fig. 3), as seen by the absence of change in antibody titers following vaccination.

Having determined the humoral response induced by Pfizer BNT-162b2, we then examined how emerging RBD mutations present in different variants of concern impact antibody binding. For this, we included RBD mutants for the UK (501Y), South African (417N, 484K, and 510Y), Mink (453F), and LA (452R) variants in MULTICOV-AB. For the UK variant, nearly identical antibody response was observed for vaccinated and infected individuals compared with wild-type variant (Kendall's tau 0.965) (Fig. 3a). In contrast, a varied and reduced immune response was visible for the South African variant in both groups (Kendall's tau 0.844) (Fig. 3b). Both the Mink and LA variants had a similar response as the wild-type variant (Supplementary Fig. 4). Having seen that antibody-binding responses were reduced in the context of RBD mutants in the South African variant, we examined its neutralizing potential on samples from vaccinated individuals using a virus neutralization test (VNT)[34], employing a patient-derived South African variant of SARS-CoV-2. Despite the detectable variation, the VNT revealed substantially reduced neutralization for the South African variant for sera obtained from vaccinated and infected individuals (Fig. 4a). We further confirmed these findings using an ACE2 inhibition assay (Fig. 4b). Here, we additionally observed increased neutralization capacities for both wild-type (Fig. 4c) and the South African variant (Fig. 4d), in all samples derived from vaccinated individuals following the second dose, which was further confirmed by the NeutrobodyPlex[35] (Supplementary Fig. 5). Overall, our results showed individual differences in neutralization capacity for RBD mutations found in variants (Supplementary Fig. 6), with minimal to no change in neutralization for the UK, Mink, or LA variants. Conversely, neutralization capacity versus the South African variant was severely compromised.

Discussion

RBD mutants are particularly important to track and study due to the role of the RBD:ACE2 interaction site in virus transmission and neutralization[13,30] and their potentially increased infectivity[12] or lethality[28]. This tracking has led to the identification of several variants of concern, notably the UK[12], South African[24], Mink[26], and LA[27] variants. We initiated this study to reveal the vaccine-induced immune response and most importantly to shed light on the still controversial question of how efficiently antibodies can bind and neutralize SARS-CoV-2 variants of concern. The presence of large titers of IgG antibodies within the saliva of vaccinated individuals far exceeded those seen in convalescent individuals. This was both surprising and welcome as it could indicate that vaccination might confer a

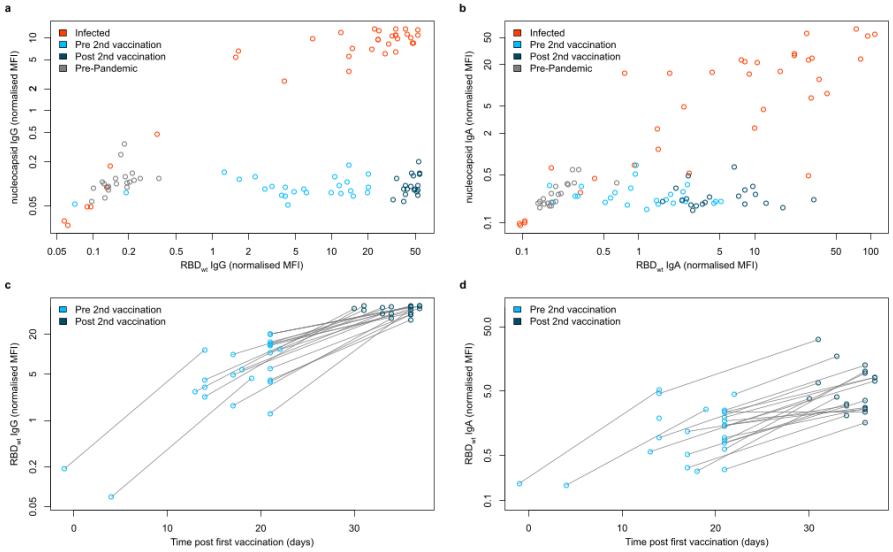

Fig. 1 IgG and IgA response in serum samples of vaccinated, infected, and negative individuals. IgG (**a**, **c**) and IgA (**b**, **d**) response in sera from vaccinated (pre second vaccination (light blue, $n = 25$), post second vaccination (dark blue, $n = 20$)), infected (red) ($n = 35$), and negative (gray) ($n = 20$) individuals were measured with MULTICOV-AB. IgG (**a**) and IgA (**b**) response is shown as normalized RBD wild-type (wt) versus normalized nucleocapsid MFI values allowing for visualization of separation between the different groups. Increasing antibody titers in vaccinated individuals for IgG (**c**) and IgA (**d**) is shown with increasing days post vaccination, with samples colored based on whether they are before (light blue) or after (dark blue) the second dose. Lines indicate paired samples from the same donor. Source data are provided as a Source Data file.

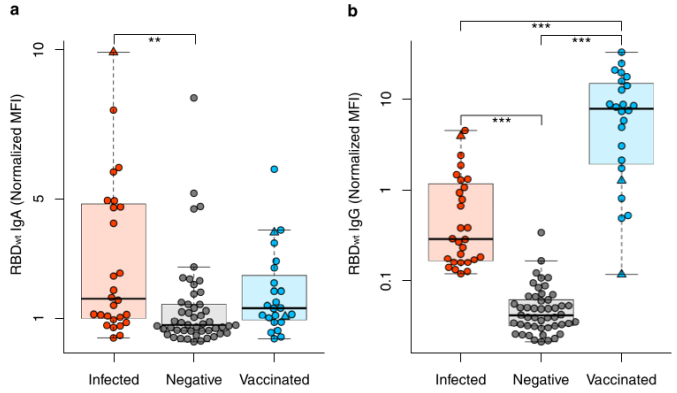

Fig. 2 IgA and IgG response in saliva samples of vaccinated, infected, and negative individuals. Box and whisker plots for the IgA (**a**) and IgG (**b**) response in the saliva of vaccinated (blue, $n = 22$), infected (red, $n = 26$), and negative (gray, $n = 45$) individuals. All samples were measured three times using MULTICOV-AB, normalized against QC values to remove confounding effects, and the mean calculated and displayed. Panel **b** is presented using a logarithmic scale for clarity. As additional controls, one infected and then vaccinated sample and two vaccinated samples from individuals not in contact with active COVID-19 infections are displayed as triangles. Boxes represent the median, 25th and 75th percentiles, whiskers show the largest and smallest non-outlier values. Outliers were determined by 1.5 times IQR. Statistical significance was calculated by Mann–Whitney *U* (two-sided) with significance determined as being < 0.01. **< 0.001; ***< 0.0001. Source data are provided as a Source Data file.

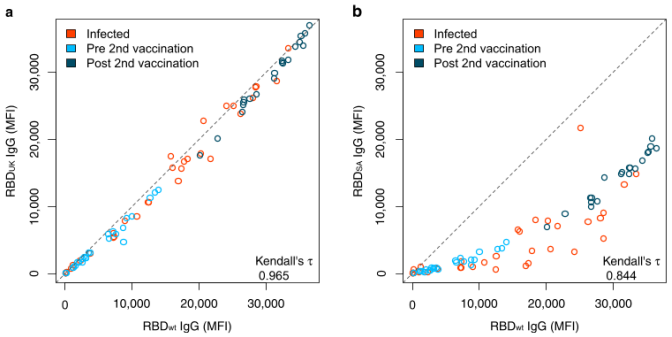

Fig. 3 South African RBD mutant has a reduced response compared to UK RBD mutant. UK (**a**) and South African (SA) RBD mutants (**b**) have differing effects upon antibody binding. RBD mutant antigens were generated and added to MULTICOV-AB to measure the immune response towards them in sera from vaccinated pre-second dose (light blue, $n = 25$), post second dose (dark blue, $n = 20$), and infected (red, $n = 35$) individuals, compared to the wild-type (wt) RBD. A linear curve ($y = x$) is shown as a dashed gray line to indicate an identical response between wild-type and mutant. Kendall's tau was calculated to measure the ordinal association between the mutant and wild-type. Source data are provided as a Source Data file.

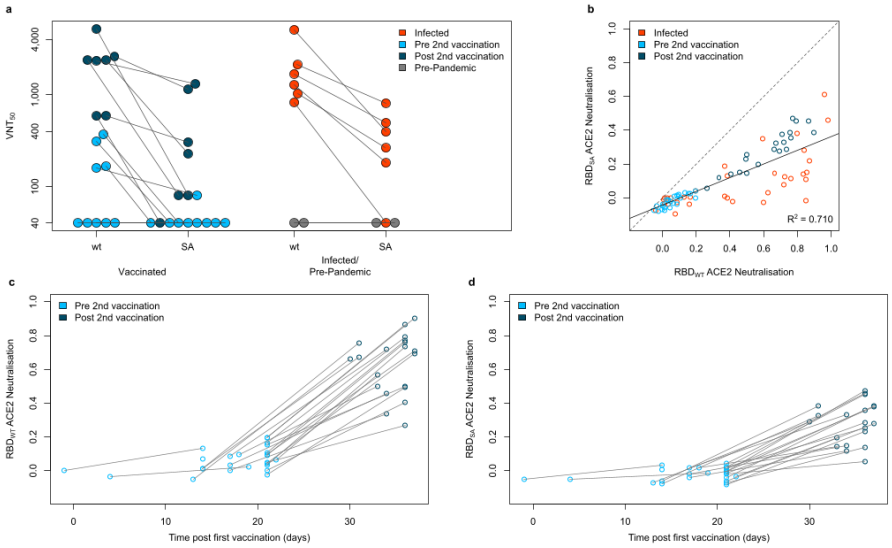

Fig. 4 South African RBD variant has decreased neutralization compared to wild-type in vaccinated and infected samples. Neutralization for the South African variant (SA) displayed as virus neutralizing titers (VNT_{50}) was measured in a virus neutralization assay compared to a wild-type variant (wt) (**a**) with sera from vaccinated (pre second vaccination (light blue, $n = 9$), post second vaccination (dark blue, $n = 7$)), infected (red, $n = 6$), and negative (pre-pandemic) (gray, $n = 2$) individuals. To confirm the reduction in neutralization seen, an ACE2 competition assay was developed and used to measure neutralization capacity for wild-type RBD (wt) and the South African RBD mutant (SA) (**b**) on sera from vaccinated (pre second vaccination (light blue, $n = 25$), post second vaccination (dark blue, $n = 20$)), infected (red, $n = 35$) and negative (pre-pandemic, gray, $n = 20$) individuals. 0 indicates that no neutralization is present while 1 indicates maximum neutralization. A linear regression ($y = -0.044 + 0.408x$) for all samples is shown in gray with the R^2 included. When examining vaccinated samples only, wild-type neutralization (**c**) is significantly increased following the second vaccine dose. For South African neutralization (**d**), while it is increased following the second dose, there is a significant reduction when compared to wild-type. Lines in (**a**), (**c**), and (**d**) indicate paired samples from the same donor. Source data are provided as a Source Data file.

sterilizing immune response in the oral cavity and thereby lower virus transmission. Focusing on antibody response, we examined in detail the effects of RBD mutations observed in emerging variants of concern. While only minor differences were detectable for the UK, Mink, and LA variants, a substantial reduction in RBD-binding antibodies was observed for the South African variant. These findings were confirmed at the functional level by a VNT using patient-derived viral isolates, showing a significant decrease in the neutralizing capacity of sera from vaccinated or infected individuals for the South African variant, in accordance with other recently published studies[36–39]. This could provide a reasonable explanation for infection in vaccinated or convalescent individuals with the South African variant and suggests a potential reduction in the efficacy of the Pfizer BNT-162b2 vaccine from a B-cell perspective.

This study is limited by the sample size, the restriction to only two time points after vaccination for data analysis, and the lack of paired saliva and serum samples for our infected and negative groups. However, we want to note that our sample size examined is similar to or larger than most other sample sets used to examine immune response to mutants in detail[40] and that we examined paired serum and saliva samples for all of our vaccinated subjects. Furthermore, we performed VNT assays comparing wild-type to the South African variant with authentic virus isolates on human cells, in contrast to utilizing a pseudotype neutralization assay[40] or genetically engineered wild-type variant[37]. Notably, we focused our study on a detailed characterization of the humoral immune response, as a proxy of an individual's immune response, as T-cell immunity has already been extensively studied[21,41]. Future work should investigate the antibody response and their persistence from different vaccines (i.e., AstraZeneca-Oxford, Moderna) against similar or newly emerging RBD mutants over a longer timeframe with increased sample size.

Viewed in a larger context, the impaired RBD-binding capacity to mutations in emerging variants of concern highlights the importance of updating current vaccines accordingly. Particular attention should be paid to the South African variant, because of the reduced neutralizing potency identified, while spontaneous independent enrichments of the E484K mutation have been observed in several countries[42].

Methods

Data reporting. No statistical analysis was used to determine the sample size. The experiments were not randomized, and the investigators were not blinded during either experimentation or data analysis.

Study recruitment, sample collection, and ethics statement. Serum and saliva samples were collected from healthcare workers, vaccinated with the Pfizer BNT-162b2 vaccine. Two serum samples were collected from each individual. The first collection took place on average 17 days following administration of the first dose, while the second collection took place on average 12 days following administration of the second dose. Saliva samples were collected 7–10 days following the second serum sampling. Infected serum and saliva samples were collected from different groups of individuals. Serum samples were collected from individuals hospitalized at Universität Klinikum Tübingen between March 25, 2020 and January 22, 2021. All individuals tested positive for SARS-CoV-2 by PCR. Saliva samples were collected from individuals who had previously been infected with SARS-CoV-2 between March 7, 2020 and June 19, 2020. All individuals had previously tested positive by PCR, or were confirmed as being previously infected by ELISA measurements plus the presence of at least one key symptom (i.e., coughing, fever). Negative serum and saliva samples were also from different groups of individuals. Negative serum samples were purchased from Central Biohub. All of these samples were collected pre-pandemic. Negative saliva samples were collected at the Institute of Tropical Medicine, Universität Tübingen from negative individuals and were confirmed to be anti-SARS-CoV-2 negative by serum ELISA. As additional controls, serum and saliva samples were collected from two individuals vaccinated with Pfizer BNT-162b2, who do not have contact with active SARS-CoV-2 infected patients, and one individual who had been previously infected with SARS-CoV-2 and was later vaccinated.

For serum collection, blood was taken by venipuncture, the serum extracted, and then frozen at −80 °C until use. For saliva collection, all individuals spat directly into a collecting tube. To inactive the samples, TnBP and Triton X-100 were added to final concentrations of 0.3% and 1×, respectively. Saliva samples were then frozen at −80 °C until further use.

This study was approved by the Ethics Committee of Eberhard Karls University Tübingen and the University Hospital Tübingen under the approval number 222/2020BO2 to Dr. Karina Althaus, Institute for Clinical and Experimental Transfusion Medicine, University Hospital Tübingen, and 312/2020BO1 (Coro-Buddy) to Dr. Andrea Kreidenweiss, Institute of Tropical Medicine, University Hospital Tübingen and Eberhard Karls University Tübingen. All participants gave written informed consent. Characteristics of vaccinated and infected serum donors can be found in Supplementary Table 1. Characteristics of vaccinated, infected, and negative saliva donors can be found in Supplementary Table 2.

Expression of RBD mutants. The pCAGGS plasmid encoding the receptor-binding domain (RBD) of SARS-CoV-2 was kindly provided by F. Krammer[43]. RBDs of SARS-CoV-2 variants of concern were generated by PCR amplification of fragments from wild-type DNA template followed by fusion PCRs to introduce described mutation N501Y for the UK variant and additional mutations K417N and E484K for the South African variant[28,44]. Forward primer RBDfor and reverse primer N501Yrev were used for amplification of fragment 1, forward primer N501Yfor and reverse primer RBDrev were used for amplification of fragment 2. Both fragments containing an overlap sequence at the 3′ and 5′ end were fused by an additional PCR using forward primer RBDfor and RBDrev. Based on cDNA for the UK variant, additional mutations of the South African Variant were introduced by PCR amplification of three fragments using forward primer RBD-for and reverse primer K417Nrev, forward primer K417Nfor and reverse primer E484Krev, forward primer E484Kfor and reverse primer RBDrev. Amplified fragments were assembled by subsequent fusion PCR using forward primer RBDfor and RBDrev. RBD mutation L452R as recently reported for the SARS-CoV-2 variant of concern identified in Southern California (referred to in this manuscript as "LA"), was introduced using primer RBD-for and reverse primer L452Rrev for amplification of fragment 1 and forward primer L452Rfor for fragment 2. Both fragments were subsequently fused using primers RBDfor and RBDrev. DNA coding for mutant RBDs (amino acids 319–541 of respective spike proteins) was cloned into Esp3I and EcoRI site of pCDNA3.4 expression vector with the N-terminal signal peptide (MGWTLVFLFLLSVTAGVHS) for the secretory pathway that comprises Esp3I site. All expression constructs were verified by sequence analysis. A full list of primers used in this study can be found in Supplementary Table 3. Confirmed constructs were expressed in Expi293 cells[33]. Briefly, cells were cultivated (37 °C, 125 rpm, 8% (v/v) CO_2) to a density of 5.5×10^6 cells/mL, diluted with Expi293F expression medium and transfection of the corresponding plasmids (1 µg/mL) with expifectamine as per the manufacturer's instructions. 20 h post transfection enhancers were added as per the manufacturer's instructions. Cell suspensions were then cultivated for 2–5 days (37 °C, 125 rpm, 8 % (v/v) CO_2) and then centrifuged (4 °C, 23,900×*g*, 20 min) to clarify the supernatant. Supernatants were then filtered with a 0.22-µm membrane (Millipore, Darmstadt, Germany) and supplemented with His-A buffer stock solution (20 mM Na2HPO4, 300 mM NaCl, 20 mM imidazole, pH 7.4). The solution was then applied to a HisTrap FF crude column on an Äkta pure system (GE Healthcare, Freiburg, Germany), extensively washed with His-A buffer, and eluted with an imidazole gradient (50–400 mM). Eluted proteins were dialyzed against PBS.

Bead coupling. Coupling of RBD mutant antigens was done by Anteo coupling (#A-LMPAKMM-10, Anteo Tech Reagents) following the manufacturer's instructions. Briefly, 100 µL of spectrally distinct populations of MagPlex beads (1.25×10^6) (Luminex) were activated in 100 µL of AnteoBind Activation Reagent for 1 h at room temperature. The activated beads were washed twice with 100 µL of Coupling Buffer using a magnetic separator. Following this, 50 µg/mL of antigen (diluted in Coupling buffer) was added to the beads and incubated for 1 h at room temperature. The beads were then washed twice with 100 µL Coupling buffer and blocked for 1 h at room temperature in 0.1% BSA in Coupling Buffer. After washing twice in storage buffer, the beads were stored at 4 °C until further use.

MULTICOV-AB. MULTICOV-AB[33], a multiplex immunoassay that simultaneously analyses 20 antigens was performed on all samples. In addition to the antigens presently included in MULTICOV-AB (Supplementary Table 4), RBD mutants from variants of concern were also included for measurements of all serum samples. All RBD mutants except the Mink variant (#40592-V08H80, Sino Biological) were produced in-house. Both IgG and IgA were measured for all serum samples. To adapt MULTICOV-AB to analyze antibodies in saliva, the dilution factor was changed from 1:400 for the serum to 1:12 for saliva. Samples were diluted into assay buffer (1:4 Low Cross Buffer (Candor Bioscience GmBH) in CBS (1× PBS + 1% BSA) + 0.05% Tween20) inside a sterile workbench. In total, 25 µL of diluted sample was then added to 25 µL of 1× Bead Mix[33] using a 96-well plate (#3600, Corning). Samples were incubated for 2 h at 20 °C, 750 rpm on a Thermomixer (Eppendorf), after which the unbound antibodies were removed by washing three times with Wash Buffer (1× PBS, 0.05% Tween20) using a

microplate washer (Biotek 405TS, Biotek Instruments GmBH). Bound antibodies were detected using either 3 µg/mL RPE-huIgG (#109-116-098, Dianova) or 5 µg/mL RPE-huIgA (#109-115-011, Dianova) by incubation for 45 min at 20 °C, 750 rpm on a thermomixer. Following another washing step, beads were re-suspended in 100 µL of Wash Buffer and re-shaken for 3 mins at 20 °C, 1000 rpm. Plates were then measured using a FLEXMAP3D instrument (Luminex) using the following settings: 80 µL (no timeout), 50 events, Gate:7500–15000 and Report Gain:Standard PMT. Each sample was measured in three independent experiments. Three cut-off (CO) samples with a known MFI value were generated as in ref. [45] and included on each plate as a quality control. CO2 was used to generate the plate-by-plate CO value for the IgG Spike and wtRBD of SARS-CoV-2, with CO3 being used for the same purpose but for IgA. Raw median fluorescence intensity (MFI) values were divided by the mean MFI of CO2 (for IgG) or CO3 (for IgA), included on each plate to produce a normalization value. For serum measurements of the Spike and wtRBD of SARS-CoV-2, a normalized MFI value > 1 indicates positivity.

Saliva IgG ELISA. To validate saliva measurements by MULTICOV-AB, samples were re-measured using an in-house ELISA established by the Institute of Tropical Medicine, Universität Tübingen. Saliva samples were analyzed for SARS-CoV-2 wild-type RBD reactive IgG antibodies by an in-house ELISA developed at the Institute of Tropical Medicine, University of Tübingen. SARS-CoV-2 RBD recombinant protein was dissolved in PBS to a final concentration of 2 µg/mL. In all, 50 µL was then coated into 96-well Costar microtiter high binding plates (#3590, Corning) and blocked at 4 °C overnight with The Blocking Solution (Candor Bioscience GmBH), at room temperature on a microplate shaker set to 700 rpm. Before each of the following steps, wells were washed with PBS/0.1% Tween20. Saliva samples were diluted using The Blocking Solution (1:3–1:729) and 100 µL added to each well. Plates were then incubated at room temperature for 1 h. For detection, 1:20,000 biotinylated anti-human IgG (#109-065-008, Jackson Immuno Research Laboratories) and 1:20,000 Streptavidin-HRP (#109-035-098) were added and incubated for 1 h and 30 min, respectively. For visualization, TMB was added and the reaction was stopped using 1 M HCl. The plate was read at 450 nm and 620 nm using a microplate reader (CLARIOstar, BMG LABTECH, running Software Version 5.40 R2). To estimate the concentration of the IgG antibodies in the saliva, a dilution series of highly pure human IgG (#31154, ThermoFisher) was in parallel coated on the ELISA plates and quantified using the secondary antibodies. A four-parameter logistic curve using MARS Data Analysis Software Version 3.31 was fitted to the respective OD values and the antibody concentrations in the sample specimen calculated[46].

Neutralization assays. Viral neutralization assays[34] for the wild-type (Tü1) variant and the South African variant were performed on 16 vaccinated, 6 infected, and 2 negative serum samples. Briefly, Caco-2 cells were cultured at 37 °C with 5% CO_2 in Dulbecco's modified Eagle medium (DMEM), supplemented with 10% fetal calf serum (FCS), 2 mM L-glutamine, 100 mg/mL penicillin–streptomycin, and 1% non-essential amino acids (NEAA). The clinical isolate (200325_Tü1)[34] which belongs to the lineage B.1.126 is referred to as "wild-type" in this manuscript. The South African variant (210211_SaV) was isolated from a throat swab collected in January 2021 at the Institute for Medical Virology and Epidemiology of Viral Diseases, University Hospital Tübingen, from a PCR-positive patient. In total, 100 µL of patient material was diluted in medium and used to directly inoculate 150,000 Caco-2 cells in a six-well plate. At 48 h post infection, the supernatant was collected, centrifuged, and stored at −80 °C. After two consecutive passages, the supernatant was tested by qRT-PCR confirming the presence of three point mutations (N501Y, K417N, and E484K). NGS confirmed that the clinical isolate belongs to the lineage B.1.351. Sequence comparison of the Spike protein of 200325_Tü1 and 210211_SaV can be found as Supplementary Data 1. Caco-2 cell infection with 210211_SAv was detected by western blotting, using sera from a convalescent patient. The multiplicity of infection determination (MOI) was conducted by titration using serial dilutions of both virus stocks. The number of infectious virus particles per millimeter was calculated as (MOI x cell number)/(infection volume), where MOI = -ln (1 – infection rate). For neutralization experiments, 1×10^4 Caco-2 cells/well were seeded in 96-well plates the day before infection in a medium containing 5% FCS. Cells were co-incubated with SARS-CoV-2 clinical isolate 200325_Tü1 or SARS-CoV-2 clinical isolate 210211_SAv at an MOI of 0.7. Patient sera were added in serial twofold dilutions from 1:40 to 1:5120. At 48 h post infection, cells were fixed with 80% acetone for 5 min, washed with PBS, and blocked for 1 h at room temperature (RT) with 10% normal goat serum (NGS). Cells were incubated for 1 h at RT with 100 µL of serum from a hospitalized convalescent donor in a 1:10,000 dilution and washed three times with PBS. In total, 100 µL of goat anti-human Alexa594 (1:2000) in PBS was used as a secondary antibody for 1 h at RT. Cells were then washed three times with PBS and counterstained with 1:20,000 DAPI solution (2 mg/mL) for 10 min at RT. For quantification of infection rates, images were taken with the Cytation3 (BioTek) and DAPI-positive and Alexa594-positive cells were automatically counted by the Gen5 software (BioTek). Virus neutralizing titers (VNT_{50}) were calculated as the half-maximal inhibitory dose (ID_{50}) using 4-parameter nonlinear regression (GraphPad Prism). An overview of the VNT assay and examples of cells treated with both variants from one vaccinated and one infected individual's serum can be found in Supplementary Fig. 7.

ACE2 competition assay. Biotinylated recombinant human ACE2 (#10108-H08H-B, Sino Biological) was diluted to a final concentration of 571.4 ng/mL in assay buffer (1:4 Low Cross Buffer (Candor Bioscience GmBH) in CBS (1× PBS + 1% BSA) + 0.05% Tween20) to create ACE2 buffer. Plasma samples were diluted 1:50 in assay buffer and then to a final concentration of 1:400 in ACE2 buffer under a sterile workbench, resulting in a final ACE2 concentration of 500 ng/mL in all samples. In all, 25 µL of diluted plasma samples were then added to 25 µL of 1× BeadMix[33] per well of a 96-well plate (#3642, Corning). In addition to the standard bead mix used in MULTICOV-AB, all bead coupled RBD mutants were included. As a control, 500 ng/mL ACE2 was also used. Samples were incubated at 21 °C, 750 rpm for 2 h on a thermomixer. Samples were then washed using a microplate washer with Wash Buffer (1× PBS + 0.05% Tween20). 30 µL of 2 µg/mL Streptavidin-PE (#SAPE-001, Moss) was added to each well and incubated for 45 min, 21 °C, 750 rpm in darkness on a thermomixer. Following incubation, samples were washed again and then resuspended in 100 µL of Wash Buffer, before being shaken again for 3 min at 1000 rpm. Samples were read individually on a FLEXMAP3D instrument under the following settings: 80 µL (no timeout), 50 events, Gate: 7500–15,000, Reporter Gain: Standard PMT. MFI values were then normalized against the control wells. All samples were measured in duplicates and the mean is reported.

Neutrobody Plex. For further validation of the neutralization response, all samples were analyzed using the NeutrobodyPlex[35] using a final Nanobody (NMI1267) concentration of 2 nM. Samples were diluted 1:25 into assay buffer (same as MULTICOV-AB) and then a further 1:8 in neutrobody buffer (MULTICOV-AB assay buffer + 4.56 nM nanobody). In total, 25 µL of diluted sample was then added to 25 µL of 1× MULTICOV-AB Bead Mix[33] using a 96-well plate (#3600, Corning). Samples were incubated for 2 h at 21 °C, 750 rpm on a thermomixer (Eppendorf), after which the unbound antibodies were removed by washing three times with Wash Buffer (1× PBS, 0.05% Tween20) using a microplate washer (Biotek 405TS, Biotek Instruments GmBH). Bound antibodies were detected using 3 µg/mL RPE-huIgG (#109-116-098, Dianova) by incubation for 45 mins at 21 °C, 750 rpm on a thermomixer. Following another washing step, beads were re-suspended in 100 µL of Wash Buffer and re-shaken for 3 min at 21 °C, 1000 rpm. Plates were then measured using a FLEXMAP3D instrument (Luminex) using the same settings as in MULTICOV-AB above. Samples were measured on the same plate with their respective MULTICOV-AB IgG measurement. In addition to MULTICOV-AB controls, for plate-to-plate qualification one control sample was processed on all plates.

Data analysis. Data analysis and figure generation were performed in RStudio (Version 1.2.5001), running R (version 3.6.1) with the additional packages "beeswarm" and "RcolorBrewer" for data depiction purposes only. The type of statistical analysis performed (when appropriate) is listed in the figure legends. Figures were generated in Rstudio and then edited for clarity in Inkscape (Inkscape 0.92.4). Mann–Whitney *U* test was used to determine the difference between signal distributions from different sample groups using the "wilcox.test" function from R's "stats" library. Kendall's τ coefficient was calculated in order to determine the ordinal association between the observed antibody responses towards RBD mutant and wild-type proteins using the "cor" function from R's "stats" library. Linear regression was performed to assess the reduction in ACE2 neutralization observed for RBD mutants compared to wild-type proteins using the "lm" function from R's "stats" library. Pre-processing of data such as matching sample metadata and collecting results from multiple assay runs was performed in Excel 2016. GraphPad Prism version 8.4.0 was used to process VNT data.

Reporting summary. Further information on research design is available in the Nature Research Reporting Summary linked to this article.

Data availability

Source data are provided with this paper.

Code availability

Custom analysis code in R and required input files have been deposited on GitHub: https://github.com/BeckerMatthias/Vaccination_VoC_Publication.

Received: 8 March 2021; Accepted: 28 April 2021;
Published online: 25 May 2021

References

1. Zhou, P. et al. A pneumonia outbreak associated with a new coronavirus of probable bat origin. *Nature* **579**, 270–273 (2020).
2. Zhu, N. et al. A novel coronavirus from patients with pneumonia in China, 2019. *N. Engl. J. Med.* **382**, 727–733 (2020).

3. Pan, K.-Y. et al. The mental health impact of the COVID-19 pandemic on people with and without depressive, anxiety, or obsessive-compulsive disorders: a longitudinal study of three Dutch case-control cohorts. *Lancet Psychiatry* **8**, 121–129 (2021).
4. Pierce, M. et al. Mental health before and during the COVID-19 pandemic: a longitudinal probability sample survey of the UK population. *Lancet Psychiatry* **7**, 883–892 (2020).
5. Mofijur, M. et al. Impact of COVID-19 on the social, economic, environmental and energy domains: lessons learnt from a global pandemic. *Sustain. Prod. Consum.* **26**, 343–359 (2021).
6. Baden, L. R. et al. Efficacy and safety of the mRNA-1273 SARS-CoV-2 Vaccine. *N. Engl. J. Med.* **384**, 403–416 (2021).
7. Voysey, M. et al. Safety and efficacy of the ChAdOx1 nCoV-19 vaccine (AZD1222) against SARS-CoV-2: an interim analysis of four randomised controlled trials in Brazil, South Africa, and the UK. *Lancet* **397**, 99–111 (2021).
8. Polack, F. P. et al. Safety and efficacy of the BNT162b2 mRNA Covid-19 vaccine. *N. Engl. J. Med.* **383**, 2603–2615 (2020).
9. Mulligan, M. J. et al. Phase I/II study of COVID-19 RNA vaccine BNT162b1 in adults. *Nature* **586**, 589–593 (2020).
10. Korber, B. et al. Tracking changes in SARS-CoV-2 spike: evidence that D614G increases infectivity of the COVID-19 virus. *Cell* **182**, 812–827.e819 (2020).
11. Volz, E. et al. Assessing transmissibility of SARS-CoV-2 lineage B.1.1.7 in England. *Nature* https://doi.org/10.1038/s41586-021-03470-x (2021).
12. Graham, M. S. et al. Changes in symptomatology, reinfection, and transmissibility associated with the SARS-CoV-2 variant B.1.1.7: an ecological study. *Lancet Public Health* https://doi.org/10.1016/S2468-2667(21)00055-4 (2021).
13. Davies, N. G. et al. Estimated transmissibility and impact of SARS-CoV-2 lineage B.1.1.7 in England. *Science* **372**, eabg3055 (2021).
14. Collier, D. A. et al. Sensitivity of SARS-CoV-2 B.1.1.7 to mRNA vaccine-elicited antibodies. *Nature* https://doi.org/10.1038/s41586-021-03412-7 (2021).
15. Kemp, S. A. et al. SARS-CoV-2 evolution during treatment of chronic infection. *Nature* **592**, 277–282 (2021).
16. Schrörs, B. et al. Large-scale analysis of SARS-CoV-2 spike-glycoprotein mutants demonstrates the need for continuous screening of virus isolates. Preprint at *bioRxiv* https://doi.org/10.1101/2021.02.04.429765 (2021).
17. Ou, J. et al. Emergence of SARS-CoV-2 spike RBD mutants that enhance viral infectivity through increased human ACE2 receptor binding affinity. Preprint at *bioRxiv* https://doi.org/10.1101/2020.03.15.991844 (2020).
18. Sun, C. et al. SARS-CoV-2 and SARS-CoV spike-RBD structure and receptor binding comparison and potential implications on neutralizing antibody and vaccine development. Preprint at *bioRxiv* https://doi.org/10.1101/2020.02.16.951723 (2020).
19. Cerutti, G. et al. Potent SARS-CoV-2 neutralizing antibodies directed against spike N-terminal domain target a single supersite. *Cell Host Microbe* https://doi.org/10.1016/j.chom.2021.03.005 (2021).
20. Ibarrondo, F. J. et al. Rapid decay of anti-SARS-CoV-2 antibodies in persons with mild Covid-19. *N. Engl. J. Med.* **383**, 1085–1087 (2020).
21. Dan, J. M. et al. Immunological memory to SARS-CoV-2 assessed for up to 8 months after infection. *Science* **371**, eabf4063 (2021).
22. Tea, F. et al. SARS-CoV-2 neutralizing antibodies; longevity, breadth, and evasion by emerging viral variants. Preprint at *medRxiv* https://doi.org/10.1101/2020.12.19.20248567 (2020).
23. Flehmig, B. et al. Persisting neutralizing activity to SARS-CoV-2 over months in sera of COVID-19 patients. *Viruses* **12**, https://doi.org/10.3390/v12121357 (2020).
24. Tegally, H. et al. Detection of a SARS-CoV-2 variant of concern in South Africa. *Nature* https://doi.org/10.1038/s41586-021-03402-9 (2021).
25. Sabino, E. C. et al. Resurgence of COVID-19 in Manaus, Brazil, despite high seroprevalence. *Lancet* **397**, 452–455 (2021).
26. Larsen, H. D. et al. Preliminary report of an outbreak of SARS-CoV-2 in mink and mink farmers associated with community spread, Denmark, June to November 2020. *Eurosurveillance* **26**, 2100009 (2021).
27. Zhang, W. et al. Emergence of a novel SARS-CoV-2 variant in Southern California. *J. Am. Med. Assoc.* https://doi.org/10.1001/jama.2021.1612 (2021).
28. Davies, N. G. et al. Increased mortality in community-tested cases of SARS-CoV-2 lineage B.1.1.7. *Nature* https://doi.org/10.1038/s41586-021-03426-1 (2021).
29. Shen, X. et al. SARS-CoV-2 variant B.1.1.7 is susceptible to neutralizing antibodies elicited by ancestral spike vaccines. *Cell Host Microbe* https://doi.org/10.1016/j.chom.2021.03.002 (2021).
30. Yan, R. et al. Structural basis for the recognition of SARS-CoV-2 by full-length human ACE2. *Science* **367**, 1444 (2020).
31. Gu, H. et al. Adaptation of SARS-CoV-2 in BALB/c mice for testing vaccine efficacy. *Science* **369**, 1603 (2020).
32. Planas, D. et al. Sensitivity of infectious SARS-CoV-2 B.1.1.7 and B.1.351 variants to neutralizing antibodies. *Nat. Med.* https://doi.org/10.1038/s41591-021-01318-5 (2021).
33. Becker, M. et al. Exploring beyond clinical routine SARS-CoV-2 serology using MultiCoV-Ab to evaluate endemic coronavirus cross-reactivity. *Nat. Commun.* **12**, 1152 (2021).
34. Ruetalo, N. et al. Antibody response against SARS-CoV-2 and seasonal coronaviruses in nonhospitalized COVID-19 patients. *mSphere* **6**, https://doi.org/10.1128/mSphere.01145-20 (2021).
35. Wagner, T. R. et al. NeutrobodyPlex—nanobodies to monitor a SARS-CoV-2 neutralizing immune response. *EMBO Rep.* **22**, e52325 https://doi.org/10.15252/embr.202052325 (2021).
36. Zhou, D. et al. Evidence of escape of SARS-CoV-2 variant B.1.351 from natural and vaccine-induced sera. *Cell* https://doi.org/10.1016/j.cell.2021.02.037.
37. Liu, Y. et al. Neutralizing activity of BNT162b2-elicited serum—preliminary report. *N. Engl. J. Med.* https://doi.org/10.1056/NEJMc2102017 (2021).
38. Wang, P. et al. Antibody resistance of SARS-CoV-2 variants B.1.351 and B.1.1.7. *Nature* https://doi.org/10.1038/s41586-021-03398-2 (2021).
39. Kuzmina, A. et al. SARS-CoV-2 spike variants exhibit differential infectivity and neutralization resistance to convalescent or post-vaccination sera. *Cell Host Microbe* https://doi.org/10.1016/j.chom.2021.03.008 (2021).
40. Wang, Z. et al. mRNA vaccine-elicited antibodies to SARS-CoV-2 and circulating variants. *Nature* https://doi.org/10.1038/s41586-021-03324-6 (2021).
41. Nelde, A. et al. SARS-CoV-2-derived peptides define heterologous and COVID-19-induced T cell recognition. *Nat. Immunol.* **22**, 74–85 (2021).
42. Rambaut, A. et al. A dynamic nomenclature proposal for SARS-CoV-2 lineages to assist genomic epidemiology. *Nat. Microbiol.* **5**, 1403–1407 (2020).
43. Amanat, F. et al. A serological assay to detect SARS-CoV-2 seroconversion in humans. *Nat. Med.* **26**, 1033–1036 (2020).
44. Lauring, A. S. & Hodcroft, E. B. Genetic variants of SARS-CoV-2—what do they mean? *J. Am. Med. Assoc.* **325**, 529–531 (2021).
45. Planatscher, H. et al. Systematic reference sample generation for multiplexed serological assays. *Sci. Rep.* **3**, 1–5 (2013).
46. Sulyok, Z. et al. Heterologous protection against malaria by a simple chemoattenuated PfSPZ vaccine regimen in a randomizedtrial. *Nat. Commun.* **12**, 2518, https://doi.org/10.1038/s41467-021-22740-w (2021).

Acknowledgements

We thank Johanna Griesbaum for technical assistance, Florian Krammer for providing us with expression plasmids for the Spike Trimer and RBD, Tina Ganzenmüller and the diagnostic department of the Institute for Medical Virology, University Hospital Tübingen for providing patient samples, and the NGS competence center of the University Hospital Tübingen for rapid sequencing. This work was financially supported by the State Ministry of Baden-Württemberg for Economic Affairs, Labour and Housing Construction (grant numbers FKZ 3–4332.62-NMI-67 and FKZ 3–4332.62-NMI-68), the Ministerium für Wissenschaft und Kunst Baden-Württemberg, the Initiative and Networking Fund of the Helmholtz Association of German Research Centres (grant number SO-96), the Deutsche Forschungsgemeinschaft (DFG-KO 3884/5-1) and the EU Horizon 2020 research and innovation programme (grant agreement number 101003480—CORESMA). The funders had no role in study design, data collection, data analysis, or the decision to publish.

Author contributions

U.R., M.K., M.B., A.D., and N.S.M. conceived the study. M.B., A.D., Ja.H., R.F., A.K., Mi.S., U.R., and N.S.M. designed the experiments. K.S.L., Mo.S., G.K., Mi.S., M.K., and N.S.M. procured funding. M.B., A.D., D.J., N.R., C.H., Ju.H., and M.L. performed experiments. Y.T.P., M.M., V.M., T.B., K.A., R.F., A.K., M.K., U.R., and N.S.M. collected samples or organized their collection. P.D.K., B.T., and T.W. produced the RBD mutants. H.P., M.B., and D.J. produced and analyzed the QC samples in MULTICOV-AB. M.B., A.D., N.R., and Mi.S. performed the data analysis. M.B., A.D., D.J., and N.S.M. generated the figures. A.D. wrote the first draft of the manuscript with input from M.B., D.J., Ja.H., K.S.L., Mo.S., R.F., A.K., Mi.S., U.R., and N.S.M. A.D., M.B., R.F., Mi.S., U.R., and N.S.M. revised the manuscript. All authors approved the final version of the manuscript.

Competing interests

T.R.W., P.K., N.S.M., and U.R. are named as inventors on a patent application (EP 20 197 031.6) claiming the use of the described Nanobodies used in the NeutrobodyPlex for diagnosis and therapeutics filed by the Natural and Medical Sciences Institute. N.S.-M. was a speaker at Luminex user meetings in the past. The Natural and Medical Sciences Institute at the University of Tuebingen is involved in applied research projects as a fee for services with Luminex. The remaining authors declare no competing interests.

Additional information

Supplementary information The online version contains supplementary material available at https://doi.org/10.1038/s41467-021-23473-6.

Correspondence and requests for materials should be addressed to U.R., M.S. or N.S-M.

Peer review information *Nature Communications* thanks Fridtjof Lund-Johansen and the other, anonymous, reviewer(s) for their contribution to the peer review of this work. Peer reviewer reports are available.

Reprints and permission information is available at http://www.nature.com/reprints

Publisher's note Springer Nature remains neutral with regard to jurisdictional claims in published maps and institutional affiliations.

Supplementary Information – Immune response to SARS-CoV-2 variants of concern in vaccinated individuals

Matthias Becker[1#], Alex Dulovic[1#], Daniel Junker[1], Natalia Ruetalo[2], Philipp D. Kaiser[1], Yudi T. Pinilla[3], Constanze Heinzel[3], Julia Haering[1], Bjoern Traenkle[1], Teresa R. Wagner[1,4], Mirjam Layer[2], Martin Mehrlaender[5], Valbona Mirakaj[5], Jana Held[3,6], Hannes Planatscher[7], Katja Schenke-Layland[1,8,9,10], Gérard Krause[11,12], Monika Strengert[11,12], Tamam Bakchoul[13], Karina Althaus[13], Rolf Fendel[3,6], Andrea Kreidenweiss[3,6], Michael Koeppen[5], Ulrich Rothbauer[1,4*], Michael Schindler[2*], Nicole Schneiderhan-Marra[1*]

Author Affiliations

1 NMI Natural and Medical Sciences Institute at the University of Tübingen, Reutlingen, Germany

2 Institute for Medical Virology and Epidemiology, University Hospital Tübingen, Tübingen, Germany

3 Institute of Tropical Medicine, University of Tübingen, Germany

4 Pharmaceutical Biotechnology, University of Tübingen, Germany

5 Department of Anaesthesiology and Intensive Care Medicine, University Hospital Tübingen, Tübingen, Germany

6 German Center for Infection Research (DZIF), partner site Tübingen, Germany

7 Signatope GmbH, Reutlingen, Germany

8 Cluster of Excellence iFIT (EXC2180) “Image-Guided and Functionally Instructed Tumor Therapies”, University of Tübingen, Tübingen, Germany

9 Department of Women’s Health, Research Institute for Women’s Health, University of Tübingen, Tübingen, Germany

10 Department of Medicine/Cardiology, Cardiovascular Research Laboratories, David Geffen School of Medicine at UCLA, Los Angeles, USA

11 Helmholtz Centre for Infection Research, Braunschweig, Germany

12 TWINCORE GmbH, Centre for Experimental and Clinical Infection Research, a joint venture of the Hannover Medical School and the Helmholtz Centre for Infection Research, Hannover, Germany

13 Institute for Clinical and Experimental Transfusion Medicine, University Hospital Tübingen, Tübingen, Germany

# these authors contributed equally to this work

* corresponding authors.

Contact Information

Nicole Schneiderhan-Marra – Phone number +49 (0)7121 51530 815. Email Address Nicole.schneiderhan@nmi.de Postal Address – Markwiesenstrasse 55, 72770 Reutlingen, Germany.

Michael Schindler – Phone number +49 (0)7071 2987459. Email Address Michael.Schindler@med.uni-tuebingen.de Postal Address – Elfriede-Aulhorn-Strasse 6, 72076 Tübingen, Germany

Ulrich Rothbauer – Phone number +49 (0)7121 51530 415. Email Address Ulrich.rothbauer@nmi.de Postal Address – Markwiesenstrasse 55, 72770 Reutlingen, Germany

Competing Interests

T.R.W., P.K., N.S.M. and U.R. are named as inventors on a patent application (EP 20 197 031.6) claiming the use of the described Nanobodies used in the NeutrobodyPlex for diagnosis and therapeutics filed by the Natural and Medical Sciences Institute. The other authors declare no competing interest.

Supplementary Table 1 – Characteristics of Vaccinated and Infected sera

Characteristic	Vaccinated	Infected
Number of donors	23	35
Median age (IQR) – years	42 (16)	59 (19)
Female sex (%)	5 (21.7)	10 (28.6)
1st sample collection – median ΔT post first vaccination (range)	21 days (-1 to 22 days)	Not applicable
2nd sample collection – median ΔT post second vaccination (range)	15 days (-7 to 16 days)	Not applicable
Median ΔT post positive PCR test (range)	Not applicable	14 days (2 – 85 days)

For both vaccinated and infected groups, the number of donors, median age in years (including inter-quartile range) and number of females are provided. For vaccinated groups, the median time post-first vaccination is provided for the first sample, and the median time post-second vaccination is provided for the second sample. The full range is included for both samples. A total of 45 samples from 23 vaccinated donors were included in this study. For one individual a second sample was not taken. One individual had their first sample collected before they received a vaccination and so they have a negative ΔT for the first sample. Similarly, two individuals had their second sample collected before they received their second vaccination and so they have a negative ΔT for the second sample. For the infected group, the median ΔT for time between positive PCR test and sample collection is given including the full range.

Supplementary Table 2 – Characteristics of Vaccinated, Infected and Negative saliva samples

Characteristic	Vaccinated	Infected	Negative
Number of donors	22	27	49
Median age (IQR) – years	43 (16)	38 (25 – 58)	29 (25 – 38)
Female sex (%)	5 (22.7)	17 (63)	27 (55)

For all three groups, the total number of samples, median age in years (including inter-quartile range) and number of females are provided. The vaccinated samples are from the same sample group as the serum samples. Infected samples were confirmed by either PCR test or ELISA (EuroImmun) plus the presence of at least one identifying COVID-19 symptom. Negative samples were confirmed to be negative by ELISA (EuroImmun).

Supplementary Table 3 – Full list of primers used in this study

Primer Name	Sequence (5' to 3')
RBDfor	ATATCTAGAGCCACCATGTTCGTGTTTCTGG
N501Yrev	CCACGCCATATGTGGGCTGAAAGCCGTAG
N501Yfor	GGCTTTCAGCCCACATATGGCGTGGGCTATCAGC
RBDrev	AAGATCTGCTAGCTCGAGTCGC
K417Nrev	GTTGTAGTCGGCGATGTTGCCTGTCTGTCCAGGG
K417Nfor	GACAGACAGGCAACATCGCCGACTACAACTACAAGC
E484Krev	GCAGTTGAAGCCTTTCACGCCGTTACAAGGGGT
E484Kfor	GTAACGGCGTGAAAGGCTTCAACTGCTACTTCCC
L452Rrev	CGGTACCGGTAATTGTAGTTGCCGCCG
L452Rfor	GGCAACTACAATTACCGGTACCGGCTGTTCCGGAAG

Full List of primers used in this study for the production of RBD Mutants

Supplementary Table 4 – Antigens included in MULTICOV-AB

Disease	Antigen	Manufacturer	Category number
SARS-CoV-2	Spike Trimer	NMI	-
SARS-CoV-2	RBD	NMI	-
SARS-CoV-2	S1 domain	NMI	-
SARS-CoV-2	S2 domain	Sino	40590
SARS-CoV-2	Nucleocapsid	Aalto	6404-b
SARS-CoV-2	Nucleocapsid N-terminal domain	NMI	-
hCoV-OC43	Spike	Sino	40607-V08B
hCoV-OC43	S1 domain	NMI	-
hCoV-OC43	Nucleocapsid	NMI	-
hCoV-OC43	Nucleocapsid N-terminal domain	NMI	-
hCoV-HKU1	S1 domain	NMI	-
hCoV-HKU1	Nucleocapsid	NMI	-
hCoV-HKU1	Nucleocapsid N-terminal domain	NMI	-
hCoV-NL63	Spike Trimer	NMI	-
hCoV-NL63	S1 domain	NMI	-
hCoV-NL63	Nucleocapsid	NMI	-
hCoV-NL63	Nucleocapsid N-terminal domain	NMI	-
hCoV-229E	S1 domain	NMI	-
hCoV-229E	Nucleocapsid	NMI	-
hCoV-229E	Nucleocapsid N-terminal domain	NMI	-

Full list of antigens included as standard in MULTICOV-AB (minus controls), their manufacturer, and if available, their category number. Full details on all NMI produced antigens can be found in [1].

Supplementary Figure 1 – High serum antibody titers after the second vaccination dose

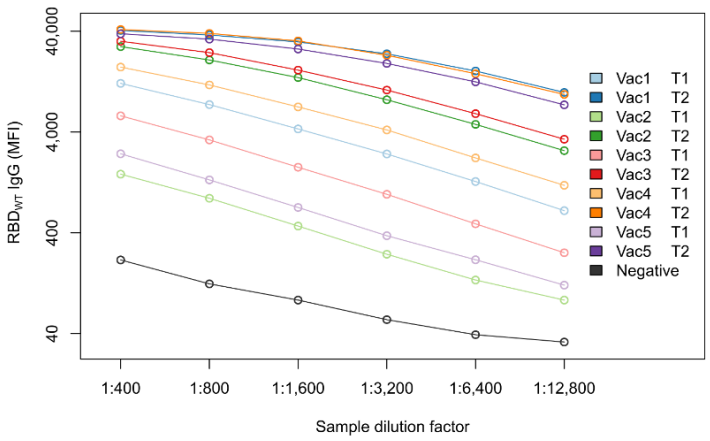

The second vaccination appears to plateau the serum antibody response at the Upper Limit of Detection for MULTICOV-AB. To confirm this, 11 samples consisting of 10 paired samples from five vaccinated individuals (shown in paired colours) and one negative individual (shown in black) were examined in a dilution series. Due to the wide range of samples, a log curve is used for the y axis. The three sera with the highest response maintained a similarly high response for the initial dilution, indicating a plateau in the range of >40,000 MFI, therefore suggesting that even for donors with high responses in the first sample, the second vaccination strongly increased the antibody response. A uniform curve shape for all samples (including the negative control) confirmed reliability of the generated data. Source data are provided as a Source Data file.

Supplementary Figure 2 – RBD reactive IgG detected by ELISA.

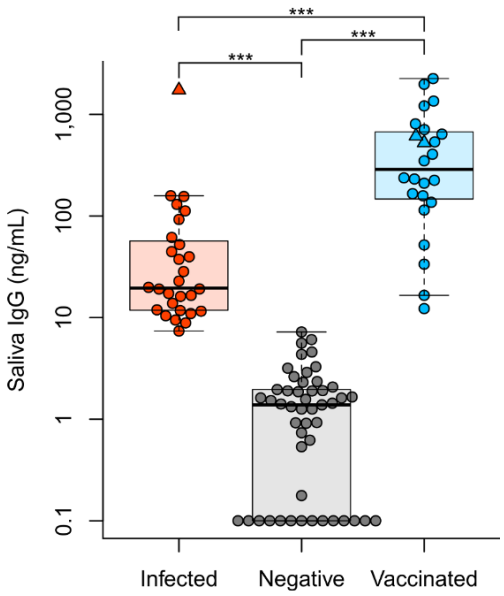

To confirm results for MULTICOV-AB, anti-RBD IgG antibodies in saliva were measured by an in-house ELISA. As in Fig 2, saliva IgG response was highest in vaccinated individuals. Results for vaccinated (blue, n=22), infected (red, n=26) and negative (grey, n=45) individuals are displayed as a Box and whisker plot. Two vaccinated sera samples from individuals not in contact with active SARS-CoV-2 infected individuals and one sera sample from an individual who was previously infected with SARS-CoV-2 and then later vaccinated are included as triangles. Boxes represent the median, 25th and 75th percentiles, whiskers show the largest and smallest non-outlier values. Outliers were determined by 1.5 times IQR. Negative samples that measured 0 were raised to 0.1 for display purposes only. For statistical analysis, their true value was used. Mann-Whitney U (two-sided) was used to determine statistical significance between the groups. *** indicates p-values lower than 0.0001. Source data are provided as a Source Data file.

Supplementary Figure 3 – Cross-reactivity of antibodies to endemic coronaviruses in vaccinated individuals

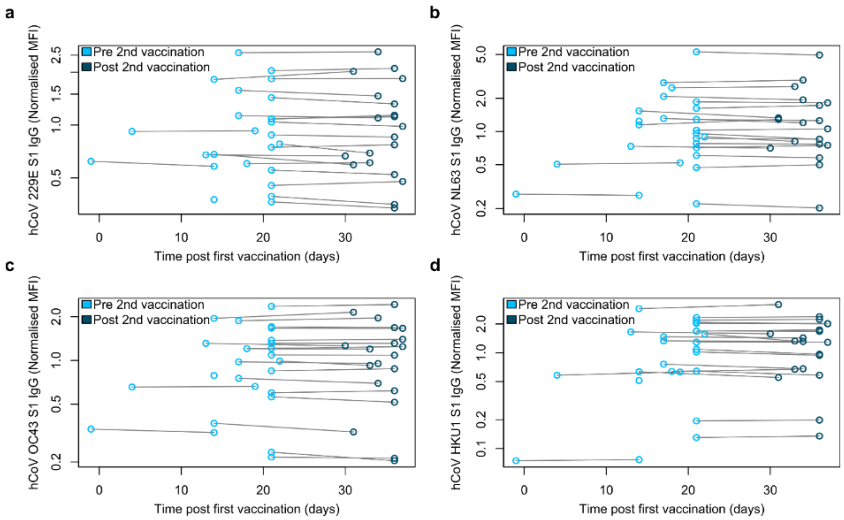

Vaccinated individuals did not have an increased antibody response towards S1 proteins of the endemic coronaviruses 229E (**a**), NL63 (**b**), OC43 (**c**) and HKU1 (**d**). All samples were measured using MULTICOV-AB. Light blue (n=25) indicates samples are pre second vaccination, while dark blue (n=20) indicates samples are post second vaccination. Lines indicated paired samples from the same donor. Source data are provided as a Source Data file.

Supplementary Figure 4 – RBD mutants for the LA and Mink variants have similar antibody binding compared to the wild-type variant.

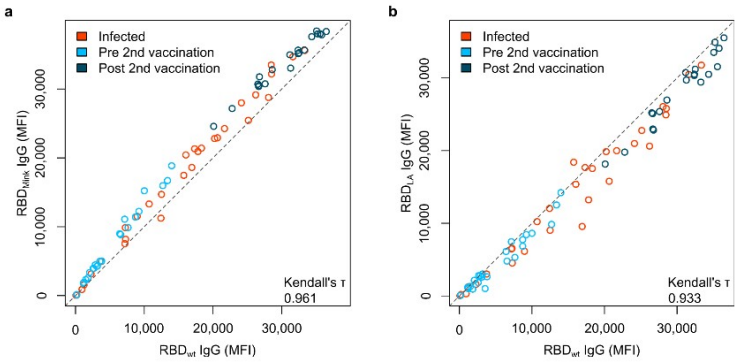

When compared to wild-type (wt), RBD mutants for both the Mink (**a**) and LA (**b**) variants of concern resulted in similar response. RBD mutant antigens were generated (LA) or purchased (Mink) and added to MULTICOV-AB to measure the immune response towards them from vaccinated (blue, n=45) and infected (red, n=35) sera, compared to the wild-type RBD. A linear curve (y=x) is shown as a dashed grey-line to indicate identical response between wild-type and mutant. Kendall's tau was calculated to measure ordinal association between the mutant and wild-type. Source data are provided as a Source Data file.

Supplementary Figure 5 – NeutrobodyPlex confirms reduced neutralization potential of vaccinated and infected sera for the wild-type variant

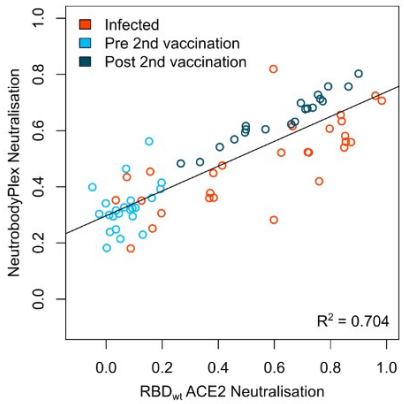

To further validate the results of the VNT and ACE2 competition assay, NeutrobodyPlex was used to examine neutralization potential of sera from vaccinated (pre-second dose (light blue, n=23), post-second dose (dark blue, n=20)) and infected individuals (red, n=28) for wild-type (wt) RBD. The correlation between NeutrobodyPlex and ACE2 competition assay results is shown. A linear regression (y=x) was calculated with the R^2 value shown. Source data are provided as a Source Data file.

Supplementary Figure 6 – Neutralization as measured by ACE2 inhibition assay for the UK, Mink and LA RBD mutants compared to wild-type RBD

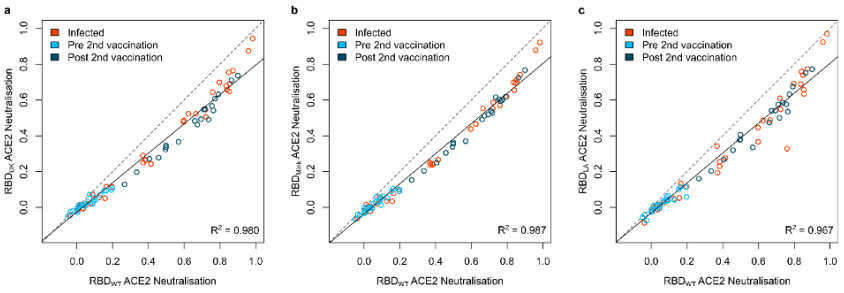

To determine the effect variants of concern had upon neutralization potential, an ACE2 competition assay was developed. RBD mutants for all variants of concern included within this manuscript (UK (**a**), Mink (**b**), LA (**c**)) were examined as well as the wild-type (wt) variant on sera from infected (red, n=35) and vaccinated (pre second vaccination (light blue, n=25), post second vaccination (dark blue, n=20)) individuals. Linear regression (y=x) was calculated for each panel, with the R^2 value shown. Linear regressions had the following equations for the different figure panels: (**a**) y = -0.026 + 0.820x (**b**) y = -0.036 + 0.840x (**c**) y = -0.03 + 0.835x. Source data are provided as a Source Data file.

Supplementary Figure 7 – Overview of VNT

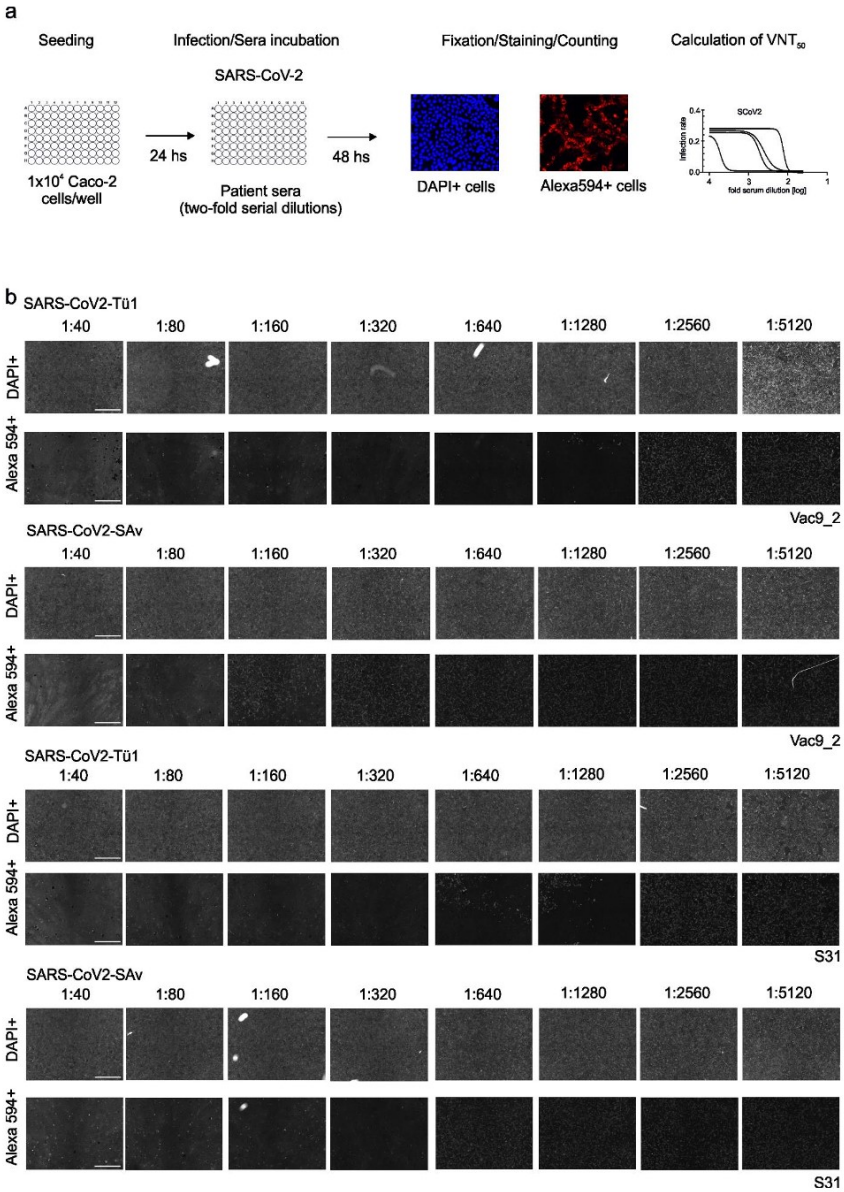

Simple overview of the VNT protocol (**a**) with examples (**b**) for cells treated with the wild-type (SARS-CoV-2-Tü1) and South African (SARS-CoV-2-SAv) for sera from one vaccinated (Vac9_2) and one infected (S31) individual. A dilution series (1:40 – 1:5120) is shown with the corresponding images for DAPI-positive and Alexa 594-positive cells. Scale bar = 1000 µm.

References

1 Becker, M. *et al.* Exploring beyond clinical routine SARS-CoV-2 serology using MultiCoV-Ab to evaluate endemic coronavirus cross-reactivity. *Nature Communications* **12**, 1152, doi:10.1038/s41467-021-20973-3 (2021).

Appendix V: Robust and durable serological response following pediatric SARS-CoV-2 infection

Renk H*, Dulovic A*, Seidel A*, Becker M, Fabricius D, Zernickel M, **Junker D**, Groß R, Müller J, Hilger A, Bode SFN, Fritsch L, Frieh P, Haddad A, Görne T, Remppis J, Ganzemueller T, Dietz A, Huzly D, Hengel H, Kaier K, Weber S, Jacobsen EM, Kaiser PD, Traenkle B, Rothbauer U, Stich M, Tönshoff B, Hoffmann GF, Müller B, Ludwig C, Jahrsdörfer B, Schrezenmeier H, Peter A, Hörber S, Iftner T, Münch J, Stamminger T, Groß HJ, Wolkewitz M, Engel C, Liu W, Rizzi M, Hahn BH, Henneke P, Franz AR, Debatin KM, Schneiderhan-Marra N, Janda A, Elling R.

Nature Communications. 2022. 13(1):128

https://doi.org/10.1038/s41467-021-27595-9

nature COMMUNICATIONS

ARTICLE

https://doi.org/10.1038/s41467-021-27595-9 OPEN

Robust and durable serological response following pediatric SARS-CoV-2 infection

Hanna Renk[1,21], Alex Dulovic[2,21], Alina Seidel[3,21], Matthias Becker[2], Dorit Fabricius[4], Maria Zernickel[4], Daniel Junker[2], Rüdiger Groß[3], Janis Müller[3], Alexander Hilger[5], Sebastian F. N. Bode[4], Linus Fritsch[5], Pauline Frieh[5], Anneke Haddad[5], Tessa Görne[5], Jonathan Remppis[1], Tina Ganzemueller[6], Andrea Dietz[7], Daniela Huzly[8], Hartmut Hengel[8], Klaus Kaier[9], Susanne Weber[9], Eva-Maria Jacobsen[4], Philipp D. Kaiser[2], Bjoern Traenkle[2], Ulrich Rothbauer[2], Maximilian Stich[10], Burkhard Tönshoff[10], Georg F. Hoffmann[10], Barbara Müller[11], Carolin Ludwig[12,13,14], Bernd Jahrsdörfer[12,13,14], Hubert Schrezenmeier[12,13,14], Andreas Peter[15], Sebastian Hörber[15], Thomas Iftner[6], Jan Münch[3], Thomas Stamminger[7], Hans-Jürgen Groß[16], Martin Wolkewitz[9], Corinna Engel[1,17], Weimin Liu[18], Marta Rizzi[19], Beatrice H. Hahn[18], Philipp Henneke[5,20], Axel R. Franz[1,17], Klaus-Michael Debatin[4], Nicole Schneiderhan-Marra[2], Ales Janda[4,22] & Roland Elling[5,20,22]✉

The quality and persistence of children's humoral immune response following SARS-CoV-2 infection remains largely unknown but will be crucial to guide pediatric SARS-CoV-2 vaccination programs. Here, we examine 548 children and 717 adults within 328 households with at least one member with a previous laboratory-confirmed SARS-CoV-2 infection. We assess serological response at 3–4 months and 11–12 months after infection using a bead-based multiplex immunoassay for 23 human coronavirus antigens including SARS-CoV-2 and its Variants of Concern (VOC) and endemic human coronaviruses (HCoVs), and additionally by three commercial SARS-CoV-2 antibody assays. Neutralization against wild type SARS-CoV-2 and the Delta VOC are analysed in a pseudotyped virus assay. Children, compared to adults, are five times more likely to be asymptomatic, and have higher specific antibody levels which persist longer (96.2% versus 82.9% still seropositive 11–12 months post infection). Of note, symptomatic and asymptomatic infections induce similar humoral responses in all age groups. SARS-CoV-2 infection occurs independent of HCoV serostatus. Neutralization responses of children and adults are similar, although neutralization is reduced for both against the Delta VOC. Overall, the long-term humoral immune response to SARS-CoV-2 infection in children is of longer duration than in adults even after asymptomatic infection.

A full list of author affiliations appears at the end of the paper.

To date, our knowledge of children's immune response to infection with severe acute respiratory syndrome coronavirus type 2 (SARS-CoV-2) remains incomplete. In light of current debates on vaccination strategies and non-pharmaceutical preventative measures (e.g. school closures), a comprehensive understanding of protective immunity after natural infection in children is required. As with other viral infections, immune control of SARS-CoV-2 is achieved through a concerted interplay of humoral and cellular immunity[1]. Neutralizing antibodies in children are of particular interest in this context, given their role in blocking virus entry into cells by inhibiting the interaction between the viral receptor binding domain (RBD) within the S-glycoprotein and the angiotensin-converting enzyme 2 (ACE2) receptor[2].

Previous longitudinal studies of the humoral response have found that neutralizing antibodies peak within 3–5 weeks post-infection with a calculated half-life of up to 8 months, suggesting long-term protection in convalescent individuals[1,3–5]. However, most studies only included adults, and longitudinal studies on SARS-CoV-2 infections in children had limited sample size and duration of follow-up post-infection[6–15]. Furthermore, it remains unclear as to whether any form of cross-protection is offered by endemic human coronaviruses (HCoVs) that regularly circulate in the pediatric population, with some studies identifying cross-protection and others not[16,17].

To provide an in-depth characterization of the humoral response in children, we initiated a multi-center longitudinal study, encompassing 328 households each with at least one SARS-CoV-2-infected member, which were followed for up to 12 months after the first infection in each household. This cohort is unique as the subjects exhibited mainly asymptomatic or mild disease with uninfected family members serving as environmental and age-matched controls. We performed an extensive serological evaluation of SARS-CoV-2 infection in all household members, comprising analyses of production of antibodies against various SARS-CoV-2 antigens, including Variants of Concern (VOCs), production of neutralizing antibodies and the role of HCoVs.

Results

A total of 548 children and 717 adults from 328 households were examined at T1 and 279 households including 402 children and 569 adults were followed to T2 (see Methods and Appendix for full details, Table 1 for a description of the study population, Fig. S2 in the Supplementary Appendix for details on the age structure of the study population). Children were substantially less often seropositive (33.0% at T1, 37.3% at T2) than adults (57.7% at T1, 49.4% at T2) (Table 1). Seropositive participants were almost exclusively mildly or asymptomatically infected. In seropositive individuals, asymptomatic infections were five times more common in children (44.8% T1, 46.0% T2) than in adults (8.7% T1, 11.0% T2) (Table 1), with the proportion of asymptomatic infections decreasing with increasing age (Fig. S3). Overall, hospitalization was rare (3·6% of adults, 0% of children, Table 1). The performance of the four serological assays for children and adults at T1 and T2 is shown in Table S1 and Fig. S4.

The detailed humoral immune response against different SARS-CoV-2 antigens, assessed by MULTICOV-AB is shown in Fig. 1. Children had significantly higher antibody titers against spike ($p < 0.001$), RBD ($p < 0.001$), S1 domain ($p < 0.001$) and nucleocapsid ($p = 0.01$) compared to adults at T1. This increased response was confirmed by the three commercial assays (Fig. S5). In addition, we observed a large difference in seroreversion, with only 3.8% of children, but 17.1% of adults seroreverting between T1 and T2 (Table 1). Seroreversion was not associated with the response to particular antigens, although the largest and smallest decay in antibody concentrations were observed for antibodies against the S2 domain and nucleocapsid, respectively, regardless of age (Fig. S6).

For both children and adults, there was no significant difference in antibody response between symptomatic and asymptomatic infections (Figs. 2a, b, S7). The frequency of reported symptoms differed between adults and children and the predictive value of each symptom varied between both groups (Fig. 2c, d). While any of the symptoms fever, cough, diarrhea or dysgeusia proved to be a good indicator of infection in adults, dysgeusia was by far the best predictive symptom in children (87.50% of children with dysgeusia were seropositive; 95% CI 71.4–95.2%, 30.5% of children without dysgeusia were seropositive for SARS-CoV-2, 95% CI 29.7–31.3% Fig. 2d). Conversely, cough was a poor predictor of SARS-CoV-2 infection in children (37.4% of children with a cough were seropositive; 95% CI 29.3–46.3%, 33.0% of children without a cough were seropositive; 95% CI 31.0–35.2%, Fig. 2d). Further examination of predictive symptoms among children showed that in contrast to dysgeusia, cough only gained predictive value in children above the age of 12 and the predictive value of fever increased with age (Table S2). There was no difference in the humoral response associated with the presence of particular symptoms in either adults or children (Fig. S8).

To further explore differences in the antibodies produced by children and adults, we analyzed their neutralization potential as well as their binding towards VOCs. The neutralizing potential of a subset of children's sera exceeded that of a subset of adults' at T1 ($p < 0.001$) and T2 ($p = 0.02$) (Fig. 3a). However, this could be attributed to antibody titers, as neutralization in children correlated with the S1-directed antibody response (Spearman's rank 0.86, Fig. 3b). There was no difference in antibody binding responses to the RBD of Alpha and Beta VOCs between adults and children, with an identical binding for the Alpha variant compared to wild-type (Spearman's rank 0.95, Fig. 3c) and a reduction in binding for the Beta variant (Spearman's rank 0.69, Fig. 3d). Neutralization capacity in the pseudotyped virus assay was significantly reduced against the Delta VOC compared to wild-type in both children and adults ($p < 0.01$, Fig. 3e, f). However, neutralization was present in the majority of the seropositive participants–both adults (77.5%) and children (82.0%).

Seroprevalence against endemic coronaviruses rose sharply with age in early childhood, and was stable in older children, adolescents and adults independent of age (Figs. 4a and S9). In contrast to SARS-CoV-2 seroreversion, HCoV antibody titers decreased faster in younger children than in adults (Fig. S10). There were HCoV naïve samples in this cohort and some individuals showed a substantial increase in HCoV antibody response indicating exposure towards endemic HCoVs between the two time points (Fig. 4b in red, Fig. S11). Amongst SARS-CoV-2 exposed individuals in households with a defined index case (index cases excluded from the analysis, see Methods), there was no difference in HCoV antibody titers between SARS-CoV-2 seropositive and seronegative children or adults ($p = 0.21$, Figs. 4c and S12). In addition, we assessed whether SARS-CoV-2 infection boosted HCoV antibody responses, however there was no evidence for an association between HCoV antibody responses and SARS-CoV-2 antibody responses in exposed children or adults (Spearman's rank 0.03, Fig. 4d).

Discussion

To our knowledge, this is the largest prospective multi-center study comprehensively comparing the adult and pediatric longitudinal humoral immune response following SARS-CoV-2

Table 1 Demographics and key information for the study cohort.

	Time point T1	Time point T1	Time point T2	Time point T2
Number of participants by age group (n)	Adult (717)	Children (548)	Adult (569)	Children (402)
Median Age - years (IQR)	44 (37-49)	10 (6-13)	45 (38-50)	10 (6-14)
Number of females (%)	362 (50.5)	277 (50.6)	297 (52.2)	202 (50.3)
BMI (IQR)	25.4 (22.2-27.7)	17.4 (14.9-19.5)	24.7 (22.3-28.1)	17.0 (15.0-19.7)
Number of seropositive participants	414 (57.7)	181 (33.0)	281 (49.4)	150 (37.3)
• Asymptomatic (%)	36 (8.7)	81 (44.8)	31 (11.0)	69 (46.0)
• Symptomatic (%)	378 (91.3)	100 (55.2)	250 (89.0)	81 (54.0)
Seroreverted at T2 (%)	NA	NA	71 (17.1)	7 (3.8)
Symptoms at disease onset (of seropositive)	..	..	..	..
• Fever (%)	217 (52.4)	66 (36.5)	151 (53.7)	49 (32.7)
• Cough (%)	221 (53.4)	37 (20.4)	154 (54.8)	33 (22.0)
• Dysgeusia (%)	266 (64.3)	28 (15.5)	176 (62.6)	24 (16.0)
• Diarrhea (%)	75 (18.1)	18 (9.9)	55 (19.6)	16 (10.7)
Median (IQR) days from positive PCR test result to timepoint	96 (63-120)	96 (63-120)	333 (319-353)	333 (319-353)
Median (IQR) days from symptoms onset to timepoint (of seropositive)	109 (67-122)	109 (67-122)	340 (322-356)	340 (322-356)
Hospitalized (of seropositive) (%)	15 (3.6)	0 (0.0)	NA	NA
Vaccinated (%)	NA	NA	24 (4.2)	1 (0.3)
Number of households	328	328	279	279
Median (IQR) number of household members	4 (3-4)	4 (3-4)	4 (3-4)	4 (3-4)

See methods for definition of how samples were defined as being seropositive, asymptomatic or symptomatic. Median time from positive PCR test to time point ($n = 368$ at T1, $n = 310$ at T2) and median time from symptoms onset to time point ($n = 349$ at T1, $n = 243$ at T2) are calculated using adult samples for which this data was available. Percentages of seropositive participants refer to the sample size at Time point 1 and Time point 2, respectively.
BMI Body Mass Index, *IQR* Interquartile Range, *NA* not applicable, *PCR* Polymerase Chain Reaction.

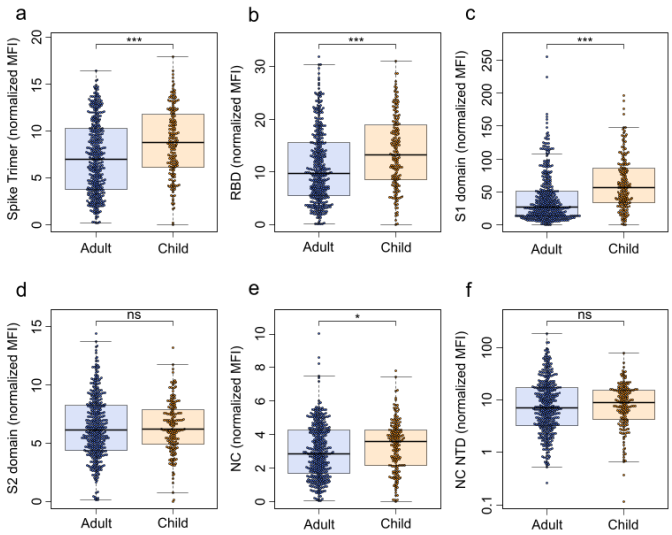

Fig. 1 Children have a significantly higher humoral response to SARS-CoV-2 than adults. The humoral response generated following SARS-CoV-2 household exposure with seroconversion was examined using MULTICOV-AB. Children (orange, $n = 181$) produced significantly more antibodies against the Spike (**a** $p = 6.00 \times 10^{-6}$), Receptor Binding Domain (RBD) (**b** $p = 2.86 \times 10^{-6}$), S1 domain (**c** $p = 3.00 \times 10^{-14}$) and nucleocapsid (NC) (**e** $p = 1.76 \times 10^{-2}$) than adults (blue, $n = 414$). There was no significant difference for either the S2 domain (**d** $p = 0.66$) or the N-terminal domain of the nucleocapsid (NC NTD) (**f** $p = 0.40$). Only samples from T1 with a seropositive status (see Methods) are shown. Box and whisker plots with the box representing the median, 25th and 75th percentiles, while whiskers show the largest and smallest non-outlier values. Outliers were identified using upper/lower quartile ±1.5 times IQR. Statistical significance was calculated using Mann–Whitney-*U* (two-sided) with significance defined as being *<0.05, ***<0.001. Values >0.05 were defined as non-significant (ns). MFI Median Fluorescence Intensity.

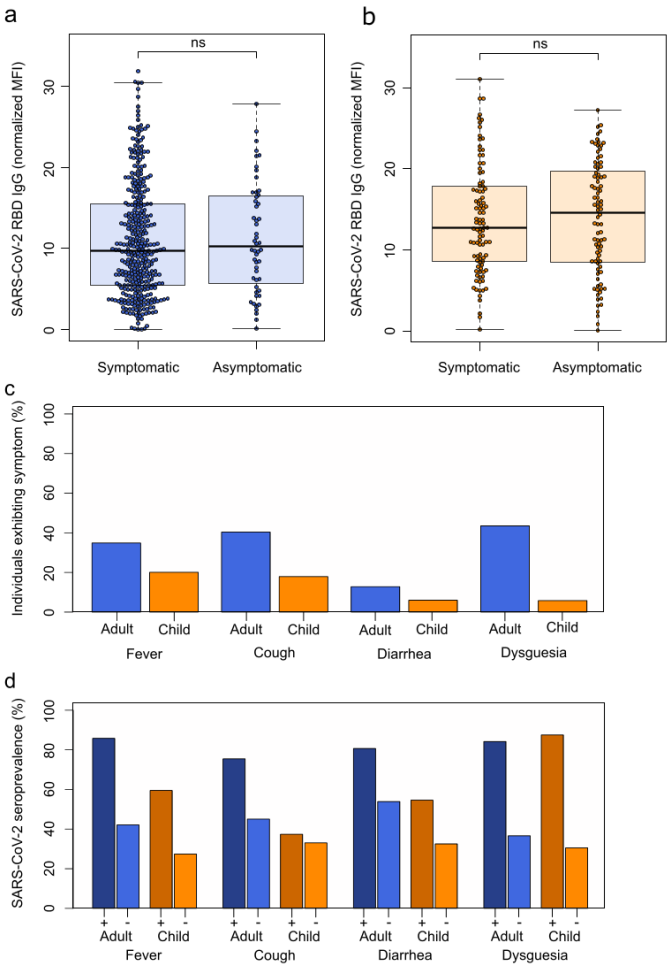

Fig. 2 SARS-CoV-2 infections in children are more often asymptomatic than in adults, although dysgeusia is a good indicator of SARS-CoV-2 infection in both adults and children. Box and whisker plots showing that there is no difference in antibody response between asymptomatic and symptomatic SARS-CoV-2 infections in adults (**a** in blue, $p = 0.684$, $n = 414$) or children (**b** in orange, $p = 0.712$, $n = 181$), as assessed by MULTICOV-AB. The receptor binding domain (RBD) is shown as an example, all other SARS-CoV-2 antigens are shown in Fig. S7. Boxes represent the median, 25th and 75th percentiles, while whiskers show the largest and smallest non-outlier values. Outliers were identified using upper/lower quartile ±1.5 times IQR. Statistical significance was calculated using Mann–Whitney-*U* (two-sided). ns indicates a non-significant *p* value >0.05. The four symptoms reported in this study were then examined for their frequency within the study population (**c**), with all symptoms more commonly reported in seropositive adults (in blue) than seropositive children (in orange). Each symptom was then examined for its predictive ability to indicate SARS-CoV-2 infection (**d**), with dysgeusia a strong predictor in both adults (dark blue, 84.2%) and children (dark orange, 87·5%). All other symptoms were poor predictors in children (fever 59.5%, cough 37.4%, diarrhea 54.6%) compared to adults (fever 85.8%, cough 75.0%, diarrhea 80.7%). Only samples from T1 were analyzed for this figure ($n = 717$ adults, 548 children). "+" indicates presence of the symptom "−" indicates absence of the symptom. MFI Median Fluorescence Intensity.

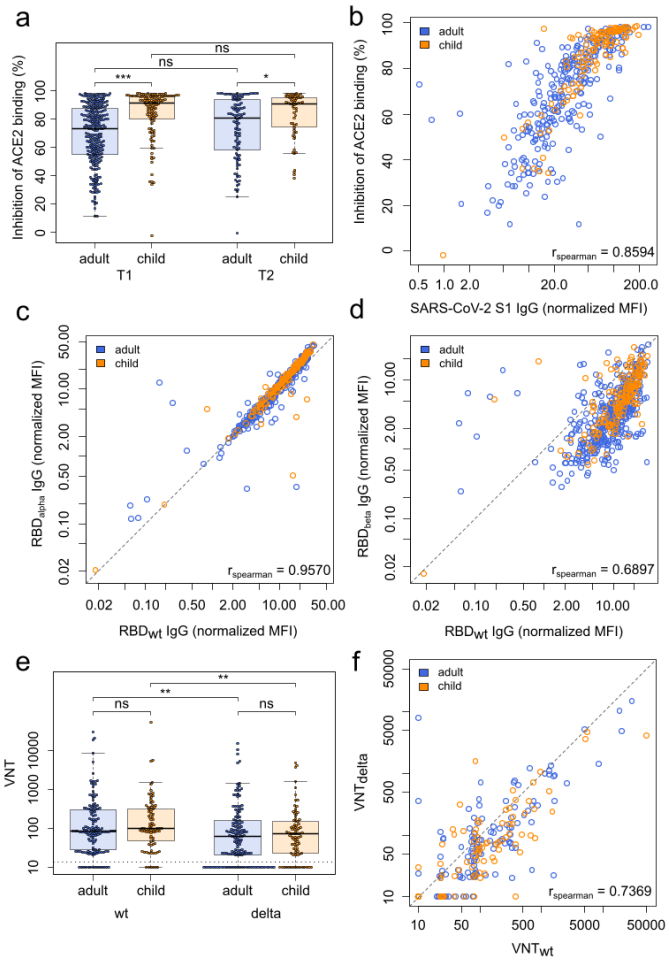

household exposure. As the humoral immunity against SARS-CoV-2 is now increasingly accepted as the central correlate of protection[18–20], improving our incomplete understanding in children[21,22] is of considerable value for public health and vaccination strategies. Importantly, our outpatient cohort has high epidemiological relevance, as a mild course is the most frequent outcome of SARS-CoV-2 infection overall[23]. Our findings identify several unique features of the pediatric serological immune response against SARS-CoV-2.

Children had a lower seroprevalence after household exposure and seropositivity followed asymptomatic infection more frequently than in adults. This is in agreement with our previous report of a different cohort consisting of parent–child pairs[24]. In light of potential pediatric vaccination campaigns, children's humoral response to SARS-CoV-2 is markedly increased in both quantity and longevity, with children seroreverting at a significantly lower pace than adults. Children generated higher titers of SARS-CoV-2 antibodies than their parents after being exposed to likely same viral strain, and antibody titers negatively correlated with age. Of particular interest are the increase in antibodies produced against the S1 domain and RBD, both of which are associated with higher neutralization capacity, indicating that children produce a high quality humoral response against SARS-CoV-2[2,18,25]. The quality of the pediatric humoral response is further illustrated by the similar binding capacity against the SARS-CoV-2 Alpha and Beta VOCs and a similar neutralization capacity towards the Delta VOC compared to adults. These data argue for the generation of a protective long-term humoral

Fig. 3 Children and adults produce antibodies with equal neutralizing potential and their antibodies offer the same protection against Variants of Concern. a Box and whisker plot showing that antibodies produced by children (orange, $n = 118$) have a significantly higher inhibition of ACE2 binding than those produced by adults (blue, $n = 267$, $p = 4.37 \times 10^{-13}$) at T1 and T2 ($p = 0.02$, child $n = 59$, adult $n = 106$) as determined by the sVNT assay. Boxes represent the median, 25th and 75th percentiles, while whiskers show the largest and smallest non-outlier values. Outliers were identified using upper/lower quartile ±1.5 times IQR. Statistical significance was calculated using Mann–Whitney-*U* (two-sided) with *** indicating a p value < 0.001, * indicating a p value < 0.05, and ns indicating a non-significant p value > 0.05. To determine whether this was due to the higher titers in children, SARS-CoV-2 S1 humoral response was determined using MULTICOV-AB for T1 and plotted against the results of the sVNT assay (**b**). Spearman's rank was calculated to measure the ordinal association between them, confirming that the increase in neutralization is due to higher titers. Protection against the Alpha (**c**) and Beta (**d**) VOCs was determined by MULTICOV-AB and plotted as a linear regression against the antibody binding response to the wild-type (wt) receptor binding domain (RBD), with Spearman's rank calculated to measure the ordinal association. There was no difference in antibody response between children ($n = 166$, T1 samples only) and adults ($n = 381$, T1 samples only) for either variant. (**e**) Box and whisker plot showing reduced neutralization responses in both adults (blue, $n = 142$, $p = 4.38 \times 10^{-3}$) and children (orange, $n = 83$, $p = 6.36 \times 10^{-3}$) against Delta VOC as compared to WT as determined by a pseudotype virus assay (VNT). Boxes represent the median, 25th and 75th percentiles, while whiskers show the largest and smallest non-outlier values. Outliers were identified using upper/lower quartile ±1.5 times IQR. Statistical significance was calculated using Mann–Whitney-*U* (two-sided) with ** indicating a p value < 0·01 and ns indicating a non-significant value >0.05. Titers are given as serum dilution factor resulting in 50% pseudovirus neutralization (PVNT50). The dashed line represents the lower limit of detection. **f** Linear regression comparing wild-type (VNTwt) and delta (VNTdelta) neutralization responses with Spearman's rank calculated to measure the ordinal association. ACE2 angiotensin-converting enzyme 2, MFI Median Fluorescence Intensity, (s)VNT (surrogate) Virus Neutralization Test, wt wild type.

immune response also against VOCs after wild-type SARS-CoV-2 infection, but the quality and duration of this protection can only be estimated following known exposure to VOCs. Children also had significantly higher neutralizing antibody titers than adults, indicating increased protection. This increase in neutralization was directly correlated with higher antibody titers in the other assays, and therefore may not be due to substantial qualitative changes of the pediatric antibody profiles. These findings are in line with one preprinted study[26] but in contrast to two previous studies, which found that children generated a lower humoral response to SARS-CoV-2 than adults, with a corresponding reduction in neutralization activity[10,12]. However, compared to our cohort, all three studies were substantially smaller in sample size and the latter two investigated a different disease spectrum comprising mostly hospitalized children or those diagnosed with hyperinflammatory MIS-C syndrome, and sampled blood at earlier time points after presumed infection.

It is striking that antibody levels in seropositive individuals were independent of fever, cough or diarrhea, as clinical proxies for systemic or localized inflammation of the respiratory or gastrointestinal tract, respectively. Previous studies have reported a clear correlation between disease severity and neutralizing antibody titers in adults[5,27]. At the other end of the disease spectrum with mildly affected younger adults and children as in our cohort, this association was not detectable irrespective of age. This diverges from the classical infection immunology dogma that systemic pathogen–host interaction is required for the generation of robust immune memory. While titers themselves did not differ between asymptomatic and symptomatic infections, we found substantial differences in titers between adults and children. Presence of any symptom was predictive of seropositivity in adults, whereas children showed substantial differences in both the prevalence of symptoms in seropositive individuals and the predictive values of symptoms with respect to SARS-CoV-2 seropositivity. Since cough was a relatively common symptom in children irrespective of seroconversion, it was not useful in predicting SARS-CoV-2 infection. In contrast, dysgeusia, an infrequent symptom among children, was highly accurate in predicting infection. These findings suggest that symptom criteria used for subsequent PCR testing need to be different for children and adults.

Similarly to other authors[28], we identified that exposure to HCoVs, as measured by seropositivity typically happens within the first five years of life. The relatively small decline of HCoV antibody levels during the study period, especially in the adult population, in comparison to the decline in SARS-CoV-2 antibody levels after a single infection suggests that long-term serological immunity against HCoVs may be driven by recurrent exposure. We observed HCoV infections in previously naïve individuals, indicating that endemic HCoVs still circulated between T1 and T2 despite SARS-CoV-2 related distancing and hygiene measures. Although cross-reactivity and/or cross-protection between SARS-CoV-2 and HCoVs have been hypothesized, our analyses did not find evidence for such effects. For both Alpha- and Beta-coronaviruses, HCoV antibody responses were not associated with a lower likelihood of seroconversion following SARS-CoV-2 exposure. Along with frequent HCoV seronegativity in younger childhood, this strongly argues that the lower incidence of SARS-CoV-2 infection in children is not due to HCoV cross-protection. Moreover, there was no evidence for boosting of HCoV titers following SARS-CoV-2 infection. In contrast to other studies which did identify an effect for endemic HCoV infection, our cohort is composed of intensely exposed individuals from within the same households, which is a substantial strength compared to previous studies that have used pre-pandemic sera or indirect control groups[16,26,29].

Limitations of our study include the potential recall-bias inherent to retrospective self- or parent-reporting of symptoms via questionnaires and physician-interviews. Additionally, PCR tests for SARS-CoV-2 during the first wave in Germany were mostly limited to the household index case, meaning it is possible that infected individuals were not identified as such, despite the multi-assay serological approach. However, the in-depth characterization of the humoral response provides valuable data for clinicians, public health officials and the public, at a time when children are increasingly viewed as a potential viral reservoir due to exclusion of pediatric populations from current vaccination strategies. Moreover, the limited PCR capacities make it also possible that non-index study participants were additionally exposed to unknown infection sources outside of their household. Given the relatively low incidence in Germany during the first wave (peak incidence spring 2020 45 cases/100.000/7 days) and the strict lockdown measures including school closures, this scenario can be assumed to be a rare event. Similarly, while PCR testing was not available for all individuals, the strength of this cohort comes from the comparatively large number of children, inclusion of children and adults from the same household, the inclusion of seronegative household members as well-matched controls, and the prospective longitudinal analysis of the humoral response in children for up to one year post-infection. The

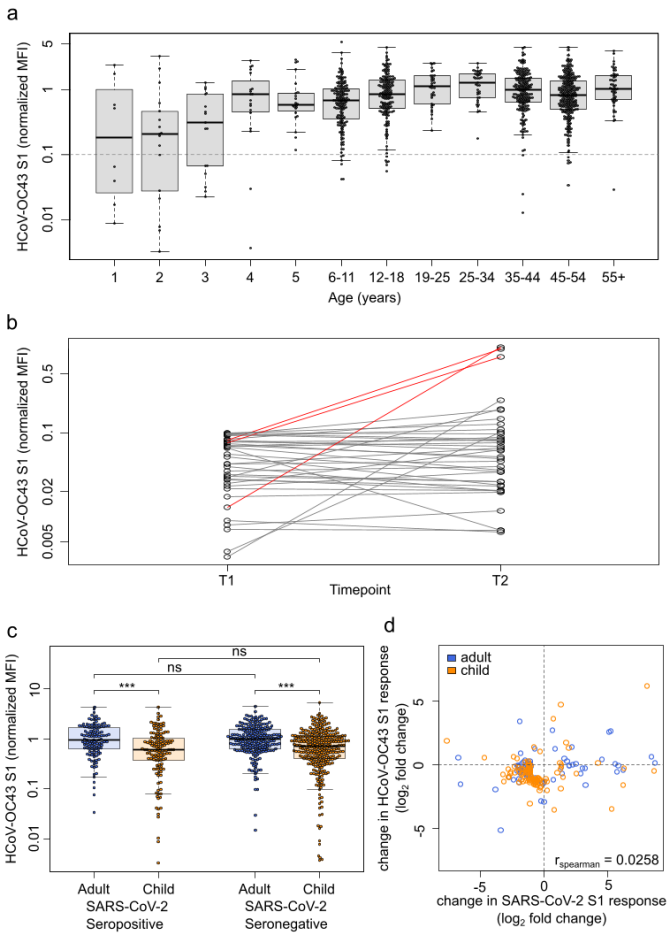

seropositive cohort also comprises almost exclusively individuals with mild or asymptomatic infections and so provides real-world data representative for the majority of SARS-CoV-2 infections in the community. It should be also stated that while all samples were analysed using a range of serological assays, only a subset of samples were analysed for their neutralizing capabilities, and as such, caution should be applied in extrapolating the implications regarding the neutralizing response to all study participants.

In summary, although children mostly show mild or even asymptomatic clinical courses following SARS-CoV-2 infection, they mount a strong and enduring humoral immune response. This strongly argues for sustained protection after infection, and might inform the design of vaccination strategies for SARS-CoV-2 convalescent children.

Methods

Cohort. This study forms part of a non-interventional, prospective observational national multi-center cohort study[30], including 548 children and 717 adults from 328 households each with at least one individual with a SARS-CoV-2 reverse-transcriptase polymerase chain reaction (RT-PCR) proven infection and/or a symptomatic and later serologically proven infection. Participants were recruited during the first wave of the pandemic (May to August 2020) via local health authorities and an in-hospital database of households with at least one laboratory-confirmed SARS-CoV-2 infection. Due to restrictions in obtaining a SARS-CoV-2 RT-PCR test during the first wave (children and asymptomatic contacts of an index case were not tested routinely), serological assays were the only means to identify previous infection. This study was initiated by the four University Children's Hospitals of Freiburg, Heidelberg, Tübingen and Ulm and approved by the independent ethics committees of each center. Sera and data for this substudy were collected at the study sites in Freiburg, Tübingen and Ulm. Participants were asked to fill a questionnaire at time point 1 (May– August 2020) and follow-up time point 2 (February–March 2021).

Fig. 4 HCoVs offer no protection against SARS-CoV-2, nor do they show a boost-back antibody response following SARS-CoV-2 infection. Samples from households with a known index case ($n = 971$) were examined with MULTICOV-AB to determine whether the antibody response to endemic coronaviruses (HCoV) provides any protection against infection with SARS-CoV-2. Initial screening of the population showed that seroprevalence increases with age, although several samples were within the blank range of the HCoV assays, indicating the presence of naïve samples (**a**). Naïve samples were defined as those having less than one-tenth the mean antibody response (indicated by dotted line), with the majority of these samples occurring in children under the age of five. HCoV-OC43 is shown as an example, all other HCoVs can be found as Fig. S9. Boxes represent the median, 25th and 75th percentiles, while whiskers show the largest and smallest non-outlier values. Outliers were identified using upper/lower quartile ±1.5 times IQR. **b** Line graph showing the longitudinal response of these naïve samples from T1 to T2, with new infections in HCoV-OC43 shown in red. **c** Box and whisker plot showing there is no significant difference in HCoV-OC43 antibody response between SARS-CoV-2 seropositive and seronegative individuals, among either adults (blue, $n = 440$, $p = 0.974$) or children (orange, $n = 436$, $p = 0{\cdot}214$). Boxes represent the median, 25th and 75th percentiles, while whiskers show the largest and smallest non-outlier values. Outliers were identified using upper/lower quartile ±1·5 times IQR. Statistical significance was calculated by Mann–Whitney-*U* (two-sided) with *** indicating a p value < 0·001 and ns indicating a p value > 0·05. **d** When comparing paired samples longitudinally within the SARS-CoV-2 seropositive subgroup, there was no increase in HCoV-OC43 S1 response in either adults (blue, $n = 76$) or children (orange, $n = 103$) following SARS-CoV-2 infection. Change in response is presented as log2-fold change from T1 to T2 and only samples with either log2-fold change greater than 1 or smaller than −1 are shown. Spearman's rank was used to calculate the ordinal association between the change in response for HCoV-OC43 and SARS-CoV-2. The same figures for the endemic coronaviruses HCoV-NL63, HCoV-HKU1 and HCoV-229E can be found as Figs. S9, S11 and S12. HCoV human Coronavirus, MFI Median Fluorescence Intensity, S1 Spike S1 domain., S1 Spike S1.

Study participants and eligibility criteria. Families were identified during the first wave of the pandemic between May and August 2020 in the region of Baden–Württemberg, Germany.

Inclusion criteria:

(i) Children (male or female) aged 1–18 years.
(ii) Parents and other adults (male or female) living in the same household with the investigated children (without age limit).
(iii) Residency in the state of Baden-Württemberg.
(iv) Written consent to the study.

Key exclusion criteria:

(i) Severe congenital diseases (e.g. infantile cerebral palsy, severe congenital malformations).
(ii) Congenital or acquired immunodeficiencies.
(iii) Insufficient comprehension of German language.

Data collection. Children and adults within eligible households completed a questionnaire containing demographic information (date of birth, gender, height, weight, smoking), the presence of symptoms (fever, cough, dysgeusia or diarrhea) in plausible temporal association (max. two weeks prior or later) with the onset of the SARS-CoV-2 infection within the household or around the time of a positive SARS-CoV-2 RT-PCR, and symptom duration. For younger children, parents provided symptom information. They additionally provided serum samples for immunological analysis at time point 1 and at follow-up time point 2 after the SARS-CoV-2 infection within the household. Data on vaccination and potential re-infection within the household were collected at time point 2. We investigated all invited households with at least one child to avoid selection bias. Questionnaires were checked for missing or inadequate data and inconsistencies; where possible, these points were clarified retrospectively with the families. To predetermine the sample size, we used a one-factor variance analysis design. Assuming 1.5 children per household participating in the study and three different age ranges, we aimed at a sample size of ≈200 households to reveal small effect sizes of about 0.1 at a significance level of 5% and a test strength of 80%.

Data variables. Samples were defined as being "symptomatic" on the basis of having at least one of four (fever, cough, diarrhea and dysgeusia) symptoms, in addition to a positive serology result. "Asymptomatic" samples were defined as those without any of the above symptoms and a positive serology result. For some households ($n = 272$) an "index case" was defined. This is the first household member to test positive for SARS-CoV-2 by RT-PCR. The majority of index cases in this study were adults (249 of 272). No index was defined for households where additional household members tested positive by RT-PCR within 48 hours of the first positive test or where infection was identified by the combination of positive serology and symptoms only. If a household had a defined index case, then all other household members were considered "exposed". "Time post symptom onset" within a household was calculated as the number of days between the first date of symptom onset in any seropositive individual within a household and the sampling date at T1 and T2 respectively.

Study oversight. This part of the study was conducted by the University Children's Hospitals in Freiburg, Tübingen and Ulm, Germany. Ethics approval was obtained from the respective Medical Faculties' independent ethics committees (University of Freiburg: 256/20_201553; University of Tübingen: 293/2020BO2; University of Ulm: 152/20). Written informed consent was obtained from adult participants and from parents or legal guardians on behalf of their children at both sampling time points. Children's preferences on whether or not to provide a blood sample were respected throughout. This study was registered at the German Clinical Trials Register (DRKS), study ID 00021521, conducted according to the Declaration of Helsinki, and designed, analyzed and reported according to the Strengthening the Reporting of Observational Studies in Epidemiology (STROBE) reporting guidelines. The full study protocol can be found at (https://www.drks.de/drks_web/navigate.do?navigationId=trial.HTML&TRIAL_ID=DRKS00021521).

Blood sample collection. Samples were collected at two separate time points, an early time point (T1) at a median of 109 days (IQR 67–122 days) after earliest symptom onset in household and a late time point (T2) at 340 days (IQR 322–356 days) post-symptom onset (Table 1, Fig. S1 in Supplementary Appendix). Blood samples were collected by venipuncture from all consenting adults and children within the study. Serum was separated on the same day by centrifugation, aliquoted and frozen at −80 °C until used.

Serological assays. Antibodies against SARS-CoV-2 in 2236 samples were detected using the following four assays: (1) EuroImmun-Anti-SARS-CoV-2 ELISA IgG (S1), (2) Siemens Healthineers SARS-CoV-2 IgG (RBD), (3) Roche Elecsys Ig (Nucleocapsid Pan Ig) and (4) MULTICOV-AB, a previously published bead-based multiplex immunoassay that simultaneously analyses antibody binding to 23 antigens from SARS-CoV-2 (including VOCs)[31,32]. Seropositivity was defined as any three of the four SARS-CoV-2 assays being positive. The MULTICOV-AB assay also analyses antibody binding to endemic coronavirus antigens (i.e. HCoV-OC43, -NL63, -HKU1 and −229E)[31,32].

EuroImmun Anti-SARS-CoV-2 ELISA. The EuroImmun Anti-SARS-CoV-2 ELISA (IgG) was performed as the manufacturer's instructions to detect IgG antibodies against the S1 domain of the SARS-CoV-2 spike protein. All 2236 samples used in the final analysis were measured with this assay. All samples were processed with the specified controls and calibrators. Serological analysis was performed blinded for all clinical covariables.

Siemens Healthineers SARS-CoV-2 IgG (sCOVG). The Siemens sCOVG assay was performed as per the manufacturer's instructions on an Advia Centaur XPT platform to detect IgG antibodies against the receptor-binding-domain (RBD) of the SARS-CoV-2 spike protein. All 2,236 samples used in the final analysis were measured with this assay. All samples were processed with the specified controls and calibrators. Serological analysis was performed blinded for all clinical covariables.

Roche Elecsys Electrochemiluminescence immunoassay (ECLIA). The Roche Elecsys ECLIA was performed as per the manufacturer's instruction on a Cobas e411 or e811 platform to detect IgG, IgA and IgM antibodies against the nucleocapsid of SARS-CoV-2. All 2236 samples used in the final analysis were measured with this assay. All samples were processed with the specified controls and calibrators. Serological analysis was performed blinded for all clinical covariables.

MULTICOV-AB™. All 2236 samples used in the final analysis were analyzed using MULTICOV-AB™[1], a bead-based multiplex immunoassay that simultaneously analyzes 23 antigens from SARS-CoV-2 (including RBDs from variants of concern and endemic human coronaviruses)[31]. A full list of antigens used in this study can

be found in Table S3. Samples were measured in 384-well plates, with all pipetting steps performed using a Beckmann Coulter i7 pipetting robot. Antigens were coupled by EDC/s-NHS or Anteo coupling to spectrally distinct populations of MagPlex beads (Luminex Technology). Samples were diluted in assay buffer (1:4 Low Cross Buffer (Candor Bioscience GmBH) in CBS (1x PBS + 1% BSA) + 0.05% Tween20) and added to bead mix to a final dilution factor of 1:400, before being incubated for 2 hours at 21 °C on a thermomixer (1500rpm). Unbound antibodies were then removed by washing with Wash buffer (1x PBS, 0.05% Tween20). Bound antibodies were detected using RPE-conjugated human IgG (3 µg/mL) and IgA (5 µg/mL) (both Biozol) by incubation for 45 mins at 21 °C, 1800 rpm on a thermomixer. Following a further washing step, beads were resuspended in 80 µL of washing buffer and shaken briefly for 3 mins at 1500 rpm. Plates were then measured using a FLEXMAP-3D (Luminex Technology) instrument running xPONENT Software (version 4.3) with the following settings: 60 µL, 80 s timeout, 35 events, Gate 7500-15000 and Reporter Gain: Standard PMT. For quality control, eight wells for each QC sample plus eight blank wells (negative control) were included on each 384-well plate[31–33]. Additionally, control beads coupled with human IgG, goat-anti-human IgG, human IgA and goat-anti-human IgA were included in each well to act as controls for both sample addition and signal system addition. To pass QC, each sample had to meet the minimum threshold for number of beads per ID (35), have a sample and signal system control bead value within normal range and pass plate-by-plate QC sample controls. Any plate or sample that failed QC was re-measured (83/2,390). Normalization values for each antigen were generated by dividing the raw median fluorescence intensity (MFI) value by the mean plate-by-plate MFI of QC2 (IgG) or QC3 (IgA). For SARS-CoV-2, normalization values >1 for the trimeric spike and wild-type RBD indicate positivity. To reduce analytical variations, all samples were analyzed in the same run. Serological analysis was performed blinded for all clinical covariables. Technical questions regarding the MULTICOV-AB"assay should be directed to nicole.schneiderhan@nmi.de.

Surrogate SARS-CoV-2 Neutralization Test. A subset of 385 samples were analyzed for neutralization with the surrogate SARS-CoV-2 neutralization test (GenScript) as per the manufacturer's instructions and as published previously[34]. Briefly, samples and controls were incubated with an HRP-conjugated RBD fragment. Following this, the mixture was added to wells of a capture plate coated with human ACE2 protein. The plate was then washed three times to remove any complexes or non-bound antibodies. TMB was added and then stopped with the addition of a stop reagent. The plate was then read by a microtiter plate reader (POLARstar Omega) at 450 nm. The absorbance of the sample is inversely correlated with the amount of SARS-CoV-2 neutralizing antibodies. Positive and negative controls served as internal assay quality controls. The test was considered valid only if the OD450 for each control fell within the respective range (OD450negative control >1.0, OD450positive control <0.3). For final interpretation, inhibition rates were calculated as follows: Inhibition score (%) = (1 − (OD valuesample/OD valuenegative control) × 100%). Scores <30% were considered negative, scores ≥30% were considered positive.

Cell culture. Vero E6 (African green monkey, female, kidney; CRL-1586, ATCC, RRID:CVCL_0574) cells were grown in Dulbecco's modified Eagle's medium (DMEM, Gibco) supplemented with 2.5% heat-inactivated fetal calf serum (FCS), 100 units/ml penicillin, 100 µg/ml streptomycin, 2 mM L-glutamine, 1 mM sodium pyruvate, and 1x non-essential amino acids. HEK293T (human, female, kidney; ACC-635, DSMZ, RRID: CVCL_0063) cells were grown in DMEM supplemented with 10% FCS, 100 units/ml penicillin, 100 µg/ml streptomycin, and 2 mM L-glutamine. All cells were grown at 37 °C in a 5% CO2 humidified incubator.

Preparation of pseudotyped particles. Rhabdoviral pseudotype particles were prepared as previously described[34]. A replication-deficient VSV vector in which the genetic information for VSV-G is replaced by genes encoding enhanced green fluorescent protein and firefly luciferase 3 (kindly provided by Gert Zimmer, Institute of Virology and Immunology, Mittelhäusern, Switzerland) was used for pseudotyping. HEK293T cells were transfected with expression plasmids encoding SARS-CoV-2 spike variants D614G 4 (pCG1_SARS-2-Sdel18_D614G, kindly provided by Stefan Pöhlmann) or B.1.617.2/Delta[35], containing the spike mutations T19R, G142D, E156-, F157-, R158G, L452R, T478K, D614G, P681R, D950N and a 19AA C-terminal deletion (pcDNA3.1-S2S-IN2(B.1.617.2)Δ19. 24 h post transfection, cells were inoculated with VSV vector. After 2 h incubation at 37 °C, the inoculum was removed, cells were washed with PBS and fresh medium added. After 16–18 h, the supernatant was collected and centrifuged (2,000 × g, 5 min, room temperature) to remove cellular debris. Cell culture medium containing anti-VSV-G antibody (I1-hybridoma cells; ATCC no. CRL-2700) was added to block residual VSV-G-containing particles. Samples were then aliquoted and stored at −80 °C.

Pseudovirus neutralization assay. A subset of 225 samples were examined by Pseudovirus neutralization assay against Wild-type (B1 isolate) and the delta VOC (B.1.617.2). For pseudovirus neutralization experiments, Vero E6 cells were seeded in 96-well plates one day prior. Heat-inactivated (56 °C, 30 min) sera were serially diluted in PBS, mixed with pseudovirus stocks (1:1, v/v) and incubated for 30 min at 37 °C before being added to cells. After 16-18 h, firefly luciferase activity was quantified as a readout for transduction efficiency. For this, cells were lysed by incubation with Cell Culture Lysis Reagent (Promega) at room temperature. Lysates were then transferred into white 96-well plates and luciferase activity was measured using a commercially available substrate (Luciferase Assay System, Promega) and a plate luminometer (Orion II Microplate Luminometer running Simplicity Software v4.2, Berthold). For analysis, background signal of untreated cells was subtracted and values normalized to pseudovirus mixed with PBS only. Results are given as serum dilution resulting in 50% pseudovirus neutralization (PVNT50) on cells, calculated by nonlinear regression ([Inhibitor] vs. normalized response–Variable slope) in GraphPad Prism Version 9.1.1. The upper and lower cutoff values of this assay were set at PVNT50 >81,920 and PVNT50 <20, respectively.

Data analysis. Initial data collection was done using Microsoft Excel and Access. Formal data analysis was performed on RStudio (Version 1.2.5001, running R 3.6.1) with the following additional packages: "RColorBrewer", "beeswarm", "gplots", "VennDiagram", all of which were used solely for data depiction and not statistical analysis. Figures were generated in RStudio and then edited for clarity in Inkscape (Inkscape 0.92.4). Only samples for which full data for MULTICOV-AB was available were included in the analysis. Furthermore, only samples from time point 1 were used for all non-longitudinal analyses. For longitudinal analyses, only those participants for whom both T1 and T2 samples were available were included and all participants who were vaccinated prior to T2 were excluded. For analysis of potential cross-protection though endemic coronaviruses, only households with a known index case were used and the index case itself was excluded. Statistical analyses performed are described in the figure legends. For comparison of signal distribution between sample groups, Mann–Whitney-*U* tests were performed using the "wilcox.test" function from R's "stats" library. For correlation analysis, Spearman's rank was calculated using the "cor" function from R's "stats" library. p values < 0.05 were considered to be significant.

Reporting summary. Further information on research design is available in the Nature Research Reporting Summary linked to this article.

Data availability

A short version of the study protocol is available at the German Clinical Trials Register (DRKS, www.drks.de), study ID 00021521. The full study protocol is available from https://www.drks.de/drks_web/navigate.do?navigationId=trial.HTML&TRIAL_ID=DRKS00021521. Individual participant data, including data dictionaries will not be available, since we did not seek parental consent for data sharing.

Code availability

Code will be available upon reasonable request.

Received: 26 August 2021; Accepted: 22 November 2021;
Published online: 10 January 2022

References

1. Sette, A. & Crotty, S. Adaptive immunity to SARS-CoV-2 and COVID-19. *Cell* **184**, 861–880 (2021).
2. Robbiani, D. F. et al. Convergent antibody responses to SARS-CoV-2 in convalescent individuals. *Nature* **584**, 437–442 (2020).
3. Dan, J. M. et al. Immunological memory to SARS-CoV-2 assessed for up to 8 months after infection. *Science* **371**, eabf4063 (2021).
4. Wheatley, A. K. et al. Evolution of immune responses to SARS-CoV-2 in mild-moderate COVID-19. *Nat. Commun.* **12**, 1162 (2021).
5. Seow, J. et al. Longitudinal observation and decline of neutralizing antibody responses in the three months following SARS-CoV-2 infection in humans. *Nat. Microbiol.* **5**, 1598–1607 (2020).
6. Bartsch, Y. C. et al. Humoral signatures of protective and pathological SARS-CoV-2 infection in children. *Nat. Med.* **27**, 454–462 (2021).
7. Bloise S. et al. Serum IgG levels in children 6 months after SARS-CoV-2 infection and comparison with adults. *Eur. J. Pediatr.* **180**, 1–8 (2021).
8. Bavaro, D. F. et al. Anti-spike S1 receptor-binding domain antibodies against SARS-CoV-2 persist several months after infection regardless of disease severity. *J. Med Virol.* **93**, 3158–3164 (2021).
9. Cotugno, N. et al. Virological and immunological features of SARS-CoV-2-infected children who develop neutralizing antibodies. *Cell Rep.* **34**, 108852 (2021).
10. Pierce, C. A. et al. Immune responses to SARS-CoV-2 infection in hospitalized pediatric and adult patients. *Sci. Transl. Med.* **12**, 5487 (2020).
11. Selva, K. J. et al. Systems serology detects functionally distinct coronavirus antibody features in children and elderly. *Nat. Commun.* **12**, 2037 (2021).

12. Weisberg, S. P. et al. Distinct antibody responses to SARS-CoV-2 in children and adults across the COVID-19 clinical spectrum. *Nat. Immunol.* **22**, 25–31 (2021).
13. Yang, H. S. et al. Association of age with SARS-CoV-2 antibody response. *JAMA Netw. Open* **4**, e214302 (2021).
14. Waterfield, T. et al. Seroprevalence of SARS-CoV-2 antibodies in children: a prospective multicentre cohort study. *Arch. Dis. Child* **106**, 680–686 (2021).
15. Gudbjartsson, D. F. et al. Humoral immune response to SARS-CoV-2 in Iceland. *N. Engl. J. Med.* **383**, 1724–1734 (2020).
16. Anderson, E. M. et al. Seasonal human coronavirus antibodies are boosted upon SARS-CoV-2 infection but not associated with protection. *Cell* **184**, 1858–1864.e10 (2021).
17. Sagar, M. et al. Recent endemic coronavirus infection is associated with less-severe COVID-19. *J. Clin. Invest* **131**, e143380 (2021).
18. Khoury D. S. et al. Neutralizing antibody levels are highly predictive of immune protection from symptomatic SARS-CoV-2 infection. *Nat. Med.* **27**, 1205–1211 (2021).
19. Hall, V. J. et al. SARS-CoV-2 infection rates of antibody-positive compared with antibody-negative health-care workers in England: a large, multicentre, prospective cohort study (SIREN). *Lancet* **397**, 1459–1469 (2021).
20. Earle, K. A. et al. Evidence for antibody as a protective correlate for COVID-19 vaccines. *Vaccine* **39**, 4423–4428 (2021).
21. Zimmermann, P. & Curtis, N. Why is COVID-19 less severe in children? A review of the proposed mechanisms underlying the age-related difference in severity of SARS-CoV-2 infections. *Arch. Dis. Child* **106**, 429–439 (2021).
22. Viner, R. M. et al. Susceptibility to SARS-CoV-2 infection among children and adolescents compared with adults: a systematic review and meta-analysis. *JAMA Pediatr.* **175**, 143–156 (2021).
23. Götzinger, F. et al. COVID-19 in children and adolescents in Europe: a multinational, multicentre cohort study. *Lancet Child Adolesc. Heal* **4**, 653–661 (2020).
24. Tönshoff, B. et al. Prevalence of SARS-CoV-2 infection in children and their parents in Southwest Germany. *JAMA Pediatr.* **175**, 586–593 (2021).
25. Feng S. et al. Correlates of protection against symptomatic and asymptomatic SARS-CoV-2 infection. *Nat Med.* 2021. Epub ahead of print.
26. Dowell A. C. et al. Children develop strong and sustained cross-reactive immune responses against Spike protein following SARS-CoV-2 infection, with enhanced recognition of variants of concern. April 29, 2021. medRxiv. (https://doi.org/10.1101/2021.04.12.21255275). Preprint.
27. Hansen, C. B. et al. SARS-CoV-2 antibody responses are correlated to disease severity in COVID-19 convalescent individuals. *J. Immunol.* **206**, 109–117 (2021).
28. Huang, A. T. et al. A systematic review of antibody mediated immunity to coronaviruses: kinetics, correlates of protection, and association with severity. *Nat. Commun.* **11**, 4704 (2020).
29. Guo, L. et al. Cross-reactive antibody against human coronavirus OC43 spike protein correlates with disease severity in COVID-19 patients: a retrospective study. *Emerg. Microbes Infect.* **10**, 664–676 (2021).
30. Stich M. et al. Transmission of severe acute respiratory syndrome coronavirus 2 in households with children, Southwest Germany, May-August 2020. *Emerg Infect Dis.* 2021 25;27. Epub ahead of print.
31. Becker, M. et al. Immune response to SARS-CoV-2 variants of concern in vaccinated individuals. *Nat. Commun.* **12**, 3109 (2021).
32. Becker, M. et al. Exploring beyond clinical routine SARS-CoV-2 serology using MultiCoV-Ab to evaluate endemic coronavirus cross-reactivity. *Nat. Commun.* **12**, 1152 (2021).
33. Planatscher, H. et al. Systematic reference sample generation for multiplexed serological assays. *Sci. Rep.* **3**, 3259 (2013).
34. Jahrsdörfer, B. et al. Characterization of the SARS-CoV-2 neutralization potential of COVID-19–convalescent donors. *J. Immunol.* **206**, 2614–2622 (2021).
35. Wang, L. et al. Ultrapotent antibodies against diverse and highly transmissible SARS-CoV-2 variants. *Science* **373**, eabh1766 (2021). Aug 13.

Acknowledgements

We thank Carmen Blum, Sevil Essig, Ulrike Formentini, Jens Gruber, Andrea Hänsler, Simone Hock, Ann Kathrin Horlacher, Jennifer Juengling, Gudrun Kirsch, Ingrid Knape, Helgard Knauss, Sonja Landthaler, Alexandra Niedermeyer, Bianca Rippberger, Andrea Schuster, Boram Song, Ulrike Tengler, Mareike Walenta and Linda Wolf for assistance with sample processing and patient material storage. We are grateful for the FREEZE and HILDA biobank Freiburg for sample processing, in particular Ali-Riza Kaya, Marco Teller and Dirk Lebrecht. We thank Sandra Steinmann, Yvonne Müller, Vanessa Missel at the University Hospital Ulm, Andrea Evers-Bischoff, Andrea Bevot and the CPCS at the University Hospital Tübingen for organizational support in conducting the study. We thank Steffen Keul for assistance with data processing. This work was financially supported by the State Ministry of Baden-Württemberg for Economic Affairs, Labor and Housing Construction (grant numbers FKZ-3-4332.62-NMI-67 and FKZ-3-4332.62-NMI-68) to NSM, the Ministry of Science, Research and the Arts Baden-Württemberg within the framework of the special funding line for COVID-19 research to the Freiburg, Tübingen, Ulm and Heidelberg centers, the Federal Ministry of Health to the Freiburg study site (PH and RE) and the NIH (R01 AI 050529 and R37 AI 150590 to B.H.H). Additional funding by the German Federal Ministry of Education and Research (BMBF 01GL1746B) to PH. The funders had no role in study design, data collection, data analysis or the decision to publish. The funding agencies of the study, the Ministry of Science of the State of Baden-Württemberg, the NIH, and the Ministry for Economic Affairs, Labor and Housing Construction of the State of Baden-Württemberg had no role in study design, data collection, data analysis, interpretation of data, writing of the report, and in the decision to submit the paper for publication.

Author contributions

R.E., H.R., A.J., D.F., P.H., A.R.F. and K.M.D. conceived the study. H.R., A.D., R.E., A.J., P.H., A.R.F., K.M.D. and N.S.M. designed the experiments. R.E., H.R., A.J., B.H.H., P.H., A.R.F., K.M.D. and N.S.M. procured funding. A.D., M.B., D.J., A.S., R.G., J.M., J.M., A.H., C.L., T.G., A.D., D.H., H.H., A.P., S.H., T.I., T.S., W.L. and H.-J.G. performed experiments. R.E., H.R., A.J., D.F., M.Z., S.B., L.F., P.F., A.H., J.R., E.-M.J., C.E., M.W., T.G. and M.R. collected samples or organized their collection. B.J., H.S., M.S., B.T., G.F.H. and B.M. supported the sample collection and provided key resources. P.K., B.T. and U.R. produced the R.B.D. mutants. H.R., A.J., A.D., M.B., D.F., A.H., A.D., K.K., S.W., E.-M.J., A.P., T.I., T.S., H.-J.G., M.W., C.E., K.M.D. and M.R. curated the data. M.B. and A.D. performed the data analysis. A.D. and M.B. generated the figures. A.D., H.R., A.J. and R.E. wrote the first draft of the manuscript. All authors approved the final version of the manuscript. All authors confirm that they had full access to all the data in the study and accept responsibility to submit for publication.

Funding

Open Access funding enabled and organized by Projekt DEAL.

Competing interests

N.S.M. was a speaker at Luminex user meetings in the past. The Natural and Medical Sciences Institute at the University of Tübingen is involved in applied research projects as a fee for services with Luminex. The other authors report no competing interests.

Additional information

Supplementary information The online version contains supplementary material available at https://doi.org/10.1038/s41467-021-27595-9.

Correspondence and requests for materials should be addressed to Roland Elling.

Peer review information *Nature Communications* thanks Karin Nielsen and the other, anonymous, reviewer(s) for their contribution to the peer review of this work. Peer reviewer reports are available.

Reprints and permission information is available at http://www.nature.com/reprints

Publisher's note Springer Nature remains neutral with regard to jurisdictional claims in published maps and institutional affiliations.

[1]University Children's Hospital Tübingen, Tübingen, Germany. [2]NMI Natural and Medical Sciences Institute at the University of Tübingen, Reutlingen, Germany. [3]Institute of Molecular Virology, Ulm University Medical Center, Ulm, Germany. [4]Department of Pediatrics and Adolescent Medicine, Ulm University Medical Center, Ulm University, Ulm, Germany. [5]Center for Pediatrics and Adolescent Medicine, Medical Center Freiburg, Germany and Faculty of Medicine, University of Freiburg, Freiburg, Germany. [6]Institute for Medical Virology and Epidemiology of Viral Diseases, University Hospital Tübingen, Tübingen, Germany. [7]Institute of Virology, Ulm University Medical Center, Ulm, Germany. [8]Institute of Virology, Medical Center Freiburg, Germany and Faculty of Medicine, University of Freiburg, Freiburg, Germany. [9]Institute of Medical Biometry and Statistics, Medical Center Freiburg, Germany and Faculty of Medicine, University of Freiburg, Freiburg, Germany. [10]Department of Pediatrics I, University Children's Hospital Heidelberg, Heidelberg, Germany. [11]Department of Infectious Diseases, Virology, Heidelberg University Hospital, Heidelberg, Germany. [12]Institute of Transfusion Medicine, Ulm University, Ulm, Germany. [13]Institute for Clinical Transfusion Medicine and Immunogenetics, Ulm, Germany. [14]German Red Cross Blood Transfusion Service, Baden-Württemberg-Hessen, Germany. [15]Institute for Clinical Chemistry and Pathobiochemistry, University Hospital Tübingen, Tübingen, Germany. [16]Institute of Clinical Chemistry, Ulm University, Ulm, Germany. [17]Center for Pediatric Clinical Studies, University Hospital Tübingen, Tübingen, Germany. [18]Department of Microbiology and Department of Medicine, University of Pennsylvania, Philadelphia, USA. [19]Department of Rheumatology and Clinical Immunology, Medical Center Freiburg, Germany and Faculty of Medicine, University of Freiburg, Freiburg, Germany. [20]Institute for Immunodeficiency, Medical Center Freiburg, Germany and Faculty of Medicine, University of Freiburg, Freiburg, Germany. [21]These authors contributed equally: Hanna Renk, Alex Dulovic, Alina Seidel. [22]These authors jointly supervised this work: Ales Janda, Roland Elling. ✉email: roland.elling@uniklinik-freiburg.de

Supplementary Information – Robust and durable serological response following pediatric SARS-CoV-2 infection

Hanna Renk MD[1*], Alex Dulovic Dr.rer.nat[2*], Alina Seidel M.Sc[3*], Matthias Becker M.Sc[2], Dorit Fabricius MD[4], Maria Zernickel M.Sc[4], Daniel Junker M.Sc[2], Rüdiger Groß M.Sc[3], Janis A. Müller Dr.rer.nat[4], Alexander Hilger M.Sc[5], Sebastian F.N. Bode MD[4], Linus Fritsch[5], Pauline Frieh[5], Anneke Haddad DPhil[5], Tessa Görne[5], Jonathan Remppis MD[1], Tina Ganzemueller MD[7], Andrea Dietz Dr.biol.hum[6], Daniela Huzly MD[8], Hartmut Hengel MD[8], Klaus Kaier PhD[9], Susanne Weber Dipl.Math[9], Eva-Maria Jacobsen Dr.rer.physiol[4], Philipp D. Kaiser Dr.rer.nat[2], Bjoern Traenkle Dr.rer.nat[2], Ulrich Rothbauer Dr.rer.nat[2], Maximilian Stich MD[10], Burkhard Tönshoff MD[10], Georg F. Hoffmann MD[10], Barbara Müller PhD[11], Carolin Ludwig[12,13,14], Bernd Jahrsdörfer MD[12,13,14], Hubert Schrezenmeier MD[12,13,14], Andreas Peter MD[15], Sebastian Hörber MD[15], Thomas Iftner PhD[7], Jan Münch PhD[3], Thomas Stamminger MD[6], Hans-Jürgen Groß MD[16], Martin Wolkewitz PhD[9], Corinna Engel Dr.biol.hum[1,17], Marta Rizzi MD[18], Weimin Liu MD[19], Beatrice H. Hahn MD[19], Philipp Henneke MD[5,20], Axel R. Franz MD[1,17], Klaus-Michael Debatin MD[4], Nicole Schneiderhan-Marra Dr.rer.nat[2], Ales Janda MD[4,#] and Roland Elling MD[5,20,#,†]

1 – University Children's Hospital Tübingen, Tübingen, Germany

2 – NMI Natural and Medical Sciences Institute at the University of Tübingen, Reutlingen, Germany

3 – Institute of Molecular Virology, Ulm University Medical Center, Ulm University, Ulm, Germany

4 – Department of Pediatrics and Adolescent Medicine, Ulm University Medical Center, Ulm University, Ulm, Germany

5 – Center for Pediatrics and Adolescent Medicine, Medical Center Freiburg, Germany and Faculty of Medicine, University of Freiburg, Freiburg, Germany

6 – Institute of Virology, Ulm University Medical Center, Ulm, Germany

7 – Institute for Medical Virology and Epidemiology of Viral Diseases, University Hospital Tübingen, Tübingen, Germany

8 – Institute of Virology, Medical Center Freiburg, Germany and Faculty of Medicine, University of Freiburg, Freiburg, Germany

9 – Institute of Medical Biometry and Statistics, Medical Center Freiburg, Germany and Faculty of Medicine, University of Freiburg, Freiburg, Germany

10 – Department of Pediatrics I, University Children's Hospital Heidelberg, Heidelberg, Germany

11 - Department of Infectious Diseases, Virology, Heidelberg University Hospital, Heidelberg, Germany

12 – Department of Transfusion Medicine, Ulm University, Ulm, Germany

13 – Institute for Clinical Transfusion Medicine and Immunogenetics, Ulm, Germany

14– German Red Cross Blood Transfusion Service, Baden-Württemberg-Hessen, Germany

15 – Institute for Clinical Chemistry and Pathobiochemistry, University Hospital Tübingen, Tübingen, Germany

16 – Institute of Clinical Chemistry, Ulm University, Ulm, Germany

17 – Center for Pediatric Clinical Studies, University Hospital Tübingen, Tübingen, Germany

2

18 - Department of Rheumatology and Clinical Immunology, Medical Center Freiburg, Germany and Faculty of Medicine, University of Freiburg, Freiburg, Germany

19 - Department of Microbiology and Department of Medicine, University of Pennsylvania, Philadelphia, USA

20 – Institute for Immunodeficiency, Medical Center Freiburg, Germany and Faculty of Medicine, University of Freiburg, Freiburg, Germany

*These authors contributed equally

#These authors jointly supervised this work

†indicates corresponding author

Supplementary Figures

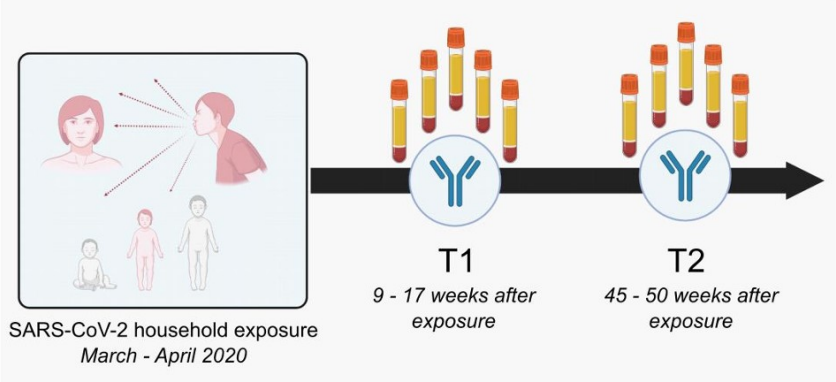

Figure S1: **Overview of the time points within the study population.** Illustration of study design, from exposure to study participation time points. Times shown are the IQR for each time point. T1 – Time point 1, T2 – Time point 2.

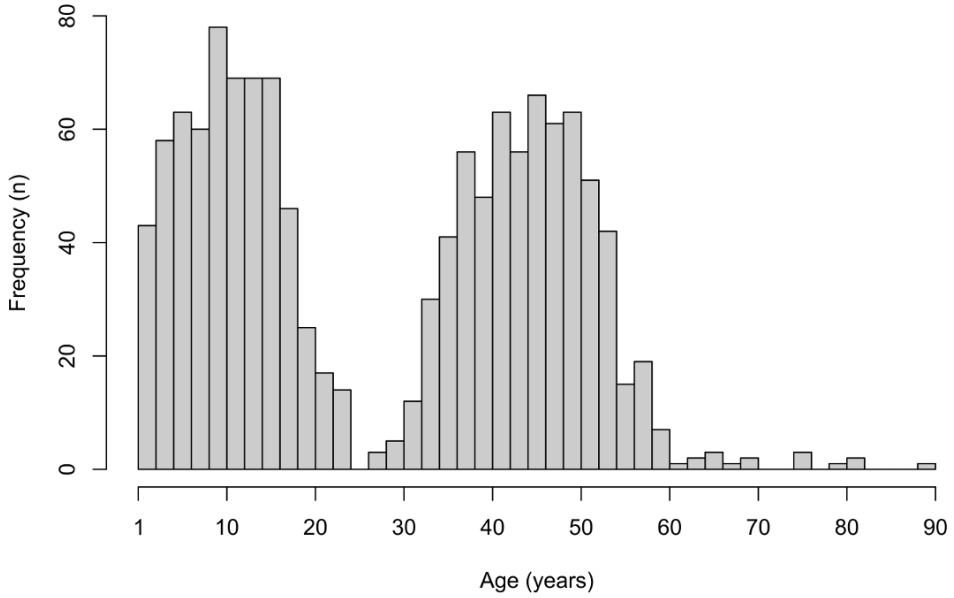

Figure S2 – **Study population age distribution**. Histogram showing age distribution within the study population at T1 (n=1265).

5

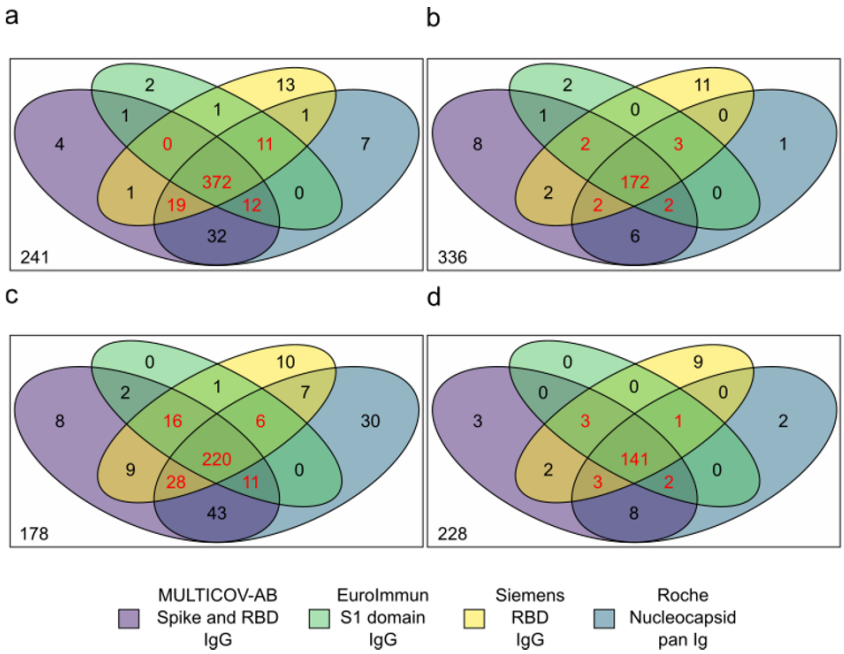

Figure S4 – **Comparative performance of the different serology assays used in this study**. 4-way Venn diagrams showing how each assay classified samples as being seropositive for T1 (a and b) and T2 (c and d) for adults (a and c) and children (b and d). Samples were classified as being positive if three or more assays classified them as being positive (shown in red). Negative samples for all assays are indicated in the bottom left corner of the boxes. Assays are color-coded as defined by the key including the manufacturer or name of the assay, which antigen it uses as a target and which Ig-isotype it measures. RBD – receptor binding domain.

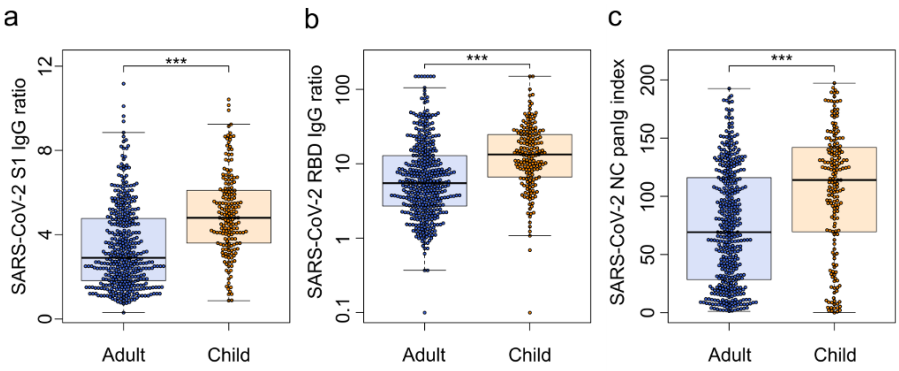

Figure S5 – **Children have higher antibody responses than adults**. Seropositive children (orange, n=181) had significantly higher IgG antibody titres against S1 (a, $p=1.52x10^{-18}$), receptor binding domain (RBD) (b, $p=7.05x10^{-14}$) and nucleocapsid (NC) (c, $p=7.55x10^{-10}$) than seropositive adults (blue, n=414) as determined using the commercial EuroImmun (a), Siemens (b) and Roche (c) assays at T1. The Ig isotype measured with each assay is indicated on the axis. Seropositive adults and children were identified using the multi-assay definition of seropositivity explained in the Method section. Box and whisker plots with the box representing the median, 25th and 75th percentiles, while whiskers show the largest and smallest non-outlier values. Outliers were identified using upper/lower quartile ± 1·5 times IQR. Statistical significance was calculated by Mann-Whitney-U (two-sided) with *** indicating a p-value <0·001.

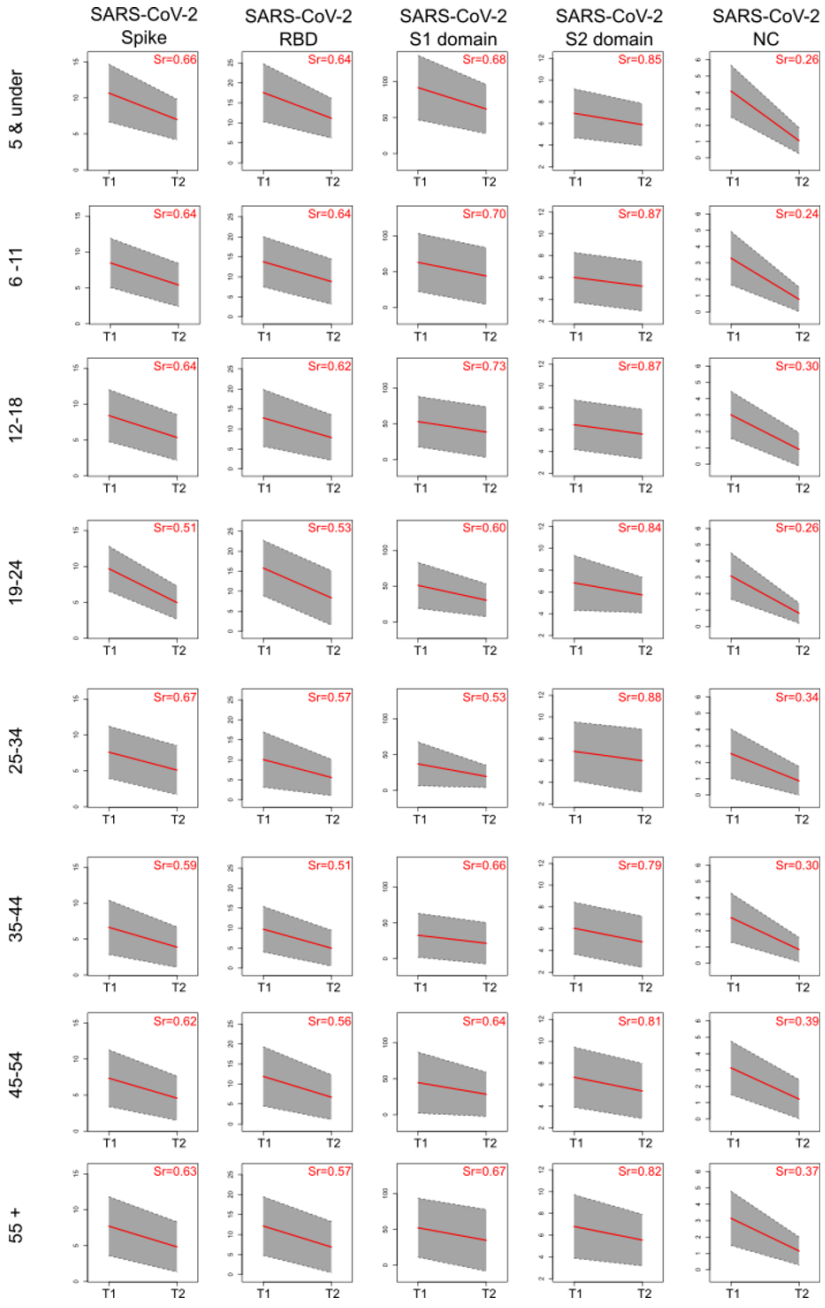
SARS-CoV-2 Spike
SARS-CoV-2 RBD
SARS-CoV-2 S1 domain
SARS-CoV-2 S2 domain
SARS-CoV-2 NC
5 & under
6 -11
12-18
19-24
25-34
35-44
45-54
55 +
Sr=0.66
Sr=0.64
Sr=0.68
Sr=0.85
Sr=0.26
Sr=0.64
Sr=0.64
Sr=0.70
Sr=0.87
Sr=0.24
Sr=0.64
Sr=0.62
Sr=0.73
Sr=0.87
Sr=0.30
Sr=0.51
Sr=0.53
Sr=0.60
Sr=0.84
Sr=0.26
Sr=0.67
Sr=0.57
Sr=0.53
Sr=0.88
Sr=0.34
Sr=0.59
Sr=0.51
Sr=0.66
Sr=0.79
Sr=0.30
Sr=0.62
Sr=0.56
Sr=0.64
Sr=0.81
Sr=0.39
Sr=0.63
Sr=0.57
Sr=0.67
Sr=0.82
Sr=0.37
T1
T2

9

Figure S6 – **Antibody decay occurs at the same rate in adults and children.** Longitudinal comparison of T1 and T2 samples using MULTICOV-AB to determine the rate of antibody decay. The IgG antibodies against spike trimer, receptor binding domain (RBD), S1 domain, S2 domain and nucleocapsid (NC) of SARS-CoV-2 are shown. Samples are separated into distinct age groups: under 5 years old (n=28), 6-11 (n=61), 12-18 (n=68), 19-24 (n=14), 25-34 (n=21), 35-44 (n=117), 45-54 (n=148) and over 55 years old (n=31). All y-axis show the normalized MFI. Red lines indicate mean rates of decrease; grey boxes indicate ±1 standard deviation. Sr indicates proportion of signal remaining, calculated as the ratio of the mean MFI at T2 compared to the mean MFI at T1. MFI – median fluorescence intensity.

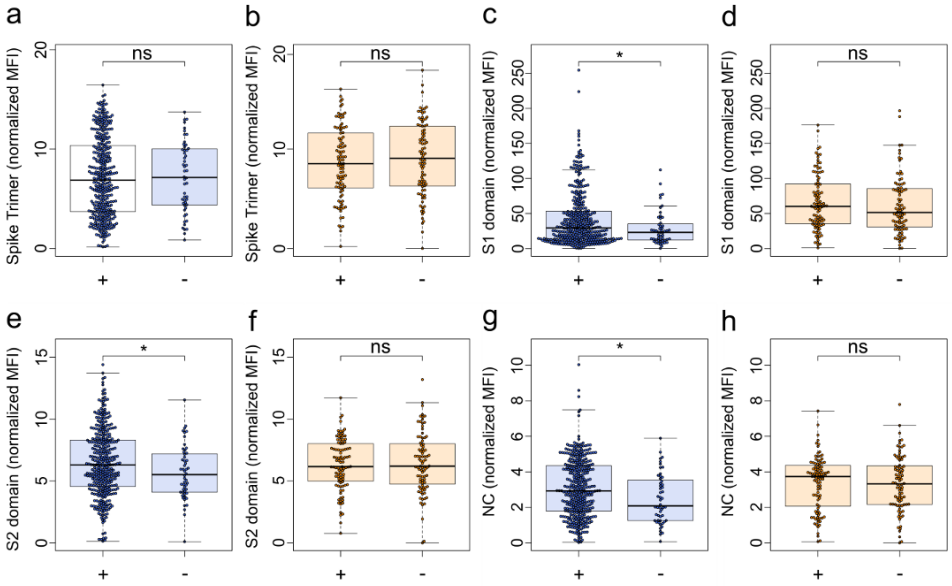

Figure S7 – **There is no difference in antibody response between asymptomatic and symptomatic infections in children**. Box and whisker plots with the box representing the median, 25th and 75th percentiles, while whiskers show the largest and smallest non-outlier values. Outliers were identified using upper/lower quartile ±1·5 times IQR. Statistical significance was calculated by Mann-Whitney-U (two-sided) with * indicating a p-value <0·05. and ns indicating a non-significant p-value >0·05. "+" indicates a symptomatic infection while "-" indicates an asymptomatic infection. There were no significant differences between symptomatic and asymptomatic seropositive children (orange, n=185) in terms of antibody response for the spike trimer (b, p=0·43), S1 domain (d, p=0·34), S2 domain (f, p=0·87) or Nucleocapsid (NC) (h, p=0·78). Symptomatic and asymptomatic seropositive adults (blue, n=414) showed no significant difference for the spike trimer (a, p=0·94), although there were small significant differences in the S1 domain (c, p=0·03) and S2 domain (e, p=0·05) and NC (g, p=0·01). MFI – median fluorescence intensity.

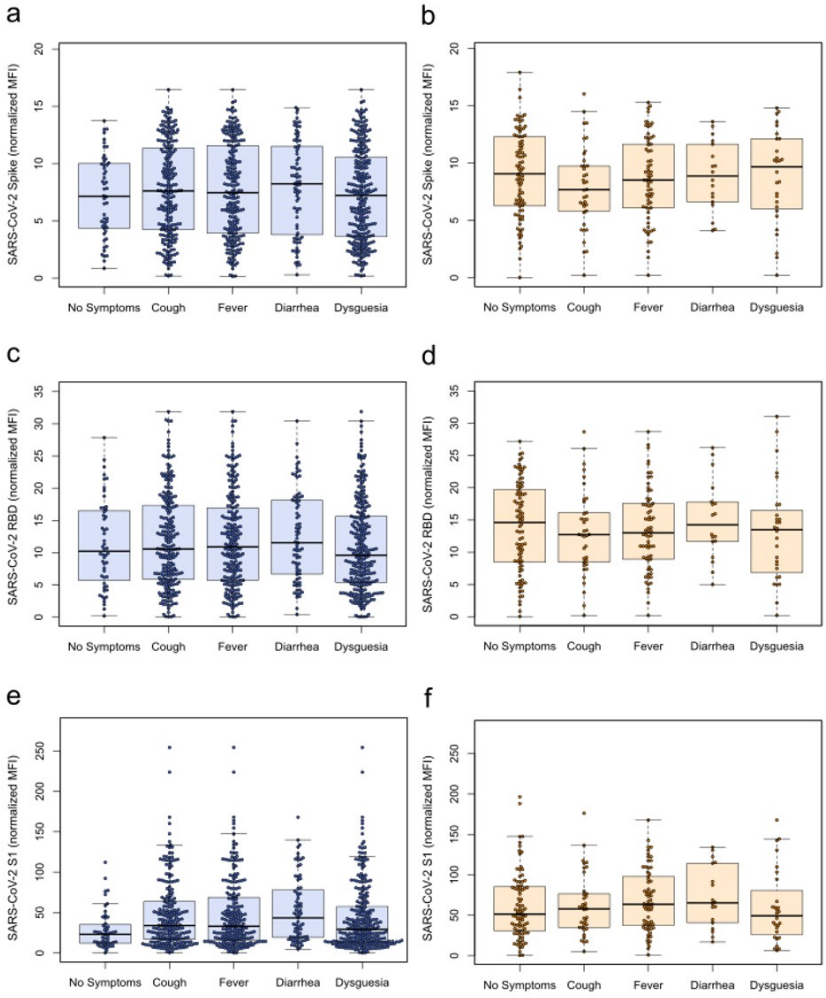

Figure S8 – **Symptoms do not moderate antibody response amongst seropositive individuals after mild COVID-19**. Box and whisker plots with the box representing the median, 25th and 75th percentiles, while whiskers show the largest and smallest non-outlier values. Outliers were identified using upper/lower quartile ±1·5 times IQR. Within the seropositive subgroups, neither adults (blue, a, c, e) nor children (orange, b, d, f) showed any difference in response based on presence of

symptoms for either the spike trimer (a and b), receptor binding domain (RBD) (c and d) or S1 domain (e and f) of SARS-CoV-2. Symptom group sizes: no symptoms – adults n=36, children n=83, cough – adults n=221, children n=37, fever – adults n=217, children n=66, diarrhea – adults n=75, children n=18, dysgeusia – adults n=266, children n=28. MFI – median fluorescence intensity.

a

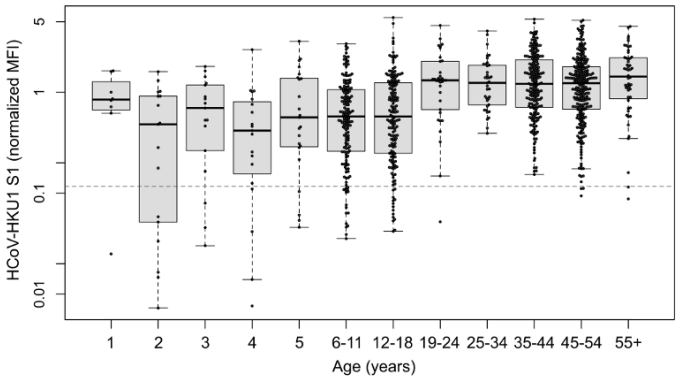
HCoV-HKU1 S1 (normalized MFI)
0.01
0.1
1
5
1
2
3
4
5
6-11
12-18
19-24
25-34
35-44
45-54
55+
Age (years)

b

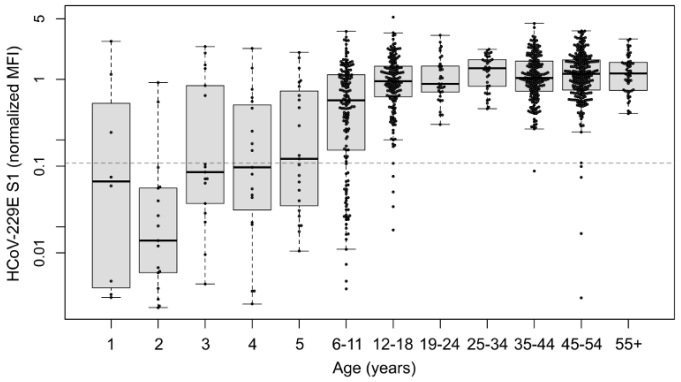
HCoV-229E S1 (normalized MFI)
0.01
0.1
1
5
1
2
3
4
5
6-11
12-18
19-24
25-34
35-44
45-54
55+
Age (years)

c

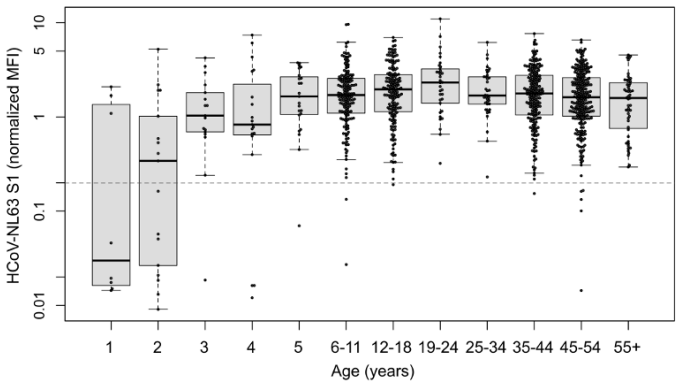
HCoV-NL63 S1 (normalized MFI)
0.01
0.1
1
5
10
1
2
3
4
5
6-11
12-18
19-24
25-34
35-44
45-54
55+
Age (years)

14

Figure S9 – **Initial HCoV infection often occurs during the first five years of life**. Box and whisker plots with the box representing the median, 25th and 75th percentiles, while whiskers show the largest and smallest non-outlier values. Outliers were identified using upper/lower quartile ±1·5 times IQR. Single ages from 1 to 5 are shown (1 – n=8, 2 – n=17, 3 – n=17, 4 – n=19, 5 – n=23) with age then grouped into: 6-11 (n=160), 12-18 (n=163), 19-24 (n=34), 25-34 (n=37), 35-44 (n=195), 45-54 (n=346) and over 55 years olds (n=52). For all HCoVs (a – HKU1, b – 229E, c – NL63), the majority of naïve samples are children. Dashed line indicates one-tenth of the mean response of all samples. All samples below the dashed line are considered to be naïve. HCoV – human endemic Coronavirus, MFI – median fluorescence intensity.

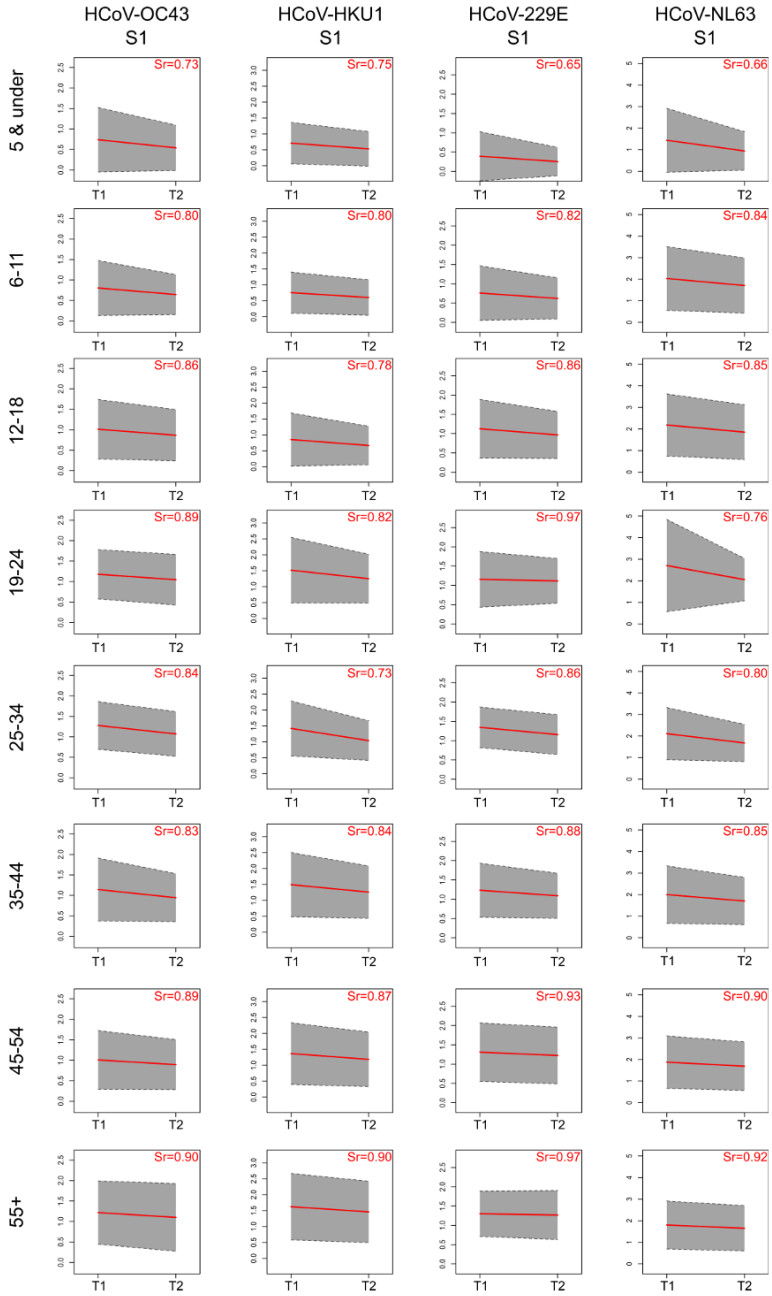
HCoV-OC43
S1
HCoV-HKU1
S1
HCoV-229E
S1
HCoV-NL63
S1
5 & under
6-11
12-18
19-24
25-34
35-44
45-54
55+
Sr=0.73
Sr=0.75
Sr=0.65
Sr=0.66
Sr=0.80
Sr=0.80
Sr=0.82
Sr=0.84
Sr=0.86
Sr=0.78
Sr=0.86
Sr=0.85
Sr=0.89
Sr=0.82
Sr=0.97
Sr=0.76
Sr=0.84
Sr=0.73
Sr=0.86
Sr=0.80
Sr=0.83
Sr=0.84
Sr=0.88
Sr=0.85
Sr=0.89
Sr=0.87
Sr=0.93
Sr=0.90
Sr=0.90
Sr=0.90
Sr=0.97
Sr=0.92
T1
T2

16

Figure S10 – **Children seroreverted faster for HCoVs than adults**. Longitudinal comparison of T1 and T2 samples using MULTICOV-AB to determine the rate of seroreversion. The S1 domain of HCoV-OC43, HCoV-HKU1, HCoV-229E and HCoV-NL63 are shown. Samples are separated into distinct age groups: five years old and under (n=84), 6-11 (n=160), 12-18 (n=162), 19-24 (n=32), 25-34 (n=36), 35-44 (n=182), 45-54 (n=228) and over 55 years old (n=48). Red lines indicate mean rate of decrease; grey boxes indicate ±1 standard deviation. Sr indicates the proportion of signal remaining, calculated as the ratio of the mean MFI at T2 compared to the mean MFI at T1. HCoV – human endemic Coronavirus, MFI – median fluorescence intensity.

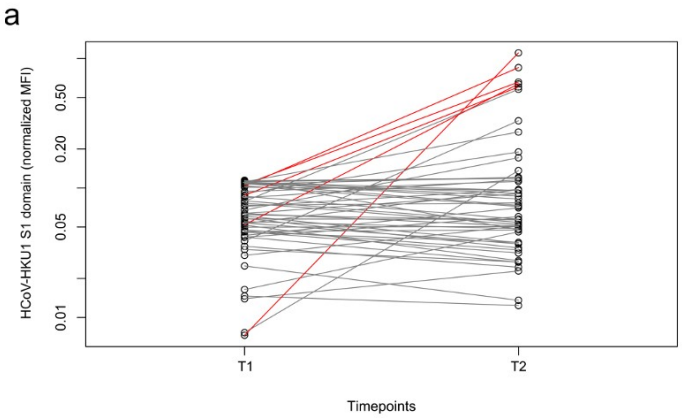
a
HCoV-HKU1 S1 domain (normalized MFI)
0.01
0.05
0.20
0.50
T1
T2
Timepoints

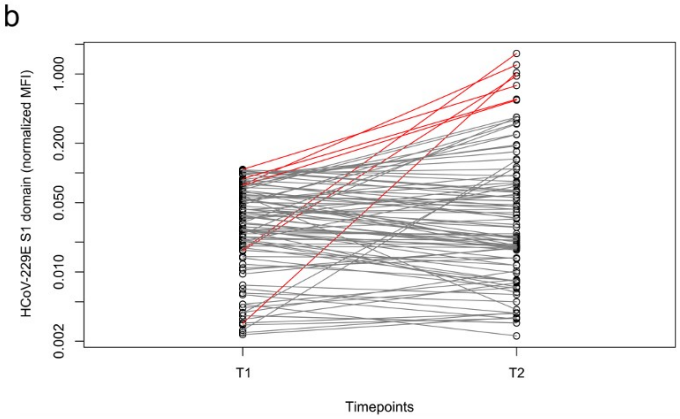
b
HCoV-229E S1 domain (normalized MFI)
0.002
0.010
0.050
0.200
1.000
T1
T2
Timepoints

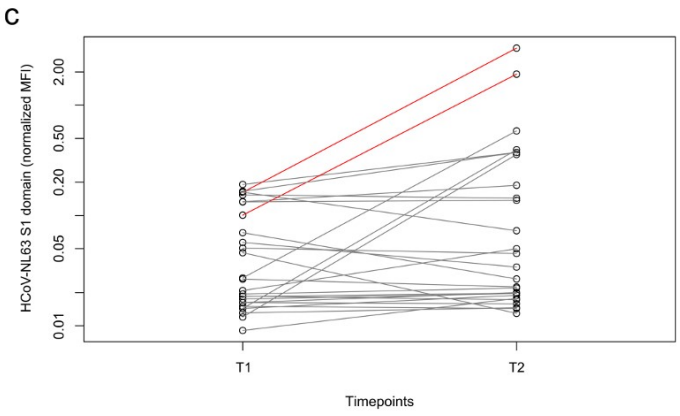
c
HCoV-NL63 S1 domain (normalized MFI)
0.01
0.05
0.20
0.50
2.00
T1
T2
Timepoints

18

Figure S11 – **Naïve samples are present within the study, although endemic coronavirus infections persisted during the SARS-CoV-2 pandemic**. Line graphs showing longitudinal antibody response from T1 to T2 for samples defined as naïve at T1. Individuals who remain naïve are shown in grey, individuals who seroconvert between T1 and by T2 are shown in red. Not all individuals who show increased HCoV antibody levels at T2 compared to T1 are considered to have been infected, as some remain within the negative range for the assay at T2. Normalized MFI is shown on a logscale for clarity. Although there is variation in the number of naïve samples between the different HCoVs (a – HKU1, b – 229E, c – NL63), new HCoV infections are seen across all HCoVs. HCoV – human endemic Coronavirus, MFI – median fluorescence intensity.

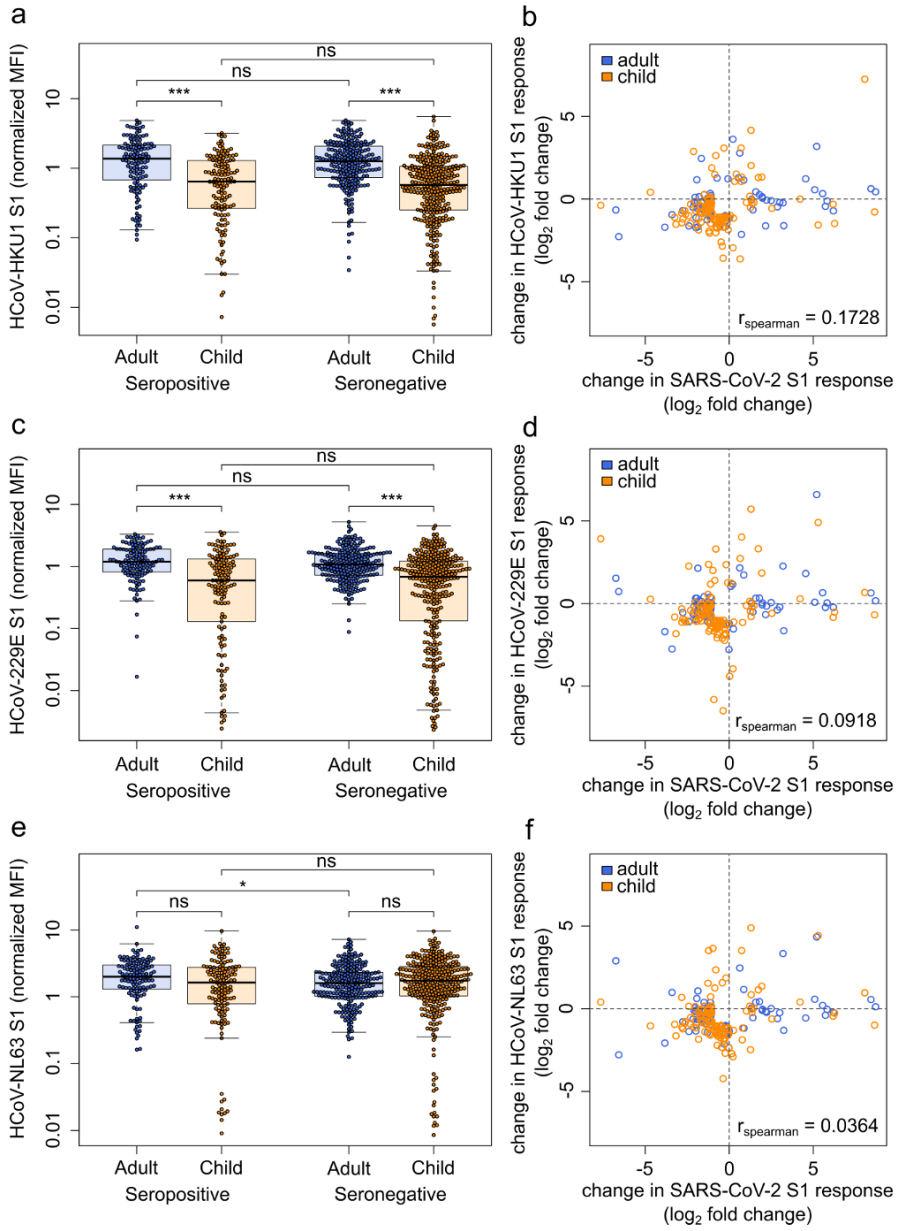
a
HCoV-HKU1 S1 (normalized MFI)
0.01
0.1
1
10
ns
ns
***
***
Adult
Child
Adult
Child
Seropositive
Seronegative
b
change in HCoV-HKU1 S1 response
(log2 fold change)
adult
child
rspearman = 0.1728
-5
0
5
change in SARS-CoV-2 S1 response
(log2 fold change)
c
HCoV-229E S1 (normalized MFI)
d
change in HCoV-229E S1 response
(log2 fold change)
rspearman = 0.0918
e
HCoV-NL63 S1 (normalized MFI)
*
f
change in HCoV-NL63 S1 response
(log2 fold change)
rspearman = 0.0364

Figure S12 – **HCoVs offer no cross protection towards SARS-CoV-2, nor do they show a boost-back antibody response following SARS-CoV-2 infection**. Samples from households with a known index case were examined with MULTICOV-AB to determine whether the antibody response to endemic coronaviruses (HCoV) provides any protection against SARS-CoV-2. (a, c and e) Box and whisker plots demonstrating no significant difference between SARS-CoV-2 seropositive and seronegative adults (blue, n=440) or children (orange, n=436) in terms of HCoV-HKU1 (a, adult p=0·67, child p=0·47) or HCoV-229E (c, adult p=0·14, child p=0·99). For HCoV-NL63, there was a small significant difference for adults only (e, adults p=0·01, children p=0·35). Boxes represent the median, 25th and 75th percentiles, and whiskers show the largest and smallest non-outlier values. Outliers were identified using upper/lower quartile ± 1·5 times IQR. Statistical significance was calculated by Mann-Whitney-U (two-sided) with *** indicating a p-value <0·001, * indicating a p-value <0·05 and ns indicating a p-value >0·05 (b, d and f). When comparing paired samples longitudinally within the SARS-CoV-2 seropositive subgroup, there was no association between change in SARS-CoV-2 antibody level and change in HCoV antibody level for HCoV-HKU1 (b), HCoV-229E (d) or HCoV-NL63 (f) and in either adults (b - n=79, d – n=74, f – n=80) or children (b - n=117, d – n=114, f – n=118). Change in response is presented as log2-fold change from T1 to T2 and only samples with a log2-fold change > 1 or < -1 are shown. Spearman's rank was used to calculate ordinal associations between the changes in HCoV antibody level and change in SARS-CoV-2 antibody level. MFI – median fluorescence intensity.

Supplementary Tables

Table S1 – **Comparative seroprevalence between different assays used in the study**

Assay	Seropositive	Seronegative	Total	% of Seropositive
EuroImmun S1 IgG	991	1245	2236	44.3
Roche Elecsys N pan Ig	1149	1087	2236	51·4
Siemens RBD IgG	1067	1169	2236	47·7
MULTICOV S and RBD IgG	1142	1094	2236	51·1

Only samples that were measured with all four assays are considered. For each assay, the manufacturer or name of the assay is stated, as well as the target antigen and Ig-isotype detected. N – Nucleocapsid, RBD – receptor binding domain, S – spike protein.

Table S2 **– Symptom frequency and diagnostic performance in children under 18**

		Age group						All children	
		Under 5		6 to 11		12 to 18			
Symptom	Present or Absent	n (%)	Seropositive (PPV, 95% CI)	n (%)	Seropositive (PPV, 95% CI)	n (%)	Seropositive (PPV, 95% CI)	n (%)	Seropositive (PPV, 95% CI)
Fever	Present	37 (28·03)	17 (0·46, 0·33-0·59)	46 (21·70)	28 (0·61, 0·48-0·72)	28 (13·40)	21 (0·75, 0·57-0·87)	111 (20·07)	66 (0·59, 0·51-0·67)
	Absent	95 (71·97)	23 (0·24, 0·19-0·30)	166 (78·30)	45 (0·27, 0·24-0·31)	181 (86·60)	53 (0·29, 0·27-0·32)	442 (79·93)	121 (0·27, 0·25-0·29)
Cough	Present	28 (21·21)	9 (0·32, 0·19-0·48)	43 (20·28)	14 (0·33, 0·21-0·46)	28 (13·40)	14 (0·50, 0·34-0·66)	99 (17·90)	37 (0·37, 0·29-0·46)
	Absent	104 (78·79)	31 (0·30, 0·25-0·35)	169 (79·72)	59 (0·35, 0·31-0·38)	181 (86·60)	60 (0·33, 0·30-0·36)	454 (82·10)	150 (0·33, 0·31-0·35)
Diarrhea	Present	8 (6·06)	3 (0·38, 0·13-0·71)	17 (8·02)	11 (0·65, 0·41-0·83)	8 (3·83)	4 (0·50, 0·20-0·80)	33 (5·97)	18 (0·55, 0·38-0·70)
	Absent	124 (93·94)	37 (0·30, 0·27-0·32)	195 (91·98)	62 (0·32, 0·30-0·34)	201 (96·17)	70 (0·35, 0·33-0·36)	520 (94·03)	169 (0·33, 0·31-0·34)
Dysguesia	Present	1 (0·76)	1 (1·00, n/a)	7 (3·30)	6 (0·86, 0·42-0·98)	24 (11·48)	21 (0·88, 0·68-0·96)	32 (5·79)	28 (0·88, 0·71-0·95)
	Absent	131 (99·24)	39 (0·30, 0·29-0·30)	205 (69·70)	67 (0·33, 0·32-0·34)	185 (88·52)	53 (0·29, 0·27-0·31)	521 (94·21)	159 (0·31, 0·30-0·31)

The frequency of each symptom within the study population, shown number of individuals (n, also as %) either with (present) or without (absent) this symptom, and the number of individuals (n, also as %) within these groups who were seropositive for SARS-CoV-

2. Children are split into three groups: under 5-year olds (n=132), 6- to 11-year olds (n=212) and 12- to 18-year olds (n=209). Positive Predictive Value (PPV) for seropositivity in the presence or absence of each symptom, 95% Confidence Intervals (CI) are standard logit confidence intervals[1].

Table S3 – **List of antigens used in MULTICOV-AB**

Disease	Antigen	Manufacturer	Cat. No.
SARS-CoV-2	Spike Trimer	NMI	-
SARS-CoV-2	RBD	NMI	-
SARS-CoV-2	S1 domain	NMI	-
SARS-CoV-2	S2 domain	Sino	40590
SARS-CoV-2	Nucleocapsid	Aalto	6404-b
SARS-CoV-2	Nucleocapsid N-terminal domain	NMI	-
SARS-CoV-2	RBD alpha variant	NMI	-
SARS-CoV-2	RBD beta variant	NMI	-
HCoV-OC43	S1 domain	NMI	-
HCoV-OC43	Nucleocapsid	NMI	-
HCoV-OC43	Nucleocapsid N-terminal domain	NMI	-
HCoV-HKU1	S1 domain	NMI	-
HCoV-HKU1	Nucleocapsid	NMI	-
HCoV-HKU1	Nucleocapsid N-terminal domain	NMI	-
HCoV-NL63	S1 domain	NMI	-
HCoV-NL63	Nucleocapsid	NMI	-
HCoV-NL63	Nucleocapsid N-terminal domain	NMI	-
HCoV-229E	S1 domain	NMI	-
HCoV-229E	Nucleocapsid	NMI	-
HCoV-229E	Nucleocapsid N-terminal domain	NMI	-

List of antigens included in MULTICOV-AB in this study, including information about their manufacturer, and if available, their category number. Full information on the NMI produced antigens can be found at[2,3].

Supplementary References

1. Mercaldo N.D, Lau K.F and Zhou X.H. Confidence intervals for predictive values with an emphasis to case-control studies. Statist Med 2007;26:2170-2183.
2. Becker M, Dulovic A, Junker D, et al. Immune response to SARS-CoV-2 variants of concern in vaccinated individuals. Nat Commun 2021;12(1):3109.
3. Becker M, Strengert M, Junker D, et al. Exploring beyond clinical routine SARS-CoV-2 serology using MultiCoV-Ab to evaluate endemic coronavirus cross-reactivity. Nat Commun 2021;12(1):1152.

Appendix VI: Antibody Binding and Angiotensin-Converting Enzyme 2 Binding Inhibition Is Significantly Reduced for Both the BA.1 and BA.2 Omicron Variants

Junker D*, Becker M*, Wagner TR*, Kaiser PD, Maier S, Grimm TM, Griesbaum J, Marsall P, Gruber J, Traenkle B, Heinzel C, Pinilla YT, Held J, Fendel R, Kreidenweiss A, Nelde A, Maringer Y, Schroeder S, Walz JS, Althaus K, Uzun G, Mikus M, Bakchoul T, Schenke-Layland K, Bunk S, Haeberle H, Göpel S, Bitzer M, Renk H, Remppis J, Engel C, Franz AR, Harries M, Kessel B, Lange B, Strengert M, Krause G, Zeck A, Rothbauer U, Dulovic A, Schneiderhan-Marra N.

Clinical Infectious Diseases. 2023. 76(3):e240-e249
https://doi.org/10.1093/cid/ciac498

Clinical Infectious Diseases
MAJOR ARTICLE

Antibody Binding and Angiotensin-Converting Enzyme 2 Binding Inhibition Is Significantly Reduced for Both the BA.1 and BA.2 Omicron Variants

Daniel Junker,[1,a] Matthias Becker,[1,a] Teresa R. Wagner,[1,2,a] Philipp D. Kaiser,[1] Sandra Maier,[1] Tanja M. Grimm,[1] Johanna Griesbaum,[1] Patrick Marsall,[1] Jens Gruber,[1] Bjoern Traenkle,[1] Constanze Heinzel,[3] Yudi T. Pinilla,[3] Jana Held,[3] Rolf Fendel,[3,4,5] Andrea Kreidenweiss,[3,4,5] Annika Nelde,[6,7,8,9] Yacine Maringer,[6,7,8,9] Sarah Schroeder,[6,8,10] Juliane S. Walz,[6,7,8,9] Karina Althaus,[11,12] Gunalp Uzun,[11] Marco Mikus,[11] Tamam Bakchoul,[11,12] Katja Schenke-Layland,[1,8,13,14] Stefanie Bunk,[15] Helene Haeberle,[16] Siri Göpel,[4,15] Michael Bitzer,[15,17] Hanna Renk,[18] Jonathan Remppis,[18] Corinna Engel,[18,19] Axel R. Franz,[18,19] Manuela Harries,[20] Barbora Kessel,[20] Berit Lange,[20] Monika Strengert,[20,21] Gerard Krause,[20,21] Anne Zeck,[1] Ulrich Rothbauer,[1,2] Alex Dulovic,[1,b,©] and Nicole Schneiderhan-Marra[1,b]

[1]NMI Natural and Medical Sciences Institute at the University of Tuebingen, Reutlingen, Germany; [2]Pharmaceutical Biotechnology, University of Tuebingen, Tuebingen, Germany; [3]Institute of Tropical Medicine, University Hospital Tuebingen, Tuebingen, Germany; [4]German Center for Infection Research, partner site Tuebingen, Tuebingen, Germany; [5]Centre de Recherches Médicales de Lambaréné, Lambaréné, Gabon; [6]Department of Peptide-Based Immunotherapy, University of Tuebingen and University Hospital Tuebingen, Tuebingen, Germany; [7]Department of Internal Medicine, Clinical Collaboration Unit Translational Immunology, German Cancer Consortium, University Hospital Tuebingen, Tuebingen, Germany; [8]Department of Immunology, Institute for Cell Biology, University of Tuebingen, Tuebingen, Germany; [9]Cluster of Excellence iFIT (EXC2180) "Image-Guided and Functionally Instructed Tumor Therapies," University of Tuebingen, Tuebingen, Germany; [10]Department of Otorhinolaryngology, Head and Neck Surgery, University of Tuebingen, Tuebingen, Germany; [11]Center for Clinical Transfusion Medicine, Tuebingen, Germany; [12]Institute of Clinical and Experimental Transfusion Medicine, University Hospital Tuebingen, Tuebingen, Germany; [13]Department for Medical Technologies and Regenerative Medicine, Institute of Biomedical Engineering, University of Tuebingen, Tuebingen, Germany; [14]Division of Cardiology, Department of Medicine, University of California, Los Angeles, Los Angeles, California, USA; [15]Infectious Diseases, Department of Internal Medicine I, University Hospital Tuebingen, Tuebingen, Germany; [16]Department of Anaesthesiology and Intensive Care Medicine, University Hospital Tuebingen, Tuebingen, Germany; [17]Center for Personalized Medicine, University of Tuebingen, Tuebingen, Germany; [18]University Children's Hospital, Tuebingen, Germany; [19]Center for Pediatric Clinical Studies, University Hospital Tuebingen, Tuebingen, Germany; [20]Helmholtz Centre for Infection Research, Braunschweig, Germany; and [21]TWINCORE, Centre for Experimental and Clinical Infection Research, a joint venture of Hannover Medical School and the Helmholtz Centre for Infection Research, Hannover, Germany

Background. The rapid emergence of the Omicron variant and its large number of mutations led to its classification as a variant of concern (VOC) by the World Health Organization. Subsequently, Omicron evolved into distinct sublineages (eg, BA.1 and BA.2), which currently represent the majority of global infections. Initial studies of the neutralizing response toward BA.1 in convalescent and vaccinated individuals showed a substantial reduction.

Methods. We assessed antibody (immunoglobulin G [IgG]) binding, ACE2 (angiotensin-converting enzyme 2) binding inhibition, and IgG binding dynamics for the Omicron BA.1 and BA.2 variants compared to a panel of VOCs/variants of interest, in a large cohort (N = 352) of convalescent, vaccinated, and infected and subsequently vaccinated individuals.

Results. While Omicron was capable of efficiently binding to ACE2, antibodies elicited by infection or immunization showed reduced binding capacities and ACE2 binding inhibition compared to wild type. Whereas BA.1 exhibited less IgG binding compared to BA.2, BA.2 showed reduced inhibition of ACE2 binding. Among vaccinated samples, antibody binding to Omicron only improved after administration of a third dose.

Conclusions. Omicron BA.1 and BA.2 can still efficiently bind to ACE2, while vaccine/infection-derived antibodies can bind to Omicron. The extent of the mutations within both variants prevents a strong inhibitory binding response. As a result, both Omicron variants are able to evade control by preexisting antibodies.

Keywords. SARS-CoV-2; Omicron; antibody binding; multiplex; variants of concern.

Since its initial outbreak in late 2019, severe acute respiratory syndrome coronavirus 2 (SARS-CoV-2) has evolved into a global pandemic, characterized by multiple waves of infection within countries and regions. Following the initial global wave, subsequent waves were often triggered by the emergence of variants of concern (VOCs) [1] that outcompeted earlier variants. These emerging VOCs are presumed to have an increased rate of transmission or the ability to escape vaccine and infection-induced immunity [2–7]. Due to concerns that its numerous spike protein mutations would render it able to escape immune control and its rapid spread in South Africa, the World Health Organization classified Omicron as a VOC on 26 November 2021 [8]. Within days of this classification,

Received 11 January 2022; editorial decision 08 June 2022; published online 15 July 2022

[a]D. J., M. B., and T. R. W. contributed equally to this work.

[b]A. D. and N. S.-M. contributed equally to this work.

Correspondence: A. Dulovic, Natural and Medical Sciences Institute at the University of Tuebingen, Markwiesenstrasse 55, Reutlingen, 72770 Germany (alex.dulovic@nmi.de).

Clinical Infectious Diseases® 2023;76(3):e240–e9

https://doi.org/10.1093/cid/ciac498

Omicron had already been reported in multiple other countries and as of 26th April 2022, it is the dominant global variant [9]. The BA.2 lineage has now surpassed BA.1 [9], which is not only genetically distinct in key regions of the spike glycoprotein [10, 11], but has also evolved to give rise to BA.4, BA.5, and BA.2.12.1. Early studies at the end of 2021 of neutralization against BA.1 found a substantial reduction in neutralizing activity, particularly in individuals who did not receive 3 vaccine doses [12–17]. Because of the urgency of these studies to establish real-time data of whether there is an evasion toward vaccine-induced responses or therapeutics, they often included limited sample numbers, diversity of sample types (eg, only those vaccinated with Pfizer BNT162b2), or only directly compared Omicron to wild-type (WT) or a single other VOC. Complementary to these studies, we provide here a comprehensive analysis of the binding capacity, binding dynamics, and angiotensin-converting enzyme 2 (ACE2) binding inhibition of Omicron BA.1 and BA.2 against antibodies generated either by vaccination or natural infection compared to WT, currently recognized VOCs, and the Lambda and Mu variants of interest (VOIs). We also analyzed samples from a range of vaccines and dosing schemes currently available within the European Union, including booster vaccines, as well as convalescent samples from both adults and children from the first, second, and third waves of infection in Germany.

METHODS

Sample Cohort

Serum samples used in this study were originally collected for use in several other studies [18–21]. The sample set was designed to include a broad representation of samples from infected individuals (hereafter referred to as "convalescent") from the different waves of SARS-CoV-2 within Germany, as well as vaccinated samples. We separated our cohort into 4 groups: vaccinated samples, convalescent samples, infected and later vaccinated samples, and prepandemic samples as controls.

Vaccinated study participants received either 2 homologous doses of AZD1222, BNT162b2, or mRNA-1273; 2 heterologous doses of AZD1222 and BNT162b2 or AZD1222 and mRNA-1273; or 3 doses of BNT162b2. To examine how antibody dynamics changed over time, we included samples from both 1–2 months post–second dose and 5–6 months post–second dose. We also included samples from vaccinated individuals who had a previous polymerase chain reaction (PCR)–confirmed infection and then received a single dose of BNT162b2 as per national guidelines. Samples from convalescent study participants were collected approximately 3 months after positive PCR. To assess differences between variants of SARS-CoV-2, we collected samples from those with a WT, Alpha, or Delta infection. WT samples came from both adults and children. To be considered a WT sample, the infection had to occur during the first wave of the SARS-CoV-2 pandemic in Germany (spring–summer 2020). Alpha samples were confirmed by PCR sequencing and were collected between January and May 2021. Delta samples were either confirmed by PCR sequencing, or where collected during a time period when all infections in Germany were considered to be Delta (September–November 2021). To represent naive samples, negative prepandemic samples were obtained from Central BioHub. An overview of the characteristics for each cohort subgroup can be found in Table 1.

Table 1. Overview of Sample Characteristics for the Study Population

Sample Type	Subgroup	No. of Samples	Median dT, Days (IQR)	No. (%) of Females	Median Age, Years (IQR)	History of Immunosuppressive Condition or Medication, No. (%)
Convalescent	WT (adults)	30	104 (94–119)	14 (47)	62 (51–69)	0 (0)
	WT (children)	20	124 (116–129)	7 (35)	11 (7–14)	0 (0)
	Alpha	30	88 (47–104)	12 (40)	56 (42–65)	14 (47)
	Delta	6	18 (10–23)	5 (83)	65 (56–73)	4 (67)
Infected and vaccinated	…	25	54 (23–91)	16 (64)	55 (48–59)	1 (4)
Vaccinated	A/A (1–2 mo)	30	49 (48–52)	20 (67)	64 (60–66)	2 (7)
	A/A (4–6 mo)	30	154 (146–158)	23 (77)	55 (48–60)	0 (0)
	M/M (1–2 mo)	30	51 (48–54)	20 (67)	59 (49–61)	1 (3)
	M/M (4–6 mo)	16	139 (131–145)	9 (56)	70 (51–83)	1 (6)
	P/P (1–2 mo)	30	51 (49–54)	20 (67)	58 (52–66)	1 (3)
	P/P (4–6 mo)	30	152 (141–160)	25 (83)	38 (30–53)	0 (0)
	A/M	20	153 (150–154)	16 (80)	41 (29–56)	0 (0)
	A/P	20	151 (144–157)	19 (95)	48 (42–56)	0 (0)
	P/P/P	20	14 (14–26.5)	13 (65)	33 (29–44)	2 (12)
Negative	…	15	…	8 (53)	37 (29–41)	0 (0)

Abbreviations: A/A, 2-dose AZD1222; A/M, first dose AZD1222, second dose mRNA-1273; A/P, first dose AZD1222, second dose BNT162b2; dT, time post-infection/last vaccination dose; IQR, interquartile range; M/M, 2-dose mRNA-1273; P/P, 2-dose BNT162b2; P/P/P, 3-dose BNT162b2; WT, wild-type (B.1 isolate).

Ethical Oversight

Informed written consent was obtained from all study participants. Ethical approval and oversight for the samples used in this study was provided by the following ethics committees: the Ethics Committee of the University Hospital Tuebingen (293/2020BO2, 764/2020/BO2 [amended 6 December 2021], B312/2020BO1 [amended 2 June 2021], 556/2021BO1), the Ethics Committee of the University of Tuebingen (179/2020/BO2, 188/2020A), and the Ethics Committee of Hannover Medical School (9086_BO_S_2020).

Mass Spectrometry of Omicron Receptor-Binding Domain

Receptor-binding domain (RBD) Omicron protein samples had their structure verified by liquid chromatography–mass spectrometry (LC-MS). In brief, samples were *N*-deglycosylated using PNGaseF reducing kit (New England Biolabs), diluted 1:3 with His-NaCl buffer and analyzed by liquid chromatography coupled to electrospray ionization quadrupole time-of-flight mass spectrometry. For full details, please consult the Supplementary Methods.

MULTICOV-AB Assay

MULTICOV-AB, a previously published multiplex immunoassay, was performed as described previously [22]. A full list of antigens included within the assay is shown in Table 2. Samples were randomly allocated to plates to ensure that at least 3 samples of every sample group were included on each plate. All samples were measured twice in 2 independent experiments. No sample failed quality control (QC). Raw median fluorescence intensity values were normalized to a QC sample for all antigens as per Becker et al [23]. Please consult the Supplementary Methods for full details.

RBDCoV-ACE2 Assay

RBDCoV-ACE2, a previously published multiplex ACE2 inhibition assay [19], analyzes neutralizing antibody activity through ACE2 binding inhibition. A full list of antigens included in this assay can be found in Table 2. ACE2 binding inhibition was calculated as a percentage, with 100% indicating maximum ACE2 binding inhibition and 0% indicating no ACE2 binding inhibition. Samples with an ACE2 binding inhibition <20% are classified as nonresponders [19]. Please consult the Supplementary Methods for full details.

Biolayer Interferometry

Analysis of binding kinetics of RBD-specific antibodies in serum samples were performed using the Octet RED96e system (Sartorius) as per the manufacturer's recommendations. Purified RBDs of WT, Delta, and Omicron were biotinylated with Sulfo-NHS-LC-LC-Biotin (Thermo Fisher Scientific) in 5 molar excess at ambient temperature for 30 minutes. Excess of biotin was removed by size exclusion chromatography using Zeba Spin Desalting Columns 7K MWCO 0.5 mL (Thermo Fisher Scientific) according to the manufacturer's protocol. Data were analyzed using the Octet Data Analysis HT 12.0 software applying the 1:1 fitting model for the dissociation step.

Table 2. Overview of Antigens Used in MULTICOV-AB and RBDCoV-ACE2 Assays

Antigen	Manufacturer	Category Number	Mutations Covered
Spike WT (B.1)	NMI	…	…
RBD WT (B.1)	NMI	…	…
S1 domain WT (B.1)	NMI	…	…
S2 domain WT (B.1)	Sino Biological	40590-V08B	…
Nucleocapsid WT (B.1)	Aalto Bioreagents	6404-b	…
RBD Alpha (B.1.1.7)	NMI	…	N501Y
RBD Beta (B.1.351)	NMI	…	K417N, E484K, N501Y
RBD Gamma (P1)	NMI	…	K417T, E484K, N501Y
RBD Delta (B.1.617.2)	NMI	…	L452R, T478K
RBD Omicron (B.1.529/BA.1)	Sino Biological	40592-V08H121	G339D, S371L, S373P, S375F, K417N, N440K, G446S, S477N, T478K, E484A, Q493R, G496S, Q498R, N501Y, Y505H
Spike Omicron (B.1.1.529/BA.1)	Sino Biological	40589-V08H26	A67V, del HV69/70, T95I, G142D, del VYY 143-145, del N211, L212I, ins214EPE, G339D, S371L, S373P, S375F, K417N, N440K, G446S, S477N, T478K, E484A, Q493R, G496S, Q498R, N501Y, Y505H, T547K, H655Y, N679K, P681H, N764K, D796Y, F817P, N856K, A892P, A899P, A942P, Q954H, N969K, L981F, K986P, V987P
RBD Omicron (B.1.1.529/BA.2)	Sino Biological	40592-V08H123	G339D, S371F, S373P, S375F, T376A, D405N, R408S, K417N, N440K, S477N, T478K, E484A, Q493R, Q498R, N501Y, Y505H
Nucleocapsid Omicron (B.1.1.529/BA.2)	Sino Biological	40588-V07E35	P13L, del ERS 31-33, R203K, G204R, S413R
RBD Lambda (C.37)	NMI	…	L452Q, F490S
RBD Mu (B.1.621)	NMI	…	R346K, E484K, N501Y

Mutations present within each antigen are provided. Where appropriate, the manufacturer category number is provided. For details on the NMI antigen production, please see [19, 22, 23].
Abbreviations: NMI, Natural and Medical Sciences Institute; RBD, receptor-binding domain; WT, wild-type.

The binding profile response of each sample is illustrated as the mean wavelength shift in nm. For affinity determination, the 1:1 global fit of the Data Analysis HT 12.0 software was used. Please consult the Supplementary Methods for full details.

Statistical Analysis

Data were collated and matched to metadata in Excel 2016. Data visualization was done in RStudio (version 1.2.5001 running R version 3.6.1). Additional packages gplots and beeswarm were used for specific displays. The "lm" function of R's stats library was used for linear regression analyzes. Correlation analyzes were performed using the "cor" function of R's stats library. The "wilcox.test" function from R's stats library was used to perform either Mann–Whitney *U* tests (2-sided) to estimate significance of observed differences between different groups, or Wilcoxon signed-rank tests (2-sided) to estimate significance of observed different between antigens. Graphs were exported from RStudio and further edited in Inkscape (version 0.92.4) to generate final figures. Biolayer inferometry graphical representation was prepared using GraphPad Prism Software (version 9.0.0).

RESULTS

Initially, we examined immunoglobulin G (IgG) binding using MULTICOV-AB [22], a previously published SARS-CoV-2 multiplex immunoassay that was adapted to analyze binding

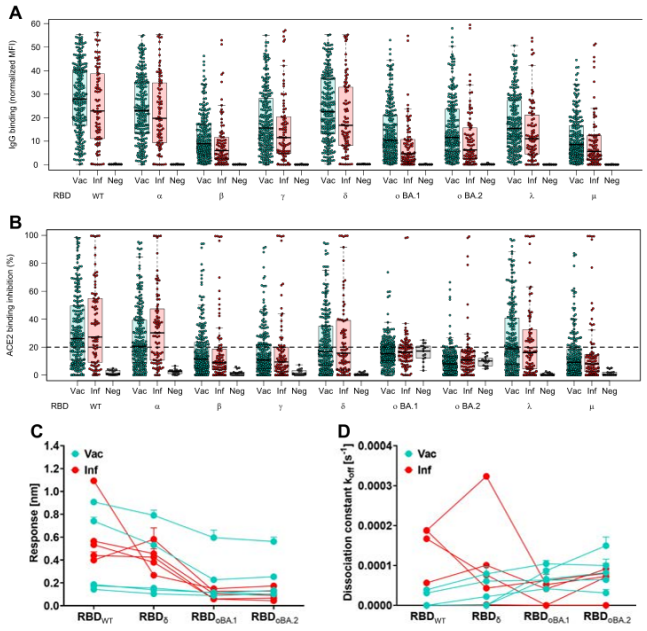

Figure 1. Antibody binding response is significantly reduced for both BA.1 and BA.2. Binding response by preexisting antibodies generated through either infection or vaccination was measured with MULTICOV-AB (*A*) and RBDCoV-ACE2 (*B*) assays and Biolayer interferometry (*C* and *D*). *A*, Boxplot showing that immunoglobulin G binding is significantly reduced for both BA.1 and BA.2 as compared to other variants of concern (VOCs)/variants of interest (VOIs) for convalescent (n = 86) and vaccinated (n = 226) samples. Negative samples are included as controls (n = 15). *B*, Boxplot showing that ACE2 binding inhibition is significantly reduced for both BA.1 and BA.2 as compared to other VOCs/VOIs for both convalescent and vaccinated samples. Boxes represent the median with 25th and 75th percentiles; whiskers show the largest and smallest non-outlier values. Outliers were determined by 1.5 interquartile range. *C* and *D*, Binding kinetics of receptor-binding domain (RBD)–specific antibodies from serum samples of convalescent and vaccinated individuals (both n = 5). Binding response (*C*) and dissociation constant (*D*) were determined by 1:1 fitting model of the individual serum samples between the different RBD variants. Median fold reductions for both (*A*) and (*B*) can be found as Supplementary Tables 1–3 and 5. Statistical differences between all variants was analyzed by Wilcoxon signed-rank test for both (*A*) and (*B*) and is available as Supplementary Tables 4 and 7. The response rate for (*B*) is available as Supplementary Table 6. Abbreviations: ACE2, angiotensin-converting enzyme 2; IgG, immunoglobulin G; Inf, infected; MFI, median fluorescence intensity; Neg, negative; RBD, receptor-binding domain; Vac, vaccinated; WT, wild-type.

toward RBDs from VOC/VOIs (a full list of antigens analyzed and their mutations contained within can be found in Table 2). For both vaccinated and convalescent samples, IgG binding toward both Omicron BA.1 and BA.2 for preexisting antibodies was significantly reduced compared to WT (BA.1: 2.3–4.1 median fold reduction, $P < .001$; BA.2: 2.1–3.0 median fold reduction, $P < .001$) (Figure 1, Supplementary Tables 1–4). This is similar to the statistically significant reduction in binding toward Beta (2.8–3.5 median fold reduction, $P < .001$) and Mu (3.0–3.6 median fold reduction, $P < .001$, Figure 1, Supplementary Tables 1–4). Within Omicron, BA.1 had a significantly increased reduction in IgG binding compared to BA.2 (1.1–1.2 median fold reduction, $P < .001$) (Figure 1, Supplementary Tables 2–4).

Next, we analyzed ACE2 binding inhibition to determine how effective the antibodies were at blocking the RBD-ACE2 interaction, using RBDCoV-ACE2 [19], a multiplex ACE2-RBD inhibition assay. This assay mimics the interaction between ACE2 and the RBD, while the multiplex format allows for the simultaneous measurement of all VOCs/VOIs in a single well. To evaluate binding against other antigens of SARS-CoV-2, we also include the spike and S1 domain of WT and the spike and nucleocapsid of Omicron. In line with IgG binding, ACE2 binding inhibition against Omicron was significantly reduced compared to WT (Omicron BA.1: median, 15.2%–16.4% and BA.2: median, 8.0%–10.9%; WT: median, 26.1%–27.2%; both $P < .001$) (Figure 1, Supplementary Table 5), with less than half as many samples considered responsive (WT: 62.8%; BA.1: 30.1%–32.6%; BA.2: 8.4%–14.0%) (Figure 1*B*, Supplementary Table 6). Interestingly, although BA.2 revealed reduced ACE2 binding inhibition and sample response rate compared to BA.1, this was not significant ($P = .08$, Supplementary Table 7). While BA.2 had the lowest response rate of all variants examined, the median ACE2 binding inhibition and response rate for BA.1 was greater than for Beta (median, 8.9–11.4; response, 22.1%–31.0%), Gamma (median, 9.4–10.8; response, 25.5%–30.1%), and Mu (median, 8.1–9.1; response, 19.8%–22.6%).

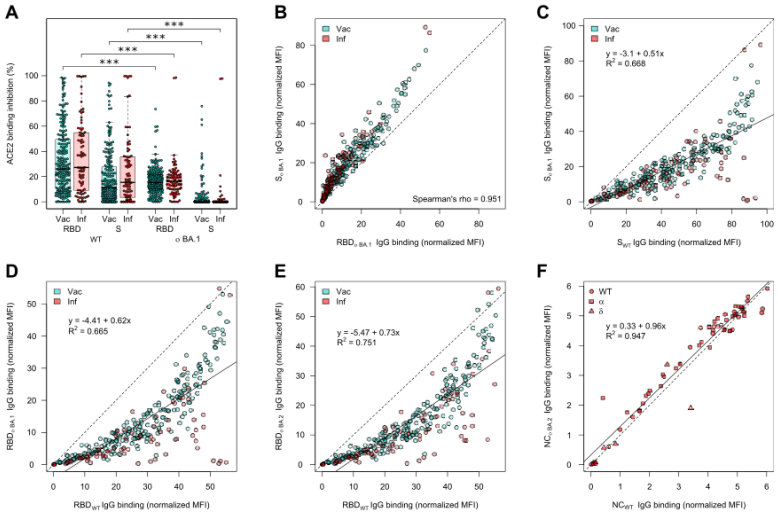

Figure 2. Angiotensin-converting enzyme 2 (ACE2) binding inhibition and correlations of binding capacity between BA.1, BA.2, and wild-type (WT) for different antigens. ACE2 binding inhibition (*A*) and immunoglobulin G (IgG) binding capacity (*B*–*F*) were compared for the Omicron BA.1 and BA.2 receptor-binding domain (RBD), and spike (S) to the WT RBD and S. *A*, Boxplot showing that ACE2 binding inhibition is significantly reduced toward BA.1 for both RBD and S for both vaccinated (n = 226) and convalescent (n = 86) samples. Boxes represent the median with 25th and 75th percentiles; whiskers show the largest and smallest nonoutlier values. Outliers were determined by 1.5 interquartile range. Statistical significance was calculated by Wilcoxon signed-rank test; ***$P < .001$. *B*, Correlation analysis of IgG binding capacity for the BA.1 spike compared to the BA.1 RBD. Spearman rank was calculated to assess ordinal association between the variables. *C*–*F*, Linear regressions of IgG binding capacity for the BA.1 S compared to WT S (*C*), BA.1 RBD compared to wild-type RBD (*D*), BA.2 RBD compared to WT RBD (*E*), and BA.2 nucleocapsid compared to WT nucleocapsid (*F*). R^2 is included to indicate the correlation. Abbreviations: ACE2, angiotensin-converting enzyme 2; IgG, immunoglobulin G; Inf, infected; MFI, median fluorescence intensity; NC, nucleocapsid; RBD, receptor-binding domain; S, spike; Vac, vaccinated; WT, wild-type.

To investigate the RBD binding of BA.1 and BA.2 further, we analyzed the binding kinetics of RBD-specific antibodies from vaccinated (2 doses of BNT162b2) and convalescent (WT) study participants by biolayer interferometry analysis (Figure 1*C* and 1*D*). Binding response and dissociation constant were measured for each sample as an indicator of amount and binding strength. Binding response toward BA.1 and BA.2 was reduced compared to both WT and Delta (Figure 1*C*), while most samples showed increased dissociation kinetics for Omicron (Figure 1*D*). Despite high variation observed for both the vaccinated and convalescent samples, Omicron always showed the lowest binding response (Supplementary Figure 1, Supplementary Table 8). When binding toward ACE2 itself was examined, Omicron BA.1 and BA.2 were still able to bind ACE2 with high affinity (Supplementary Figure 2).

As mutations toward Omicron are not limited to the RBD, we also analyzed ACE2 binding toward the full-length spike protein. Omicron BA.1 ACE2 binding inhibition toward the spike protein was significantly reduced compared to WT ($P <$ .001). Interestingly, the response rate underwent a similar 30% reduction from RBD to S for both WT (62.8% to 34.5%–43.0%) and Omicron (30.1%–32.6% to 3.5%–4.9%) (Figure 2*A*, Supplementary Table 9). IgG binding capacity toward spike appears to be conserved to a similar degree as the RBD (Figure 2*B*–*D*). However, this is substantially reduced compared to the nucleocapsid of BA.2, for which there was no change in binding capacity compared to WT for convalescent samples, regardless with which strain they had been previously infected (Figure 2*E*, samples highlighted according to strain).

Next, we analyzed whether vaccine type (AZD1222, mRNA-1273, or BNT162b2) and number of doses (homologous or heterologous 2 dose, or homologous 3 dose) received resulted in differences with respect to Omicron binding response. To analyze how this response changed as time postvaccination increased, we also compared the responses at

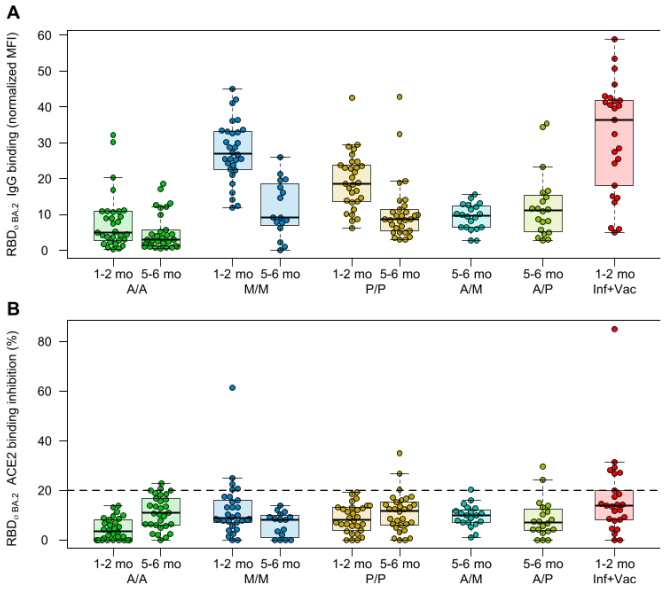

Figure 3. Differences in Omicron binding response among different populations of vaccinated samples. Binding response toward Omicron BA.2 was analyzed by either MULTICOV-AB (*A*) or RBDCoV-ACE2 (*B*) assays for samples from different vaccine schemes (n = 30 for all samples, except for mRNA-1273 at 5–6 months (n = 16), heterologous vaccine schemes (both n = 20), and infected and vaccinated (n = 25). To determine the effect of time postvaccination, samples from both 1–2 months and 5–6 months postvaccination were included. Boxes represent the median with 25th and 75th percentiles; whiskers show the largest and smallest nonoutlier values. Outliers were determined by 1.5 interquartile range. The 20% cutoff for nonresponders is indicated by the dashed line on (*B*). The equivalent data for BA.1 are provided as Supplementary Figure 3. Abbreviations: A/A, AZD1222; ACE2, angiotensin-converting enzyme 2; A/M, first dose AZD1222, second dose mRNA-1273; A/P, first dose AZD1222, second dose BNT162b2; IgG, immunoglobulin G; Inf, infected; MFI, median fluorescence intensity; M/M, mRNA-1273; P/P, BNT162b2; RBD, receptor-binding domain; Vac, vaccinated.

1–2 months post–second dose and 5–6 months post–second dose for the homologous recipients. IgG binding capacity at 5–6 months was low for all recipients regardless of the administered vaccine, although homologous mRNA-based vaccination still had higher binding capacity at this timepoint than 1–2 months post–second dose for vector-based vaccination (median of 9.16, 8.7, and 5.04 for mRNA-1273, BNT-162b2, and AZD1222, respectively; Figure 3*A*). Among samples from 1–2 months postdosing, infected and then vaccinated had the greatest IgG binding capacity (median, 36.5), followed by 2-dose mRNA-1273 (median, 27.0), BNT162b2 (median, 18.7), and AZD1222 (median, 2.3). This pattern was consistent for both BA.1 (Supplementary Figure 3) and BA.2 (Figure 3). ACE2 binding inhibition was consistently low regardless of type received and timeframe postdose (Figure 3*B*).

To determine whether a third dose results in increased binding responses against Omicron, we analyzed samples from individuals who had received a third dose of BNT162b2 and compared it to those who had received their second dose in a similar timeframe and individuals 5–6 months post–second dose, who would be eligible to receive a third dose (Figure 4). Further boosting was associated with higher Omicron ACE2 binding inhibition compared to 2 doses (27% and 0% of samples were responders toward BA.1 and BA.2 post–second dose, respectively; 55% and 25% were responders after boosting) suggesting that boosting offers increased protection against Omicron (Figure 4). However, this increase in protection was not limited to Omicron and was present for all VOCs (Figure 4). Compared to the second dose from a similar timepoint (30% and 10% responders to BA.1 and BA.2, respectively), boosting with the third dose increased ACE2 binding inhibition, substantially confirming this effect is generated by the third dose itself, and not by time postvaccination alone (Figure 4*C*).

Last, we analyzed whether natural infection with different variants resulted in differences in binding responses. There was no difference in ACE2 binding inhibition between convalescent individuals infected with either WT or Alpha, with both having minimal inhibition against Omicron (Figure 5*A*, Supplementary Figure 3). While some samples with a previous Delta infection showed substantially more activity compared to WT or Alpha, they had been collected much sooner after the infection (median dT, 18 days) than WT (median dT, 104 days) or Alpha (median dT, 88 days). To evaluate whether children's antibodies were more effective at binding toward Omicron than adults, we compared convalescent samples 3–4 months post-PCR from the first wave in children (n = 20), to convalescent samples 3 months post–positive PCR from the same wave in adults (n = 30) (Figure 5*B* and 5*C*, Supplementary Figure 4). There was no significant difference between adults and children in ACE2 binding inhibition ($P = .48$; Figure 5*B*), although children did have significantly reduced binding capacity toward Omicron ($P = .01$; Figure 5*C*).

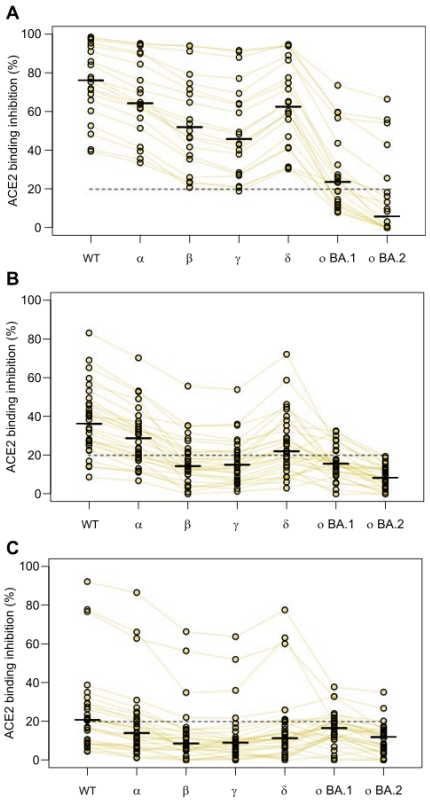

Figure 4. Angiotensin-converting enzyme 2 (ACE2) binding inhibition toward Omicron is boosted by a third vaccine dose. Changes in ACE2 binding response following the third dose of BNT162b2 for all variants within the study. Samples come from either boosted (n = 20, *A*), 1–2 months post–second dose of BNT162b2 (n = 20, *B*), or 5–6 months post–second dose of BNT162b2 (n = 20, *C*). Individual samples are highlighted by connected lines with bars representing medians. The 20% cutoff for nonresponders is indicated by the dashed line. Abbreviations: ACE2, angiotensin-converting enzyme 2; WT, wild-type.

DISCUSSION

In this study, we provide an in-depth characterization of antibody binding to Omicron BA.1 and BA.2 compared to WT and all other VOCs and variants under investigation in a large, diverse sample cohort. The use of an ACE2 inhibition assay enabled the comparison of multiple variants of interest simultaneously, while also producing comparable results to classical virus neutralization assays [19]. Similar to others, we

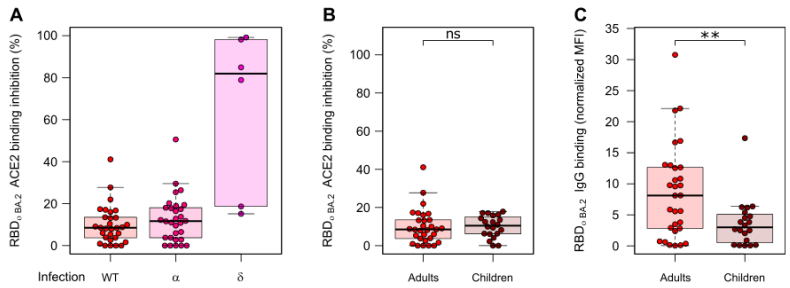

Figure 5. Differences in immunoglobulin G (IgG) binding response and angiotensin-converting enzyme 2 (ACE2) binding inhibition toward BA.2 among different populations of convalescent samples. Comparative ACE2 binding inhibition (*A* and *B*) and IgG binding capacity (*C*) between convalescent samples from different pandemic waves (*A*) and adults and children (*B* and *C*) for BA.2. *A*, There are no differences in ACE2 binding inhibition toward BA.2 for individuals infected with wild-type (WT) (n = 30), Alpha (n = 30), or Delta (n = 6). *B*, Children (n = 20) and adults (n = 30) have similar ACE2 binding inhibition toward BA.2 following WT infection, although they have significantly reduced IgG binding capacity ($P = .01$). *C*, Boxes represent the median with 25th and 75th percentiles; whiskers show the largest and smallest nonoutlier values. Outliers were determined by 1.5 interquartile range. Statistical significance was calculated by Mann–Whitney *U* test: $^{**}P < .01$; ns, $P < .05$. The equivalent data for BA.1 are provided as Supplementary Figure 4. Abbreviations: ACE2, angiotensin-converting enzyme 2; IgG, immunoglobulin G; MFI, median fluorescence intensity; RBD, receptor-binding domain; WT, wild-type.

identified that antibody binding and ACE2 binding inhibition toward both Omicron BA.1 and BA.2 elicited by either immunization or previous infection were significantly reduced [14, 16, 24–28]. However, we provide here additional information on IgG binding capacity and ACE2 binding inhibition by the inclusion of a large variety of subcohorts representing the present diversity of immunity against SARS-CoV-2, the comparison of the Omicron variant to all other VOCs/VOIs, and the comparison between BA.1 and BA.2.

We found that both IgG binding capacity and ACE2 binding inhibition was significantly reduced for BA.1 and BA.2, similar to reductions for Beta and Mu, with the majority of samples being classified as nonresponsive toward Omicron for ACE2 binding inhibition. Like others researchers [15, 24, 28], we found that antibody binding responses toward Omicron were significantly increased upon administration of a booster dose. Boosting increases were not restricted to just Omicron IgG binding capacity and ACE2 binding inhibition, but were present against all VOCs/VOIs. No significant difference was present between BA.1 and BA.2. However, data regarding the longitudinal response post–third dose remains lacking, with some countries now offering a fourth dose for certain groups (eg, immunocompromised individuals). The increased responses following boosting also appear to apply for convalescent individuals, as seen by the increased IgG binding capacity and ACE2 binding inhibition for previously infected individuals who received a single dose, compared to those who had received any 2 vaccine doses. This increase in responses for individuals who have been both infected and vaccinated is in agreement with Pajon et al [29], who found that infections prior to vaccination resulted in a greater breadth of immune response, while Lechmere et al [26] found that breakthrough Delta infections among vaccinated individuals acted like a booster dose. Thus, both reinfection and a booster dose leads to appropriate affinity maturation of elicited antibodies. Among those who had received 2 doses, binding responses were consistent with other reports (eg, [16]) in identifying a significant decrease for those who received homologous 2-dose vector vaccination as opposed to homologous mRNA vaccination or heterologous vaccination.

We identified no significant difference in ACE2 binding inhibition toward Omicron for children compared to adults, although IgG binding capacity was significantly reduced. This is in contrast to previous research that has identified that children's antibody titers are higher than adults following infection [21]; however, a limitation of our study is that the children and adult groups were not well-matched in terms of time post–positive PCR (median dT, 104 for adults and 124 for children) or disease severity (majority hospitalized adults vs asymptomatic/mildly symptomatic children). A larger investigation including vaccinated samples from children is needed to investigate any possible protective effect from previous infection and the antibody response toward Omicron itself in children in more detail.

Similar to Carreño et al [27], we identified that IgG binding capacity toward Omicron was not as severely reduced as ACE2 binding inhibition. Interestingly, while BA.2 had significantly increased IgG binding capacity to BA.1, it had reduced ACE2 binding inhibition. While mutations in BA.1 and BA.2 are not limited to the RBD, their reduction in activity was limited to the trimeric spike, with near-identical binding compared to WT for the nucleocapsid. Our analysis of both the spike- and

RBD-derived ACE2 binding inhibition suggests that while both epitopes are sufficiently conserved to enable binding, their divergent mutated sequences affect their inhibitory response. Further investigation into this pattern and particularly the role of S1-derived antibodies in neutralization is required to understand the inhibitory protection offered against Omicron.

Overall, our results identify that while Omicron can efficiently bind ACE2 and vaccine/infection-induced antibodies can bind Omicron, the extent of the mutations within the RBD appear too divergent to enable RBD-directed antibodies to mount an inhibitory response. The dramatic reductions in both IgG binding and ACE2 binding inhibition toward Omicron, as opposed to other VOCs/VOIs, confirm that this variant remains capable of immune escape and requires careful sequence monitoring to identify any further sequence evolution. Importantly, booster doses elicit a significant increase in antibody response, which correlates with a significant increase in both IgG binding and ACE2 binding inhibition against Omicron. Our data add weight to a growing body of evidence that the continuous adaptation of vaccines toward novel highly contagious variants needs to be considered in order to control SARS-CoV-2.

Supplementary Data

Supplementary materials are available at *Clinical Infectious Diseases* online. Consisting of data provided by the authors to benefit the reader, the posted materials are not copyedited and are the sole responsibility of the authors, so questions or comments should be addressed to the corresponding author.

Notes

Author contributions. D. J., M. Be., A. D., and N. S.-M. conceived the study. D. J., M. Be., T. R. W., P. D. K., S. M., A. Z., U. R., A. D., and N. S. M. planned experiments. A. D. and N. S. M. supervised the study. D. J., M. Be., P. D. K., T. R. W., S. M., T. M. G., J. Gri., P. M., J. Gru., and B. T. performed experiments. C. H., Y. T. P., J. H., R. F., A. K., A. N., Y. M., S. S., J. S. W., K. A., G. U., M. M., T. B., K. S.-L., H. H., S. G., M. Bi., H. R., J. R., C. E., A. R. F., M. H., B. K., M. S., and G. K. collected samples or organized their collection. K. S.-L. and N. S. M. obtained funding. M. Be., T. R. W., and A. D. performed data analysis and generated the figures. A. D. wrote the first draft of the manuscript. All authors approved the manuscript prior to submission.

Acknowledgments. The authors thank other members of the Multiplex Immunoassays, Biological Development Center and Bioanalytics groups at the Natural and Medical Sciences Institute at the University of Tuebingen (NMI) for their support on this project. The authors also thank Joop van der Heuvel for his expertise in protein production; Ann Kathrin Horlacher and Mareike Walenta for assistance with sample processing and patient material storage; Ulrike Schmidt, Iris Schaefer, Richard Schaad, and Hannah Zug for technical support; Katharina Kienzle, Hartmut Mahrhofer, Hardy Richter, and Stefanie Döbele for help with sample collection; Andrea Evers-Bischoff, Andrea Bevot, and the Centre for Pediatric Clinical Studies at the University Hospital Tuebingen for organizational support in conducting the study; and all those involved in the organization of the MuSPAD and TuSeRe sample collection.

Disclaimer. The funders had no role in study design, data collection, and analysis; preparation of the manuscript; or the decision to submit the manuscription for publication.

Financial support. This work was supported by the State Ministry of Baden-Württemberg for Economic Affairs, Labour and Tourism (grant numbers FKZ 3-4332.62-NMI-67, FKZ 3-4332.62-NMI-68, and 7-4332.62-NMI/55); the Initiative and Networking Fund of the Helmholtz Association of German Research Centres (grant number SO-96); the European Union Horizon 2020 research and innovation program (grant agreement number 101003480, CORESMA), and the State Ministry of Lower Saxony for Science and Culture (grant agreement number 14-76103-1841, MWK HZI COVID-19).

Potential conflicts of interest. N. S. M. was a speaker at previous Luminex user meetings. The NMI is involved in applied research projects as a fee for services with the Luminex Corporation. M. Bi. reports payment or honoraria from MSD Sharp & Dohme GmbH for symposia; and also reports participation on advisory boards for Roche Pharma AG, Incyte Biosciences Germany GmbH, Bayer Vital GmbH, Bristol-Myers Squibb GmbH & Co KgaA, and MSD Sharp & Dohme GmbH. C. E. reports support for the present manuscript from MWK Sonderfördermaßnahme Kinderstudie (Kap. 1499 TG 93). B. L. reports receiving funding for the present manuscript from NaFOUniMedCovid19 (FKZ: 01KX2021) supported by the German Federal Ministry of Education and Research; and reports a leadership or fiduciary role for the German Center for Infection Research (TI BBD, DZIF), Transplant Cohort, and Steering Committee TBNet. A. Z. reports state technology funding for device infrastructure (7-4332.62-NMI/55), outside the conduct of this study. N. S.-M. reports support for the present manuscript from LAND BW (MULTICOV-AB and LAND BW, Automation in SARS-CoV-2) and payment or honoraria from Luminex Corporation for being a speaker at previous user meetings (the NMI is also involved in applied research projects as a fee for services with the Luminex Corporation). All other authors report no potential conflicts.

All authors have submitted the ICMJE Form for Disclosure of Potential Conflicts of Interest. Conflicts that the editors consider relevant to the content of the manuscript have been disclosed.

References

1. World Health Organization. Tracking SARS-CoV-2 variants. Available at: https://www.who.int/en/activities/tracking-SARS-CoV-2-variants/. Accessed 1 May 2022.
2. Korber B, Fischer WM, Gnanakaran S, et al. Tracking changes in SARS-CoV-2 spike: evidence that D614G increases infectivity of the COVID-19 virus. Cell **2020**; 182:812–27.e19.
3. Graham MS, Sudre CH, May A, et al. Changes in symptomatology, reinfection, and transmissibility associated with the SARS-CoV-2 variant B.1.1.7: an ecological study. Lancet Public Health **2021**; 6:E335–45.
4. Davies NG, Abbott S, Barnard RC, et al. Estimated transmissibility and impact of SARS-CoV-2 lineage B.1.1.7 in England. Science **2021**; 372:eabg3055.
5. Collier DA, De Marco A, Ferreira IATM, et al. Sensitivity of SARS-CoV-2 B.1.1.7 to mRNA vaccine-elicited antibodies. Nature **2021**; 593:136–41.
6. Tao K, Tzou PL, Nouhin J, et al. The biological and clinical significance of emerging SARS-CoV-2 variants. Nat Rev Genet **2021**; 22:757–73.
7. Pegu A, O'Connell SE, Schmidt SD, et al. Durability of mRNA-1273 vaccine-induced antibodies against SARS-CoV-2 variants. Science **2021**; 373:1372–7.
8. World Health Organization. Classification of Omicron (B.1.1.529): SARS-CoV-2 variant of concern. **2021**. Available at: https://www.who.int/news/item/26-11-2021-classification-of-omicron-(b.1.1.529)-sars-cov-2-variant-of-concern. Accessed 1 May 2022.
9. CoVariants. Shared mutations. Available at: https://covariants.org/shared-mutations/. Accessed 1 May 2022.
10. Rambaut A, Holmes EC, O'Toole Á, et al. A dynamic nomenclature proposal for SARS-CoV-2 lineages to assist genomic epidemiology. Nat Microbiol **2020**; 5:1403–7.
11. cov-lineages.org. Lineage B.1.1.529. **2022**. Available at: https://cov-lineages.org/lineage.html?lineage=B.1.1.529. Accessed 1 May 2022.
12. Cele S, Jackson L, Khoury DS, et al. SARS-CoV-2 Omicron has extensive but incomplete escape of Pfizer BNT162b2 elicited neutralization and requires ACE2 for infection. medRxiv [Preprint]. Posted online 17 December **2021**. doi:10.1101/2021.12.08.21267417.
13. Cao Y, Wang J, Jian F, et al. Omicron escapes the majority of existing SARS-CoV-2 neutralizing antibodies. Nature **2022**; 602:657–63.
14. Nemet I, Kliker L, Lustig Y, et al. Third BNT162b2 vaccination neutralization of SARS-CoV-2 Omicron infection. N Engl J Med **2022**; 386:492–4.
15. Garcia-Beltran WF, StDenis KJ, Hoelzemer A, et al. mRNA-based COVID-19 vaccine boosters induce neutralizing immunity against SARS-CoV-2 Omicron variant. Cell **2022**; 185:457–66.e4.

16. Schmidt F, Muecksch F, Weisblum Y, et al. Plasma neutralization of the SARS-CoV-2 Omicron variant. N Engl J Med **2022**; 386:599–601.
17. Aggarwal A, Stella AO, Walker G, et al. SARS-CoV-2 Omicron: evasion of potent humoral responses and resistance to clinical immunotherapeutics relative to viral variants of concern. medRxiv [Preprint]. Posted online 15 December **2021**. doi:10.1101/2021.12.14.21267772.
18. Gornyk D, Harries M, Glöckner S, et al. SARS-CoV-2 seroprevalence in Germany. Dtsch Arztebl Int **2021**; 118:824–31.
19. Junker D, Dulovic A, Becker M, et al. COVID-19 patient serum less potently inhibits ACE2-RBD binding for various SARS-CoV-2 RBD mutants. Sci Rep **2021**; 12: 7168.
20. Heinzel C, Pinilla YT, Elsner K, et al. Non-invasive antibody assessment in saliva to determine SARS-CoV-2 exposure in young children. Front Immunol **2021**; 12: 753435.
21. Renk H, Dulovic A, Seidel A, et al. Robust and durable serological response following pediatric SARS-CoV-2 infection. Na Commun **2022**; 13:128.
22. Becker M, Strengert M, Junker D, et al. Exploring beyond clinical routine SARS-CoV-2 serology using MultiCoV-Ab to evaluate endemic coronavirus cross-reactivity. Nat Commun **2021**; 12:1152.
23. Becker M, Dulovic A, Junker D, et al. Immune response to SARS-CoV-2 variants of concern in vaccinated individuals. Nat Commun **2021**; 12:3109.
24. Gruell H, Vanshylla K, Tober-Lau P, et al. mRNA booster immunization elicits potent neutralizing serum activity against the SARS-CoV-2 Omicron variant. Nat Med **2022**; 28:477–80.
25. Wilhelm A, Widera M, Grikscheit K, et al. Reduced neutralization of SARS-CoV-2 Omicron variant by vaccine sera and monoclonal antibodies. medRxiv [Preprint]. Posted online 8 December **2021**. doi:10.1101/2021.12.07.21267432.
26. Lechmere T, Snell LB, Graham C, et al. Broad neutralization of SARS–CoV–2 variants, including Omicron, following breakthrough infection with Delta in COVID–19–vaccinated individuals. mBio **2022**; 13:e0379821.
27. Carreño JM, Alshammary H, Tcheou J, et al. Activity of convalescent and vaccine serum against SARS-CoV-2 Omicron. Nature **2022**; 602:682–8.
28. Pajon R, Doria-Rose NA, Shen X, et al. SARS-CoV-2 Omicron variant neutralization after mRNA-1273 booster vaccination. N Engl J Med **2022**; 386:1088–91.
29. Goel RR, Apostolidis SA, Painter MM, et al. Distinct antibody and memory B cell responses in SARS-CoV-2 naive and recovered individuals following mRNA vaccination. Sci Immunol **2021**; 6:eabi6950.

Supplementary Information - Antibody binding and ACE2 binding inhibition is significantly reduced for both the BA1 and BA2 omicron variants

Daniel Junker[1,*], Matthias Becker[1,*], Teresa R. Wagner[1,2,*], Philipp D. Kaiser[1], Sandra Maier[1], Tanja M. Grimm[1], Johanna Griesbaum[1], Patrick Marsall[1], Jens Gruber[1], Bjoern Traenkle[1], Constanze Heinzel[3], Yudi T. Pinilla[3], Jana Held[3], Rolf Fendel[3,4,5], Andrea Kreidenweiss[3,4,5], Annika Nelde[6,7,8,9], Yacine Maringer[6,7,8,9], Sarah Schroeder[6,8,10], Juliane S. Walz[6,7,8,9], Karina Althaus[11,12], Gunalp Uzun[11], Marco Mikus[11], Tamam Bakchoul[11,12], Katja Schenke-Layland[1,8,13,14], Stefanie Bunk[15], Helene Haeberle[16], Siri Göpel[4,15], Michael Bitzer[15,17], Hanna Renk[18], Jonathan Remppis[18], Corinna Engel[18,19], Axel R. Franz[18,19], Manuela Harries[20], Barbora Kessel[20], Berit Lange[20], Monika Strengert[20,21], Gerard Krause[20,21], Anne Zeck[1], Ulrich Rothbauer[1,2], Alex Dulovic[1,§,#] and Nicole Schneiderhan-Marra[1,§,#]

Author affiliations

1 – NMI Natural and Medical Sciences Institute at the University of Tuebingen, Reutlingen, Germany

2 – Pharmaceutical Biotechnology, University of Tuebingen, Tuebingen, Germany

3 – Institute of Tropical Medicine, University Hospital Tuebingen, Tuebingen, Germany

4 – German Center for Infection Research (DZIF), Partner Site Tuebingen, Tuebingen, Germany

5 - Centre de Recherches Médicales de Lambaréné (CERMEL), Gabon

6- Department of Peptide-based Immunotherapy, University of Tuebingen and University Hospital Tuebingen, Tuebingen, Germany

7 – Clinical Collaboration Unit Translational Immunology, German Cancer Consortium (DKTK), Department of Internal Medicine, University Hospital Tuebingen, Tuebingen, Germany

8 – Institute for Cell Biology, University of Tuebingen, Tuebingen, Germany

9 – Cluster of Excellence iFIT (EXC2180) “Image-Guided and Functionally Instructed Tumor Therapies”, University of Tuebingen, Tuebingen, Germany

10 – Department of Otolaryngology, Head and Neck Surgery, University of Tuebingen, Tuebingen, Germany

11 – Center for Clinical Transfusion Medicine, Tuebingen, Germany

12 – Institute of Clinical and Experimental Transfusion Medicine, University Hospital Tuebingen, Tuebingen, Germany

13 – Institute of Biomedical Engineering, Department for Medical Technologies and Regenerative Medicine, University of Tuebingen, Tuebingen, Germany

14 – Department of Medicine/Cardiology, University of California Los Angeles (UCLA), Los Angeles, USA

15 – Infectious Diseases, Department Internal Medicine I, University Hospital Tuebingen, Tuebingen, Germany

16 – Department of Anaesthesiology and Intensive Care Medicine, University Hospital Tuebingen, Tuebingen, Germany

17 – Center for Personalized Medicine, University of Tuebingen, Tuebingen, Germany

18 – University Children's Hospital, Tuebingen, Germany

19 – Center for Pediatric Clinical Studies, University Hospital Tuebingen, Tuebingen, Germany

20 – Helmholtz Centre for Infection Research, Braunschweig, Germany

21 – TWINCORE, Centre for Experimental and Clinical Infection Research, a joint venture of Hannover Medical School and the Helmholtz Centre for Infection Research, Hannover, Germany

* indicates shared first authorship

§ indicates shared last authorship

# indicates corresponding author

Corresponding author Information

Alex Dulovic – alex.dulovic@nmi.de, +49 (0)7121 51530 580

Nicole Schneiderhan-Marra – nicole.schneiderhan@nmi.de, +49 (0)7121 51530 815

Supplementary Methods

Mass Spectrometry of omicron receptor binding domain (RBD)

The RBD omicron protein samples (5 µg) were N-deglycosylated using a PNGaseF reducing kit (Rapid PNGaseF reducing kit, New England Biolabs, Frankfurt am Main, Germany) by adding ¼ of the volume of reducing buffer included in the kit and denaturation and reduction for 5 minutes at 80 °C. Subsequently, 0.125 µL PNGaseF enzyme preparation, included in the kit, were added and deglycosylation was performed for 10 minutes at 50 °C. Prior to Liquid chromatography-mass spectrometry (LC-MS) analysis, the samples were diluted 1:3 with HisNaCl buffer (20 mmM His 140 mM NaCl, pH 6.0) and analyzed by liquid chromatography (HPLC) coupled to electrospray ionization (ESI) quadrupole time-of-flight (QTOF) MS. Samples (0.4 µg per injection) was desalted using reversed phase chromatography on a Dionex U3000 RSLC system (Thermo Scientific, Dreieich, Germany) using a Acquity BEH300 C4 column (1mm x 50mm, Waters, Eschborn, Germany) at 75°C and 150 µl/min flow rate applying a 11-min linear gradient with varying slopes. In detail, the gradient steps were applied as follows (min/% Eluent B): 0/5, 0.4/5, 2.55/30, 7/50, 7.5/99, 8/5, 8.75/99, 9.5/5, 10/99, 10.25/5 and 11/5. Eluent B was acetonitrile with 0.1% formic acid, and solvent A was water with 0.1% formic acid. To avoid contamination of the mass spectrometer with buffer salts, the HPLC eluate was directed into waste for the first 2 min. Continuous MS analysis was performed using a QTOF mass spectrometer (Maxis UHR-TOF; Bruker, Bremen, Germany) with an ESI source operating in positive ion mode. Spectra were taken in the mass range of 600–2000 m/z. External calibration was applied by infusion of tune mix via a syringe pump during a short time segment at the beginning of the run. Raw MS data were lock-mass corrected (at m/z 1221.9906) and further processed using Data Analysis 5.3 and MaxEnt Deconvolution software tools (Bruker).

Antigen Immobilisation on beads

SARS-CoV-2 wild-type Spike, RBD, S1 domain, S2 domain and Nucleocapsid were immobilised on magnetic MagPlex beads (Luminex) by EDC-sNHS coupling as previously described(1).RBDs from variants of concern and the Omicron Spike protein were immobilised on magnetic MagPlex beads (Luminex) by Anteo coupling (AMG Activation Kit for Multiplex Microspheres, #A-LMPAKMM-400, Anteo Technologies) as previously described(2). Following coupling, beads were stored at 4°C. Prior to experimentation, beads were then combined into a 25x Bead Mix and stored at 4°C until used. The antigens used in these experiments can be found in Table 2.

MULTICOV-AB

MULTICOV-AB, a previously published multiplex immunoassay was performed as described(1). A full list of antigens included within the assay are listed in Table 2. Samples were randomly allocated to plates to ensure that at least three sample of every sample group was included on each plate. Briefly, samples were thawed at room temperature, vortexed and then diluted 1:200 in assay buffer before being mixed 1:1 with 1x Bead Mix in a 96-well plate (final dilution 1:400). Samples were then incubated in darkness on a Thermomixer (20°C, 750 rpm, 2 hours) before being washed three times to remove unbound antibodies. To ensure retention of beads, a magnetic plate washer was used. To detect bound IgG, 3 µg/mL RPE-goat anti-human IgG was added to each well and then incubated for a further 45 mins on a Thermomixer. After another washing step, beads were resuspended in 100 µL of wash buffer, shaken for 3 mins at 1000 rpm, and then measured on a FLEXMAP3D instrument (No Timeout, Gate 7500-15000, Reporter Gain Standard PMT, 50 events). 3 Quality control samples were included in duplicate on each plate. All

samples were measured twice in two independent experiments. No sample failed QC. Raw median fluorescence intensity (MFI) values were normalized to a QC sample for all antigens as per(3) .

RBDCoV-ACE2

RBDCoV-ACE2, a previously published multiplex ACE2 inhibition assay(2), analyzes neutralizing antibody activity through ACE2 binding inhibition. A full list of antigens included in this assay can be found as Table 2. Briefly, 1:25 diluted samples from MULTICOV-AB, were further diluted to 1:200 in ACE2 buffer(2), which contains 300 ng/mL biotinylated ACE2. Samples were then mixed 1:1 with 1x VOC bead mix in 96 well plates and incubated for 2 hours in darkness on a thermomixer (750 rpm, 20°C). Following this initial incubation, samples were washed to remove unbound ACE2 using an automated magnetic plate washer. Bound ACE2 was detected by adding 2 µg/mL RPE-labelled streptavidin and incubating for a further 45 mins. After washing to remove unbound fluorophores, beads were resuspended in 100 µL washing buffer and shaken for 3 mins at 1000 rpm. Plates were measured once on a FLEXMAP3D instrument (No Timeout, Gate 7500-15000, Reporter Gain Standard PMT, 50 events). As controls, 3 wells with 150 ng/mL ACE2, 2 blank wells and 3 wells with a QC sample were included. ACE2 binding inhibition was calculated as a percentage, with 100% indicating maximum ACE2 binding inhibition and 0% indicating no ACE2 binding inhibition. Samples with an ACE2 binding inhibition less than 20% are classified as non-responders(2).

Biolayer Interferometry (BLI)

Purified RBD_{wt}, RBD_{δ}, RBD_{oBA1} and RBD_{oBA2} were biotinylated with Sulfo-NHS-LC-LC-Biotin (Thermo Fisher Scientific) in 5 molar excess at ambient temperature for 30 min. Excess of biotin was removed by size exclusion chromatography using Zeba™

Spin Desalting Columns 7K MWCO 0.5 ml (Thermo Fisher Scientific) according to the manufacturer's protocol. Analysis of binding kinetics of RBD specific antibodies in serum samples were performed using the Octet RED96e system (Sartorius) as per the manufacturer's recommendations. In brief, 5 µg/ ml of each biotinylated RBD diluted in Octet buffer (PBS, 0.1% BSA, 0.02% Tween20) was immobilized on streptavidin coated biosensor tips (SA, Sartorius) for 20 s. In the association step, serum samples at a 1:100 dilution were reacted for 720 s followed by dissociation in Octet buffer for 1200 s. Every run was normalized to a healthy control sample (pre-pandemic) lacking RBD specific antibodies and for each sample technical duplicates (n = 2) were performed. Data were analyzed using the Octet Data Analysis HT 12.0 software applying the 1:1 fitting model for the dissociation step. The binding profile response of each sample is illustrated as the mean wavelength shift in nm. Binding kinetics for ACE2 were performed by immobilizing 5 µg/ ml of each biotinylated RBD diluted in Octet buffer on streptavidin coated biosensor tips (SA, Sartorius) for 20 s. Dilution series ranging from 50 to 6.25 nM of ACE2 (Sino Biological) were applied for 300 s and one reference was included per run, followed by a dissociation step in Octet buffer (480s). For affinity determination, the 1:1 global fit of the Data Analysis HT 12.0 software was used.

Data Analysis

Data was collated and matched to metadata in Excel 2016. Data visualisation was done in RStudio (Version 1.2.5001 running R version 3.6.1). Additional packages "gplots" and "beeswarm" were used for specific displays. The "lm" function of R's "stats" library was used for linear regression analyzes. Correlation analyzes were performed using the "cor" function of R's "stats" library. The "wilcox.test" function from R's "stats" library was used to perform both Mann-Whitney-U Tests (two-sided) in order to estimate significance of observed differences between different groups, and

Wilcoxon Signed Rank Analysis (two-sided) to estimate the significance of observed differences between antigens for the same samples. Graphs were exported from RStudio and further edited in Inkscape (Version 0.92.4) to generate final figures. Biolayer inferometry graphical representation was prepared using GraphPad Prism Software (Version 9.0.0).

Supplementary Figures

Supplementary Figure 1: **Binding kinetics of RBD specific antibodies from serum samples of vaccinated and convalescent individuals.**

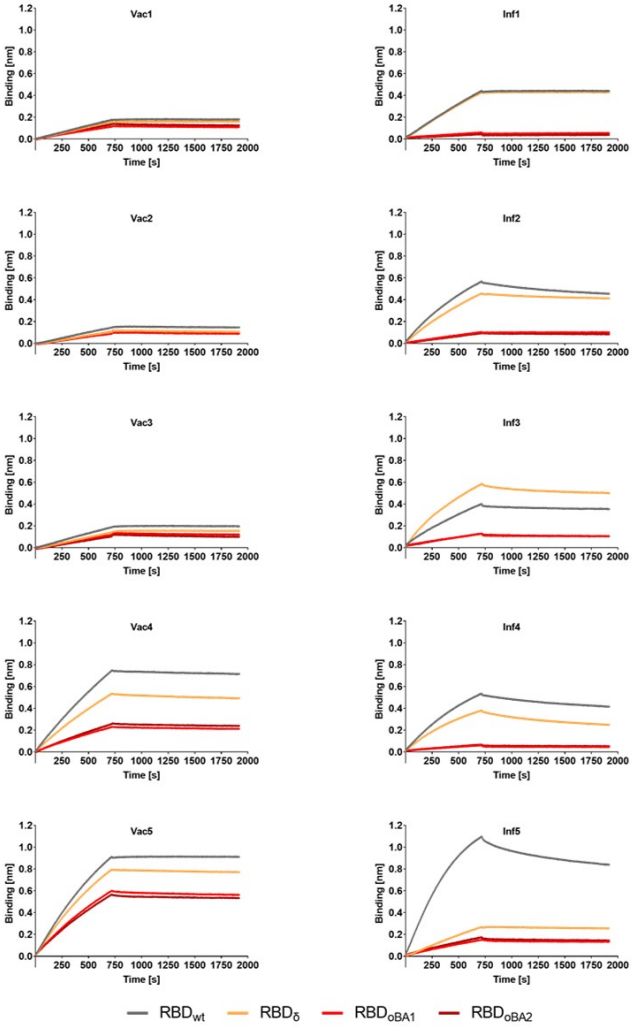

Biotinylated RBD_{wt}, RBD_{δ}, RBD_{oBA1}, RBD_{oBA2} were immobilized on streptavidin biosensor tips and binding kinetics of serum samples from vaccinated (n = 5, Vac) and convalescent (n =5, Inf) individuals were analyzed using BLI. All sensograms are illustrated as mean of technical duplicates (n = 2).

Supplementary Figure 2: **Binding kinetics of ACE2 to RBD_{wt}, RBD_{δ}, RBD_{oBA1} and RBD_{oBA2} using BLI.**

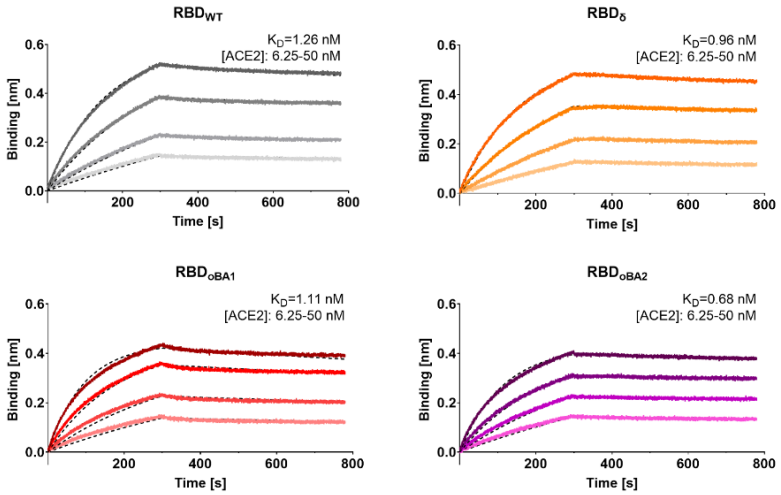

	K_D [nM]	k_{on} [10^5 M^{-1} s^{-1}]	k_{off} [10^{-4} s^{-1}]
RBD_{wt}	1.26 ± 0.01	1.37 ± 0.00	1.72 ± 0.01
RBD_{δ}	0.96 ± 0.01	1.24 ± 0.00	1.19 ± 0.01
RBD_{oBA1}	1.11 ± 0.01	2.10 ± 0.01	2.32 ± 0.02
RBD_{oBA2}	0.68 ± 0.01	1.75 ± 0.00	1.19 ± 0.02

For biolayer interferometry (BLI)-based affinity measurements, biotinylated RBD_{wt}, RBD_{δ}, RBD_{oBA1} and RBD_{oBA2} were immobilized on streptavidin biosensors. Kinetic measurements were performed using four concentrations of purified ACE2 ranging from 6.25 nM to 50 nM (illustrated with gradually lighter shades). The table summarizes affinities (K_D), association (k_{on}), and dissociation constants (k_{off}) of ACE2 determined for the different RBD variants.

Supplementary Figure 3: **IgG binding capacity and ACE2 binding inhibition for vaccinated samples towards BA1**.

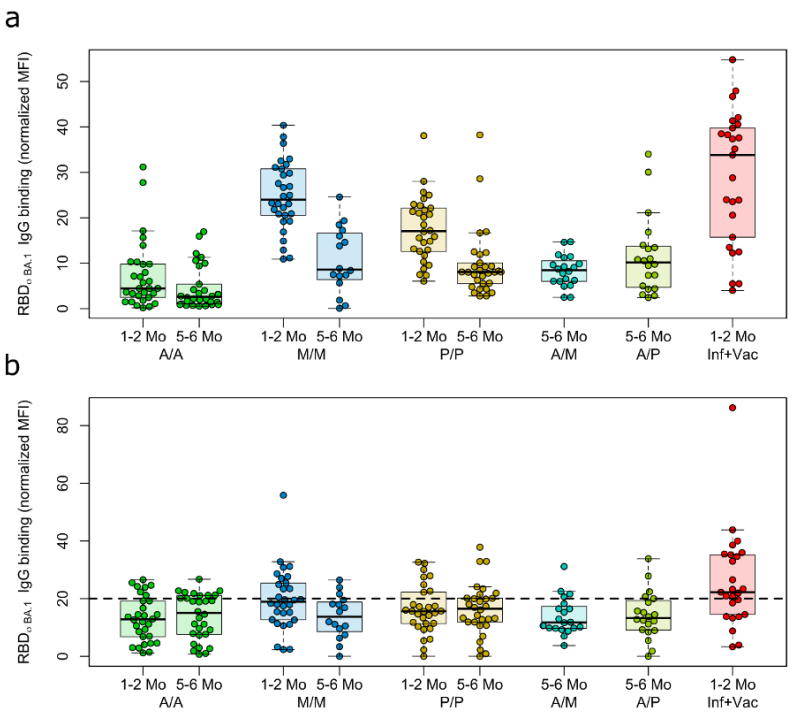

Binding response towards omicron was analyzed by either MULTICOV-AB (a) or RBDCoV-ACE2 (b) for samples from different vaccine schemes (n=30 for all sample groups, except for mRNA-1273 5-6 months (n=16), heterologous vaccine schemes (both n=20) and infected and vaccinated (Inf+vac, n=25). To determine the effect of time post-vaccination, samples from both 1-2 months and 5-6 months post-vaccination were included. A/A = AZD1222. M/M = mRNA-1273. P/P = BNT162b2. A/M = first dose AZD1222, second dose mRNA-1273. A/P = first dose AZD1222, second dose BNT162b2. Boxes represent the median, 25th and 75th percentiles, whiskers show the largest and smallest non-outlier values. Outliers were determined

by 1.5 IQR. The 20% cut off for non-responders is indicated by the dashed line on b.

The equivalent data for BA2 is shown in the main manuscript file as Figure 3.

Supplementary Figure 4: **Differences in IgG binding response and ACE2 binding inhibition towards BA1 among different populations of convalescent samples.**

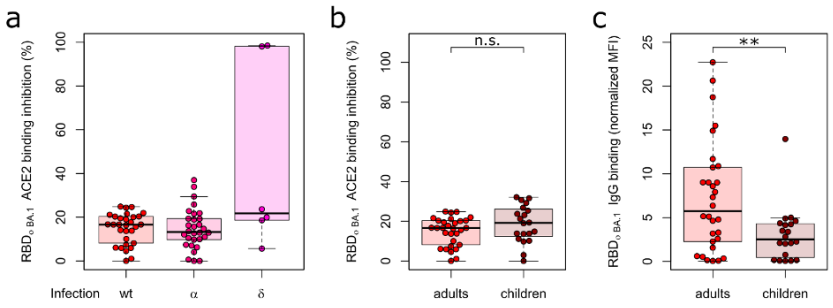

Comparative ACE2 binding inhibition (a and b) and IgG binding capacity (c) between convalescent samples from different pandemic waves (a) and adults and children (b and c) for Omicron BA1. (a) ACE2 binding inhibition towards BA1 for individuals infected with WT (n=30), alpha (n=30) or delta (n=6). (b) There is no significant difference (p=0.18) in ACE2 binding inhibition between adults (n=30) and children (n=20). (c) Adults have significantly higher IgG binding capacity (p=0.01) towards BA1 than children. Boxes represent the median, 25th and 75th percentiles, whiskers show the largest and smallest non-outlier values. Outliers were determined by 1.5 IQR. Statistical significance was calculated by two-sided Mann-Whitney U.

Supplementary Table 1: **Median fold reduction in IgG binding capacity from wild-type to respective variant**

Group	Vaccinated	Convalescent
WT	1	1
alpha	1.19 (1.06 – 1.32)	1.17 (0.95 – 1.39)
beta	2.84 (1.80 – 3.88)	3.46 (1.24 – 5.67)
gamma	1.65 (1.17 – 2.13)	1.96 (1.03 – 2.90)
delta	1.21 (1.03 – 1.38)	1.25 (0.95 – 1.55)
omicron BA1	2.32 (0.96 – 3.68)	4.09 (1.31 – 6.87)
omicron BA2	2.14 (0.96 – 3.32)	2.99 (0.93 – 5.05)
lambda	1.73 (1.24 – 2.20)	2.03 (1.29 – 2.76)
mu	3.01 (1.60 – 4.42)	3.62 (1.25 – 5.99)

Median fold change in reduction towards WT for all other variants included within the MULTICOV-AB assay. The IQR is shown in brackets. Values are shown for both vaccinated (n=226) and convalescent (n=86) samples. WT – wild-type (B.1. isolate).

Supplementary Table 2: **Median fold reduction in IgG binding capacity from omicron BA1 to respective variant**

Group	Vaccinated	Convalescent
WT	2.32 (0.96 – 3.68)	4.09 (1.31 – 6.87)
alpha	1.91 (0.85 – 2.96)	3.16 (0.40 – 5.91)
beta	0.83 (0.62 – 1.04)	0.99 (0.67 – 1.32)
gamma	1.39 (0.97 – 1.81)	1.76 (1.07 – 2.45)
delta	1.91 (1.03 – 2.80)	3.00 (1.27 – 4.73)
omicron BA1	1	1
omicron BA2	1.10 (1.03 – 1.17)	1.18 (1.02 – 1.34)
lambda	1.31 (0.79 – 1.83)	1.69 (0.73 – 2.66)
mu	0.78 (0.57 – 1.00)	0.94 (0.50 – 1.38)

Median fold change in reduction towards omicron BA1 for all other variants included within the MULTICOV-AB assay. The IQR is shown in brackets. Values are shown for both vaccinated (n=226) and convalescent (n=86) samples. WT – wild-type (B.1. isolate).

Supplementary Table 3: **Median fold reduction in IgG binding capacity from omicron BA2 to respective variant**

Group	Vaccinated	Convalescent
WT	2.13 (0.95 – 3.32)	2.99 (0.93 – 5.05)
alpha	1.72 (0.86 – 2.58)	2.47 (0.53 – 4.41)
beta	0.76 (0.58 – 0.93)	0.84 (0.63 – 1.04)
gamma	1.26 (0.91 – 1.61)	1.45 (0.90 – 2.00)
delta	1.71 (1.00 – 2.43)	2.30 (0.87 – 3.74)
omicron BA1	0.91 (0.85 – 0.97	0.85 (0.73 – 0.96)
omicron BA2	1	1
lambda	1.18 (0.74 – 1.62)	1.32 (0.62 – 2.01)
mu	0.72 (0.54 – 0.90)	0.80 (0.52 – 1.09)

Median fold change in reduction towards omicron BA2 for all other variants included within the MULTICOV-AB assay. The IQR is shown in brackets. Values are shown for both vaccinated (n=226) and convalescent (n=86) samples. WT – wild-type (B.1. isolate).

Supplementary Table 4: **Statistical significance between variants for IgG binding capacity**

	WT	alpha	beta	gamma	delta	omicron BA1	omicron BA2	lambda	mu
WT		2.37×10^{-50}	2.50×10^{-55}	4.75×10^{-54}	1.76×10^{-49}	4.72×10^{-55}	6.86×10^{-54}	3.06×10^{-55}	2.35×10^{-55}
alpha			7.46×10^{-54}	1.88×10^{-53}	7.87×10^{-4}	1.56×10^{-54}	1.05×10^{-52}	3.75×10^{-55}	2.35×10^{-55}
beta				6.05×10^{-54}	2.35×10^{-55}	8.75×10^{-21}	1.06×10^{-39}	9.28×10^{-53}	6.44×10^{-10}
gamma					2.74×10^{-49}	1.55×10^{-52}	7.59×10^{-45}	4.08×10^{-16}	3.34×10^{-54}
delta						4.46×10^{-55}	1.61×10^{-52}	2.35×10^{-55}	2.35×10^{-55}
omicron BA1							1.26×10^{-50}	6.04×10^{-44}	5.68×10^{-24}
omicron BA2								6.01×10^{-23}	4.47×10^{-39}
lambda									2.14×10^{-53}
mu									

Statistical analysis as determined by Wilcoxon Signed Rank between all variants for IgG binding capacity. WT – wild-type (B.1. isolate).

Supplementary Table 5: **Median ACE2 binding inhibition of the respective variant**

Group	Vaccinated	Convalescent
WT	26.11 (38.7)	27.25 (45.55)
alpha	20.63 (30.37)	30.23 (36.32)
beta	11.38 (18.48)	8.87 (14.52)
gamma	10.81 (17.34)	9.41 (17.19)
delta	16.67 (27.97)	15.72 (34.75)
omicron BA1	15.26 (11.26)	16.44 (11.54)
omicron BA2	8.03 (9.92)	10.88 (12.65)
lambda	18.79 (33.09)	16.13 (27.63)
mu	9.12 (15.08)	8.07 (12.16)

Median ACE2 binding inhibition for all RBD variants included within the RBDCoV-ACE2 assay. The IQR is shown in brackets. Values are shown for both vaccinated (n=226) and convalescent (n=86) samples. WT – wild-type (B.1. isolate).

Supplementary Table 6**: Responder rate for different variants**

	WT	alpha	beta	gamma	delta	BA1	BA2	lambda	mu
Infected	54 (63)	51 (59)	19 (22)	22 (26)	38 (44)	28 (33)	12 (14)	34 (40)	17 (20)
Vaccinated	142 (63)	116 (51)	70 (31)	68 (30)	98 (43)	68 (30)	19 (8)	107 (47)	51 (23)
Negative	0 (0)	0 (0)	0 (0)	0 (0)	0 (0)	0 (0)	0 (0)	0 (0)	0 (0)

Samples were classified as responsive based on having an ACE2 binding inhibition greater than 20% within the RBDCoV-ACE2 assay. Number of samples classified as responsive is shown, with this displayed as a percentage of all samples of this type in brackets. Values are shown for both vaccinated (n=226), convalescent (n=86) and negative (n=15) samples. WT – wild-type (B.1. isolate).

Supplementary Table 7: **Statistical significance between variants for ACE2 binding inhibition**

	WT	alpha	beta	gamma	delta	omicron BA1	omicron BA2	lambda	mu
WT		0.04	8.40×10^{-17}	7.22×10^{-18}	2.12×10^{-6}	3.99×10^{-11}	5.99×10^{-29}	4.00×10^{-5}	2.76×10^{-23}
alpha			2.58×10^{-12}	3.44×10^{-13}	2.24×10^{-3}	6.88×10^{-6}	8.97×10^{-24}	0.02	8.16×10^{-19}
beta				0.77	2.77×10^{-4}	1.20×10^{-6}	0.02	1.70×10^{-5}	0.04
gamma					8.97×10^{-5}	5.61×10^{-7}	0.03	4.61×10^{-6}	0.09
delta						0.53	1.12×10^{-10}	0.50	5.10×10^{-8}
omicron BA1							1.46×10^{-20}	0.15	2.92×10^{-13}
omicron BA2								8.82×10^{-13}	0.95
lambda									1.12×10^{-9}
mu									

Statistical analysis as determined by Wilcoxon Signed Rank between all variants for ACE2 binding inhibition. WT – wild-type (B.1. isolate).

Supplementary Table 8: **Summary of the binding response and dissociation constant (k_{off}) of the individual serum samples.**

	Response [nm]				Dissociation constant k_{off} [10^{-5} s^{-1}]			
	RBD_{wt}	**$RBD_{δ}$**	**RBD_{oBA1}**	**RBD_{oBA2}**	**RBD_{wt}**	**$RBD_{δ}$**	**RBD_{oBA1}**	**RBD_{oBA2}**
Vac1	0.175 ± 0.008	0.154 ± 0.018	0.113 ± 0.002	0.134 ± 0.007	0.010 ± 0.000	0.010 ± 0.000	6.565 ± 1.280	8.205 ± 2.326
Vac2	0.143 ± 0.005	0.104 ± 0.005	0.089 ± 0.004	0.105 ± 0.008	3.895 ± 0.148	7.880 ± 1.824	10.405 ± 0.841	9.965 ± 1.605
Vac3	0.186 ± 0.011	0.139 ± 0.002	0.117 ± 0.000	0.101 ± 0.004	0.010 ± 0.000	0.010 ± 0.000	8.660 ± 0.014	14.950 ± 2.192
Vac4	0.741 ± 0.034	0.531 ± 0.020	0.227 ± 0.003	0.254 ± 0.003	3.080 ± 0.170	6.050 ± 0.269	6.325 ± 0.375	6.420 ± 0.141
Vac5	0.908 ± 0.019	0.791 ± 0.045	0.596 ± 0.066	0.562 ± 0.038	0.010 ± 0.000	2.200 ± 0.099	4.165 ± 0.120	3.110 ± 0.863
Inf1	0.439 ± 0.009	0.425 ± 0.072	0.059 ± 0.004	0.044 ± 0.003	0.010 ± 0.000	0.181 ± 0.242	0.010 ± 0.000	0.010 ± 0.000
Inf2	0.565 ± 0.015	0.456 ± 0.011	0.103 ± 0.006	0.092 ± 0.007	16.700 ± 0.141	7.630 ± 0.184	0.010 ± 0.000	7.125 ± 1.167
Inf3	0.399 ± 0.072	0.581 ± 0.099	0.126 ± 0.025	0.128 ± 0.014	5.635 ± 0.502	10.050 ± 0.071	4.105 ± 1.082	9.115 ± 0.092
Inf4	0.534 ± 0.019	0.380 ± 0.039	0.060 ± 0.002	0.067 ± 0.001	18.750 ± 0.212	32.350 ± 0.354	5.185 ± 3.882	7.245 ± 0.926
Inf5	1.094 ± 0.025	0.267 ± 0.010	0.149 ± 0.014	0.174 ± 0.000	18.800 ± 0.283	4.315 ± 0.516	6.240 ± 1.541	8.025 ± 2.157

Binding kinetics of serum samples from (n = 5, Vac) and convalescent (n =5, Inf) individuals to the different RBD variants were analyzed using BLI. Binding response and dissociation constant (k_{off}) determined by the 1:1 fitting model of the individual serum samples were summarized as mean ± SD.

Supplementary Table 9: **Differences in response rate towards the Spike and RBD for BA1 and WT**

	Spike WT	Spike BA1	RBD WT	RBD BA1
Convalescent	37 (43)	3 (3)	54 (63)	28 (33)
Vaccinated	78 (35)	11 (5)	142 (63)	68 (30)
Negative	0 (0)	0 (0)	0 (0)	0 (0)

Samples were classified as responsive based on having an ACE2 binding inhibition greater than 20% within the RBDCoV-ACE2 assay. Number of samples classified as responsive is shown, with this displayed as a percentage of all samples of this type in brackets. Values are shown for both vaccinated (n=226), convalescent (n=86) and negative (n=15) samples. WT – wild-type (B.1. isolate).

References

1. Becker M, Strengert M, Junker D, Kaiser PD, Kerrinnes T, Traenkle B, et al. Exploring beyond clinical routine SARS-CoV-2 serology using MultiCoV-Ab to evaluate endemic coronavirus cross-reactivity. Nature Communications. 2021;12(1):1152.

2. Junker D, Dulovic A, Becker M, Wagner TR, Kaiser PD, Traenkle B, et al. COVID-19 patient serum less potently inhibits ACE2-RBD binding for various SARS-CoV-2 RBD mutants. medRxiv. 2021:2021.08.20.21262328.

3. Becker M, Dulovic A, Junker D, Ruetalo N, Kaiser PD, Pinilla YT, et al. Immune response to SARS-CoV-2 variants of concern in vaccinated individuals. Nature Communications. 2021;12(1):3109.

Appendix VII: Diminishing Immune Responses against Variants of Concern in Dialysis Patients 4 Months after SARS-CoV-2 mRNA Vaccination

Dulovic A*, Strengert M*, Ramos GM*, Becker M, Griesbaum J, **Junker D**, Lürken K, Beigel A, Wrenger E, Lonnemann G, Cossmann A, Stankov MV, Dopfer-Jablonka A, Kaiser PD, Traenkle B, Rothbauer U, Krause G, Schneiderhan-Marra N, Behrens GMN.

Emerging Infectious Diseases. 2023. 76(3):e240-e249

https://doi.org/10.3201/eid2804.211907

Diminishing Immune Responses against Variants of Concern in Dialysis Patients 4 Months after SARS-CoV-2 mRNA Vaccination

Alex Dulovic,[1] Monika Strengert,[1] Gema Morillas Ramos,[1] Matthias Becker, Johanna Griesbaum, Daniel Junker, Karsten Lürken, Andrea Beigel, Eike Wrenger, Gerhard Lonnemann, Anne Cossmann, Metodi V. Stankov, Alexandra Dopfer-Jablonka, Philipp D. Kaiser, Bjoern Traenkle, Ulrich Rothbauer, Gérard Krause,[2] Nicole Schneiderhan-Marra,[2] Georg M.N. Behrens[2]

Patients undergoing chronic hemodialysis were among the first to receive severe acute respiratory syndrome coronavirus 2 (SARS-CoV-2) vaccinations because of their increased risk for severe coronavirus disease and high case-fatality rates. By using a previously reported cohort from Germany of at-risk hemodialysis patients and healthy donors, where antibody responses were examined 3 weeks after the second vaccination, we assessed systemic cellular and humoral immune responses in serum and saliva 4 months after vaccination with the Pfizer-BioNTech BNT162b2 vaccine using an interferon-γ release assay and multiplex-based IgG measurements. We further compared neutralization capacity of vaccination-induced IgG against 4 SARS-CoV-2 variants of concern (Alpha, Beta, Gamma, and Delta) by angiotensin-converting enzyme 2 receptor-binding domain competition assay. Sixteen weeks after second vaccination, compared with 3 weeks after, cellular and humoral responses against the original SARS-CoV-2 isolate and variants of concern were substantially reduced. Some dialysis patients even had no detectable B- or T-cell responses.

Persistence of vaccination-induced cellular and humoral immune responses is crucial to prevent severe acute respiratory syndrome coronavirus 2 (SARS-CoV-2) infection or at least provide protection against severe coronavirus disease (COVID-19) that requires hospitalization. As in many other countries, the SARS-CoV-2 vaccination strategy in Germany was based on prioritization by occupation, underlying medical conditions, or advanced age (*1*). Although those priority groups have been vaccinated, a debate has emerged as to whether a third booster dose may be necessary to maintain or raise levels of protection within some of these groups. Decisions on whether to recommend a third dose needed to be made within a short timeframe, because SARS-CoV-2 infection case numbers were expected to increase again in the upcoming cold season, as previously observed in late 2020 (*2*). To date, however, data are lacking regarding the longevity of vaccination responses, and most published studies only provide follow-up data until 3 months after the second dose (*3*). Only 2 studies report data on extended time frames of 6 months after a completed 2-dose scheme (*4*,*5*), and, to our knowledge, no studies have considered follow-ups in patients receiving chronic hemodialysis. Data on the actual effect of a third dose are equally scarce and, so far, limited to organ transplant recipients, where a third dose substantially increased antibody

Author affiliations: University of Tübingen Natural and Medical Sciences Institute, Reutlingen, Germany (A. Dulovic, M. Becker, J. Griesbaum, D. Junker, P.D. Kaiser, B. Traenkle, U. Rothbauer, N. Schneiderhan-Marra); Helmholtz Centre for Infection Research, Braunschweig, Germany (M. Strengert, G. Krause); TWINCORE GmbH Centre for Experimental and Clinical Infection Research, Hannover, Germany (M. Strengert, G. Krause); Hannover Medical School, Hannover (G. Morillas Ramos, A. Cossmann, M.V. Stankov, A. Dopfer-Jablonka, G.M.N. Behrens); Dialysis Centre Eickenhof, Langenhagen, Germany (K. Lürken, A. Beigel, E. Wrenger, G. Lonnemann); German Centre for Infection Research, Hannover–Braunschweig, Germany (A. Dopfer-Jablonka, G. Krause, G.M.N. Behrens); University of Tübingen Pharmaceutical Biotechnology, Tübingen (U. Rothbauer); Centre for Individualized Infection Medicine, Hannover (G.M.N. Behrens)

DOI: https://doi.org/10.3201/eid2804.211907

[1]These authors contributed equally to this article.
[2]These authors contributed equally to this article.

responses (*6*). In addition, protection offered by first-generation vaccines is reduced for SARS-CoV-2 variants of concern (VOCs) (*7*), which now account for most infections worldwide (*8*), making the decision of whether a third dose is advisable even more critical for those with underlying conditions, immunodeficiencies, or an increased exposure risk (e.g., healthcare workers).

One particular risk group for SARS-CoV-2 infection and severe COVID-19 disease is hemodialysis patients; currently, ≈80,000 persons requiring regular renal replacement therapy in Germany (*9*). Their various underlying medical conditions and dialysis therapy often lead to a state of generalized immunosuppression (*10*). At the same time, these patients bear a continuous exposure risk because of the regular need for in-center hemodialysis therapy, which prevents them from self-isolating or reducing contacts to avoid infection. We and others have identified impaired cellular and humoral responses towards several viral vaccinations (e.g., SARS-CoV-2, influenza A, or hepatitis B) (*10*–*13*); however, there is a lack of longitudinal vaccination response studies against SARS-CoV-2 within this population. To guide future vaccination strategies as to whether additional booster vaccinations for at-risk groups to prevent severe COVID-19 are required, we provide follow-up data for a previously reported cohort of 76 persons receiving hemodialysis and 23 healthcare workers with no underlying conditions (*13*) for systemic and mucosal B- and T-cell responses 16 weeks after full BNT162b2 vaccination and the neutralizing potency of vaccination-induced antibodies. Because of the emergence of VOCs, and because all currently licensed vaccines are formulated against the original wild-type isolate (B.1), we also examined antibody binding and neutralization toward the Alpha (B.1.1.7), Beta (B.1.351), Gamma (P.3) and Delta (B.1.617.2) VOCs.

Methods

Study Design and Sample Collection

We collected blood samples by using vascular access before the start of dialysis or by venipuncture for the control population 16 weeks after the standard 2-dose vaccination with a 21-day interval of BNT162b2 (Pfizer-BioNTech, https://www.pfizer.com) was completed (T2). An analysis of samples from this population that were collected 3 weeks after the second dose of BNT162b2 (T1) has been published previously (*13*). A total of 76 patients on maintenance hemodialysis and 23 healthcare workers from the same dialysis center participated in the longitudinal follow-up (*13*). Demographic characteristics (e.g., age and sex), body mass index, time on dialysis, use of immunosuppressive medications, and anti-S1 domain IgG levels at T1 of persons who did not provide a sample at T2 were not substantially different compared with persons included in this analysis (Table; Appendix Table 1, 2, https://wwwnc.cdc.gov/EID/article/28/4/21-1907-App1.pdf). We obtained plasma by using an S-Monovette lithium heparin blood collection kit (Sarstedt, https://www.sarstedt.com). We used whole-blood samples immediately for an interferon-γ (IFN-γ) release assay (IGRA). To inactivate potential pathogens, we treated collected saliva samples with Tri (n-butyl) phosphate for a final concentration of 0.3% and Triton X-100 for a final concentration of 1%.

Ethics Considerations

The study was approved by the Internal Review Board of Hannover Medical School (approval number

Table. Characteristics of participants in a study of immune response against variants of concern in dialysis patients 4 months after SARS-CoV-2 mRNA vaccination*

Characteristic	Nondialysis control group	Hemodialysis group	p value for difference between groups
No. (%) patients	23 (100)	76 (100)	NA
Median age, y (IQR)	55 (14)	70.5 (18.25)	2.78×10^{-9}
Sex			1.01×10^{-2}†
M	6 (26.09)	43 (56.58)	
F	17 (73.91)	33 (43.42)	
Median days since start of hemodialysis (IQR)	NA	1,337 (1,686.5)	NA
Using immunosuppressive medication	0	10 (13.16)	6.77×10^{-2}
Underlying condition			
Obesity, BMI >30‡	4 (17.39)	16 (21.05)	8.68×10^{-1}
Diabetes mellitus	0	19 (25)	7.30×10^{-3}
Cardiovascular disease	0	35 (46.05)	2.93×10^{-5}

*Values are no. (%) except as indicated. Percentages are for total group. BMI, body mass index; IQR, interquartile range; NA, not applicable; SARS-CoV-2, severe acute respiratory syndrome coronavirus 2.
†p value reflects difference in male-to-female ratios between the two groups, not differences explicitly for either male or female persons.
‡BMI for 1 person was not known.

8973_BO-K_2020). We obtained written informed consent from all participants before the start of the study.

Bead Coupling

We coupled antigens to spectrally distinct MagPlex beads (Luminex, https://www.luminexcorp.com) by using EDC/s-NHS coupling for all standard (MULTICOV-AB) antigens (*14*). We coupled receptor-binding domains (RBDs) from VOCs by using Anteo coupling (AnteoTech, https://www.anteotech.com) according to the manufacturer's instructions (*15*).

MULTICOV-AB

We analyzed IgG and IgA binding and levels by using MULTICOV-AB, a multiplex coronavirus immunoassay, as previously described (14). For our study, we used a panel of recombinant proteins as antigens (Appendix Table 3). In brief, we immobilized antigens on spectrally distinct populations of MagPlex beads either by EDC/s-NHS coupling (*14*) or by Anteo coupling according to the manufacturer instructions (*15*). We then incubated the combined MagPlex beads with samples. After conducting a wash step to remove unbound antibodies, we detected IgG or IgA with either R-phycoerythrin labeled goat anti-human IgG (Jackson ImmunoResearch, https://www.jacksonimmuno.com) or IgA (Jackson ImmunoResearch) as secondary antibodies. After conducting another wash step and bead resuspension, we measured samples once on a FLEXMAP 3D instrument (Luminex) by using the following settings: timeout, 80 s; gate, 7,500–15,000; reporter gain, standard photomultiplier tube; 40 events. Raw median fluorescence intensity (MFI) values or normalized values (MFI/MFI of quality control [QC] samples) (*15*) are reported. Three QC samples were measured per individual plate to monitor MULTICOV-AB performance. We measured all samples once.

Angiotensin-Converting Enzyme 2 Receptor Binding Domain Competition Assay

We carried out an angiotensin-converting enzyme 2 receptor-binding domain (ACE2-RBD) competition assay as previously described (*15*; D. Junker et al., unpub. data, https://doi.org/10.1101/2021.08.20.21262328) to determine IgG neutralization capacity against SARS-CoV-2 wild-type and the VOCs. For this assay, we combined biotinylated ACE2 with individual samples (and as a control, ACE2 alone) and incubated with the previously described MULTICOV-AB bead mix. Before and after ACE2 detection with Streptavidin-PE (Moss, Fisher Scientific, https://www.fishersci.com), we conducted washes. We measured samples once on a FLEXMAP 3D instrument with the same settings as MULTICOV-AB and analyzed them by using normalization of MFI values against the control. We considered samples with a neutralization ratio <0.2 as nonneutralizing. This cutoff is based on comparison to a classic virus neutralization test (D. Junker et al., unpub. data).

Euroimmun ELISA QuantiVac

As a control for the MULTICOV-AB results, we also analyzed plasma samples by using the Anti-SARS-CoV-2 QuantiVac ELISA IgG (Euroimmun, https://www.euroimmun.com). Samples were measured as previously described (*13*). We measured all samples once.

IGRA

We analyzed SARS-CoV-2–specific T-cell responses from whole blood by measuring IFN-γ production after stimulation with a peptide pool from the SARS-CoV-2 spike S1 with the SARS-CoV-2 Interferon Gamma Release Assay (Euroimmun) and the IFN-γ ELISA (Euroimmun), as previously described (*13*). We subtracted background signals from negative controls and calculated final results in milli-IU (mIU) per milliliter by using standard curves. Results from positive and negative controls were not statistically significantly different between timepoints T1 and T2. We considered IFN-γ concentrations >200 mIU/mL as reactive. We defined this arbitrary cutoff by using average background IFN-γ activity without antigen-stimulation in all samples of T1 multiplied with 10 for the threshold for IGRA positive. Using this cutoff, we found negative IGRA results in all of the 15 control samples (prepandemic persons) (*16*). The upper limit of reactivity was 2,000 mIU/mL.

Data Analysis and Statistics

We matched sample metadata and collected results from different assay platforms in Microsoft Excel 2016 (https://www.microsoft.com). We used GraphPad Prism 8.4.3 (https://www.graphpad.com) for statistical analysis. We generated figures in RStudio 1.2.5001 running R 3.6.1 (https://www.rstudio.com). We used the beeswarm add-on package to visualize data as strip charts with overlaying boxplots and to create nonoverlaying datapoints and used the RcolorBrewer add-on to generate specific colors for plots. We then edited the figures by using Inkscape 0.92.4 (https://inkscape.org).

RESEARCH

Results

Substantial Decrease in Antibody Titers from 3 Weeks to 4 Months Postvaccination

Because antibody levels are considered a proxy for protection, we initially examined the seroreversion rate by using MULTICOV-AB (*14*), a previously published bead-based multiplex immunoassay that simultaneously analyses >20 different SARS-CoV-2 antigens, including the RBDs of VOCs and the endemic human coronaviruses. Similar to findings from our previous report (*13*), RBD IgG responses within the dialysis group (median normalized MFI 4.26 among 76 patients) toward SARS-CoV-2 wild-type RBD were significantly reduced compared with those for the control group (median normalized MFI 13.6 among 23 persons; p<0.001) (Figure 1, panel A) 16 weeks after complete vaccination (T2). Compared with titer levels at 3 weeks after the second dose (T1), at 16 weeks after (T2), antibody titers had significantly decreased, by 61% in the control group and 75% in the dialysis group (p<0.001) (Figure 1, panel A). RBD IgG levels measured by MULTICOV-AB were additionally verified with a commercial quantitative in vitro diagnostic antibody test (Spearman rank 0.956) (Appendix Figure 1). Although none of the samples of the control group were classified as seronegative (titer below the cutoff) (Appendix Figure 2), 19.7% (15/76) of dialysis samples were defined as such 16 weeks after the second dose (T2), which constitutes a substantial increase from 3 weeks after second vaccination (T1),

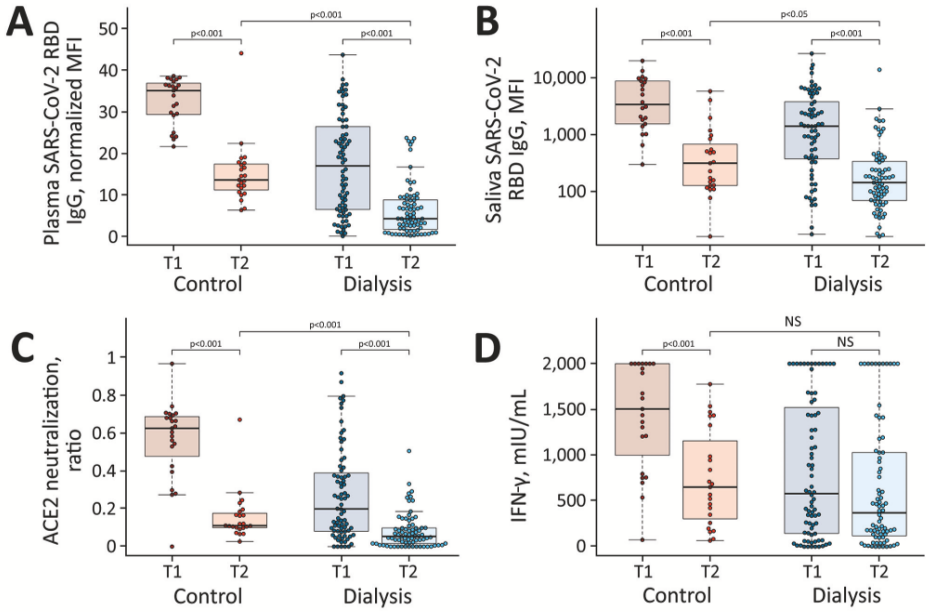

Figure 1. Significant decrease in humoral and cellular responses induced by Pfizer-BioNTech vaccine BNT162b2 (https://www.pfizer.com) against SARS-CoV-2 from 3 weeks to 16 weeks after second vaccination, observed in a study of immune response against variants of concern in dialysis patients 4 months after SARS-CoV-2 mRNA vaccination. A) IgG response in plasma; B) IgG response in saliva; C) neutralizing capacity toward SARS-CoV-2 wild type B.1; D) T-cell response measured by IFN-γ release assay. Blue circles indicate dialysis patients (n = 76) and red circles controls (n = 23). Samples were taken 3 weeks (T1) and 16 weeks (T2) after vaccination. Saliva (panel B) has reduced sample numbers in both groups because of issues in sample collection (T1 control, n = 22; T1 dialysis, n = 69; T2 control, n = 23; T2 dialysis. n = 71). T1 timepoint data has been published previously (*13*) and is reproduced here for clarity. Horizontal lines within boxes indicate medians; box tops and bottoms indicate the 25th and 75th percentiles; whiskers show the largest and smallest nonoutlier values. Outliers were determined by 1.5 times interquartile range. Statistical significance was calculated by Wilcoxon matched-pairs signed rank test when comparing T1 and T, and 2-sided Mann–Whitney–U test when comparing control and dialysis groups. ACE2, angiotensin-converting enzyme 2; IFN-γ, interferon γ; MFI; median fluorescence intensity; NS, not significant; RBD, receptor-binding domain; SARS-CoV-2, severe acute respiratory syndrome coronavirus 2; T1, timepoint 1; T2, timepoint 2.

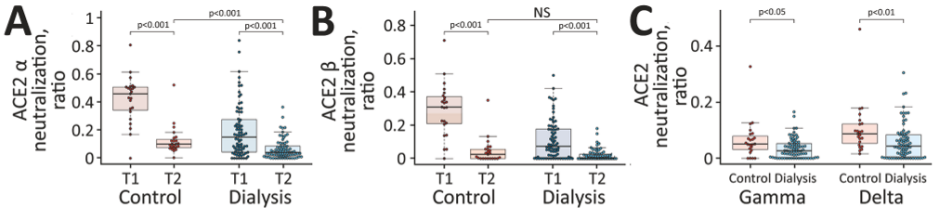

Figure 2. Reduced neutralizing capacity against SARS-CoV-2 variants of concern observed in a study of immune response against variants of concern in dialysis patients 4 months after SARS-CoV-2 mRNA vaccination. Neutralizing capacity of plasma IgG toward SARS-CoV-2 variants of concern Alpha (A), Beta (B), and Gamma and Delta (C) in the dialysis (blue circles, n = 76) and control (red circles, n = 23) groups 16 weeks after second vaccination with Pfizer-BioNTech vaccine BNT162b2 (https://www.pfizer.com). Neutralization capacity is displayed as ratio, where 1 indicates maximum neutralization and 0 no neutralization. Horizontal lines within boxes indicate medians; box tops and bottoms indicate the 25th and 75th percentiles; whiskers show the largest and smallest nonoutlier values. Outliers were determined by 1.5 times interquartile range. Statistical significance was calculated by 2-sided Mann–Whitney–U test. ACE2, angiotensin-converting enzyme 2; NS, not significant; SARS-CoV-2, severe acute respiratory syndrome coronavirus 2; T1, timepoint 1; T2, timepoint 2.

at which point only 5.3% (4/76) of samples were seronegative. When examining plasma titers against nucleocapsid, we did not observe any dialysis patients, other than one who had a PCR-confirmed infection before the first dose, having a value above the cutoff that would indicate infection.

To evaluate whether this reduction in plasma RBD IgG was also present at the mucosal site, we profiled the local antibody response in saliva by using MULTICOV-AB. As observed in plasma, a significant reduction occurred in saliva RBD IgG titers in the dialysis (median 143 among 71 patients) compared with the control group (median 313.5 among 23 persons) ($p = 0.02$) (Figure 1, panel B). When comparing saliva RBD IgG levels at T1 to those at T2, we observed a statistically significant decline in both groups ($p<0.001$) (Figure 1, panel B), suggesting that the antibodies have potentially lost competence to prevent transmission if infected. When examining RBD IgA, we observed a significant difference in titers between persons in the control and dialysis groups ($p = 0.003$) (Appendix Figure 3, panel A); 47.8% of controls and 75% of dialysis patients were classified as seronegative. This more pronounced reduction in IgA versus IgG levels most likely represents the shorter IgA half-life. Saliva RBD IgA tended to be higher in the dialysis group, although not significantly ($p = 0.051$) (Appendix Figure 3, panel B).

Decreased Neutralization Capacity as Time Postvaccination Increased

We next examined whether neutralization potential was also hindered because solid evidence exists on the protective role for neutralizing serum antibodies (*17*). By using an ACE2–RBD competition assay, which assesses neutralization potency toward SARS-CoV-2 wild-type and the circulating Alpha, Beta, Gamma, and Delta VOCs, we found that neutralization against wild-type SARS-CoV-2 RBD was significantly reduced in the dialysis group compared with the controls ($p<0.001$) (Figure 1, panel C) 16 weeks after complete vaccination. We found that 82.6% (19/23) of control samples and 89.5% (68/76) of dialysis patient samples were below the 0.2 threshold, which indicates the absence of neutralizing activity (Appendix Figure 2), a threshold is based on information provided for other available ACE2 competition assays (*18*). This difference represents a substantially significant reduction ($p<0.001$ for both groups) in neutralizing activity compared with 3 weeks after second vaccination, at which point only 4.3% (1/23) of the control samples and 50.0% (38/76) of the dialysis patient samples were below the threshold (Figure 1, panel C; Appendix Figure 2).

Reduced T-cell Response after Vaccination in Dialysis Patients and Decrease Over Time

Because some persons might be able to control and clear SARS-CoV-2 infections with a strong T-cell response alone, we examined spike-specific SARS-CoV-2 T-cell responses by using a commercially available IGRA. Although absolute mean IFN-γ responses in the dialysis group compared with the control group tended to be lower (median 370 vs. 651 mIU/mL), this difference was not significant ($p = 0.13$) (Figure 1, panel D). In the control group, IFN-γ release after restimulation declined significantly from the first timepoint (median 1,505; $p<0.001$) (Figure 1, panel D), whereas for dialysis patients, this decline was not significant (median 580; $p = 0.13$) (Figure 1, panel D). This difference is probably attributable to most control samples being at the assay's upper limit

of detection at the first timepoint, when the dialysis samples already showed reduced IFN-γ release. Overall, the number of nonresponders was higher in the hemodialysis group (40.8% [31/76]) than the control group (21.7% [5/23]) (Appendix Figure 2). A lack of serologic response appears to be more driven by T-cell immunity than B-cell immunity; 2.6% (2/76) of the dialysis group having a T-cell response but no B-cell response, compared with 23.6% (18/76) who had a B-cell response but no T-cell response. In total, 17.1% (13/76) of the dialysis group were classified as complete nonresponders because of the absence of detectable SARS-CoV-2 wild-type B- and T-cell responses, compared with none in the control group.

Significantly Reduced Antibody Binding and Neutralization Capacity against VOCs

Having characterized response against wild-type SARS-CoV-2, we then assessed humoral response against the VOCs Alpha, Beta, Gamma, and Delta. As shown with classical cell-culture based virus neutralization assays (*7*), neutralization responses were also reduced for all VOCs compared with wild-type when we used the previously described ACE2-RBD competition assay. Compared levels at with the initial timepoint, neutralization decreased significantly for the Alpha and Beta VOCs ($p<0.001$ for both) (Figure 2, panel A, B). We were unable to determine these changes for Gamma and Delta because these variants were not measured in the initial analysis. In a comparison between the dialysis and the control cohort, dialysis patients had significantly reduced neutralization against Alpha ($p<0.001$) (Figure 2, panel A), Gamma ($p = 0.014$) (Figure 2, panel C), and Delta ($p = 0.002$) (Figure 2, panel C) but not for Beta ($p = 0.08$) (Figure 2, panel B). The number of nonresponders was variable between the different strains although consistently high; 87.0% of the control group and 93.4% of the dialysis group were considered nonresponders against Alpha, 95.7% of the control group and 100% of the dialysis group against Beta and Gamma, and 95.7% of the control group and 96.1% of dialysis group against Delta.

Discussion

After our initial study (*13*), which focused on humoral and cellular responses 3 weeks after administering the second BNT162b2 vaccination, we provide longitudinal data for 4 months after the second dose. In comparison with other vaccine studies, which have mostly examined peak humoral response within 1 month or alternative prime-boost vaccination schedules with BNT162b2 (*12*), our data reveal a substantial decrease in the subsequent months in hemodialysis patients and healthy controls. Overall, the decline in neutralizing anti–spike RBD antibodies was comparable in both groups, and the difference between groups was mostly driven by differences in the magnitude of the initial humoral response. Although this decrease is expected and can be attributed to the memory phase, the extent of the reduction was unpredicted because it resulted in a substantial proportion of persons being classified as seronegative. The reduction of salivary antibodies is particularly important because their presence has been linked to reduced transmission potential (*15*). This pattern of reduced antibody binding with increasing time postvaccination was also reflected in diminishing neutralization potential.

Most persons tested were classified below our defined neutralization threshold for wild-type RBD with an almost complete nonresponder rate against Delta, which was the dominant strain in many parts of the world at the time of our analysis (*8*). Although this finding does not automatically translate to a failure of vaccine efficacy, given that any active challenge of the immune system should result in expansion of memory B- and T-cell populations along with increased (neutralizing) antibody titers, it does suggest nevertheless that active protection against infection may be reduced. Although a recent study by Pfizer (*4*) indicated that BNT162b2 vaccine efficacy did only slightly decrease 6 months postvaccination in the study cohort (from 95% to 91%) in fully immunocompetent persons, data from vaccinations in Israel identified a reduction in efficacy to 40% (*19*). In combination with our data, where 17.1% of the dialysis cohort were classified as having no evidence for vaccine-elicited T- and B-cell immunity after 4 months, the Pfizer study findings suggest that vaccine efficacy may be even further reduced within this patient group. For dialysis patients, this finding is particularly concerning because they often have underlying conditions that put them at additional risk for severe COVID-19 (*10*). The lack of a considerable SARS-CoV-2 specific T-cell response in dialysis patients may result from chronic inflammatory conditions, leading to T-cell exhaustion and suppression of IFN-γ levels (*20*). Differences in anti–SARS-CoV-2 T-cell kinetics between groups presumably reflect difference in the magnitude of T-cell responses after boost and during the contraction phase. To what extent T-cell immunity contributes to protection from COVID-19 and whether our IGRA results below a cutoff provide evidence for the lack of effective adaptive T-cell immunity, requires further investigation. However, we should state that

although we see reductions in titer, neutralizing activity, and T-cell responses, we did not see any new infections by T2 within our cohort.

Our study is limited by the relatively small sample size of persons, who were not matched by age or sex. However, the sample number and compromised matching is consistent with similar studies on dialysis vaccine responses (*12*). Although studies have indicated that differences exist in protection and antibody responses (*21*) after different COVID-19 vaccination schedules, our study of Pfizer's BNT162b2 represents a real-world situation for most dialysis patients. Because of reduced anti-spike responses 4 weeks postvaccination in patients with other chronic conditions (*6*), these groups should undergo careful monitoring to determine whether their responses also decrease substantially over time.

Taken together, our results strongly argue that all persons undergoing chronic hemodialysis should be preferably administered a third dose of the BNT162b2 vaccine. Recent studies on administering a third dose to dialysis patients and transplant recipients has identified strong increases in humoral responses after vaccination, and a reduced percentage of recipients are considered nonresponders (*22*–*25*). However, longitudinal follow-up studies will be needed in early 2022 to monitor the rate of antibody decay after administration of a third dose in these and other vulnerable groups.

Acknowledgments

We thank staff and participants at the Dialysis Centre Eickenhof for their continued support to make this study possible.

This work was financially supported by the Initiative and Networking Fund of the Helmholtz Association of German Research Centers (grant no. SO-96), the EU Horizon 2020 Research and Innovation Program (grant agreement no. 101003480–CORESMA), the State Ministry of Baden–Württemberg for Economic Affairs, Labor and, Tourism (grant nos. FKZ 3–4332.62-NMI-67 and FKZ 3–4332.62-NMI-68), and the European Regional Development Fund (Defeat Corona, grant no. ZW7–8515131). The funders had no role in study design, data collection, data analysis, interpretation, writing, or submission of the manuscript. All authors had complete access to the data and hold responsibility for the decision to submit for publication.

About the Author

Dr. Dulovic is a scientist in the Multiplex Immunoassay Group at the Natural and Medical Sciences Institute at the University of Tübingen. He has a background in molecular biology and genetics of parasitic nematodes and currently works on serologic assay development for a range of pathogens, including SARS-CoV-2, hepatitis virus, and influenza virus.

References

1. European Centre for Disease Control and Prevention. Overview of the implementation of COVID-19 vaccination strategies and deployment plans in the EU/EEA. 2021 [cited 2021 Aug 18]. https://www.ecdc.europa.eu/en/publications-data/overview-implementation-covid-19-vaccination-strategies-and-deployment-plans
2. Haab BB. Methods and applications of antibody microarrays in cancer research. Proteomics. 2003;3:2116–22. https://doi.org/10.1002/pmic.200300595
3. Ibarrondo FJ, Hofmann C, Fulcher JA, Goodman-Meza D, Mu W, Hausner MA, et al. Primary, recall, and decay kinetics of SARS-CoV-2 vaccine antibody responses. ACS Nano. 2021;15:11180–91. https://doi.org/10.1021/acsnano.1c03972
4. Thomas SJ, Moreira ED Jr, Kitchin N, Absalon J, Gurtman A, Lockhart S, et al.; C4591001 Clinical Trial Group. Safety and efficacy of the BNT162b2 mRNA Covid-19 vaccine through 6 months. N Engl J Med. 2021;385:1761–73. https://doi.org/10.1056/NEJMoa2110345
5. Doria-Rose N, Suthar MS, Makowski M, O'Connell S, McDermott AB, Flach B, et al.; mRNA-1273 Study Group. Antibody persistence through 6 months after the second dose of mRNA-1273 vaccine for Covid-19. N Engl J Med. 2021;384:2259–61. https://doi.org/10.1056/NEJMc2103916
6. Kamar N, Abravanel F, Marion O, Couat C, Izopet J, Del Bello A. Three doses of an mRNA Covid-19 vaccine in solid-organ transplant recipients. N Engl J Med. 2021;385:661–2. https://doi.org/10.1056/NEJMc2108861
7. Altmann DM, Boyton RJ, Beale R. Immunity to SARS-CoV-2 variants of concern. Science. 2021;371:1103–4. https://doi.org/10.1126/science.abg7404
8. Heyse S, Vogel H, Sänger M, Sigrist H. Covalent attachment of functionalized lipid bilayers to planar waveguides for measuring protein binding to biomimetic membranes. Protein Sci. 1995;4:2532–44. https://doi.org/10.1002/pro.5560041210
9. Girndt M, Trocchi P, Scheidt-Nave C, Markau S, Stang A. The prevalence of renal failure. Results from the German Health Interview and Examination Survey for Adults, 2008–2011 (DEGS1). Dtsch Arztebl Int. 2016;113:85–91.
10. Windpessl M, Bruchfeld A, Anders HJ, Kramer H, Waldman M, Renia L, et al. COVID-19 vaccines and kidney disease. Nat Rev Nephrol. 2021;17:291–3. https://doi.org/10.1038/s41581-021-00406-6
11. Schrezenmeier E, Bergfeld L, Hillus D, Lippert J-D, Weber U, Tober-Lau P, et al. Immunogenicity of COVID-19 tozinameran vaccination in patients on chronic dialysis. Front Immunol. 2021;12:690698. https://doi.org/10.3389/fimmu.2021.690698
12. Carr EJ, Wu M, Harvey R, Wall EC, Kelly G, Hussain S, et al.; Haemodialysis COVID-19 consortium; Crick COVID Immunity Pipeline. Neutralising antibodies after COVID-19 vaccination in UK haemodialysis patients. Lancet. 2021;398:1038–41. https://doi.org/10.1016/S0140-6736(21)01854-7
13. Strengert M, Becker M, Ramos GM, Dulovic A, Gruber J, Juengling J, et al. Cellular and humoral immunogenicity of a SARS-CoV-2 mRNA vaccine in patients on haemodialysis.

EBioMedicine. 2021;70:103524. https://doi.org/10.1016/j.ebiom.2021.103524
14. Becker M, Strengert M, Junker D, Kaiser PD, Kerrinnes T, Traenkle B, et al. Exploring beyond clinical routine SARS-CoV-2 serology using MultiCoV-Ab to evaluate endemic coronavirus cross-reactivity. Nat Commun. 2021;12:1152. https://doi.org/10.1038/s41467-021-20973-3
15. Becker M, Dulovic A, Junker D, Ruetalo N, Kaiser PD, Pinilla YT, et al. Immune response to SARS-CoV-2 variants of concern in vaccinated individuals. Nat Commun. 2021;12:3109. https://doi.org/10.1038/s41467-021-23473-6
16. Stankov MV, Cossmann A, Bonifacius A, Dopfer-Jablonka A, Ramos GM, Gödecke N, et al. Humoral and cellular immune responses against severe acute respiratory syndrome coronavirus 2 variants and human coronaviruses after single BNT162b2 vaccination. Clin Infect Dis. 2021;73:2000–8. https://doi.org/10.1093/cid/ciab555
17. Khoury DS, Cromer D, Reynaldi A, Schlub TE, Wheatley AK, Juno JA, et al. Neutralizing antibody levels are highly predictive of immune protection from symptomatic SARS-CoV-2 infection. Nat Med. 2021;27:1205–11. https://doi.org/10.1038/s41591-021-01377-8
18. Lopez E, Haycroft ER, Adair A, Mordant FL, O'Neill MT, Pymm P, et al. Simultaneous evaluation of antibodies that inhibit SARS-CoV-2 variants via multiplex assay. JCI Insight. 2021;6:e150012. https://doi.org/10.1172/jci.insight.150012
19. Ng JH, Ilag LL. Biochips beyond DNA: technologies and applications. Biotechnol Annu Rev. 2003;9:1–149. https://doi.org/10.1016/S1387-2656(03)09001-X
20. Hartzell S, Bin S, Cantarelli C, Haverly M, Manrique J, Angeletti A, et al. Kidney failure associates with T cell exhaustion and imbalanced follicular helper T cells. Front Immunol. 2020;11:583702. https://doi.org/10.3389/fimmu.2020.583702
21. Garcia P, Anand S, Han J, Montez-Rath ME, Sun S, Shang T, et al. COVID-19 vaccine type and humoral immune response in patients receiving dialysis. J Am Soc Nephrol. 2022;33:33–7. https://doi.org/10.1681/ASN.2021070936
22. Ducloux D, Colladant M, Chabannes M, Yannaraki M, Courivaud C. Humoral response after 3 doses of the BNT162b2 mRNA COVID-19 vaccine in patients on hemodialysis. Kidney Int. 2021;100:702–4. https://doi.org/10.1016/j.kint.2021.06.025
23. Hall VG, Ferreira VH, Ku T, Ierullo M, Majchrzak-Kita B, Chaparro C, et al. Randomized trial of a third dose of mRNA-1273 vaccine in transplant recipients. N Engl J Med. 2021;385:1244–6. https://doi.org/10.1056/NEJMc2111462
24. Massa F, Cremoni M, Gérard A, Grabsi H, Rogier L, Blois M, et al. Safety and cross-variant immunogenicity of a three-dose COVID-19 mRNA vaccine regimen in kidney transplant recipients. EBioMedicine. 2021;73:103679. https://doi.org/10.1016/j.ebiom.2021.103679
25. Stervbo U, Blazquez-Navarro A, Blanco EV, Safi L, Meister TL, Paniskaki K, et al. Improved cellular and humoral immunity upon a second BNT162b2 and mRNA-1273 boost in prime-boost vaccination no/low responders with end-stage renal disease. Kidney Int. 2021;100:1335–7. https://doi.org/10.1016/j.kint.2021.09.015

Address for correspondence: Gérard Krause, Helmholtz Center for Infection Research, Inhoffenstrasse 7, 38124 Braunschweig, Germany; email: gerard.krause@helmholtz-hzi.de; Nicole Schneiderhan-Marra, Natural and Medical Sciences Institute at the University of Tübingen, Markwiesenstrasse 55, 72770 Reutlingen, Germany; email: nicole.schneiderhan@nmi.de; Georg M.N. Behrens, Hannover Medical School, Carl-Neuberg-Straße 1, 30625 Hannover, Germany; email: behrens.georg@mh-hannover.de

Article DOI: https://doi.org/10.3201/eid2804.211907

Diminishing Immune Responses against Variants of Concern in Dialysis Patients 4 Months after SARS-CoV-2 mRNA Vaccination

Appendix

Appendix Table 1. Therapeutic indication for hemodialysis*

Diagnosis	No. patients (%) in hemodialysis group
Total	76 (100)
Autosomal dominant polycystic kidney disease	11 (14.47)
Chronic glomerulonephritis	6 (7.90)
Diabetic nephropathy	11 (14.47)
Focal segmental glomerulosclerosis	5 (6.59)
IgA nephropathy	8 (10.53)
Interstitial nephropathy	6 (7.90)
Nephrosclerosis	16 (21.05)
Acute toxic tubular epithelial damage syndrome	1 (1.32)
Primary amyloidosis	1 (1.32)
ANCA-associated vasculitis	1 (1.32)
Cardiorenal syndrome	2 (2.64)
Medullary cystic kidney disease	1 (1.32)
Membranous glomerulonephritis	1 (1.32)
Kidney dysplasia	1 (1.32)
Obstructive nephropathy	1 (1.32)
Reflux nephropathy	1 (1.32)
Septic organ failure	1 (1.32)
Cystic kidney disease	1 (1.32)
Cyclosporin intoxication	1 (1.32)

*ANCA, antineutrophilic cytoplasmic autoantibody.

Appendix Table 2. Medication of vaccination cohort

	No. (%)	
Medication	Nondialysis control group	Hemodialysis group
Total	23 (100)	76 (100)
Angiotensin-converting enzyme inhibitors	2 (8.70)	22 (28.95)
Statins	0 (0)	45 (59.21)
Angiotensin II Receptor Blockers	5 (21.74)	25 (32.89)
Vitamin D Supplements	12 (52.17)	75 (98.68)
Immunosuppressants (dosing range per day)*		
Prednisolone (2–7.5 mg)	0	5 (6.59)
Prednisolone (50 mg) day 6–14 post 2nd vaccination	0	1 (1.32)
Prednisolone (5 mg), Tacrolimus (0.5–2 mg)	0	2 (2.64)
Prednisolone (5 mg), Tacrolimus (12 mg), Mycophenolatmofetil (500 mg)	0	1 (1.32)
Hydrocortisone (20 mg)	0	1 (1.32)

*Therapeutic indication for immunosuppression were in four patients a kidney transplant (one had received an additional liver transplant), polymyositis, polyarthritis, vasculitis and chronic obstructive pulmonary disease.

Appendix Table 3. MULTICOV-AB antigen panel

Virus	Antigen	Manufacturer	Product number
SARS-CoV-2	Spike Trimer	NMI	–
SARS-CoV-2	RBD B.1 (wild-type)	NMI	–
SARS-CoV-2	Nucleocapsid	Aalto	6404–b
SARS-CoV-2	S1 domain	NMI	–
SARS-CoV-2	S2 domain	NMI	–
SARS-CoV-2	RBD B.1.1.7 (Alpha)	NMI	–
SARS-CoV-2	RBD B.1.351 (Beta)	NMI	–
SARS-CoV-2	RBD P.3 (Gamma)	NMI	–
SARS-CoV-2	RBD B.1.617.2 (Delta)	NMI	–
hCoV-OC43	S1 domain	NMI	–
hCoV-OC43	Nucleocapsid	NMI	–
hCoV-HKU1	S1 domain	NMI	–
hCoV-HKU1	Nucleocapsid	NMI	–
hCoV-NL63	S1 domain	NMI	–
hCoV-NL63	Nucleocapsid	NMI	–
hCoV-229E	S1 domain	NMI	–
hCoV-229E	Nucleocapsid	NMI	–

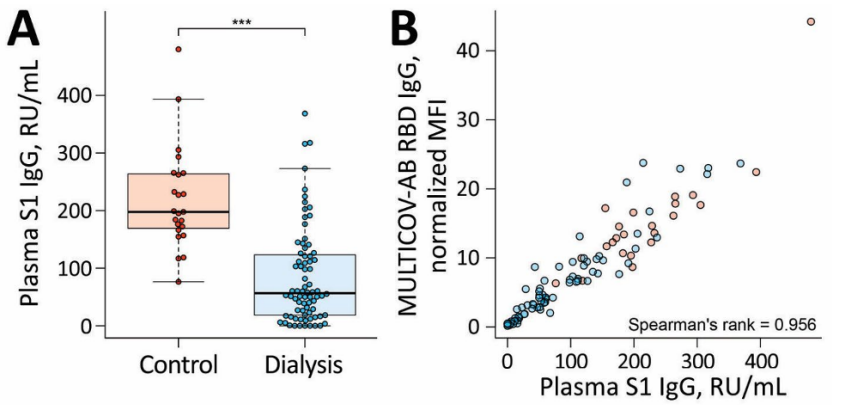

Appendix Figure 1. Quantitative plasma IgG titers 16 weeks after vaccination with Pfizer BNT162b2. A) Spike S1-specific plasma IgG (RU/mL) from control group (red, n = 23) and dialysis group (blue, n = 76) were analyzed 16 weeks post-second dose of Pfizer BNT162b2 using the QuantiVac-ELISA (Euroimmun). Samples above upper or below the ELISA's limits of detection are shown at the corresponding limit. Boxes represent the median, 25th and 75th percentiles, whiskers show the largest and smallest non-outlier values. Outliers were determined by 1.5 times IQR. Statistical significance was calculated by two-sided Mann-Whitney-U test. Significance was defined as ***<0.001. B) Correlation of MULTICOV-AB wild-type RBD B.1-IgG and QuantiVac Spike S1-IgG across the study population. Spearman's rank was used for correlation analysis.

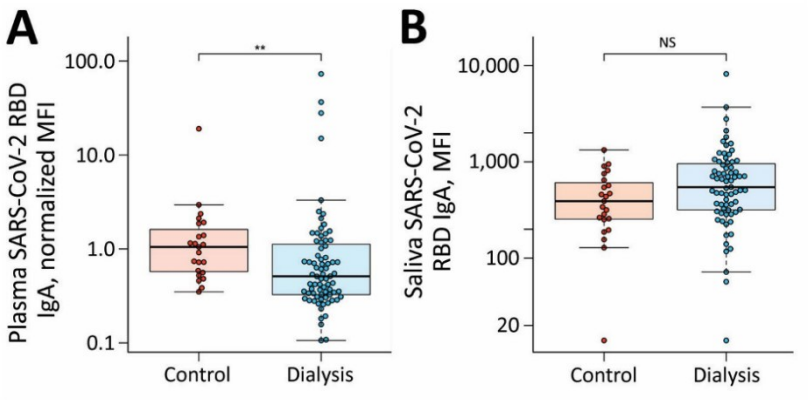
A
Plasma SARS-CoV-2 RBD IgA, normalized MFI
100.0
10.0
1.0
0.1
**
Control
Dialysis
B
Saliva SARS-CoV-2 RBD IgA, MFI
10,000
1,000
100
20
NS
Control
Dialysis

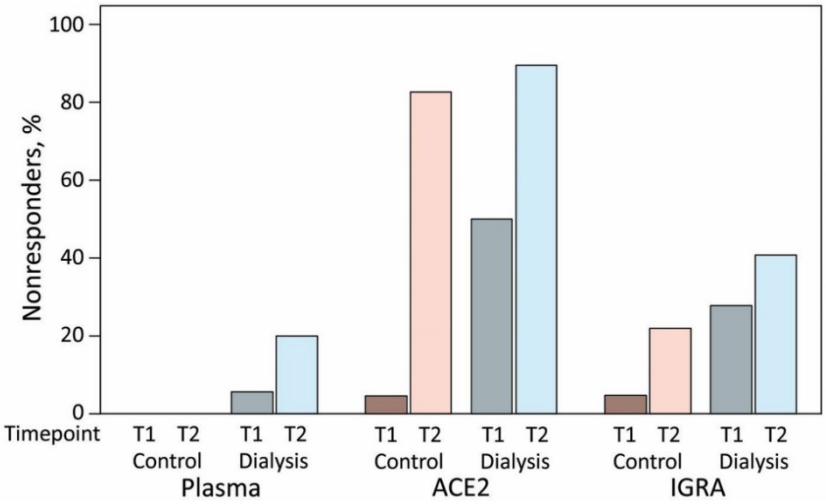

Reference

1. Strengert M, Becker M, Ramos GM, Dulovic A, Gruber J, Juengling J, et al. Cellular and humoral immunogenicity of a SARS-CoV-2 mRNA vaccine in patients on haemodialysis. EBioMedicine. 2021;70:103524. PubMed https://doi.org/10.1016/j.ebiom.2021.103524

Appendix VIII: Longitudinal cellular and humoral immune responses after triple BNT162b2 and fourth full-dose mRNA-1273 vaccination in haemodialysis patients

Becker M*, Cossmann A*, Lürken K, **Junker D**, Gruber J, Juengling J, Ramos GM, Beigel A, Wrenger E, Lonnemann G, Stankov MV, Dopfer-Jablonka A, Kaiser PD, Traenkle B, Rothbauer U, Krause G, Schneiderhan-Marra N, Strengert M, Dulovic A, Behrens GMN.

Frontiers in Immunology. 2022. 13:1004045

https://doi.org/10.3389/fimmu.2022.1004045

frontiers | Frontiers in Immunology

TYPE Original Research
PUBLISHED 06 October 2022
DOI 10.3389/fimmu.2022.1004045

OPEN ACCESS

EDITED BY
Elke Bergmann-Leitner,
Walter Reed Army Institute of Research, United States

REVIEWED BY
Tim Luetkens,
University of Maryland, Baltimore, United States
Yanmin Wan,
Fudan University, China

*CORRESPONDENCE
Monika Strengert
monika.strengert@helmholtz-hzi.de
Alex Dulovic
alex.dulovic@nmi.de
Georg M. N. Behrens
behrens.georg@mh-hannover.de

†These authors have contributed equally to this work

‡These authors have contributed equally to this work and share first authorship

SPECIALTY SECTION
This article was submitted to Vaccines and Molecular Therapeutics, a section of the journal Frontiers in Immunology

RECEIVED 26 July 2022
ACCEPTED 12 September 2022
PUBLISHED 06 October 2022

CITATION
Becker M, Cossmann A, Lürken K, Junker D, Gruber J, Juengling J, Ramos GM, Beigel A, Wrenger E, Lonnemann G, Stankov MV, Dopfer-Jablonka A, Kaiser PD, Traenkle B, Rothbauer U, Krause G, Schneiderhan-Marra N, Strengert M, Dulovic A and Behrens GMN (2022) Longitudinal cellular and humoral immune responses after triple BNT162b2 and fourth full-dose mRNA-1273 vaccination in haemodialysis patients. *Front. Immunol.* 13:1004045. doi: 10.3389/fimmu.2022.1004045

Longitudinal cellular and humoral immune responses after triple BNT162b2 and fourth full-dose mRNA-1273 vaccination in haemodialysis patients

Matthias Becker[1‡], Anne Cossmann[2‡], Karsten Lürken[3], Daniel Junker[1], Jens Gruber[1], Jennifer Juengling[1], Gema Morillas Ramos[2], Andrea Beigel[3], Eike Wrenger[3], Gerhard Lonnemann[3], Metodi V. Stankov[2], Alexandra Dopfer-Jablonka[2,4], Philipp D. Kaiser[1], Bjoern Traenkle[1], Ulrich Rothbauer[1,5], Gérard Krause[4,6,7], Nicole Schneiderhan-Marra[1], Monika Strengert[6,7*†], Alex Dulovic[1*†] and Georg M. N. Behrens[2,4,8*†]

[1]NMI Natural and Medical Sciences Institute at the University of Tübingen, Reutlingen, Germany, [2]Department for Rheumatology and Immunology, Hannover Medical School, Hannover, Germany, [3]Department of Internal Medicine and Nephrology, Dialysis Centre Eickenhof, Langenhagen, Germany, [4]German Centre for Infection Research (DZIF), partner site Hannover-Braunschweig, Hannover, Germany, [5]Pharmaceutical Biotechnology, University of Tübingen, Tübingen, Germany, [6]Department Epidemiology, Helmholtz Centre for Infection Research, Braunschweig, Germany, [7]TWINCORE GmbH, Centre for Experimental and Clinical Infection Research, a joint venture of the Hannover Medical School and the Helmholtz Centre for Infection Research, Hannover, Germany, [8]CiiM - Centre for Individualized Infection Medicine, Hannover, Germany

Haemodialysis patients respond poorly to vaccination and continue to be at-risk for severe COVID-19. Therefore, dialysis patients were among the first for which a fourth COVID-19 vaccination was recommended. However, targeted information on how to best maintain immune protection after SARS-CoV-2 vaccinations in at-risk groups for severe COVID-19 remains limited. We provide, to the best of our knowledge, for the first time longitudinal vaccination response data in dialysis patients and controls after a triple BNT162b2 vaccination and in the latter after a subsequent fourth full-dose of mRNA-1273. We analysed systemic and mucosal humoral IgG responses against the receptor-binding domain (RBD) and ACE2-binding inhibition towards variants of concern including Omicron and Delta with multiplex-based immunoassays. In addition, we assessed Spike S1-specific T-cell responses by interferon γ release assay. After triple BNT162b2 vaccination, anti-RBD B.1 IgG and ACE2 binding inhibition reached peak levels in dialysis patients, but remained inferior compared to controls. Whilst we detected B.1-specific ACE2 binding inhibition in 84% of dialysis patients after three BNT162b2 doses, binding inhibition towards the Omicron variant was only detectable in 38% of samples and

10.3389/fimmu.2022.1004045

declining to 16% before the fourth vaccination. By using mRNA-1273 as fourth dose, humoral immunity against all SARS-CoV-2 variants tested was strongly augmented with 80% of dialysis patients having Omicron-specific ACE2 binding inhibition. Modest declines in T-cell responses in dialysis patients and controls after the second vaccination were restored by the third BNT162b2 dose and significantly increased by the fourth vaccination. Our data support current advice for a four-dose COVID-19 immunisation scheme for at-risk individuals such as haemodialysis patients. We conclude that administration of a fourth full-dose of mRNA-1273 as part of a mixed mRNA vaccination scheme to boost immunity and to prevent severe COVID-19 could also be beneficial in other immune impaired individuals. Additionally, strategic application of such mixed vaccine regimens may be an immediate response against SARS-CoV-2 variants with increased immune evasion potential.

KEYWORDS

dialysis, mRNA vaccination, Omicron variant of concern, protective immunity, immunocompromised, longitudinal response, mixed mRNA vaccination, COVID-19

Introduction

To date, SARS-CoV-2 vaccinations reassuringly provide some degree of protection from severe COVID-19 independent of the currently circulating variants of concern (VoC) for the majority of healthy individuals (1). However, weaker immunogenicity and a faster decline in protection levels to standard two-dose or three-dose booster SARS-CoV-2 immunisation schemes have been widely demonstrated in immunocompromised individuals such as solid organ transplant recipients (2), dialysis patients (3) or patients suffering from other severe chronic conditions such as cancer (4). Starting in mid-2021 and more widely since the beginning of 2022, several countries recommended a fourth dose of SARS-CoV-2 mRNA vaccines for immunosuppressed populations at-risk for severe COVID-19 disease and older individuals to maintain levels of immune protection (5–8). This was driven by weaker peak vaccine responses and waning immunity in those individuals as well as continued evolution of SARS-CoV-2 variants with increasing levels of immune evasion potential as demonstrated for Omicron VoC subspecies BA.1, BA.4, BA.5, and BA.2.12.1 (9–12).

Recent studies reported improved SARS-CoV-2 humoral and cellular responses not only towards the original SARS-CoV-2 B.1 isolate but also Delta and Omicron VoC after a fourth vaccination in haemodialysis patients receiving either mRNA vaccines or vector-based formulations in combination with mRNA vaccines (13–15). However, targeted data on the most efficient dosing and vaccination scheme or even predictors of vaccination success in haemodialysis patients at-risk of severe COVID-19 and its associated mortality is limited. We aimed to comprehensively examine the magnitude and kinetics of both cellular and humoral immunity towards the most recently dominating Delta and Omicron variant's in a well-controlled longitudinal cohort of haemodialysis patients. These patients received a triple dose of BNT162b2 followed by a full-dose of mRNA-1273. Healthcare workers vaccinated three times with BNT162b2 served as controls. Our data provide preliminary evidence that in addition to heterologous vector- and mRNA-based vaccination schemes also heterologous mRNA vaccine regimens may become strategically beneficial for achieving efficient immunity against SARS-CoV-2 in immunosuppressed patients.

Methods

Study design and sample collection

This is a follow-up study in haemodialysis patients and control individuals, for which the results for haemodialysis patients after a complete two-dose BNT162b2 vaccination (16) and subsequent decline (17) have been previously reported. Blood samples were taken before start of dialysis treatment (n=50) or from healthcare workers (n=33), who participated in the COVID-19 contact (CoCo) study served (18) as non-dialysed control population. To be included in the study, participants had to be over the age of 18 and able to give

10.3389/fimmu.2022.1004045

written informed consent. For the current analysis, we only considered dialysis patients for which results from all time points after either three or four vaccine doses were available. All participants received the standard two-dose regimen of BNT162b2 three weeks apart, followed by a third BNT162b2 vaccination about six (dialysis) or 8.5 months (controls) after the second vaccination. Only dialysis patients were vaccinated a fourth time with 100 µg mRNA-1273 four months after the last BNT162b2 vaccination. The vaccination schedule and blood collection time points are depicted in Figure 1 and Figure S1. Participants with SARS-CoV-2 infection diagnosed by either PCR or anti-nucleocapsid IgG determined by MULTICOV-AB multiplex measurement (19) were excluded from the analysis. Demographic characteristics and medical information are listed in Tables 1, S1, S2. Plasma was obtained from lithium heparin blood (S-Monovette Plasma, Sarstedt, Germany). Whole blood samples were used immediately for interferon γ release assay (IGRA). For saliva collection, all individuals spat directly into a collection tube. To inactivate replication-competent SARS-CoV-2 virus particles potentially present in saliva samples, Tri(n-butyl) phosphate (TnBP) and Triton X-100 were added to final concentrations of 0.3% and 1%, respectively (20). Both plasma and saliva samples were frozen and stored at −80°C until further use.

MULTICOV-AB

IgG binding and levels were analysed using MULTICOV-AB, a multiplex coronavirus immunoassay which contains the trimeric Spike B.1, its subdomains (S1, S2, RBD), nucleocapsid B.1 and RBDs of Delta and Omicron BA.1 antigens as previously described (9, 19). Briefly, antigens were immobilised on spectrally distinct populations of MagPlex beads (Cat #MC10XXX-01, Luminex Corporation) either by EDC/s-NHS coupling (21) or by Anteo coupling (Cat #A-LMPAKMM-10, Anteo Tech Reagents) following the manufacturer's instruction (19). The combined MagPlex beads were then incubated with samples at an effective dilution of 1:3200 for plasma and of 1:12 for saliva. After a wash step to remove unbound antibodies, IgG was detected with R-phycoerythrin labelled goat-anti-human IgG (Jackson ImmunoResearch Labs, Cat #109-116-098, Lot #148837, RRID: AB_2337678) as secondary antibody. After another wash step and bead resuspension, samples were measured once on a FLEXMAP 3D instrument (Luminex Corporation) using the following settings: Timeout 80 sec, Gate: 7500-15000, Reporter Gain: Standard PMT, 50 events. Raw median fluorescence intensity (MFI) values or normalised values (MFI/MFI of quality control (QC) samples (19, 22) are reported. Three QC samples were measured per individual plate to monitor MULTICOV-AB performance.

RBDCoV-ACE2

RBDCoV-ACE2, a multiplex competitive inhibition assay, was performed as previously described (23) as surrogate assay to determine immunoglobulin neutralisation capacity against SARS-CoV-2 B.1 isolate and variants of concern. For this, biotinylated ACE2 was combined with individual samples (and as a control, ACE2 alone) and incubated with the above mentioned MULTICOV-AB bead mix. Before and after ACE2 detection with Strep-PE (Cat #SAPE-001, Moss), washes were carried out. Samples were measured once on a FLEXMAP 3D instrument with the same settings as MULTICOV-AB and analysed by normalisation of MFI values against the control. 100% ACE2 binding inhibition indicates maximum binding inhibition. Responders for ACE2 binding inhibition are classified as above a 20% ACE2 binding threshold as described in Junker et al. (23).

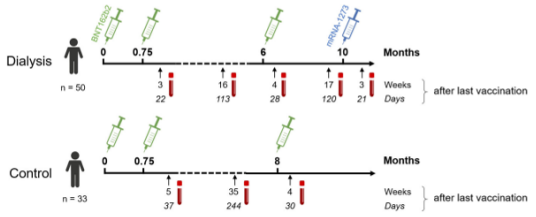

FIGURE 1
Participant recruitment scheme for longitudinal vaccination response analysis in haemodialysis patients after triple BNT162b2 and fourth full-dose mRNA-1273. Patients on haemodialysis (n = 50) and healthcare workers as controls (n = 33) were triple-vaccinated with BNT162b2 (green syringe) followed by a 100 µg (full) dose of mRNA-1273 (blue syringe) for dialysed individuals only. Sampling and vaccination schedule is given in days and weeks as indicated.

TABLE 1 Characteristics of study population.

Characteristics	Haemodialysis group (n = 50)	Non-dialysis control group (n =33)	p-value for difference between groups
Age (years), median (IQR)	69.5 (60–79)	42 (32–55)	$1.08*10^{-11}$
Sex (female: n, %)	19 (38.0)	23 (69.7)	$9.26*10^{-3}$
Days since start of haemodialysis (median, IQR)	1263 (753-2314)	n. a.	n. a.
Immunosuppressive medication (n, %)			
2021 (Vaccine dose 1-3)*	7 (14.0)	0 (0.0)	n. a.
2022 (Vaccine dose 4)*	6 (12.0)	n. a.	n. a.
Co-morbidities			
Obesity (BMI, >30)	12 (24.0)	NA	n. a.
Diabetes mellitus (n, %)	14 (28.0)	1 (3.0)	$9.27*10^{-3}$
Cardiovascular disease (n, %)	21 (42.0)	2 (6.1)	$8.69*10^{-4}$
Cancer (n, %)	1 (2.0)	0 (0.0)	n. a.
Chronic conditions (n, %)			
Ulcerative colitis (n, %)	0 (0.0)	1 (3.0)	n. a.
Goiter (n, %)	0 (0.0)	1 (3.0)	n. a.
Hashimoto's thyroiditis (n, %)	0 (0.0)	1 (3.0)	n. a.
Hypothyroidism (n, %)	0 (0.0)	1 (3.0)	n. a.
Other	0 (0.0)	1 (3.0)	n. a.

*Participants on medication when vaccinated and sampled.
IQR, Inter Quartile Range; BMI, Body Mass Index; n, absolute numbers per group; NA, Information not available; n. a., not applicable.

Anti-SARS-CoV-2 QuantiVac ELISA

Plasma samples were additionally analysed using the Anti-SARS-CoV-2-QuantiVac-ELISA IgG (Cat #EI 2606-9601-10G, Euroimmun) as previously described (16).

Interferon γ release assay

SARS-CoV-2-specific T-cell responses from whole blood were analysed by measuring IFNγ production after stimulation with a peptide pool from the SARS-CoV-2 Spike S1 with the SARS-CoV-2 Interferon Gamma Release Assay (Cat #ET-2606-3003, Euroimmun) and the IFNγ ELISA (Cat #EQ-6841-9601, Euroimmun) according to the manufacturer's description and as previously evaluated against alternative assays for antigen-specific T-cell reactivity using intracellular cytokine staining or enzyme linked immuno spot assay (24, 25). Background signals from negative controls were subtracted and final results calculated in mIU/mL using standard curves. IFNγ concentrations >200 mIU/mL were considered as reactive. We defined this arbitrary cut-off by using average background IFNγ activity without antigen-stimulation in all samples multiplied with 10 for the threshold for IGRA-positive. Using this cut-off, we found in all of the 15 controls taken from independent individuals before the COVID-19 pandemic negative IGRA results (26). The upper limit of reactivity was 16,000 mIU/mL.

Data analysis and statistics

RStudio (Version 1.2.5001), with R (version 3.6.1) was used for data analysis and figure generation. Additionally, the R add-on package "beeswarm" was utilised to visualise data as stripcharts with overlaying boxplots and to create non-overlaying data points. A second R add-on package "gplots" was used to generate specific colours for plots. Figures were exported from RStudio and then edited using Inkscape (Inkscape 1.2). Spearman's rho coefficient was calculated to determine correlation between IGRA results and ACE2 binding inhibition using the "cor" function from R's "stats" library. Mann-Whitney-U test and Wilcoxon test were used to determine difference of signal distributions between dialysed and control groups for unpaired and paired samples, respectively using the "wilcox.test" function from R's "stats" library. To assess differences in the study population, Pearson's Chi-squared test with Yates' continuity correction was used for categorical characteristics using the "chisq.test" function from R's "stats" library and Mann-Whitney-U test as above was used for difference in age. The type of statistical analysis performed

10.3389/fimmu.2022.1004045

(when appropriate) is listed in the figure legends. Pre-processing of data such as matching sample metadata and collecting results from multiple assay platforms was performed in Excel 2016.

Results

Inferior humoral responses in haemodialysis patients after triple BNT162b2 vaccination

To characterise the vaccination response after the third BN162b2 vaccination in 50 patients on maintenance haemodialysis, we had followed immunoglobulin levels longitudinally after the second dose of BNT162b2 using MULTICOV-AB, a multiplex immunoassay containing antigens from the Spike protein of SARS-CoV-2 and selected variants of concern (9). As a novel control group, 33 samples from healthcare workers with triple BNT162b2 vaccination were used for comparison. Detailed information on the study populations can be found in Tables 1, S1, S2. Consistent with our previous reports (16, 17), IgG responses towards the original B.1 isolate in vaccinated dialysis patients were significantly reduced ($p=4.68*10^{-5}$, Mann-Whitney-U test) when compared to the control group and declined after the second vaccination to comparable levels in both groups ($p=7.33*10^{-2}$, Mann-Whitney-U test, Figure 2A). A third BNT162b2 vaccination about six to eight months after the second increased the peak IgG RBD B.1 response in both groups but with higher variability in dialysis patients ($p=4.02*10^{-2}$, Mann-Whitney-U test, Figure 2A). As an additional control, quantitative S1 IgG titres were measured using a commercial assay (Figure S2), which led to a very similar pattern of significantly diminished antibody responses in dialysis patients compared to non-dialysed individuals after the second BNT162b2 dose, declining titres and a robust peak response increase after the third vaccination. There was no significant difference in male or female individuals and we did not find any association to age. Regarding the decline in anti-S IgG after the third dose, we were able to measure this in only n=10 of the control group at a comparable time point after vaccination to the haemodialysis group (Figure S3). Dialysis patients showed a mean 3-fold reduction in anti-S IgG levels 121 days (range 119-129 days) after the third vaccination (from mean 2,314 BAU/mL to mean 771 BAU/mL). This was almost identical to the 3.2-fold decline in healthy controls (from mean 5,430 BAU/mL to mean 1, 662 BAU/mL), although the time point for the follow up was somewhat later.

For a functional characterisation of vaccine-induced antibodies towards the original B.1 RBD isolate, we used RBDCoV ACE2 - a multiplex competitive inhibition assay (23). ACE2 binding inhibition was significantly reduced in dialysed compared to non-dialysed individuals ($p=2.42*10^{-6}$, Mann-Whitney-U test) after the second vaccination (Figure 2B). Responses were comparably diminished in both groups four to eight months after the second vaccination, with only 12% and 6% of samples being above the 20% responder threshold in patients on haemodialysis and controls, respectively. However, comparable to IgG binding levels, the

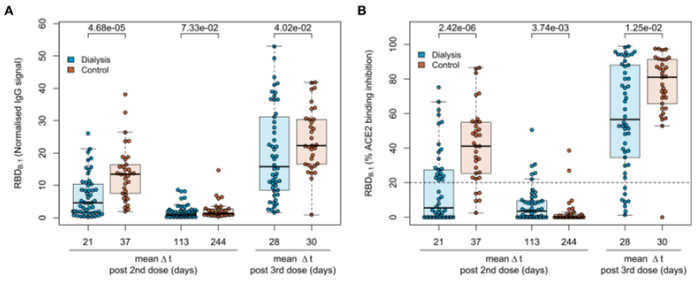

FIGURE 2
Humoral immune response in haemodialysis patients after a triple vaccination with BNT162b2. IgG response **(A)** and ACE2 binding inhibition **(B)** towards the SARS-CoV-2 B.1 RBD isolate were measured in plasma from haemodialysis patients (blue circles, n = 50) and controls (orange circles, n=33) using MULTICOV-AB **(A)** or an ACE2-RBD competition assay **(B)** after double or triple vaccination with BNT162b2 at the indicated time points. Data is displayed as normalised median fluorescence intensity (MFI) signal **(A)** for IgG binding or as % ACE2 binding inhibition where 100% indicates maximum inhibition and 0% no inhibition **(B)**. Samples with an ACE2 binding inhibition of less than 20% (dashed line) are classified as non-responders. Boxes represent the median, 25th and 75th percentiles, whiskers show the largest and smallest non-outlier values. Outliers were determined by 1.5 times IQR. Mean sampling time in days after two-dose BNT162b2 vaccination as Δt is displayed on the x-axis. Statistical significance was calculated by two-sided Mann-Whitney-U test. P-values for relevant comparisons are given above the sample groups. Significance was defined as $p < 0.05$. Response data from dialysed individuals from day 21 and day 113 after the second BNT162b2 dose were already published before as part of Strengert et al. (16) and Dulovic et al. (17).

10.3389/fimmu.2022.1004045

third BNT162b2 vaccination restored and even augmented ACE2 binding inhibition against the B.1 variant in both populations.

Strong immune responses after a fourth mRNA-1273 vaccination in haemodialysis patients

Next, we followed the anti-Spike RBD IgG levels in haemodialysis patients after the third vaccination over time and after a fourth vaccination with a full 100 µg dose of mRNA-1273, which was considered by German guidelines for immunocompromised individuals. As expected, IgG responses against the original B.1 isolate had again declined within approximately 4 months after the third vaccination (Figure 3A; Figure S2) as did the ACE2 binding inhibition activity as a surrogate for virus neutralisation (Figure 3B). Whilst the decline was not as severe as after the second BNT162b2 dose with now 64% of samples remaining above the 20% ACE2 binding inhibition threshold, only the fourth vaccination with mRNA-1273 markedly raised both anti-Spike RBD IgG levels (Figures 3A, S2; Table S3 for a complete statistical evaluation) and ACE2 binding inhibition (Figure 3B) towards the B.1 isolate above levels seen at peak response after the second and third dose of BNT162b2. 96% of samples from individuals on haemodialysis were now classified as above the 20% ACE2 responder threshold. Further, we also analysed the longitudinal development of ACE2 binding inhibition towards the dominantly circulating SARS-CoV-2 of 2021 (Delta) and 2022 (Omicron) (Figures 3C, D). ACE2 binding inhibition towards the Delta variant was slightly reduced over time compared to levels observed with the B.1 isolate. Overall, the third dose resulted in a clear increase in Delta ACE2 responder rates from 24% after two-dose BNT162b2 scheme to 64%, which was further increased to 94% after the subsequent dose of mRNA-1273 (Figure 3C). Importantly, neutralisation against the Omicron BA.1 variant, which was largely absent after the second vaccination and only transiently above threshold in 38% of dialysis patients after the third vaccination, reached high levels of ACE2 binding inhibition with an 80% responder rate at peak response after the fourth vaccination with mRNA-1273. This coincided with Omicron being the dominant SARS-CoV-2 variant circulating in Germany (Figure 3D).

We also analysed IgG binding longitudinally after a triple dose of BNT162b2 towards the RBD of B.1, Delta and Omicron

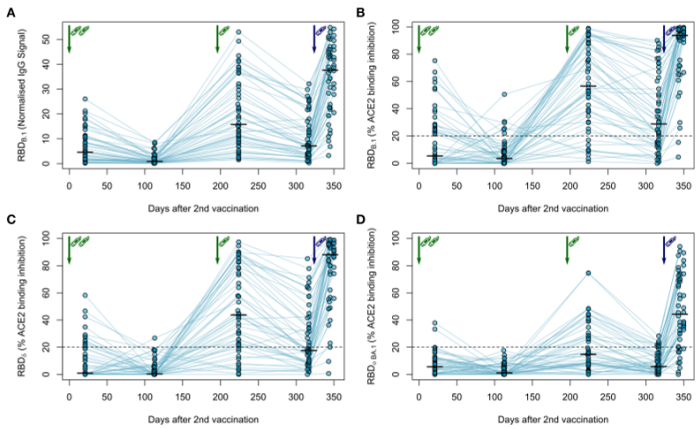

FIGURE 3
Longitudinal humoral immune response in haemodialysis patients after a triple vaccination with BNT162b2 and a fourth full-dose of mRNA-1273. IgG response **(A)** and ACE2 binding inhibition **(B–D)** towards the SARS-CoV-2 RBD of B.1 **(A, B)**, δ **(C)** and O BA.1 **(D)** isolates were measured in plasma from haemodialysis patients (n = 50) using MULTICOV-AB **(A)** or an ACE2-RBD competition assay **(B–D)** after immunisation with a triple dose of BNT162b2 (green syringe) and a fourth full-dose of mRNA-1273 (blue syringe). Data is displayed as normalised median fluorescence intensity (MFI) signal for IgG binding **(A)** or as % ACE2 binding inhibition where 100% indicates maximum inhibition and 0% no inhibition **(B–D)**. Samples with an ACE2 binding inhibition of less than 20% (dashed line) are classified as non-responders **(B–D)**. Interconnecting lines represent samples from the same individual. Sampling time points in days after the standard complete two-dose BNT162b2 vaccination is stated below the graph. Statistical significance was calculated by two-sided paired Wilcoxon rank test. Significance was defined as $p < 0.05$. All p-values for relevant comparisons are listed in Table S3.

10.3389/fimmu.2022.1004045

BA.1 VoC in saliva of haemodialysis patients to determine protection levels at the primary side of SARS-CoV-2 replication. Although anti-RBD specific IgG was readily detectable both in the peak and plateau response phase following the complete two-dose and the third booster dose of BNT162b2, IgG binding towards the Delta and Omicron BA.1 RBD was significantly reduced compared to the B.1 RBD across all time points (Figure S4). Interestingly, saliva responses across vaccinated individuals were much more widespread in saliva than in plasma.

As clinical studies suggested that both cellular and humoral response can confer protection from COVID-19 (27), we also assessed vaccination-induced T-cell responses by IFNγ release assay longitudinally. Overall, these responses were more stable over time (Figure 4A). After two BNT162b2 vaccinations, IFNγ release after *in vitro* re-stimulation was readily detectable in haemodialysis patients, but declined slightly thereafter. The third BNT162b2 vaccination increased cellular responses to levels comparable to after the second vaccination. Similar to the humoral responses, the fourth vaccination with mRNA-1273 further increased IFNγ release after Spike S1 peptide restimulation of T-cells (Figure 4A; Table S3 for a complete statistical evaluation).

Finally, we correlated B- and T-cell responses after each vaccination within our longitudinal cohort of haemodialysis patients. We overall observed moderate correlation between peak T-cell responses (measured by IGRA) and B-cell responses [determined by % ACE2 binding inhibition of the B.1 variant (Spearman's rho=0.561, Figure 4B, upper panel)], which did not increase after the third (Spearman's rho=0.405) and fourth (Spearman's rho=0.371) vaccination. We further described responder rates for T- and B-cell response by a combined cut-off as displayed in Figure 4B. Notably, responder rates among haemodialysis patients strongly increased to 72% after the triple BNT162b2 dose and further to 86% after the fourth full-dose mRNA-1273. Importantly, whilst we observed a similar trend for the correlation coefficient between Delta and Omicron BA.1 % ACE2 binding inhibition and T-cell responses (Figure 4B; middle and lower panel, Table S3 for a complete statistical evaluation), dual cellular (>200mIU/mL) and humoral (>20% ACE inhibition) responders levels equally strongly increased for both VoC after the third and fourth vaccination to a final 84% and 74%, respectively.

Discussion

Although overall case mortality rates for SARS-CoV-2 have significantly decreased since the initial wave of the pandemic, maintaining high levels of vaccine-induced protection is of paramount importance for at-risk individuals for severe COVID-19 such as haemodialysis patients. Ensuring that these and other similarly vulnerable individuals are sufficiently protected remains challenging, with high case numbers throughout 2022 as a result of successive occurrence of Omicron subvariants. Despite clear recommendations on the need for a fourth dose, worryingly this fourth dose uptake among haemodialysis patients has decreased compared to the first three doses, with disparities among demographic groups remaining in place (28). At present, recommendations by the German Standing Committee on Vaccination (STIKO) clearly endorse a fourth SARS-CoV-2 vaccine dose including a full dose of mRNA-1273 for immunocompromised individuals (5), which contrasts WHO guidelines recommending 50 µg mRNA-1273 for fourth vaccinations (29).

Several studies report of superior immunity after initial mRNA-1273 prime/boost vaccination when compared to BNT162b2 in haemodialyis patients (30, 31) or in the general population (32–34) and further improved humoral responses after triple vaccination in dialysis patients (35–39). Third dose vaccination with mRNA-1273 or BNT162b2 provided comparable protection against symptomatic SARS-CoV-2 infection in the general population, although differences between both vaccines were observed after the second dose (40). Finally, Caillard et al. found that a four-dose mRNA-1273 compared to a four-dose BNT162b2 results in increased levels of binding antibodies in kidney transplant recipients (41). In general, COVID-19 vaccine-induced humoral immune responses tend to be higher in females and lower in elderly people. Differences in anti-S IgG were prominent after the second but not after the third vaccination, whilst males remained to have inferior neutralisation activity even after the third vaccination (42). We did not find such association most likely due to the smaller samples size of our cohort.

Two studies found more durable neutralising antibody titers four or six months after a third dose of mRNA vaccine compared to two doses (43, 44). For the BNT162b2 vaccine the decline was 1.6-fold at four months. These findings indicate robust long-lived antibody production after three doses, but the durability of neutralising activity against different SARS-CoV-2 variants could be variable (43). In a third study in an Israeli population receiving the BNT162b2 vaccine, the decline over approximately four months after the third dose was much higher (5.5-fold). We observed an about 3-fold decline in both groups, which is in line with the current literature and indicates that the peak anti-S IgG responses are the main drivers for the differences between groups over time and that the anti-S IgG kinetics are likely similar in dialysis patients and controls. However, conclusions about durability of antibody responses after 3-doses mRNA vaccination remain uncertain, particularly after combination of different vaccines (45). With regard to the T-cell responses, we (24, 25, 46, 47) and others (48, 49) have described that Spike-specific T-cell responses (CD4+ or CD8+ T-lymphocytes) after infection or prime/boost vaccination are more stable as compared to the respective humoral responses in healthy

10.3389/fimmu.2022.1004045

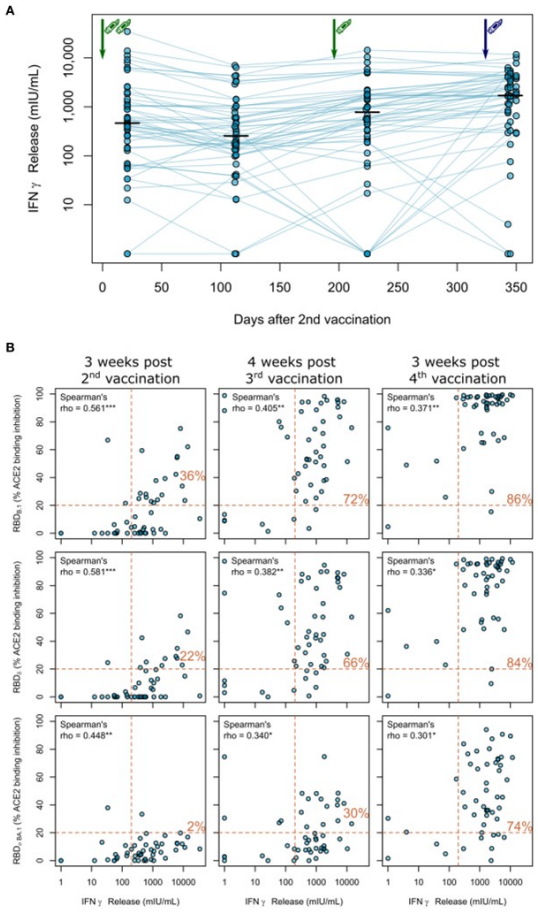

FIGURE 4
Impact of triple vaccination with BNT162b2 and a fourth full-dose of mRNA-1273 on cellular immune response in haemodialysis patients. **(A)** Whole blood from longitudinally-sampled vaccinated haemodialysis patients (n = 50) was *ex vivo* stimulated using a SARS-CoV-2 Spike S1-specific peptide pool. Supernatant fractions were then analysed by interferon γ release assay (IGRA). Interconnecting lines represent samples from the same individual. Sampling time points in days after two-dose BNT162b2 vaccination is displayed on the x-axis. Statistical significance was calculated by two-sided paired Wilcoxon rank test. Significance was defined as $p<0.05$. All p-values for relevant comparisons are listed in Table S3. Response data from dialysed individuals from day 21 after the second BNT162b2 dose were already published before as part of Strengert et al. (16) and Dulovic et al. (17). **(B)** T-cell responses assessed by IGRA and B-cell responses assessed by ACE2-RBD competition assay towards the RBD of B.1, Delta, Omicron BA.1 isolates were plotted for correlation analysis **(B)**. Correlation was calculated using Spearman's coefficient rho. P values are marked as * <0.05, ** <0.01, *** <0.001. Dashed lines indicated the respective responder thresholds for IGRA (IFNγ release >200 mIU/mL) and RBD-ACE2 binding assay (20%). Responder rates (%) for both cellular and humoral response are shown in the upper right quadrant.

10.3389/fimmu.2022.1004045

individuals. Thus, vaccine-induced long-lasting T-cell memory after two or three COVID-19 vaccination are most likely not a specific response in dialysis patients COVID-19 (45). The IGRA employed in this study reliably detects vaccine-induced Spike-specific T-cell responses and showed good correlation to other techniques for studying post-vaccination T-cell immunity including ELISpot and intracellular cytokine staining (24, 26).

Potential causes for our observations may include the higher dose of mRNA-1273. Similar doses of mRNA-1273 (25 µg) to the BNT162b2 dose (30 µg) generated comparable Spike-specific memory CD4 T-cell frequencies to natural infection and about half as strong as those seen with high-dose vaccination (100 µg) indicating that differences between cellular and humoral immunity after two mRNA vaccines most likely result from the different doses of the vaccine (48). In addition, Spike and RBD IgG+ memory B-cell frequencies increase between 3 and 6 months after immunisation with mRNA vaccine (50) and germinal centers appear to be central to the immune responses to COVID-19 vaccines (45). Kidney transplant recipients, unlike healthy subjects, presented deeply blunted SARS-CoV-2-specific germinal center B-cell responses coupled with severely hindered neutralising antibody responses. These data indicate impaired germinal center-derived immunity in immunocompromised individuals (51). Germinal centers can persist and be productive for more than six months after two doses of COVID-19 mRNA vaccines and that the quality of neutralising antibodies can improve over three to six months (52). We speculate that diminished B-cell memory generation and germinal center formation is one feature of the immune dysfunction in dialysis patients and that repetitive vaccination, mix of mRNA vaccines or increase in vaccine dose may help to overcome these limitations. Finally, we specifically looked at dialysis patients with IGRA results below threshold after the third vaccination (n=12), of which almost all were among individuals with lowest IGRA results also after the second and fourth vaccination. We classified these as "low responders", since also their anti-S IgG responses were persistently very low. These low responders comprised all patients with organ-transplantation (n=4) and 7 out of 8 individuals with immunosuppressive therapy at the time of the third vaccination. We found no other association to co-morbidities or clinical conditions in the low responder subgroup. Thus, immunosuppression as listed in Table S2 is a further explanation for the inferior humoral and cellular vaccine response in many of the low responders.

We can only speculate about the effects of mixing mRNA-based vaccines. Janssen et al. compared heterologous and homologous mRNA-1273 and BNT162b2 vaccination after the respective first vaccination in a randomised trial (53). They found the geometric mean titers of anti-Spike IgG antibodies for each heterologous regimen to be higher relative to the corresponding homologous regimen. This is consistent with data from Israel (54) and the COV-BOOST study (55), in which even half-dose mRNA-1273 as fourth dose after triple BNT162b2 vaccination appeared to have higher immunogenicity than full-dose BNT162b2. The authors suggested that this result might be due to a heterologous schedule effect or the vaccine dose. Interestingly, differences between both mRNA vaccines could be more complex, since mRNA-1273 is reported to induce higher concentrations of RBD- and N-terminal domain-specific IgA and more antibodies eliciting neutrophil phagocytosis and natural killer cell activation as compared to BNT162b2 (56).

Our study is, to our knowledge, the only study examining the longitudinal humoral and cellular immune response towards the most recent SARS-CoV-2 isolates in haemodiaylsis patients after administration of consistent vaccination regimens starting with a triple dose of BNT162b2 followed by a fourth full-dose of mRNA-1273. Whilst other studies principally support the beneficial impact of a fourth vaccination dose on both antibody titers and neutralising potency towards SARS-CoV-2 B.1 and VoC isolates, often various vaccination regimens including heterologous vector-based/mRNA regimens were pooled in cohorts (14) or vaccine dosages not provided (13).

Our data provide solid evidence that the triple vaccination resulted in mean antibody concentration and neutralising activity above levels to after the second vaccination. Interestingly, we identified significant further increases in both humoral and cellular response rates following the fourth dose, compared to the second and third. The increase in response rate from 30% to 74% from third to fourth dose for Omicron is particularly important considering it comprises almost all currently circulating variants of SARS-CoV-2. We consider this as a valid argument for a fourth vaccination in at-risk patients, especially, since T-cell immunity elicited by current vaccines is also effective against VoC including Omicron (57–59). The large range in both humoral and cellular responses illustrates however the variable nature of SARS-CoV-2 vaccination responses in dialysis patients and may be of relevance for identifying individuals with inferior responses in need for further doses.

Our study has several limitations. The number of participants within our cohort was limited, with only 50 patients on haemodialysis and a further 33 control participants, although our sample size is larger than similar studies examining the effect of the fourth dose within haemodialysis patients (15). The use of longitudinal cohort also allows us to directly identify the responses and their decline following each individual dose. Unfortunately, we were unable to obtain samples post-fourth dose for our control population, since many individuals were meanwhile infected with Omicron, additional booster vaccinations are not generally recommended and a full dose mRNA-1273 vaccination would be the unlikely regimen for the healthy controls. Although our control group was well-matched for sample collection at peak antibody levels after the second and third vaccination, they were not optimally matched for age and gender. A potential limitation of our study is that we used only peptides from a single SARS-

CoV-2 S1 protein for T-cell analysis, not taking into account reactivity against other variants including Omicron. To investigate the extent to which substitutions in spike and non-spike proteins affect T-cell recognition, several studies examined T-cells in vaccinated and convalescent individuals (49, 60–62). Overall, these studies show a high degree of preservation of T-cell epitopes between the ancestral strain, Omicron and other variants of concern. However, the degree of cross-reactivity varied among individuals, possibly as a consequence of genetic aspects of antigen presentation. Finally, it would have been interesting to directly compare homologous fourth BNT162b2 dose to mRNA-1273 in haemodialysis patients and to assess the reactogenicity, but this would have required a prospective study design for an interventional study.

Overall, a fourth full-dose of the mRNA-1273 vaccine elicits improved cellular and humoral responses compared to the triple BNT162b2 vaccination and appears to be an advisable strategy for immunocompromised patients, such as haemodialysis patients. Nevertheless, the decline after fourth vaccination and the effectivity against emerging SARS-CoV-2 variants will have to be monitored to assess the immune response duration and requirement for further booster vaccinations.

Data availability statement

The raw data supporting the conclusions of this article will be made available by the authors, without undue reservation.

Ethics statement

The studies involving human participants were reviewed and approved by the Internal Review Board of Hannover Medical School (MHH, approval number 8973_BO-K_2020, amendment Dec. 2020). The patients/participants provided their written informed consent to participate in this study.

Author contributions

GMNB, NS-M, AD, and MS conceived the study. MB, AD, MS, AD-J, GMNB, AC, NS-M, DJ, and MVS designed the experiments. NS-M, MS, GMNB, AD-J, and GK procured funding. GR, JG, JJ, DJ, and MVS performed experiments. KL, AB, EW, GL, AC, and GMNB collected samples or organised their collection. PK, BT, and UR produced and designed recombinant assay proteins. MB, KL, AD, MS, GR, MVS, and AC performed data collection and analysis. MB generated the figures. MB, MS, AD, and GMNB verified the underlying data. GMNB and MS wrote the first draft of the manuscript with input from MB, AC, KL, and AD. All authors critically reviewed and approved the final manuscript.

Funding

This work was financially supported by the Initiative and Networking Fund of the Helmholtz Association of German Research Centres (grant number SO-96), the EU Horizon 2020 research and innovation program (grant agreement number 101003480 - CORESMA), the State Ministry of Baden-Württemberg for Economic Affairs, Labour and Tourism (grant numbers FKZ 3-4332.62-NMI-67 and FKZ 3-4332.62-NMI-68) and the European Regional Development Fund (ZW7-8515131 and ZW7-85151373). The funders had no role in study design, data collection, data analysis, interpretation, writing or submission of the manuscript. All authors had complete access to the data and hold responsibility for the decision to submit for publication.

Acknowledgments

We sincerely thank all patients for their continued contribution and willingness to participate in this study. We also thank all clinical staff at the Eickenhof Dialysis Centre for their efforts to make this study possible.

Conflict of interest

NS-M was a speaker at Luminex user meetings in the past. The Natural and Medical Sciences Institute at the University of Tübingen is involved in applied research projects as a fee for services with the Luminex Corporation. GMNB was a speaker on a symposium sponsored by Moderna.

The remaining authors declare that the research was conducted in the absence of any commercial or financial relationships that could be construed as a potential conflict of interest.

Publisher's note

Supplementary material

The Supplementary Material for this article can be found online at: https://www.frontiersin.org/articles/10.3389/fimmu.2022.1004045/full#supplementary-material

References

1. Zeng B, Gao L, Zhou Q, Yu K, Sun F. Effectiveness of COVID-19 vaccines against SARS-CoV-2 variants of concern: A systematic review and meta-analysis. *BMC Med* (2022) 20(1):200. doi: 10.1186/s12916-022-02397-y

2. Manothummetha K, Chuleerarux N, Sanguankeo A, Kates OS, Hirankarn N, Thongkam A, et al. Immunogenicity and risk factors associated with poor humoral immune response of SARS-CoV-2 vaccines in recipients of solid organ transplant: A systematic review and meta-analysis. *JAMA Netw Open* (2022) 5(4):e226822. doi: 10.1001/jamanetworkopen.2022.6822

3. Galmiche S, Luong Nguyen LB, Tartour E, de Lamballerie X, Wittkop L, Loubet P, et al. Immunological and clinical efficacy of COVID-19 vaccines in immunocompromised populations: A systematic review. *Clin Microbiol Infect* (2022) 28(2):163–77. doi: 10.1016/j.cmi.2021.09.036

4. Kuderer NM, Lyman GH. COVID-19 vaccine effectiveness in patients with cancer: remaining vulnerabilities and uncertainties. *Lancet Oncol* (2022) 23(6):693–5. doi: 10.1016/S1470-2045(22)00252-2

5. Epidemiologisches Bulletin.Ständige Impfkommission: Beschluss der STIKO zur 20. Aktualisierung der COVID-19-Impfempfehlung. *Epid Bull* (2022) 21:3–19. doi: 10.25646/10076.2

6. *Update: FDA authorizes additional vaccine dose for certain immunocompromised individuals* (2021). Available at: https://www.fda.gov/news-events/press-announcements/coronavirus-covid-19-update-fda-authorizes-additional-vaccine-dose-certain-immunocompromised.

7. *Direction génèrale de la santé DGS precisions sur la vaccination IMD*. Available at: https://solidarites-sante.gouv.fr/IMG/pdf/dgs_urgent_52_precisions_sur_la_vaccination_imd.pdf.

8. Burki TK. Fourth dose of COVID-19 vaccines in Israel. *Lancet Respir Med* (2022) 10(2):e19. doi: 10.1016/S2213-2600(22)00010-8

9. Junker D, Becker M, Wagner TR, Kaiser PD, Maier S, Grimm TM, et al. Antibody binding and ACE2 binding inhibition is significantly reduced for both the BA1 and BA2 omicron variants. *Clin Infect Dis* (2022), ciac498. doi: 10.1093/cid/ciac498

10. van Gils MJ, Lavell A, van der Straten K, Appelman B, Bontjer I, Poniman M, et al. Antibody responses against SARS-CoV-2 variants induced by four different SARS-CoV-2 vaccines in health care workers in the Netherlands: A prospective cohort study. *PloS Med* (2022) 19(5):e1003991. doi: 10.1371/journal.pmed.1003991

11. Gruell H, Vanshylla K, Korenkov M, Tober-Lau P, Zehner M, Münn F, et al. SARS-CoV-2 Omicron sublineages exhibit distinct antibody escape patterns. *Cell Host Microbe* (2022) 30(9):1231–1241.e6. doi: 10.1101/2022.04.06.487257

12. van der Straten K, Guerra D, van Gils MJ, Bontjer I, Caniels TG, van Willigen HDG, et al. Antigenic cartography using sera from sequence-confirmed SARS-CoV-2 variants of concern infections reveals antigenic divergence of Omicron. *Immunity*. (2022) 55(9):1725–1731.e4. doi: 10.1016/j.immuni.2022.07.018

13. Anft M, Blazquez-Navarro A, Frahnert M, Fricke L, Meister TL, Roch T, et al. Inferior cellular and humoral immunity against omicron and delta variants of concern compared with SARS-CoV-2 wild type in hemodialysis patients immunized with 4 SARS-CoV-2 vaccine doses. *Kidney Int* (2022) 102(1):207–8. doi: 10.1016/j.kint.2022.05.004

14. Cheng CC, Platen L, Christa C, Tellenbach M, Kappler V, Bester R, et al. Improved SARS-CoV-2 neutralization of Delta and Omicron BA.1 variants of concern after fourth vaccination in hemodialysis patients. *Vaccines (Basel)* (2022) 10(8):1328. doi: 10.3390/vaccines10081328

15. Housset P, Kubab S, Hanafi L, Pardon A, Vittoz N, Bozman D-F, et al. Humoral response after a fourth "booster" dose of a coronavirus disease 2019 vaccine following a 3-dose regimen of mRNA-based vaccination in dialysis patients. *Kidney Int* (2022) 101(6):1289–90. doi: 10.1016/j.kint.2022.04.006

16. Strengert M, Becker M, Ramos GM, Dulovic A, Gruber J, Juengling J, et al. Cellular and humoral immunogenicity of a SARS-CoV-2 mRNA vaccine in patients on haemodialysis. *EBioMedicine*. (2021) 70:103524. doi: 10.1016/j.ebiom.2021.103524

17. Dulovic A, Strengert M, Ramos GM, Becker M, Griesbaum J, Junker D, et al. Diminishing immune responses against variants of concern in dialysis patients 4 months after SARS-CoV-2 mRNA vaccination. *Emerg Infect Dis* (2022) 28(4):743–50. doi: 10.3201/eid2804.211907

18. Behrens GMN, Cossmann A, Stankov MV, Schulte B, Streeck H, Förster R, et al. Strategic anti-SARS-CoV-2 serology testing in a low prevalence setting: The COVID-19 contact (CoCo) study in healthcare professionals. *Infect Dis Ther* (2020) 9(4):837–49. doi: 10.1007/s40121-020-00334-1

19. Becker M, Dulovic A, Junker D, Ruetalo N, Kaiser PD, Pinilla YT, et al. Immune response to SARS-CoV-2 variants of concern in vaccinated individuals. *Nat Commun* (2021) 12(1):3109. doi: 10.1038/s41467-021-23473-6

20. Rabenau HF, Biesert L, Schmidt T, Bauer G, Cinatl J, Doerr HW. SARS-coronavirus (SARS-CoV) and the safety of a solvent/detergent (S/D) treated immunoglobulin preparation. *Biologicals*. (2005) 33(2):95–9. doi: 10.1016/j.biologicals.2005.01.003

21. Becker M, Strengert M, Junker D, Kaiser PD, Kerrinnes T, Traenkle B, et al. Exploring beyond clinical routine SARS-CoV-2 serology using MultiCoV-ab to evaluate endemic coronavirus cross-reactivity. *Nat Commun* (2021) 12(1):1152. doi: 10.1038/s41467-021-20973-3

22. Planatscher H, Rimmele S, Michel G, Potz O, Joos T, Schneiderhan-Marra N. Systematic reference sample generation for multiplexed serological assays. *Sci Rep* (2013) 3:3259–64. doi: 10.1038/srep03259

23. Junker D, Dulovic A, Becker M, Wagner TR, Kaiser PD, Traenkle B, et al. COVID-19 patient serum less potently inhibits ACE2-RBD binding for various SARS-CoV-2 RBD mutants. *Sci Rep* (2022) 12(1):7168. doi: 10.1038/s41598-022-10987-2

24. Barros-Martins J, Hammerschmidt SI, Cossmann A, Odak I, Stankov MV, Morillas Ramos G, et al. Immune responses against SARS-CoV-2 variants after heterologous and homologous ChAdOx1 nCoV-19/BNT162b2 vaccination. *Nat Med* (2021) 27(9):1525–9. doi: 10.1038/s41591-021-01449-9

25. Behrens GMN, Barros-Martins J, Cossmann A, Ramos GM, Stankov MV, Odak I, et al. BNT162b2-boosted immune responses six months after heterologous or homologous ChAdOx1nCoV-19/BNT162b2 vaccination against COVID-19. *Nat Commun* (2022) 13(1):4872. doi: 10.1038/s41467-022-32527-2

26. Stankov MV, Cossmann A, Bonifacius A, Dopfer-Jablonka A, Ramos GM, Godecke N, et al. Humoral and cellular immune responses against severe acute respiratory syndrome coronavirus 2 variants and human coronaviruses after single BNT162b2 vaccination. *Clin Infect Dis* (2021) 73(11):2000–8. doi: 10.1093/cid/ciab555

27. Forni G, Mantovani A, Forni G, Mantovani A, Moretta L, Rappuoli R, et al. COVID-19 vaccines: where we stand and challenges ahead. *Cell Death Differentiation*. (2021) 28(2):626–39. doi: 10.1038/s41418-020-00720-9

28. Parker EPK, Tazare J, Hulme WJ, Bates C, Beale R, Carr EJ, et al. Factors associated with COVID-19 vaccine uptake in people with kidney disease: An OpenSAFELY cohort study. *medRxiv*. (2022), 2022.06.14.22276391. doi: 10.1101/2022.06.14.22276391

29. WHO. *The moderna COVID-19 (mRNA-1273) vaccine: what you need to know* (2022). Available at: https://www.who.int/news-room/feature-stories/detail/the-moderna-covid-19-mrna-1273-vaccine-what-you-need-to-know.

30. Van Praet J, Reynders M, De Bacquer D, Viaene L, Schoutteten MK, Caluwé R, et al. Predictors and dynamics of the humoral and cellular immune response to SARS-CoV-2 mRNA vaccines in hemodialysis patients: A multicenter observational study. *J Am Soc Nephrol* (2021) 32(12):3208. doi: 10.1681/ASN.2021070908

31. Yau K, Chan CT, Abe KT, Jiang Y, Atiquzzaman M, Mullin SI, et al. Differences in mRNA-1273 (Moderna) and BNT162b2 (Pfizer-BioNTech) SARS-CoV-2 vaccine immunogenicity among patients undergoing dialysis. *Can Med Assoc J* (2022) 194(8):E297. doi: 10.1503/cmaj.211881

32. Dulovic A, Kessel B, Harries M, Becker M, Ortmann J, Griesbaum J, et al. Comparative magnitude and persistence of humoral SARS-CoV-2 vaccination responses in the adult population in Germany. *Front Immunol* (2022) 13. doi: 10.3389/fimmu.2022.828053

33. Montoya JG, Adams AE, Bonetti V, Deng S, Link NA, Pertsch S, et al. Differences in IgG antibody responses following BNT162b2 and mRNA-1273 SARS-CoV-2 vaccines. *Microbiol spectrum*. (2021) 9(3):e0116221. doi: 10.1128/Spectrum.01162-21

34. Steensels D, Pierlet N, Penders J, Mesotten D, Heylen L. Comparison of SARS-CoV-2 antibody response following vaccination with BNT162b2 and mRNA-1273. *Jama*. (2021) 326(15):1533–5. doi: 10.1001/jama.2021.15125

35. Benning L, Klein K, Morath C, Bartenschlager M, Kim H, Buylaert M, et al. Neutralizing antibody activity against the B.1.617.2 (delta) variant before and after a third BNT162b2 vaccine dose in hemodialysis patients. *Front Immunol* (2022) 13. doi: 10.3389/fimmu.2022.840136

36. Espi M, Charmetant X, Barba T, Mathieu C, Pelletier C, Koppe L, et al. A prospective observational study for justification, safety, and efficacy of a third dose of mRNA vaccine in patients receiving maintenance hemodialysis. *Kidney Int* (2022) 101(2):390–402. doi: 10.1016/j.kint.2021.10.040

37. Tillmann F-P, Figiel L, Ricken J, Still H, Korte C, Plaßmann G, et al. Effect of third and fourth mRNA-based booster vaccinations on SARS-CoV-2 neutralizing antibody titer formation, risk factors for non-response, and outcome after SARS-CoV-2 omicron breakthrough infections in patients on chronic hemodialysis: A

prospective multicenter cohort study. *J Clin Med* (2022) 11(11):3187–201. doi: 10.3390/jcm11113187

38. Patyna S, Eckes T, Koch BF, Sudowe S, Oftring A, Kohmer N, et al. Impact of moderna mRNA-1273 booster vaccine on fully vaccinated high-risk chronic dialysis patients after loss of humoral response. *Vaccines* (2022) 10(4):585–94. doi: 10.3390/vaccines10040585

39. Bensouna I, Caudwell V, Kubab S, Acquaviva S, Pardon A, Vittoz N, et al. SARS-CoV-2 antibody response after a third dose of the BNT162b2 vaccine in patients receiving maintenance hemodialysis or peritoneal dialysis. *Am J Kidney Diseases.* (2022) 79(2):185–92.e1. doi: 10.1053/j.ajkd.2021.08.005

40. Niesen Michiel JM, Matson R, Puranik A, O'Horo John C, Pawlowski C, Vachon C, et al. Third dose vaccination with mRNA-1273 or BNT162b2 vaccines improves protection against SARS-CoV-2 infection. *PNAS Nexus* (2022) 1(2): pgac042. doi: 10.1093/pnasnexus/pgac042

41. Benotmane I, Gautier G, Perrin P, Olagne J, Cognard N, Fafi-Kremer S, et al. Antibody response after a third dose of the mRNA-1273 SARS-CoV-2 vaccine in kidney transplant recipients with minimal serologic response to 2 doses. *JAMA.* (2021) 326(11):1063–5. doi: 10.1001/jama.2021.12339

42. Lustig Y, Gonen T, Meltzer L, Gilboa M, Indenbaum V, Cohen C, et al. Superior immunogenicity and effectiveness of the third compared to the second BNT162b2 vaccine dose. *Nat Immunol* (2022) 23(6):940–6. doi: 10.1038/s41590-022-01212-3

43. Pajon R, Doria-Rose NA, Shen X, Schmidt SD, O'Dell S, McDanal C, et al. SARS-CoV-2 omicron variant neutralization after mRNA-1273 booster vaccination. *N Engl J Med* (2022) 386(11):1088–91. doi: 10.1056/NEJMc2119912

44. Xia H, Zou J, Kurhade C, Cai H, Yang Q, Cutler M, et al. Neutralization and durability of 2 or 3 doses of the BNT162b2 vaccine against omicron SARS-CoV-2. *Cell Host Microbe* (2022) 30(4):485–8.e3. doi: 10.1016/j.chom.2022.02.015

45. Sette A, Crotty S. Immunological memory to SARS-CoV-2 infection and COVID-19 vaccines. *Immunol Rev* (2022) 310(1):27–46. doi: 10.1111/imr.13089

46. Bonifacius A, Tischer-Zimmermann S, Dragon AC, Gussarow D, Vogel A, Krettek U, et al. COVID-19 immune signatures reveal stable antiviral T cell function despite declining humoral responses. *Immunity.* (2021) 54(2):340–54.e6. doi: 10.1016/j.immuni.2021.01.008

47. Guerrera G, Picozza M, D'Orso S, Placido R, Pirronello M, Verdiani A, et al. BNT162b2 vaccination induces durable SARS-CoV-2-specific T cells with a stem cell memory phenotype. *Sci Immunol* (2021) 6(66):eabl5344. doi: 10.1126/sciimmunol.abl5344

48. Mateus J, Dan JM, Zhang Z, Rydyznski Moderbacher C, Lammers M, Goodwin B, et al. Low-dose mRNA-1273 COVID-19 vaccine generates durable memory enhanced by cross-reactive T cells. *Science* (2021) 374(6566):eabj9853. doi: 10.1126/science.abj9853

49. Tarke A, Coelho CH, Zhang Z, Dan JM, Yu ED, Methot N, et al. SARS-CoV-2 vaccination induces immunological T cell memory able to cross-recognize variants from alpha to omicron. *Cell.* (2022) 185(5):847–59.e11. doi: 10.1016/j.cell.2022.01.015

50. Zhang Z, Mateus J, Coelho CH, Dan JM, Moderbacher CR, Galvez RI, et al. Humoral and cellular immune memory to four COVID-19 vaccines. *Cell.* (2022) 185(14):2434–51.e17. doi: 10.1016/j.cell.2022.05.022

51. Lederer K, Bettini E, Parvathaneni K, Painter MM, Agarwal D, Lundgreen KA, et al. Germinal center responses to SARS-CoV-2 mRNA vaccines in healthy and immunocompromised individuals. *Cell.* (2022) 185(6):1008–24.e15. doi: 10.1016/j.cell.2022.01.027

52. Turner JS, O'Halloran JA, Kalaidina E, Kim W, Schmitz AJ, Zhou JQ, et al. SARS-CoV-2 mRNA vaccines induce persistent human germinal centre responses. *Nature.* (2021) 596(7870):109–13. doi: 10.1038/s41586-021-03738-2

53. Janssen C, Cachanado M, Ninove L, Lachatre M, Michon J, Epaulard O, et al. Immunogenicity and reactogenicity of heterologous and homologous mRNA-1273 and BNT162b2 vaccination: A multicenter non-inferiority randomized trial. *eClinicalMedicine.* (2022) 48:101444. doi: 10.1016/j.eclinm.2022.101444

54. Regev-Yochay G, Gonen T, Gilboa M, Mandelboim M, Indenbaum V, Amit S, et al. Efficacy of a fourth dose of covid-19 mRNA vaccine against omicron. *New Engl J Med* (2022) 386(14):1377–80. doi: 10.1056/NEJMc2202542

55. Munro APS, Janani L, Cornelius V, Aley PK, Babbage G, Baxter D, et al. Safety and immunogenicity of seven COVID-19 vaccines as a third dose (booster) following two doses of ChAdOx1 nCov-19 or BNT162b2 in the UK (COV-BOOST): a blinded, multicentre, randomised, controlled, phase 2 trial. *Lancet* (2021) 398(10318):2258–76. doi: 10.1016/S0140-6736(21)02717-3

56. Kaplonek P, Cizmeci D, Fischinger S, A-r C, Suscovich T, Linde C, et al. mRNA-1273 and BNT162b2 COVID-19 vaccines elicit antibodies with differences in fc-mediated effector functions. *Sci Trans Med* (2022) 14(645):eabm2311. doi: 10.1126/scitranslmed.abm2311

57. De Marco L, D'Orso S, Pirronello M, Verdiani A, Termine A, Fabrizio C, et al. Assessment of T-cell reactivity to the SARS-CoV-2 omicron variant by immunized individuals. *JAMA Network Open* (2022) 5(4):e2210871–e. doi: 10.1001/jamanetworkopen.2022.10871

58. Jung MK, Jeong SD, Noh JY, Kim D-U, Jung S, Song JY, et al. BNT162b2-induced memory T cells respond to the omicron variant with preserved polyfunctionality. *Nat Microbiol* (2022) 7(6):909–17. doi: 10.1038/s41564-022-01123-x

59. Jergović M, Coplen CP, Uhrlaub JL, Beitel SC, Burgess JL, Lutrick K, et al. Cutting edge: T cell responses to B.1.1.529 (Omicron) SARS-CoV-2 variant induced by COVID-19 infection and/or mRNA vaccination are largely preserved. *J Immunol* (2022) 208(11):2461–5. doi: 10.4049/jimmunol.2200175

60. Naranbhai V, Nathan A, Kaseke C, Berrios C, Khatri A, Choi S, et al. T Cell reactivity to the SARS-CoV-2 omicron variant is preserved in most but not all individuals. *Cell.* (2022) 185(6):1041–51.e6. doi: 10.1016/j.cell.2022.01.029

61. Keeton R, Tincho MB, Ngomti A, Baguma R, Benede N, Suzuki A, et al. T Cell responses to SARS-CoV-2 spike cross-recognize omicron. *Nature.* (2022) 603 (7901):488–92. doi: 10.1038/s41586-022-04460-3

62. GeurtsvanKessel CH, Geers D, Schmitz KS, Mykytyn AZ, Lamers MM, Bogers S, et al. Divergent SARS-CoV-2 omicron-reactive T and b cell responses in COVID-19 vaccine recipients. *Sci Immunol* (2022) 7(69):eabo2202. doi: 10.1126/sciimmunol.abo2202

Supplementary Material

Longitudinal cellular and humoral immune responses after triple BNT162b2 and fourth full-dose mRNA-1273 vaccination in haemodialysis patients

Matthias Becker[1#], Anne Cossmann[2#], Karsten Lürken[3], Daniel Junker[1], Jens Gruber[1], Jennifer Juengling[1], Gema Morillas Ramos[1], Andrea Beigel[3], Eike Wrenger[3], Gerhard Lonnemann[3], Metodi V. Stankov[2], Alexandra Dopfer-Jablonka[2,4], Philipp D. Kaiser[1], Bjoern Traenkle[1], Ulrich Rothbauer[1,5], Gérard Krause[4,6,7], Nicole Schneiderhan-Marra[1], Monika Strengert[6,7,*], Alex Dulovic[1,*], Georg M.N. Behrens[2,4,8,*]

Author Affiliations

1. NMI Natural and Medical Sciences Institute at the University of Tübingen, Reutlingen, Germany
2. Department for Rheumatology and Immunology, Hannover Medical School, Hannover, Germany
3. Dialysis Centre Eickenhof, Langenhagen, Germany
4. German Centre for Infection Research (DZIF), partner site Hannover-Braunschweig, Germany
5. Pharmaceutical Biotechnology, University of Tübingen, Tübingen, Germany
6. Helmholtz Centre for Infection Research, Braunschweig, Germany
7. TWINCORE GmbH, Centre for Experimental and Clinical Infection Research, a joint venture of the Hannover Medical School and the Helmholtz Centre for Infection Research, Hannover, Germany
8. CiiM - Centre for Individualized Infection Medicine, Hannover, Germany

#,* these authors contributed equally to this work.

* corresponding authors.

Corresponding authors contact details:

Monika Strengert, Phone number: +49 (0)531 3103 Email address: monika.strengert@helmholtz-hzi.de, Postal address: Inhoffenstraße 7, 38124 Braunschweig, Germany.

Alex Dulovic, Phone number: +49 (0)7121 51530 580, Email address: alex.dulovic@nmi.de, Postal address: Markwiesenstraße 55, 72770 Reutlingen, Germany.

Georg M.N. Behrens, Phone number: +49 (0)511 532 5337, Email address: behrens.georg@mh-hannover.de, Postal address: Carl-Neuberg-Straße 1, 30625 Hannover, Germany.

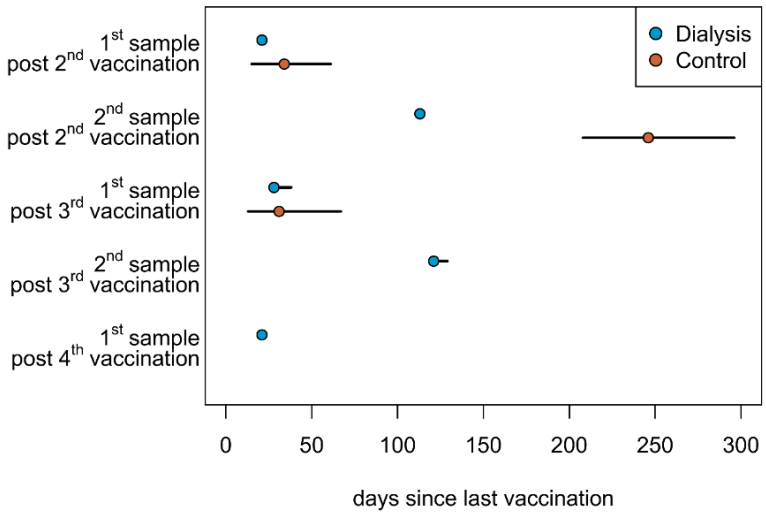

Figure S1. Sampling time points after COVID-19 vaccination in the study population.
Graphic display of median and absolute range of sampling times after the indicated vaccination of haemodialysis patients (n=50, blue circles) and healthcare workers (n=33, orange circles), who served as controls. Controls were triple-vaccinated with BNT162b2 (vaccination 1-3) whereas haemodialysed individuals received an additional full-dose of mRNA-1273 (vaccination 4).

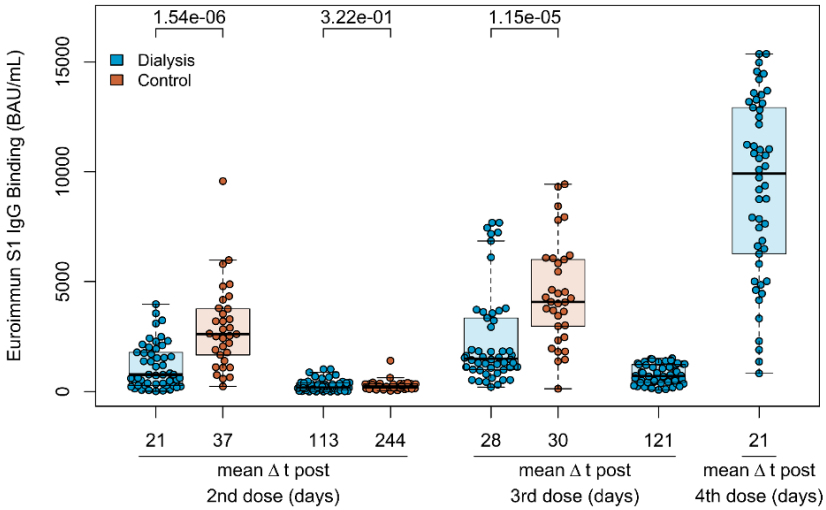

Figure S2. Development of quantitative plasma IgG titres after COVID-19 vaccination.
Spike subdomain 1 (S1)-plasma IgG from haemodialysis patients (blue circles, n=50) and controls (orange circles, n=33) were analysed using the QuantiVac-ELISA from Euroimmun (BAU/mL) after a triple vaccination with BNT162b2. For haemodialysed individuals, S1 IgG titres are additionally shown after a fourth 100 µg (full) dose of mRNA-1273. Mean sampling time in days after the respective vaccination is displayed as Δt on the x-axis. Boxes represent the median, 25th and 75th percentiles, whiskers show the largest and smallest non-outlier values. Outliers were determined by 1.5 times IQR. Statistical significance was calculated by two-sided Mann-Whitney-U test. P-values for relevant comparisons are given above the sample groups. Significance was defined as $p<0.05$. Response data from dialysed individuals from day 21 and day 113 after the second BNT162b2 dose were already published before as part of Strengert *et al.* (1) and Dulovic *et al.* (2).

2

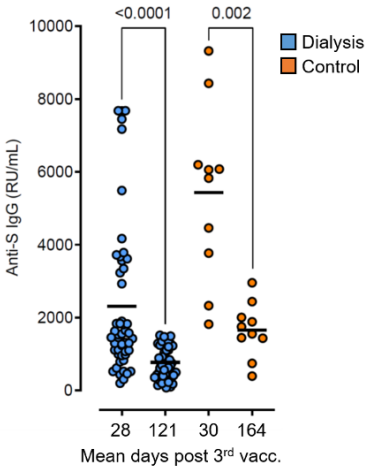

Figure S3. Decline in anti-S1 IgG after the third vaccination.
Spike subdomain 1 (S)-plasma IgG of dialysis patients (n=50) and a subgroup of healthy controls (n=10) after the third vaccination. Note that the second time point was slightly different with mean 121 days (range 119-129 days) for dialysis patients and mean 164 days (range 112-223 days) in healthy controls. Reduction mean anti-S1 IgG in dialysis patients and the control group was 3-fold and 3.2-fold, respectively. Statistical significance was calculated by two-sided paired Wilcoxon rank test. Significance was defined as $p<0.05$.

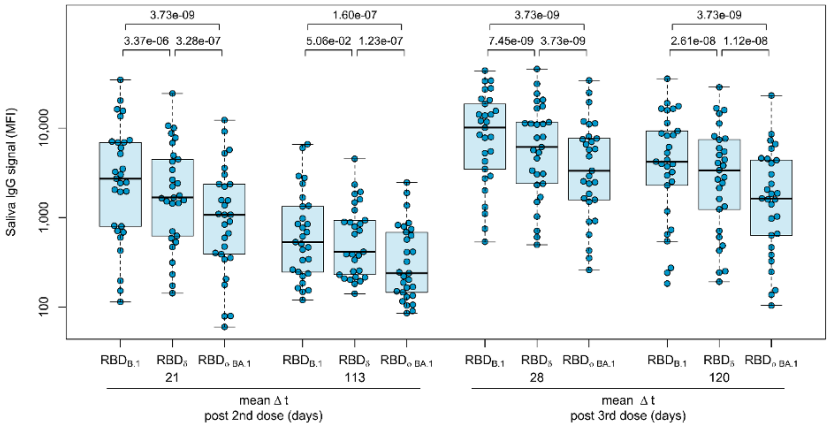

Figure S4. Mucosal immune response in haemodialysis patients after triple vaccination with BNT162b2. IgG response in saliva of haemodialysis patients (n=29) towards the SARS-CoV-2 RBD of B.1, Delta and Omicron BA.1 isolates were measured using MULTICOV-AB. Data is displayed as median fluorescence intensity (MFI) signal for IgG binding. Sampling time points in days after a completed standard two-dose BNT162b2 vaccination is stated on the x-axis. Statistical significance was calculated by two-sided paired Wilcoxon rank test. Significance was defined as $p<0.05$. P-values for relevant comparisons are given above the sample groups. Response data from dialysed individuals from day 21 and day 113 after the second BNT162b2 dose were already published before as part of Strengert *et al.* (1) and Dulovic *et al.* (2).

Table S1. Indication for haemodialysis in the study population.

Characteristics	Haemodialysis group (n=50)
Diagnosis (n, %)	
Autosomal dominant polycystic kidney disease	7 (14.0)
Chronic glomerulonephritis	3 (6.0)
Diabetic nephropathy	8 (16.0)
Focal segmental glomerulosclerosis	3 (6.0)
IgA nephropathy	7 (14.0)
Interstitial nephritis	4 (8.0)
Nephrosclerosis	11 (22.0)
Acute toxic tubular epithelial damage syndrome	1 (2.0)
Anti-Neutrophilic Cytoplasmic Autoantibody (ANCA)-associated vasculitis	1 (2.0)
Medullary cystic kidney disease	1 (2.0)
Membranous glomerulonephritis	1 (2.0)
Kidney dysplasia	1 (2.0)
Obstructive nephropathy	1 (2.0)
Cystic kidney disease	1 (2.0)
Cyclosporin intoxication	1 (2.0)

Table S2. Medication of study participants. NA - Information not available.

Medication (n, %)	Haemodialysis group (n=50)	Non-dialysis control group (n=33)
Angiotensin-converting enzyme inhibitor	15 (30.0)	2 (6.1)
Statins	28 (56.0)	0 (0.0)
Angiotensin II Receptor Blocker	16 (32.0)	1 (3.0)
Vitamin D Supplements	49 (98.0)	NA
L-Thyroxine	0 (0.0)	3 (9.1)
Ca^{2+} channel antagonist	0 (0.0)	2 (6.1)
5-aminosalicylic acid	0 (0.0)	1 (3.0)
DPP4 inhibitor + metformin	0 (0.0)	1 (3.0)
Factor Xa inhibitor	0 (0.0)	1 (3.0)
Immunosuppressants (dosing range per day)		
Prednisolone (2 mg; every second day)	1 (2.0)	0 (0.0)
Prednisolone (5 mg)*	2 (4.0)	0 (0.0)
Prednisolone (7.5 mg)	1 (2.0)	0 (0.0)
Prednisolone (5 mg), Tacrolimus (1-2 mg)	2 (4.0)	0 (0.0)
Prednisolone (5 mg), Tacrolimus (12 mg), Mycophenolatmofetil (500 mg)**	1 (2.0)	0 (0.0)
Hydrocortisone (20 mg)	1 (2.0)	0 (0.0)
5-Fluorouracil***	1 (2.0)	0 (0.0)

* One patient discontinued prednisolone 128 days after the second and 68 days before the third BNT162b2 dose.
** Mycophenolatmofetil discontinued 166 days after the second and 30 days before the third BNT162b2 dose.
*** First treatment cycle started 63 days before the fourth vaccination with mRNA-1273.

Table S3. Statistical comparison of longitudinal cellular and humoral vaccination responses in haemodialysis patients.

Assay	Variant	Figure	Sample 1 vs 2	Sample 1 vs 3	Sample 3 vs 4	Sample 3 vs 5
MULTICOV-AB	B.1	3a	$1.51*10^{-9}$	$1.61*10^{-9}$	$2.44*10^{-9}$	$1.05*10^{-9}$
RBDCoV-ACE2	B.1	3b	0.005	$7.79*10^{-10}$	$4.38*10^{-9}$	$7.79*10^{-10}$
RBDCoV-ACE2	Delta	3c	0.013	$1.15*10^{-9}$	$1.20*10^{-8}$	$7.79*10^{-10}$
RBDCoV-ACE2	Omicron BA.1	3d	0.002	$3.52*10^{-7}$	$8.48*10^{-7}$	$1.15*10^{-9}$
IGRA	B.1	4a	$1.38*10^{-5}$	0.564	NA	0.0005

References

1. Strengert M, Becker M, Ramos GM, Dulovic A, Gruber J, Juengling J, et al. Cellular and humoral immunogenicity of a SARS-CoV-2 mRNA vaccine in patients on haemodialysis. EBioMedicine. 2021;70:103524.
2. Dulovic A, Strengert M, Ramos GM, Becker M, Griesbaum J, Junker D, et al. Diminishing Immune Responses against Variants of Concern in Dialysis Patients 4 Months after SARS-CoV-2 mRNA Vaccination. Emerg Infect Dis. 2022;28(4):743-50.

Appendix IX: STAR SIGN study: Evaluation of COVID-19 vaccine efficacy against the SARS-CoV-2 variants BQ.1.1 and XBB.1.5 in patients with inflammatory bowel disease

Woelfel S, Dütschler J, König M, Dulovic A, Graf N, **Junker D**, Oikonomou V, Krieger C, Truniger S, Franke A, Eckhold A, Forsch K, Koller S, Wyss J, Krupka N, Oberholzer M, Frei N, Geissler N, Schaub P; STAR SIGN Study Investigators; Albrich WC, Friedrich M, Schneiderhan-Marra N, Misselwitz B, Korte W, Bürgi JJ, Brand S.

Alimentary Pharmacology and Therapeutics. 2023. 58(7):678-691

https://doi.org/10.1111/apt.17661

Received: 3 July 2023 | First decision: 6 July 2023 | Accepted: 26 July 2023

DOI: 10.1111/apt.17661

AP&T Alimentary Pharmacology & Therapeutics WILEY

STAR SIGN study: Evaluation of COVID-19 vaccine efficacy against the SARS-CoV-2 variants BQ.1.1 and XBB.1.5 in patients with inflammatory bowel disease

Simon Woelfel[1,2] | Joel Dütschler[2,3] | Marius König[2] | Alex Dulovic[4] | Nicole Graf[5] | Daniel Junker[4] | Vasileios Oikonomou[6] | Claudia Krieger[2] | Samuel Truniger[2,3] | Annett Franke[2,3] | Annika Eckhold[2] | Kristina Forsch[2] | Seraina Koller[2] | Jacqueline Wyss[6] | Niklas Krupka[6] | Melanie Oberholzer[7] | Nicola Frei[2] | Nora Geissler[2] | Peter Schaub[2] | STAR SIGN Study Investigators | Werner C. Albrich[8] | Matthias Friedrich[9] | Nicole Schneiderhan-Marra[4] | Benjamin Misselwitz[6] | Wolfgang Korte[7] | Justus J. Bürgi[7] | Stephan Brand[2]

[1]Max von Pettenkofer Institute of Hygiene and Medical Microbiology, Faculty of Medicine, Ludwig Maximilian University of Munich (LMU Munich), Munich, Germany

[2]Department of Gastroenterology and Hepatology, Cantonal Hospital St. Gallen, St. Gallen, Switzerland

[3]Outpatient Clinic, Ambulatory Services Rorschach, Rorschach, Switzerland

[4]NMI Natural and Medical Sciences Institute at the University of Tübingen, Reutlingen, Germany

[5]Clinical Trials Unit, Cantonal Hospital St. Gallen, St. Gallen, Switzerland

[6]Department of Visceral Surgery and Medicine, Inselspital Bern University Hospital, University of Bern, Bern, Switzerland

[7]Center for Laboratory Medicine, St. Gallen, Switzerland

[8]Division of Infectious Diseases & Hospital Epidemiology, Cantonal Hospital St. Gallen, St. Gallen, Switzerland

[9]Translational Gastroenterology Unit, Nuffield Department of Medicine, University of Oxford, Oxford, UK

Correspondence
Stephan Brand, Department of Gastroenterology and Hepatology, Cantonal Hospital St. Gallen, St. Gallen, Switzerland.
Email: stephan.brand@kssg.ch

Funding information
Cantonal Hospital St. Gallen; HORIZON EUROPE European Research Council, Grant/Award Number: 101003480-CORESMA; State Ministry of Baden-Württemberg for Economic Affairs, Labour and Tourism, Grant/Award Number: FKZ-3-4332.62-NMI-67 and FKZ 3-4332.62-NMI-68; University of Oxford

Summary

Background: Vaccine-elicited immune responses are impaired in patients with inflammatory bowel disease (IBD) treated with anti-TNF biologics.

Aims: To assess vaccination efficacy against the novel omicron sublineages BQ.1.1 and XBB.1.5 in immunosuppressed patients with IBD.

Methods: This prospective multicentre case–control study included 98 biologic-treated patients with IBD and 48 healthy controls. Anti-spike IgG concentrations and surrogate neutralisation against SARS-CoV-2 wild-type, BA.1, BA.5, BQ.1.1, and XBB.1.5 were measured at two different time points (2–16 weeks and 22–40 weeks) following third dose vaccination. Surrogate neutralisation was based on antibody-mediated blockage of ACE2-spike protein–protein interaction. Primary outcome was surrogate neutralisation against tested SARS-CoV-2 sublineages. Secondary outcomes were proportions of participants with insufficient surrogate neutralisation, impact of breakthrough infection, and correlation of surrogate neutralisation with anti-spike IgG concentration.

The Handling Editor for this article was Professor Colin Howden, and it was accepted for publication after full peer-review.

Results: Surrogate neutralisation against all tested sublineages was reduced in patients with IBD who were treated with anti-TNF biologics compared to patients treated with non-anti-TNF biologics and healthy controls (each $p \leq 0.001$) at visit 1. Anti-TNF therapy (odds ratio 0.29 [95% CI 0.19–0.46]) and time since vaccination (0.85 [0.72–1.00]) were associated with low, and mRNA-1273 vaccination (1.86 [1.12–3.08]) with high wild-type surrogate neutralisation in a β-regression model. Accordingly, higher proportions of patients treated with anti-TNF biologics had insufficient surrogate neutralisation against omicron sublineages at visit 1 compared to patients treated with non-anti-TNF biologics and healthy controls (each $p \leq 0.015$). Surrogate neutralisation against all tested sublineages decreased over time but was increased by breakthrough infection. Anti-spike IgG concentrations correlated with surrogate neutralisation.

Conclusions: Patients with IBD who are treated with anti-TNF biologics show impaired neutralisation against novel omicron sublineages BQ.1.1 and XBB.1.5 and may benefit from prioritisation for future variant-adapted vaccines.

1 | INTRODUCTION

SARS-CoV-2 vaccines have proven to be effective and powerful tools in the combat against the COVID-19 pandemic by saving millions of lives.[1,2] However, the increase in SARS-CoV-2 immunisation world-wide positively selected for new virus subvariants which can overcome vaccine-elicited immune defences and have increased transmissibility.[3–7] Therefore, it is important to continue the surveillance of immune responses against such subvariants in the population in order to identify and protect vulnerable patient groups with an impaired response to SARS-CoV-2 vaccines.

One of such groups are patients with inflammatory bowel diseases (IBD), a multifactorial immune disorder that often requires treatment with immunomodulatory biologic agents.[8] It was shown that patients with IBD who are treated with biologics that antagonise the proinflammatory cytokine TNF-alpha (anti-TNF), such as infliximab or adalimumab, have impaired humoral immunity following SARS-CoV-2 mRNA vaccination, when compared to healthy controls.[9–11] In contrast, immunogenicity is not altered by treatment with other biologics such as vedolizumab or ustekinumab which antagonise α4β7-integrin and interleukin-12 and -23, respectively.[9,10,12] Recently, we and others demonstrated that impaired immune responses in anti-TNF-treated patients with IBD manifest even after a third dose of SARS-CoV-2 mRNA vaccines.[13–16] This impaired humoral vaccine response correlates with a higher rate of SARS-CoV-2 breakthrough infections in anti-TNF-treated patients with IBD, highlighting the increased risk faced by these patients.[15,17] Vaccination with a fourth dose of omicron-adapted bivalent vaccines can protect from severe COVID-19 and is recommended for at risk immunosuppressed patients including anti-TNF-treated patients with IBD.[18] Such vaccines were shown to induce substantial neutralisation against omicron sublineages BA.1 and to a lesser extent against BA.5 in healthy individuals.[19,20] However, vaccination hesitancy is high and vaccine fatigue poses a threat to further containment of the SARS-CoV-2 pandemic.[21–24] Moreover, the novel SARS-CoV-2 omicron sublineages BQ, XBB, and their derivatives display alarming levels of neutralisation escape and caused recent surges of COVID-19 infections worldwide.[25–27]

To this date, no data on neutralisation against these subvariants in patients with IBD are available. Therefore, it remains unknown if the conventional three dose SARS-CoV-2 vaccination scheme sufficiently protects patients with IBD on immunosuppressive treatment during current COVID-19 waves. To our knowledge, this collaborative study between several Swiss tertiary IBD centres, NMI Reutlingen, and the University of Oxford is the first study to assess neutralisation against the novel omicron sublineages BQ.1.1 and XBB.1.5 in patients with IBD and in anti-TNF-treated patients in general.

2 | METHODS

2.1 | Study design

STAR SIGN (Systemic and T cell-Associated Responses to SARS-CoV-2 booster Immunisation in Gut iNflammation) is a national multi-centre case–control study investigating the impact of biologic treatment in patients with IBD on immunogenicity towards SARS-CoV-2 vaccination.[13] It is designed as an observational trial combining prospective data from patient questionnaires and blood sample analysis with retrospective data collected manually from electronic medical records. The study protocol received approval by the Ethics Committee of Eastern Switzerland under the project-ID 2021-02511.

2.2 | Study population

Patients were recruited during regular hospital visits at the IBD outpatient clinic of the Cantonal Hospital St. Gallen, the outpatient

clinic Rorschach, and the IBD outpatient clinic of the Inselspital Bern University Hospital. Healthy subjects were recruited from staff of the Cantonal Hospital St. Gallen, excluding those who are directly involved in the study. Inclusion criteria were age of 18 years or older and third dose SARS-CoV-2 mRNA vaccination 2–16 weeks before study inclusion. For patients, a diagnosis of UC, CD or indeterminate colitis and therapy with either anti-TNF- (infliximab, adalimumab, golimumab, and certolizumab pegol), or non-anti-TNF-targeting (vedolizumab and ustekinumab) biologics were additional requirements. Absence of IBD was required for healthy subjects. Study exclusion criteria were incapability to answer the questionnaire, absence of signed consent, pregnancy at the time of SARS-CoV-2 third dose vaccination or between vaccination and study inclusion, and administration of SARS-CoV-2 vaccines other than BNT162b2 or mRNA-1273. Furthermore, study exclusion criteria for control subjects were use of immunosuppressive medication (steroids, immunomodulators, and biologics) within 6 months before third-dose vaccination, or between vaccination and study inclusion. Upon study inclusion, participant information on vaccine type (BNT162b2, mRNA-1273), demographics (age, gender, ethnicity, education, BMI, smoking status, and comorbidities), IBD diagnosis (CD, UC, and indeterminate colitis), disease duration, age at disease diagnosis, concomitant medication, disease activity, and SARS-CoV-2 infection status based on PCR or antigen testing were recorded. Study population characteristics are described in Table 1.

2.3 | Study outcomes

The primary outcome was to determine if surrogate neutralisation against SARS-CoV-2 wild-type and omicron sublineages BA.1, BA.5, BQ.1.1, and XBB.1.5 following third-dose vaccination differs in anti-TNF-treated patients with IBD compared to patients with IBD who are treated with non-anti-TNF biologics and healthy controls.

Secondary outcomes were:

(i) proportion of participants having non-inhibitory surrogate neutralisation of less than 20% against SARS-CoV-2 wild-type and omicron sublineages, stratified by study group,
(ii) impact of omicron breakthrough infection on surrogate neutralisation against SARS-CoV-2 wild-type and omicron sublineages, and
(iii) correlation of serum anti-spike IgG concentrations with surrogate neutralisation against SARS-CoV-2 wild-type and omicron sublineages.

2.4 | Definitions of SARS-CoV-2 infection status, severe infection, and steroid use

Individuals with no detectable anti-nucleocapsid IgG antibodies who did not report PCR- or antigen-test confirmed SARS-CoV-2 infection were considered SARS-CoV-2-naïve.

Third dose breakthrough infection was based on several parameters and was considered proven in participants who:

(i) reported infection between 12 days post third-dose vaccination and visit 1 or between visits 1 and 2 based on positive PCR- or antigen-test,
(ii) had detectable anti-nucleocapsid IgG at visit 2 but not at visit 1,
(iii) or had higher anti-spike IgG concentrations at visit 2 compared to visit 1, if data were available.

Infection before vaccination was based on reported positive SARS-CoV-2 PCR- or antigen-test before third vaccination.

Severe COVID-19 was based on reported hospitalisation due to SARS-CoV-2 infection.

Steroid use was defined as the application of systemic or topical steroids at the time of SARS-CoV-2 vaccination.

2.5 | Measurement of SARS-CoV-2 spike protein- and nucleocapsid-reactive antibody concentrations

Antibody measurements were performed in the ISO/IEC accredited Center of Laboratory Medicine in St. Gallen, Switzerland, by trained laboratory staff. Serum of study participants was isolated after coagulation for 20 min by centrifugation for 10 min at 2800*g*. SARS-CoV-2 spike protein-reactive IgG was quantified using the chemiluminescence immunoassay LIAISON® SARS-CoV-2 TrimericS IgG assay (DiaSorin Inc.) in accordance with manufacturer's instructions and as described earlier.[13] Briefly, serum anti-spike IgG antibodies bind to trimeric spike protein immobilised on magnetic particles and are detected using isoluminol-conjugated anti-human IgG antibodies. Bound IgG are quantified by measuring the Relative Light Units released by the conjugated luminol in a flash chemiluminescence reaction. For conversion of Relative Light Units to the WHO international standard BAU/ml (BAU = binding antibody units), the numerical factor 2.6 was used, as recommended by the manufacturer. Where needed, samples were diluted 1:20 in LIAISON® TrimericS IgG Diluent Accessory.

SARS-CoV-2 nucleocapsid-reactive IgG in participant sera was qualitatively measured using the Biomerica COVID-19 IgG/IgM Rapid Test (Biomerica) in accordance with manufacturer's instructions and as described before.[13] Briefly, this lateral flow chromatographic immunoassay is based on binding of serum antibodies by a SARS-CoV-2 nucleocapsid antigen-gold conjugate, and subsequent reaction with human-directed IgM and IgG upon membrane migration.

2.6 | Determination of surrogate neutralisation against SARS-CoV-2 wild-type and omicron sublineages

Surrogate neutralisation against SARS-CoV-2 wild-type and BA.1, BA.5, BQ.1.1, and XBB.1.5 subvariants was determined as

TABLE 1 Baseline characteristics of participants included in the analyses of this study.

Variable	Level	Anti-TNF-treated IBD patients	Non-anti-TNF-treated IBD patients	Healthy controls
n		59	39	48
Type of vaccine (%)	BNT162b2 (Pfizer-BioNTec)	44 (74.6)	30 (76.9)	44 (91.7)
	mRNA-1273 (Moderna)	15 (25.4)	9 (23.1)	4 (8.3)
Age, years (mean (SD))		44.39 (14.71)	50.15 (17.03)	47.77 (11.61)
Gender (%)	Female	28 (47.5)	12 (30.8)	28 (58.3)
	Male	31 (52.5)	27 (69.2)	20 (41.7)
Ethnicity (%)	European	56 (94.9)	39 (100.0)	46 (95.8)
	Asian	0 (0.0)	0 (0.0)	1 (2.1)
	African	1 (1.7)	0 (0.0)	0 (0.0)
	Other	2 (3.4)	0 (0.0)	1 (2.1)
Education (%)	Primary	10 (16.9)	3 (7.7)	1 (2.1)
	Secondary	28 (47.5)	19 (48.7)	11 (22.9)
	Tertiary	21 (35.6)	17 (43.6)	36 (75.0)
BMI, kg/m^2 (mean (SD))		24.45 (3.63)	25.81 (5.32)	24.34 (3.42)
Smoking (%)	Current	11 (18.6)	5 (12.8)	10 (20.8)
	Former	24 (40.7)	16 (41.0)	12 (25.0)
	Never	24 (40.7)	18 (46.2)	26 (54.2)
Diagnosis (%)	Crohn's Disease	44 (74.6)	24 (61.5)	
	Indeterminate Colitis	0 (0.0)	1 (2.6)	
	Ulcerative Colitis	15 (25.4)	14 (35.9)	
Disease duration, years (median [IQR])		11.00 [6.00, 21.00]	11.50 [6.25, 21.50]	
Age at diagnosis, years (median [IQR])		26.00 [20.00, 39.00]	29.00 [21.25, 49.75]	
Steroids (%)	Yes	15 (25.4)	7 (17.9)	
	No	44 (74.6)	32 (82.1)	
Immunomodulator (%)	Yes	1 (1.7)	1 (2.6)	
	No	58 (98.3)	38 (97.4)	
ASA-5 (%)	Yes	12 (20.3)	13 (33.3)	
Disease activity (PRO2) (%)	Remission	40 (69.0)	23 (59.0)	
	Mild	10 (17.2)	8 (20.5)	
	Moderate	8 (13.8)	7 (17.9)	
	Severe	0 (0.0)	1 (2.6)	
Faecal calprotectin concentrations within two months before SARS-CoV-2 vaccination in µg/g (median [IQR])		73.50 [38.50, 166.25] *n* = 22	218.50 [68.75, 448.25] *n* = 20	
Faecal calprotectin concentrations within two months after SARS-CoV-2 vaccination in µg/g (median [IQR])		105.50 [33.25, 373.75] *n* = 28	361.00 [54.00, 803.00] *n* = 21	
Heart disease (%)	Yes	2 (3.4)	4 (10.3)	
	No	57 (96.6)	35 (89.7)	
Hypertension (%)	Yes	4 (6.8)	9 (23.1)	
	No	55 (93.2)	30 (76.9)	
Pulmonary disease (%)	Yes	1 (1.7)	3 (7.7)	
	No	58 (98.3)	36 (92.3)	
Kidney disease (%)	Yes	2 (3.4)	3 (7.7)	
	No	57 (96.6)	36 (92.3)	

(Continues)

TABLE 1 (Continued)

Variable	Level	Anti-TNF-treated IBD patients	Non-anti-TNF-treated IBD patients	Healthy controls
Diabetes (%)	Yes	1 (1.7)	0 (0.0)	
	No	58 (98.3)	39 (100.0)	
Hyperlipidemia (%)	Yes	0 (0.0)	1 (2.6)	
	No	59 (100.0)	38 (97.4)	
Arthritis (%)	Yes	7 (11.9)	0 (0.0)	
	No	52 (88.1)	39 (100.0)	
Reported infection before vaccination (%)	Yes	6 (10.2)	2 (5.1)	7 (14.6)
	No	53 (89.8)	37 (94.9)	41 (85.4)
Breakthrough infection between visits 1 and 2 (%)	Yes	31 (52.5)	20 (51.3)	20 (41.7)
	No	28 (47.5)	19 (48.7)	28 (58.3)
Breakthrough infection between visits 1 and 2 resulting in severe COVID-19 (%)	Yes	1 (1.7)	0 (0.0)	0 (0.0)
	No	58 (98.3)	39 (100.0)	48 (100.0)
Fourth vaccination between visits 1 and 2 (%)	Yes	3 (5.1)	0 (0.0)	1 (2.1)
	No	56 (94.9)	39 (100.0)	47 (97.9)
Neutralisation measurements for both visits 1 and 2 (%)		29 (49.2)	21 (53.8)	28 (58.3)

described before using the ACE2-RBD inhibition assay RBDCoV-ACE2.[28,29] This assay quantifies antibody-mediated blockage of ACE2-spike protein–protein interaction as a surrogate for virus neutralisation. In detail, thawed serum samples were diluted 1:25 in assay buffer (Low Cross Buffer diluted 1:4 in CBS (1×PBS+1% BSA)+0.05% Tween20)) and further 1:8 in ACE2 buffer (assay buffer containing 342.9 ng/mL biotinylated human ACE2 (Sino Biological); final concentration: 300 ng/μL). MagPlex beads (Luminex) with distinct spectral properties and coupled to RBD proteins of SARS-CoV-2 wild-type, BA.1, BA.5, BQ.1.1, or XBB.1.5 were pooled to achieve a bead mix with a concentration of 40 beads/μL per bead population. 25 μL of diluted serum were mixed 1:1 with bead mix in wells of a 96 well plate (Corning). Duplicate wells containing 300 ng/mL ACE2 in assay buffer without added serum were used as normalisation control. Two quality control samples were measured in duplicate wells of each 96 well plate. Two wells containing 25 μL assay buffer instead of diluted serum served as blanks. After incubation for 2 h at 21°C and 750 rpm agitation, beads were washed three times with 100 μL wash buffer (1×PBS+0.05% Tween20) using a microplate washer (Biotek 405TS, Biotek Instruments GmbH). 30 μL of streptavidin-RPE conjugate were added to each well, followed by incubation for 45 min at 21°C and 750 rpm agitation. After washing three times as described earlier, the plate was agitated for 3 min at 1000 rpm. For quantification of bead-attached biotinylated ACE2, mean fluorescence intensity (MFI) emitted by conjugated RPE was measured using a FLEXMAP 3D instrument (Luminex) with the following settings: 80 μL (no timeout), 50 events, gate: 7500–15,000, reporter gain: standard PMT. ACE2-binding inhibition was defined as percentage of sample MFI relative to normalisation control MFI deducted from 100%. Negative MFI values were considered as zero. ACE2 binding inhibition was validated as a surrogate of virus neutralisation in numerous studies.[30–32] Therefore, in this study, ACE2-binding inhibition is referred to as surrogate neutralisation. Participant sera with surrogate neutralisation of <20% were considered non-inhibiting, which has been validated with virus neutralisation assays for the tested SARS-CoV-2 subvariants.[33]

2.7 | Statistical analysis

Surrogate neutralisation against SARS-CoV-2 wild-type and omicron sublineages BA.1, BA.5, BQ.1.1, and XBB.1.5 was compared between study groups using Kruskal-Wallis and Holm corrected Dunn's post-hoc tests. The proportion of participants with non-inhibitory surrogate neutralisation was compared between the study groups with Holm corrected Fisher's exact tests. For the intra-individual comparison of wild-type, BA.1, BA.5, BQ.1.1, and XBB.1.5 surrogate neutralisation, Wilcoxon signed rank tests were performed with Holm correction for each of ten comparisons. Likewise, for the intra-individual comparison of non-inhibitory surrogate neutralisation, Holm corrected McNemar tests were performed. A β-regression model with logit link function was fitted for wild-type surrogate neutralisation. The following predictors were included: type of biologic treatment, infection status before vaccination, time since vaccination, age, smoking status, type of IBD, time between second and third vaccination, and type of vaccination. No β-regression was run for the omicron sublineages, as there were many zero values. However, for BA.1, a logistic regression was calculated with non-inhibitory surrogate neutralisation as a dependent variable and all

the predictors that proved to be significant in the β-regression as independent variables. For other omicron sublineages, the number of patients with inhibitory surrogate neutralisation was too low to run logistic regressions. For the comparison of visits 1 and 2 measurements, Wilcoxon signed-rank tests were used. Spearman's rho was calculated for pairwise correlation of logarithmized anti-spike IgG and surrogate neutralisation against wild-type and omicron sublineages. Except for analyses where SARS-CoV-2 naïve individuals were compared to individuals with SARS-CoV-2 breakthrough infection, participants with breakthrough infection and fourth vaccination were excluded. All analyses were performed in the R programming language (version 4.2.2; R Core Team, 2022). Packages "tableone", "dunn. test", and "betareg" were used to compute descriptive statistics, calculate Dunn's post-hoc tests, and calculate the beta regression model, respectively.

3 | RESULTS

3.1 | Study population

The STAR SIGN study includes a total of 225 study participants who were recruited from the outpatient clinics and hospital staff of Cantonal Hospital St. Gallen, Ambulatorium Rorschach, and Inselspital Bern between January 2022 and April 2022. Of those, SARS-CoV-2 neutralisation data were available for 98 patients with IBD and 48 healthy controls who were used for the analyses of this study (Figure S1). Among patients with IBD, 59 received anti-TNF treatment with infliximab, adalimumab, or golimumab and 39 received non-anti-TNF biologic treatment with vedolizumab or ustekinumab. The STAR SIGN study protocol is summarised in Figure 1. Detailed characteristics of participants used for the analyses of this study are listed in Table 1. Baseline characteristics of participants who were excluded due to missing neutralisation data were comparable to those of included participants (Table S2).

3.2 | Anti-TNF-treatment impairs functional immunity against BQ.1.1 and XBB.1.5 following SARS-CoV-2 vaccination

When comparing surrogate neutralisation against SARS-CoV-2 wild-type, BA.1, BA.5, BQ.1.1, and XBB.1.5 in sera from participants without breakthrough infection, surrogate neutralisation against each tested strain was reduced in anti-TNF-treated patients with IBD compared to patients under non-anti-TNF therapy ($p \leq 0.001$ for each strain) and healthy controls ($p < 0.001$ for each strain) (Figure 2A and Table 2). Treatment with non-anti-TNF biologics had no effect on surrogate neutralisation compared to healthy controls ($p > 0.05$ for each strain). Interestingly, wild-type surrogate neutralisation was higher than surrogate neutralisation against each tested omicron sublineage (each $p < 0.001$), and BA.1 surrogate neutralisation was higher than BA.5, BQ.1.1, and XBB.1.5 surrogate neutralisation (each $p < 0.001$) in each study group (Table 3). In anti-TNF treated patients with IBD, BQ.1.1 surrogate neutralisation was lower compared to XBB.1.5 surrogate neutralisation ($p = 0.005$) (Table 3). At visit 2 (22–40 weeks after vaccination), similar trends were observed, and anti-TNF-treated patients with IBD had the lowest neutralisation against tested subvariants (Figure S2). However, interpretation is aggravated by limited availability of data points. The negative association of anti-TNF-treatment with surrogate neutralisation was confirmed in a β-regression model with wild-type surrogate neutralisation at visit 1 as outcome which included several potential confounders (odds ratio 0.29 [95% CI 0.19–0.46] $p < 0.001$). This model also identified a positive effect on wild-type surrogate neutralisation for vaccination with mRNA-1273 versus BNT162b2 (1.86 [1.12–3.08] $p = 0.016$) (Figure 2B) but no effects for infection before vaccination, age per decade, current smoker (vs. former and never smokers), Crohn's disease (vs. ulcerative colitis), and time between second and third vaccination. Similarly, no effect was found for age above 60 years and steroid use when adjusting for these factors in a separate β-regression model (Table S3). Within our study cohort,

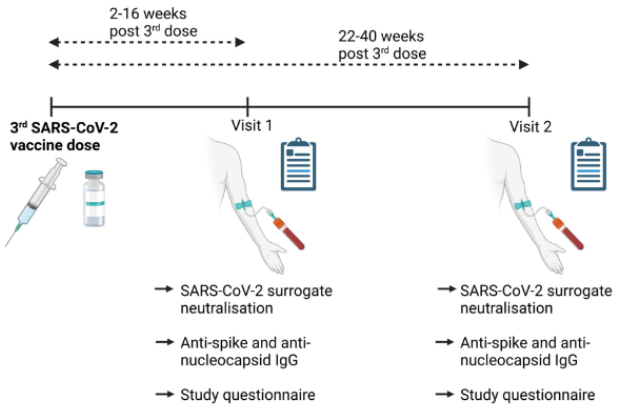

FIGURE 1 Participant recruitment strategy and outline of study procedures. Study protocol of the STAR SIGN study. Patients were enrolled at visit 1, 2–16 weeks after third dose SARS-CoV-2 vaccination. Visit 2 was 22–40 weeks after third-dose vaccination. At each visit, blood was drawn for analysis of surrogate neutralisation, anti-spike IgG, and anti-nucleocapsid IgG, and questionnaires were filled.

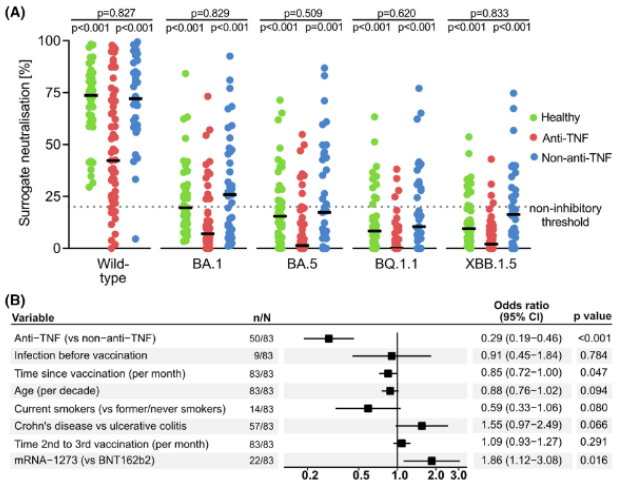

FIGURE 2 Functional immunity based on surrogate neutralisation against BQ.1.1 and XBB.1.5 is impaired in anti-TNF-treated patients with IBD. (A) Surrogate neutralisation against wild-type and omicron sublineages BA.1, BA.5, BQ.1.1, and XBB.1.5 at visit 1 (2–16 weeks) after SARS-CoV-2 vaccination, stratified by study group. Thick lines indicate the median, and statistical analysis is based on Dunn's post-hoc test with Holm correction. Dotted line represents the threshold for inhibitory surrogate neutralisation (=20%). Individuals with fourth vaccination or SARS-CoV-2 infection before or after vaccination were excluded from this analysis. (B) β-regression model with wild-type surrogate neutralisation as outcome. Coefficients and 95% confidence intervals were exponentiated. The analysis population consisted of patients with Crohn's disease or ulcerative colitis without breakthrough infection. A total of 14 individuals were not included due to missing data.

TABLE 2 Surrogate neutralisation against wild-type and omicron sublineages, stratified by study group and presented in percentages.

SARS-CoV-2 variant	Healthy controls ($n=48$)	Anti-TNF-treated IBD patients ($n=59$)	Non-anti-TNF-treated IBD patients ($n=39$)
Wild-type (median [IQR])	73.71 [60.71, 83.54]	42.28 [24.83, 71.15]	72.12 [58.81, 89.95]
BA.1 (median [IQR])	19.60 [13.23, 32.22]	7.00 [4.00, 13.20]	25.88 [9.00, 47.06]
BA.5 (median [IQR])	15.52 [5.88, 28.89]	1.34 [0.00, 11.21]	17.28 [0.63, 43.67]
BQ.1.1 median [IQR])	8.56 [2.23, 22.02]	0.00 [0.00, 3.16]	10.48 [4.06, 30.83]
XBB.1.5 (median [IQR])	10.16 [5.39, 22.01]	2.01 [0.00, 6.86]	16.27 [3.82, 28.74]

one anti-TNF-treated patient with IBD had a breakthrough infection that resulted in severe COVID-19 (Table 1).

3.3 | Anti-TNF-treated patients with IBD face increased risk of non-inhibitory surrogate neutralisation against BQ.1.1 and XBB.1.5 following SARS-CoV-2 vaccination

A greater proportion of anti-TNF-treated patients with IBD showed non-inhibitory surrogate neutralisation against omicron sublineages (BA.1 47/59 [79.7%]; BA.5 50/59 [84.7%]; BQ.1.1 55/59 [93.2%]; XBB.1.5 55/59 [93.2%]) when compared to patients receiving non-anti-TNF biologic therapy (BA.1 17/39 [43.6%] $p=0.001$; BA.5 22/39 [56.4%] $p=0.007$; BQ.1.1 25/39 [64.1%] $p=0.001$; XBB.1.5 24/39 [61.5%] $p<0.001$), and healthy controls (BA.1 25/48 [52.1%] $p=0.007$; BA.5 29/48 [60.4%] $p=0.015$; BQ.1.1 35/48 [72.9%] $p=0.013$; XBB.1.5 33/48 [68.8%] $p=0.003$) (Figure 3). The proportion of participants with non-inhibitory wild-type surrogate neutralisation was similar in anti-TNF-treated patients (0/48 [0.0%]) when compared to non-anti-TNF-treated patients with IBD (vs. 1/39 [2.6%] $p=0.096$) but was smaller when compared to healthy controls

SARS-CoV-2 variant	Healthy controls ($n=48$)	Anti-TNF-treated IBD patients ($n=59$)	Non-anti-TNF-treated IBD patients ($n=39$)
Wild-type vs. BA.1 (p-value)	<0.001	<0.001	<0.001
Wild-type vs. BA.5 (p-value)	<0.001	<0.001	<0.001
Wild-type vs. BQ.1.1 (p-value)	<0.001	<0.001	<0.001
Wild-type vs. XBB.1.5 (p-value)	<0.001	<0.001	<0.001
BA.1 vs. BA.5 (p-value)	<0.001	<0.001	<0.001
BA.1 vs. BQ.1.1 (p-value)	<0.001	<0.001	<0.001
BA.1 vs. XBB.1.5 (p-value)	<0.001	<0.001	<0.001
BA.5 vs. BQ.1.1 (p-value)	<0.001	<0.001	<0.001
BA.5 vs. XBB.1.5 (p-value)	<0.001	0.083	0.011
BQ.1.1 vs. XBB.1.5 (p-value)	0.22	0.005	0.147

TABLE 3 Multiple comparisons of surrogate neutralisation against SARS-CoV-2 wild-type and omicron sublineages at visit 1 (2–16 weeks after vaccination) in individuals without breakthrough infection. Statistical analysis is based on Wilcoxon signed rank tests with Holm correction for each of ten comparisons.

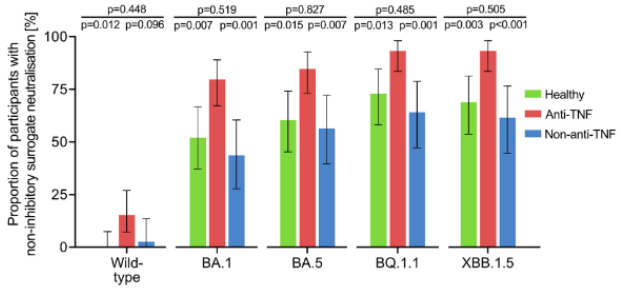

FIGURE 3 Risk of developing non-inhibitory surrogate neutralisation against BQ.1.1 and XBB.1.5 following SARS-CoV-2 vaccination is increased in anti-TNF-treated patients with IBD. Proportion of individuals with non-inhibitory surrogate neutralisation against wild-type and omicron sublineages BA.1, BA.5, BQ.1.1, and XBB.1.5 at visit 1 (2–16 weeks) after SARS-CoV-2 vaccination, stratified by study group. Error bars represent 95% confidence intervals based on exact Clopper-Pearson method. Statistical analysis is based on Fisher's exact post-hoc test with Holm correction. Individuals with fourth vaccination or SARS-CoV-2 infection before or after vaccination were excluded from this analysis.

SARS-CoV-2 variant	Healthy controls ($n=48$)	Anti-TNF-treated IBD patients ($n=59$)	Non-anti-TNF-treated IBD patients ($n=39$)
Wild-type vs. BA.1 (p-value)	<0.001	<0.001	0.001
Wild-type vs. BA.5 (p-value)	<0.001	<0.001	<0.001
Wild-type vs. BQ.1.1 (p-value)	<0.001	<0.001	<0.001
Wild-type vs. XBB.1.5 (p-value)	<0.001	<0.001	<0.001
BA.1 vs. BA.5 (p-value)	0.686	0.248	0.294
BA.1 vs. BQ.1.1 (p-value)	0.027	0.067	0.080
BA.1 vs. XBB.1.5 (p-value)	0.134	0.067	0.116
BA.5 vs. BQ.1.1 (p-value)	0.308	0.221	0.744
BA.5 vs. XBB.1.5 (p-value)	0.402	0.221	1.000
BQ.1.1 vs. XBB.1.5 (p-value)	0.686	NA	1.000

TABLE 4 Multiple comparisons of proportions of individuals with non-inhibitory surrogate neutralisation against SARS-CoV-2 wild-type and omicron sublineages at visit 1 (2–16 weeks after vaccination) in individuals without breakthrough infection. Statistical analysis is based on McNemar tests with Holm correction for each comparison.

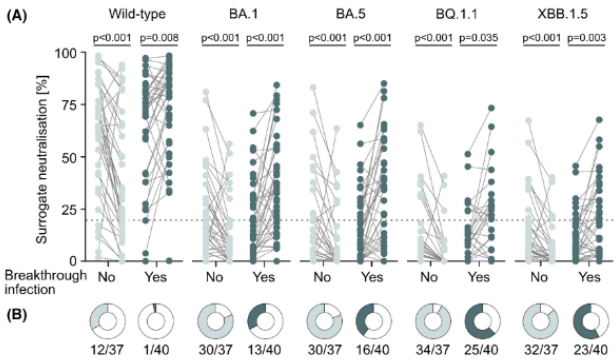

FIGURE 4 Vaccine-elicited surrogate neutralisation against BQ.1.1 and XBB.1.5 wanes over time but is increased by omicron breakthrough infection. (A) Surrogate neutralisation against wild-type and omicron sublineages BA.1, BA.5, BQ.1.1, and XBB.1.5 at visit 1 (2–16 weeks) and visit 2 (22–40 weeks) after SARS-CoV-2 vaccination, in SARS-CoV-2 naïve study participants (light teal) and participants with SARS-CoV-2 breakthrough infection between visit 1 and 2 (dark teal). Individuals with fourth vaccination, SARS-CoV-2 infection before vaccination, or with breakthrough infection before visit 1 were excluded from this analysis. Dotted line indicates threshold for inhibitory surrogate neutralisation (=20%). Statistical analysis is based on Wilcoxon signed rank test (B) Proportions of individuals with non-inhibitory surrogate neutralisation against indicated SARS-CoV-2 variants at visit 2 in individuals without (light teal) and with (dark teal) breakthrough infection between visits 1 visit 2.

(vs. 9/59 [15.3%] $p=0.012$). No difference was observed for patients with IBD treated with non-anti-TNF biologic agents when compared with healthy controls (wild-type $p=0.448$; BA.1 $p=0.519$; BA.5 $p=0.827$; BQ.1.1 $p=0.485$; XBB.1.5 $p=0.505$). Greater proportions of participants from each study group showed non-inhibitory surrogate neutralisation against omicron sublineages compared to wild-type (each $p<0.001$), while proportions were comparable between the tested omicron sublineages in patients with IBD independent of treatment (each $p>0.05$; Figure 3 and Table 4). At visit 2 (22–40 weeks after vaccination), while limited availability of data points limits interpretation of results, similar trends were observed (supplementary Figure S3). Logistic regression modelling with non-inhibitory BA.1 surrogate neutralisation as dependent variable and confounders identified in the β-regression model (Figure 2B) as independent variables, confirmed that anti-TNF treatment increases the risk of developing non-inhibitory surrogate neutralisation (odds ratio 6.467 [95% CI 2.410, 18.970] $p<0.001$) following SARS-CoV-2 vaccination (Table S4). No association was found for vaccination with mRNA-1273 (0.350 [0.105–1.090]) and time since vaccination (1.007 [0.995–1.020]).

3.4 | SARS-CoV-2 breakthrough infection counteracts waning surrogate neutralisation against BQ.1.1 and XBB.1.5 following vaccination

Looking at study participants from all study groups, SARS-CoV-2 naïve individuals had reduced wild-type and omicron sublineage surrogate neutralisation at visit 2 (22–40 weeks after vaccination) compared to visit 1 (2–16 weeks after vaccination) (each $p<0.001$), indicating waning of virus neutralisation over time (Figure 4A). However, in patients who experienced SARS-CoV-2 breakthrough infection between visits 1 and 2, surrogate neutralisation against each tested virus strain was increased at visit 2 compared to visit 1 (wild-type $p=0.008$; BA.1 $p<0.001$; BA.5 $p<0.001$; BQ.1.1 $p=0.035$; XBB.1.5 $p=0.003$) (Figure 4A and Table 5). Nevertheless, 62.5% (25/40) and 57.5% (23/40) of participants with breakthrough infection had non-inhibitory surrogate neutralisation against BQ.1.1 and XBB.1.5, respectively (Figure 4B).

3.5 | Anti-spike IgG strongly correlates with surrogate neutralisation against SARS-CoV-2 wild-type and omicron sublineages

In order to assess the contribution of serum anti-spike IgG antibodies to SARS-CoV-2 wild-type and omicron sublineage surrogate neutralisation, Spearman's rho was calculated for pairwise correlation of anti-spike IgG and the rate of surrogate neutralisation against each SARS-CoV-2 strain. When assessing the correlation between anti-spike IgG concentrations and wild-type surrogate neutralisation, at visit 1 (2–16 after vaccination) and visit 2 (22–40 weeks after vaccination) in our study population, a strong positive correlation was found at both timepoints (visit 1 $r_1=0.81$ $p_1<0.001$; visit 2 $r_2=0.87$, $p_2<0.001$; Figure 5). Similarly, anti-spike IgG concentrations correlated with surrogate neutralisation against BA.1 ($r_1=0.73$ $p_1<0.001$; $r_2=0.76$ $p_2<0.001$), BA.5 ($r_1=0.73$ $p_1<0.001$; $r_2=0.77$ $p_2<0.001$), BQ.1.1 ($r_1=0.66$ $p_1<0.001$; $r_2=0.68$ $p_2<0.001$), and

TABLE 5 Surrogate neutralisation against SARS-CoV-2 wild-type and omicron sublineages BA.1, BA.5, BQ.1.1, and XBB.1.5 at visit 1 (2–16 weeks after vaccination) and visit 2 (22–40 weeks after vaccination) in participants with and without breakthrough infection between visits and measurements for each visit.

	Visit 1		Visit 2	
SARS-CoV-2 variant	Infection: yes ($n=40$)	Infection: no ($n=37$)	Infection: yes ($n=40$)	Infection: no ($n=37$)
Wild-type (median [IQR])	72.18 [54.39, 81.98]	64.82 [41.97, 84.53]	80.93 [63.10, 90.07]	31.74 [16.19, 66.03]
BA.1 (median [IQR])	13.87 [5.66, 30.38]	16.46 [7.86, 30.28]	33.49 [16.33, 53.32]	8.27 [0.24, 17.38]
BA.5 (median [IQR])	9.68 [0.65, 26.88]	9.46 [0.15, 23.12]	31.67 [7.25, 48.97]	0.00 [0.00, 10.74]
BQ.1.1 (median [IQR])	5.72 [0.00, 13.72]	4.91 [0.00, 10.95]	5.63 [0.00, 26.20]	0.00 [0.00, 0.00]
XBB.1.5 (median [IQR])	6.94 [0.97, 17.62]	6.11 [1.94, 18.04]	11.18 [3.54, 30.48]	0.96 [0.00, 7.79]

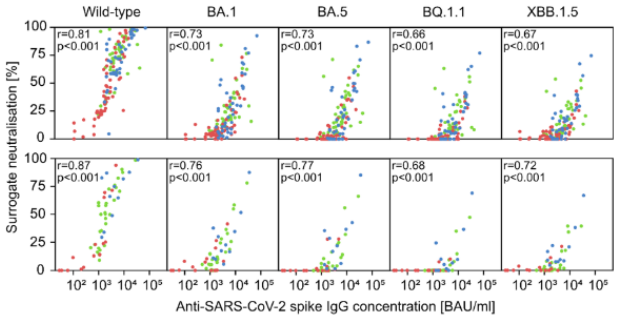

FIGURE 5 Correlation of systemic anti-spike IgG concentration with surrogate neutralisation against SARS-CoV-2 wild-type and omicron sublineages following vaccination. Pairwise correlation of anti-spike IgG and surrogate neutralisation against wild-type and omicron sublineages BA.1, BA.5, BQ.1.1, and XBB.1.5 at visit 1 (2–16 weeks; top) and visit 2 (22–40 weeks; bottom) after SARS-CoV-2 vaccination. Healthy control subjects, anti-TNF-, and non-anti-TNF-treated patients with IBD are depicted in green, red, and blue, respectively. Individuals with fourth vaccination or SARS-CoV-2 infection before or after vaccination were excluded from this analysis. Spearman's rho (r) and p-values are displayed.

XBB.1.5 ($r_1=0.67$ $p_1<0.001$; $r_2=0.72$ $p_2<0.001$) at both timepoints (Figure 5). Interestingly, however, correlation coefficients were lower in omicron sublineages compared to wild-type, suggesting that anti-spike IgG antibodies elicited by SARS-CoV-2 vaccination are less efficient in neutralising omicron sublineages compared to wild-type.

4 | DISCUSSION

Novel SARS-CoV-2 omicron subvariants such as XBB.1.5 are predominant in most countries and display alarming potential of vaccine-elicited immune evasion with unknown implications for immunosuppressed patient groups.[34–36]

Here, we show that neutralisation against BQ.1.1 and XBB.1.5 is impaired in anti-TNF-treated patients with IBD, compared to patients treated with non-anti-TNF biologics and healthy controls. Wild-type surrogate neutralisation was associated negatively with anti-TNF therapy and time since vaccination, and positively with mRNA-1273 vaccination. In line with previous research, no association was found for steroid use.[17] Contrasting previous research, no impact of age on SARS-CoV-2 neutralisation was found.[17] However, this study was not primarily designed to evaluate the influence of old age on vaccine efficacy. Therefore, this finding may be related to the limited number of study participants older than 60 years ($n=18$).

Although our study focuses on neutralising antibodies targeting SARS-CoV-2 wild-type and omicron sublineages, reduced humoral wild-type immunity in anti-TNF-treated patients with IBD following second and third dose vaccination has been reported before.[9,12,13,15,16,37,38] Interestingly, similar effects were observed for the JAK inhibitor tofacitinib.[9,16,37] During SARS-CoV-2 waves with pre-omicron variants, neutralising antibody titres were strong predictors of protection against symptomatic SARS-CoV-2 infection.[39,40] Since emergence of the omicron variant, robust protection correlates are yet to be established. Due to its high immune-evasive potential, vaccine-elicited neutralising antibodies may be less potent in protecting individuals from omicron infection and severe disease.[41] It is suggested that a combination of neutralising antibodies, robust CD8+ T cells, and virus-directed mucosal IgA play a role in protection against omicron.[40,42,43] Recently, low concentrations of neutralising NT50s against BA.4/5 were associated with a shorter

time to breakthrough infection in patients with IBD.[17] Therefore, our results indicate a potentially elevated risk for anti-TNF-treated patients with IBD during ongoing BQ.1.1 and XBB.1.5 waves. Given that in patients with IBD neutralisation against BQ.1.1 was reduced compared to BA.5 and BA.1 independent of treatment, infection risk could be higher compared to previous COVID-19 waves. It will be interesting to see if our findings translate into increased infection risk or altered infection severity in anti-TNF-treated patients during ongoing COVID-19 waves. Previous research suggests that anti-TNF treatment is not associated with increased disease severity after SARS-CoV-2 infection but with an increased risk of SARS-CoV-2 infection during omicron waves.[15,17,44] However, according to a recent systematic review and meta-analysis, 43% of SARS-CoV-2-infected individuals suffer from symptoms related to long COVID.[45] Therefore, in addition to the immediate personal impact on the quality of life of affected individuals, increased infection rates in anti-TNF-treated individuals may pose a substantial burden to economies and healthcare systems worldwide.[46] In contrast to previous studies, our study fundamentally improves the current state of knowledge about SARS-CoV-2 humoral immunity in two ways. First, the inclusion of a healthy control group enables the assessment of potential IBD-specific confounders of SARS-CoV-2 neutralisation other than type of biologic treatment. Second, this is the first study to demonstrate impaired vaccine-elicited immune responses towards the novel omicron sublineages BQ.1.1 and XBB.1.5 in patients with IBD and anti-TNF-treated patient groups in general.

Consistent with previous research in healthy individuals, high proportions of each study group showed insufficient surrogate neutralisation against BA.1, BA.5, BQ.1.1, and XBB.1.5 2–16 weeks post-vaccination.[47] This finding could explain recent surges in COVID-19 infections caused by XBB and BQ derivatives and is facilitated by their strong capability to evade vaccine-elicited immune responses.[25] Among anti-TNF-treated patients with IBD, 93.2% had non-inhibitory surrogate neutralisation against BQ.1.1 and XBB.1.5 which was a greater proportion than in healthy individuals and patients with IBD treated with non-anti-TNF biologics. Accordingly, anti-TNF therapy was associated with a higher risk of non-inhibitory BA.1 surrogate neutralisation in a logistic regression model. Calculation of comparable models for BA.5, BQ.1.1, and XBB.1.5 was hindered by the low percentage of individuals with inhibitory surrogate neutralisation against these subvariants. Interpretation of neutralisation data at visit 2 (22–40 weeks after vaccination) was limited by the small number of available data points. However, the trend that anti-TNF-treated patients with IBD are least protected against most tested subvariants holds true at visit 2. Insufficient SARS-CoV-2 immunity in immunosuppressed patients bears the risk of virus evolution towards new variants with increased transmissibility and unpredictable severity.[48,49] Considering our findings, it may be advised to foster approaches to increase BQ.1.1- and XBB.1.5-targeting neutralising antibodies, especially in anti-TNF-treated patient groups. Previous research showed that fourth dose vaccination with bivalent omicron-adapted mRNA vaccines potently increases breadth of virus neutralisation and improves BQ.1.1 neutralisation in haemodialysis patients with impaired virus neutralisation after three vaccine doses.[50,51] Furthermore, the STOP COVID-19 in IBD study reported an increase of anti-spike IgG concentrations in patients with IBD vaccinated with a fourth dose of BNT-162b2 or mRNA-1273.[52] Despite recommendations of fourth dose vaccination in immunosuppressed patients with IBD, only four out of 146 participants received a fourth vaccine dose by the end of the study, which highlights the urge of continued vaccination campaigns. It will be interesting to see whether bivalent fourth dose vaccination will result in reduced clinically relevant infection rates and disease severity. Importantly, bivalent fourth dose vaccination increased protection against BQ.1.1 but not against XBB.1.5 in immunocompromised hematologic and solid cancer patients, which indicates that continuous vaccine adaptation to novel variants might be required to fully protect at risk patient groups. Recently, the first country reached emergency approval of a trivalent vaccine targeting XBB, BA.5, and delta.[27] Moreover, Pfizer and BioNTech submitted applications to FDA for approval of an XBB.1.5-adapted monovalent COVID-19 vaccine. Our results support prioritisation of anti-TNF-treated patients with IBD for such variant-adapted vaccines.

We show that neutralisation against BQ.1.1 and XBB.1.5 wanes over time but is increased by breakthrough infection during the 2022 omicron wave. Nevertheless, even among individuals with breakthrough infection, over 50% had non-inhibitory surrogate neutralisation against the novel omicron sublineages BQ.1.1 and XBB.1.5 22–40 weeks after vaccination, while surrogate neutralisation against BA.1 and BA.5 was efficient in most participants. This is in line with previous studies in healthy individuals showing that levels of neutralisation antibodies against BQ.1.1 and XBB-derivatives are lower than against BA.5 after omicron breakthrough infection, with neutralisation antibodies targeting XBB-derivatives being lowest.[25,53] An explanation for poor XBB.1.5 and BQ.1.1 neutralisation after breakthrough infection might be that most participants were infected with BA.1, BA.2, or BA.5 during the study period, while XBB.1.5 and BQ.1.1 emerged only after data collection was finished (supplementary Figure S4). As BQ.1 is a sublineage of BA.5 and XBB emerged via genetic recombination of BA.2.10.1 and BA.2.75, neutralisation against these subvariants is increased, albeit less strongly, by breakthrough infections with their parent subvariants BA.2 and BA.5.[35] It will be interesting to see if breakthrough infection with BQ.1.1 and XBB.1.5 will further increase surrogate neutralisation against these subvariants.

Whether anti-spike or anti-RBD IgG concentrations elicited by wild-type-based vaccines are a reliable predictor of omicron, neutralisation is still controversial and depends on the magnitude of neutralisation antibody escape by the tested SARS-CoV-2 subvariant.[54,55] In our study population, we found a strong pairwise correlation between anti-spike IgG concentrations and surrogate virus neutralisation against all tested SARS-CoV-2 subvariants at both timepoints. Spearman's rho was greater at visit 2 compared to visit 1 for all subvariants and greater for wild-type than for each omicron sublineage, respectively. These findings are in line with previous research and might be explained by antibody maturation over

time and the increased potential of omicron sublineages to evade vaccine-elicited neutralising antibodies, respectively.[56,57] Strong positive correlation between surrogate neutralisation and anti-spike IgG antibodies reassuringly suggests validity of the utilised surrogate neutralisation assay.

We acknowledge the lack of patients on combination therapy with anti-TNF biologics and immunomodulators, the small number of participants with fourth dose vaccination, and the small sample size of our cohort as limitations of this study.

In conclusion, our findings highlight the importance of continued vaccine efficacy surveillance, targeted vaccination campaigns, and adaptation of vaccines to novel omicron sublineages. Recently, WHO and FDA recommended the use of XBB.1.5-specific SARS-CoV-2 vaccines in preparation of upcoming COVID-19 waves. Our study demonstrates the first proof of concept that even three doses of conventional mRNA vaccines provide minimal protection against XBB.1.5, with particularly poor outcomes for anti-TNF-treated patients with IBD. Our results support the current recommendation of bivalent fourth dose vaccination in patients treated with anti-TNF biologics and indicate that these patients may benefit from prioritisation for XBB-specific and future variant-adapted SARS-CoV-2 vaccines.

AUTHOR CONTRIBUTIONS

Simon Woelfel: Conceptualization (equal); data curation (supporting); formal analysis (supporting); funding acquisition (supporting); investigation (supporting); methodology (supporting); visualization (lead); writing – original draft (lead); writing – review and editing (lead). **Joel Dütschler:** Conceptualization (equal); funding acquisition (lead); investigation (lead); project administration (equal); writing – review and editing (supporting). **Marius König:** Investigation (supporting); resources (supporting); writing – review and editing (supporting). **Alex Dulovic:** Funding acquisition (supporting); investigation (supporting); methodology (supporting); supervision (supporting); validation (supporting); writing – review and editing (supporting). **Nicole Graf:** Data curation (lead); formal analysis (lead); methodology (supporting); validation (lead); visualization (supporting); writing – review and editing (supporting). **Daniel Junker:** Investigation (supporting); methodology (supporting); validation (supporting); writing – review and editing (supporting). **Vasileios Oikonomou:** Investigation (supporting); writing – review and editing (supporting). **Claudia Krieger:** Investigation (supporting); resources (supporting); writing – review and editing (supporting). **Samuel Truniger:** Investigation (supporting); resources (supporting); writing – review and editing (supporting). **Annett Franke:** Investigation (supporting); resources (supporting); writing – review and editing (supporting). **Annika Eckhold:** Data curation (supporting); project administration (lead); resources (equal). **Kristina Forsch:** Project administration (supporting); resources (supporting). **Seraina Koller:** Project administration (supporting); resources (supporting). **Jacqueline Wyss:** Investigation (supporting); resources (supporting); writing – review and editing (supporting). **Niklas Krupka:** Investigation (supporting); resources (supporting); writing – review and editing (supporting). **Melanie Oberholzer:** Investigation (supporting); resources (supporting). **Nicola Frei:** Investigation (supporting); resources (supporting); writing – review and editing (supporting). **Nora Geissler:** Investigation (supporting); resources (supporting); writing – review and editing (supporting). **Peter Schaub:** Investigation (supporting); resources (supporting); writing – review and editing (supporting). **Werner C. Albrich:** Supervision (supporting); writing – review and editing (supporting). **Matthias Friedrich:** Funding acquisition (supporting); investigation (supporting); resources (supporting); supervision (supporting); writing – review and editing (supporting). **Nicole Schneiderhan-Marra:** Methodology (supporting); resources (supporting); supervision (supporting). **Benjamin Misselwitz:** Investigation (supporting); resources (supporting); supervision (supporting); writing – review and editing (supporting). **Wolfgang Korte:** Investigation (supporting); funding acquisition (equal); resources (supporting); supervision (supporting); writing – review and editing (supporting). **Justus J. Bürgi:** Data curation (supporting); investigation (supporting); resources (supporting); supervision (supporting); validation (supporting); writing – review and editing (supporting). **Stephan Brand:** Funding acquisition (equal); investigation (supporting); methodology (supporting); project administration (supporting); resources (lead); supervision (lead); visualization (supporting); writing – original draft (supporting); writing – review and editing (supporting).

ACKNOWLEDGEMENTS

Declaration of personal interests: SB has consulted to Abbvie, Celgene, Ferring, Gilead, Janssen, MSD, Pfizer, Roche, UCB, Takeda, and Vifor; SB has received speaker's honoraria from Abbvie, Falk, Ferring, Janssen, MSD, Takeda, UCB, and Vifor; SB has received an educational grant from Takeda. JD has served on advisory boards for Takeda. BM has served on advisory boards for Abbvie, Gilead, and Novigenix. He has received speaking fees from Vifor, MSD, and Takeda and travelling fees from Vifor, Novartis, Gilead, and Takeda. This study was funded by a research grant from the Cantonal Hospital St. Gallen (Switzerland) to JD, SW, and SB, by a grant from the University of Oxford (UK) to MF, by funding of the Center for Laboratory Medicine St. Gallen (Switzerland), and by grants from the State Ministry of Baden-Württemberg for Economic Affairs, Labour, and Tourism (FKZ-3-4332.62-NMI-67 and FKZ 3-4332.62-NMI-68) and the EU Horizon 2020 Research and Innovation Programme (grant agreement number 101003480-CORESMA). The sole role of the funding sources was to finance the biochemical assays and to cover the costs for the Clinical Trial Unit (CTU) statistician as well as the study personnel. No other aspect pertaining to the study was influenced by the funding sources. No pharmaceutical company or other agency was involved in the preparation or funding of this manuscript. All authors approved the final version of this manuscript.

AUTHORSHIP

Guarantor of the article: Stephan Brand.

ORCID

Simon Woelfel https://orcid.org/0000-0003-2528-0582
Stephan Brand https://orcid.org/0000-0001-7011-0430

REFERENCES

1. Watson OJ, Barnsley G, Toor J, Hogan AB, Winskill P, Ghani AC. Global impact of the first year of COVID-19 vaccination: a mathematical modelling study. Lancet Infect Dis. 2022;22:1293–302.
2. Bhurwal A, Mutneja H, Bansal V, Goel A, Arora S, Attar B, et al. Effectiveness and safety of SARS-CoV-2 vaccine in inflammatory bowel disease patients: a systematic review, meta-analysis and meta-regression. Aliment Pharmacol Ther. 2022;55:1244–64.
3. Wall EC, Wu M, Harvey R, Kelly G, Warchal S, Sawyer C, et al. Neutralising antibody activity against SARS-CoV-2 VOCs B.1.617.2 and B.1.351 by BNT162b2 vaccination. Lancet. 2021;397:2331–3.
4. Viana R, Moyo S, Amoako DG, Tegally H, Scheepers C, Althaus CL, et al. Rapid epidemic expansion of the SARS-CoV-2 Omicron variant in Southern Africa. Nature. 2022;603:679–86.
5. Andrews N, Stowe J, Kirsebom F, Toffa S, Rickeard T, Gallagher E, et al. Covid-19 vaccine effectiveness against the omicron (B.1.1.529) variant. N Engl J Med. 2022;386:1532–46.
6. Cele S, Jackson L, Khoury DS, Khan K, Moyo-Gwete T, Tegally H, et al. Omicron extensively but incompletely escapes Pfizer BNT162b2 neutralization. Nature. 2022;602:654–6.
7. Harvey WT, Carabelli AM, Jackson B, Gupta RK, Thomson EC, Harrison EM, et al. SARS-CoV-2 variants, spike mutations and immune escape. Nat Rev Microbiol. 2021;19:409–24.
8. Danese S, Vuitton L, Peyrin-Biroulet L. Biologic agents for IBD: practical insights. Nat Rev Gastroenterol Hepatol. 2015;12:537–45.
9. Alexander JL, Kennedy NA, Ibraheim H, Anandabaskaran S, Saifuddin A, Castro Seoane R, et al. COVID-19 vaccine-induced antibody responses in immunosuppressed patients with inflammatory bowel disease (VIP): a multicentre, prospective, case-control study. Lancet Gastroenterol Hepatol. 2022;7:342–52.
10. Edelman-Klapper H, Zittan E, Bar-Gil Shitrit A, Rabinowitz KM, Goren I, Avni-Biron I, et al. Lower serologic response to COVID-19 mRNA vaccine in patients with inflammatory bowel diseases treated with anti-TNFα. Gastroenterology. 2022;162:454–67.
11. Doherty J, Fennessy S, Stack R, O' Morain N, Cullen G, Ryan EJ, et al. Review article: vaccination for patients with inflammatory bowel disease during the COVID-19 pandemic. Aliment Pharmacol Ther. 2021;54:1110–23.
12. Kennedy NA, Lin S, Goodhand JR, Chanchlani N, Hamilton B, Bewshea C, et al. Infliximab is associated with attenuated immunogenicity to BNT162b2 and ChAdOx1 nCoV-19 SARS-CoV-2 vaccines in patients with IBD. Gut. 2021;70:1884–93.
13. Woelfel S, Dütschler J, König M, Graf N, Oikonomou V, Krieger C, et al. Systemic and T cell-associated responses to SARS-CoV-2 immunisation in gut inflammation (STAR SIGN study): effects of biologics on vaccination efficacy of the third dose of mRNA vaccines against SARS-CoV-2. Aliment Pharmacol Ther. 2023;57:103–16.
14. Quan J, Ma C, Panaccione R, Hracs L, Sharifi N, Herauf M, et al. Serological responses to three doses of SARS-CoV-2 vaccination in inflammatory bowel disease. Gut. 2023;72:802–4.
15. Kennedy NA, Janjua M, Chanchlani N, Lin S, Bewshea C, Nice R, et al. Vaccine escape, increased breakthrough and reinfection in infliximab-treated patients with IBD during the Omicron wave of the SARS-CoV-2 pandemic. Gut. 2023;72:295–305.
16. Alexander JL, Liu Z, Muñoz Sandoval D, Reynolds C, Ibraheim H, Anandabaskaran S, et al. COVID-19 vaccine-induced antibody and T-cell responses in immunosuppressed patients with inflammatory bowel disease after the third vaccine dose (VIP): a multicentre, prospective, case-control study. Lancet Gastroenterol Hepatol. 2022;7:1005–15.
17. Liu Z, Le K, Zhou X, Alexander JL, Lin S, Bewshea C, et al. Neutralising antibody potency against SARS-CoV-2 wild-type and omicron BA.1 and BA.4/5 variants in patients with inflammatory bowel disease treated with infliximab and vedolizumab after three doses of COVID-19 vaccine (CLARITY IBD): an analysis of a prospective multicentre cohort study. Lancet Gastroenterol Hepatol. 2023;8:145–56.
18. Arbel R, Peretz A, Sergienko R, Friger M, Beckenstein T, Duskin-Bitan H, et al. Effectiveness of a bivalent mRNA vaccine booster dose to prevent severe COVID-19 outcomes: a retrospective cohort study. Lancet Infect Dis. 2023;23:914–21.
19. Chalkias S, Harper C, Vrbicky K, Walsh SR, Essink B, Brosz A, et al. A bivalent Omicron-containing booster vaccine against Covid-19. N Engl J Med. 2022;387:1279–91.
20. Winokur P, Gayed J, Fitz-Patrick D, Thomas SJ, Diya O, Lockhart S, et al. Bivalent omicron BA.1–adapted BNT162b2 booster in adults older than 55 years. N Engl J Med. 2023;388:214–27.
21. Barouch DH. Covid-19 vaccines — immunity, variants, boosters. N Engl J Med. 2022;387:1011–20.
22. Lazarus JV, Wyka K, White TM, Picchio CA, Gostin LO, Larson HJ, et al. A survey of COVID-19 vaccine acceptance across 23 countries in 2022. Nat Med. 2023;29:366–75.
23. Stamm TA, Partheymüller J, Mosor E, Ritschl V, Kritzinger S, Alunno A, et al. Determinants of COVID-19 vaccine fatigue. Nat Med. 2023;29:1164–71.
24. Su Z, Cheshmehzangi A, McDonnell D, da Veiga CP, Xiang Y-T. Mind the "vaccine fatigue". Front Immunol. 2022;13:839433.
25. Wang Q, Iketani S, Li Z, Liu L, Guo Y, Huang Y, et al. Alarming antibody evasion properties of rising SARS-CoV-2 BQ and XBB subvariants. Cell. 2023;186:279–286.e8.
26. Uraki R, Ito M, Furusawa Y, Yamayoshi S, Iwatsuki-Horimoto K, Adachi E, et al. Humoral immune evasion of the omicron subvariants BQ.1.1 and XBB. Lancet Infect Dis. 2023;23:30–2.
27. Ye Y. China's rolling COVID waves could hit every six months—infecting millions. Nature. 2023;618:442–3.
28. Junker D, Becker M, Wagner TR, Kaiser PD, Maier S, Grimm TM, et al. Antibody binding and angiotensin-converting enzyme 2 binding inhibition is significantly reduced for both the BA.1 and BA.2 omicron variants. Clin Infect Dis. 2023;76:e240–9.
29. Junker D, Dulovic A, Becker M, Wagner TR, Kaiser PD, Traenkle B, et al. COVID-19 patient serum less potently inhibits ACE2-RBD binding for various SARS-CoV-2 RBD mutants. Sci Rep. 2022;12:7168.
30. Tan CW, Chia WN, Qin X, Liu P, Chen MIC, Tiu C, et al. A SARS-CoV-2 surrogate virus neutralization test based on antibody-mediated blockage of ACE2–spike protein–protein interaction. Nat Biotechnol. 2020;38:1073–8.
31. Abe KT, Li Z, Samson R, Samavarchi-Tehrani P, Valcourt EJ, Wood H, et al. A simple protein-based surrogate neutralization assay for SARS-CoV-2. JCI Insight. 2020;5:e142362.
32. Walker SN, Chokkalingam N, Reuschel EL, Purwar M, Xu Z, Gary EN, et al. SARS-CoV-2 assays to detect functional antibody responses that block ACE2 recognition in vaccinated animals and infected patients. J Clin Microbiol. 2020;58:e01533-20.
33. Roth N, Gergen J, Kovacikova K, Mueller SO, Ulrich L, Schön J, et al. Assessment of immunogenicity and efficacy of CV0501 mRNA-based omicron COVID-19 vaccination in small animal models. Vaccine. 2023;11:318.
34. Zhang X, Chen LL, Ip JD, Chan WM, Hung IFN, Yuen KY, et al. Omicron sublineage recombinant XBB evades neutralising antibodies in recipients of BNT162b2 or CoronaVac vaccines. Lancet Microbe. 2023;4:e131.
35. Hoffmann M, Arora P, Nehlmeier I, Kempf A, Cossmann A, Schulz SR, et al. Profound neutralization evasion and augmented host cell entry are hallmarks of the fast-spreading SARS-CoV-2 lineage XBB.1.5. Cell Mol Immunol. 2023;20:419–22.
36. Dewald F, Pirkl M, Paluschinski M, Kühn J, Elsner C, Schulte B, et al. Impaired humoral immunity to BQ.1.1 in convalescent and vaccinated patients. Nat Commun. 2023;14:2835.
37. Liu Z, Alexander JL, Lin KW, Ahmad T, Pollock KM, Powell N, et al. Infliximab and tofacitinib attenuate neutralizing antibody

responses against SARS-CoV-2 ancestral and omicron variants in inflammatory bowel disease patients after 3 doses of COVID-19 vaccine. Gastroenterology. 2023;164:300–303.e3.
38. Jena A, James D, Singh AK, Dutta U, Sebastian S, Sharma V. Effectiveness and durability of COVID-19 vaccination in 9447 patients with IBD: a systematic review and meta-analysis. Clin Gastroenterol Hepatol. 2022;20:1456–1479.e18.
39. Cromer D, Steain M, Reynaldi A, Schlub TE, Wheatley AK, Juno JA, et al. Neutralising antibody titres as predictors of protection against SARS-CoV-2 variants and the impact of boosting: a meta-analysis. Lancet Microbe. 2022;3:e52–e61.
40. Regev-Yochay G, Lustig Y, Joseph G, Gilboa M, Barda N, Gens I, et al. Correlates of protection against COVID-19 infection and intensity of symptomatic disease in vaccinated individuals exposed to SARS-CoV-2 in households in Israel (ICoFS): a prospective cohort study. Lancet Microbe. 2023;4:e309–18.
41. Willett BJ, Grove J, MacLean OA, Wilkie C, de Lorenzo G, Furnon W, et al. SARS-CoV-2 Omicron is an immune escape variant with an altered cell entry pathway. Nat Microbiol. 2022;7:1161–79.
42. Chandrashekar A, Yu J, McMahan K, Jacob-Dolan C, Liu J, He X, et al. Vaccine protection against the SARS-CoV-2 Omicron variant in macaques. Cell. 2022;185:1549–1555.e11.
43. Bruel T, Pinaud L, Tondeur L, Planas D, Staropoli I, Porrot F, et al. Neutralising antibody responses to SARS-CoV-2 omicron among elderly nursing home residents following a booster dose of BNT162b2 vaccine: a community-based, prospective, longitudinal cohort study. eClinicalMedicine. 2022;51:101576.
44. Ungaro RC, Brenner EJ, Gearry RB, Kaplan GG, Kissous-Hunt M, Lewis JD, et al. Effect of IBD medications on COVID-19 outcomes: results from an international registry. Gut. 2021;70:725–32.
45. Chen C, Haupert SR, Zimmermann L, Shi X, Fritsche LG, Mukherjee B. Global prevalence of post-coronavirus disease 2019 (COVID-19) condition or long COVID: a meta-analysis and systematic review. J Infect Dis. 2022;226:1593–607.
46. Gandjour A. Long COVID: costs for the German economy and health care and pension system. BMC Health Serv Res. 2023;23:641.
47. Qu P, Faraone JN, Evans JP, Zheng YM, Carlin C, Anghelina M, et al. Enhanced evasion of neutralizing antibody response by Omicron XBB.1.5, CH.1.1, and CA.3.1 variants. Cell Rep. 2023;42:112443.
48. Corey L, Beyrer C, Cohen MS, Michael NL, Bedford T, Rolland M. SARS-CoV-2 variants in patients with immunosuppression. N Engl J Med. 2021;385:562–6.
49. Markov PV, Katzourakis A, Stilianakis NI. Antigenic evolution will lead to new SARS-CoV-2 variants with unpredictable severity. Nat Rev Microbiol. 2022;20:251–2.
50. Scheaffer SM, Lee D, Whitener B, Ying B, Wu K, Liang CY, et al. Bivalent SARS-CoV-2 mRNA vaccines increase breadth of neutralization and protect against the BA.5 Omicron variant in mice. Nat Med. 2023;29:247–57.
51. Platen L, Liao BH, Tellenbach M, et al. Longitudinal SARS-CoV-2 neutralization of Omicron BA.1, BA.5 and BQ.1.1 after four vaccinations and the impact of break-through infections in hemodialysis patients. Clin Kidney J. 2023;sfad147. https://doi.org/10.1093/ckj/sfad147
52. Quan J, Ma C, Panaccione R, Hracs L, Sharifi N, Herauf M, et al. Serological responses to the first four doses of SARS-CoV-2 vaccine in patients with inflammatory bowel disease. Lancet Gastroenterol Hepatol. 2022;7:1077–9.
53. Chen J-J, Li LB, Peng HH, Tian S, Ji B, Shi C, et al. Neutralization against XBB.1 and XBB.1.5 after omicron subvariants breakthrough infection or reinfection. Lancet Reg Health - West Pac. 2023;33:100759.
54. Tran TT, Vaage EB, Mehta A, Chopra A, Tietze L, Kolderup A, et al. Titers of antibodies against ancestral SARS-CoV-2 correlate with levels of neutralizing antibodies to multiple variants. Npj Vaccines. 2022;7:174.
55. Takheaw N, Liwsrisakun C, Chaiwong W, Laopajon W, Pata S, Inchai J, et al. Correlation analysis of anti-SARS-CoV-2 RBD IgG and neutralizing antibody against SARS-CoV-2 omicron variants after vaccination. Diagnostics. 2022;12:1315.
56. Grunau B, Prusinkiewicz M, Asamoah-Boaheng M, Golding L, Lavoie PM, Petric M, et al. Correlation of SARS-CoV-2 viral neutralizing antibody titers with anti-spike antibodies and ACE-2 inhibition among vaccinated individuals. Microbiol Spectr. 2022;10:e01315-22.
57. Fu J, Shen X, Anderson M, Stec M, Petratos T, Cloherty G, et al. Correlation of binding and neutralizing antibodies against SARS-CoV-2 omicron variant in infection-naïve and convalescent BNT162b2 recipients. Vaccine. 2022;10:1904.

SUPPORTING INFORMATION

Additional supporting information will be found online in the Supporting Information section.

How to cite this article: Woelfel S, Dütschler J, König M, Dulovic A, Graf N, Junker D, et al. STAR SIGN study: Evaluation of COVID-19 vaccine efficacy against the SARS-CoV-2 variants BQ.1.1 and XBB.1.5 in patients with inflammatory bowel disease. Aliment Pharmacol Ther. 2023;58:678–691. https://doi.org/10.1111/apt.17661

Appendix X: Dynamics of humoral response towards SARS-CoV-2 from vaccination and breakthrough infection

Becker M*, Dulovic A*, Uzun G, Bareiß A, Mikus M, **Junker D**, Griesbaum J, Michel T, Fandrich M, Schenke-Layland K, Althaus K, Bakchoul T, Schneiderhan-Marra N.

Unpublished Manuscript

Dynamics of humoral response towards SARS-CoV-2 from vaccination and breakthrough infection

Matthias Becker Dr.rer.nat[1,*], Alex Dulovic Dr.rer.nat[1,*], Gunalp Uzun MD[2], Alan Bareiß MD[2], Marco Mikus MTA[2], Daniel Junker MSc[1], Johanna Griesbaum MTA[1], Tanja Michel Dr.rer.nat[1], Madeleine Fandrich MSc[1], Katja Schenke-Layland Dr.rer.nat[1,3,4], Karina Althaus MD[2,5], Tamam Bakchoul MD[2,5,#], Nicole Schneiderhan-Marra Dr.rer.nat[1,#]

1 – NMI Natural and Medical Sciences Institute at the University of Tübingen, Reutlingen, Germany

2 – Centre for Clinical Transfusion Medicine, Tübingen, Germany

3 – Institute of Biomedical Engineering, Department for Medical Technologies and Regenerative Medicine, Eberhard Karls University Tübingen, Tübingen, Germany

4 – Cluster of Excellence iFIT (EXC 2180) "Image-Guided and Functionally Instructed Tumor Therapies", Eberhard Karls University Tübingen, Tübingen, Germany

5 – Institute for Clinical and Experimental Transfusion Medicine, Medical Faculty of Tübingen, University Hospital Tübingen, Tübingen, Germany

*contributed equally to the manuscript and share first authorship

#indicates shared last authorship and corresponding author

Corresponding author

Tamam Bakchoul – Otfried-Müller-Straße 4/1, 72076 Tübingen, Germany.
tamam.bakchoul@med.uni-tuebingen.de. +49 7071 2981601

Nicole Schneiderhan-Marra – Markwiesenstrasse 55, 72770 Reutlingen, Germany.
Nicole.schneiderhan@nmi.de. +49 7121 51530815

Keywords: SARS-CoV-2, vaccine, humoral immunity, breakthrough

Statements and Declarations

Competing Interests

TB has received research funding from CoaChrom Diagnostica GmbH, DFG, Robert Bosch GmbH, Stiftung Transfusionsmedizin und Immunhämatologie e.V.: Ergomed, DRK Blutspendedienst, Deutsche Herzstiftung, Ministerium fuer Wissenschaft, Forschung und Kunst Baden-Wuerttemberg, has received lecture honoraria from Aspen Germany GmbH, Bayer Vital GmbH, Bristol-Myers Squibb GmbH & Co., Doctrina Med AG, Meet The Experts Academy UG, Schoechl medical education GmbH, Stago GmbH, Mitsubishi Tanabe Pharma GmbH, Novo Nordisk Pharma GmbH, Leo Pharma GmbH, Swedish Orphan Biovitrum

GmbH, has provided consulting services to: Terumo, has provided expert witness testimony relating to heparin induced thrombocytopenia (HIT) and non-HIT thrombo-cytopenic and coagulopathic disorders. All of these are outside the current work. The other authors declare no conflicts of interest.

Abstract

Purpose: The broad variety of vaccination schemes against SARS-CoV-2 and waves of breakthrough infections have led to a heterogenous immune landscape. This study aims to assess and identify potential differences in humoral immunity following diverse vaccination schema and breakthrough infections

Methods: As part of an ongoing longitudinal cohort study in Southwest Germany (TüSeRe:exact), healthcare workers and medical researchers who had been vaccinated against SARS-CoV-2 were followed from September 2021 until September 2022 for IgG titer and ACE2 binding inhibition (pseudoneutralization).

Results: Humoral immunity was highly diverse and individualistic. Boosting only temporarily increased humoral immunity among individuals who had low responses after two doses. Breakthrough infections resulted in durable, broader humoral immune responses, regardless of how many prior doses had been received.

Conclusion: The humoral immune landscape towards SARS-CoV-2 is highly variable, although breakthrough infections do result in a broad sustained humoral response, regardless of the number of vaccine doses also received, indicating sustained protection. Future vaccination campaigns should target specific groups (e.g. low responders, those without breakthrough infections). Investigating differences between individuals who revert compared to those who can sustain their humoral response are of particular interest in designing future vaccines.

Trial Registration: TüSeRe:exact is registered in the German Clinical Trial Register (https://drks.de, registration number: DRKS00029013).

Introduction

Since the outbreak of SARS-CoV-2 in late 2019 (1), the virus has continued to mutate into variants and sub-variants of concern (2, 3), resulting in subsequent local, national and global waves of infection. At the same time, unprecedented research efforts have led to the development of several different vaccines against SARS-CoV-2 (4-6), the use of which have led to significant reductions in mortality(7, 8). However, vaccine recommendations have consistently changed over time in response to safety concerns (9, 10), vaccine availability and diminishing immune protection against new SARS-CoV-2 variants (11, 12), while the presence of large numbers of breakthrough infections with several different variants(13, 14) means that immunity towards SARS-CoV-2 is largely heterogenous. While humoral immunity is only part of the immune response, given the continual evolution of new viral variants each of which could potentially escape pre-existing immunity, it is important to determine if there are significant differences within the current humoral immunological landscape. For this purpose, we analysed humoral responses (antibody titre and ACE2 binding inhibition (as a proxy for virus neutralization)) in individuals with and without breakthrough infections, and with and without a booster (3rd) vaccination, as part of an ongoing prospective cohort study.

Methods

TüSeRe:exact

This study is part of TüSeRe:exact (Tübinger Monitoring Studie zur exakten Analyse der Immunantwort nach Vakzinierung), a non-interventional, prospective longitudinal cohort study. TüSeRe:exact aims to investigate the longitudinal changes in antibody levels following SARS-CoV-2 vaccination. Employees from the University Hospital Tübingen, the Center for Clinical Transfusion Medicine, and the Natural and Medical Sciences Institute at the University of Tübingen were invited by email to participate. Ethical approval for the study was obtained from the ethics committee of the Medical Faculty of the Eberhard Karls University Tübingen and the University Hospital Tübingen under the study number 556/2021BO1 (granted on 08.09.21 to TB). The study protocol was amended to include additional timepoints for blood collection following booster vaccination (556/2021BO2 granted on 03.12.2021 to TB). TüSeRe:exact is registered in the German Clinical Trial Register (https://drks.de, registration number: DRKS00029013).

The following inclusion criteria applied to be eligible to enrol within the study.

- Employment relationship with one of the above listed medical institutes
- Age between 18 and 75 years at time of enrolment
- Must have received either at least two approved vaccine doses against SARS-CoV-2 (for naïve individuals) or at least one approved vaccine dose against SARS-CoV-2 (for convalescent individuals)

The following exclusion criteria was applied.

- Being pregnant or breastfeeding at time of enrolment
- Body weight <50 kg
- Have been vaccinated with a non-approved vaccine in Germany

All participants completed an online questionnaire (see Supplementary Information) which collected basic demographic information (e.g. age, gender), SARS-CoV-2 vaccination history (dates and types of vaccines received), SARS-CoV-2 infection history (date and method used to detect infection), basic medical history (medications, conditions etc) and side effects post-vaccination (this part of the study has already been published as (15)). Participants were invited to submit a blood sample on at least three occasions. At each timepoint, participants were asked to update their online questionnaire to account for new vaccinations, infections or changes in medical history. Blood samples were collected by venepuncture, with serum separated on the same day by centrifugation, aliquoted and then frozen at -80°C until used.

For use in this manuscript, samples were only used from individuals that fulfilled the following criteria:

- At least three samples available
- Consistent metadata free from discrepancies
- Not participated in any vaccine trial
- Not received the Janssen vaccine
- Had received at least three vaccine doses or two doses and been infected
- No evidence of unknown prior infection (Nucleocapsid titre value >0.5)

An overview of how samples were considered for inclusion in this manuscript is provided as **Supplementary Figure 1**. All samples used in this manuscript were collected between 28.09.21 and 19.09.22.

Primary and secondary outcomes

The primary outcome of this study was to measure the humoral immune response longitudinally following vaccination. Antibody effect (binding and inhibition) towards newly emergent variants were evaluated in addition to the overall response. The secondary outcome was to investigate antibody interaction with platelets following vaccination, which is beyond the scope of the current publication.

Laboratory Analysis

Antibody binding titre and ACE2 binding inhibition as a proxy for neutralization were analysed using MULTICOV-AB and RBDCoV-ACE2. Both assays are multiplex bead-based assays that either detect antibody titre towards a range of different SARS-CoV-2 antigens (MULTICOV-AB) (16) or ACE2 binding inhibition towards the RBD of various SARS-CoV-2 variants of concern (RBDCoV-ACE2) (17). The full list of analytes used in both assays can be found as **Supplementary Table 1**. Both assays were performed as previously described in a semi-automated format using a Biomek i7 pipetting robot (18). For a subset of samples used in Figures 1 and 2, IgG avidity measurements were performed. A full method is included within the **Supplementary Information**. Investigators were blinded when performing the laboratory analysis.

Statistical Analysis

Metadata was merged with analytical data in Excel, after which statistical analysis and data visualization was performed in RStudio (version 2022.7.1, running R v4.2.1), using functions from the “stats” package. Neutralizing breadth index, a measure of how effective antibodies are at inhibiting a wide range of variants, (19) was manually calculated by dividing WT ACE2 binding inhibition, by the average of beta, delta and BA2 binding inhibition. To avoid including

non-neutralizing values, values for all variants within a sample had to be >20%. The exact statistical test used is stated in each figure legend. Assessment of significant differences between groups was analysed using either One-way ANOVA “aov”, with Tukey HSD post-HOC “TukeyHSD” or Mann-Whitney-U “wilcox.test”. Linear models were generated using “lm” to estimate peak response and decay over time and estimate interaction effects between groups, with Spearman ρ statistic was used to estimate a rank-based association of two variables using “cor”. “gplots” and “beeswarm” were used for data visualization only. Analysis code is available from the authors upon request and will be made publically available upon acceptance.

155 **Results**

156 Initially, we evaluated how humoral responses changed following booster vaccination, and
157 whether individuals who had low responses to two doses (hereon referred to as "non-
158 sustained responders"), would remain so after boosting (**Figure 1**).

159 **Figure 1 - Humoral immunity reverts for non-sustained responders even after booster**
160 **vaccination**
161

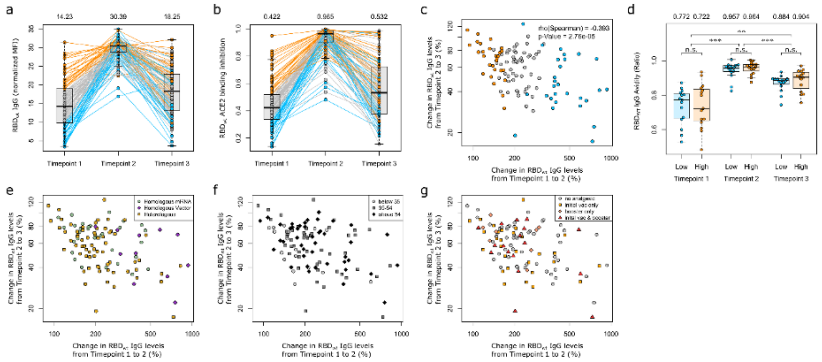

162

163 Longitudinal samples from 117 individuals were collected at three timepoints (T1= 126-189
164 days post 2nd dose, T2= 14 to 42 days post 3rd dose and T3= 182 to 238 days post 3rd dose),
165 see Supplementary Figure 2 for further details. RBD antibody titre (a) and ACE2 binding
166 inhibition towards WT SARS-CoV-2 (b) are shown to assess the humoral response. The
167 bottom 25% ("non-sustained responders") are coloured blue, the middle 50% grey and the
168 top 25% orange. Non-sustained responders had the largest fold change increase in titre
169 (displayed as %) directly after booster vaccination, but also the largest decrease in titre 6
170 months after booster vaccination (c). (d) IgG antibody avidity at all timepoints was analysed
171 for a subset of sustained (n=15) and non-sustained (n=15) responders. Immunisation
172 scheme received (e), age (f) and use of painkillers after vaccination (g) were assessed as
173 potential indicator of non-sustained response. Keys within each panel (e-g) indicate the
174 differing groups depicted. (a, b and d) box and whisker plots with where boxes represent the
175 1st to 3rd quartiles, whiskers represent 1.5 IQR and the line represents the median. Outliers
176 are shown. Median are depicted above the box. Statistically significant differences in d were
177 determined by MWU with Tukey Adhoc significance testing. ** indicates p<0.01, *** indicates
178 p<0.001 and n.s. indicates a non-significant value >0.05.

179

180 To enable this, we defined a sub-cohort which had three longitudinal samples with similar
181 dTs post vaccination (**Supplementary Figure 2**). While boosting did significantly increase
182 titre and ACE2 binding inhibition directly following booster vaccination (**Figure 1a and b**),
183 non-sustained responders 4-6 months post-2nd dose largely reverted 6 to 8 months post-3rd

dose, with a strong significant negative correlation (Spearman = -0.39, p<0.001, **Figure 1c**) between how much antibody titres increased directly following boosting versus the long-term change in titre. Avidity was analysed for a subset of samples at each timepoint, with no significant difference in avidity between sustained and non-sustained responders at each timepoint (**Figure 1d**). We then evaluated whether being a non-sustained responder was associated with either vaccination scheme (**Figure 1e**). While individuals who had received AZD1222 for their primary immunisation were only present within the non-sustained or normal (1st to 3rd quartile) responder groups, there was no significant difference in titre 5-7 months post-3rd dose between those who received two doses of AZD1222 and those who received 1 (p=0.88) or none (p=0.09) (**Supplementary Figure 3**). We also examined non-sustained responders in relation to age (**Figure 1f**) or use of painkillers following vaccination (**Figure 1g**), finding no significant association between any of them.

Figure 2 – Breakthrough Infections led to increased breadth and longevity of the humoral response

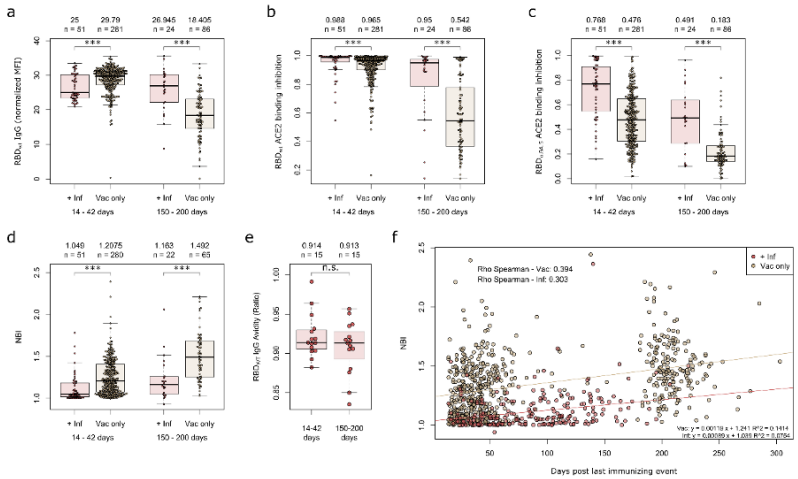

Antibody titre (a), ACE2 binding inhibition towards WT (b) and BA5 (c), neutralizing breadth index (d) were compared in samples from individuals with or without a breakthrough infection following 3 vaccine doses. Samples were compared at two timepoints: 14 to 42 days post most recent immunizing event to capture the peak response and 150 to 200 days to capture the long term "lag" response (see **Supplementary Figure 4** for further details on sample selection). For a subset of samples with a breakthrough infection, IgG avidity was also analysed (e). To evaluate how NBI changed over time, NBI was plotted as days post immunizing event increased (f), with Spearman's rank used to determine the correlation. The equation of the line and R^2 value are included within the panel. The same plot was produced for RBD titre and is available as **Supplementary Figure 5**. (a-e) box and whisker plots

where boxes represent the 1st to 3rd quartiles, whiskers represent 1.5 IQR and the line represents the median. Outliers are shown. MWU was used to identify statistically significant differences between the two groups with *** indicating p<0.001 and n.s. indicating a non-significant p value >0.05. N's and medians for each group are included within the figure panels.

We then examined how infections in addition to vaccination changed the humoral response, by examining antibody titre as well as ACE2 binding inhibition towards omicron variants that were not present when the samples were collected. To analyse how these antibody dynamics changed over time, we evaluated samples collected 14 to 42 days (for peak response) and 150 to 200 days (for lag response) post the most recent immunizing event (**Supplementary Figure 4**). At the peak response time, while antibody titre was significantly higher for vaccinated only individuals (median RBD titre 29.79±3.92 vs 25.00±3.71, p<0.001, **Figure 2a**), ACE2 inhibitory responses towards WT and BA5 were significantly lower (median ACE2 binding inhibition WT 0.97±0.11 vs 0.99±0.09, p<0.001, **Figure 2b,** BA5 0.48±0.22 vs 0.77±0.23, p<0.001 **Figure 2c**). Antibodies from individuals who had also been infected had significantly increased breadth of inhibitory activity (median NBI 1.05±0.17, p<0.001, **Figure 2d**) than those from vaccinated only individuals (median NBI 1.21±0.22). In contrast to the peak response, antibody titre at the lag response was significantly higher in infected individuals (median RBD titre 26.95±6.24) than vaccinated individuals (18.41±6.71, p<0.001, **Figure 2a**), with vaccinated only individuals having a significantly faster rate of antibody waning (p<0.001, **Supplementary Figure 5**). In line with the peak response, ACE2 binding inhibition for WT (0.54±0.25 vs 0.95±0.25, p<0.001, **Figure 2b**) and BA5 (0.18±0.16 vs 0.49±0.25, p<0.001, **Figure 2c**) were all significantly higher in infected and vaccinated individuals compared to those who had only been vaccinated at the lag response, while NBI indicated broader neutralisation (1.49±0.29 vs 1.16±0.25, p<0.001, **Figure 2d**). IgG avidity for infected individuals did not change from peak response (median 0.91±0.03) to lag response (median 0.91±0.03, **Figure 2e**). While the NBI was significantly higher for vaccinated individuals, it waned at the same rate as that for infected individuals (**Figure 2f**, p=0.36).

Lastly, as some individuals were not recommended to receive a booster vaccination due to having had a previous infection, we investigated whether there were differences in humoral response between individuals who had received two doses and had an infection (hereon referred to as "hybrid immunity") and individuals who had received three vaccine doses (**Figure 3**). Much like responses following an infection and three vaccine doses, antibody titre for hybrid immunity samples were decreased compared to vaccine-only samples directly following the most recent immunizing event, however they wane at a significantly slower rate (Spearman hybrid =-0.22, Spearman vaccine =-0,54, p=0.001, **Figure 3a**). ACE2 binding

inhibition for WT (Spearman hybrid = -0.52, Spearman vaccine =-0.61, p=0.03, **Figure 3b**) also followed the same pattern, with hybrid immunity responses being more durable as time post-immunizing event increased. ACE2 binding inhibition for BA5 was significantly higher for hybrid immunity than for vaccine immunity (p<0.001, **Figure 3c**), although decay was technically faster for hybrid than vaccine immunity (p=0.03), largely due most samples becoming non-inhibiting. Hybrid immunity also had increased breadth of inhibitory responses compared to vaccine immunity directly following the latest immunizing event, although this difference did decline as time post immunizing event increased (**Figure 3d**).

Figure 3 – Hybrid immunity confers increased antibody function compared to vaccine-elicited immunity

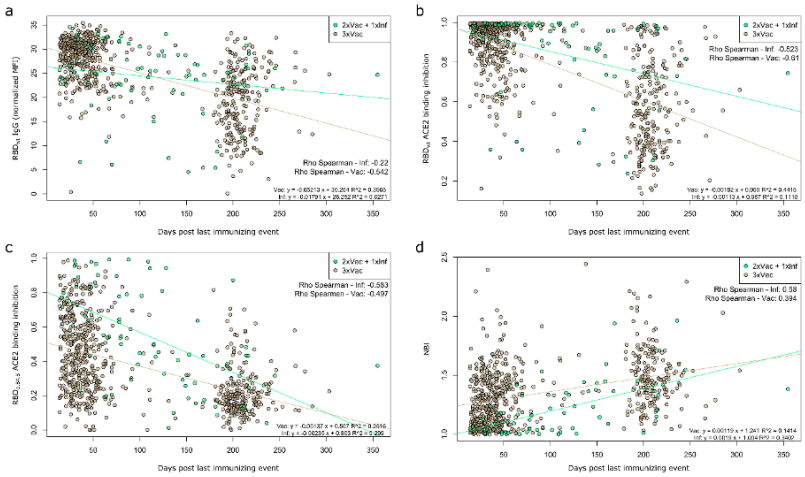

Antibody titre (a), ACE2 binding inhibition against WT (b) and BA5 (c) and NBI (d) were compared between individuals who had received three immunisations (either three vaccine doses (n=674, gold) or two vaccine doses and an infection (n=67, green)), as time post last immunizing event increased. Changes in humoral response are depicted as linear regressions, with Spearman's rank calculated to show the correlation, and linear modelling used to determine significant differences between the two lines. The equations of the line and R^2 value are included within each panel.

Discussion

In our study, we found that the humoral response to SARS-CoV-2 vaccination appears to be self-limiting, with individuals who had low titre and activity post-2nd dose, also having low titre and activity post-3rd dose. Although a booster dose did as expected temporarily increase antibody levels, inhibitory activity and avidity, most non-sustained responders reverted long-term post booster immunisation. While this direct increase post booster for non-sustained responders has been reported previously (20, 21), to our knowledge this is the first-time report investigating them for more than 3 months post boosting. Low titres were previously found to be linked to fewer SARS-CoV-2 specific B cells and a reduced T cell repertoire, implicating that premature lymphocyte aging may contribute to a less effective humoral response (21). While these parameters were not investigated within this manuscript, our results would appear to agree, as those with low responses reverted as time increased post immunisation. Interestingly we found no link between age and being a non-sustained responder, even though increased age is implicated in accelerated waning of immunity and decreased humoral responses (22, 23). However, this may be due to our cohort consisting of healthcare workers and those engaged in medical research, meaning most participants were young and middle-aged adults (only 11% over the age of 60 with a maximum age of 69). While there were no individuals with the highest humoral responses who received AZD1222 for primary immunisation and only 17% of non-sustained responders received mRNA vaccines only, it is unlikely that this was a key factor, as we saw no significant difference in titre or ACE2 binding inhibition 5-7 months post-booster between different vaccine regimens. Further investigation into the specific characteristics of non-sustained responders, particularly if they continue to revert following further vaccine doses, will be of interest for developing both more effective future vaccines as well as individualised vaccine plans for SARS-CoV-2.

In line with other studies (24-27), humoral responses generated from both infection and vaccination had significantly higher inhibitory activity than those elicited by vaccination only. Breakthrough infection with Omicron variants, which contain over 30 spike protein mutations(28), unsurprisingly led to a broader inhibitory response. Interestingly however, antibody titre themselves were significantly higher directly post-immunising event in those who had only been vaccinated, as opposed to those who had also been infected. This suggests that infection does not result in a significant increase in titre, rather a significant broadening of the antibody repertoire. Further antibody titre and avidity remained stable over 5 months post-immunising event, suggesting continual replenishment by B cells. It should be noted that while antibody levels themselves are considered generally correlative with protection (29), there remains no clearly defined threshold for infection so we can only speculate whether these individuals who have been infected once are likely to be infected

again in the future. However, as reports of double breakthrough infections remain rare, it appears that breakthrough-generated immunity provides ongoing protection against SARS-CoV-2.

When examining the direct difference in humoral response following three immunising events (either 3 vaccine doses or two doses and an infection), we found that while hybrid humoral responses produced a lower antibody titre, they had significantly increased ACE2 inhibition towards omicron, significantly increased breadth of neutralizing response and significantly reduced waning. While investigations into long-lasting hybrid immunity are limited, it has been shown that breakthrough rates were significantly reduced for these individuals compared to those who had received three vaccine doses (30). Our results therefore also appear to confirm the recommended strategy from the RKI, that individuals who had received two doses plus had an infection need not have received an additional vaccination in late 2021. It is particularly interesting that these hybrid individuals had significant increased ACE2 inhibition for BA5, given the majority had infections with either the delta variant or earlier variants.

Our study has several limitations. Firstly, as all participants were either healthcare workers or those working actively in medical research, the majority were female, younger and healthier than the general population. A large proportion also received AZD1222 as their primary immunisation which is in contrast to the rest of the German population. Samples were also collected based upon defined dates of subject availability, as opposed to consistent timepoints post-immunisation, meaning that we could only use subsets of the cohort for certain analyses (e.g. Figure 1). However, this also means that we have a highly comprehensive and wide-ranging dataset, with data available for the majority of days for up to day 303 post-third dose. The collection of metadata for this study was also performed using an online questionnaire, which led to issues with quality control. To correct for this, we excluded any samples from this publication that contained false or incomplete metadata. This however led to a substantial reduction in the number of available samples. Our study also only considers humoral immune responses in the form of antibody titre, avidity and inhibitory function, and does not inform about cellular immunity or mucosal IgA, both of which are involved in the immune response to infection. Lastly, our study also only examines data up to approximately 8 months after the initial booster dose. While booster vaccinations did significantly increase both the immune response (31-33) and vaccine efficacy compared to the second dose (8), the longevity of this response also significantly decreased over time leading to recommendations at the end of 2022 for a second booster dose, making some of our data unrepresentative of the current immunological landscape.

Conclusions

This cohort study found that humoral responses towards SARS-CoV-2 following vaccination and infection are highly individualistic. Given their lack of sustained response following boosting, our results suggest that further investigation into non-sustained responders is warranted to develop more effective future vaccines, as well as personalized vaccine regimens to optimise efficacy and protection. Our study also found that breakthrough infection resulted in a broad durable humoral response, regardless of number of vaccine doses received, suggesting that this group may not need continual re-vaccination. However, given the continuous mutation of SARS-CoV-2, tracking antibody quantity, quality and function change as time post-immunizing event increases, will be of importance to identify whether further vaccinations are required.

Acknowledgements

We thank Carmen Farber, Barbara Gübitz and Dr. Egon Klatt for helping to organize the TüSeRe:exact study. We thank the physicians and staff of the Tübingen Blood Donor Center for their help with participant recruitment and blood collection.

MB, AD, GU, KSL, KA, TB and NSM designed the project. GU, AB, MM, KA and TB collected samples or was involved in their collection. MB, AD, DJ, JG, TM and MF performed laboratory analysis. KSL, TB and NSM acquired funding. MB, AD, GU, AB and MM analysed the data. MB generated the figures. AD wrote the first draft of the manuscript with input from MB, GU, TM and KSL. All authors approved the final draft of the manuscript.

This work was supported by grants from the German Research Foundation (BA5158/4 to TB); the Herzstiftung (TSG-Study to TB); the State Ministry of Baden-Württemberg for Economic Affairs, Labor and Tourism (FKZ 3-4332.62-NMI-67 and FKZ-3-4332.62-NMI-68 to NSM); as well as special funds from the state of Baden-Württemberg for coagulation research (to TB); and Blood donation service of the German Red Cross (to TB). Data will be made available upon publication.

References

1. Zhu N, Zhang D, Wang W, Li X, Yang B, Song J, et al. A Novel Coronavirus from Patients with Pneumonia in China, 2019. New England Journal of Medicine. 2020;382(8):727-33.
2. Tao K, Tzou PL, Nouhin J, Gupta RK, de Oliveira T, Kosakovsky Pond SL, et al. The biological and clinical significance of emerging SARS-CoV-2 variants. Nature Reviews Genetics. 2021;22(12):757-73.
3. Tegally H, Wilkinson E, Giovanetti M, Iranzadeh A, Fonseca V, Giandhari J, et al. Detection of a SARS-CoV-2 variant of concern in South Africa. Nature. 2021.
4. Voysey M, Clemens SAC, Madhi SA, Weckx LY, Folegatti PM, Aley PK, et al. Safety and efficacy of the ChAdOx1 nCoV-19 vaccine (AZD1222) against SARS-CoV-2: an interim analysis of four randomised controlled trials in Brazil, South Africa, and the UK. The Lancet. 2021;397(10269):99-111.
5. Baden LR, El Sahly HM, Essink B, Kotloff K, Frey S, Novak R, et al. Efficacy and Safety of the mRNA-1273 SARS-CoV-2 Vaccine. N Engl J Med. 2021;384(5):403-16.
6. Polack FP, Thomas SJ, Kitchin N, Absalon J, Gurtman A, Lockhart S, et al. Safety and Efficacy of the BNT162b2 mRNA Covid-19 Vaccine. New England Journal of Medicine. 2020;383(27):2603-15.
7. Scobie HM, Johnson AG, Suthar AB, Severson R, Alden NB, Balter S, et al. Monitoring Incidence of COVID-19 Cases, Hospitalizations, and Deaths, by Vaccination Status - 13 U.S. Jurisdictions, April 4-July 17, 2021. MMWR Morbidity and mortality weekly report. 2021;70(37):1284-90.
8. Tenforde MW, Patel MM, Gaglani M, Ginde AA, Douin DJ, Talbot HK, et al. Effectiveness of a Third Dose of Pfizer-BioNTech and Moderna Vaccines in Preventing COVID-19 Hospitalization Among Immunocompetent and Immunocompromised Adults - United States, August-December 2021. MMWR Morbidity and mortality weekly report. 2022;71(4):118-24.
9. Greinacher A, Thiele T, Warkentin TE, Weisser K, Kyrle PA, Eichinger S. Thrombotic Thrombocytopenia after ChAdOx1 nCov-19 Vaccination. New England Journal of Medicine. 2021;384(22):2092-101.
10. Althaus K, Möller P, Uzun G, Singh A, Beck A, Bettag M, et al. Antibody-mediated procoagulant platelets in SARS-CoV-2-vaccination associated immune thrombotic thrombocytopenia. Haematologica. 2021;106(8):2170-9.
11. Dulovic A, Strengert M, Ramos GM, Becker M, Griesbaum J, Junker D, et al. Diminishing immune responses against variants of concern in dialysis patients four months after SARS-CoV-2 mRNA vaccination. medRxiv. 2021:2021.08.16.21262115.
12. Link-Gelles R, Levy ME, Gaglani M, Irving SA, Stockwell M, Dascomb K, et al. Effectiveness of 2, 3, and 4 COVID-19 mRNA Vaccine Doses Among Immunocompetent Adults During Periods when SARS-CoV-2 Omicron BA.1 and BA.2/BA.2.12.1 Sublineages Predominated - VISION Network, 10 States, December 2021-June 2022. MMWR Morbidity and mortality weekly report. 2022;71(29):931-9.
13. Pulliam JRC, van Schalkwyk C, Govender N, von Gottberg A, Cohen C, Groome MJ, et al. Increased risk of SARS-CoV-2 reinfection associated with emergence of the Omicron variant in South Africa. medRxiv. 2021:2021.11.11.21266068.
14. CoVariants. Shared Mutations (https://covariants.org/shared-mutations) [
15. Bareiß A, Uzun G, Mikus M, Becker M, Althaus K, Schneiderhan-Marra N, et al. Vaccine Side Effects in Health Care Workers after Vaccination against SARS-CoV-2: Data from TüSeRe:exact Study. Viruses. 2023;15(1):65.
16. Becker M, Strengert M, Junker D, Kaiser PD, Kerrinnes T, Traenkle B, et al. Exploring beyond clinical routine SARS-CoV-2 serology using MultiCoV-Ab to evaluate endemic coronavirus cross-reactivity. Nature Communications. 2021;12(1):1152.
17. Junker D, Dulovic A, Becker M, Wagner TR, Kaiser PD, Traenkle B, et al. COVID-19 patient serum less potently inhibits ACE2-RBD binding for various SARS-CoV-2 RBD mutants. Scientific reports. 2022;12(1):7168.

18. Renk H, Dulovic A, Seidel A, Becker M, Fabricius D, Zernickel M, et al. Robust and durable serological response following pediatric SARS-CoV-2 infection. Nature Communications. 2022;13(1):128.
19. Moriyama S, Adachi Y, Sato T, Tonouchi K, Sun L, Fukushi S, et al. Temporal maturation of neutralizing antibodies in COVID-19 convalescent individuals improves potency and breadth to circulating SARS-CoV-2 variants. Immunity. 2021;54(8):1841-52.e4.
20. Lake DF, Roeder AJ, Gonzalez-Moa MJ, Koehler M, Kaleta E, Jasbi P, et al. Third COVID-19 vaccine dose boosts neutralizing antibodies in poor responders. Communications Medicine. 2022;2(1):85.
21. Huang Y, Shin JE, Xu AM, Yao C, Joung S, Wu M, et al. Evidence of premature lymphocyte aging in people with low anti-spike antibody levels after BNT162b2 vaccination. iScience. 2022;25(10).
22. Collier DA, Ferreira IATM, Kotagiri P, Datir RP, Lim EY, Touizer E, et al. Age-related immune response heterogeneity to SARS-CoV-2 vaccine BNT162b2. Nature. 2021;596(7872):417-22.
23. Levin EG, Lustig Y, Cohen C, Fluss R, Indenbaum V, Amit S, et al. Waning Immune Humoral Response to BNT162b2 Covid-19 Vaccine over 6 Months. New England Journal of Medicine. 2021;385(24):e84.
24. Hoffmann M, Behrens GMN, Arora P, Kempf A, Nehlmeier I, Cossmann A, et al. Effect of hybrid immunity and bivalent booster vaccination on omicron sublineage neutralisation. The Lancet Infectious Diseases. 2023;23(1):25-8.
25. Muik A, Lui BG, Bacher M, Wallisch AK, Toker A, Finlayson A, et al. Omicron BA.2 breakthrough infection enhances cross-neutralization of BA.2.12.1 and BA.4/BA.5. Sci Immunol. 2022;7(77):eade2283.
26. Quandt J, Muik A, Salisch N, Lui BG, Lutz S, Krüger K, et al. Omicron BA.1 breakthrough infection drives cross-variant neutralization and memory B cell formation against conserved epitopes. Sci Immunol. 2022;7(75):eabq2427.
27. Kaku CI, Bergeron AJ, Ahlm C, Normark J, Sakharkar M, Forsell MNE, et al. Recall of preexisting cross-reactive B cell memory after Omicron BA.1 breakthrough infection. Sci Immunol. 2022;7(73):eabq3511.
28. Tegally H, Moir M, Everatt J, Giovanetti M, Scheepers C, Wilkinson E, et al. Emergence of SARS-CoV-2 Omicron lineages BA.4 and BA.5 in South Africa. Nature Medicine. 2022;28(9):1785-90.
29. Feng S, Phillips DJ, White T, Sayal H, Aley PK, Bibi S, et al. Correlates of protection against symptomatic and asymptomatic SARS-CoV-2 infection. Nature Medicine. 2021.
30. Ntziora F, Kostaki EG, Karapanou A, Mylona M, Tseti I, Sipsas NV, et al. Protection of vaccination versus hybrid immunity against infection with COVID-19 Omicron variants among Health-Care Workers. Vaccine. 2022;40(50):7195-200.
31. Gilboa M, Mandelboim M, Indenbaum V, Lustig Y, Cohen C, Rahav G, et al. Early Immunogenicity and Safety of the Third Dose of BNT162b2 Messenger RNA Coronavirus Disease 2019 Vaccine Among Adults Older Than 60 Years: Real-World Experience. J Infect Dis. 2022;225(5):785-92.
32. Lustig Y, Gonen T, Meltzer L, Gilboa M, Indenbaum V, Cohen C, et al. Superior immunogenicity and effectiveness of the third compared to the second BNT162b2 vaccine dose. Nature Immunology. 2022;23(6):940-6.
33. Nemet I, Kliker L, Lustig Y, Zuckerman N, Erster O, Cohen C, et al. Third BNT162b2 Vaccination Neutralization of SARS-CoV-2 Omicron Infection. N Engl J Med. 2022;386(5):492-4.

Supplementary Information -

Dynamics of humoral response towards SARS-CoV-2 from vaccination and breakthrough infection

Matthias Becker[1,*], Alex Dulovic[1,*], Gunalp Uzun[2], Alan Bareiß[2], Marco Mikus[2], Daniel Junker[1], Johanna Griesbaum[1], Tanja Michel[1], Madeleine Fandrich[1], Katja Schenke-Layland[1,3,4], Karina Althaus[2,5], Tamam Bakchoul[2,5,#], Nicole Schneiderhan-Marra[1,#]

1 – NMI Natural and Medical Sciences Institute at the University of Tübingen, Reutlingen, Germany

2 – Centre for Clinical Transfusion Medicine, Tübingen, Germany

3 – Institute of Biomedical Engineering, Department for Medical Technologies and Regenerative Medicine, Eberhard Karls University Tübingen, Tübingen, Germany

4 – Cluster of Excellence iFIT (EXC 2180) “Image-Guided and Functionally Instructed Tumor Therapies”, Eberhard Karls University Tübingen, Tübingen, Germany

5 – Institute for Clinical and Experimental Transfusion Medicine, Medical Faculty of Tübingen, University Hospital Tübingen, Tübingen, Germany

*contributed equally to the manuscript and share first authorship

#indicates shared last authorship and corresponding author

Corresponding author

Tamam Bakchoul – Otfried-Müller-Straße 4/1, 72076 Tübingen, Germany.
tamam.bakchoul@med.uni-tuebingen.de. +49 7071 2981601

Nicole Schneiderhan-Marra – Markwiesenstrasse 55, 72770 Reutlingen, Germany.
Nicole.schneiderhan@nmi.de. +49 7121 51530815

Supplementary Methods

IgG avidity assay

For a subset of samples used in Figure 1 and 2, IgG avidity was assessed using a modified version of MULTICOV-AB. Briefly, serum samples were diluted 1:800 in assay buffer and mixed with beads coated with WT RBD to a final dilution factor of 1:1600. Samples were then incubated for 2 hours on a thermomixer (750 rpm, 20°C) to enable antibody binding to the beads. Following washing with a magnetic plate washer to remove unbound antibodies, the beads were separated into two plates, with either 100µL of PBS or 100µL of 6M Urea added to each well. The plates were then incubated for 10 mins on a thermomixer under the same conditions and then washed. Bound antibodies were detected by adding 3mM Strep-PE conjugated IgG to each well and incubating under the same conditions for 45 mins. Unbound detection antibody was then removed by washing, the beads resuspended in 100µL of wash buffer and then analysed using a FLEXMAP 3D instrument under the following settings: standard PMT, volume 60µL, gating 7000-15000, timeout 60 secs. A minimum of 40 beads per well were analysed. Median fluorescence intensity (MFI) was used to assess antibody binding to the beads. To calculate avidity of each sample, the MFI from the urea-treated beads was divided by the MFI of the PBS-treated beads. Samples were measured twice in two independent experiments. Avidity is displayed as a mean percentage of both experiments.

Supplementary Table 1 – List of analytes used in MULTICOV-AB and RBDCoV-ACE2 analysis

Analyte	Assay used	Manufacturer	Cat #
Spike trimer	MULTICOV-AB	NMI	
RBD WT	MULTICOV-AB and RBDCoV-ACE2	NMI	
S1 domain	MULTICOV-AB	NMI	
S2 domain	MULTICOV-AB	Sino Biological	
Nucleocapsid	MULTICOV-AB	Aalto Bioreagents	
Human IgG	MULTICOV-AB		
Goat anti-human IgG	MULTICOV-AB		
RBD beta	RBDCoV-ACE2	NMI	
RBD delta	RBDCoV-ACE2	NMI	
RBD omicron BA2	RBDCoV-ACE2	Sino Biological	
RBD omicron BA5	RBDCoV-ACE2	Sino Biological	

Supplementary Figure 1 – Flowchart of sample inclusion/exclusion for use in this publication

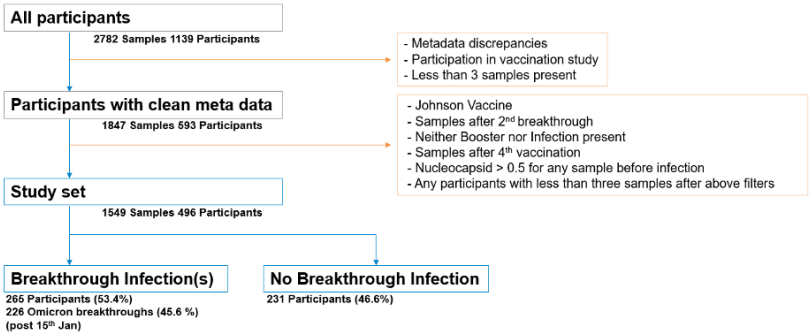

Flowchart detailing inclusion and exclusion criteria for use in this publication. Overall, 2782 samples from 1139 study participants were reduced to 1549 samples from 496 study participants. Samples used in all figures were then further defined on the basis of individual criteria (e.g. dT, number of doses received, see Supplementary Figure 2 and 4 for details).

Supplementary Figure 2 – Sample selection for use in Figure 1

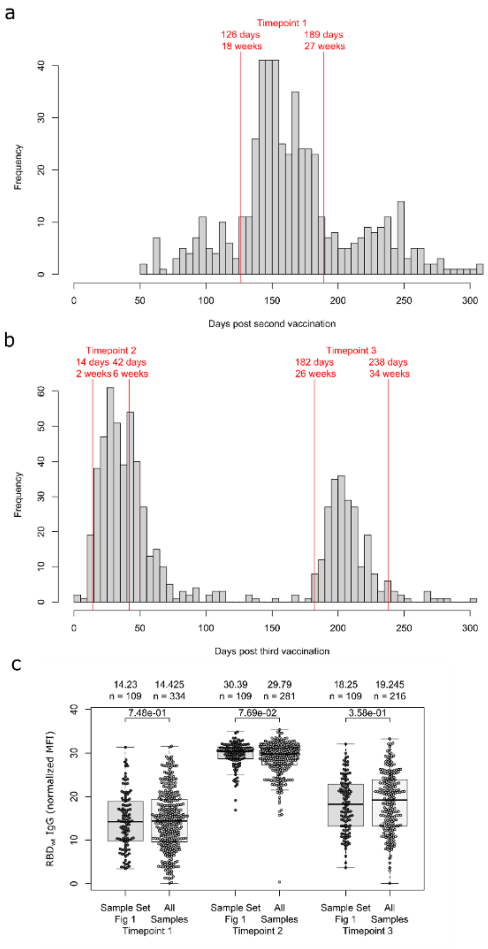

Longitudinal samples used in Figure 1 were selected to provide the largest number of study participants within the shortest time window possible. (a and b) histograms showing number of available samples for each day post second (a) or third (b) vaccination. No samples included had been infected at time of collection. As only samples from individuals with a sample present in all 3 timepoints were used, we compared RBD titre between these samples and all other samples available within the same timepoint (c) to confirm that they are representative of our study population. There was no significant difference in titre between samples used in Figure 1, and samples with from the same timepoint that were not used in Figure 1. (c) box and whisker plot with boxes to represent the 1st to 3rd quartiles, lines represent the median and whiskers are 1.5 IQR with outliers shown. MWU was used to calculate statistical significance between the two groups.

Supplementary Figure 3 – No long-term difference in antibody titre between different primary immunisations schemes

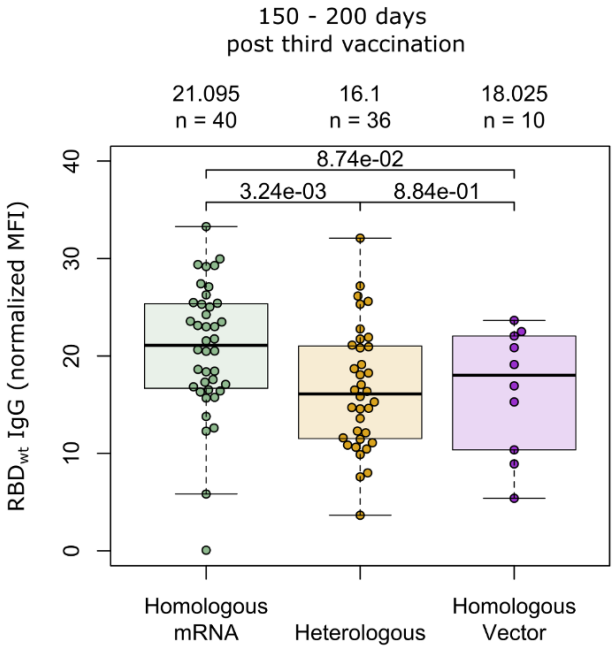

Box and whisker plot demonstrating differences in RBD antibody titre at timepoint 3 based upon primary immunisation scheme. Individuals received either two doses of either mRNA-1273 or BNT162b2 (homologous mRNA), one dose of AZD1222 and one dose of an mRNA vaccine (heterologous) or two doses of AZD1222 (homologous vector). All booster vaccinations were with either mRNA-1273 or BNT162b2. Box and whisker plots with boxes representing the 1st to 3rd quartiles, lines representing the median and whiskers are 1.5 IQR with outliers shown. One way ANOVA was used to compare differences between the groups.

Supplementary Figure 4 – Sample selection for use in Figure 2

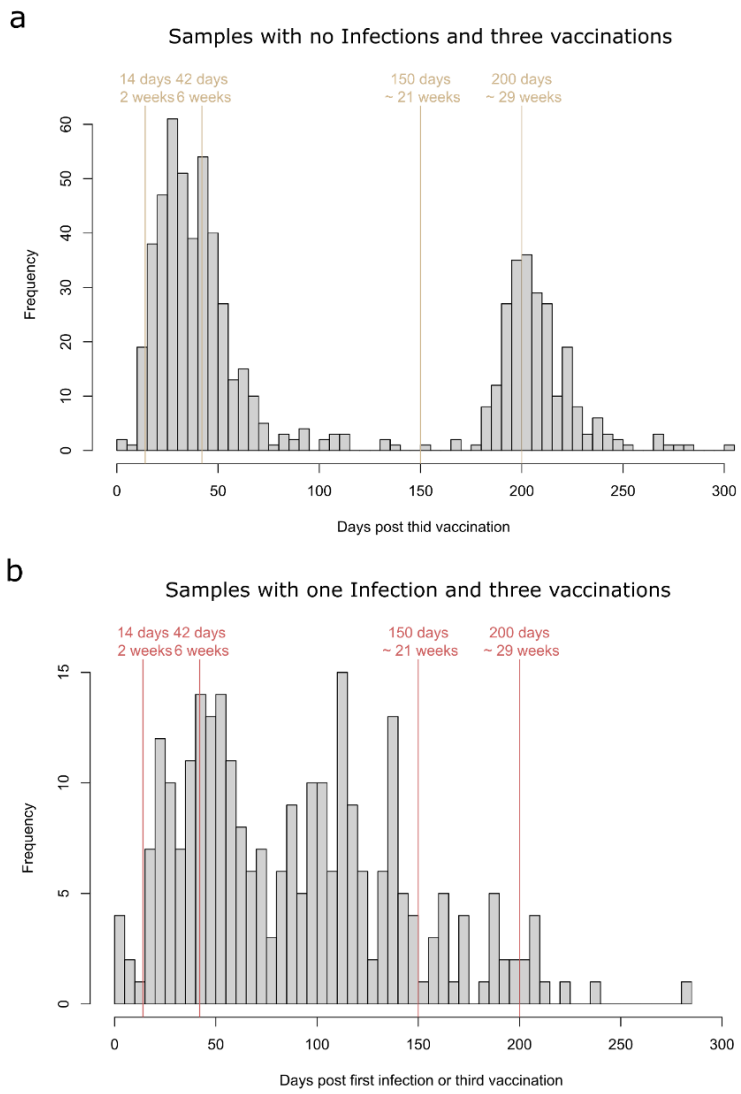

Longitudinal samples used in Figure 2 were selected to provide the largest number of study participants within the shortest time window possible. (a and b) histograms showing number of available samples for each day post third vaccination (a) or third vaccination/breakthrough infection (b).

Supplementary Figure 5 – RBD antibodies decay more slowly following a breakthrough infection.

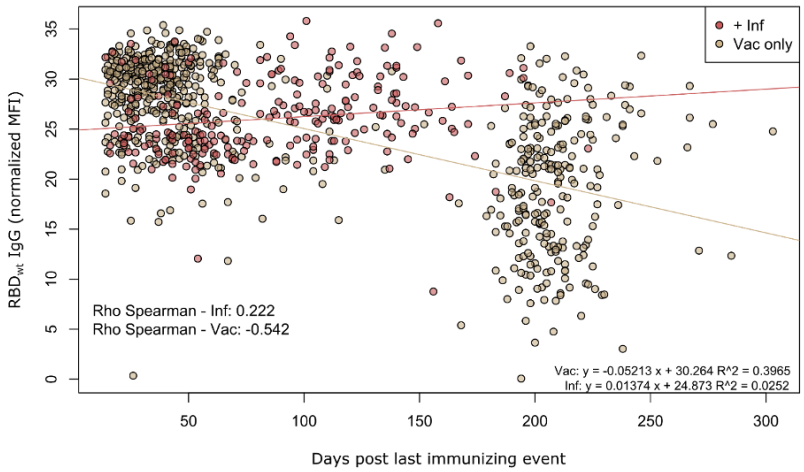

Differences in RBD antibody titre as time post last immunizing increases for vaccinated (3x, shown in gold) and vaccinated (3x) and infected individuals (shown in red). Spearman's rank was calculated to show the correlation with linear modelling used to analyse differences in antibody decay.